



**Anionic polymerization of aziridines:
Tuning block- and gradient-copolymer architectures
and applications of linear polyaziridines**

**Dissertation zur Erlangung des akademischen Grades eines
Doctor rerum naturalium**

vorgelegt von

TASSILO GLEEDE

geboren in Wiesbaden

Dekan: [REDACTED]

Erster Gutachter: [REDACTED]

Zweiter Gutachter: [REDACTED]

Die vorliegende Arbeit wurde in der Zeit vom Mai 2016 bis zum Oktober 2019 am Max Planck-Institut für Polymerforschung sowie dem Institut für Organische Chemie der Johannes Gutenberg-Universität Mainz unter Anleitung von [REDACTED] im Arbeitskreis von [REDACTED] [REDACTED] angefertigt.

Hiermit versichere ich, die vorliegende Arbeit selbstständig und ohne Benutzung anderer als der angegebenen Hilfsmittel angefertigt zu haben. Alle Stellen, die wörtlich oder sinngemäß aus Veröffentlichungen oder anderen Quellen entnommen sind, wurden als solche eindeutig kenntlich gemacht. Diese Arbeit ist in gleicher oder ähnlicher Form noch nicht veröffentlicht und auch keiner anderen Prüfungsbehörde vorgelegt worden.

Tassilo Gleede Mainz, 18.01.2020

Danksagung

[Redacted text block containing multiple lines of blacked-out content]

[REDACTED]

[REDACTED]

[REDACTED]

[REDACTED]

[REDACTED]

[REDACTED]

[REDACTED]

[REDACTED]

[REDACTED]

[REDACTED]

[REDACTED]

[REDACTED]

[REDACTED]

Table of Contents

DANKSAGUNG	V
TABLE OF CONTENTS	VII
MOTIVATION AND OBJECTIVES	1
GRAPHICAL ABSTRACT	4
ABSTRACT	7
ZUSAMMENFASSUNG	11
1 AZIRIDINES AND AZETIDINES: BUILDING BLOCKS FOR POLYAMINES BY ANIONIC AND CATIONIC RING-OPENING POLYMERIZATION	15
1.1 INTRODUCTION.....	17
1.2 CATIONIC RING-OPENING POLYMERIZATION OF AZIRIDINES AND AZETIDINES	20
1.3 ANIONIC POLYMERIZATION OF AZIRIDINES	30
1.4 ANIONIC POLYMERIZATION OF AZETIDINES	43
1.5 ORGANOCATALYTIC RING-OPENING POLYMERIZATION (OROP) OF ACTIVATED AZIRIDINES	46
1.6 DESULFONYLATION REACTIONS	48
1.7 COMBINATION OF AZIRIDINES AND AZETIDINES WITH OTHER POLYMERIZATION TECHNIQUES: COPOLYMERS AND POLYMER ARCHITECTURES.....	50
1.8 CONCLUSIONS	58
1.9 REFERENCES CHAPTER 1	59
2 ALCOHOL- AND WATER-TOLERANT LIVING ANIONIC POLYMERIZATION OF AZIRIDINES	65
2.1 ABSTRACT	67
2.2 INTRODUCTION.....	68
2.3 RESULTS AND DISCUSSION	70
2.4 REFERENCES CHAPTER 2.....	79
2.5 SUPPORTING INFORMATION FOR ALCOHOL- AND WATER-TOLERANT LIVING ANIONIC POLYMERIZATION OF AZIRIDINES	81
2.6 MATERIALS AND METHODS	81
2.7 SECTION A: MECHANISTIC EXPLANATION OF AAROP WITH PROTIC ADDITIVES.....	83
2.8 SECTION B. KINETICS.....	83
2.9 SECTION C. ¹³ C-NMRs AND 2D-NMRs OF THE KINETICS	88
2.10 SECTION D. POLYMERIZATION IN OPEN VIALS	98

2.11	SECTION E. MALDI-TOF SPECTRA	109
2.12	SECTION F. CHAIN EXTENSION EXPERIMENTS.....	111
2.13	SECTION G: COMPUTATIONAL DETAIL	115
2.14	SECTION H. POLYMERIZATION OF UNPROTECTED HYDROXYL-FUNCTIONALIZED SULFONYL AZIRIDINE	119
2.15	ADDITIONAL REFERENCES CHAPTER 2	122
3	FAST ACCESS TO AMPHIPHILIC MULTIBLOCK ARCHITECTURES BY THE ANIONIC COPOLYMERIZATION OF AZIRIDINES AND ETHYLENE OXIDE	123
3.1	ABSTRACT	124
3.2	INTRODUCTION.....	125
3.3	RESULTS AND DISCUSSION	126
3.4	SUMMARY.....	133
3.5	REFERENCES CHAPTER 3	134
3.6	SUPPORTING INFORMATION FOR FAST ACCESS TO AMPHIPHILIC MULTI-BLOCK ARCHITECTURES BY ANIONIC COPOLYMERIZATION OF AZIRIDINES AND ETHYLENE OXIDE	137
3.7	ADDITIONAL REFERENCES CHAPTER 3	165
4	COMPETITIVE COPOLYMERIZATION: ACCESS TO AZIRIDINE COPOLYMERS WITH ADJUSTABLE GRADIENT STRENGTHS	167
4.1	ABSTRACT	168
4.2	INTRODUCTION.....	169
4.3	EXPERIMENTAL SECTION	172
4.4	RESULTS AND DISCUSSION	177
4.5	CONCLUSION	190
4.6	REFERENCES CHAPTER 4	191
4.7	SUPPORTING INFORMATION FOR: COMPETITIVE COPOLYMERIZATION: ACCESS TO AZIRIDINE COPOLYMERS WITH ADJUSTABLE GRADIENT STRENGTHS	195
5	LINEAR WELL-DEFINED POLYAMINES VIA ANIONIC RING-OPENING POLYMERIZATION OF ACTIVATED AZIRIDINES: FROM MILD DESULFONYLATION TO CELL TRANSFECTION.....	217
5.1	ABSTRACT	218
5.2	INDRODUCTION	219
5.3	RESULTS AND DISSCUSSION	221
5.4	SUMMARY.....	227
5.5	REFERENCES CHAPTER 5	228

5.6	SUPPORTING INFORMATION FOR LINEAR WELL-DEFINED POLYAMINES VIA ANIONIC RING-OPENING POLYMERIZATION OF ACTIVATED AZIRIDINES: FROM MILD DESULFONYLATION TO CELL TRANSFECTION	230
5.7	MATERIALS AND ANALYTIC METHODS	230
5.8	SYNTHESIS PROCEDURES	232
5.9	ADDITIONAL REFERENCES CHAPTER 5.....	242
6	4-STYRENESULFONYL-(2-METHYL)AZIRIDINE: THE FIRST BIVALENT AZIRIDINE-MONOMER FOR ANIONIC AND RADICAL POLYMERIZATION	243
6.1	ABSTRACT	244
6.2	INTRODUCTION.....	245
6.3	EXPERIMENTAL SECTION.....	246
6.4	RESULTS AND DISCUSSION	249
6.5	REFERENCES CHAPTER 6.....	258
6.6	SUPPORTING INFORMATION FOR 4-STYRENESULFONYL-(2-METHYL)AZIRIDINE: THE FIRST BIVALENT AZIRIDINE-MONOMER FOR ANIONIC AND RADICAL POLYMERIZATION	259
6.7	ANALYTICAL DATA OF STMAZ	259
6.8	ANALYTICAL DATA OF HOMO AND CO-POLYMERS.....	261
6.9	ANALYTIC OF THIOL-ENE FUNCTIONALIZATION.....	264
7	TACTICITY CONTROL IN POLY(SULFONYL AZIRIDINE)S: TOWARDS TUNING CRYSTALLINITY AND SUPRAMOLECULAR INTERACTIONS	273
7.1	INTRODUCTION.....	274
7.2	EXPERIMENTAL SECTION.....	277
7.3	RESULTS AND DISCUSSION	281
7.4	SUMMARY.....	284
7.5	REFERENCES CHAPTER 7	285
7.6	SUPPORTING INFORMATION FOR TACTICITY CONTROL IN POLY(SULFONYL AZIRIDINE)S: TOWARDS TUNING CRYSTALLINITY AND SUPRAMOLECULAR INTERACTIONS	287
8	APPENDIX.....	295
8.1	PUBLICATIONS OF COOPERATION PROJECTS.....	295

Motivation and Objectives

Using a sulfonyl group to substitute the *N*-proton of aziridines activates the aziridine and allows anionic ring-opening reactions. Sulfonyl groups act as both an activation and protecting group. Sulfonyl activated aziridines are a compatibly new class of monomers that have been explored in 2005. To determine their properties and application in anionic ring-opening polymerization (AROP) more novel monomers carrying functionalities should be designed to expand the existing scope of activated aziridines. Currently, most monomers functionalities are introduced in the aziridine side group instead of the *N*-activation group itself. The inclusion of different functionalities enables a greater range of potential applications of polyaziridines to be achieved. This functionality can be used to give adjustable solubility or thermal properties of the polysulfonamides. New functional aziridine monomers have been developed, and the properties of the resulting polymers have been studied. Polymers formed from activated aziridines are polysulfonamides which belong to a class of polyamines, due to the presence of nitrogen in the polymer backbone.

The most popular strategy to access linear polyamines is the cationic ring-opening polymerization (CROP) of 2-oxazolines. The CROP methodology has been developed several years ago and is applied in industry and performs very well. Nevertheless, AROP does not suffer of increased chain transfer, termination or recombination reactions, and is by this superior to CROP. One major goal of this thesis was the deprotection of polysulfonamides to show a mild synthetic alternative to the L-PEI strategy *via* CROP from 2-oxazolines. Several methods to desulfonylate these polymers have already been reported. Due to the strength of the sulfonyl-amine bond most of them suffer from low yields or require very toxic chemicals and harsh conditions. This makes further application in biological studies challenging. The monomer, which was developed in this work, allows a mild nucleophilic desulfonylation mechanism. Moreover, the ring is sufficiently activated to enable efficient initiation and controllable polymerization.

In addition, the electron withdrawing (EWD) nature of activating groups pull electron density from the active chain end of the polymers. This effects the nucleophilicity as well as the basicity of the active species. In previous studies, only the effect of the EWD groups on the monomer activity was partly analyzed and discussed. Investigating the effect EWD groups have on the active polymer chain-end during polymerization gives us a better understanding of the role of the activating group. A strong nucleophilicity of the chain-end is required to ensure propagation. While conversely, strong nucleophilicity increases the probability of termination by electrophiles or protons.

Using a systematic library of different electron withdrawing substituents, allows tuning of monomer reactivities. This enables the production of different gradient polymer microstructures in copolymerization mixtures. As part of this thesis, the concept of tuning polymer gradient will be revealed and correlations between the monomer activation and propagation rates will be discussed. The precise control of the polymer structure enables a gradual distribution of functionalities in the polymer microstructure to be obtained. We see adjustable gradient strength in copolymers as a central goal in polymer synthesis according to adjust polymer properties. Tuning the gradient over this enormous range from statistical to block copolymers with copolymerizations is a synthetic challenge. The conventional strategy to access gradient copolymers uses monomer-dosing apertures. Detailed understanding of the copolymerization behavior and the correlations to monomer properties allows the access this polymer structures by single-step and one-pot reactions. Building on the concept of copolymerizing different activated aziridines and single-step polymerization set-ups, the copolymerization of aziridines with ethylene oxide (EO), as representative of the oxyanionic polymerization, was a major goal, which was tested, but not achieved before this thesis.

Chapter 1: The first chapter introduces the anionic polymerization of activated aziridines. It further gives an overview of the state of the art research and how polyaziridines are obtained by anionic and other polymerization methods. Copolymerization techniques to novel polysulfonamides and various monomers are introduced.

Chapter2: The impact of the electron withdrawing activation groups on the active chain-end is studied in this chapter. Different EWD groups are used to study the influence of homopolymerization kinetics according to the presents of additives such as protic solvents (alcohols and water). Furthermore, the influence on polymerization kinetic, polymer dispersities and secondary initiation should be explored to understand the AROP of activated aziridines with focus on the active chain-end in detail.

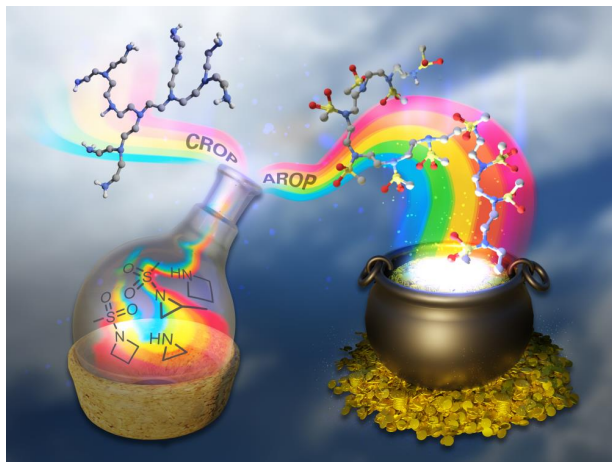
Chapter 3: To achieve a copolymerization of activated aziridines ethylene oxide is the priority in the third chapter. As monomers appear to be very similar, both are three membered rings with a heteroatom, both polymerize *via* AROP, both have a similar ring tension, the copolymerization and analysis of the microstructure a major importance of this chapter. EO and the tested aziridines showed to have highly different monomer reactivities; therefore the copolymerization could be used to generate amphiphilic multiblock systems. Additionally, routes and applications of novel water-soluble polymers with diverse architectures should be explores in this chapter.

Chapter 4: The intention of the fourth chapter was to further expand the scope of the different activation groups to understand and practically observe the detailed effect of the reactivity difference and gradient strength of the copolymer microstructure. The co-monomers library and the correlations between the reactivity differences could be used to prepare more different gradient structures. Gradient systems are used as functional polyamines after removal of the sulfonyl group or directly as compatibilizer for polysulfonamides.

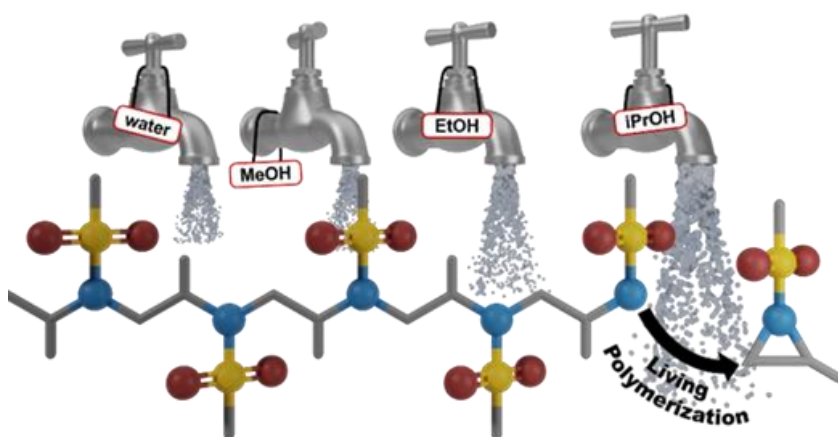
Chapter 5: The fifth chapter is dedicated to the desulfonylation reaction of the polysulfonamides. Developing novel activation groups, which are covalent attached on the nitrogen of the aziridine rings, can be used to fine-tune the propagation rates, like in chapter 4 and 3. Seeing the sulfonyl group as a protecting group and not as a simple activating group should be in the focus of this chapter. Depending also on the EWD behavior of the sulfonyl group of the monomers, the polymer is deprotectable. A method should be designed to use the polysulfonamides as a precursor for linear, functionalized polyamines. PEI derivatives synthesized *via* AROP should be tested as cell transfection agent.

Chapter 6: The last chapter is about the great variety of functional activated aziridine monomers. The activation group of the aziridines cannot only be used to trigger the reactivity. Here, the activation group should also act a functional group allowing further post modification, which were previously only introduced *via* the 2-position. Bearing a styrene moiety the anionically synthesized polysulfonamides should be further functionalized and simultaneously the vinyl moiety should act as a polymerizable group for radical polymerization, which makes this activated aziridine become an orthogonal bivalent monomer for both, radical and AROP.

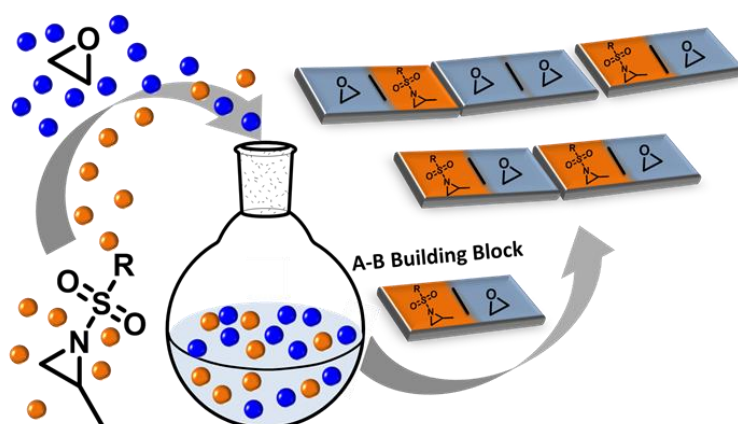
Graphical Abstract



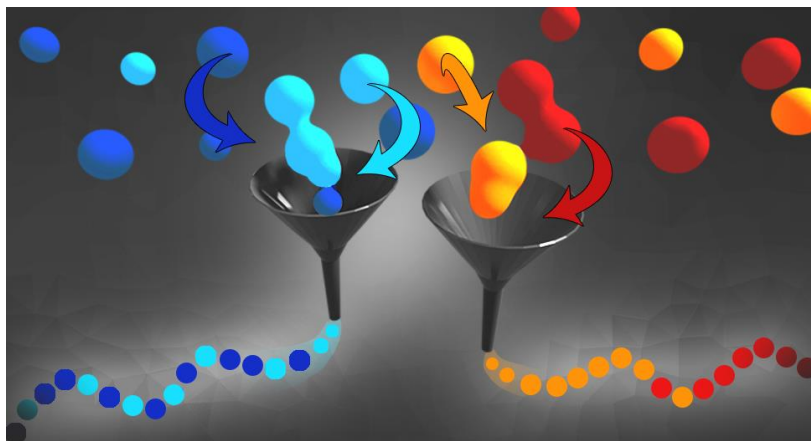
TOC 1: Table of content, symbolizing the wide spectra of polymerizing activated aziridines and azetidines to novel linear polyethyleneimines by anionic ring-opening polymerization (from the flask to the right, and the polymerization of aziridine and azetidine by cationic ring-opening polymerization (left side)



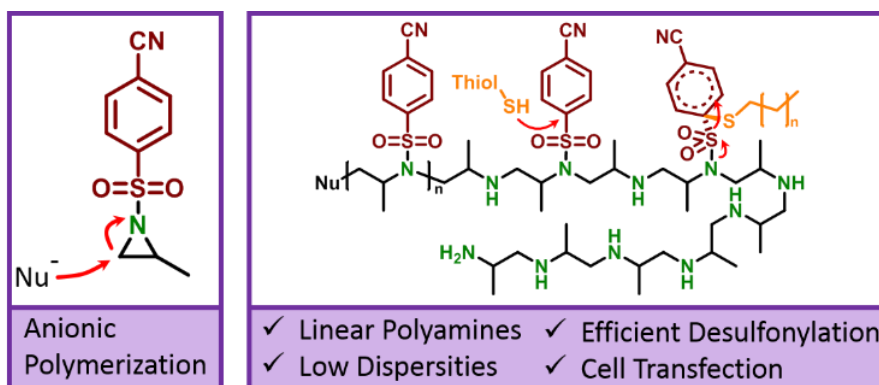
TOC 2: Table of content, symbolizing the robust polymerization of activated aziridines, resistant against protic additives (alcohols and water)



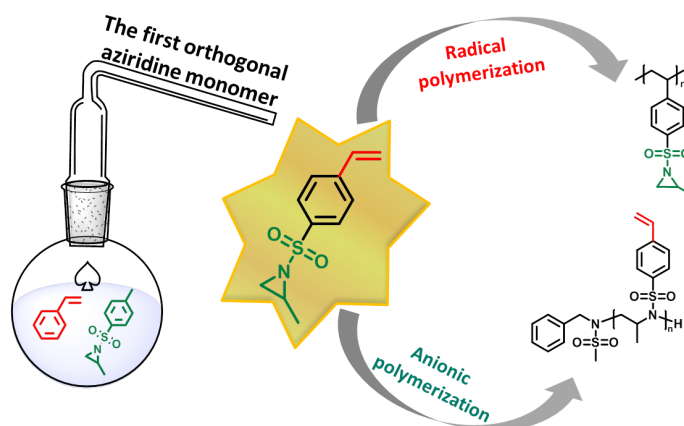
TOC 3: Table of content, symbolizing fast an easy synthesis of amphiphilic multiblock architectures from EO (blue) and Aziridines (orange)



TOC 4: Table of content, symbolizing the combination different monomers for a copolymerization: Depending on the activation difference between two copolymers the microstructure is adjustable from statistical over gradient to block-copolymers.



TOC 5: The TOC illustrates the desulfonation of the polysulfonamide, which was polymerized by anionic ring-opening polymerization.



TOC 6: Table of content, symbolizing the combination of two different monomers (Styrene and tosyl activated 2-methylaziridine) to access bivalent monomer with orthogonal moieties for radical (red) and anionic (green) polymerization.

Abstract

14 Years after anionic ring-opening polymerization was applied to activated aziridines for the first time, this rather novel monomer class became interesting for more and more research groups. The polymer class originated from activated aziridines offers several hidden potentials to be further explored e.g. their unique properties concerning the polymerization behavior and expanding the scope of new aziridine monomers to study functional polyamine derivatives. In contrast to cationic polymerization, anionic polymerization requires proton-free conditions, why the *N*-terminal hydrogen is substituted with a sulfonyl group which withdraws electrons from the aziridine ring and thereby allows nucleophilic attacks and consequently, living anionic polymerization. The polymers from activated aziridines represent functionalizable, linear polyamine derivatives or polysulfonamides.

This PhD thesis focuses primarily on a deeper understanding of synthesizing gradient and block copolymers with aziridines as well as further explain the nature of aza-anionic polymerization to classify it next to other anionic polymerizations. In addition, this novel class of linear polyamine derivatives were investigated in fundamental studies on potential applications as cell transfection agents or as amphiphilic surfactants. The thesis itself is divided in six main chapters of published results, an outlook and appendix. The **first Chapter** is an introduction on polyamines synthesized from aziridines and azetidines. It provides an overview of different routes to access polyamines with various structures and refer to applications of those polyamine classes, introduces the different routes to synthesize the activated aziridines and summarizes the different polymerization techniques to access the polysulfonamides.

The **second chapter** focus on the unique finding that anionic polymerization of aziridines appears to be tolerant and robust towards protic impurities. Further, this polymerization technique does not require inert atmosphere and stays living in the presence of large amounts of water or alcohols. Different activated aziridines were polymerized with up to 100-fold excess of an added protic impurity (like water or alcohols), proven to be active and fulfilling the requirements of a living polymerization. The electron withdrawing effect of the activating groups causes this unique tolerance towards protic additives. This effect decreases the basicity of the propagating species, while maintaining a strong nucleophilic character. Alcohol or water is only slightly involved in the polymerization, which further allows the direct preparation of polyols by anionic polymerization without protective groups.

The **third chapter** demonstrates the first single step one pot copolymerization of activated aziridines with ethylene oxide (EO). Copolymerization of these two highly strained three-membered heterocycles results by a one-pot copolymerization to well-defined amphiphilic block copolymers with a single step. The polymerization was followed by real-time ^1H NMR spectroscopy, finding the biggest reactivity difference of $r_1 = 265$ and $r_2 = 0.004$ for 2-methyl-*N*-tosylaziridine/EO and $r_1 = 151$ and $r_2 = 0.013$ for 2-methyl-*N*-mesylaziridine/EO ever reported for anionic copolymerizations. The obtained amphiphilic diblock copolymers were used to stabilize emulsions and to prepare polymeric nanoparticles by mini-emulsion polymerization. Synthesis strategies towards amphiphilic penta- and tetrablock copolymers in one or two steps are presented additionally in this section. These example of epoxide and aziridine copolymerizations represent a novel strategy to produce sophisticated macromolecular architectures. They are an ideal system to study stimuli-responsive and amphiphilic (block) polymers consisting of polyamines and water soluble polyglycols.

The **fourth chapter** is dedicated to the individual copolymerizations of activated aziridines with two different activation groups. Due to the beneficial living nature of anionic polymerization, gradient copolymers can be obtained with low dispersities and adjustable molar mass. The great variety of the activation groups allows tuning the electron withdrawing behavior precisely and thereby the degree of the monomer activation. The combination of different activating groups allows further fine-tuning the gradient strength of copolymers. Sulfonyl activated aziridines are to date the only monomer class providing access to gradient copolymers with microstructures ranging from statistical to block-copolymers solely by adjusting the activation groups. This detailed study allowed correlations between the monomer activation given by Hammett parameters and the propagation parameters of the individual homo polymerizations. This is used to predict polymerization rates (k_p) for aziridines, not synthesized so far. For the first time correlation of copolymerization ratios for ring-opening polymerization with the EWD nature of the monomers was possible. This knowledge allows accessing various tailored gradient copolymers with controlled monomer sequence in a single step and predicting copolymer structures of not synthesized monomers.

The last two chapters (**chapter 5 & 6**) represent the synthesis of lately developed functional activated aziridines. In both chapters the obtained polysulfonamides were further used for post modification. As the anionic polymerization of sulfonamide-activated aziridines leads to polymers with a linear polyamine backbone, this pathway is after a successful desulfonylation an alternative to the 2-oxazoline route. Poly (2-oxazoline)s are usually used to access linear polyethyleneimine (L-PEI) after acidic hydrolysis from. The 1-(4-cyanobenzenesulfonyl) 2-methyl-

aziridine, an aziridine containing a highly electron withdrawing activation group was found to polymerize as good as the other monomers of the aziridine family. Additionally, the 4-cyanobenzenesulfonyl allows mild reaction conditions to cleave the nitrogen – sulfur bond to convert the polysulfonamide into linear polypropyleneimine (L-PPI). The high control over molecular weight and weight dispersities achieved by living anionic polymerization are the key advantages of this strategy, especially if used for biomedical applications, as molecular weight correlates with toxicity. The synthesized polypropylene-imine showed further to be an adequate cell transfection agent.

4-Styrenesulfonyl-(2-methyl)aziridine (StMAz) is a monomer containing a functional activation group. This makes it the first orthogonal aziridine monomer, applicable for both anionic ring-opening and radical polymerization. Both polymerization pathways are accessible without using protective groups. While azaanionic ring-opening polymerization (AAROP) of StMAz and other methyl-aziridine derivatives provides multifunctional polyaziridines, radical polymerization of the vinyl group gives access to polyalkylenes with aziridine side groups, which are known to be efficiently addressable *via* nucleophiles.

Chapter 7 contains unpublished results on the synthesis and polymerization of enantiomerically pure aziridines. These and discussed applications correspond to an outlook on further research with activated aziridines.

Zusammenfassung

14 Jahre nach dem die anionische Ringöffnungspolymerisation erstmals an aktivierten Aziridinen angewandt wurde, gewinnt diese Monomerkategorie der aktivierten Aziridine immer mehr an Bedeutung. Die aus aktivierten Aziridinen stammende Polymerklasse bietet weiterhin verborgenes Potential, um die einzigartigen Eigenschaften hinsichtlich der Polymerisation und des Anwendungsbereichs neuer Aziridinmonomere weiter zu erforschen. Im Gegensatz zur kationischen Polymerisation erfordert die anionische Polymerisation in der Regel strikt aprotische Bedingungen, weshalb der *N*-terminale Wasserstoff durch eine Sulfonylgruppe substituiert ist. Diese Schutzgruppe entzieht dem Aziridinring Elektronen und ermöglicht nukleophile Angriffe. Somit wird eine lebende anionische Polymerisation an Aziridinen ermöglicht. Bei den Polymeren von aktivierten Aziridinen handelt es sich um lineare funktionalisierbare Polyaminderivate, hier auch als Polysulfonamide und Polyaziridine bezeichnet.

Diese Doktorarbeit beschäftigt sich in erster Linie damit, ein tieferes Verständnis für die Synthese von Gradienten- und Blockcopolymeren mit Aziridinen zu erhalten, sowie die azaanionische Polymerisation zwischen den anderen anionischen Polymerisationsklassen einzuordnen. Darüber hinaus wurde diese neue Klasse von linearen Polyaminderivaten grundlegenden Studien unterzogen, um die Anwendungen als Zelltransfektionsmittel oder den Nutzen als amphiphile Tenside zu zeigen. Die Arbeit selbst ist in sechs Kapitel mit publizierten Ergebnissen gegliedert und enthält ein Ausblick mit unpublizierten Ergebnissen, sowie ein Appendix. Das **erste Kapitel** dient zur Einführung in Polyamine, welche aus Aziridinen und Azetidinen synthetisiert werden können. Es bietet zudem einen Überblick über diverse Wege zu Polyaminen mit verschiedenen Strukturen und bezieht sich auch auf Anwendungen von Polyaminen. Es werden verschiedene Wege zur Synthese von aktivierten Aziridinen erläutert und die verschiedenen Polymerisationstechniken, welche die Synthese von Polysulfonamiden ermöglichen, zusammengefasst.

Das **zweite Kapitel** befasst sich mit der einzigartigen Erkenntnis, dass die anionische Polymerisation von Aziridinen robust gegenüber protischen Verunreinigungen ist und Wasser sowie Alkohole toleriert werden. Zusätzlich verlangt diese Polymerisationstechnik keine inerte Atmosphäre und bleibt in Gegenwart großer Mengen von Wasser oder Alkoholen nachweislich lebend. Verschiedene aktivierte Aziridine wurden mit einem bis zu 100-fachen Überschuss einer zugesetzten protischen Verunreinigung (wie Wasser oder Alkohole) polymerisiert. Die Kettenenden blieben dabei aktiv und die Polymerisationen erfüllten die Anforderungen einer lebenden Polymerisation. Der elektronenziehende Effekt der Aktivierungsgruppen ist

verantwortlich für die einzigartige Toleranz gegenüber protischen Additiven. Er verringert die Basizität des aktiven Kettenendes, während der stark nukleophile Charakter erhalten bleibt. Alkohole oder Wasser sind nur geringfügig an der Polymerisation beteiligt, was die direkte Herstellung von Polyolen durch anionische Polymerisation ohne Schutzgruppen ermöglicht.

Das **dritte Kapitel** zeigt die erste Einschnitt-Eintopfcopolymerisation von aktivierten Aziridinen und Ethylenoxid (EO). Die Copolymerisation dieser beiden hochgespannten dreigliedrigen Heterozyklen führt auf schnellem und einfachem Weg zu definierten amphiphilen Blockcopolymeren. Die Polymerisation wurde durch Echtzeit ^1H NMR-Spektroskopie verfolgt, wobei der, für anionische Copolymerisationen, größte Reaktivitätsunterschied von $r_1 = 265$ und $r_2 = 0,004$ für 2-Methyl-*N*-tosylaziridin / EO, sowie $r_1 = 151$ und $r_2 = 0,013$ für 2-Methyl-*N*-mesylaziridin / EO gefunden wurde. Die erhaltenen amphiphilen Diblockcopolymeren wurden verwendet, um Emulsionen zu stabilisieren und Nanopartikel durch Miniemulsionspolymerisation herzustellen. In diesem Kapitel werden zusätzlich Synthesestrategien für amphiphile Penta- und Tetrablockcopolymeren in wenigen Syntheseschritten vorgestellt. Diese Copolymerisation von EO und Aziridinen ermöglicht neue Strategien zur Herstellung komplexer makromolekularer Architekturen. Diese sind ein ideales System zur weiteren Erforschung von responsiven und amphiphilen Blockcopolymeren, welche aus Polyaminen und wasserlöslichen Polyethern bestehen.

Das **vierte Kapitel** behandelt die Copolymerisationen von aktivierten Aziridinen mit zwei verschiedenen Aktivierungsgruppen. Aufgrund des lebenden Charakters der anionischen Polymerisation können Gradientencopolymeren mit geringen Dispersitäten und einstellbaren Molmassen erhalten werden. Die große Vielfalt der Aktivierungsgruppen ermöglicht es das elektronenziehende Verhalten und damit die Monomeraktivität exakt einzustellen. Die Kombination von verschiedenen aktivierenden Gruppen ermöglicht es, die Gradientenstärke der Copolymeren zu beeinflussen. Die Klasse der sulfonamidaktivierten Aziridine ist bis heute die einzige Monomerklasse, welche es erlaubt, durch Wahl der Aktivierungsgruppen, Gradientencopolymeren mit unterschiedlichen Mikrostrukturen von statistisch bis zu blockartig zu synthetisieren. Diese detaillierte Studie ermöglichte Korrelationen zwischen dem durch den Hammett-Parameter beschriebenen Elektronenzug und der Monomeraktivität, wiedergespiegelt durch die Propagationsparameter (k_p) der einzelnen Homopolymerisationen zu erkennen. Die gefundenen Gesetzmäßigkeiten lassen sich nutzen, um die Polymerisationsgeschwindigkeiten für Aziridine vorherzusagen, welche bislang noch nicht synthetisiert wurden. Dieses Wissen erlaubt den Zugriff auf verschiedene maßgeschneiderte Gradientencopolymeren mit einstellbarer

Monomersequenz, welche in einem Schritt synthetisiert werden können. Darüber hinaus können auch Copolymerstrukturen von noch nicht synthetisierten Monomeren vorhergesagt werden.

Die letzten beiden Kapitel (**Kapitel 5 und 6**) beschreiben die Synthese kürzlich entwickelter funktionalisierter Aziridine. In beiden Kapiteln wurden die erhaltenen Polysulfonamide modifiziert. Da die anionische Polymerisation aktivierter Aziridine zu Polymeren mit linearen Polyamingrundgerüst führt, ist dieser Weg nach einer erfolgreichen Desulfonylierung eine mögliche Alternative zu dem Weg über 2-Oxazoline. Poly-(2-oxazoline) werden üblicherweise verwendet, um lineares Polyethylenimin (L-PEI) nach saurer Hydrolyse zu erhalten. 1-(4-Cyanobenzolsulfonyl)-2-methylaziridin, ein neues Aziridinmonomer, welches eine stark elektronenziehende Aktivierungsgruppe enthält, polymerisiert ähnlich gut wie die anderen Monomere der Aziridinfamilie. Zusätzlich ermöglicht die 4-Cyanobenzolsulfonylgruppe die Spaltung der Stickstoff-Schwefel-Bindung unter milden Reaktionsbedingungen. Somit kann lineares Polypropylenimin (L-PPI) aus Polysulfonamiden erhalten werden. Die gute Kontrolle des Molekulargewichts und der Molmassendispersitäten, welche durch lebende anionische Polymerisation ermöglicht werden, sind die Hauptvorteile dieser Strategie. Insbesondere wenn L-PPI für biomedizinische Anwendungen verwendet wird, ist eine gute Molekulargewichtseinstellung erforderlich, da die Molmasse von L-PEI mit der Toxizität korreliert. Das synthetisierte Polypropylenimin erwies sich als adäquates Zelltransfektionsmittel.

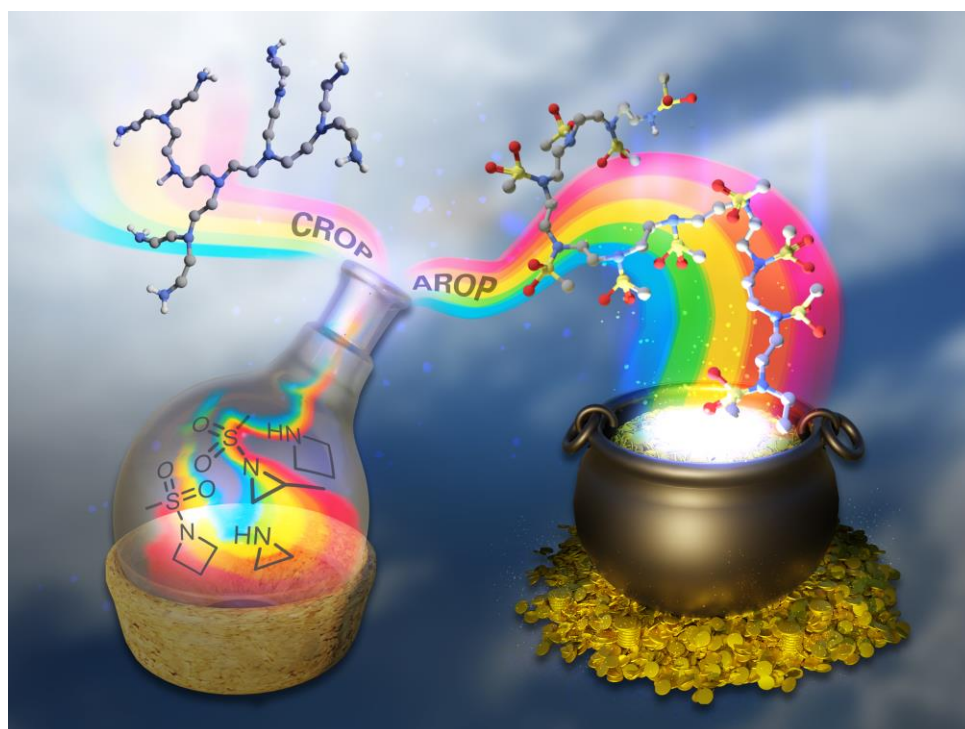
4-Styrolsulfonyl-(2-methyl)aziridin (StMAz) ist ein Monomer mit einer funktionellen Aktivierungsgruppe. Damit ist es das erste orthogonale Aziridinmonomer, das sowohl für die anionische Ringöffnungspolymerisation als auch für die radikalische Polymerisation geeignet ist. Beide Polymerisationsmethoden sind ohne Verwendung von zusätzlichen Schutzgruppen möglich. Während die azaanionische Co- und Homoringöffnungspolymerisation von StMAz werden funktionalisierbare Polyaziridine erhalten. Die radikalische Polymerisation der Vinylgruppe ermöglicht wiederum den Zugang zu Polyalkylenen mit Aziridinseitengruppen, welche bekanntermaßen effizient über Nucleophile modifizierbar sind.

Kapitel 7 enthält unpublizierte Ergebnisse zu der Synthese und der Polymerisation von enantiomerenreinen Aziridinen. Diese und diskutierte Anwendungen entsprechen einem Ausblick auf weitere Forschung mit diesen Monomeren.

1 Aziridines and azetidines: building blocks for polyamines by anionic and cationic ring-opening polymerization

Tassilo Gleede, Louis Reisman, Elisabeth Rieger, Pierre Canisius Mbarushimana,

*Paul A. Rugar and Frederik R. Wurm**



TOC 1: Table of content, symbolizing the wide spectra of polymerizing activated aziridines and azetidines to novel linear polyethyleneimines by anionic ring-opening polymerization (from the flask to the right, and the polymerization of aziridine and azetidine by cationic ring-opening polymerization (left side)

Note: This work was conducted in cooperation with Louis Reisman, Elisabeth Rieger, Pierre Canisius Mbarushimana, Paul A. Rugar, Frederik R. Wurm and me (Tassilo Gleede). The Review is divided in nine Parts.

Louis Reisman, Pierre Canisius Mbarushimana, Paul A. Rugar were responsible for following paragraphs:

- Cationic ring-opening polymerization of aziridines and azetidines
- Anionic polymerization of azetidines

Tassilo Gleede, Elisabeth Rieger, Frederik R. Wurm were responsible for following paragraphs:

- Anionic polymerization of aziridines
- Organocatalytic ring-opening polymerization (OROP) of activated aziridines
- Desulfonylation reactions
- Combination of aziridines and azetidines with other polymerization techniques: copolymers and polymer architectures
- Polymer architectures

All authors contributed to the content of the review, they wrote and edited the review.

This chapter is based on an open access review article under the terms of the Creative Commons Attribution-Non-Commercial License: Tassilo Gleede, Louis Reisman, Elisabeth Rieger, Pierre Canisius Mbarushimana, Paul A. Rugar and Frederik R. Wurm *Aziridines and azetidines: building blocks for polyamines by anionic and cationic ring-opening polymerization* *Polym. Chem.*, **2019**, *10*, 3257-3283.

Content: Despite the difficulties associated with controlling the polymerization of ring-strained nitrogen containing monomers, the resulting polymers have many important applications, such as antibacterial and antimicrobial coatings, CO₂ adsorption, chelation and materials templating, and non-viral gene transfection. This review highlights the recent advances on the polymerizations of aziridine and azetidine. It provides an overview of the different routes to produce polyamines, from aziridine and azetidine, with various structures (i.e. branched vs. linear) and degrees of control. We summarize monomer preparation for cationic, anionic and other polymerization mechanisms. This comprehensive review on the polymerization of aziridine and azetidine monomers will provide a basis for the development of future macromolecular architectures using these relatively exotic monomers.

1.1 Introduction

Despite being structural analogs with comparable ring strain (Figure 1.1), aziridine and oxirane have very different polymerization chemistries. Oxirane can be polymerized *via* a variety of mechanisms, including cationic ring-opening polymerization (CROP)¹ and anionic ring-opening polymerization (AROP)^{2,3} to form linear poly(ethylene oxide) (PEO) with high degrees of control. In contrast, aziridine can only polymerize *via* CROP to produce (hyper)branched polyethylenimine (hbPEI) with little control over molecular weight, dispersity, and microstructure.^{4–8} The situation is similar with azetidine (Figure 1.1), the nitrogen analog of oxetane, which also only forms hyperbranched poly(trimethylenimine) (hbPTMI) *via* CROP.⁹

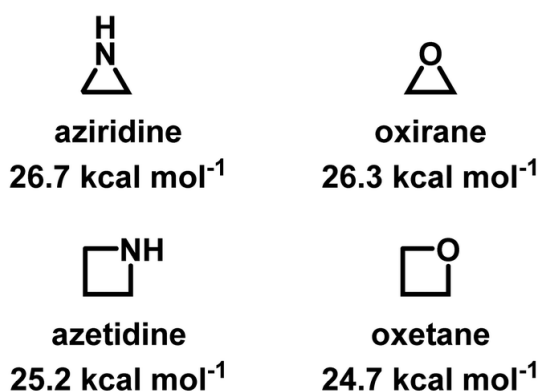


Figure 1.1: Chemical structures of aziridine, azetidine, oxirane, and oxetane and their ring-strains.^{10,11}

Even with the challenges in controlling its polymerization, the high amine density of hbPEI lends its use in a wide range of applications including non-viral gene-transfection,^{7,12–44} anti-microbial and anti-viral coatings,^{37,45–52} CO₂ capture,^{53–63} flocculation of negatively charged fibers in paper-making industries,^{64–66} metal chelation in waste water treatments,⁶⁷ as additives for inkjet paper production,¹⁶ as electron injection layers in organic light-emitting diodes,^{68,69} and materials templating.⁷⁰ As such, hbPEI is made industrially, initially under the commercial name Polymin, and today is marketed under the trade name Lupasol® by BASF.⁷¹ Aziridine is produced at a rate of ~9000 t/a (2006),⁷² where, due to its toxicity, it is usually converted directly into its nontoxic intermediates and branched polymers.

The lack of control over aziridine polymerizations has significantly limited the research of linear PEI (L-PEI), especially when compared to PEO and related polymers.^{6,73} Polyethers, especially PEO, are produced on the scale of several million tons per year and found in many everyday applications,⁷⁴ while linear polyaziridines are barely used today (Figure 2.2).⁷⁵ This is unfortunate as the potential structural diversity of aziridines is notably greater than oxygen-containing analogs as substitution on aziridines can occur both at the carbon and nitrogen atoms of aziridine.

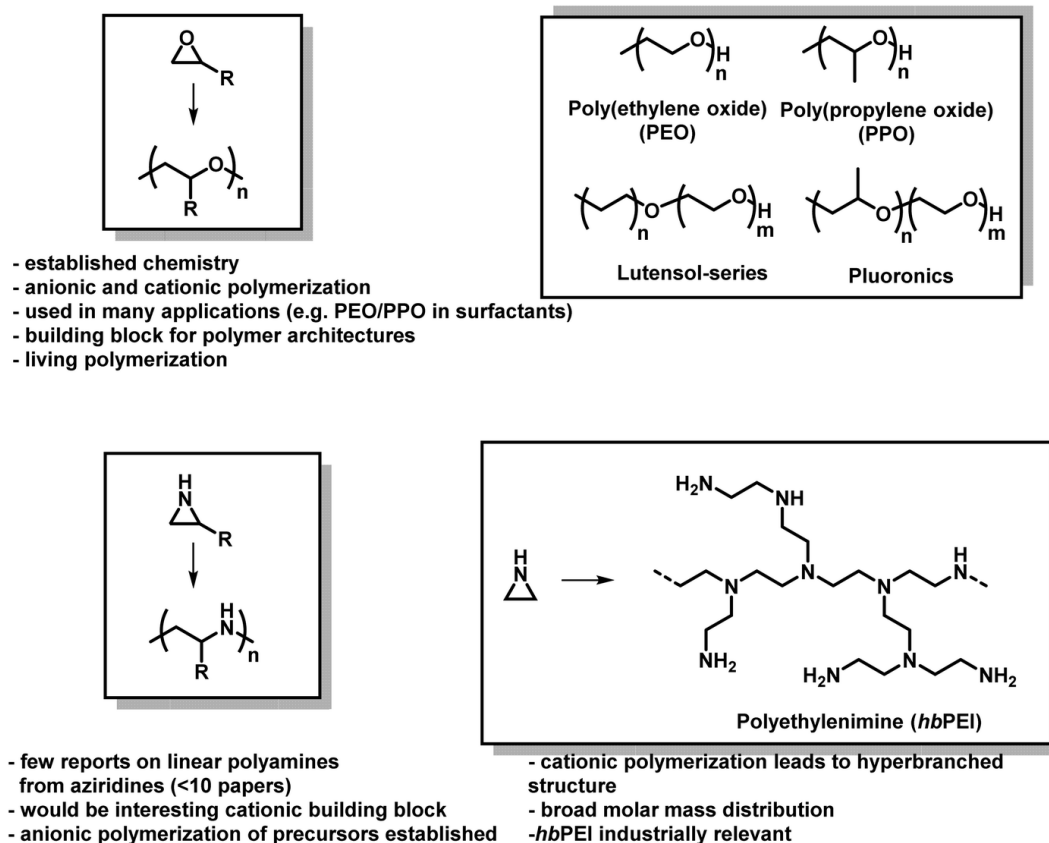
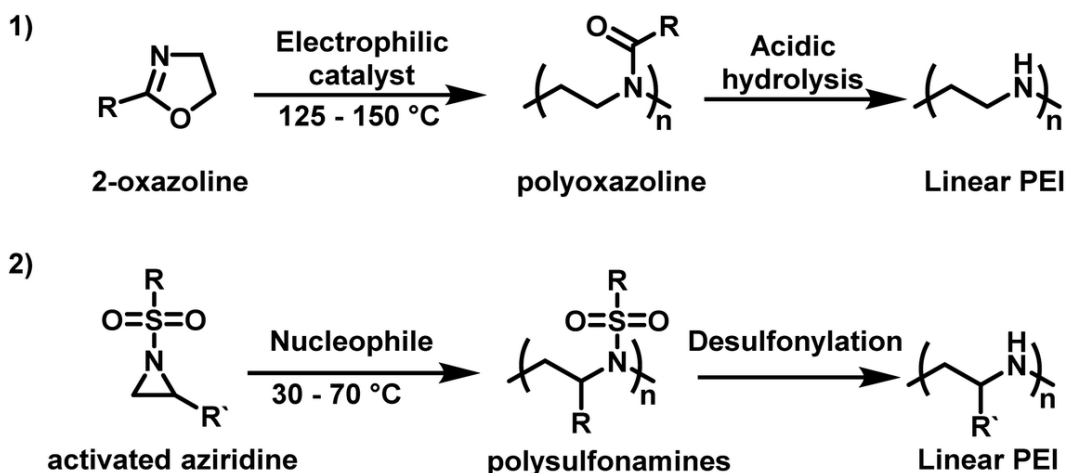


Figure 2.2: Epoxides vs. aziridines. General polymerization scheme and important facts about both material classes.

Use in non-viral gene-transfection has sparked renewed academic and pharmaceutical interest in PEI, especially L-PEI. L-PEI is attractive compared to hbPEI as it can have a well-defined architecture with narrow molecular weight distributions. This makes it ideal for structure–property relationship studies and its incorporation into polymer–drug conjugates. However, since L-PEI cannot be made from aziridine, it is instead synthesized indirectly *via* polyoxazolines.¹⁴ Typically, 2-oxazoline-based monomers, such as 2-ethyl-2-oxazoline, in the presence of cationic initiators, such as stannic chloride and boron trifluoride etherate, undergo a controlled CROP.^{76–78} Conversion of poly(2-oxazoline)s to L-PEI can occur under acidic or alkaline conditions (Scheme 1.1).^{79–81} However, this route to L-PEI has drawbacks in that the polymerization is difficult to control when targeting high degrees of polymerization and it is challenging to achieve quantitative removal of the acyl groups.⁷



Scheme 1.1: (1) Synthesis of linear polyethylenimine (L-PEI) from 2-oxazoline by cationic ring-opening polymerization in comparison to (2) anionic ring-opening polymerization of sulfonyl aziridines as an alternative pathway to linear PEI derivatives.^{82,83}

The new appreciation for the applications of L-PEI and unresolved challenges associated with aziridine polymerization means that it remains an active area of research. Since there have been no recent reviews on aziridine polymerizations (Kobayashi⁶ was published in 1990), we feel that such a review is warranted. This is especially true given the recent breakthroughs in the AROP of activated aziridines, which have yet to be summarized in the literature.

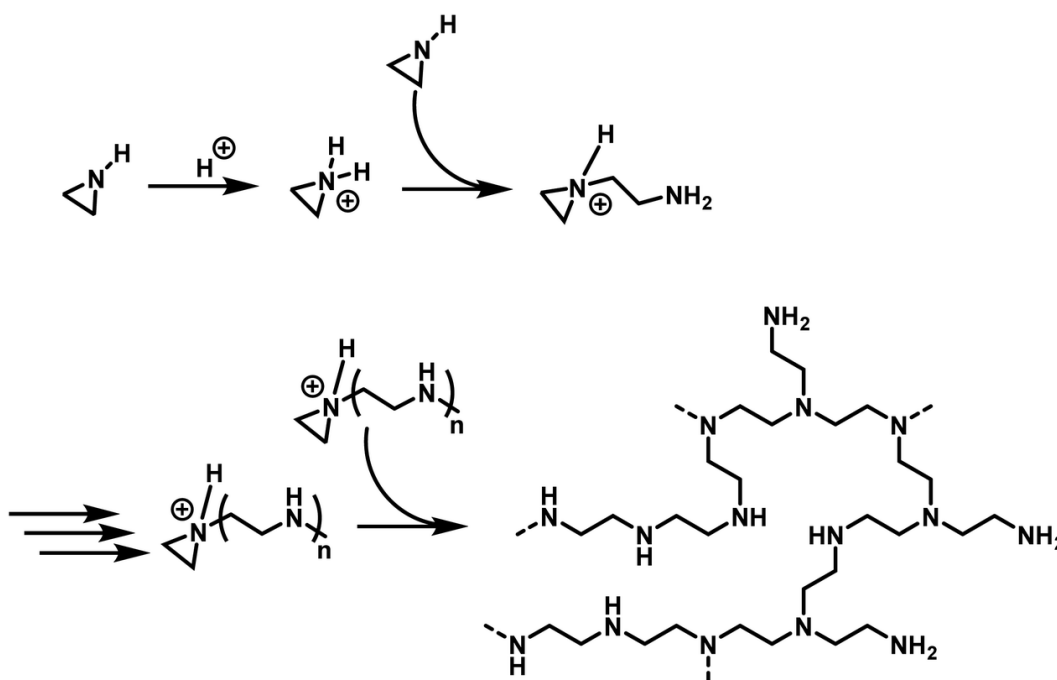
This review gives a comprehensive overview on the synthesis of polymers based on both aziridines and azetidines. We have chosen to include azetidines in this review as their polymerization chemistry closely mirrors that of aziridines and the resulting polymers are structurally similar to that of aziridine derived polymers. We first discuss the early literature on the CROP of aziridines and azetidines. Next, we highlight recent work on the AROP and organocatalytic ring-opening polymerization (OROP) of *N*-sulfonyl aziridines and azetidines and strategies to produce linear polyamines from these monomers. We conclude with routes to aziridine and azetidine copolymers and highlight the possibilities for functionalization or preparation of various polyamine structures. Spaced through the review are summaries of the synthetic methods to synthesize the aziridine and azetidine monomers. Detailed analysis of the literature on gene-transfection can be found elsewhere.⁸⁴ This review will also not cover oxazoline polymerization chemistry; the interested reader is encouraged to consult recent reviews.⁸⁵⁻⁸⁷

1.2 Cationic ring-opening polymerization of aziridines and azetidines

The differences in polymerization chemistry between nitrogen and oxygen containing strained heterocycles arise due to the reduced electronegativity of nitrogen, the presence of an acidic hydrogen atom on the nitrogen atom, and the increased nucleophilicity of the lone-pair of electrons on nitrogen. The decreased electronegativity of nitrogen prevents the nucleophilic ring-opening of aziridine and azetidine in AROP and increases the nucleophilicity of the lone pair electrons on nitrogen, leading to branching and loss of control in CROP. In addition, use of very basic nucleophiles simply deprotonates the secondary amine in aziridine and azetidine rather than inducing ring-opening. Therefore, the majority of aziridine and azetidine polymerizations proceed through a cationic mechanism.

1.2.1 Cationic ring-opening polymerization of aziridine

The cationic polymerization of aziridine and related cyclic amines were recorded in the patent literature as early as 1937.⁸⁸ However, the nature of the polymerization and the structure of the resulting polymer was first thoroughly explored by Jones and coworkers in 1944.⁸⁹ Numerous studies have been performed, elaborating on this work, resulting in the mechanism, depicted in Scheme 1.2.⁵ Polymerization is initiated by electrophilic addition of an acidic catalyst to aziridine to form an aziridinium cation. An additional aziridine monomer, acting as a nucleophile, ring opens the active aziridinium ion resulting in the formation of a primary amine and a new aziridinium moiety. Subsequent aziridines attack the propagating aziridinium terminus, resulting in the linear propagation of the polymer chain. However, as the secondary amine groups in the developing polymer chain are also nucleophilic, they also ring open aziridinium species leading to branching and results in hbPEI. For hbPEI synthesized in solution, this leads to a ratio of primary : secondary : tertiary amines of 1 : 2 : 1 (determined by ¹³C NMR).⁹⁰ This ratio can be varied depending upon the reaction conditions and the molar mass of the polymer (i.e. lower molar mass hbPEI has more primary amines).⁹⁰ The polymerization of aziridine is likely more complex than that depicted in Scheme 1.2.



Scheme 1.2 Mechanism of the cationic ring-opening polymerization of aziridine, leading to hbPEI.

Barb and coworkers⁹¹ studied the kinetics and mechanism of the polymerization of ethylenimine in the presence of different catalysts, such as *p*-toluenesulfonic acid, benzoic acid and others. They noted that the polymerization proceeds much like a step-growth polymerization, and that aziridine dimer is the dominate species early in the polymerization. A recent study on the polymerization of azetidone reached similar conclusion (cf. section 2.5).⁸ Furthermore, they noted an increase in molar masses in polymerization mixtures containing no monomeric species. This suggests that both monomer and polymer molecules are capable of activation and deactivation, thus making it more difficult to control the molecular weight and architecture of the resulting hbPEI.

1.2.2 Cationic ring-opening polymerization of 2-substituted aziridines

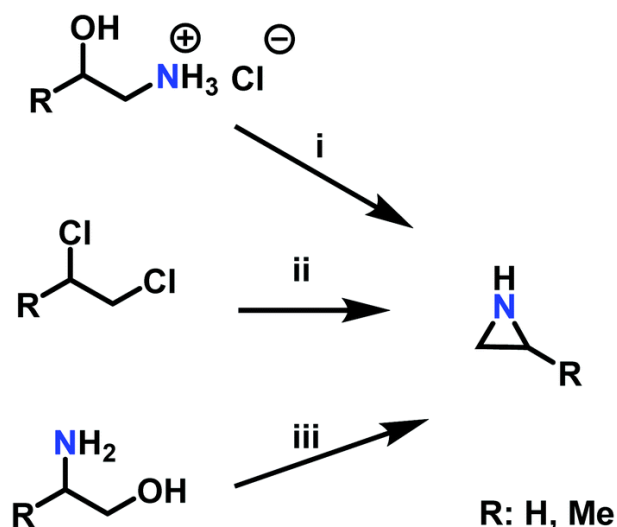
In general, the CROP of 2-substituted aziridines proceeds similarly to the parent aziridine. 2-Methylaziridine, or propylene imine, was reported to undergo polymerization initiated by $\text{BF}_3\text{Et}_2\text{O}$.⁹² The resulting polypropylenimine appeared as a viscous oil insoluble in water but soluble in CHCl_3 and DMSO. The structure of polypropylenimine formed from the cationic polymerization of 2-methylaziridine has been determined to be highly branched, similarly to hbPEI formed from the CROP of aziridine. A photoinitiated cationic polymerization of 2-methylaziridine has also been reported.⁹³ Regardless of the initiator used, the polymerization of 2-methylaziridine suffers from termination. This is due to nucleophilic addition of a tertiary amine

within the polymer to an aziridinium, resulting in the formation of an unreactive quaternary amine.

CROP of 2-phenylaziridine, initiated by methyl triflate, perchloric acid, $\text{BF}_3\text{Et}_2\text{O}$, dimethyl sulfate or hydrochloric acid, was found to form only low molecular weight polymers of $\leq 3000 \text{ g mol}^{-1}$.⁹⁴ These polymerizations did not result in full monomer consumption due to high rates of termination. Although the polymerization occurred at a much slower rate, Baklouti and coworkers found that employing methyl triflate as initiator led to the formation of the highest molecular weight polymers of 2500–3000 g mol^{-1} . Further investigation by studying the kinetics revealed this was due to an increase in the ratio of the propagation rate constant to the termination rate constant. It was proposed that this was due to the triflate counter ion stabilizing the aziridinium ion better than the counter ions of the other initiators.

1.2.3 Monomer preparation for cationic polymerization of 2-substituted aziridines

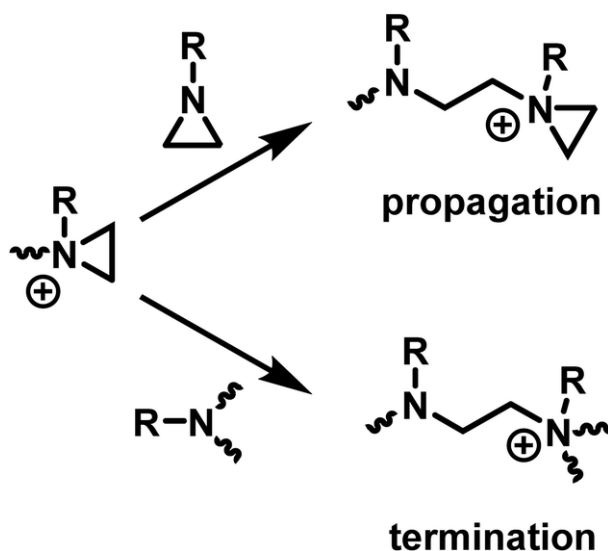
A pioneering approach to aziridines is the “ β -chloroethylamine process”, which uses vicinal chloro amine hydrochloride salts and sodium hydroxide. As corrosive hydrochloric acid (HCl) is released during the reaction, which could also lead to a CROP of aziridine, this process lost industrial relevance in 1963 (Scheme 1.3i).⁷² The “Dow Process” (Scheme 1.3ii) was used on the industrial scale beginning in 1978, but was stopped due to the drawbacks of high corrosion rates to reactors and waste stream disposal. Per one equivalent starting material, three equivalents of ammonia are necessary, which gives the Dow Process a low atom economy.⁷² Today, aziridine is prepared *via* the “Wenker synthesis” (Scheme 1.3iii). This two-step process starts with the reaction of 2-aminoethanol, or other vicinal amino alcohols, with sulfuric or chlorosulfuric acid. The sulfates are treated with 5 eq. sodium hydroxide or saturated sodium carbonate solution to give the aziridine after a nucleophilic cyclization with 2-step yields of $\sim 90\%$.⁷² Significant waste disposal problems are avoided through high atom economy and nontoxic side products.⁹⁵ For laboratory scales, sulfates can be purified by filtration and washing with excess ether. Low molecular weight aziridines such as 2-methyl aziridine can be further purified by steam distillation. If stored longer, alkali hydroxide stabilizes aziridine against spontaneous cationic polymerization. *N*-Substituted aziridines can also be obtained if secondary amines are used as starting material.^{95–97}



Scheme 1.3: Synthesis of aziridines with and without a ring substituent (R) by i: the β -chloroethylamine process, ii: the Dow Process, iii: the Wenker synthesis.

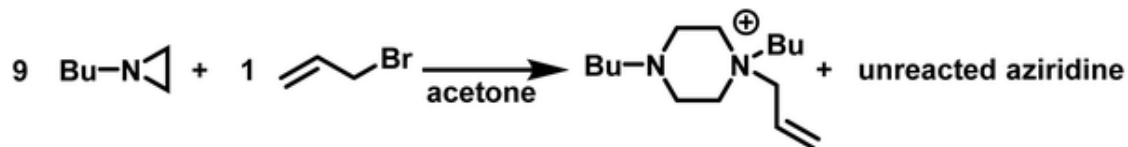
1.2.4 The cationic ring-opening polymerization of *N*-substituted aziridines

The ring-opening polymerization of *N*-substituted aziridines typically proceeds *via* a cationic mechanism. The details of the polymerization of *N*-substituted aziridines is like that of aziridine, with one important distinction: the possibility of an irreversible termination reaction.⁵ Termination occurs due to the (inter and intramolecular) nucleophilic attack of tertiary amines on aziridinium moieties, which results in the formation of unreactive, non-strained quaternary ammonium salts (Scheme 1.4).



Scheme 1.4: Competition between propagation and termination reactions during the CROP of *N*-substituted aziridines.

As such, the polymerizations of simple *N*-substituted aziridines, often proceed only to low conversions (<55%).⁵ This is exemplified by the fact that in acetone the reaction of allyl bromide with 9-fold excess of *N*-(*n*-butyl)aziridine produces the piperazinium cation in a 96% yield with excess aziridine being recovered (Scheme 1.5).⁹⁸



Scheme 1.5: Reaction of *N*-(*n*-butyl)aziridine to form a piperazinium with no detectable polymerization.

Goethals performed a series of detailed studies on the polymerization of *N*-alkylaziridines primarily focusing on the kinetics of the polymerization.⁵ A key focus of this study was to measure the propagation rate constants (k_p) vs. the rates of termination (k_t). Employing Et_3OBF_4 as a Lewis acid, due to its rapid initiation, Goethals found that alkyl substituents with low steric bulk tended to have low k_p/k_t ratios, which leads to the polymerizations proceeding to only low conversion. For instance, *N*-ethylaziridine has a k_p/k_t of 6 while the k_p/k_t for *N*-isopropylaziridine was 21. In contrast, *N*-*tert*-butylaziridine polymerized with essentially no termination ($k_p/k_t \approx \infty$) and no transfer reactions, thus allowing the polymerization to be living-like. The introduction of a methyl group in the 2-position of *N*-alkylaziridines was found to greatly reduce the rate of termination relative to propagation. For example, the polymerization of *N*-benzyl aziridine stops at very low conversion due to termination ($k_p/k_t = 85$), while *N*-benzyl-2-methylaziridine polymerizes with almost no termination ($k_p/k_t = 1100$) (Figure 1.3).

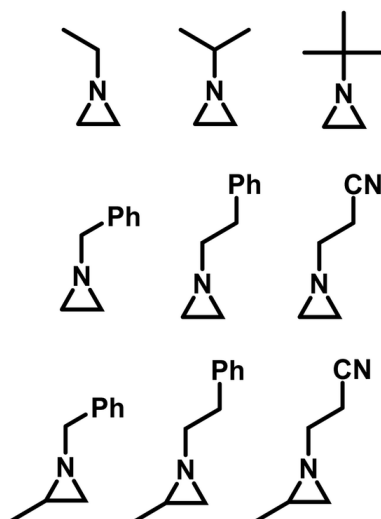
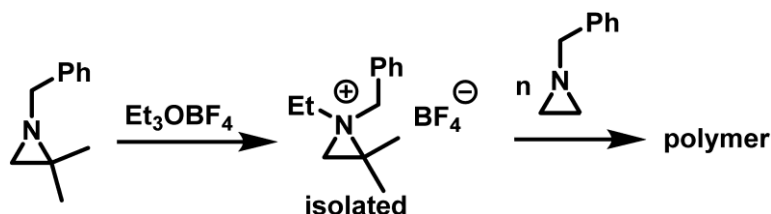


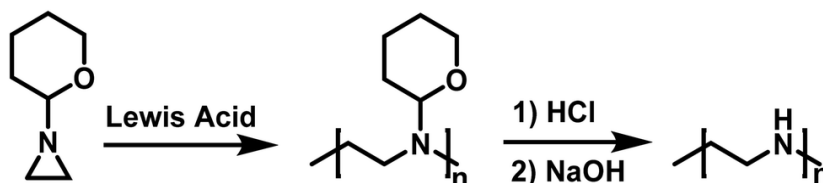
Figure 1.3 *N*-Alkyl aziridines that undergo CROP.⁵

While substitution in the 2-position greatly increases the k_p/k_t ratio, geminal substitution at the 2-position completely inhibits the polymerization. Specifically, *N*-benzyl-2,2-dimethylaziridine was only found to form *N*-benzyl-*N*-ethyl-2,2-dimethylaziridinium when reacted with Et_3OBF_4 .⁵ Interestingly, *N*-benzyl-*N*-ethyl-2,2-dimethylaziridinium could initiate the polymerization of *N*-benzylaziridine (Scheme 1.6).



Scheme 1.6: Formation of *N*-benzyl-*N*-ethyl-2,2-dimethylaziridinium and polymerization according to ref. 5.

Goethals also reported on the CROP of neat *N*-(2-tetrahydropyranyl)aziridine initiated by Lewis acids (Scheme 1.7).⁹⁹ This polymerization also appears to proceed without termination due to the bulky tetrahydropyranyl substituent. Hydrolysis of the polymer produced from *N*-(2-tetrahydropyranyl)aziridine in dilute HCl, followed by neutralization with NaOH, resulted in the formation of high molecular weight linear PEI (L-PEI). M_w for the L-PEI, as determined by LALLS, was as high as 19.6 kg mol^{-1} , which is the highest molecular weight L-PEI produced from an aziridine to date.

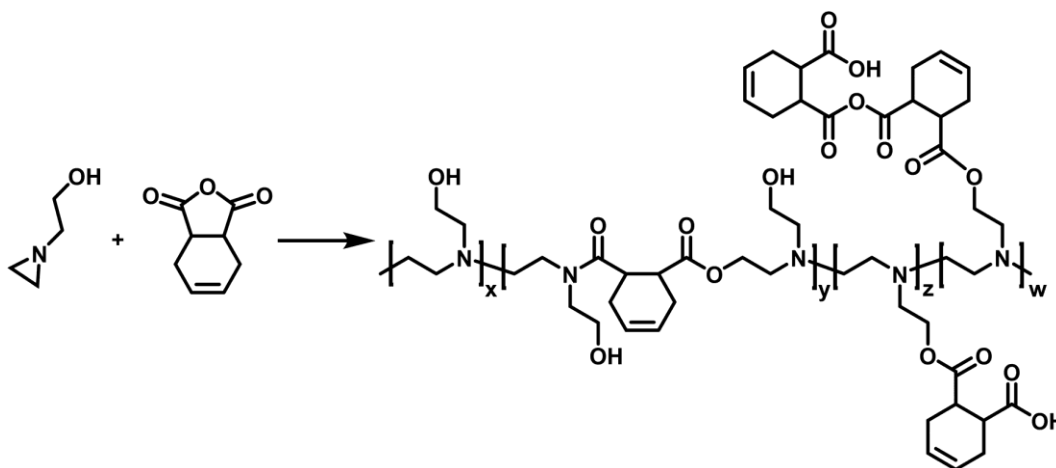


Scheme 1.7: Polymerization of *N*-(2-tetrahydropyranyl)aziridine in route to L-PEI according to ref. 99.

Polymerization of *N*-(2-hydroxyethyl)aziridine has also been reported to occur *via* traditional Lewis acid catalysts and also through electroinitiated polymerization.¹⁰⁰ The resulting poly(*N*-(2-hydroxyethyl)aziridine) (PHEA) has been shown to be an excellent chelator of metal cations. By simple adjustment of pH, PHEA can selectively remove various metals.¹⁰¹ At pH = 3, PHEA can remove Cu(II) from solution with as high as 99.5% retention. With neutral pH, Co(II), Cr(III), Fe(III), Ni(II), Zn(II), and Cd(II) can be removed from solution at as high as 99.5%. These results are similar to those of hbPEI, with the exception of Cr(III) at neutral pH, when PHEA is a much stronger chelator.

CROP of aziridines have also been employed in the synthesis of copolymers. Utilizing *N*-(2-hydroxyethyl)aziridine, Pooley and coworkers synthesized a copolymer with 1,2,3,6-tetrahydrophthalic anhydride (THPhA) (Scheme 1.8).¹⁰² This polymerization was accomplished in the absence of an initiator. These polymers are formed by employing a nucleophilic monomer with an electrophilic comonomer. These monomers form a zwitterion which leads to initiation and propagation in the polymerization. Pooley extended this work with *N*-(2-hydroxyethyl)aziridine to produce copolymers with a library of other electrophilic monomers.^{103–109}

Although not present in the open literature, there are reports in the patent literature on the CROP of sulfonylaziridines.¹¹⁰ These polymerizations were performed neat by melting the monomers and were performed in the presence of Lewis acids such as AlCl_3 , FeCl_3 , and ZnCl_2 . Employing different monomer : catalyst feeds from 200 : 1 to 10 000 : 1 polymers were obtained, but no further characterization details were given.¹¹⁰

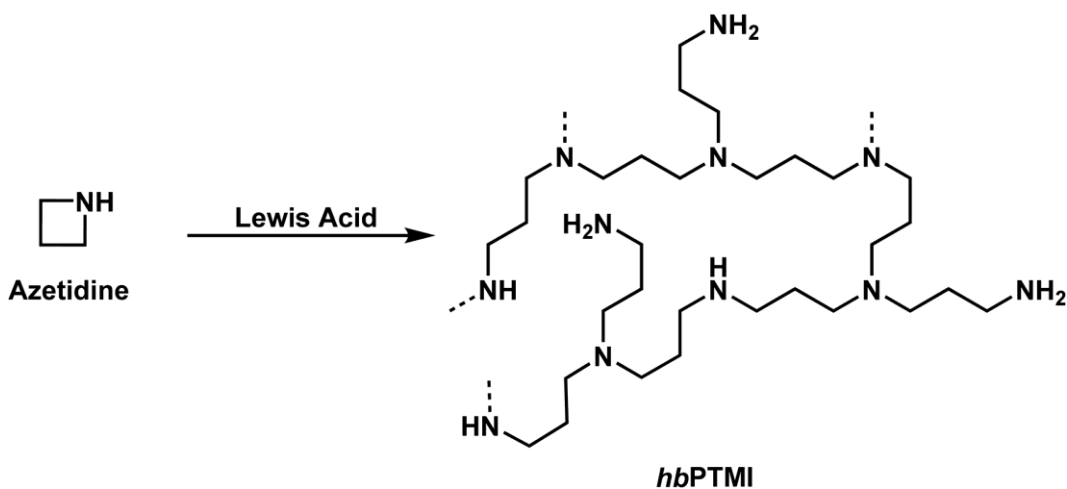


Scheme 1.8: Copolymerization of *N*-(2-hydroxyethyl)aziridine with THPhA according to ref. 102.

1.2.5 Cationic ring-opening polymerization of azetidines

While the polymerization of aziridines has been studied, there are significantly fewer examples of the four-membered ring, azetidine, in the literature. Unsurprisingly, most of this work on the polymerization of azetidines focuses on the polymerization of *N*-substituted azetidines.^{4,111–115} While the first polymerization of an azetidine ring was reported by Kornfeld, in 1960, regarding the polymerization of conidine,¹¹³ Goethals provided the greatest contributions to the field due to his studies of multiple azetidines.^{4,5,99,115–118}

In 1974, Goethals reported of the polymerization of unsubstituted azetidine (Scheme 1.9).⁴ The polymerization proceeded *via* a cationic mechanism, similar to the CROP of aziridine, to form hyperbranched poly(trimethylenimine) (hbPTMI).^{5,6} This study found that after 8 h at 70 °C in methanol nearly all monomer had been consumed. Interestingly, it was found that when all the monomer had been consumed, 70% of the reaction mixture consisted of dimer. This is explained by the pK_b difference of azetidine and *N*-methylazetidine. The pK_b of azetidine is 11.29 (ref. 115) and 10.40 (ref. 119) for *N*-methylazetidine. Due to the differences in basicity, and the similarity in structure of the azetidine dimer to *N*-methylazetidine, it is expected that a proton would transfer from the protonated tertiary amine to the more basic monomer. Because of preferential formation of dimer to propagation it was hypothesized that the resulting polymer should contain many primary and tertiary amines, rather than exclusively producing secondary amines. This can be explained by two possible reaction pathways. Propagation only occurs once the tertiary amine in the dimer is protonated. The cyclic ammonium salt can then be opened by nucleophilic addition of either a primary amine or a tertiary amine. If propagation occurred by only addition of primary amines the expected polymer would contain only secondary amines. If propagation occurred by only addition of tertiary amines the expected polymer would contain equal numbers of primary and tertiary amines but no secondary amines. ¹H NMR spectroscopy revealed that the PTMI produced contained 20% primary, 60% secondary, and 20% tertiary amines, suggesting that both mechanisms are occurring. However, tertiary amines may also be formed by the addition of secondary amines along the backbone of the polymer to the cyclic ammonium salt. Similarly, a tertiary amine along the backbone of the polymer could add to a cyclic ammonium salt. However, this is less probable due to the lower basicity of a tertiary amine to a secondary amine.¹²⁰



Scheme 1.9: The cationic ring-opening polymerization of azetidine to produce hyperbranched PTMI (hbPTMI).

Additionally, this reaction would lead to chain termination. Goethals determined in this work, by monitoring the increase in molecular weight over time, that this termination must be very slow, if occurring at all. In 2017, Goethals' initial work on the polymerization of unsubstituted azetidine was confirmed by Sarazen and Jones.⁸ They provided a report of the cationic polymerization of azetidine, which was impregnated onto a silica scaffold. These porous materials were then employed in the capturing of CO₂, which is a promising preliminary application of PTMI.

1.2.6 Cationic ring-opening polymerization of substituted azetidines

Goethal's work was not limited to unsubstituted azetidines. He also reported the polymerization of 1,3,3-trimethylazetidinium.^{4,115} In this work, Goethals studied the CROP of 1,3,3-trimethylazetidinium. After initially screening multiple solvents and initiators, the kinetics of the polymerization were studied in nitrobenzene employing Et_3OBF_4 as the initiator at temperatures $>60\text{ }^\circ\text{C}$.

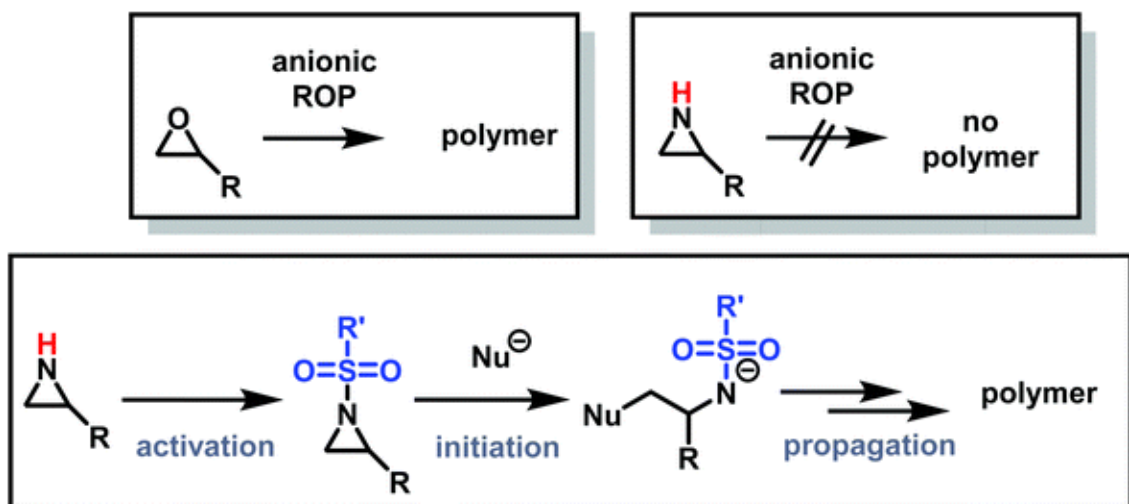
The CROP of 1,3,3-trimethylazetidinium is first-order with respect to monomer concentration and the number of active chain ends remains constant throughout the polymerization with a propagation rate constant, k_p , of $1.2 \times 10^{-4}\text{ L}/(\text{mol s})^{-1}$ at $78\text{ }^\circ\text{C}$ in nitrobenzene, making the polymerization notably slow. Additionally, molecular weights increased linearly with increase in the monomer to initiator ratio when studied using vapor pressure osmometry. This data, coupled with studies showing that initiation is significantly faster than propagation, suggests that the polymerization displays living character. Indeed, upon a second addition of monomer, following complete consumption of the initial monomer concentration, molecular weight increased following the same rate as the initial polymerization, confirming this hypothesis. This contrasts from other heterocyclic CROP, such as oxetanes,¹²¹ thietanes,¹²² and selenetanes¹²³ in which the polymerizations either slowed or stopped at low conversions. This is attributed to the reaction of the heteroatoms in the polymer backbone to the growing chain end, producing unstrained, unreactive cations. It is suggested that the polymerization of 1,3,3-trimethylazetidinium is living due to the increased basicity of 1,3,3-trimethylazetidinium compared to the tertiary amines contained in the polymer backbone.¹²⁰

Goethals further studied the polymerization kinetics of 1,3,3-trimethylazetidinium in nitrobenzene employing Et_3OBF_4 as the initiator by varying the polymerization temperature and monomer to initiator ratio. In varying the temperature, an Arrhenius plot was also constructed and the activation energy of 1,3,3-trimethylazetidinium was found to be 19 kcal mol^{-1} . Additionally, in varying the monomer to initiator ratio, little deviation was found in the value of k_p , suggesting the reaction is first order with respect to initiator, Et_3OBF_4 .

1.3 Anionic polymerization of aziridines

Recently, a number of researchers have been interested in the newly established anionic polymerization of *N*-activated aziridines to prepare linear polyaziridines. In contrast to cationic polymerization, anionic polymerization uses nucleophilic initiators and propagates through an anionic chain end. Anionic polymerizations are attractive due to the high degree of control over molecular weight and dispersity of the resulting polymers compared to other polymerization methods.

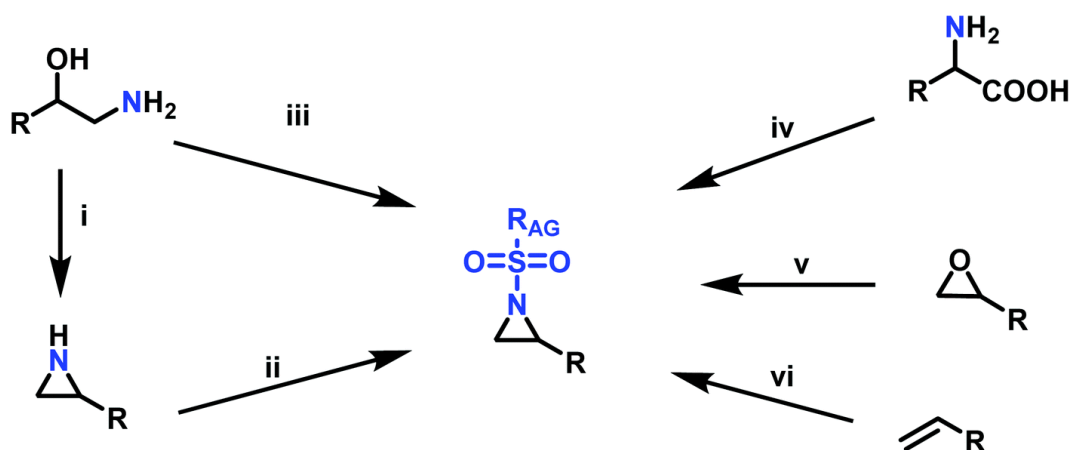
The first anionic polymerization of an aziridine, *via* an azaanion was reported by Bergman and Toste in 2005.¹²⁴ When investigating the reactivity of a nucleophilic transition metal complex, Bergman, Toste, and coworkers unexpectedly observed ring-opening polymerization of enantiopure (+)-2-benzyl-*N*-tosylaziridine to form a poly(sulfonlaziridine).¹²⁴ This molecule is activated at the ring-nitrogen by an electron-withdrawing sulfonyl group, enabling nucleophilic attack at the aziridine ring in the 3-position. The electron withdrawing effect of the sulfonyl group further stabilizes the evolving azaanion at the growing chain end by delocalization, and propagation continues *via* sulfonamide anions (Scheme 1.10). Different activating groups have also been investigated for the anionic polymerization of aziridines. Examples include diphenylphosphinyl, acetyl, and ethylcarbamoyl substituents, but exclusively the sulfonamide-aziridines were suitable for azaanionic polymerization to date.¹²⁴



Scheme 1.10: Top: Established anionic ring-opening polymerization of epoxides vs. no anionic ring-opening polymerization of aziridines. Bottom: Activation strategy of aziridines to sulfonyl-aziridines, allowing for anionic ring-opening polymerization.

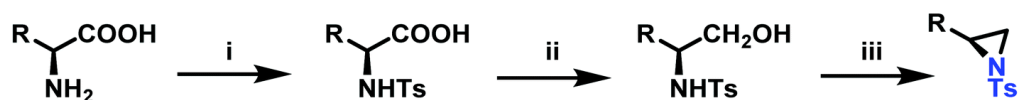
1.3.1 Preparation of sulfonyl aziridines for anionic polymerizations

Since anionic polymerization does not tolerate acidic protons, the aziridine N–H needs to be substituted with electron-withdrawing sulfonyl groups, i.e. “activation groups” (Scheme 1.11). In analogy to the Hinsberg reaction,¹²⁵ secondary amines react with sulfonyl chlorides to produce the respective sulfonyl aziridines. Xu *et al.*¹²⁶ presented an efficient microwave-assisted one-pot reaction of valinol, L-phenylalaninol, L-leucinol, L-alaninol and L-serine methylester, along with methyl-, phenyl-, and 4-methoxyphenyl-sulfonyl chlorides to yield sulfonyl aziridines. Potential solvents for this strategy were diethyl ether, THF, acetonitrile, and dichloromethane. Bases such as alkali carbonates and hydroxides are used with DMAP as catalyst. In 30 minutes Xu *et al.* were able to prepare different sulfonyl aziridines with high yields of 84%–93%.



Scheme 1.11: Synthesis of aziridine monomers for the azaanionic polymerization: i: Wenker synthesis of aziridine: (1) vicinal amino alcohol derivate, sulfuric acid or sulfuric acid chloride (2) NaOH (aq.); ii: sulfonyl chloride, TEA, DCM; iii: sulfonyl chloride, DCM, DMAP or K₂CO₃ (Microwave, 400 W); iv: (1) amino acid, NaOH (aq.), 0 °C, TsCl. (2) THF dry, BH₃–SMe₂, reflux. (3) DCM, TsCl, DMAP, Py; v: RSO₂NH₂, K₂CO₃, BnEt₃N⁺Cl[−], dioxane, 90 °C, MsCl, DCM, 0 °C to reflux; vi: (1) chloramine salts, ACN, PTAB, 12 h; (2) IPrCu(DBM), PhI=O, RSO₂–NH₂, chlorobenzene, r.t., 25 h; (3) Rh₂(cap)₄, TsNH₂, NBS, K₂CO₃.

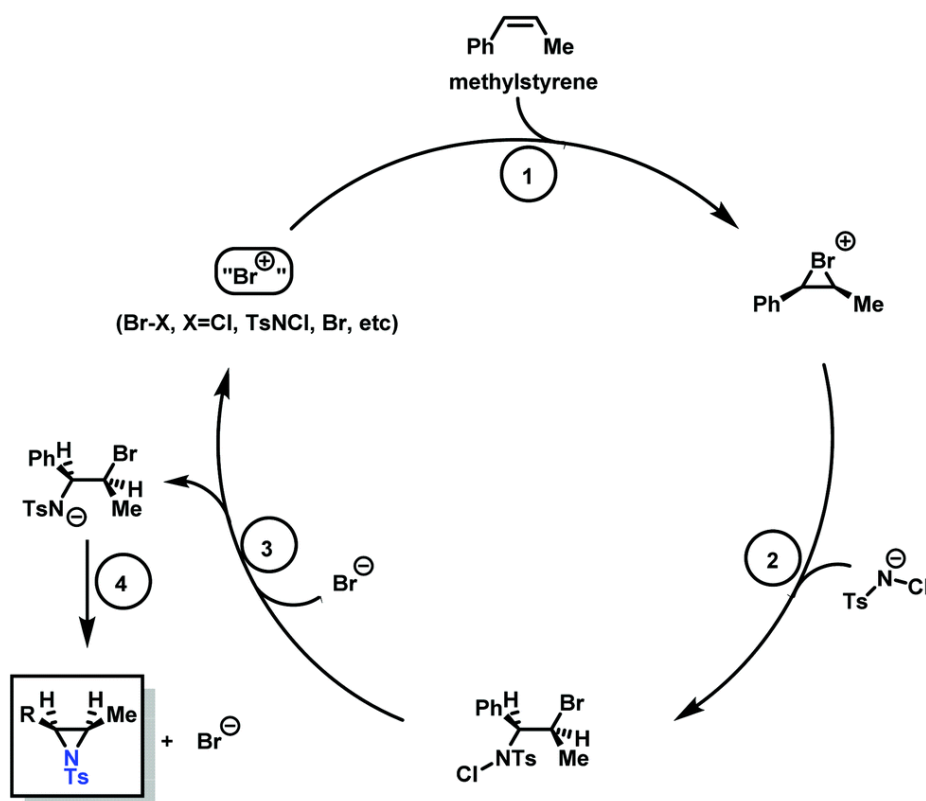
Amino acids have also been used to produce *N*-tosylaziridines in a three-step process (Scheme 1.12).¹²⁷ This was achieved by the *N*-tosylation of the amino acid, followed by reduction of the carboxylic acid to yield *N*-tosyl-2-amino alcohols and finally *O*-tosylation with an *in situ* ring-closing. Particularly interesting is that this method does not require any purification of intermediates.



R = HOCH₂, Me, iPr, iBu, PhCH₂, MeS(CH₂)₂

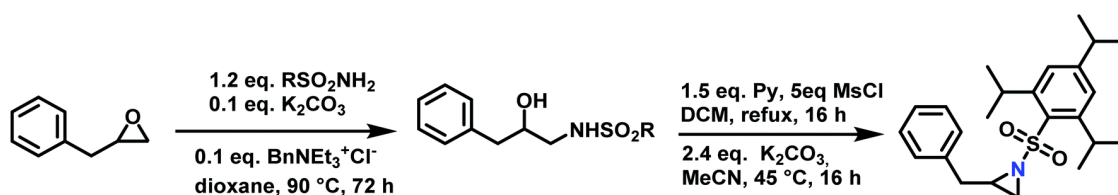
Scheme 1.12: i: Preparation of *N*-tosyl-2-aminoacids *via* *N*-tosylation with TsCl; ii: preparation of *N*-tosyl-2-aminoalcohols reduction of the carbonyl group; iii: preparation of 2-substituted *N*-tosylaziridines.

Aziridination of olefins (route (vi) in Scheme 1.11) was also utilized to produce sulfonyl aziridines. Sulfonyl aziridines with varying lengths of alkyl chains were produced in a single step that is tolerant to functional side groups, such as alcohols and acetals. An important advantage of this strategy is that toxic aziridine is avoided and the activated sulfonyl aziridines are obtained directly. This route employing non-functionalized alkenes to produce sulfonyl aziridines has high yields of 95% with rhodium catalysts and up to 93% with PTAB as catalyst, however, the yields vary depending on the pendant groups. Increasing the viability of this method, the catalysts are either commercially available or can be prepared with ease.^{128–130} Sharpless and coworkers proposed a mechanism for bromine-catalyzed aziridination (Scheme 1.13). In the first step, the olefin reacts with a Br^+ source, given by PTAB. The brominium ion is then ring-opened by TsNCl^- , to form the α -bromo-*N*-chloro-*N*-toluenesulfonamide (Step 2). Attack of the bromide anion (Br^-) (or TsNCl^-) on the *N*-Cl group of the intermediate generates the anion and a Br-X species (Step 3). Expulsion of Br^- from the anion finally yields the aziridine and the regenerated Br-X species (Step 4) initiates another turn of the catalytic cycle.¹³⁰ This synthesis route has been successfully used for monomer synthesis by the Wurm group by using chloramine-T and chloramine-M to synthesize MsDAz (49%) and TsDAz (47%)¹³¹ and acetal functionalized aziridine monomers (17%–30%).¹³²



Scheme 1.13: Catalytic cycle of the PTAB catalyzed aziridination of olefins, adopted from previous work of Sharpless. Copyright©1998 The American Chemical Society. Reprinted with permission from Journal of the American Chemical Society.¹³⁰

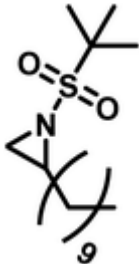
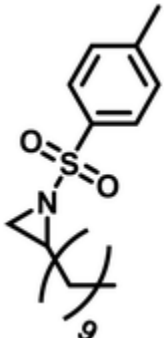
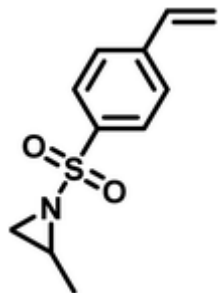
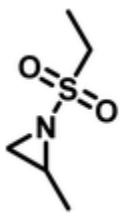
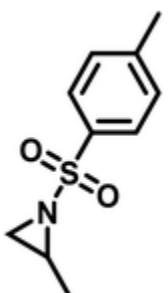
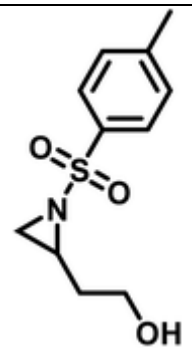
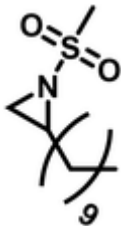
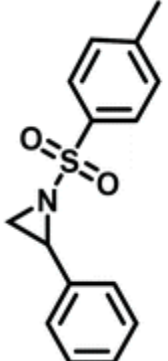
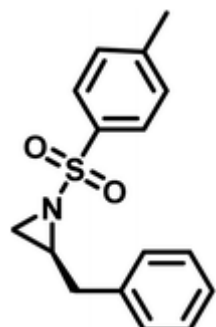
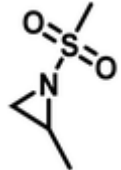
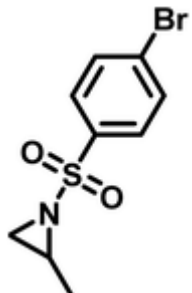
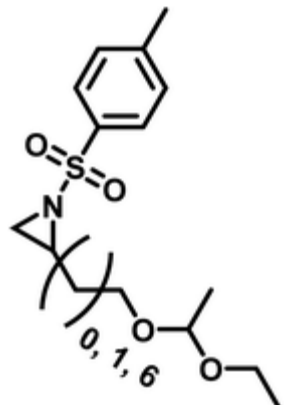
Epoxides were also used as attractive starting materials for the sulfonyl aziridine synthesis (Scheme 1.14).^{124,133} 2-Benzyl-1-(2,4,6-triisopropylbenzene-sulfonyl)aziridine was synthesized in two-steps: the first step was the nucleophilic ring-opening of 2-benzyloxirane with the primary sulfonamide (2,4,6-*i*-Pr₃C₆H₂SO₂NH₂). This reaction requires 0.1 eq. of potassium carbonate and BnNEt₃⁺Cl⁻ as catalyst in dioxane (73% yield). The subsequent mesylation–cyclization of the hydroxyl-sulfonamide was achieved by the addition of mesyl chloride to activate the hydroxy group under basic conditions (86% yield). This route might be extended to other *N*-sulfonyl groups.¹³⁴


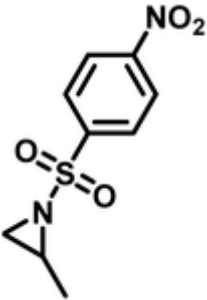
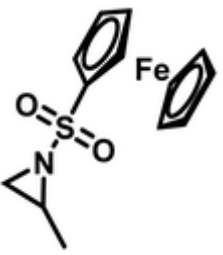
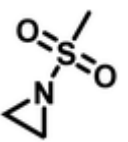
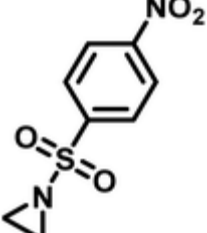
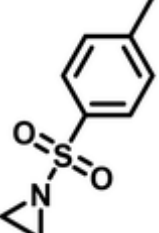
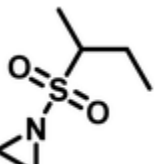
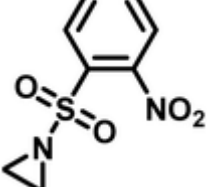
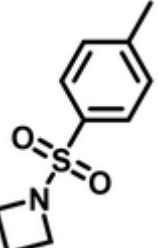
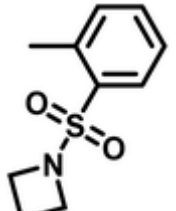
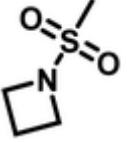


Scheme 1.14: Synthesis of 2-benzyl-1-(2,4,6-triisopropylbenzenesulfonyl)aziridine from 2-benzyloxirane, R = 2,4,6-*i*-Pr₃C₆H₂.

Another route, starting from epoxides, was used by Bergman and Toste¹²⁴ to synthesize 2-*n*-decyl-*N*-methanesulfonyl aziridine (MsDAz). Thomi and Wurm¹³³ followed this procedure to synthesize 2-(oct-7-en-1-yl)-*N*-mesylaziridine. This procedure involves three steps; first the epoxide is ring-opened with sodium azide to give the azido-hydroxyalkane as intermediate, which is converted in the second step, by a Staudinger reaction, to the corresponding alkyl aziridine. To activate the obtained aziridine for anionic polymerization mesylchloride is used to replace the *N*-terminal hydrogen in the third step. Table 1.1 summarizes activated aziridines and azetidines which were successfully polymerized *via* azaanionic polymerization to date.

Table 1.1: Activated aziridines which were successfully tested for AAROP

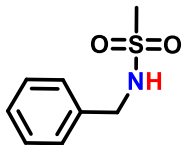
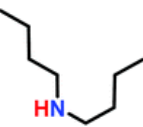
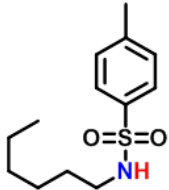
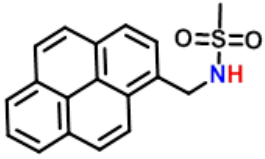

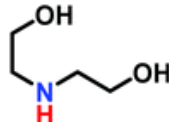
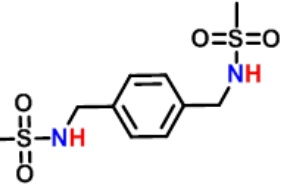

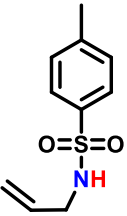
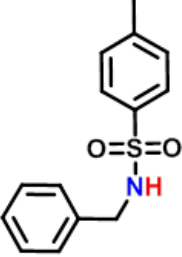
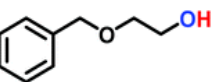
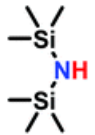
Monomer	Ref.	Monomer	Ref.	Monomer	Ref.
<i>N</i> -Activated, 2-substituted aziridines					
	131		136		137
	138		131		139
	131 and 133		138		124
	131		131		132

Monomer	Ref.	Monomer	Ref.	Monomer	Ref.
	133		131		140
N-Activated, non-substituted aziridines					
	83		141		Com.
	83		141		
N-Activated, non-substituted azetidines					
	83		83		142

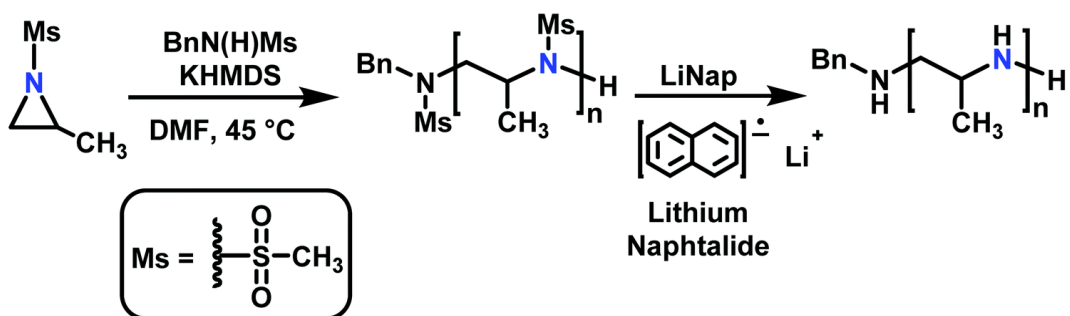
1.3.2 Initiators for the anionic polymerization of activated aziridines

The anionic ROP of sulfonyl aziridines is typically initiated by secondary *N*-sulfonamide-initiators, such as the alkali salts of *N*-benzyl-4-methylbenzenesulfonamide,¹³⁸ *N*-pyrene-methanesulfonamide,^{124,132,136} or butyl lithium (Table 1.2).^{143,144} Also a bifunctional initiator *N,N'*-(1,4-phenylenebis(methylene))dimethane-sulfonamide was introduced in 2017.¹⁴³ To date, the standard protocol uses alkali bis(trimethylsilyl)amide salts to deprotonate the sulfonamide-initiators.¹⁴³ KHMDs alone was also proven to be able to ring-open sulfonyl aziridines, but bimodal molecular weight distributions were obtained.^{132,140} With these initiators, functional poly(sulfonylaziridine)s are available. Recently, Reisman *et al.*⁸³ showed that the terminal group can be used to prepare telechelic polymers by terminating AROPs with propargyl bromide, which allows further modifications by click chemistry.

Table 1.2: Different initiators for the ring-opening polymerization of sulfonyl aziridines reported to date

Initiator	Ref.	Initiator	Ref.	Initiator	Ref.
	124		145		147
	124		143		148
	143		145		145
	138		146		140

1.3.3 Anionic polymerization of activated aziridines



Scheme 1.15: Anionic ring-opening polymerization of sulfonyl aziridines and subsequent desulfonylation (with 2-methyl-mesyloxyaziridine as an example).

When initiated with a suitable nucleophile (Table 1.1), the anionic polymerization of sulfonyl aziridines follows living conditions (Scheme 1.15).¹⁴³ The solubility of poly(sulfonylaziridine)s is highly dependent on the substituents on the sulfonyl group and the tacticity of the polymer. If (+)-2-benzyl-*N*-tosylaziridine was used as monomer, only insoluble oligomers were produced.¹²⁴ In contrast, racemic monomers produce linear polymers with degrees of polymerization (DP) of up to 200 (with $M_n = 20\,000\text{ g mol}^{-1}$) and narrow molecular weight distributions, $\mathcal{D} < 1.10$.^{124,143} Furthermore, the polymerization follows first order kinetics with respect to monomer, suggesting a living polymerization (Figure 1.4). In addition, chain extension experiments proved that the polymerization of *N*-sulfonylaziridines is living. The sulfonyl groups of the obtained poly(sulfonylaziridine)s can be removed after the polymerization with different strategies, e.g. using alkali metal naphthalides or acidic conditions to yield the corresponding polyamines (Scheme 1.15).⁸²

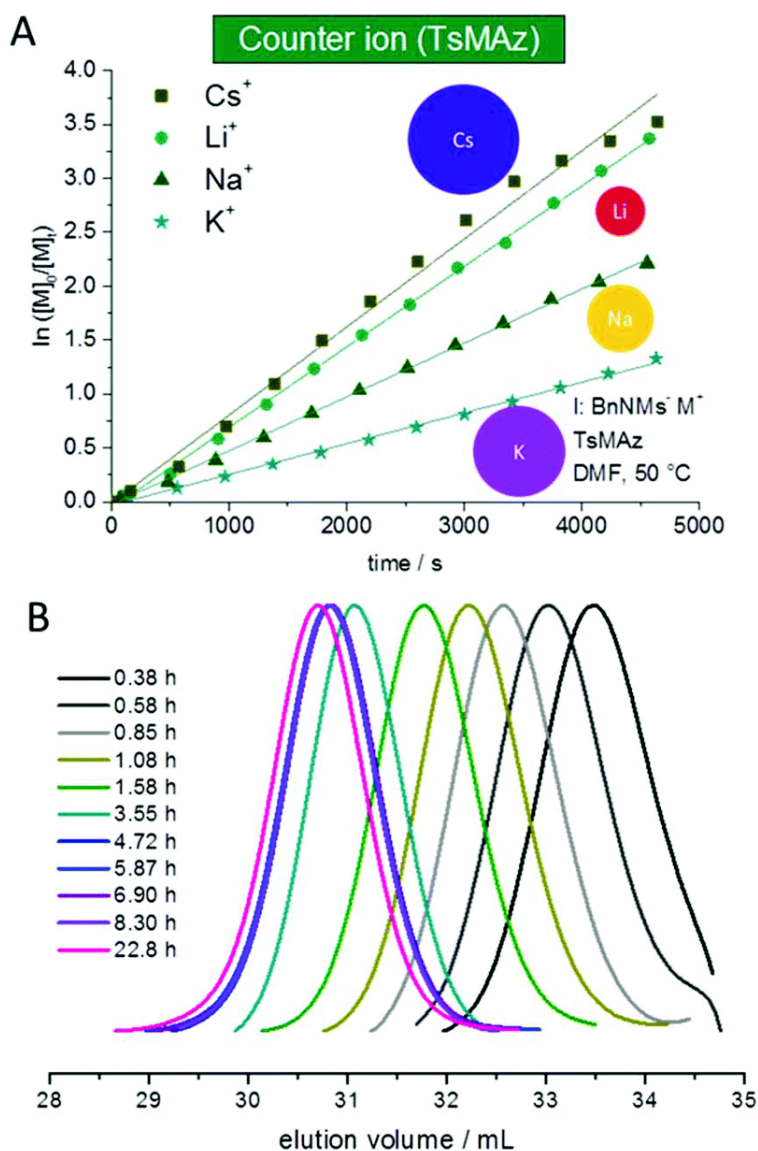
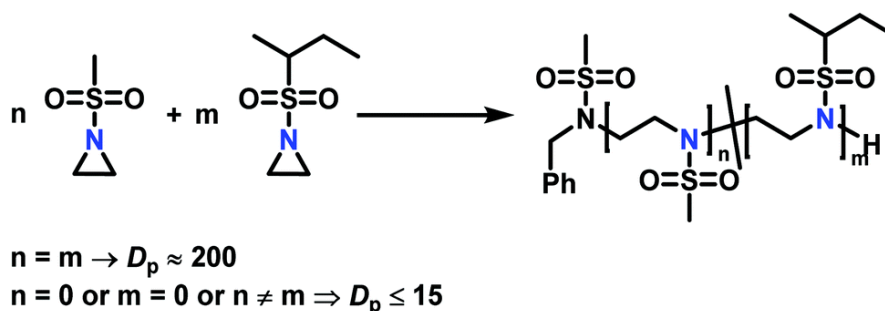


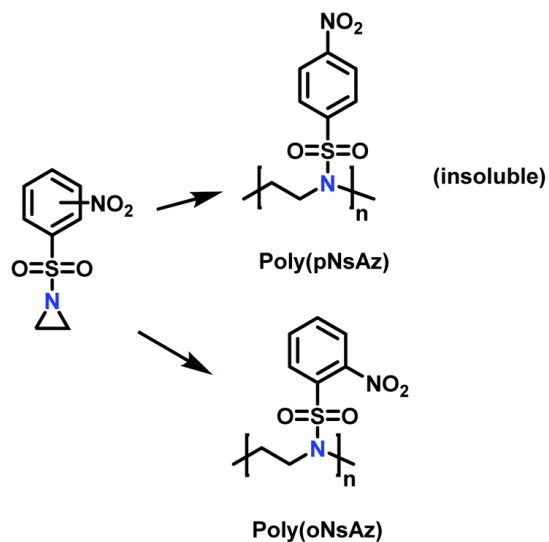
Figure 1.4: (A) Kinetic plots of $\ln([M]_0/[M]_t)$ vs. time for the azaanionic polymerization of TsMAz with BnNHMs (initiator) in DMF- d_7 at 50 °C with different bis(trimethylsilyl)amide-salts. (B) SEC-kinetics of MsMAz, BnNHMs at 50 °C in DMF (RI-signal), reproduced from ref. 143 with permission from Royal Chemical Society, copyright 2017.

The low solubility of poly(sulfonylaziridine)s was also a challenge for the polymerization of unsubstituted sulfonyl aziridines. In general, poly(sulfonylaziridine)s that lack substitution along the polymer backbone, or that have backbone substituents but are tactic, are generally insoluble in all solvents. For example, Thomi *et al.*¹⁴⁴ attempted to polymerize tosylaziridine and found that only insoluble oligomers were obtained. Later, Rupar and coworkers⁸³ were able to produce soluble polymers by copolymerizing mesylaziridine and *sec*-busylaziridine up to DP = 200. Such copolymers produced well-defined linear polyamines after desulfonylation by lithium metal (Scheme 1.16).



Scheme 1.16: Azaanionic copolymerization of unsubstituted sulfonyl aziridines as precursors for L-PEI. High degree of polymerization was only obtained when the monomers were used in a 1 : 1 ratio ($n = m$). Other ratios produced only insoluble oligomers.⁸³

Recently, Rupar and coworkers¹⁴¹ reported the first example of a poly(sulfonylaziridine) homopolymer which lacked substitution on the backbone. They studied the AROP of nitrophenylsulfonyl-activated aziridine monomers, namely *N*-((*p*-nitrophenyl)sulfonyl)aziridine (*p*NsAz) and *N*-((*o*-nitrophenyl)sulfonyl)aziridine (*o*NsAz) (Scheme 1.17). *p*NsAz formed an insoluble white powder upon heating in all attempts at polymerization. With *o*NsAz, on the other hand, the resulting poly(*o*NsAz) was soluble in both DMF and DMSO at all molecular weights, making it the first example of a soluble poly(*N*-sulfonylaziridine) homopolymer. The obtained homopolymer was subsequently deprotected using sodium thiomethoxide in DMF at 50 °C to yield an off-white residue. Although evidence was found for the formation of L-PEI from the deprotection of poly(*o*NsAz), satisfactory purification of the residue was not achievable. Control over the molecular weight of poly(*o*NsAz) was also attempted by initiating the anionic polymerization of *o*NsAz with BnN(Li)Ms. However, the resulting poly(*o*NsAz) was a mixture of the BnN(Li)Ms initiated polymer chains and hydroxyl initiated chains. This was attributed to the fact that *o*NsAz readily undergoes spontaneous polymerization, and thus could not be satisfactorily purified and dried.



Scheme 1.17: Azaanionic polymerization of nitrophenylsulfonyl-activated aziridines.¹⁴¹

Copolymerizations of different sulfonyl aziridines give access to random or gradient copolymers, depending on the nature of the sulfonyl group.¹³⁶ The reactivity ratios of 2-methyl tosyl aziridine (TsMAz) and 2-decyl tosyl aziridine (TsDAz) were determined *via* real-time ¹H NMR spectroscopy and proven to be an ideal random copolymerization with $r(\text{TsMAz}) = 1.08$ and $r(\text{TsDAz}) = 0.98$ and $r(\text{TsMAz}) \cdot r(\text{TsDAz}) = 1.05$. In contrast, combining monomers with different sulfonyl groups, resulted in (multi)gradient copolymers.¹³¹ Sulfonyl groups with stronger electron withdrawing effects increase the rate of polymerization, which led to gradient incorporation. Figure 1.5 shows the real-time ¹H NMR kinetics of a statistical terpolymerization of 2-methyl brosylaziridine (BsMAz), 2-methyl tosyl aziridine (TsMAz), and 2-methyl mesylaziridine (MsMAz), which form a copolymer with distinct domains along the polymer chain, due to the individual reactivity ratios of each monomer.¹³¹ DFT-calculations of the electrophilicity indices (ω^+) support these empirically determined comonomer reactivities, with BsMAz (2.22 eV) > TsMAz (1.98 eV) > MsMAz (1.25 eV).¹³⁹ Contrarily, the nucleophilicity (ω^-) of the azaanion at the growing chain end changes only ca. 0.14 eV, proving that the crucial factor which determines the incorporation rate is the monomer reactivity, and not the azaanion nucleophilicity.¹³⁹

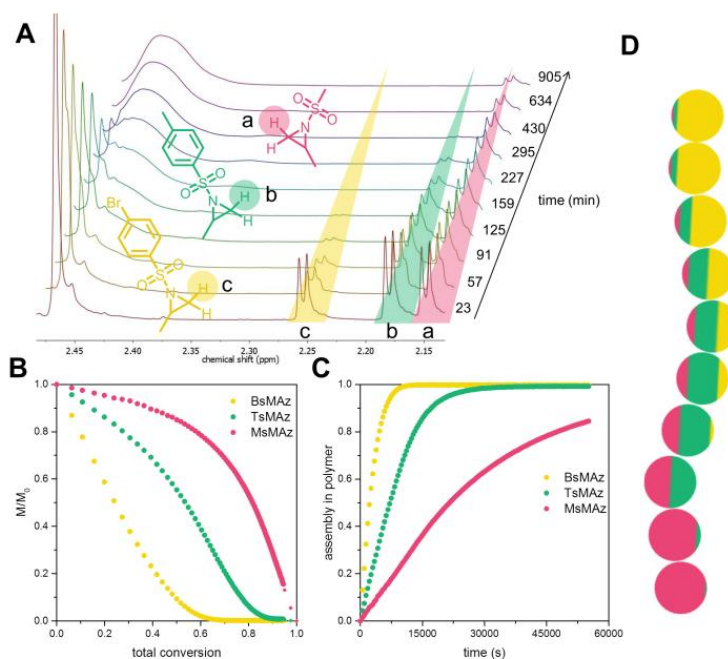


Figure 1.5: Simultaneous copolymerization of BsMAz, TsMAz, and MsMAz. (A) Real-time ¹H NMR spectra of the terpolymerization of BsMAz (yellow), TsMAz (green), MsMAz (red) showing the consumption of the monomers. (B) Normalized monomer concentrations in the reaction vs. total conversion. (C) Assembly of each monomer in the polymer vs. reaction time. (D) Visualization of a single chain for poly(BsMAz-co-TsMAz-co-MsMAz) – each sphere stands for 10% conversion. (Reproduced from ref. 131 with permission from Wiley, copyright 2016).

Gradient copolymers were also prepared by copolymerization of tosylated aziridines in emulsion.⁵⁴ The comonomer pair TsDAz and TsMAz produce random copolymers in solution, but when separated from each other by an emulsion consisting of DMSO-droplets and cyclohexane as the continuous phase, variable gradients can be obtained by partitioning of both monomers, when the continuous phase is diluted.^{136,143,149} This is represented in the apparent reactivity ratios, which are $r_{\text{app}}(\text{TsMAz}) = 4.98$ and $r_{\text{app}}(\text{TsDAz}) = 0.20$ in case of a 1 : 20-DMSO/cyclohexane emulsion, revealing the formation of strong gradient copolymers.^{150–152}

1.3.4 Functional polyaziridines prepared by anionic polymerization

Functional groups can be installed as substituents at the activating group or at the aziridine ring. 2-Oct(en)yl *N*-mesyl-aziridine (Figure 1.6a) with an olefin functionality was homo- and copolymerized *via* AROP. The olefins were post-modified by a radical thiol–ene reaction with *N*-acetyl-L-cysteine methyl ester providing quantitative conversion.¹³³ 2-Methyl-*N*-(4-styrenesulfonyl) aziridine (StMAz)¹³⁷ was the first bivalent aziridine derivative to undergo either anionic or radical polymerization (Figure 1.6d). After anionic polymerization, thiol–ene addition of mercaptoethanol or mercaptopropionic acid to the styrenic double bond was achieved. After radical polymerization, the pending sulfonyl aziridines could be further modified by nucleophilic additions, which was described for other polymers with aziridine side groups.^{153–156}

Also, polyols have been prepared by the AROP of sulfonyl aziridines. In analogy to ethoxy ethyl glycidyl ether (EEGE), the well-known precursor in oxyanionic polymerization to obtain linear poly(glycerol),^{74,157} acetal-protected *N*-tosyl-activated aziridines were introduced in 2016 (Figure 1.6b).¹³² Three different acetal-protected monomers with variable alkyl chain lengths were prepared and could be polymerized by living AROP. The hydroxyl groups were released by mild acidic hydrolysis, leaving the sulfonamides attached. Additional removal of the sulfonyl groups under reductive conditions resulted in polyamine-polyols, which might be used as chelating or transfection agents.¹³²

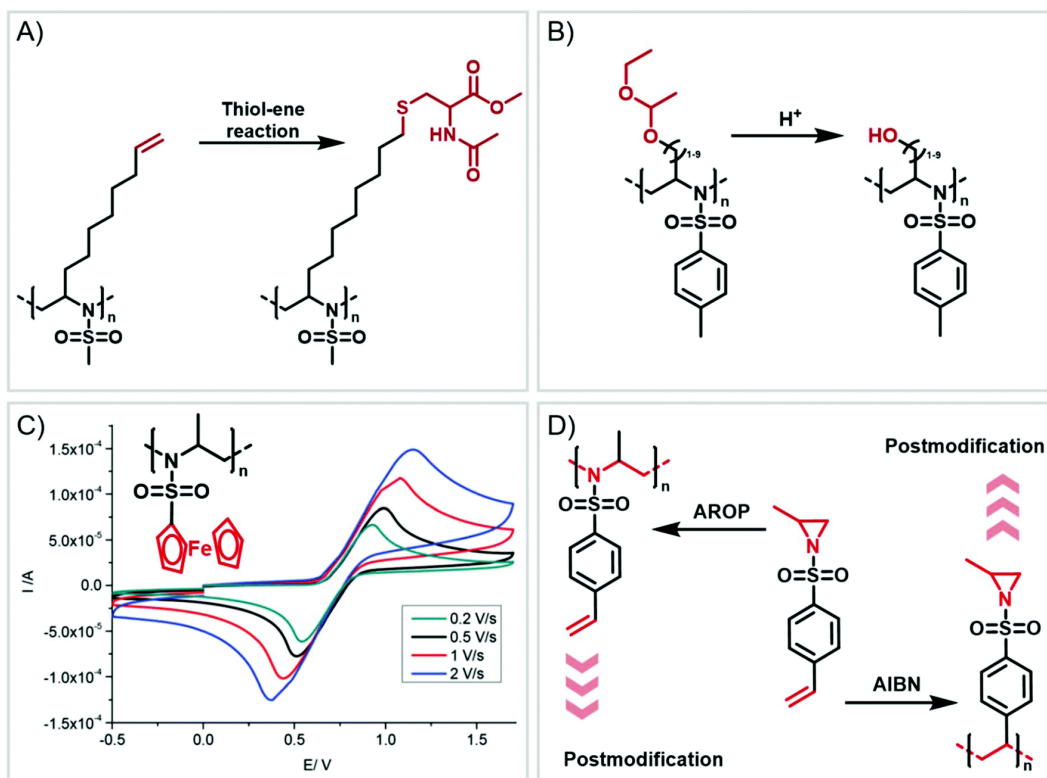
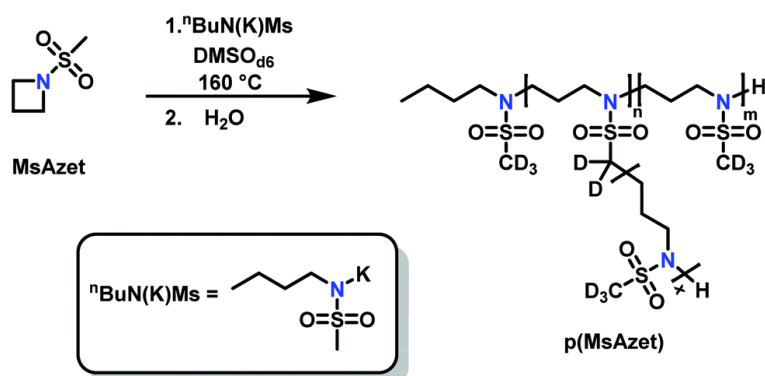


Figure 1.6: Functional polyaziridines: (A) terminal double bond can be converted *via* thiol-ene reaction. (B). Acetal-protected polyaziridines yield hydroxyl functionalities. (C) Ferrocene-containing polyaziridines are redox-responsive. (D) Orthogonal aziridine allows anionic and radical polymerization.

Organometallic 2-methyl-*N*-ferrocenylsulfonyl-aziridine was polymerized to prepare redox-responsive poly(sulfonylaziridine)s (Figure 1.6c).¹⁴⁰ Similar to other poly(sulfonylaziridine)s (see above), the homopolymerization resulted in insoluble materials. However, solid state NMR (ssNMR) and MALDI-TOF spectra supported the expected polymeric structure. Copolymerization with TsMAz or MsMAz resulted in soluble copolymers with moderate molecular weight dispersities ($\bar{D} < 1.4$), and chain extension experiments proved the living nature of the polymerization. Such organometallic polymers showed reversible oxidation/reduction by cyclic voltammetry, similar to other ferrocene-containing polymers.¹⁵⁸

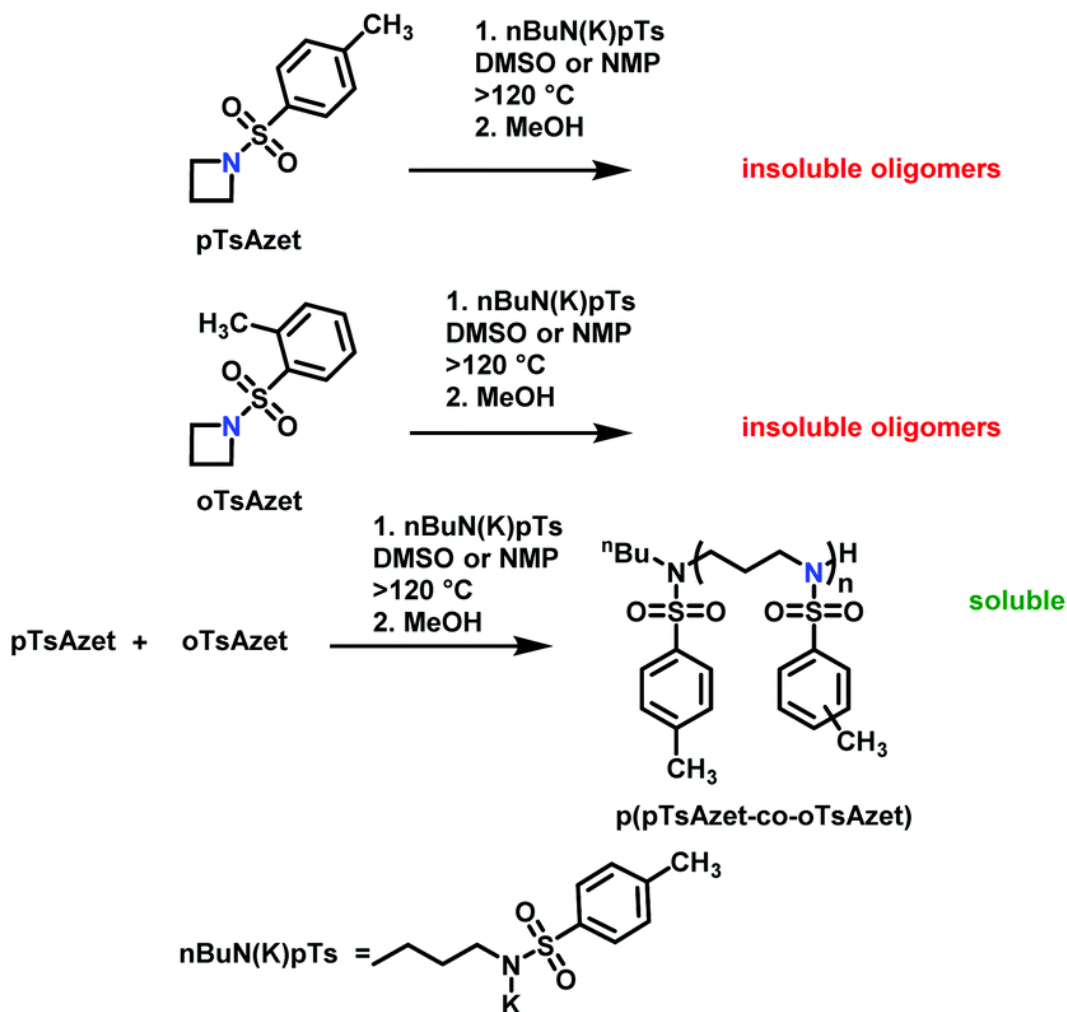
1.4 Anionic polymerization of azetidines

Reisman *et al.*¹⁴² reported the first example of AROP of an azetidine monomer, *N*-(methanesulfonyl)azetidine (MsAzet) (Scheme 1.18). Unlike the three-membered ring sulfonylaziridines, the polymerization of MsAzet required high temperatures (>100 °C) in order to polymerize. The resulting polymer, p(MsAzet), proved to contain branching due to chain transfer. As evidenced by H–D exchange experiments, this chain transfer occurs through the deprotonation of methanesulfonyl groups of the polymer backbone and the monomer to form sulfamoyl methanide anions. Evidence of minimal chain transfer to DMSO that occurs through the formation of dimsyl anions was also found. More importantly, the concentration of the active chain ends was found to be constant during the polymerization of MsAzet, which indicates that the controlled and living polymerization of sulfonylazetidines can be made possible if chain transfer can be inhibited.



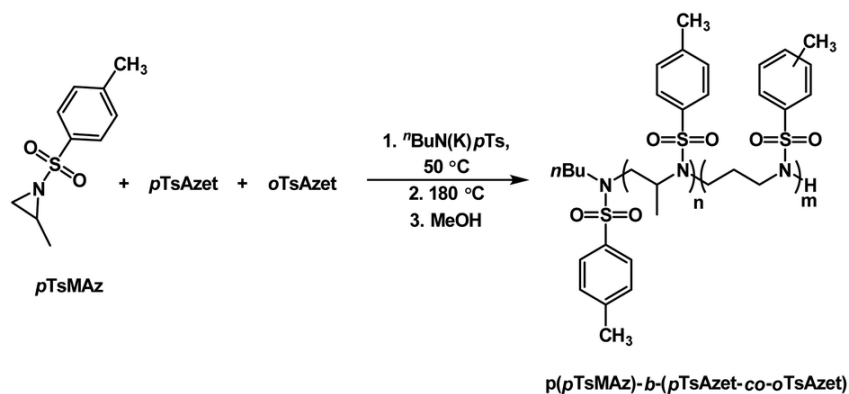
Scheme 1.18: Anionic ring-opening polymerization of *N*-(methanesulfonyl)azetidine.¹⁴²

Recently, *N*-(tolylsulfonyl)azetidines were found to undergo living AROP to form linear polymers.¹⁵⁹ These monomers do not contain protons likely to be activated under the polymerization conditions. Initial work was done by attempting to produce homopolymers from the two monomers *N*-(*p*-tolylsulfonyl)azetidine (*p*TsAzet) and *N*-(*o*-tolylsulfonyl)azetidine (*o*TsAzet) by AROP (Scheme 1.19). However, both resulting homopolymers precipitated from solution during polymerization at low molecular weight, similarly to sulfonylaziridine homopolymers.^{83,144} Drawing motivation from the literature, in which the copolymerization of two sulfonylaziridines was used to produce a soluble copolymer,⁸³ the copolymerization of *p*TsAzet with *o*TsAzet was attempted and produced the soluble copolymer, P(*p*TsAzet-*co*-*o*TsAzet) (Scheme 1.19). Similarly to MsAzet, the polymerization showed first order kinetics with respect to the total monomer concentration and the number of active chain ends remains constant. By a series of polymerizations, it was demonstrated that the polymerization was both living and controlled and produced polymers with narrow molecular weight distributions.



Scheme 1.19: Polymerization of TsAzet monomers to produce insoluble homooligomers and a soluble copolymer.¹⁵⁹

The sulfonyl groups of $P(p\text{TsAzet-co-oTsAzet})$ were removed under reductive conditions to produce the first example of LPTMI by living anionic polymerization. Additionally, due to the need for high temperatures in order to polymerize, the *N*-(tolylsulfonyl)azetidines could be used to produce block copolymers by living anionic polymerization in a closed-system in which all monomers are present at the time of initiation (Scheme 1.20, Figure 1.7).¹⁵⁹ This was accomplished by combining all monomers, $p\text{TsMAz}$, $p\text{TsAzet}$, and $o\text{TsAzet}$, in solution prior to initiation. Due to the differences in reactivities, $p\text{TsMAz}$ could be polymerized selectively at lower temperatures ($50\text{ }^\circ\text{C}$) while $p\text{TsAzet}$ and $o\text{TsAzet}$ do not polymerize. Upon total consumption of $p\text{TsMAz}$, the temperature was increased to $180\text{ }^\circ\text{C}$ to polymerize $p\text{TsAzet}$ and $o\text{TsAzet}$ to produce block copolymers. This allowed for the formation of block copolymers without homopolymer impurities. In the field of high performance block copolymers, this finding is of particular importance, as small amounts of homopolymer impurities can alter the properties of block copolymer materials.



Scheme 1.20: Block copolymerization of *p*TsMAz with *o*TsAzet and *p*TsAzet to produce $\text{P}(\text{pTsMAz})\text{-}b\text{-}\text{P}(\text{pTsAzet-co-}o\text{TsAzet})$.

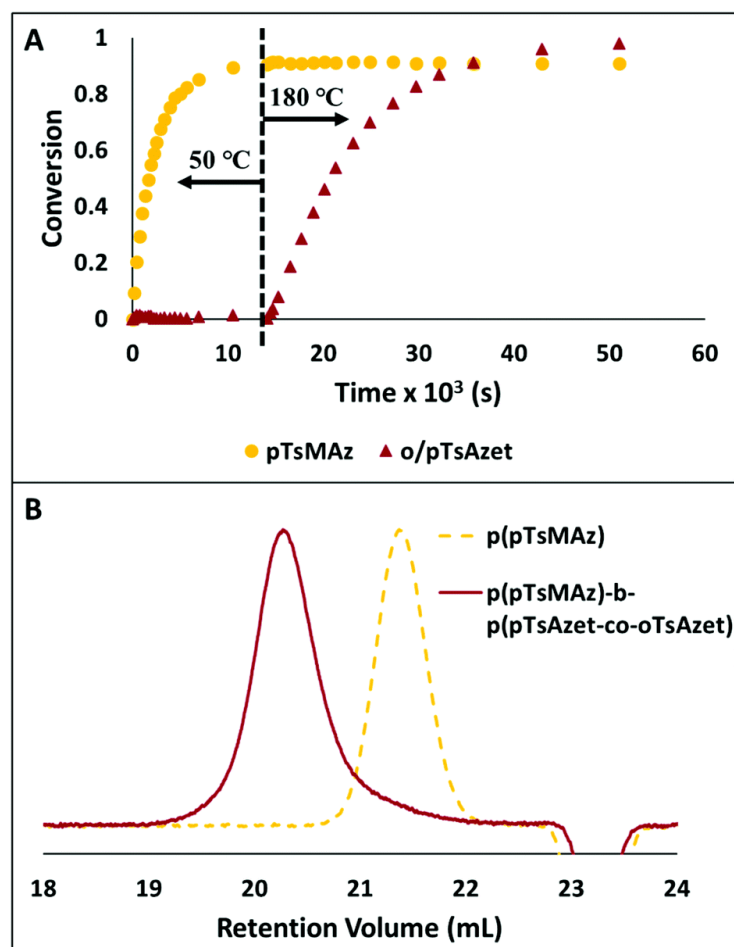
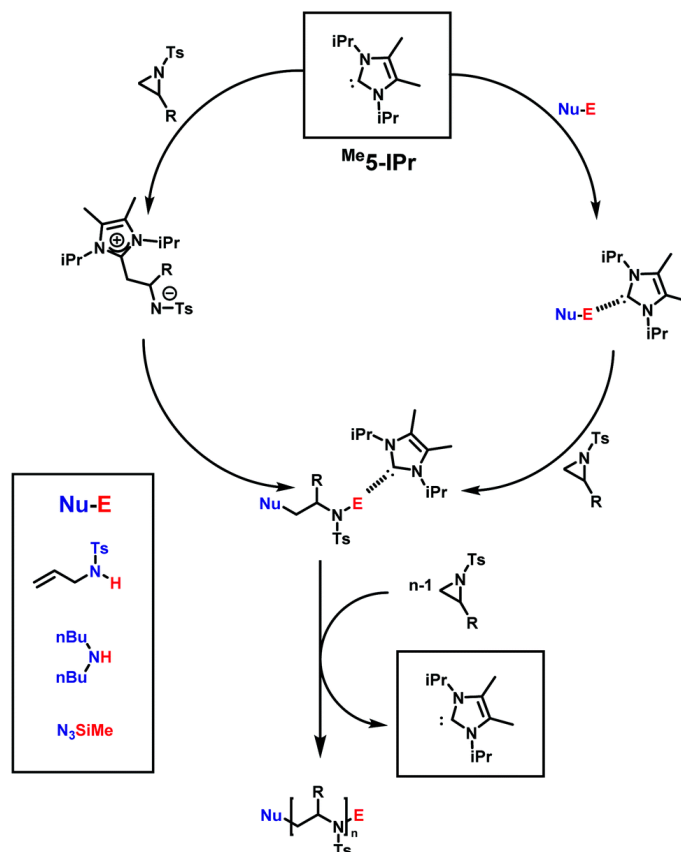


Figure 1.7: (A) Plot of conversion vs time for the block copolymerization of *p*TsMAz, *p*TsAzet, and *o*TsAzet in DMSO-d_6 to produce $\text{P}(\text{pTsMAz})_{20}\text{-}b\text{-}\text{P}(\text{pTsAzet-co-}o\text{TsAzet})_{40}$. The reaction is kept at 50 °C for 4 h, then heated to 180 °C for 10.25 h. The ^1H NMR measured conversion of *p*TsMAz appears to not reach 100% due to signal overlap between the monomer and polymer resonances in ^1H NMR spectra of the reaction mixture. (B) SEC trace of $\text{P}(\text{pTsMAz})_{20}$ prior to block copolymer chain extension (---). SEC trace of $\text{P}(\text{pTsMAz})_{20}\text{-}b\text{-}\text{P}(\text{pTsAzet-co-}o\text{TsAzet})_{80}$ (—). Block copolymerization to produce $\text{P}(\text{pTsMAz})_{20}\text{-}b\text{-}\text{P}(\text{pTsAzet-co-}o\text{TsAzet})_{80}$ was performed with a $[\text{pTsMAz}] : [\text{oTsAzet}] : [\text{pTsAzet}] : [\text{I}]$ ratio of 20 : 40 : 40 : 1 in NMP at 70 °C for 12 h, then 205 °C for 16 h. Reproduced from ref. 159 with permission from American Chemical Society, copyright 2018.

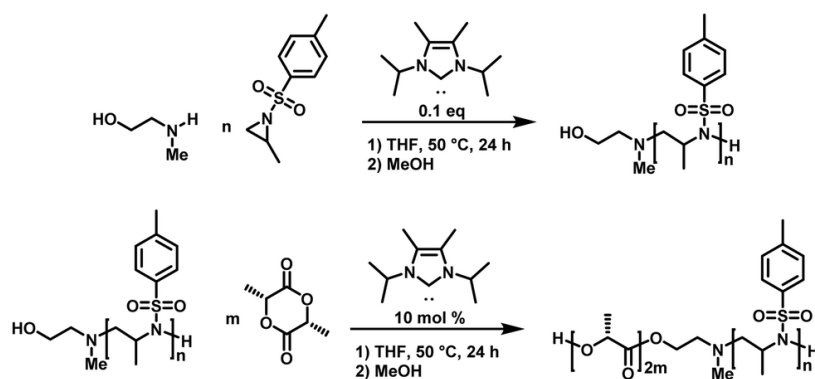
1.5 Organocatalytic ring-opening polymerization (OROP) of activated aziridines

N-Heterocyclic carbenes (NHC), such as 1,3-bis(isopropyl)-4,5(dimethyl)imidazole-2-ylidene, are powerful catalysts in many types of polymerizations. Their near unlimited structural diversity, inherent high Brønsted-basicity, and nucleophilicity make NHCs powerful organocatalysts.^{160,161} Examples of applications of NHCs include some of the most important commercial monomers in the step-growth polymerization of terephthalaldehyde,¹⁶² the group transfer polymerization of methacrylic monomers,¹⁶³ and the zwitterionic ring-opening polymerization (ZROP) of ethylene oxide (EO),¹⁶⁴ which was discovered in 2009 by Taton and coworkers. As activated aziridines polymerize with nucleophilic bases, similar to EO, *via* AROP, it was of interest if organocatalytic ring-opening polymerization (OROP) can also be successfully performed with this new monomer class. The first living OROP of 2-alkyl-*N*-sulfonyl aziridines was presented by Carlotti, Taton and coworkers in 2016 (Scheme 1.21).¹⁴⁷ The OROP of *N*-tosyl-2-substituedaziridines takes place in the presence of 1,3-bis(isopropyl)-4,5(dimethyl)imidazole-2-ylidene, as a sterically hindered organocatalyst, and activated secondary *N*-tosyl amine as the initiator. This mechanism offers a mild and metal-free route for the polymerization of activated aziridines to obtain identical polyaziridines to those from AROP, with narrow molecular weight distributions ($1.04 < \bar{D} < 1.15$) and molecular weights up to 21 000 g mol⁻¹. Depending on the steric hindrance of the ring-substituent, on the monomer, the reaction time to full conversion varies between 1 and 5 days at 50 °C in THF. Depending on the nature of the monomers, the NHCs either react as nucleophilic initiators or behave as organic catalysts by activating the initiator/active chain end. MALDI-TOF spectrometry clearly demonstrated the incorporation of the initiator (secondary *N*-tosyl amines) into the polymer, and a distribution with NHCs covalently bond to the polymer was not observed. The scope of practical initiators was expanded, when non-activated amines¹⁴⁵ and unprotected aminoalcohols were investigated, which allows further post-modification of the poly(aziridine)s.



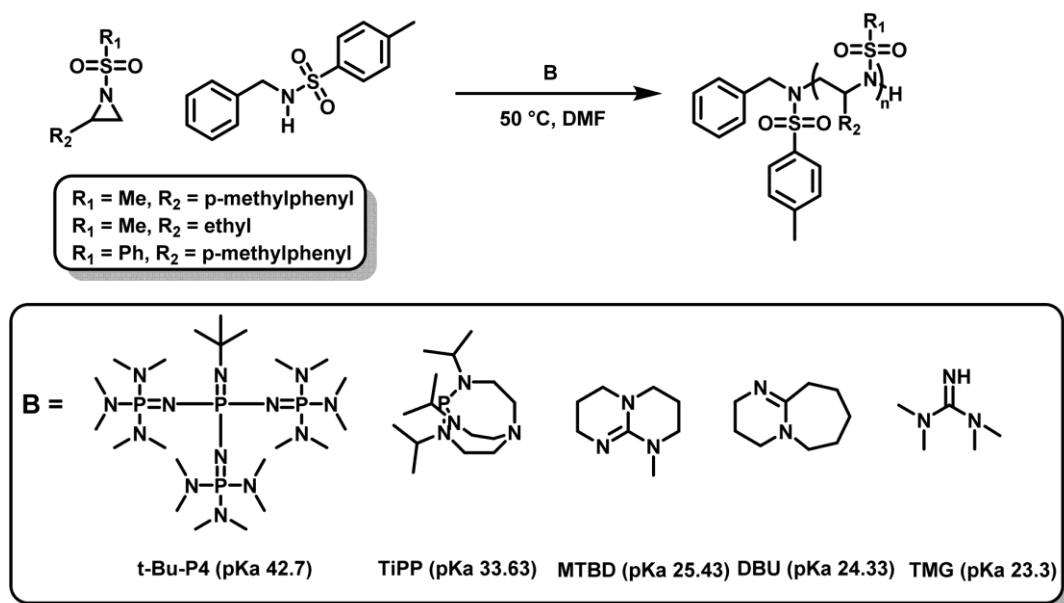
Scheme 1.21: Possible mechanism for the NHC-OROP of 2-alkyl *N-p*-toluenesulfonyl aziridines initiated by *N*-allyl *N-p*-toluenesulfonyl amine, di-*n*-butylamine and trimethylsilyl azide. Reproduced from ref. 145 with permission from Elsevier, copyright 2017.

Carbene-organocatalyzed ring-opening polymerization (NHC-OROP) of activated aziridines has also been conducted with an unprotected aminoalcohol as the initiator. The NHC catalyst selectively initiated the polymerization at the secondary amine, while the alcohol group remained untouched.¹⁴⁸ This allows for the synthesis of hydroxyl-functionalized poly(sulfonylaziridine)s which can be employed as macroinitiators for the synthesis of block copolymers. The hydroxyl group was used to initiate the ROP of lactide, catalyzed by the same carbene, to prepare PAz-*b*-PLLA diblock copolymers (Scheme 1.22).¹⁴⁸



Scheme 1.22: NHC-OROP of TsMAz initiated by 2-(methyl amino) ethanol, synthesis of poly(TsMAz)-*b*-poly(L-lactide) by sequential NHC-OROP with ^{Me}5-IPr as organocatalyst.¹⁴⁸

Recently, another metal-free azaanionic polymerization of sulfonyl aziridines was reported,¹³⁸ relying on different organic superbases, namely TMG, DBU, MTBD, TiPP and *t*-Bu-P₄ (Scheme 1.23). The basicity (pK_a-values of the conjugated acids) of these compounds increases in the order TMG < DBU < MTBD < TiPP < *t*-Bu-P₄ and correlates with their increasing catalytic activity. The OROP performed best (regarding reaction time (20 min), conversion, and dispersity ($\mathcal{D} = 1.05$)) using the most basic organic base, *t*-Bu-P₄, but TiPP also showed satisfactory results. The remaining three bases were found to catalyze the polymerization of sulfonyl aziridines but showed higher molecular weight distributions (\mathcal{D} up to 1.4). This is caused by the increased nucleophilicity of the bases leading to multiple initiators with varying rates of initiation. Overall, the strongest bases had the best catalytic activity. Moreover, the amount of catalyst could be lowered to 0.05% respect to the initiator, which indicates a very fast proton exchange, similar to oxyanionic polymerizations.⁷⁴

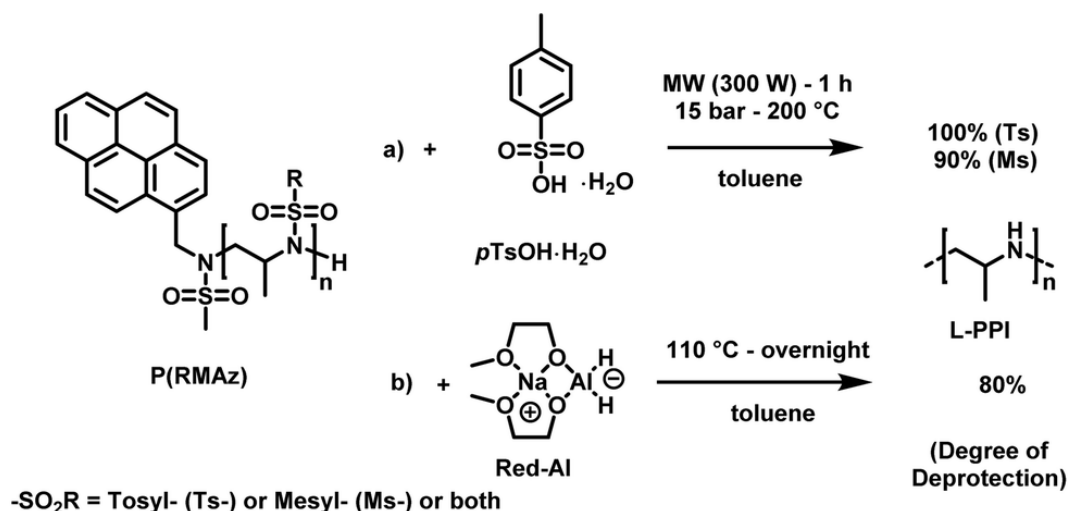


Scheme 1.23: AROP of *N*-sulfonyl aziridines mediated by organic superbases.¹³⁸

1.6 Desulfonylation reactions

L-PEI is a linear polyamine, which is of high interest for applications in non-viral gene transfection and as polyelectrolytes.¹⁶⁷ Today L-PEI is produced from polyoxazolines following hydrolysis of the pendant amides (see above).^{16,26,165,166} The primary attraction to synthesizing linear PEI *via* the oxazoline route is due to the controlled character of the cationic polymerization of poly(2-oxazoline)s, which allows control over molar masses and dispersity.¹⁶⁸ Generally, strongly acidic or alkaline media, and temperatures as high as 100 °C are required to transform acylated poly(2-oxazoline)s into L-PEI, a process that is difficult to drive to completion.

In a recent publication, Tauhardt and coworkers reported 99% hydrolysis of poly(2-oxazoline)s using 6 M HCl at 130 °C in a microwave synthesizer; the closest to complete conversion to L-PEI from a poly(2-oxazoline) yet reported.¹⁶⁹ In contrast, if aziridines or azetidines are polymerized by an anionic or organocatalytic route, desulfonation of the poly(sulfonamide)s needs to be achieved. Many published strategies exist in the literature for the reduction of low molecular weight sulfonamides to amines.^{170,171} According to Bergman and Toste,¹²⁴ a successful desulfonation of poly(sulfonylaziridine) was achieved by lithium naphthalenide. However, no spectral analyses or molecular weight distributions of the obtained structures were given. In another approach from Wurm's group,¹⁴⁴ tosylamides were cleaved by acidic hydrolysis with hydrobromic acid (HBr) and phenol. In spite of the harsh reaction conditions, the method was reported to be successful. Later, Wurm and coworkers were able to remove tosylamides with sodium bis(2-methoxyethoxy)aluminiumhydride (Red-Al) to ~80% (Scheme 1.24).¹³² Rupar and coworkers were able to prepare L-PEI under reductive conditions, using elemental lithium (Li), with *tert*-butanol (*t*-BuOH) in hexamethylphosphoramide (HMPA) and THF at low temperatures.⁸³ Acidic hydrolysis under microwave irradiation, which proved to be efficient for hydrolysis of polyoxazolines,^{171,172} also produced desulfonated linear polypropylenimine (L-PPI, 100% desulfonation for tosyl groups and ca. 90% for mesyl groups).⁸² However, chain scission could not be prevented under these harsh conditions.

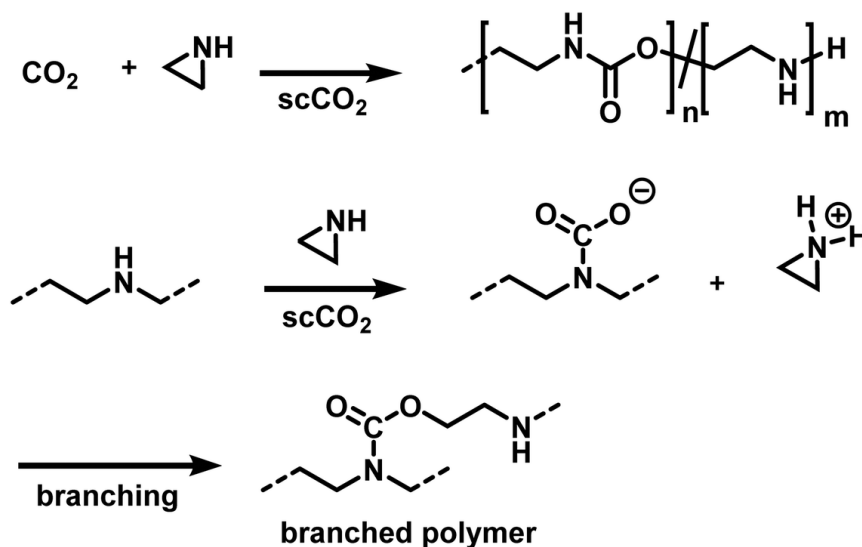


Scheme 1.24: Desulfonation methods for PAz: (a) acidic hydrolysis, using *p*TsOH in toluene under microwave irradiation. (b) Reductive deprotection using Red-Al in toluene.⁸²

1.7 Combination of aziridines and azetidines with other polymerization techniques: copolymers and polymer architectures

1.7.1 Copolymers of aziridines with CO₂

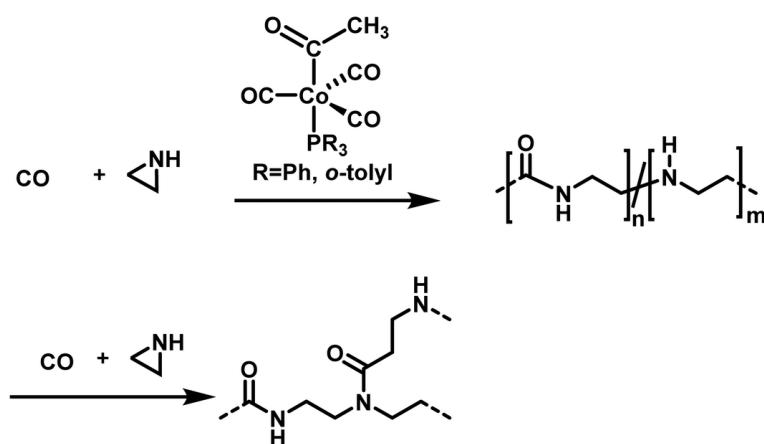
Ihata *et al.* synthesized poly(urethane-*co*-amine)s by copolymerization of several aziridines with CO₂ (Scheme 1.25).^{173,174} The polymerizations were performed without the addition of catalyst or initiator in supercritical CO₂ as the solvent, producing branched polymers of molar masses between 7000 and 15 000 g mol⁻¹. Branching occurs during the polymerization, when the secondary amines react with CO₂, resulting in a carbamate and a protonated aziridine. The latter is ring-opened by nucleophilic attack, leading to branched polymers. The ratio of urethane to amine linkages in the poly(urethane-*co*-amine)s is affected by the CO₂ pressure. By variation of the CO₂ pressure from 3 to 22 MPa, copolymers with urea contents from 32 to 62% were produced. The reported yields were <35% and decreased further when the aziridine was substituted with sterically demanding side groups (i.e. 2,2 dimethylaziridine, 2-cyclohexylaziridine, etc.). The copolymers of methylaziridine and CO₂ exhibited lower critical solution temperatures in water between 34 to 85 °C, which might be beneficial for the development of smart nanomaterials.



Scheme 1.25: Copolymerization of aziridines and CO₂ to branched poly(urethane-*co*-amine)s.^{173,174}

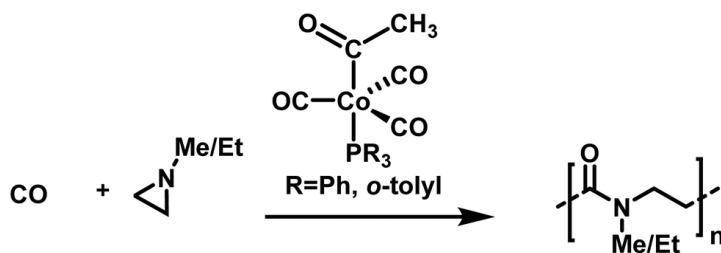
1.7.2 Copolymers of aziridines with CO

Jia *et al.* explored the alternating copolymerization of aziridine with carbon monoxide mediated by a cobalt catalyst to prepare polyamides (Scheme 1.26).¹⁷⁵ High CO pressures of up to 69 bar were necessary to obtain high polymer yields of ca. 90%. High molecular weight polyamides between 14 100 and 63 300 g mol⁻¹ were synthesized. However, molar mass dispersities of up to 11.5 indicate low degrees of control over the polymerization. The authors further proposed a mechanism, in which consecutive aziridine attacks during the polymerization could lead to an amide–amine copolymer, to rationalize the broad distributions of the polymers. The amine linkages act also as nucleophiles and thereby induce branching or crosslinking.¹⁷⁶



Scheme 1.26: Copolymerization of aziridine and carbon monoxide towards branched poly(amide-co-amine)s.¹⁷⁵

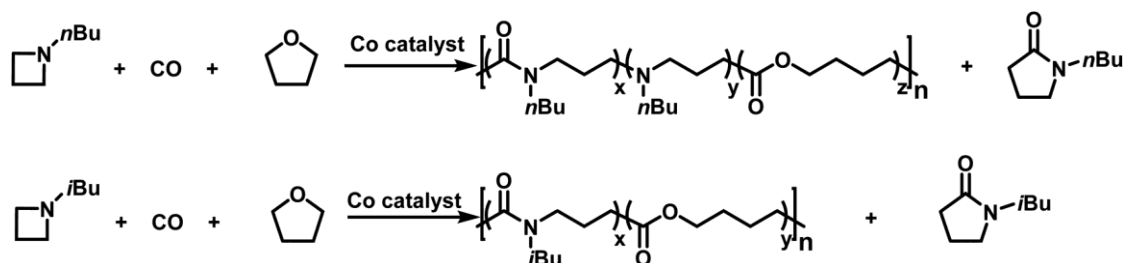
Well-defined poly- β -peptoids can be obtained in quantitative yields with $\mathcal{D} = 1.11$ when *N*-alkylated aziridines are copolymerized with carbon monoxide (Scheme 1.27).¹⁷⁷ *N*-Methyl and *N*-ethyl groups enhance the selectivity of the cobalt catalyst and improve the alternating copolymerization. The mechanism involves aziridine insertion into the cobalt–acyl bond, with the rate determining step being the ring-opening of the aziridine, followed by a migratory CO insertion.¹⁷⁸ As crossover reactions, chain transfer, or combination reactions were not observed, the copolymerization of *N*-substituted aziridines with CO seems to follow the characteristics of a living alternating copolymerization.



Scheme 1.27: Alternating copolymerization of alkylated aziridines and carbon monoxide towards well-defined poly- β -peptoides.¹⁷⁷

1.7.3 Copolymers of azetidines with CO

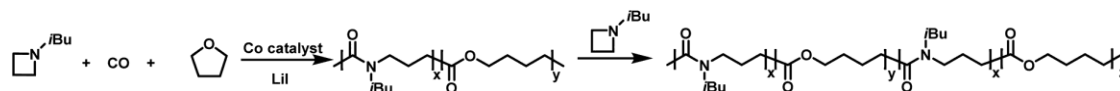
More recently, Jia provided the first example of a transition metal catalyzed azetidine polymerization.¹⁷⁹ This work provided a route to poly(γ -lactams) by overcoming the difficulties associated with the ring-opening polymerization of γ -lactams.¹⁸⁰ This was accomplished by using a cobalt catalyst to perform a carbonylative polymerization with *N*-*n*-butylazetidine and *N*-*iso*-butylazetidine. While the polymer contains only amide units for *N*-*iso*-butylazetidine, in the case of *N*-*n*-butylazetidine, it was discovered that CO is unincorporated in some instances, leaving tertiary amines along the back bone of the polymer.¹⁸¹ Interestingly, it was discovered that THF also participates in the reaction, leading to the formation of ester units in the polymers produced (Scheme 1.28).



Scheme 1.28: Co catalyzed carbonylative polymerization of azetidine with THF to produce poly(amide-co-ester)s.¹⁷⁹

This was a significant finding as the incorporation of THF does not occur in the related aziridine systems.^{175–177,182,183} Further probing of the incorporation of THF led to the finding that increased azetidine concentration produced polymers with lower degrees of ester incorporation. This suggests that the reaction of the active chain end with THF is favored when the azetidine concentration is low. The living character, displayed by narrow molecular weight distributions and the linear increase in molecular weight with increase in conversion, coupled with *in situ* IR spectroscopy, suggests that the incorporation of ester units into the polymer backbone likely occurs in a gradient manner. The cobalt catalyzed carbonylative polymerization of azetidine does have a drawback in that the formation of γ -lactam also occurs. This reaction was attributed to “back-biting”,¹⁷⁸ rather than catalyst decomposition¹⁸³ due to the continued living character of the polymerizations. Jia further hypothesized that this back-biting reaction occurs at the acylazetidinium intermediate, and not the acyl-Co(CO)₄ intermediate.¹⁸⁰ This hypothesis was tested by the addition of nucleophilic I⁻ anions to facilitate ring-opening of the acylazetidinium intermediate. The addition of LiI (2 eq. relative to Co catalyst) eliminated the γ -lactam side-product, confirming Jia's hypothesis. Curiously, it was also found that the Li counter ion also played a role in the polymerizations. This was discovered because while *n*Bu₄NI also suppressed the formation of γ -lactam, it greatly slowed the rate of polymerization. Interestingly, the addition

of LiI also prevented the formation of ester linkages prior to complete consumption of azetidine. This finding allowed for the formation of block copolymers (Scheme 1.29). To further support the hypothesis of the Li^+ cation being instrumental in the polymerization, no ester linkages were formed when $n\text{Bu}_4\text{NI}$ was used as an iodide source.

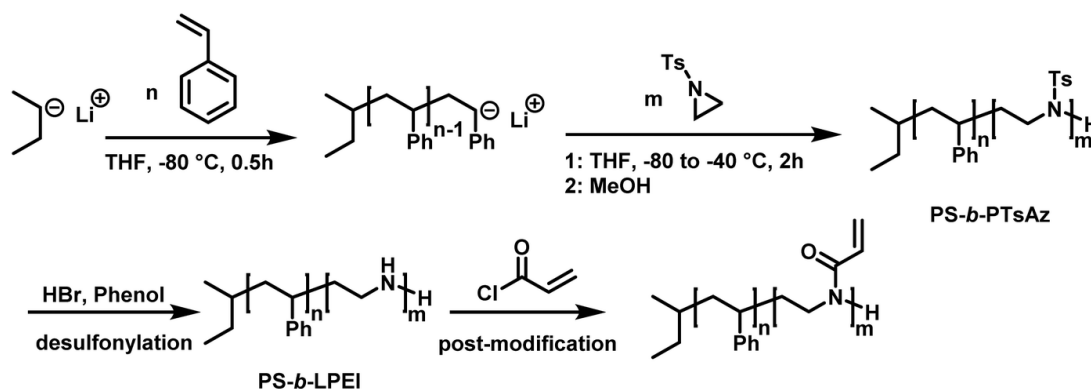


Scheme 1.29: Synthesis of poly(amide-*co*-ester) block copolymers with LiI and sequential addition of azetidine.¹⁸⁰

Due to the cobalt catalyzed carbonylative polymerization of azetidine having a living character, equal feeds of monomer were added over time in order to produce alternating amide and ester blocks. These polymers yielded narrow molecular weight distributions (<1.23) and produced low molecular weight polymers with similar dispersities (1.11–1.30) upon methanolysis under acidic conditions at room temperature. Complete degradation of the resulting polyamides could be further achieved by refluxing the polymers in aqueous acidic conditions. This allows for poly(amide-*co*-ester) block copolymers to undergo a two-stage degradation.

1.7.4 Combination of aziridines with other anionic polymerization techniques

In living anionic polymerization (LAP) no termination occurs, allowing the synthesis of block copolymers by sequential addition of the monomers. Thomi *et al.*¹⁴⁴ prepared polystyrene-block-poly(*N*-tosylaziridine) by consecutive living anionic polymerization of styrene and *N*-tosyl aziridine (Scheme 1.30).

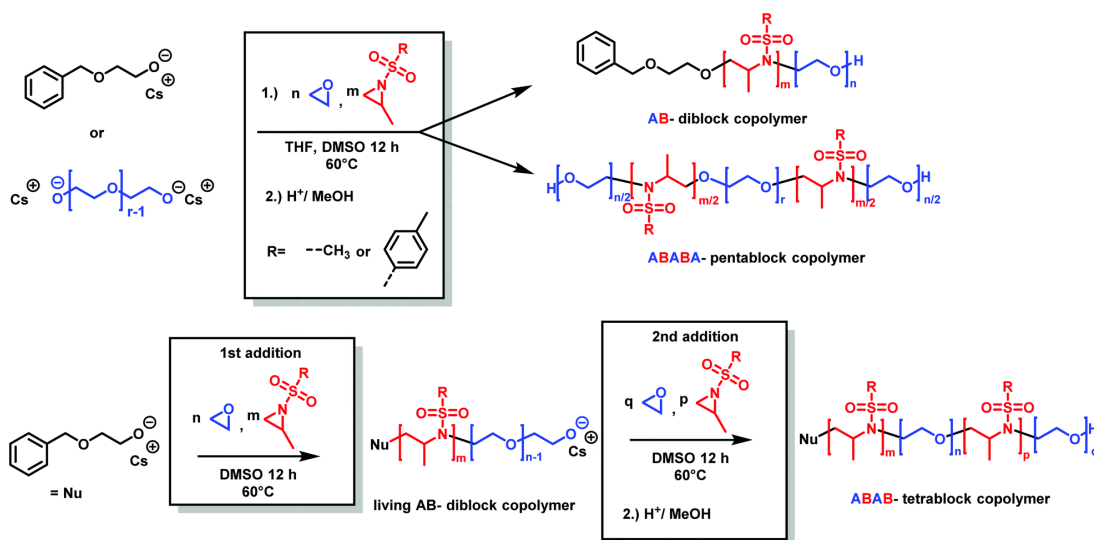


Scheme 1.30: Two step synthesis of polystyrene-block-polytosylaziridine and desulfonation to polystyrene-block-polyethylenimine.¹⁴⁴

Quantitative transfer from the carbanions to azaanions was proven and oligomerization of the sulfonyl-activated aziridine was confirmed. Thomi *et al.* further demonstrated the quantitative removal of the sulfonyl groups by acidic hydrolysis with hydrobromic acid and phenol, releasing the amino groups attached to polystyrene to produce PS-*b*-LPEI.¹⁴⁴ The introduced amine functionalities are a suitable platform for further efficient modifications which was shown by reaction with acryloyl chloride (Scheme 1.30). Short oligomers of the second block ($1 < m < 5$) were easily obtained, but block copolymers (up to 30 repeat units TsAz) with an increasing number of TsAz needed longer reaction times, due to the insolubility which inhibits further propagation.¹⁴⁴

Copolymers of aziridine and ethylene oxide are interesting materials for biomedical applications or as surfactants. Attempts for the cationic ring-opening copolymerization of epoxides and *N*-substituted aziridines failed.¹⁸⁴ Very recently, the anionic copolymerization of sulfonyl aziridines and ethylene oxide was achieved (Scheme 1.31).¹⁴⁶ In a single step, well-defined amphiphilic block copolymers were obtained by a one-pot copolymerization. The highest difference of reactivity ratios ever reported for an anionic copolymerization (with $r_1 = 265$ and $r_2 = 0.004$ for 2-methyl-*N*-tosylaziridine/EO and $r_1 = 151$ and $r_2 = 0.013$ for 2-methyl-*N*-mesylaziridine/EO) led to the formation of block copolymers in a closed system. The amphiphilic diblock copolymers were used as a novel class of nonionic and responsive surfactants. In addition, this unique comonomer reactivity allowed fast access to multiblock copolymers: we prepared the

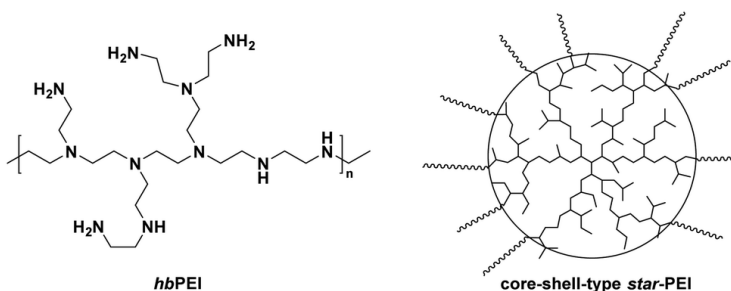
first amphiphilic penta- or tetrablock copolymers containing aziridines in only one or two steps, respectively. These examples render the combination of epoxide and aziridine copolymerization to be a powerful strategy to sophisticated macromolecular architectures and nanostructures.



Scheme 1.31: Synthesis of poly(aziridine)-*b*-poly(ethylene glycol) block copolymers by anionic copolymerization (2-methyl-*N*-tosylaziridine (TsMAz), 2-methyl-*N*-mesylaziridine (MsMAz), and *N*-tosylaziridine (TsMAz) were used in this study). Top: In a single step, either AB-diblock or ABABA-pentablock copolymers can be prepared. Bottom: Sequential addition of aziridine/EO mixture produces ABAB-tetrablock copolymers. Reproduced from ref. 146 with permission from American Chemical Society, copyright 2018.

1.7.5 Polymer architectures

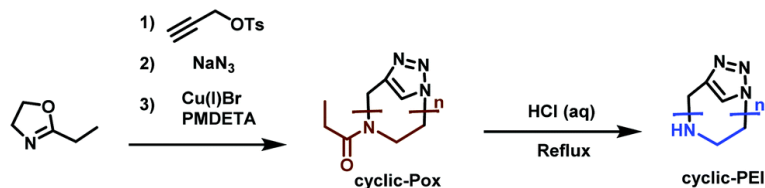
The aziridine building block can be used to prepare three-dimensional, polymer architectures. The typical polymer architectures for polyethylenimine-derivatives are, however, only hyperbranched (from CROP of aziridine) or linear (from CROP of oxazolines or AROP of sulfonyl aziridines). Few more complex copolymer architectures are reported to date. Current literature has studied the influence of different PEI architectures and molar masses on DNA complexation behavior, cell transfection efficiency, and toxicity.^{135,185–187} Various multiarm star polymers with hbPEI as core were synthesized (Scheme 1.32). The arms of shell type star-PEIs can be obtained by different synthetic strategies. ROP allows the use of hbPEI as a macroinitiator to graft several different “shell-polymers” to the core. The most well known are: polyamide-12, ϵ -caprolactone, polylactide, and other polyesters. Multiarm star polymers can be afforded as well-defined nanoparticles with potential uses in nanomedicine, catalysis, and drug or gene delivery. Furthermore, star-like topologies were studied due to their unusual physical and rheological properties. These properties were found to be mainly dependant on the number of end groups, molecular weight, and the length of the arms.¹⁸⁸



Scheme 1.32: Illustration of hbPEI and core shell type star-PEI.

Since the polymerization of ethyleneimine was first developed by Zomlefer and co workers⁸⁹ in 1943, tuning and adjusting of the hbPEI architecture has been investigated. Comparing low molecular weight hbPEI (12 kg mol^{-1}) (LMW-PEI) and high molecular weight hbPEI (1600 kg mol^{-1}) (HMW-PEI) shows that the degree of branching increases with the degree of polymerization. Commercially available high molecular mass hbPEI exhibits a ratio of primary : secondary : tertiary amines close to 1 : 1 : 1, which indicates a very dense polymer structure with a branching unit on every second nitrogen.¹²⁹ This ratio changes towards an excess of primary amines when decreasing the molecular weight; the amine ratio of this PEI, is mostly independent of molar masses from $8600\text{--}24\,300 \text{ g mol}^{-1}$, is close to 3 : 5 : 2. Commercial PEI (DP = 16) has an amine ratio of $\sim 4 : 3 : 3$. Such LMW-PEI is usually synthesized in dilute acidic aqueous environment. The less dense structure consists on average of two linear repeating units.^{129,187,189} Kissel and coworkers¹⁸⁹ demonstrated, that by varying the reaction temperature from $35 \text{ }^\circ\text{C}$ to $100 \text{ }^\circ\text{C}$, the molecular weight of PEI can be adjusted from $24\,300$ to 8610 g mol^{-1} . Though certain relationships between molar mass, synthetic route, and degree of branching are known, systematic studies of these polymers regarding their properties remain challenging due to increasing dispersities with increasing DP caused by uncontrolled crosslinking.

Cyclic PEI (c-PEI) was first synthesized by Grayson *et al.*¹⁹⁰ (Scheme 1.33). They used propargyl *p*-toluene-sulfonate as initiator to polymerize ethyloxazoline under anhydrous conditions. To minimize termination and chain transfer reactions caused by aqueous impurities, the polymerization was performed in a microwave reactor. Selective termination by adding sodium azide gives α -, ω -functionalized polyoxazoline. Subsequent click-chemistry, to cyclize the polymers, followed by acidic hydrolysis, leads to c-PEI. The effect of polymer structure (i.e. linear, cyclic, branched, etc.) on DNA complexation was studied and it was determined that c-PEI polymers showed reduced toxicity and stronger complexation. This is most likely contributed to the higher charge density compared to the linear analogue. Grayson's study precisely points out the need to develop new strategies for new PEI architectures for increased understanding in terms of their properties and potential applications.



Scheme 1.33: Synthesis route towards c-PEI.¹⁹⁰

Haag and coworkers¹⁹¹ investigated the influence of the length of the alkylene spacer, as an efficient complexation agent for DNA needs to optimize the number of phosphate units bound. Their study investigated the complexation behavior of ethylene, propylene, and butylene spacers synthesized with different strategies (Figure 1.8). Polyamines containing a butylene spacer showed stronger DNA complexation as well as decreased cytotoxicity. It was proposed, due to calculations, that the N–N distance aligns more precisely with the P–P distance of the DNA in polymers with a butylene spacer than in those with an ethylene spacer. Additionally, the increasing hydrophobicity likely also effects the biological properties.

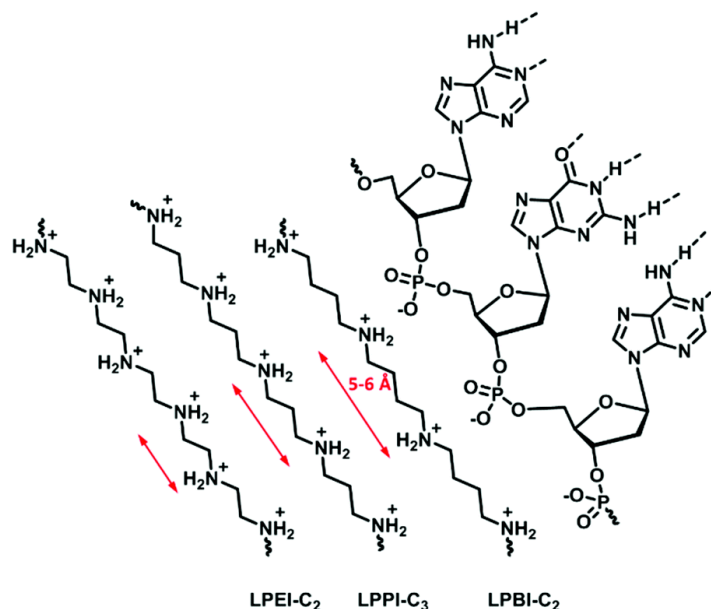


Figure 1.8: Schematic representation of the nitrogen spacing in polyamine analogs and their interaction with RNA.

1.8 Conclusions

The polymerization of aziridines (especially ethylenimine) has had industrial relevance for several decades and polyethylenimine is used in a wide range of applications from chelators to biomedical applications. Hyperbranched PEI is available commercially at low cost, however its molecular characteristics, molar mass, and dispersity are only poorly controlled by the industrial cationic ring-opening polymerization of ethylenimine. Due to these issues, aziridine polymerizations have been sparsely studied over the course of the last couple decades. Azetidine polymers are even more exotic in both industrial and academic polymer research.

However, with the development of the living anionic polymerization of sulfonyl aziridines and azetidines, the possibility to install well-defined polyamine building blocks in different macromolecular architectures has been achieved. However, to date, only very few of these polysulfonamides have been transformed into the respective polyamines, as the desulfonation step is challenging and proceeds typically under harsh conditions, but some recent efforts have paved the way to feasible synthetic routes with control over molar mass and dispersity. While these polyamines contain high value, the polysulfonamides are also interesting, novel polymers that have been only scarcely characterized for their potential applications.

The development of the living polymerization of aziridine- and azetidine-derivatives was a milestone to develop polymer architectures with these building blocks and will open the possibility to a plethora of future applications.

1.9 References Chapter 1

1. S. Penczek, P. Kubisa and K. Matyjaszewski, *Oxiranes*, Springer Berlin Heidelberg, Berlin, Heidelberg, **1985**.
2. G. Gee, W. C. E. Higginson, P. Levesley and K. J. Taylor, *J. Chem. Soc.*, **1959**, 1338–1344.
3. G. Gee, W. C. E. Higginson and G. T. Merrall, *J. Chem. Soc.*, **1959**, 1345–1352.
4. E. H. Schacht and E. J. Goethals, *Makromol. Chem.*, **1974**, 175, 3447–3459.
5. E. J. Goethals, E. H. Schacht, P. Bruggeman and P. Bossaer, in *Ring-Opening Polymerization*, American Chemical Society, **1977**, vol. 59, ch. 1, pp. 1–12
6. S. Kobayashi, *Prog. Polym. Sci.*, **1990**, 15, 751–823.
7. M. Jäger, S. Schubert, S. Ochrimenko, D. Fischer and U. S. Schubert, *Chem. Soc. Rev.*, **2012**, 41, 4755–4767.
8. M. L. Sarazen and C. W. Jones, *Macromolecules*, **2017**, 50, 9135–9143.
9. In the literature, polytrimethylenimine (PTMI) is also called polypropylenimine (PPI). We prefer PTMI.
10. S. W. Benson, F. R. Cruickshank, D. M. Golden, G. R. Haugen, H. E. O'Neal, A. S. Rodgers, R. Shaw and R. Walsh, *Chem. Rev.*, **1969**, 69, 279–324.
11. H. K. Eigenmann, D. M. Golden and S. W. Benson, *J. Phys. Chem.*, **1973**, 77, 1687–1691.
12. T. Li, L. Wu, J. Zhang, G. Xi, Y. Pang, X. Wang and T. Chen, *ACS Appl. Mater. Interfaces*, **2016**, 8, 31311–31320.
13. J. Pan, Z. Lyu, W. Jiang, H. Wang, Q. Liu, M. Tan, L. Yuan and H. Chen, *ACS Appl. Mater. Interfaces*, **2014**, 6, 14391–14398.
14. X. Ding, W. Wang, Y. Wang, X. Bao, Y. Wang, C. Wang, J. Chen, F. Zhang and J. Zhou, *Mol. Pharm.*, **2014**, 11, 3307–3321.
15. Y.-L. Lo, K.-H. Sung, C.-C. Chiu and L.-F. Wang, *Mol. Pharm.*, **2013**, 10, 664–676.
16. M. Jaeger, S. Schubert, S. Ochrimenko, D. Fischer and U. S. Schubert, *Chem. Soc. Rev.*, **2012**, 41, 4755–4767.
17. S. C. De Smedt, J. Demeester and W. E. Hennink, *Pharm. Res.*, **2000**, 17, 113–126.
18. D. W. Pack, A. S. Hoffman, S. Pun and P. S. Stayton, *Nat. Rev. Drug Discovery*, **2005**, 4, 581.
19. C. T. De Ilarduya, Y. Sun and N. Düzgüneş, *Eur. J. Pharm. Sci.*, **2010**, 40, 159–170.
20. M. D. Giron-Gonzalez, R. Salto-Gonzalez, F. J. Lopez-Jaramillo, A. Salinas-Castillo, A. B. Jodar-Reyes, M. Ortega-Muñoz, F. Hernandez-Mateo and F. Santoyo-Gonzalez, *Bioconjugate Chem.*, **2016**, 27, 549–561.
21. M. A. Mintzer and E. E. Simanek, *Chem. Rev.*, **2008**, 109, 259–302.
22. M. Neu, D. Fischer and T. Kissel, *J. Gene Med.*, **2005**, 7, 992–1009.
23. C. Raymond, R. Tom, S. Perret, P. Moussouami, D. L'Abbé, G. St-Laurent and Y. Durocher, *Methods*, **2011**, 55, 44–51.
24. E. Altuntaş, K. Knop, L. Tauhardt, K. Kempe, A. C. Crecelius, M. Jäger, M. D. Hager and U. S. Schubert, *J. Mass Spectrom.*, **2012**, 47, 105–114.
25. S. M. Moghimi, P. Symonds, J. C. Murray, A. C. Hunter, G. Debska and A. Szewczyk, *Mol. Ther.*, **2005**, 11, 990–995.
26. O. Boussif, F. Lezoualc'h, M. A. Zanta, M. D. Mergny, D. Scherman, B. Demeneix and J.-P. Behr, *Proc. Natl. Acad. Sci. U. S. A.*, **1995**, 92, 7297–7301.
27. M. Thomas and A. M. Klibanov, *Proc. Natl. Acad. Sci. U. S. A.*, **2003**, 100, 9138–9143.
28. M. S. Shim and Y. J. Kwon, *Bioconjugate Chem.*, **2009**, 20, 488–499.
29. M.-E. Bonnet, P. Erbacher and A.-L. Bolcato-Bellemin, *Pharm. Res.*, **2008**, 25, 2972.
30. L. Wightman, R. Kircheis, V. Rössler, S. Carotta, R. Ruzicka, M. Kurska and E. Wagner, *J. Gene Med.*, **2001**, 3, 362–372.
31. H. Yin, R. L. Kanasty, A. A. Eltoukhy, A. J. Vegas, J. R. Dorkin and D. G. Anderson, *Nat. Rev. Genet.*, **2014**, 15, 541–555.
32. T. K. Kim and J. H. Eberwine, *Anal. Bioanal. Chem.*, **2010**, 397, 3173–3178.
33. L. Xie, Y. Tan, Z. Wang, H. Liu, N. Zhang, C. Zou, X. Liu, G. Liu, J. Lu and H. Zheng, *ACS Appl. Mater. Interfaces*, **2016**, 8, 29261–29269.
34. H. Nguyen, P. Lemieux, S. Vinogradov, C. Gebhart, N. Guerin, G. Paradis, T. Bronich, V. Alakhov and A. Kabanov, *Gene Ther.*, **2000**, 7, 126.

35. H. Petersen, P. M. Fechner, A. L. Martin, K. Kunath, S. Stolnik, C. J. Roberts, D. Fischer, M. C. Davies and T. Kissel, *Bioconjugate Chem.*, **2002**, 13, 845–854.
36. M. Breunig, U. Lungwitz, R. Liebl and A. Goepferich, *Proc. Natl. Acad. Sci. U. S. A.*, **2007**, 104, 14454–14459.
37. N. M. Milović, J. Wang, K. Lewis and A. M. Klibanov, *Biotechnol. Bioeng.*, **2005**, 90, 715–722.
38. M. Thomas and A. M. Klibanov, *Proc. Natl. Acad. Sci. U. S. A.*, **2002**, 99, 14640–14645.
39. M. Wang, P. Lu, B. Wu, J. D. Tucker, C. Cloer and Q. Lu, *J. Mater. Chem.*, **2012**, 22, 6038–6046.
40. P. Xu, G. K. Quick and Y. Yeo, *Biomaterials*, **2009**, 30, 5834–5843.
41. B.-K. Kim, D. Kim, G. Kwak, J. Y. Yhee, I.-C. Kwon, S. H. Kim and Y. Yeo, *ACS Biomater. Sci. Eng.*, **2017**, 3, 990–999.
42. Y. Zhou, F. Yu, F. Zhang, G. Chen, K. Wang, M. Sun, J. Li and D. Oupický, *Biomacromolecules*, **2018**, 19(2), 392–401.
43. F. Wang, L. Gao, L.-Y. Meng, J.-M. Xie, J.-W. Xiong and Y. Luo, *ACS Appl. Mater. Interfaces*, **2016**, 8, 33529–33538.
44. L. Tauhardt, K. Kempe, K. Knop, E. Altuntaş, M. Jäger, S. Schubert, D. Fischer and U. S. Schubert, *Macromol. Chem. Phys.*, **2011**, 212, 1918–1924.
45. V. P. Dhende, S. Samanta, D. M. Jones, I. R. Hardin and J. Locklin, *ACS Appl. Mater. Interfaces*, **2011**, 3, 2830–2837.
46. J. Gao, E. M. White, Q. Liu and J. Locklin, *ACS Appl. Mater. Interfaces*, **2017**, 9, 7745–7751.
47. J. Haldar, D. An, L. A. de Cienfuegos, J. Chen and A. M. Klibanov, *Proc. Natl. Acad. Sci. U. S. A.*, **2006**, 103, 17667–17671.
48. A. M. Bieser and J. C. Tiller, *Macromol. Biosci.*, **2011**, 11, 526–534.
49. S. A. Koplín, S. Lin and T. Domanski, *Biotechnol. Prog.*, **2008**, 24, 1160–1165.
50. R. Kügler, O. Bouloussa and F. Rondelez, *Microbiology*, **2005**, 151, 1341–1348.
51. J. Lin, J. C. Tiller, S. B. Lee, K. Lewis and A. M. Klibanov, *Biotechnol. Lett.*, **2002**, 24, 801–805.
52. A. M. Bieser and J. C. Tiller, *Macromol. Biosci.*, **2011**, 11, 526–534.
53. S. Choi, J. H. Drese and C. W. Jones, *ChemSusChem*, **2009**, 2, 796–854.
54. J. C. Hicks, J. H. Drese, D. J. Fauth, M. L. Gray, G. Qi and C. W. Jones, *J. Am. Chem. Soc.*, **2008**, 130, 2902–2903.
55. P. Li, B. Ge, S. Zhang, S. Chen, Q. Zhang and Y. Zhao, *Langmuir*, **2008**, 24, 6567–6574.
56. F.-Q. Liu, L. Wang, Z.-G. Huang, C.-Q. Li, W. Li, R.-X. Li and W.-H. Li, *ACS Appl. Mater. Interfaces*, **2014**, 6, 4371–4381.
57. Q. Wang, J. Luo, Z. Zhong and A. Borgna, *Energy Environ. Sci.*, **2011**, 4, 42–55.
58. X. Xu, C. Song, B. G. Miller and A. W. Scaroni, *Fuel Process. Technol.*, **2005**, 86, 1457–1472.
59. W. Chaikittisilp, R. Khunsupat, T. T. Chen and C. W. Jones, *Ind. Eng. Chem. Res.*, **2011**, 50, 14203–14210.
60. N. MacDowell, N. Florin, A. Buchard, J. Hallett, A. Galindo, G. Jackson, C. S. Adjiman, C. K. Williams, N. Shah and P. Fennell, *Energy Environ. Sci.*, **2010**, 3, 1645–1669.
61. R. Sanz, G. Calleja, A. Arencibia and E. S. Sanz-Pérez, *J. Mater. Chem. A*, **2013**, 1, 1956–1962.
62. X. Xu, C. Song, J. M. Andresen, B. G. Miller and A. W. Scaroni, *Energy Fuels*, **2002**, 16, 1463–1469.
63. S. Satyapal, T. Filburn, J. Trela and J. Strange, *Energy Fuels*, **2001**, 15, 250–255.
64. E. Bayer, B. Y. Spivakov and K. Geckeler, *Polym. Bull.*, **1985**, 13, 307–311.
65. S. Kobayashi, K. Hiroishi, M. Tokunoh and T. Saegusa, *Macromolecules*, **1987**, 20, 1496–1500.
66. A. Von Zelewsky, L. Barbosa and C. Schlöpfer, *Coord. Chem. Rev.*, **1993**, 123, 229–246.
67. B. A. Bolto, *Prog. Polym. Sci.*, **1995**, 20, 987–1041.
68. H.-C. Chen, S.-W. Lin, J.-M. Jiang, Y.-W. Su and K.-H. Wei, *ACS Appl. Mater. Interfaces*, **2015**, 7, 6273–6281.
69. S. Stolz, Y. Zhang, U. Lemmer, G. Hernandez-Sosa and H. Aziz, *ACS Appl. Mater. Interfaces*, **2017**, 9, 2776–2785.
70. G. F. Zou, J. Zhao, H. M. Luo, T. M. McCleskey, A. K. Burrell and Q. X. Jia, *Chem. Soc. Rev.*, **2013**, 42, 439–449.
71. <https://www.chempoint.com/products/basf/lupasol-polyethylenimine-adhesion-promoters/lupasol-polyethylenimine>.
72. U. Steuerle and R. Feuerhake, *Ullmann's Encyclopedia of Industrial Chemistry*, 2001.
73. J. B. Sweeney, *Chem. Soc. Rev.*, **2002**, 31, 247–258.
74. J. Herzberger, K. Niederer, H. Pohlitz, J. Seiwert, M. Worm, F. R. Wurm and H. Frey, *Chem. Rev.*, **2016**, 116, 2170–2243.

75. B. D. Monnery and R. Hoogenboom, *Cationic Polymers in Regenerative Medicine*, **2014**, pp. 30–61.
76. D. A. Tomalia and D. P. Sheetz, *J. Polym. Sci., Part A-1: Polym. Chem.*, **1966**, *4*, 2253–2265.
77. W. Seeliger, E. Aufderhaar, W. Diepers, R. Feinauer, R. Nehring, W. Thier and H. Hellmann, *Angew. Chem., Int. Ed. Engl.*, **1966**, *5*, 875–888.
78. T. Kagiya, S. Narisawa, T. Maeda and K. Fukui, *J. Polym. Sci., Part B: Polym. Lett.*, **1966**, *4*, 441–445.
79. R. Tanaka, I. Ueoka, Y. Takaki, K. Kataoka and S. Saito, *Macromolecules*, **1983**, *16*, 849–853.
80. H. M. L. Lambermont-Thijs, F. S. van der Woerd, A. Baumgaertel, L. Bonami, F. E. Du Prez, U. S. Schubert and R. Hoogenboom, *Macromolecules*, **2009**, *43*, 927–933.
81. T. Saegusa, A. Yamada, H. Taoda and S. Kobayashi, *Macromolecules*, **1978**, *11*, 435–436.
82. E. Rieger, T. Gleede, A. Manhart, M. Lamla and F. R. Wurm, *ACS Macro Lett.*, **2018**, *7*, 598–603.
83. L. Reisman, C. P. Mbarushimana, S. J. Cassidy and P. A. Rugar, *ACS Macro Lett.*, **2016**, *5*, 1137–1140.
84. H. Yin, R. L. Kanasty, A. A. Eltoukhy, A. J. Vegas, J. R. Dorkin and D. G. Anderson, *Nat. Rev. Genet.*, **2014**, *15*, 541–555.
85. P. Wilson, P. C. Ke, T. P. Davis and K. Kempe, *Eur. Polym. J.*, **2017**, *88*, 486–515.
86. L. Tauhardt, K. Kempe, M. Gottschaldt and U. S. Schubert, *Chem. Soc. Rev.*, **2013**, *42*, 7998–8011.
87. M. A. Mees and R. Hoogenboom, *Polym. Chem.*, **2018**, *9*, 4968–4978.
88. J. Y. Johnson and G. W. Johnson, *Great Britain Pat.*, GB461666 (A), **1937**.
89. G. D. Jones, A. Langsjoen, S. M. M. C. Neumann and J. Zomlefer, *J. Org. Chem.*, **1944**, *09*(2), 125–147.
90. D. R. Holycross and M. Chai, *Macromolecules*, **2013**, *46*, 6891–6897.
91. W. G. Barb, *J. Chem. Soc.*, **1955**, 2564–2577.
92. B. L. Rivas and B. Barría, *Polym. Bull.*, **1996**, *36*, 157–164.
93. T. Toshikazu, Y. Z. Menciloglu and E. Takeshi, *J. Polym. Sci., Part A: Polym. Chem.*, **1992**, *30*, 501–504.
94. M. Baklouti, R. Chaabouni, J. Sledz and F. Schué, *Polym. Bull.*, **1989**, *21*, 243–250.
95. J. Xu, X. Li and N. Chen, *Synthesis*, **2010**, 3423–3428.
96. J. A. Deyrup, in *The Chemistry of Heterocyclic Compounds, Part 1*, ed. A. Hassner, Wiley, New York, **1983**, vol. 42, pp. 1–214.
97. E. Goethals, E. Schacht, P. Bruggeman and P. Bossaer, *Cationic Polymerization of Cyclic Amines*, ACS Publications, **1977**, vol. 59.
98. C. R. Dick, *J. Org. Chem.*, **1967**, *32*, 72–75.
99. K. F. Weyts and E. J. Goethals, *Polym. Bull.*, **1988**, *19*, 13–19.
100. J. J. Jakubowski and R. V. Subramanian, *Polymer*, **1980**, *21*, 230–232.
101. K. E. Geckeler, B. L. Rivas and R. Zhou, *Angew. Makromol. Chem.*, **1991**, *193*, 195–203.
102. S. A. Pooley, G. S. Canessa and B. L. Rivas, *Makromol. Chem. Phys.*, **1998**, *199*, 2293–2299.
103. B. L. Rivas, G. S. Canessa and S. A. Pooley, *Makromol. Chem., Rapid Commun.*, **1987**, *8*, 365–372.
104. S. A. Pooley, G. S. Canessa, B. L. Rivas and E. Espejo, *Polym. Bull.*, **1995**, *35*, 271–277.
105. S. A. Pooley, G. S. Canessa, B. L. Rivas and E. Espejo, *Polym. Bull.*, **1996**, *36*, 415–422.
106. S. A. Pooley, G. S. Canessa, B. L. Rivas and E. Espejo, *Polym. Bull.*, **1997**, *39*, 407–414.
107. S. A. Pooley, G. S. Canessa, B. L. Rivas and E. Espejo, *Bol. Soc. Chil. Quim.*, **1996**, *41*, 261–270.
108. S. A. Pooley, G. S. Canessa, B. L. Rivas and E. Espejo, *Bol. Soc. Chil. Quim.*, **1994**, *39*, 305–313.
109. S. A. Pooley, G. S. Canessa, B. L. Rivas and E. Espejo, *Bol. Soc. Chil. Quim.*, **1996**, *41*, 71–78.
110. 1967.
111. S. Hashimoto and T. Yamashita, *J. Macromol. Sci., Chem.*, **1986**, *23*, 295–304.
112. S. Hashimoto, T. Yamashita and J. Hino, *Polym. J.*, **1977**, *9*, 19.
113. E. R. Lavagnino, R. R. Chauvette, W. N. Cannon and E. C. Kornfeld, *J. Am. Chem. Soc.*, **1960**, *82*, 2609–2613.
114. H. Oike, M. Washizuka and Y. Tezuka, *Makromol. Chem. Phys.*, **2000**, *201*, 1673–1678.
115. E. H. Schacht and E. J. Goethals, *Makromol. Chem.*, **1973**, *167*, 155–169.
116. E. J. Goethals and B. Dervaux, in *Polymer Science: A Comprehensive Reference*, ed. M. Möller, Elsevier, Amsterdam, **2012**, pp. 309–330.
117. E. J. Goethals, E. H. Schacht, Y. E. Bogaert, S. I. Ali and Y. Tezuka, *Polym. J.*, **1980**, *12*, 571.
118. T. Saegusa and E. Goethals, *Ring-Opening Polymerization*, American Chemical Society, **1977**.
119. A. T. Bottini and J. D. Roberts, *J. Am. Chem. Soc.*, **1958**, *80*, 5203–5208.
120. H. K. Hall, *J. Am. Chem. Soc.*, **1957**, *79*, 5441–5444.
121. S. Penczek and P. Kubisa, *Makromol. Chem.*, **1969**, *130*, 186–209.

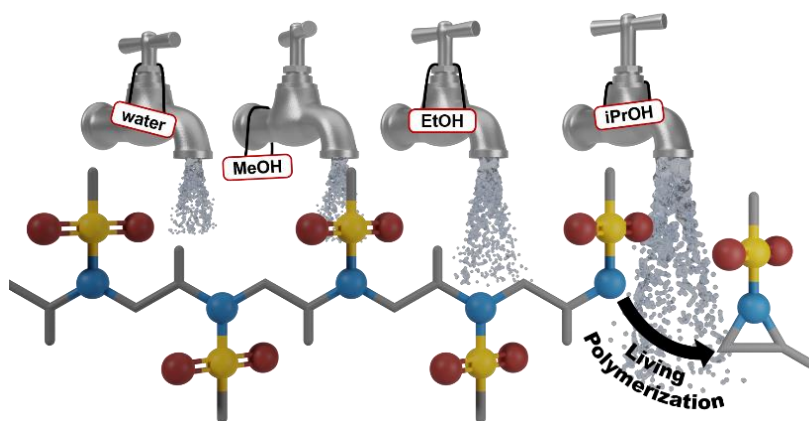
122. E. J. Goethals, G. G. Trossaert, P. J. Hartmann and K. Engelen, *Makromol. Chem., Macromol. Symp.*, **1993**, 73, 77–89.
123. E. J. Goethals, E. Schacht and D. Tack, *J. Polym. Sci., Part A-1: Polym. Chem.*, **1972**, 10, 533–539.
124. I. C. Stewart, C. C. Lee, R. G. Bergman and F. D. Toste, *J. Am. Chem. Soc.*, **2005**, 127, 17616–17617.
125. Z. Wang, *Comprehensive Organic Name Reactions and Reagents*, John Wiley & Sons, Inc., **2009**, vol. 3, ISBN: 978-0-471-70450-8.
126. H. Xu, H. Tian, L. Zheng, Q. Liu, L. Wang and S. Zhang, *Tetrahedron Lett.*, **2011**, 52, 2873–2875.
127. M. B. Berry and D. Craig, *Synlett*, **1992**, 41–44.
128. A. J. Catino, J. M. Nichols, R. E. Forslund and M. P. Doyle, *Org. Lett.*, **2005**, 7, 2787–2790.
129. A. V. Gontcharov, H. Liu and K. B. Sharpless, *Org. Lett.*, **1999**, 1, 783–786.
130. J. U. Jeong, B. Tao, I. Sagasser, H. Henniges and K. B. Sharpless, *J. Am. Chem. Soc.*, 1998, 120, 6844–6845.
131. E. Rieger, A. Alkan, A. Manhart, M. Wagner and F. R. Wurm, *Macromol. Rapid Commun.*, **2016**, 37, 833–839.
132. E. Rieger, A. Manhart and F. R. Wurm, *ACS Macro Lett.*, **2016**, 5, 195–198.
133. L. Thomi and F. R. Wurm, *Macromol. Symp.*, **2015**, 349, 51–56.
134. P. O'Brien and J. Huang, *Synthesis*, **2006**, 425–434.
135. Y. Zhao, F. Sakai, L. Su, Y. Liu, K. Wei, G. Chen and M. Jiang, *Adv. Mater.*, **2013**, 25, 5215–5256.
136. E. Rieger, J. Blankenburg, E. Grune, M. Wagner, K. Landfester and F. R. Wurm, *Angew. Chem., Int. Ed.*, **2018**, 57, 2483–2487.
137. T. Gleede, E. Rieger, T. Homann-Müller and F. R. Wurm, *Macromol. Chem. Phys.*, **2017**, 1700145.
138. X. Wang, Y. Liu, Z. Li, H. Wang, H. Gebru, S. Chen, H. Zhu, F. Wei and K. Guo, *ACS Macro Lett.*, **2017**, 6, 1331–1336.
139. T. Gleede, E. Rieger, L. Liu, C. Bakkali-Hassani, M. Wagner, S. Carlotti, D. Taton, D. Andrienko and F. R. Wurm, *Macromolecules*, **2018**, 51, 5713–5719.
140. T. Homann-Müller, E. Rieger, A. Alkan and F. R. Wurm, *Polym. Chem.*, **2016**, 7, 5501–5506.
141. P. C. Mbarushimana, Q. Liang, J. M. Allred and P. A. Rupar, *Macromolecules*, **2018**, 51(3), 977–983.
142. L. Reisman, E. A. Rowe, Q. Liang and P. A. Rupar, *Polym. Chem.*, **2018**, 9, 1618–1625.
143. E. Rieger, T. Gleede, K. Weber, A. Manhart, M. Wagner and F. R. Wurm, *Polym. Chem.*, **2017**, 8, 2824–2832.
144. L. Thomi and F. R. Wurm, *Macromol. Rapid Commun.*, **2014**, 35, 585–589.
145. C. Bakkali-Hassani, E. Rieger, J. Vignolle, F. R. Wurm, S. Carlotti and D. Taton, *Eur. Polym. J.*, **2017**, 95, 746–755.
146. T. Gleede, E. Rieger, J. Blankenburg, K. Klein and F. R. Wurm, *J. Am. Chem. Soc.*, **2018**, 140, 13407–13412.
147. C. Bakkali-Hassani, E. Rieger, J. Vignolle, F. R. Wurm, S. Carlotti and D. Taton, *Chem. Commun.*, **2016**, 52, 9719–9722.
148. C. Bakkali-Hassani, C. Coutouly, T. Gleede, J. Vignolle, F. R. Wurm, S. Carlotti and D. Taton, *Macromolecules*, **2018**, 51, 2533–2541.
149. E. Rieger, T. Gleede, K. Weber, A. Manhart, M. Wagner and F. R. Wurm, *Polym. Chem.*, **2017**, 8, 2824–2832.
150. V. Jaacks, *Angew. Chem.*, **1967**, 79, 419.
151. F. T. Wall, *J. Am. Chem. Soc.*, **1941**, 63, 1862–1866.
152. J. Blankenburg, M. Wagner and H. Frey, *Macromolecules*, **2017**, 50, 8885–8893.
153. D. C. McLeod and N. V. Tsarevsky, *Macromol. Rapid Commun.*, **2016**, 37, 1694–1700.
154. H.-J. Jang, J. T. Lee and H. J. Yoon, *Polym. Chem.*, **2015**, 6, 3387–3391.
155. H. K. Moon, S. Kang and H. J. Yoon, *Polym. Chem.*, **2017**, 8, 2287–2291.
156. T. Suzuki, J.-i. Kusakabe, K. Kitazawa, T. Nakagawa, S. Kawauchi and T. Ishizone, *Macromolecules*, **2010**, 43, 107–116.
157. A. Thomas, S. S. Muller and H. Frey, *Biomacromolecules*, **2014**, 15, 1935–1954.
158. A. Alkan, R. Klein, S. I. Shylin, U. Kemmer-Jonas, H. Frey and F. R. Wurm, *Polym. Chem.*, **2015**, 6, 7112–7118.
159. L. Reisman, E. A. Rowe, E. M. Jackson, C. Thomas, T. Simone and P. A. Rupar, *J. Am. Chem. Soc.*, **2018**, 140, 15626–15630.
160. M. K. Kiesewetter, E. J. Shin, J. L. Hedrick and R. M. Waymouth, *Macromolecules*, **2010**, 43, 2093–2107.
161. S. Naumann and A. P. Dove, *Polym. Chem.*, **2015**, 6, 3185–3200.

162. J. Pinaud, K. Vijayakrishna, D. Taton and Y. Gnanou, *Macromolecules*, **2009**, 42, 4932–4936.
163. J. Raynaud, Y. Gnanou and D. Taton, *Macromolecules*, **2009**, 42, 5996–6005.
164. J. Raynaud, C. Absalon, Y. Gnanou and D. Taton, *J. Am. Chem. Soc.*, **2009**, 131, 3201–3209.
165. I. Perevyazko, A. S. Gubarev, L. Tauhardt, A. Dobrodumov, G. M. Pavlov and U. S. Schubert, *Polym. Chem.*, **2017**, 8, 7169–7179.
166. A. Akinc, M. Thomas, A. M. Klibanov and R. Langer, *J. Gene Med.*, **2005**, 7, 657–663.
167. S. Taranejoo, J. Liu, P. Verma and K. Hourigan, *J. Appl. Polym. Sci.*, **2015**, 132, 42096.
168. K. Aoi and M. Okada, *Prog. Polym. Sci.*, **1996**, 21, 151–208.
169. L. Tauhardt, K. Kempe, K. Knop, E. Altuntaş, M. Jäger, S. Schubert, D. Fischer and U. S. Schubert, *Macromol. Chem. Phys.*, **2011**, 212, 1918–1924.
170. D. A. Alonso and P. G. Andersson, *J. Org. Chem.*, **1998**, 63, 9455–9461.
171. H. Senboku, K. Nakahara, T. Fukuhara and S. Hara, *Tetrahedron Lett.*, **2010**, 51, 435–438.
172. I. V. Kubrakova, A. A. Formanovsky and I. V. Mikhura, *Mendeleev Commun.*, **1999**, 9, 65–66.
173. O. Ihata, Y. Kayaki and T. Ikariya, *Macromolecules*, **2005**, 38, 6429–6434.
174. O. Ihata, Y. Kayaki and T. Ikariya, *Angew. Chem., Int. Ed.*, **2004**, 43, 717–719.
175. L. Jia, E. Ding and W. R. Anderson, *Chem. Commun.*, **2001**, 1436–1437.
176. J. Zhao, E. Ding, A. M. Allgeier and L. Jia, *J. Polym. Sci., Part A: Polym. Chem.*, **2003**, 41, 376–385.
177. L. Jia, H. Sun, J. T. Shay, A. M. Allgeier and S. D. Hanton, *J. Am. Chem. Soc.*, **2002**, 124, 7282–7283.
178. D. J. Darensbourg, A. L. Phelps, N. L. Gall and L. Jia, *J. Am. Chem. Soc.*, **2004**, 126, 13808–13815.
179. G. Liu and L. Jia, *Angew. Chem., Int. Ed.*, **2006**, 45, 129–131.
180. H. Sekiguchi, P. Tsourkas, F. Carriere and R. Audebert, *Eur. Polym. J.*, **1974**, 10, 1185–1193.
181. Due to this finding, *N*-isopropylazetidone was used throughout the study.
182. G. Liu and L. Jia, *J. Am. Chem. Soc.*, **2004**, 126, 14716–14717.
183. H. Xu, N. LeGall, L. Jia, W. W. Brennessel and B. E. Kucera, *J. Organomet. Chem.*, **2005**, 690, 5150–5158.
184. C. G. Overberger and M. Tobkes, *J. Polym. Sci.*, **1964**, 2, 2181–2187.
185. A. Hall, L. Parhamifar, M. K. Lange, K. D. Meyle, M. Sanderhoff, H. Andersen, M. Roursgaard, A. K. Larsen, P. B. Jensen, C. Christensen, J. Bartek and S. M. Moghimi, *Biochim. Biophys. Acta, Bioenerg.*, **2015**, 1847, 328–342.
186. B. R. Twaites, C. de las Heras Alarcón, D. Cunliffe, M. Lavigne, S. Pennadam, J. R. Smith, D. C. Górecki and C. Alexander, *J. Controlled Release*, **2004**, 97, 551–566.
187. D. Fischer, T. Bieber, Y. Li, H.-P. Elsässer and T. Kissel, *Pharm. Res.*, **1999**, 16, 1273–1279.
188. B. W. Tylkowski, K. Wieszczycka and R. Jastrzab, *Polymer Engineering*, De Gruyter, **2017**, ISBN 978-3-11-046828-1.
189. A. von Harpe, H. Petersen, Y. Li and T. Kissel, *J. Controlled Release*, **2000**, 69, 309–322.
190. M. A. Cortez, W. T. Godbey, Y. Fang, M. E. Payne, B. J. Cafferty, K. A. Kosakowska and S. M. Grayson, *J. Am. Chem. Soc.*, **2015**, 137, 6541–6549.
191. W. Fischer, B. Brissault, S. Prévost, M. Kopaczynska, I. Andreou, A. Janosch, M. Gradzielski and R. Haag, *Macromol. Biosci.*, **2010**, 10, 1073–1083.

2 *Alcohol- and water-tolerant living anionic polymerization of aziridines*

Tassilo Gleede, Elisabeth Rieger, Lei Liu, Camille Bakkali-Hassani, Manfred Wagner, Stéphane

*Carlotti, Daniel Taton, Denis Andrienko, and Frederik R. Wurm**



TOC 2: Table of content, symbolizing the robust polymerization of activated aziridines, resistant against protic additives (alcohols and water)

Note: This work was done in close collaboration with Elisabeth Rieger, **E. Rieger** and **T. Gleede** Designed, conducted and evaluated all experiments, and shared writing the manuscript.

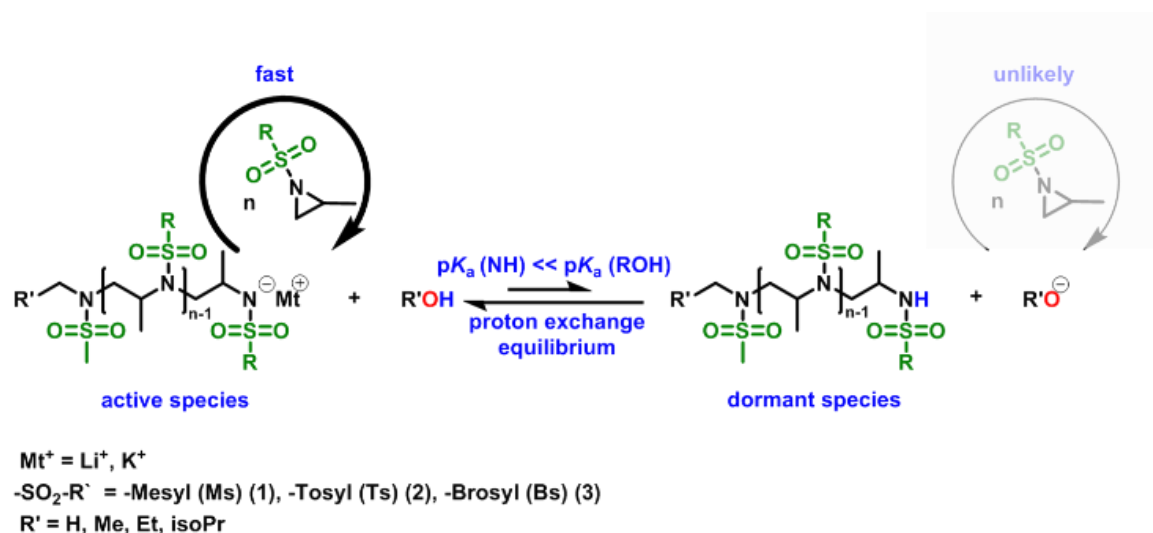
Lei Liu and **Denis Andrienko** are responsible for the DFT-calculations. **Camille Bakkali-Hassani**, measured the MALDI-TOF spectra. **Manfred Wagner** assisted with the ^1H NMR kinetic experiments. **Stéphane Carlotti**, **Daniel Taton** assisted with helpful discussions. **Frederik R. Wurm supervised the project.**

All Authors edited the manuscript.

This chapter is based on a published article under the terms of the Copyright this chapter is used with the permission of ACS Publications: Tassilo Gleede, Elisabeth Rieger, Lei Liu, Camille Bakkali-Hassani, Manfred Wagner, Stéphane Carlotti, Daniel Taton, Denis Andrienko, and Frederik R. Wurm Alcohol- and water-tolerant living anionic polymerization of aziridines, *Macromolecules* **2018**, 51, 15, 5713-5719

2.1 Abstract

Living anionic polymerization gives access to well-defined polymers, but demands strict purification of reagents and solvents. This work presents the azaanionic polymerization (AAROP) of aziridines as a robust living polymerization technique, with the ease of controlled radical polymerizations. AAROP does not require inert atmosphere and remains living in the presence of large amounts of water or alcohols. Mesyl-, tosyl-, or brosyl-activated aziridines were polymerized with up to 100-fold excess of a protic impurity and still being active for chain extension. This allowed the preparation of polyols by anionic polymerization without protective groups, as only minor initiation occurred from the alcohols. The tolerance towards protic additives lies in the electron withdrawing effect of the activating groups, decreasing the basicity of the propagating species, while maintaining a strong nucleophilic character. In this way, competing alcohols and water are only slightly involved in the polymerization, making living anionic polymerization an easy-to-conduct technique to well-defined polyamides and –amines (Scheme 2.1)



Scheme 2.1: Schematic overview of the AAROP with protic additives showing the dormant polymer species and active polymer species.

2.2 Introduction

Living anionic polymerization (LAP) is the best technique to control molar mass, chain-end fidelity, and to achieve a well-defined (co)polymers.¹⁻² It also provides a precise way for introducing of heteroatoms in the polymer backbone.³⁻⁴ LAP is, however, sensitive to protic impurities and, in many cases, oxygen. Thorough drying of reagents and solvents, high vacuum and inert gas purifications make it much more difficult to carry out than, for example, a controlled radical polymerization.⁵⁻⁶ It would therefore be beneficial to combine the robustness of the controlled radical polymerization with the precision of the living ionic polymerization. Ionic polymerizations can be terminated by moisture, protic solvents or CO₂.⁷ In the epoxide polymerization water or alcohols act as initiator and only low molecular weight products are obtained.⁸⁻¹⁰ Importantly, protic impurities at concentrations above the initiator concentration inhibit the propagation, which makes protecting groups, e.g. for alcohols, essential.

A robust LAP that can tolerate protic solvents, especially water, while maintaining the living character, is not known. To circumvent the demanding conditions of LAP, emulsion polymerization elegantly exploits the hydrophobic nature of monomers and polymers and separates the active chain end from the protic aqueous phase. As a result, the polymerization takes place at the interface or inside of the hydrophobic dispersed phase and is the only strategy for conducting an ionic polymerization in the presence of protic solvents. Unfortunately, it cannot suppress termination or transfer reactions, as reported for the aqueous emulsion polymerization of cyclic siloxanes¹¹⁻¹² or phenyl glycidyl ether, leading to oligomers.¹³ Similar approaches of anionic polymerizations of α -carbonyl acids¹⁴ or glycidol in the presence of water¹⁵ bypass the typical anionic polymerization mechanism, e.g., by monomer-activation.

We present the first living anionic polymerization that proceeds in open air and in the presence of large amounts of protic impurities, such as water and alcohols. The azaanionic ring-opening polymerization (AAROP) is chosen as a unique technique to access well-defined polysulfonamides or -amines (Scheme 1). The exceptional tolerance towards water and alcohols during the polymerization allows, for the first time, synthesis of polyols without using any protective groups. Such polyols might be interesting for the preparation of polyurethanes or for antifouling surface coatings.

Polysulfonamides, prepared from the AAROP of sulfonyl-activated aziridines, have been first polymerized *via* living polymerization in 2005.¹⁶ The monomer family has been significantly expanded since then,¹⁷⁻¹⁸ and new methods were developed to polymerize sulfonamides *via* organocatalytic¹⁹⁻²² or anionic polymerization in solution²³⁻²⁵ and in emulsion.²⁶ After cleavage of the sulfonyl groups, polysulfonamides are an alternative pathway to linear polyethylene imine (L-

PEI),^{24, 27} which, together with hyperbranched PEI (*hbPEI*), is a standard synthetic cationic transfection agent.²⁸⁻³¹

The role of the sulfonamide activating groups is two-fold: they control the microstructure of copolymers,²⁵ as well as regulate the nucleophilicity and basicity of the active chain end. The latter allows tuning reaction tolerance to additives, protic solvents, or nucleophilic functionalities in the monomers, which is the focus of this contribution. We believe that the ease of conducting a living anionic polymerization to access well-defined polyamines will contribute to diverse fields, such as gene delivery or the preparation of chelating agents or polyols for polyurethane fabrication.

To control the polymerization of sulfonyl aziridines, all previously published articles highlighted the necessity to strictly avoid moisture, impurities and the protection of nucleophilic monomer functionalities. Preparation of the experiment were thus conducted in a glovebox or with Schlenk techniques under an inert gas atmosphere.^{19-20, 23-24} Concerning the water content of solvents, an *in situ* distillation from elemental sodium or calcium hydride is established for anionic polymerization, but it is known that some solvents are difficult to dry efficiently.^{6, 9} A method that sustains the presence of protic compounds is necessary. The tolerance of the active chain end in an anionic polymerization towards nucleophilic impurities (such as water or alcohols) strongly depends on the pK_b -value of the growing chain end and the propagation rate constants. For sulfonyl-aziridines, both factors can be tuned by the choice of the activating group that influences the basicity of the azaanionic chain end, but at the same time, also the propagation rates and thus controls the chance of initiation of protic impurities in the reaction mixture. We selected three different monomers, in order of their increasing propagation rates and different nucleophilicity of the chain end: 2-methyl-*N*-mesyl-aziridine (**MsMAz**, **1**) 2-methyl-*N*-tosylaziridine (**TsMAz**, **2**), 2-methyl-*N*-brosylaziridine (**BsMAz**, **3**) (Scheme 2.1).²⁵ Monomers **1-3** have all been previously shown to undergo AAROP under an inert environment.

2.3 Results and Discussion

Strikingly, we found that polymerizations could be carried out in open vials in DMF (without any purification or drying), resulting in narrowly distributed PAz ($\mathcal{D} \leq 1.11$), which remained living and allowed further chain extension, proving the living nature under such wet conditions, without recognizable initiation of water and achieving the targeted degree of polymerization (see SEC's in SI 2 Section F). Additionally, the AAROP followed living characteristics in reactive solvents, which would inhibit other anionic polymerizations ($P(\mathbf{2})_{50}$ was prepared in acetone ($\mathcal{D} = 1.16$), ethyl acetate ($\mathcal{D} = 1.18$) and iPrOH ($\mathcal{D} = 1.23$)). The low dispersity from the polymers prepared in open air or such solvents prove that the AAROP is unaffected by CO_2 and O_2 remains living in "non-conventional" solvents of anionic polymerization (Figure S2.25, S2.30, S2.31).

In order to understand the influence of chain-end and monomer reactivity on the control of the AAROP, (**1**) and (**2**) were polymerized in the presence of protic additives. Different amounts (1 eq. – 1000 eq. relatively to the initiator) of water (H_2O), methanol (MeOH), ethanol (EtOH) and isopropanol (iPrOH), which usually act as transfer- or as terminating agents for other anionic polymerizations, were added to the reaction medium. The maximum amount of each additive was limited due to the solubility of the polymers in polar solvent mixtures (see experimental for details in the SI 2). However, if the amounts of water were increased to 1170 eq. for (**2**) and 740 eq. for (**1**), a significant reduction in the molar mass from targeted 5500 to 1200 g/mol and from 4000 to 500 g mol⁻¹ of the final polymer was detected, indicating a non-negligible amount of competitive initiation by the additive (Figure S2.22, S2.27). Lower amounts of the additive had no or only little influence on the molar mass as similar elution times by SEC were detected for the polymers (Figure S2.26, Table S2.8). In all cases, chain extension experiments with additives were performed (90 – 360 equivalents depending on the solvent), proving that the chain ends remained reactive for further monomer addition with reasonable final dispersities ($\mathcal{D} \leq 1.25$) and quantitative conversions $\geq 99\%$ for **1** with all additives tested (see SI 2 Section F, Figure S2.38 – S2.41). Taking a closer look at the monomers **1** and **2**, TsMAz (**2**), with its stronger electron withdrawing group, demonstrated a higher tolerance to the presence of additives, as propagation rates were fivefold faster compared to MsMAz (compare Figure S 2.22 – S 2.25 for (**1**) and Figure S 2.26 – S 2.30 for (**2**)). The influence of counter ions (K^+ , Li^+) was also studied with all additives tested, showing no significant difference; both indeed show full monomer conversion and low molecular weight distributions ($\mathcal{D} < 1.25$, compare Figure S2.26 – S2.30, S2.32, S2.33).

The polymerization kinetics and the amount of the PAz initiated by the additive were determined *via* real-time ^1H NMR spectroscopy of the polymerizations of **1**, **2**, and BsMAz (**3**) in the presence of ^{13}C -labeled alcohols. In Figure 2.1, the polymerization kinetics of **2** are summarized, proving an influence of the protic additives on the overall reaction rates. Within the presence of 100 eq. of isopropanol (green), almost the same k_p -value was determined as for the polymerization in dry DMF (black) without any additive. However, propagation rates decreased in the presence of ethanol (orange), water (blue) and methanol (red), probably due to an increased concentration of initiating species from the additives and the equilibrium between active and dormant species, since the rate constant depends on the nature of the alcohol. Nevertheless, in all cases, the degrees of polymerization were close to the control (typically above 95%) and had narrow molecular weight distributions ($D \leq 1.18$, Figure 2.1b).

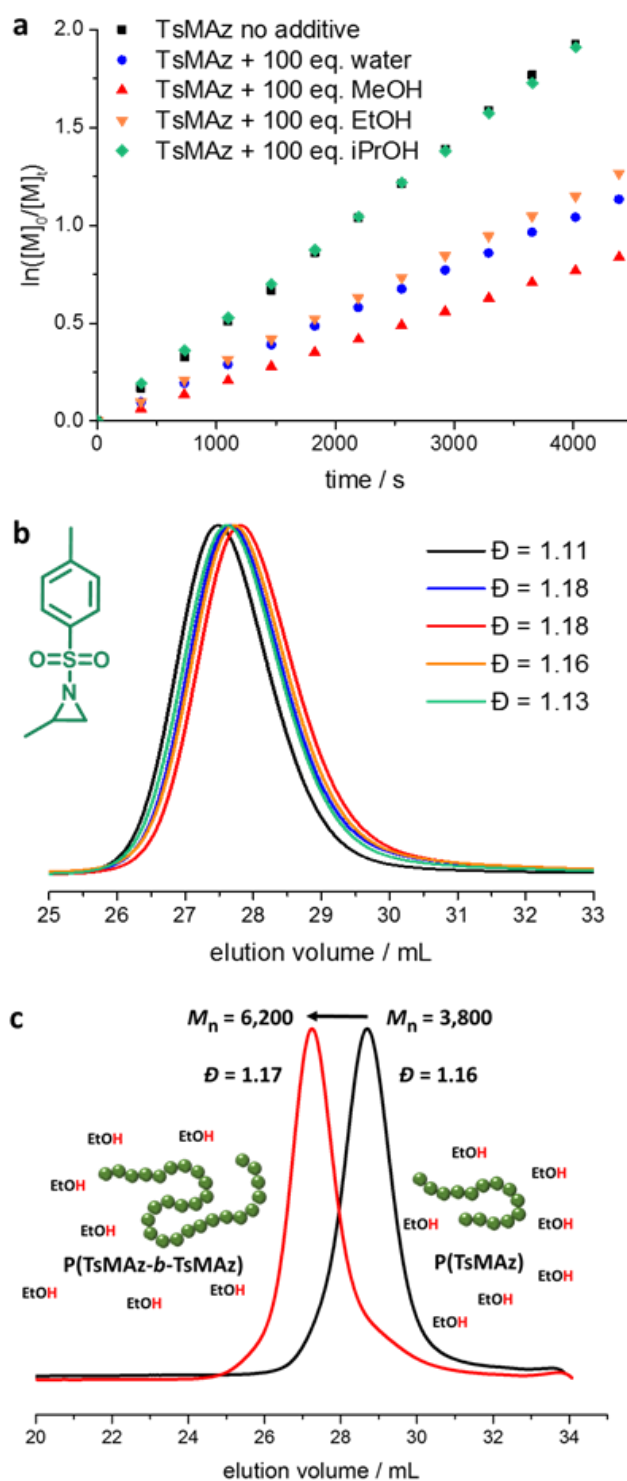


Figure 2.1: a) Kinetic plots of $\ln([M]_0/[M]_t)$ vs. time of TsMAz (2) and 100 equivalents of different additives in DMF-d7 at 50 °C. b) SEC traces in DMF (RI signal) (data listed in Table 2.1.). c) SEC traces (RI signal) of chain extension of P(TsMAz) and P(TsMAz-*b*-TsMAz), polymerization was performed with 90 equivalent excess of ethanol (compared to 1 equivalent initiator).

Table 2.1 summarizes the data from the real-time NMR measurements of TsMAz. The trend observed from the kinetic plots in Figure 2.1A is reflected in the propagation rates (k_p), that range between $22.9 \pm 1.4 \cdot 10^{-3} \text{ L mol}^{-1} \text{ s}^{-1}$ for methanol to $49.9 \pm 3.6 \cdot 10^{-3} \text{ L mol}^{-1} \text{ s}^{-1}$ for the pure reaction mixture (Figure 2.2). Also reaction times from 2.6 h (pure) to 9.4 h (MeOH) for full conversion, indicate the presence of the dormant species, as the protonation of the chain end is reversible (Scheme S 2.1). For the other two monomers (1 and 3), similar trends were observed (see SI 2, Section B). A comparison of their propagation rates (k_p) in Figure 2.2 (solid line, points) depicts that the general reactivity of the monomers increases from MsMAz (1, red) to TsMAz (2, green) to BsMAz (3, yellow), as reported earlier.²⁵ The trend of decreasing molar mass (M_n) (Figure 2.2, dotted line, squares) is in accordance to the decreasing propagation rates, which is due to a certain side initiation by the additives. MALDI-TOF-spectra of P(TsMAz) obtained in the presence of 100 equivalents of additives (H_2O , MeOH, EtOH, iPrOH) (see SI 2, Section E), show a narrowly distributed main population of PAz chains initiated with the sulfonamide initiator. In all cases, a smaller fraction can be identified as TsMAz initiated by the additive. Notably, iPrOH as a secondary alcohol does not influence the k_p -value, with only a minor influence on M_n or \bar{D} .

Table 2.1: Overview of the polymerization kinetics of TsMAz (2) in DMF- d_7 with the respective additive, including SEC-analyses and calculated propagation rates (k_p).

Monomer	TsMAz	TsMAz	TsMAz	TsMAz	TsMAz
Additive	Pure	H ₂ O	MeOH	EtOH	iPrOH
$k_p / 10^{-3} \text{ L mol}^{-1} \text{ s}^{-1}$	49.9 ± 3.6	28.1 ± 2.0	22.9 ± 1.4	29.6 ± 2.1	48.6 ± 3.5
$M_n^a / \text{g mol}^{-1}$	5500	4700	4400	4800	5100
DP / units	56	--	55.8	53.7	55.4
$DP / \%$	100	--	99.6	95.9	98.9
\bar{D}^a	1.11	1.18	1.18	1.16	1.13
Reaction time / h	2.6	5.5	9.4	4.7	2.8
Conversion / %	>99	>99	>99	>99	>99

^a Number-average molar mass and molecular weight dispersities determined via SEC in DMF (vs. PEO standards).

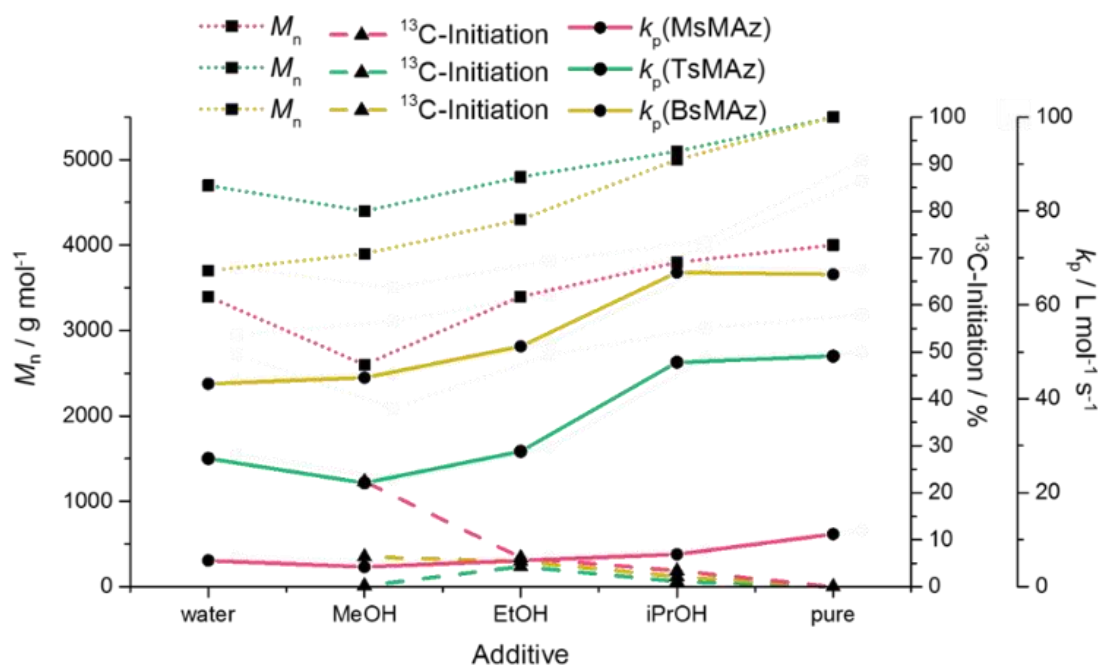


Figure 2.2: Comparison of the molar mass (M_n) (dotted line, squares, left y-axis), amount of ^{13}C -initiation (dashed line, triangles, first right y-axis) and propagation rates (k_p) (solid line, points, right y-axis) of all online NMR-kinetics of the three monomers MsMAz (1, red), TsMAz (2, green) and BsMAz (3, yellow) with the respective additives (pure, water, MeOH, EtOH, iPrOH).

As MALDI is not quantitative, we used ^{13}C NMR to quantify the amount of alcohol-initiated polymers from the integral of the ether signal of ^{13}C -labeled alcohols, used as additives. HSQC-spectra proved the existence of ^{13}C -labeled ethers (see SI, Section C). Distinctive ^{13}C -ether resonances below 10% (except for MsMAz with MeOH as additive) were detected, as depicted in Figure 2.2 (dashed line, triangles) and summarized in Table S2.3. TsMAz (2) is the most tolerant monomer, as all ^{13}C -ether signals are below the quantification limit of NMR-spectroscopy ($\leq 1\%$), determined by a high signal / noise ratio (S/N). For all three monomers, the signals of ^{13}C -isopropyl ether are also below the quantification limit of NMR-spectroscopy, showing a negligible amount of initiation for this secondary alcohol. The more acidic and nucleophilic the additive, the higher the amount of secondary initiation.

Because of the much lower pK_a value of the sulfonamide compared to the protic additives, the majority of living chains remains on the aza-anion, and only an almost negligible amount of the additive is deprotonated and can initiate the polymerization (Figure 2.3B, and Scheme S2.1 for a detailed mechanistic explanation).

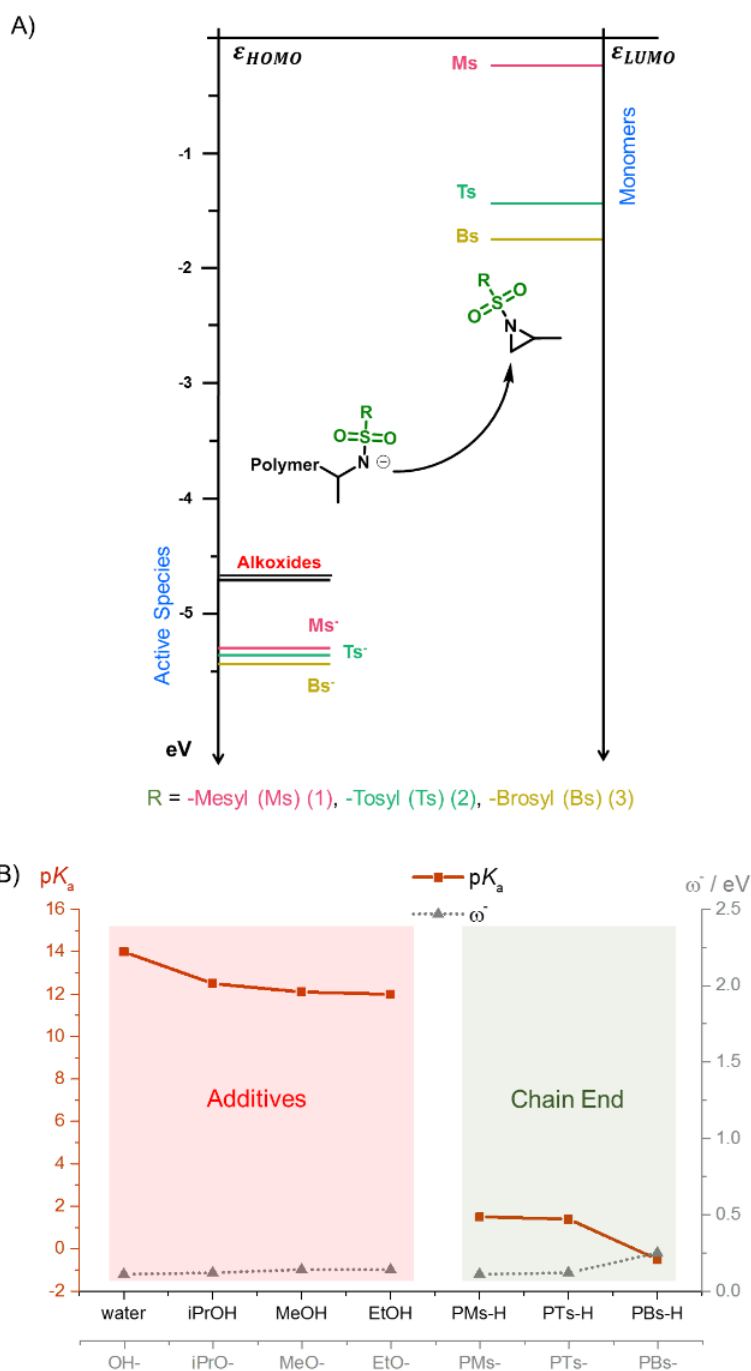


Figure 2.3. DFT (B3LYP/6-311++G**(SCRF, DMF)//B3LYP/6-31+G*) calculations of: A) HOMO levels of the active species: chain ends and alkoxides (left), and LUMO levels of the monomers (right). B) $\text{p}K_a$ -values (DMF, calculated) (dark red solid line, squares, left y-axis) and the nucleophilicity index (ω^-) (grey dotted line, triangles, right y-axis and grey x-axis on the bottom) for the additives – highlighted in red (left) - and the chain ends – highlighted in green (right).

Such amounts of “undesired” initiation can be circumvented by working under absolute inert conditions as typical for anionic polymerizations. However, compared to controlled radical polymerizations, where up to 10% of all chain ends can be undesirably initiated (in RAFT), even without including “dead” polymers by radical termination,³²⁻³⁴ we believe the ease of reaction conditions makes the AROP of aziridines an attractive alternative. In most cases, the secondary initiation was below 10%, (MsMAz with MeOH around 22%), but without “dead” polymers, i.e. the chain end remains always active. The highest percentage of secondary initiation was demonstrated for MsMAz (**1**), because its slow reaction kinetics allows also the slow initiation of alkoxides to occur. Whereas, BsMAz (**3**) (the most reactive monomer), reveals a higher percentage of ¹³C-signals than TsMAz (**2**), most likely due to its stronger electrophilic character, which makes the monomer susceptible for nucleophilic attacks. Concluding, TsMAz (**2**) is well balanced between fast reaction kinetic and susceptibility for nucleophilic attacks, (**2**) is the most robust monomer of the three tested sulfonyl aziridines (Figure 2.3).

2.3.1 DFT Calculations.

To rationalize the effect of initiation of different additives, we performed density functional theory (DFT) calculations for the propagation steps. The results are summarized in Figure 2.3 and Table S2.19-S2.21 (for computational details see SI 2, Section G). The chain end and monomer reactivity can be elaborated from the comparison of the energies of the frontier orbitals (Figure 2.3A). The highest occupied molecular orbitals (HOMO) of the active chain ends were calculated from corresponding model compounds of deprotonated *sec*-butyl(-R-)amides ((Table S2.20), R = brosyl (Bs), tosyl (Ts) or mesyl (Ms)). The activating groups proved to have a stronger effect on the monomer reactivity compared to the active chain ends, as the difference (-0.24 to -1.75 eV) in LUMO levels are larger than the HOMO levels (-5.30 to -5.44 eV). In addition, calculations show that the alkoxides (from deprotonation of the added alcohols) exhibit more reactive HOMO levels of ca. -4.7 eV, which are around 0.7 eV higher in energy than the HOMO levels of the chain ends. These findings go along with the expectations that lower LUMO levels are easier to be occupied by nucleophiles with higher HOMO levels, i.e. the alkoxides should preferably act as an initiator for the azaanionic polymerization, as soon as they are formed in solution. Moreover, we have computed the electrophilicity index ω^+ and the nucleophilicity index ω^- regarding the homopolymerization of each monomer (Figure 2.3B and Table S2.19, S2.20). The nucleophilicity of additives and sulfonamides varies in the range of 0.13 to 0.27 eV, which show that alkoxides are strong competitors to the active chain ends, especially if the concentration of alcohol exceeds the initiator concentration. However, due to the enormous difference in the pK_a -

values of a sulfonamide ($pK_a = -0.5$ to 1.5 in DMF) and the additives ($pK_a = 12.0$ to 14.0 in DMF) propagation *via* the azaanion is clearly favored over the deprotonation and initiation by additives (Figure 2.3B and Table S2.21, pK_a values were calculated using equation 5 in the SI 2, section G). DFT calculations therefore help to rationalize the fact that additives such as alcohols or water can be tolerated by the azaanionic ring-opening polymerization.

2.3.2 Synthesis of Polyols without Protective Group.

Since hydroxyl groups are relatively inert during the anionic ROP of sulfonyl aziridines, there is no need to protect protic functionalities in the monomers. This allows a direct access to polyols *via* living AROP.²⁷ Indeed, the unprotected 2-*ω*-propanol-*N*-tosylaziridine (**6**) was polymerized with full monomer conversion and reasonable molecular weight distributions ($\mathcal{D} = 1.26$ - 1.37) were obtained under standard conditions of AAROP (compare SI 2, Section H). A small amount of branching cannot be ruled out, but neither ^1H , ^{13}C NMR spectra (Figure S2.44, S2.45) nor SEC-data (Figure 2.4) can provide this information, since the monomer is not ^{13}C -labeled and from the experiments in the presence of alcohols, only a small amount of branching can be assumed.

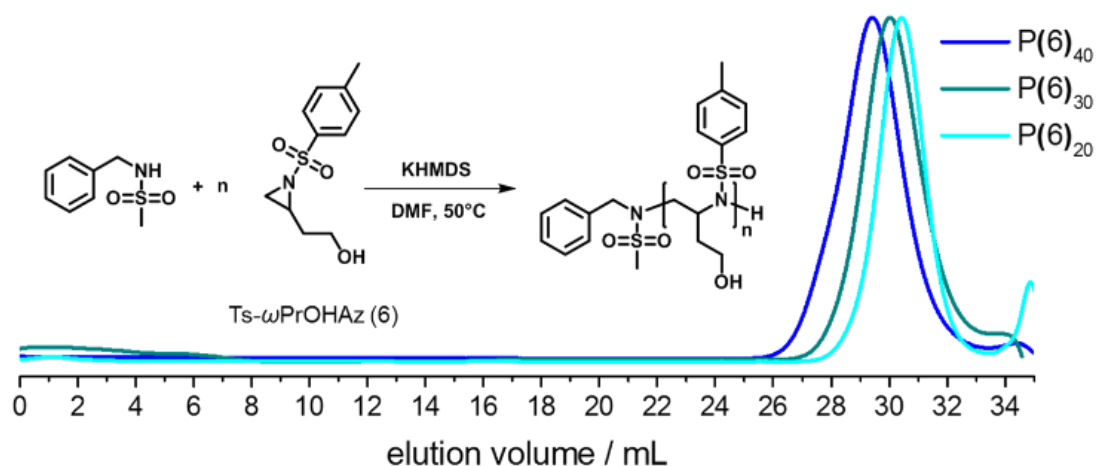


Figure 2.4: Anionic polymerization of **6**, including SEC traces of three different polymers of **6** with theoretical repeating units (20, 30, 40) in DMF (RI signal) (data listed in Table S2.22).

2.3.3 Conclusion

To conclude, the AROP of aziridines eliminates the tedious purification steps and high-vacuum techniques, which make an anionic polymerization unattractive compared to controlled radical polymerizations. Herein, we systematically investigated the influence of protic additives that are water and different alcohols (methanol, ethanol, isopropanol) on the AROP of different sulfonyl aziridines. Even at large excess of the protic impurity (more than 100 eq. compared to the initiator), the AROP of sulfonyl aziridines leads to quantitative monomer conversion and retains excellent control over molar mass and dispersity. The combination of different analyses (real-time ^1H NMR spectroscopy, MALDI-TOF, SEC, and ^{13}C NMR) and additional DFT-calculations confirmed a second slow initiation of protic solvents, of up to 10% with 100 eq. of additives (except for MsMAz with MeOH as additive). In spite of the high nucleophilicity of additives, but their high $\text{p}K_{\text{a}}$ -values, the propagation of the aza-anions (with much lower $\text{p}K_{\text{a}}$ -values) remained almost unaffected by the presence of additives (especially for TsMAz) and the polymerization keeps its living character. As a high control over molar mass, chain fidelity, size distribution and quantitative monomer conversion remains, the access to well-defined polyamides (and polyamines after hydrolysis) is still guaranteed. With this robust AROP polyols are accessible without the need of protection groups, which are interesting materials for future applications. The AROP of sulfonyl aziridines offers the simplicity of a controlled radical polymerization, where less than 10% of initiator- initiated polymers are accepted, and any termination is avoided.

2.4 References Chaper 2

1. Frey, H.; Ishizone, T., Living Anionic Polymerization Celebrates 60 Years: Unique Features and Polymer Architectures. *Macromolecular Chemistry and Physics* **2017**, *218* (12), 1700217.
2. Hirao, A.; Goseki, R.; Ishizone, T., Advances in Living Anionic Polymerization: From Functional Monomers, Polymerization Systems, to Macromolecular Architectures. *Macromolecules* **2014**, *47* (6), 1883-1905.
3. Matyjaszewski, K.; Müller, A. H. E., *Controlled and Living Polymerizations: From Mechanisms to Applications*. John Wiley & Sons: Weinheim, Germany, 2009; p 634.
4. Braunecker, W. A.; Matyjaszewski, K., Controlled/living radical polymerization: Features, developments, and perspectives. *Progress in Polymer Science* **2007**, *32* (1), 93-146.
5. Hadjichristidis, N.; Hirao, A., *Anionic Polymerization*. Springer Japan: Japan, 2015; p 1082.
6. Hadjichristidis, N.; Iatrou, H.; Pispas, S.; Pitsikalis, M., Anionic polymerization: high vacuum techniques. *Journal of Polymer Science Part A: Polymer Chemistry* **2000**, *38* (18), 3211-3234.
7. Szwarc, M., Living polymers and mechanisms of anionic polymerization. In *Living Polymers and Mechanisms of Anionic Polymerization*, Springer: 1983; pp 1-177.
8. Asami, R.; Khanna, S.; Levy, M.; Szwarc, M., The rate of dissociation of anthracene-living polystyrene complex. The nature of the complex. *Transactions of the Faraday Society* **1962**, *58*, 1821-1826.
9. Herzberger, J.; Niederer, K.; Pohlit, H.; Seiwert, J.; Worm, M.; Wurm, F. R.; Frey, H., Polymerization of Ethylene Oxide, Propylene Oxide, and Other Alkylene Oxides: Synthesis, Novel Polymer Architectures, and Bioconjugation. *Chemical Reviews* **2016**, *116* (4), 2170-2243.
10. Odian, G., *Principles of Polymerization*. 4. ed.; John Wiley & Sons, Inc. : Hoboken, New Jersey, USA, 2004.
11. Barrere, M.; Ganachaud, F.; Bendejacq, D.; Dourges, M.-A.; Maitre, C.; Hémerly, P., Anionic polymerization of octamethylcyclotetrasiloxane in miniemulsion II. Molar mass analyses and mechanism scheme. *Polymer* **2001**, *42* (17), 7239-7246.
12. Barrère, M.; Maitre, C.; Dourges, M.; Hémerly, P., Anionic polymerization of 1, 3, 5-tris (trifluoropropylmethyl) cyclotrisiloxane (F3) in miniemulsion. *Macromolecules* **2001**, *34* (21), 7276-7280.
13. Maitre, C.; Ganachaud, F.; Ferreira, O.; Lutz, J. F.; Paintoux, Y.; Hémerly, P., Anionic polymerization of phenyl glycidyl ether in miniemulsion. *Macromolecules* **2000**, *33* (21), 7730-7736.
14. Kimura, H., A simple method for the anionic polymerization of α -carbonyl acids in water. *Journal of Polymer Science Part A: Polymer Chemistry* **1998**, *36* (1), 189-193.
15. Spears, B. R.; Marin, M. A.; Montenegro-Burke, J. R.; Evans, B. C.; McLean, J.; Harth, E., Aqueous Epoxide Ring-Opening Polymerization (AEROP): Green Synthesis of Polyglycidol with Ultralow Branching. *Macromolecules* **2016**, *49* (6), 2022-2027.
16. Stewart, I. C.; Lee, C. C.; Bergman, R. G.; Toste, F. D., Living ring-opening polymerization of *N*-sulfonylaziridines: Synthesis of high molecular weight linear polyamines. *Journal of the American Chemical Society* **2005**, *127* (50), 17616-17617.
17. Gleede, T.; Rieger, E.; Homann-Müller, T.; Wurm, F. R., 4-Styrenesulfonyl-(2-methyl)aziridine: The First Bivalent Aziridine-Monomer for Anionic and Radical Polymerization. *Macromolecular Chemistry and Physics* **2017**, 1700145.
18. Homann-Müller, T.; Rieger, E.; Alkan, A.; Wurm, F. R., *N*-Ferrocenylsulfonyl-2-methylaziridine: the first ferrocene monomer for the anionic (co)polymerization of aziridines. *Polym. Chem.* **2016**, *7* (35), 5501-5506.
19. Wang, X.; Liu, Y.; Li, Z.; Wang, H.; Geburu, H.; Chen, S.; Zhu, H.; Wei, F.; Guo, K., Organocatalyzed Anionic Ring-Opening Polymerizations of *N*-Sulfonyl Aziridines with Organic Superbases. *ACS Macro Letters* **2017**, *6* (12), 1331-1336.
20. Bakkali-Hassani, C.; Rieger, E.; Vignolle, J.; Wurm, F. R.; Carlotti, S.; Taton, D., The organocatalytic ring-opening polymerization of *N*-tosyl aziridines by an *N*-heterocyclic carbene. *Chem Commun (Camb)* **2016**, *52* (62), 9719-9722.
21. Bakkali-Hassani, C.; Rieger, E.; Vignolle, J.; Wurm, F. R.; Carlotti, S.; Taton, D., Expanding the scope of *N*-heterocyclic carbene-organocatalyzed ring-opening polymerization of *N*-tosyl aziridines using functional and non-activated amine initiators. *European Polymer Journal* **2017**, *95*, 746-755.

22. Bakkali-Hassani, C.; Coutouly, C.; Gleede, T.; Vignolle, J.; Wurm, F. R.; Carlotti, S.; Taton, D., Selective Initiation from Unprotected Aminoalcohols for the *N*-Heterocyclic Carbene-Organocatalyzed Ring-Opening Polymerization of 2-Methyl-*N*-tosyl Aziridine: Telechelic and Block Copolymer Synthesis. *Macromolecules* **2018**, *51* (7), 2533-2541.
23. Rieger, E.; Gleede, T.; Weber, K.; Manhart, A.; Wagner, M.; Wurm, F. R., The living anionic polymerization of activated aziridines: a systematic study of reaction conditions and kinetics. *Polym. Chem.* **2017**, *8* (18), 2824-2832.
24. Reisman, L.; Mbarushimana, C. P.; Cassidy, S. J.; Rugar, P. A., Living Anionic Copolymerization of 1-(Alkylsulfonyl)aziridines to Form Poly(sulfonylaziridine) and Linear Poly(ethylenimine). *ACS Macro Letters* **2016**, *5* (10), 1137-1140.
25. Rieger, E.; Alkan, A.; Manhart, A.; Wagner, M.; Wurm, F. R., Sequence-Controlled Polymers via Simultaneous Living Anionic Copolymerization of Competing Monomers. *Macromolecular Rapid Communications* **2016**, *37* (10), 833-839.
26. Rieger, E.; Blankenburg, J.; Grune, E.; Wagner, M.; Landfester, K.; Wurm, F. R., Controlling the polymer microstructure in anionic polymerization by compartmentalization. *Angewandte Chemie International Edition* **2017**.
27. Rieger, E.; Manhart, A.; Wurm, F. R., Multihydroxy Polyamines by Living Anionic Polymerization of Aziridines. *ACS Macro Lett.* **2016**, *5* (2), 195-198.
28. Lungwitz, U.; Breunig, M.; Blunk, T.; Gopferich, A., Polyethylenimine-based non-viral gene delivery systems. *Eur J Pharm Biopharm* **2005**, *60* (2), 247-66.
29. Boussif, O.; Lezoualc'h, F.; Zanta, M. A.; Mergny, M. D.; Scherman, D.; Demeneix, B.; Behr, J.-P., A versatile vector for gene and oligonucleotide transfer into cells in culture and in vivo: polyethylenimine. *Proceedings of the National Academy of Sciences* **1995**, *92* (16), 7297-7301.
30. Perevyazko, I. Y.; Bauer, M.; Pavlov, G. M.; Hoepfner, S.; Schubert, S.; Fischer, D.; Schubert, U. S., Polyelectrolyte complexes of DNA and linear PEI: formation, composition and properties. *Langmuir* **2012**, *28* (46), 16167-16176.
31. Islam, M. A.; Park, T. E.; Singh, B.; Maharjan, S.; Firdous, J.; Cho, M.-H.; Kang, S.-K.; Yun, C.-H.; Choi, Y. J.; Cho, C.-S., Major degradable polycations as carriers for DNA and siRNA. *Journal of Controlled Release* **2014**, *193*, 74-89.
32. Li, Y.; Schadler, L.; Benicewicz, B.; Barner-Kowollik, C., Handbook of RAFT Polymerization. Wiley-VCH: Weinheim: 2008.
33. Perrier, S. B., 50th Anniversary Perspective: RAFT Polymerization: A User Guide. *Macromolecules* **2017**, *50* (19), 7433-7447.
34. Matyjaszewski, K., Atom transfer radical polymerization (ATRP): Current Status and Future Perspectives. *Macromolecules* **2012**, *45* (10), 4015-4039.

2.5 Supporting Information for Alcohol- and water-tolerant living anionic polymerization of aziridines

2.6 Materials and Methods

2.6.1 Chemicals

All solvents and reagents were purchased from Sigma-Aldrich, Acros Organics or Fluka and used as received unless otherwise mentioned. All deuterated solvents were purchased from Deutero GmbH and were distilled from CaH₂ or sodium and stored over molecular sieve prior to use. The ¹³C-labeled solvents were purchased from Sigma-Aldrich and dried with molecular sieves. All monomers and initiators were dried extensively by azeotropic freeze drying with benzene prior to polymerization unless otherwise mentioned. 2-methyl-*N*-mesyl-aziridine (MsMAz, 1) 2-methyl-*N*-tosylaziridine (TsMAz, 2), 2-methyl-*N*-brosyl aziridine (BsMAz, 3), *N*-pyrene-methanesulfonamide (PyNHMs, 4) and *N*-benzyl sulfonamide (BnNHMs, 5) were synthesized according to our previously published protocol.¹⁻²

2.6.2 Methods.

NMR. ^1H NMR spectra were recorded using a Bruker Avance 300, a Bruker Avance III 500 or a Bruker Avance III 700 spectrometer. All spectra were referenced internally to residual proton signals of the deuterated solvent.

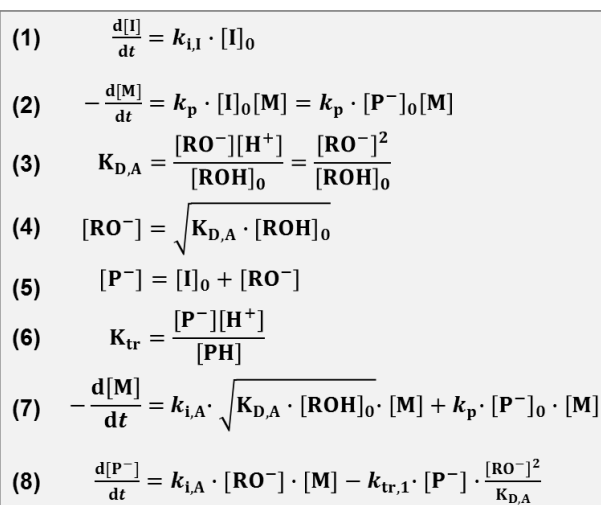
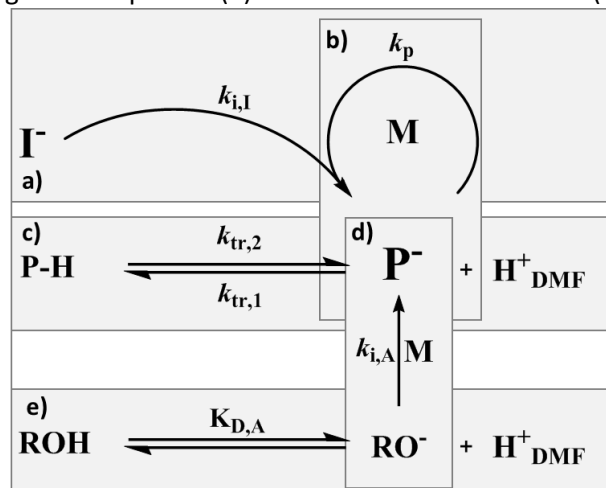
SEC. Size exclusion chromatography (SEC) measurements of standard polymers were performed in DMF (1 g L⁻¹ LiBr added) at 60°C and a flow rate of 1 mL min⁻¹ with an PSS SECcurity as an integrated instrument, including a PSS GRAM 100-1000 column and a refractive index (RI) detector. Calibration was carried out using poly(ethylene glycol) standards provided by Polymer Standards Service.

MALDI-TOF. MALDI TOF spectra were performed by the CESAMO (Bordeaux, France) on a Voyager mass spectrometer (Applied Biosystems). Spectra were recorded in the positive-ion mode using the reflectron and with an accelerating voltage of 20 kV. Samples were dissolved in THF at 10 mL min⁻¹. The matrix solution (trans-3-indoleacrylic acid, IAA) was prepared by dissolving 10 mg in 1 mL of THF. A MeOH-solution of cationization agent (NaI, 10 mL min⁻¹) was also prepared. Solutions were combined in a 10:1:1 volume ratio of matrix to sample to cationization agent.

General procedure for the azaanionic polymerization. All polymerizations were run in screw cap vials if not otherwise noted. Vials were taken directly from the box, not flame dried neither treated *in vacuo* or using standard Schlenk technique. Neither monomers nor the initiators and the bases (bis(trimethylsilyl)amide salts) were pretreated for purification. The monomers and the initiator were dissolved in dry *N,N*-dimethylformamide (DMF). The initiator solution was added to the bis(trimethylsilyl)amide salt under normal atmosphere, the initiator-solution was transferred to the reaction flask, containing the monomer. The resulting concentration was kept constant by 10 wt.% monomer in DMF. The mixture was stirred at the desired temperature and over the desired time (to ensure complete reaction: 18 h Reaction time at 50 °C). The polymers were obtained as off-white powders after evaporation of the solvent. Colorless dry powders can be obtained if the polymers are precipitation of the reaction mixture into 30 mL methanol and after drying at reduced pressure.¹⁻³ For experiments with different amount of protic solvents the above mentioned general procedure for the azaanionic polymerization was followed. After initiation (5 to 10 seconds) the protic solvent was added by an Eppendorf Pipette.

2.7 Section A: Mechanistic explanation of AAROP with protic additives.

Scheme S 2 shows a proposed, schematic mechanism for the AAROP with protic additives, including a dormant species: boxes a) and b) illustrate the initiation ($k_{i,I}$) and propagation (k_p) of the polymerization. For a living polymerization,⁴ the initiation needs to be faster than the propagation ($k_{i,I} \gg k_p$), resulting in first-order kinetics, therefore, equation (1) can be neglected. Additionally, every initiator (I) starts a growing chain (P^-), the starting initiator-concentration $[I]_0$ is equal to $[P^-]_0$, resulting in the overall equation (2) for the reaction kinetics.³ This set of equations is expanded, when protic additives (ROH) in DMF are introduced that take part in deprotonation equilibria, depending on their respective pK_a -value ((Scheme 2 (e), equation 3). The concentration of the competing nucleophiles (RO^-), which act as a secondary initiator, is given in equation (4) and illustrated in Scheme 2 (d). Due to the strong nucleophilic character of



Scheme S 2.1. Simplified scheme including the involved protic species (ROH), followed by their equations.

deprotonated additives, very fast initiation is expected ($k_{i,A} \gg k_p$). The concentration of propagating chain ends would then increase to $[P^-]$, (equation 5). Consequently, protons (H^+) from the additives will form a dormant species of the original living chain end (PH) (Scheme 2 (c)). Equation (6) illustrates, the equilibrium between active and dormant species highly depends on the amount of protons, which are only released by additives. To fully describe the system, the monomer consumption and the chain concentration of the active chain ends are expressed in equations 7 and 8.

2.8 Section B. Kinetics Monitoring polymerizations by real-time ^1H NMR spectroscopy

All polymerizations were carried out in analogy to the conventional procedure in a Schlenk flask and already described in previous publications.^{1,3} All glassware was dried by *in vacuo* for at least three times. All reactants (except the bis(trimethylsilyl)amide salts) were dried from benzene *in vacuo* for at least 4 h. Inside of a glovebox in a nitrogen-atmosphere, the respective monomer was dissolved in DMF- d_7 as a total volume of 5.0 mL of DMF- d_7 , calculated for a monomer to the initiator of $[M]_0:[I]_0 = 50:1$. The initiator-solution in 1 mL DMF- d_7 was prepared separately. Therefore 1 eq. of PyNHMs was solved in 1 mL DMF- d_7 and transferred to Lithium bis(trimethylsilyl)-amide (LiHMDS) 0.95 eq. The active initiator was then transferred to the monomer-solution to yield a 10 wt.% solution. Previously dried (drying oven at 50 °C under vacuum) conventional NMR-tubes were equipped with 100 eq. of the protic additives (none, H_2O , ^{13}C -MeOH, ^{13}C -EtOH, ^{13}C -iPrOH). The NMR-tubes were filled with the reaction mixture and sealed by melting the top of the NMR-tube with a hot flame. To prevent polymerization of the samples, which were monitored the following days, the NMR-tubes were shock frosted in liquid nitrogen and stored at -80 °C (below the melting point of DMF).

The NMR-tubes were one after another warmed up to room temperature and all ^1H NMR kinetics were recorded using a Bruker Avance III 700. All spectra were referenced internally to residual proton signals of the deuterated solvent dimethylformamide- d_7 at 8.03 ppm. The $\pi/2$ -pulse for the proton measurements was 13.1 μs . The spectra of the polymerizations were recorded at 700 MHz with 16 scans (equal to 404 s (acquisition time of 2.595 s and a relaxation time of 20 s after every pulse)) over a period of time until the polymerization had full conversion. No B-field optimizing routine was used over the kinetic measurement time. The spin-lattice relaxation rate (T_1) of the ring-protons, which are used afterward for integration, was measured before the kinetic run with the inversion recovery method.⁵

The method for the evaluation of the NMR-data to calculate the respective k_p -values is followed as described in previous publications.³

2.8.1 Kinetics of MsMAz (1)

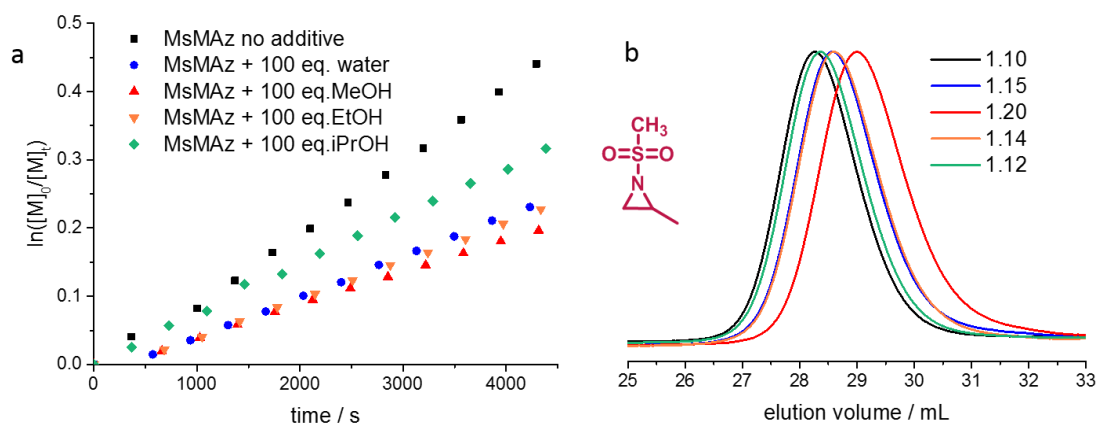


Figure S2.1. a) Kinetic plots of $\ln([M]_0/[M]_t)$ vs. time of MsMAz (1) and different additives in DMF-*d*₇ at 50 °C. b) SEC traces in DMF (RI signal) (data listed in Table S1).

Table S2.1. Overview of the polymerization kinetics of MsMAz (1) in DMF-*d*₇ with the respective additive, including SEC-analyses and calculated propagation rates (k_p).

Monomer	MsMAz (1)	MsMAz (1)	MsMAz (1)	MsMAz (1)	MsMAz (1)
Additive	Pure	H ₂ O	MeOH	EtOH	iPrOH
$k_p / 10^{-3} \text{ L mol}^{-1} \text{ s}^{-1}$	12.0±0.8	6.4±0.5	5.0±0.4	6.4±0.4	7.7±0.5
$M_n^a / \text{g mol}^{-1}$	4000	3400	2600	3400	3800
DP^b / units	50	--	40.8	46.9	48.4
$DP^b / \%$	100	--	81.6	93.8	96.8
\bar{D}^a	1.10	1.15	1.20	1.14	1.12
Reaction time / h	10.3	23	>23.9	22.2	17.5
Conversion / %	>99	>99	98	>99	>99

^a Number-average molecular weight and molecular weight dispersity determined *via* SEC in DMF (vs. PEO standards). ^b calculated from ¹³C ether initiation.

2.8.2 Kinetics of BsMAz (3)

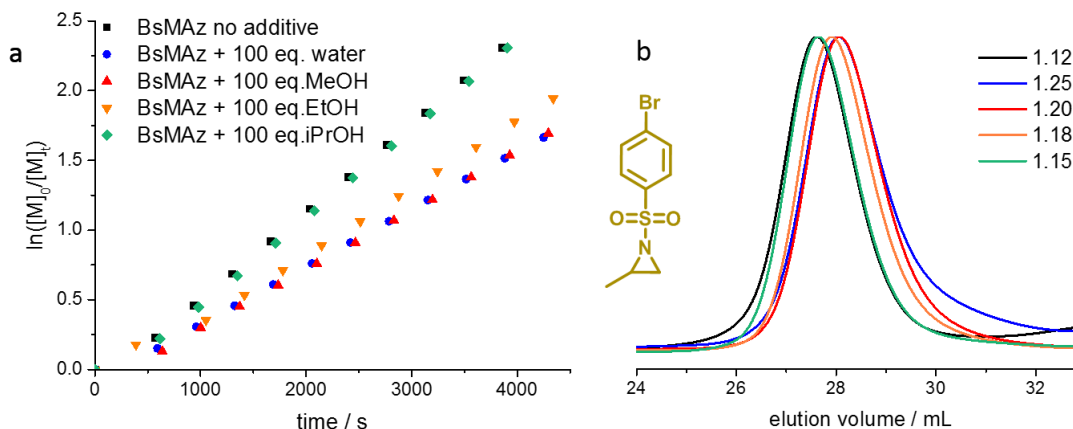


Figure S2.2. a) Kinetic plots of $\ln([M]_0/[M]_t)$ vs. time of BsMAz (3) and different additives in DMF- d_7 at 50 °C. b) SEC traces in DMF (RI signal) (data listed in Table S2).

Table S2.2. Overview of the polymerization kinetics of BsMAz (3) in DMF- d_7 with the respective additive, including SEC-analyses and calculated propagation rates (k_p).

Monomer	BsMAz (3)	BsMAz (3)	BsMAz (3)	BsMAz (3)	BsMAz (3)
Additive	Pure	H ₂ O	MeOH	EtOH	iPrOH
$k_p / 10^{-3} \text{ L mol}^{-1} \text{ s}^{-1}$	67.3±4.6	44.0±3.0	45.3±3.1	52.0±3.6	67.7±4.6
$M_n^a / \text{g mol}^{-1}$	5500	3700	3900	4300	5000
DP^b / units	56	--	52.6	53.1	54.8
$DP^b / \%$	100	--	93.9	94.8	97.9.8
\mathcal{D}^a	1.12	1.25	1.20	1.18	1.15
Reaction time / h	2.1	3.3	3.0	2.8	2.1
Conversion / %	>99	>99	>99	>99	>99

^a Number-average molecular weight and molecular weight dispersity determined *via* SEC in DMF (vs. PEO standards). ^b calculated from ¹³C ether initiation.

Table S2.3. Overview of the performed polymerization kinetics regarding initiation *via* alkoxides:

Sample	eq (monomer) ^a	Integral ¹³ C ether ^b	S/N (rms) ¹³ C ether ^c	S/N (rms) reference signal ^c	¹³ C ether / % ^d	Relative standard deviation / % ^e
P(MsMAz)-MeOH	50	0.57	83.6	18.2	22.4	4.5
P(MsMAz)-EtOH	50	0.14	22.1	18.0	6.6	4.5
P(MsMAz)-iPrOH	50	0.07	1.8	19.6	3.4*	≥20.0
P(TsMAz)-MeOH	56	0.003	3.6	82.4	0.2*	≥20.0
P(TsMAz)-EtOH	56	0.08	4.0	106.0	4.3*	≥20.0
P(TsMAz)-iPrOH	56	0.02	3.9	78.0	1.1*	≥20.0
P(BsMAz)-MeOH	56	0.12	15.8	80.8	6.4	≥4.5
P(BsMAz)-EtOH	56	0.10	14.4	147.7	5.4	≥4.5
P(BsMAz)-iPrOH	56	0.04	7.5	170.0	2.2*	≥20.0

^a Determined by ¹H NMR from stock solution without additives. ^b Determined by ¹³C NMR normalized to repeating unit (reference signal, integral = 1). ^c Determined with Top Spin software.

^d Calculated by the equation below. ^e Estimation refers to literature.⁶⁻⁷ * Value of ¹³C ether is overestimated due to high signal to noise ratios (S/N).

$$= \frac{\int \frac{{}^{13}\text{C ether}}{99} \cdot eq(\text{monomer})}{1 + \int \frac{{}^{13}\text{C ether}}{99} \cdot eq(\text{monomer})} \cdot 100\%$$

Example P(MsMAz)-MeOH:

$$\frac{\frac{0.57}{99} \cdot 50}{1 + \frac{0.57}{99} \cdot 50} \cdot 100\% = 22.4\%$$

2.9 Section C. ^{13}C -NMRs and 2D-NMRs of the kinetics

To quantify the amount of alcohol acted as an initiator, ^{13}C -labeled additives were used to follow this process by NMR. After evaporating the solvent and residual ^{13}C -labeled alcohols at reduced pressure, quantification of polymers with ^{13}C -labeled ethers, which are formed after initiation, is possible by ^{13}C NMR- and HSQC NMR-spectroscopy.

2.9.1 P(TsMAz)

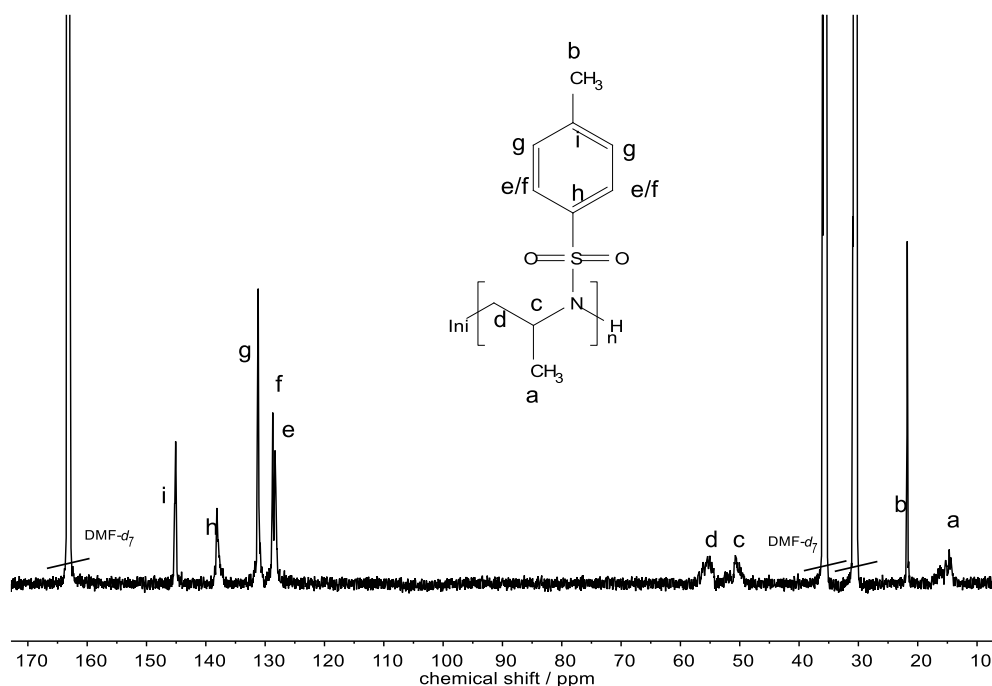


Figure S2.3. ^{13}C NMR, quantitative (176 MHz, 323 K, $\text{DMF-}d_7$) of P(TsMAz), H_2O as additive. δ [ppm] = 145.07 (s, 1C, arom., i), 138.04 (s, 1C, arom., h), 131.16 (s, 2C, arom., g), 128.70 (s, 1C, arom., f), 128.31 (s, 1C, arom., e), 56.32-54.19 (m, 1C, backbone, d), 49.06 – 52.62 (m, 1C, backbone, c), 21.75 (s, 1C, arom- CH_3 , b), 13.76-17.58 (m, 1C, backbone- CH_3 , a).

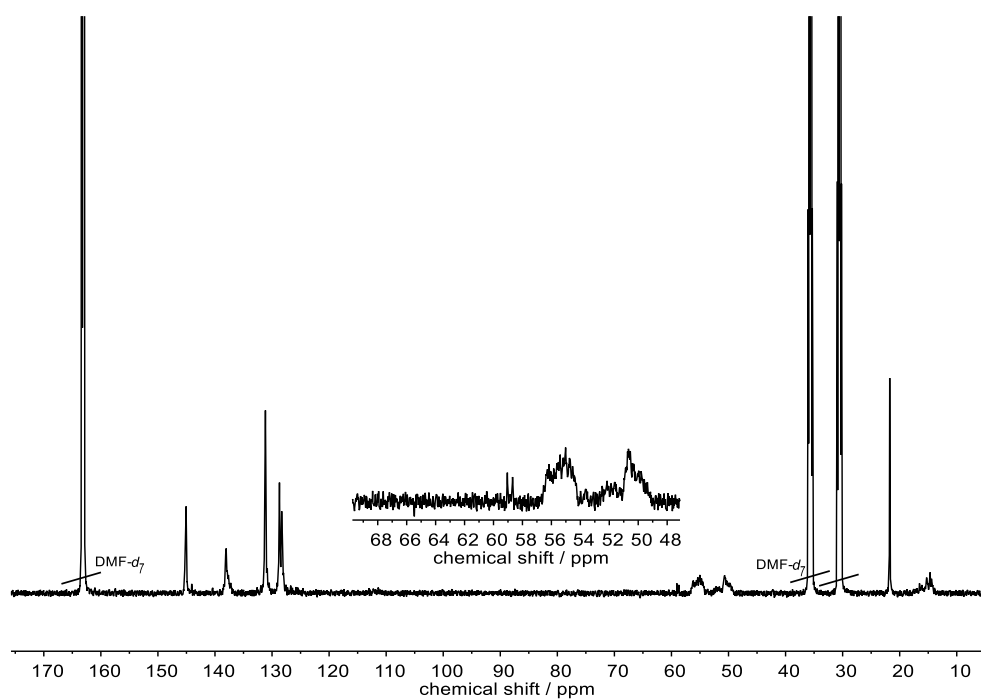


Figure S2.4. ^{13}C NMR, quantitative (176 MHz, 323 K, $\text{DMF-}d_7$) of P(TsMAz), methanol- ^{13}C as additive. δ [ppm] = 145.07 (s, 1C, arom.), 138.04 (s, 1C, arom.), 131.16 (s, 2C, arom.), 128.70 (s, 1C, arom.), 128.31 (s, 1C, arom.), 58.68-59.04 (m, 0.03, methyl- ^{13}C -ether) 56.32-54.19 (m, 1C, backbone), 49.06 – 52.62 (m, 1C, backbone) 21,75 (s, 1C, arom- CH_3), 13.76-17.58 (m, 1C, backbone- CH_3).

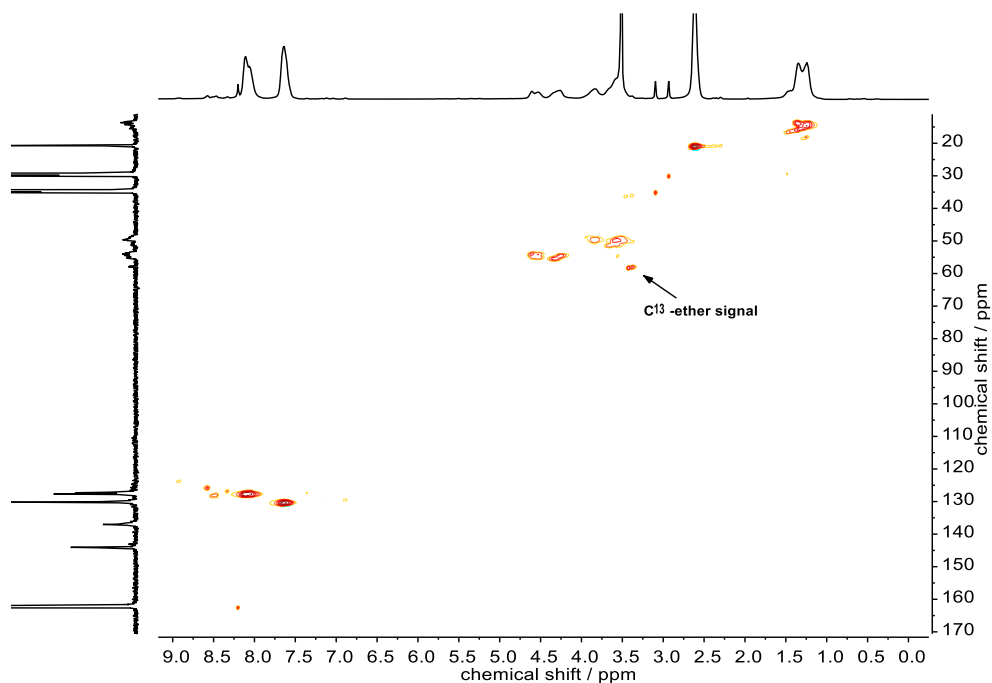


Figure S2.5. HSQC NMR (700, 176 MHz, $\text{DMF-}d_7$) of P(TsMAz), methanol- ^{13}C as additive.

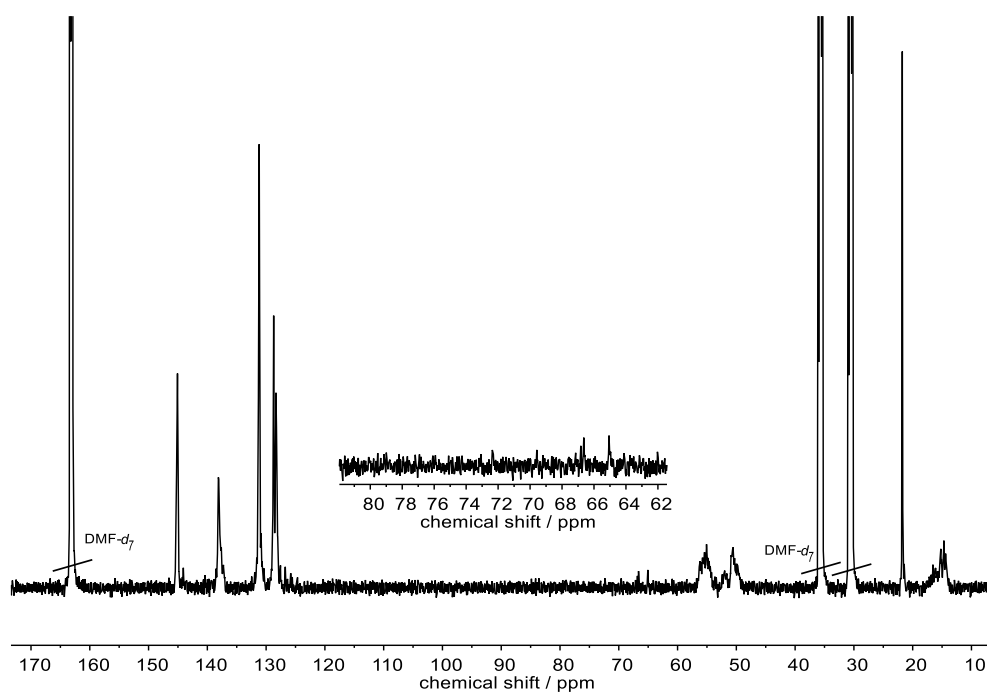


Figure S2.6. ^{13}C NMR, quantitative (176 MHz, 323 K, $\text{DMF-}d_7$) of P(TsMAz), ethanol-1- $^{13}\text{C}_1$ as additive. δ [ppm] = 145.07 (s, 1C, arom.), 138.04 (s, 1C, arom.), 131.16 (s, 2C, arom.), 128.70 (s, 1C, arom.), 128.31 (s, 1C, arom.), 66.10 (m, 0.05, ethyl-1- $^{13}\text{C}_1$ -ether) 56.32-54.19 (m, 1C, backbone), 49.06 – 52.62 (m, 1C, backbone) 21,75 (s, 1C, arom- CH_3), 13.76-17.58 (m, 1C, backbone- CH_3).

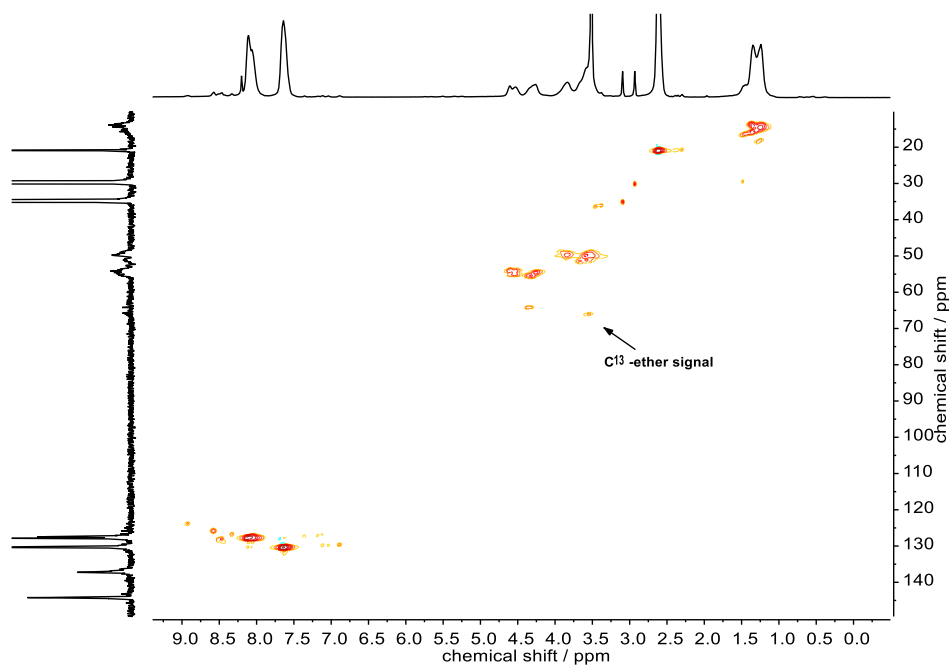


Figure S2.7. HSQC NMR (700, 176 MHz, $\text{DMF-}d_7$) of P(TsMAz), ethanol-1- $^{13}\text{C}_1$ as additive.

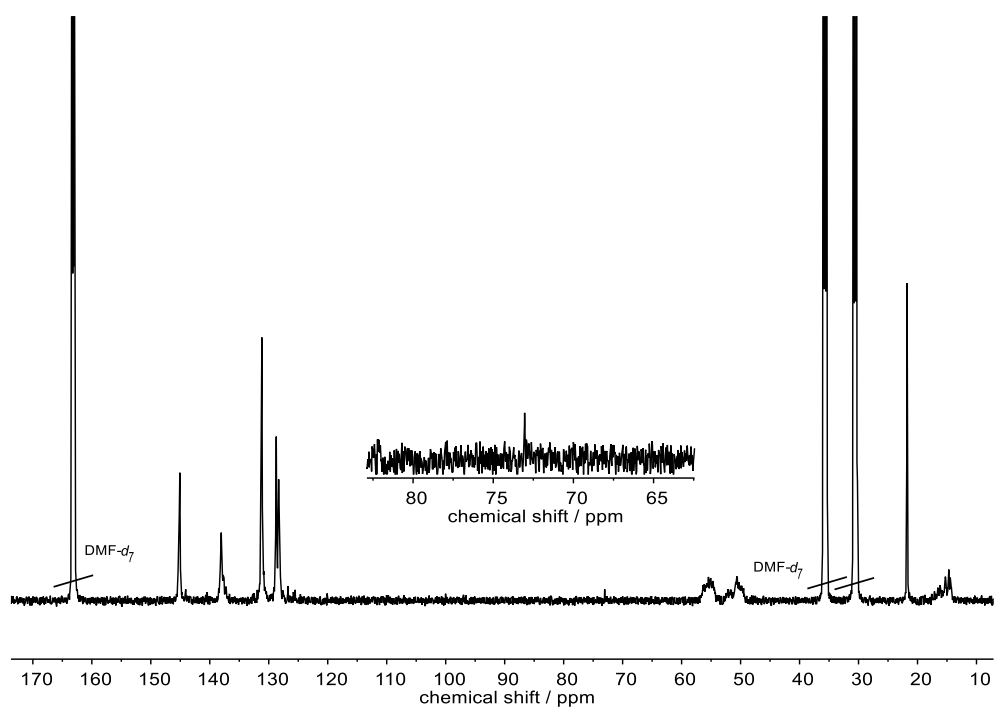


Figure S2.8. ^{13}C NMR, quantitative (176 MHz, 323 K, $\text{DMF-}d_7$) of P(TsMAz), isopropanol-2- $^{13}\text{C}_1$ as additive. δ [ppm] = 145.07 (s, 1C, arom.), 138.04 (s, 1C, arom.), 131.16 (s, 2C, arom.), 128.70 (s, 1C, arom.), 128.31 (s, 1C, arom.), 73.04 (s, 0.03, isopropyl-2- $^{13}\text{C}_1$ -ether) 56.32-54.19 (m, 1C, backbone), 49.06 – 52.62 (m, 1C, backbone) 21,75 (s, 1C, arom- CH_3), 13.76-17.58 (m, 1C, backbone- CH_3).

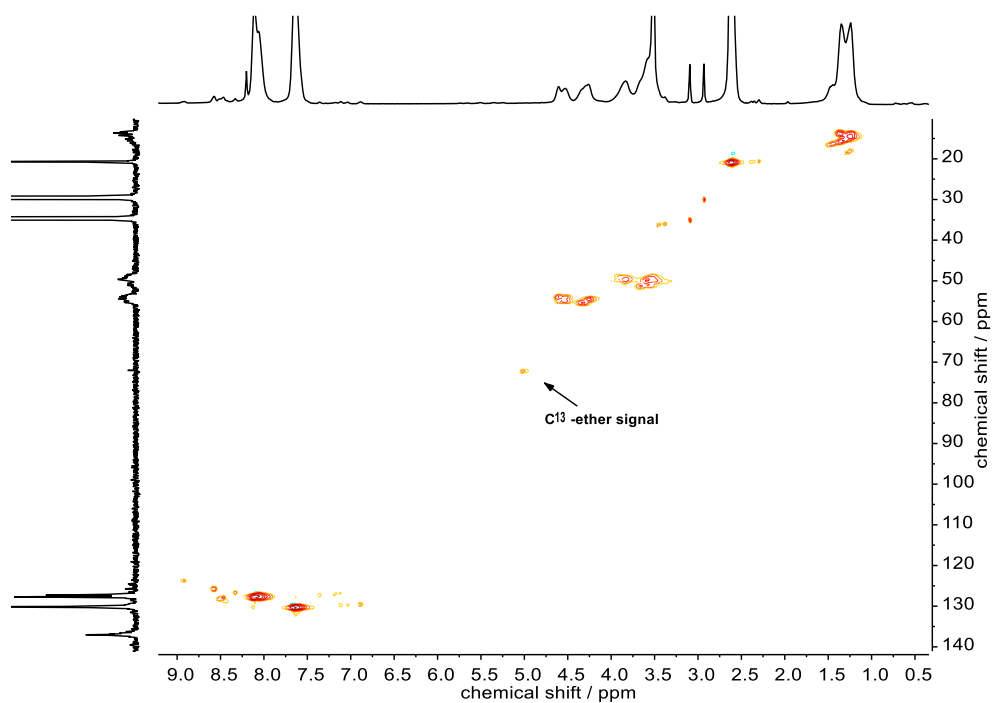


Figure S2.9. HSQC NMR (700, 176 MHz, $\text{DMF-}d_7$) of P(TsMAz), isopropanol-2- $^{13}\text{C}_1$ as additive.

2.9.2 P(BsMAz)

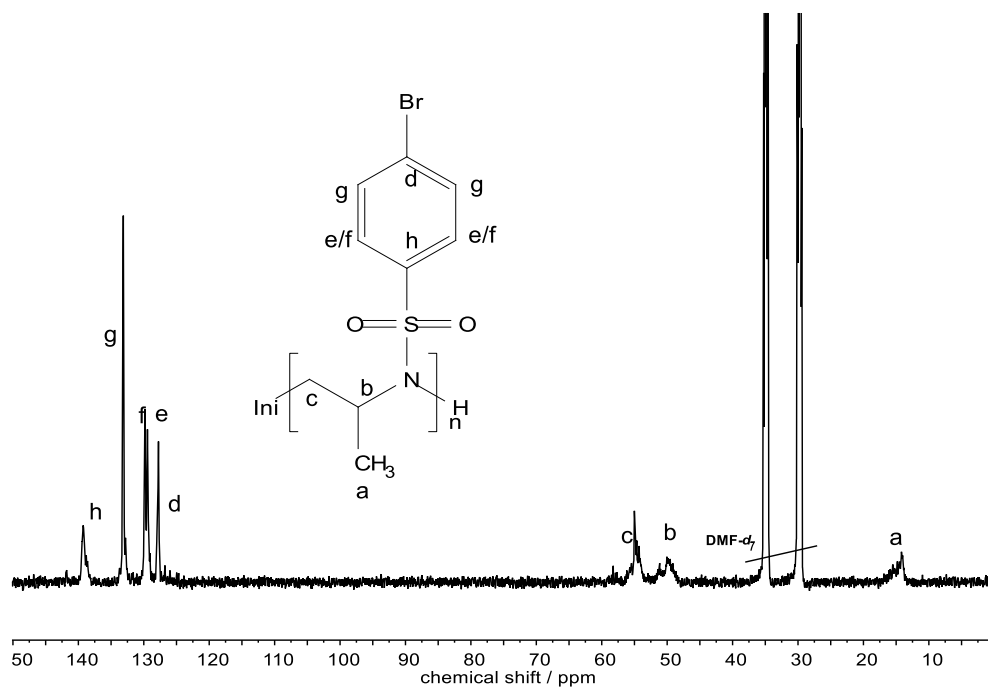


Figure S2.10. ^{13}C NMR, quantitative (176 MHz, 323 K, $\text{DMF-}d_7$) of P(BsMAz), methanol- ^{13}C as additive. δ [ppm] = 139.26 (s, 1C, arom., h), 133.08 (s, 2C, arom., g), 129.81 (s, 1C, arom., f), 129.41 (s, 1C, arom., e), 127.82 (s, 1C, arom., d), 58.24, 55.10 (m, 0.29, methyl- ^{13}C -ether) 56.83-53.51 (m, 1C, backbone, c), 52.19 – 47.99 (m, 1C, backbone, b), 17.55-13.35 (m, 1C, backbone- CH_3 , a).

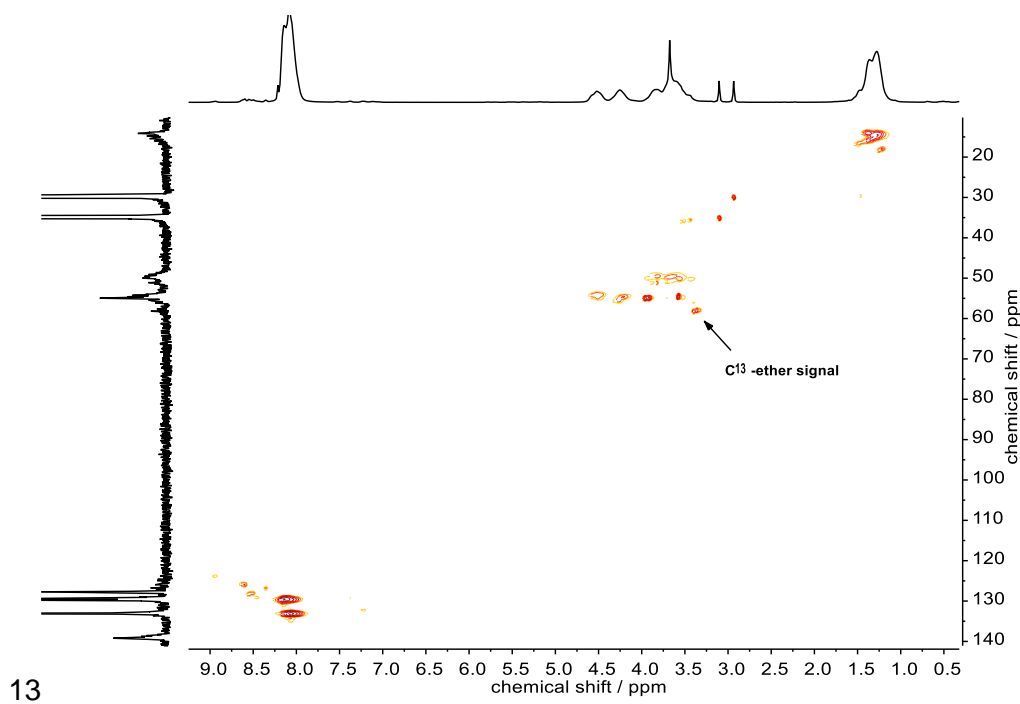


Figure S2.11. HSQC NMR (700, 176 MHz, $\text{DMF-}d_7$) of P(BsMAz), methanol- ^{13}C as additive.

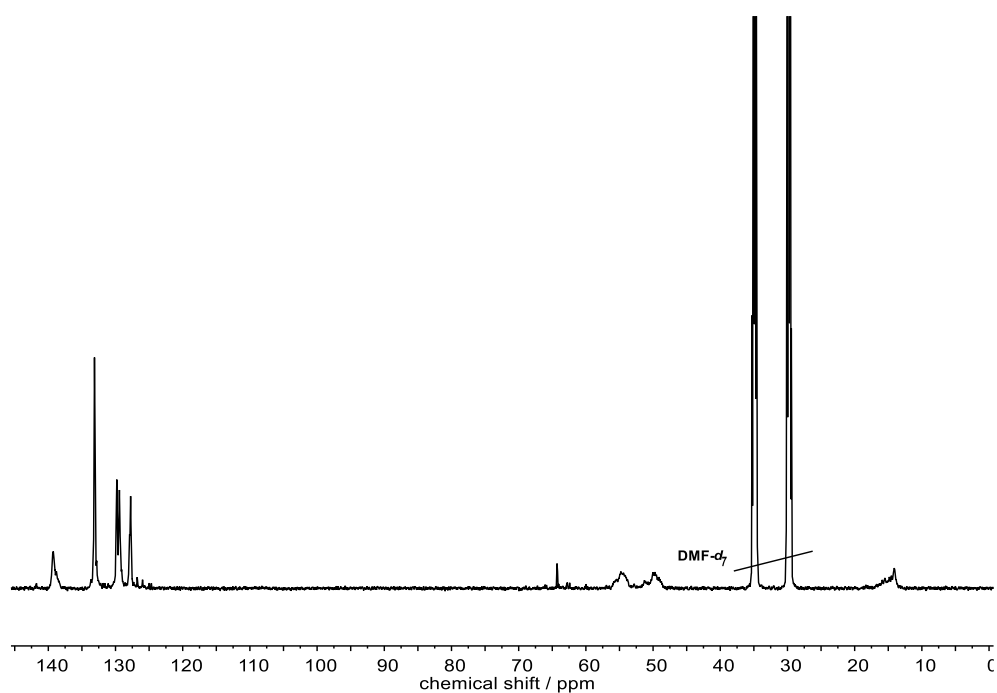


Figure S2.12. ^{13}C NMR, quantitative (176 MHz, 323 K, $\text{DMF-}d_7$) of P(BsMAz), ethanol- $1\text{-}^{13}\text{C}_1$ as additive. δ [ppm] = 139.26 (s, 1C, arom.), 133.08 (s, 2C, arom.), 129.81 (s, 1C, arom.), 129.41 (s, 1C, arom.), 127.82 (s, 1C, arom.), 58.24, 64.17 (s, 0.14, methyl- ^{13}C -ether) 56.83-53.51 (m, 1C, backbone), 52.19 – 47.99 (m, 1C, backbone), 17.55-13.35 (m, 1C, backbone- CH_3).

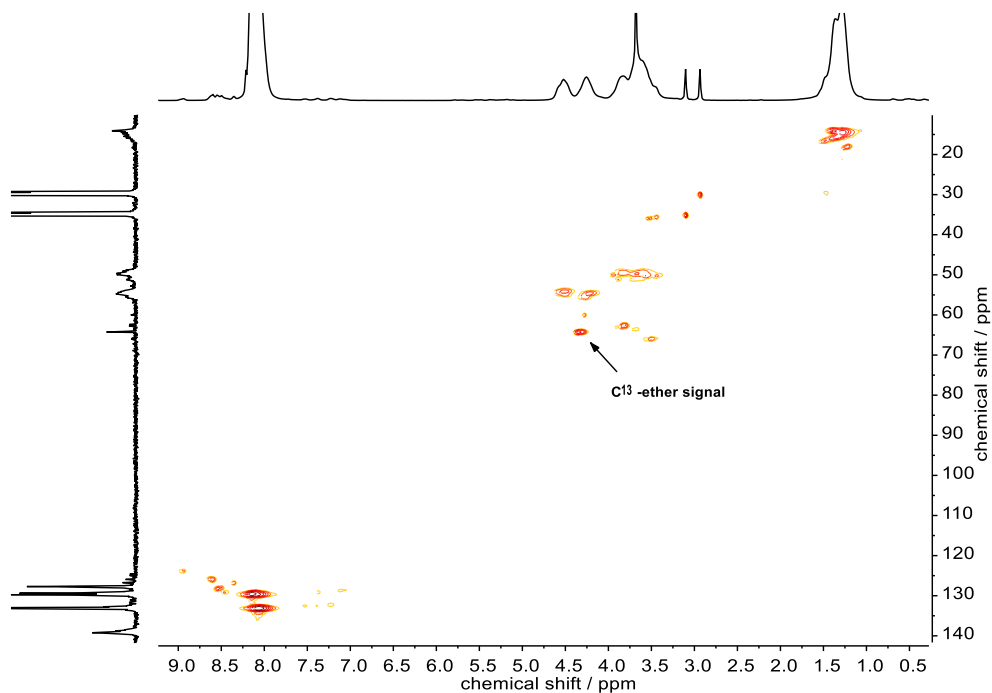


Figure S2.13. HSQC NMR (700, 176 MHz, $\text{DMF-}d_7$) of P(BsMAz), ethanol- $1\text{-}^{13}\text{C}_1$ as additive.

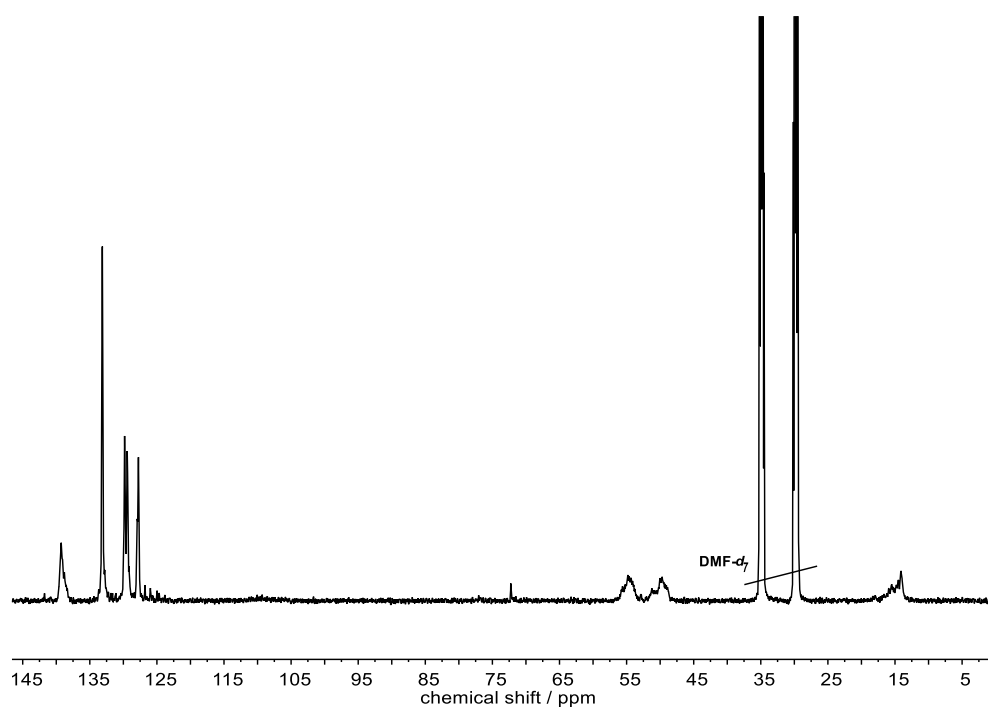


Figure S2.14. ^{13}C NMR, quantitative (176 MHz, 323 K, DMF- d_7) of P(BsMAz), isopropanol-2- $^{13}\text{C}_1$ as additive. δ [ppm] = 139.26 (s, 1C, arom.), 133.08 (s, 2C, arom.), 129.81 (s, 1C, arom.), 129.41 (s, 1C, arom.), 127.82 (s, 1C, arom.), 58.24, 72.27 (s, 0.07, methyl- ^{13}C -ether) 56.83-53.51 (m, 1C, backbone), 52.19 – 47.99 (m, 1C, backbone), 17.55-13.35 (m, 1C, backbone- CH_3).

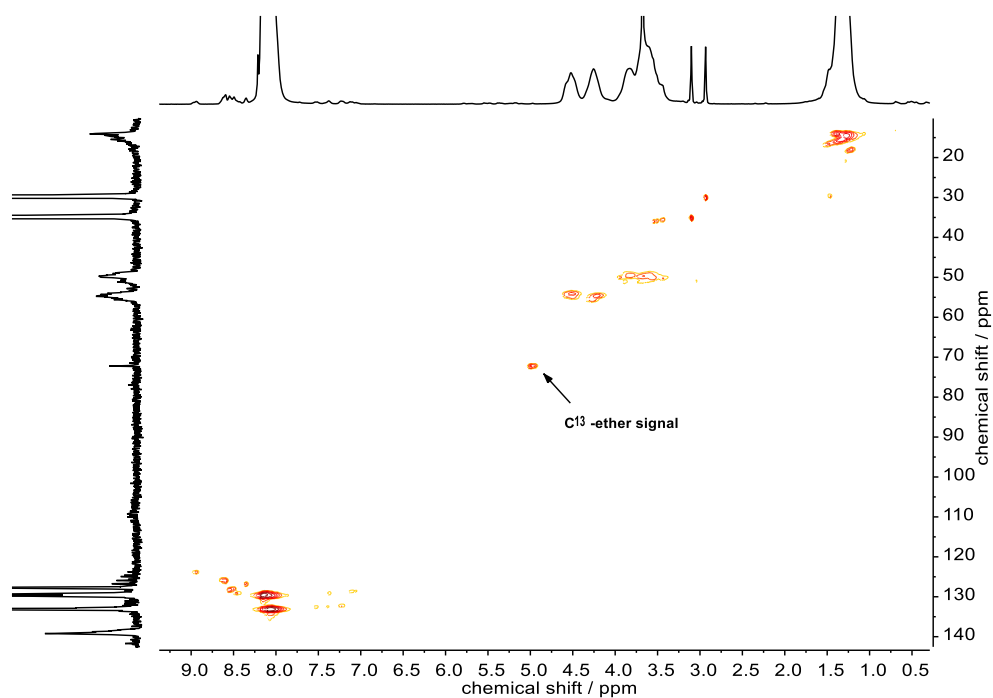


Figure S2.15. HSQC NMR (700, 176 MHz, DMF- d_7) of P(BsMAz), isopropanol-2- $^{13}\text{C}_1$ as additive.

2.9.3 P(MsMAz)

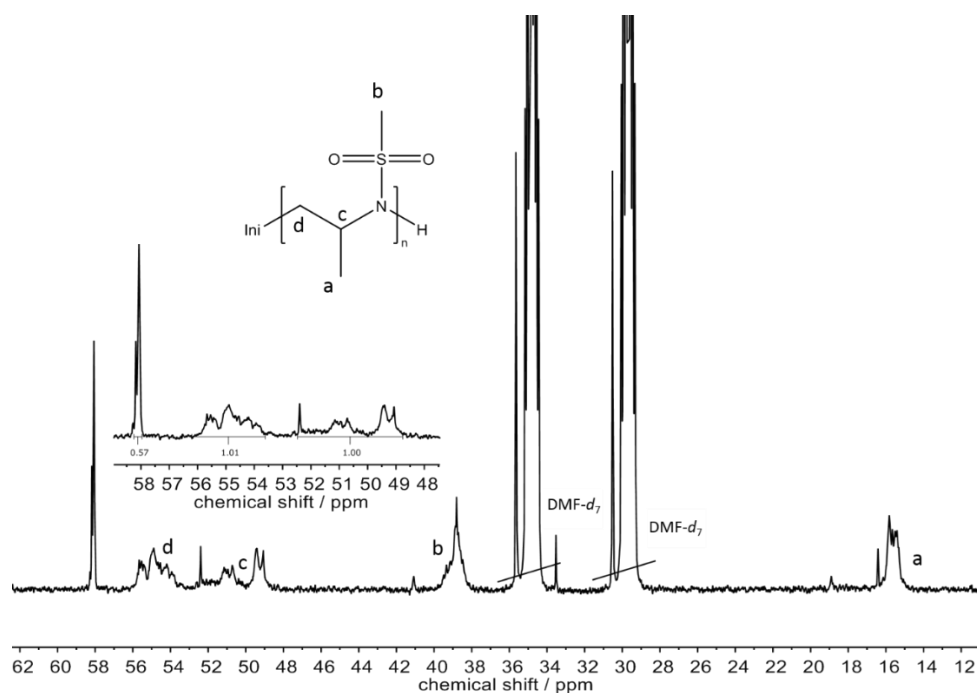


Figure S2.16. ^{13}C NMR, quantitative (176 MHz, 323 K, $\text{DMF-}d_7$) of P(MsMAz), methanol ^{13}C as additive. δ [ppm] = 58.14 (m 0.57, methyl- ^{13}C -ether), 56.06–53.20 (m, 1C, backbone, d), 51.87 – 48.62 (m, 1C, backbone, c) 40.13–37.96 (m, 1C, mesyl- CH_3 , b), 16.86–14.81 (m, 1C, backbone- CH_3 , a).

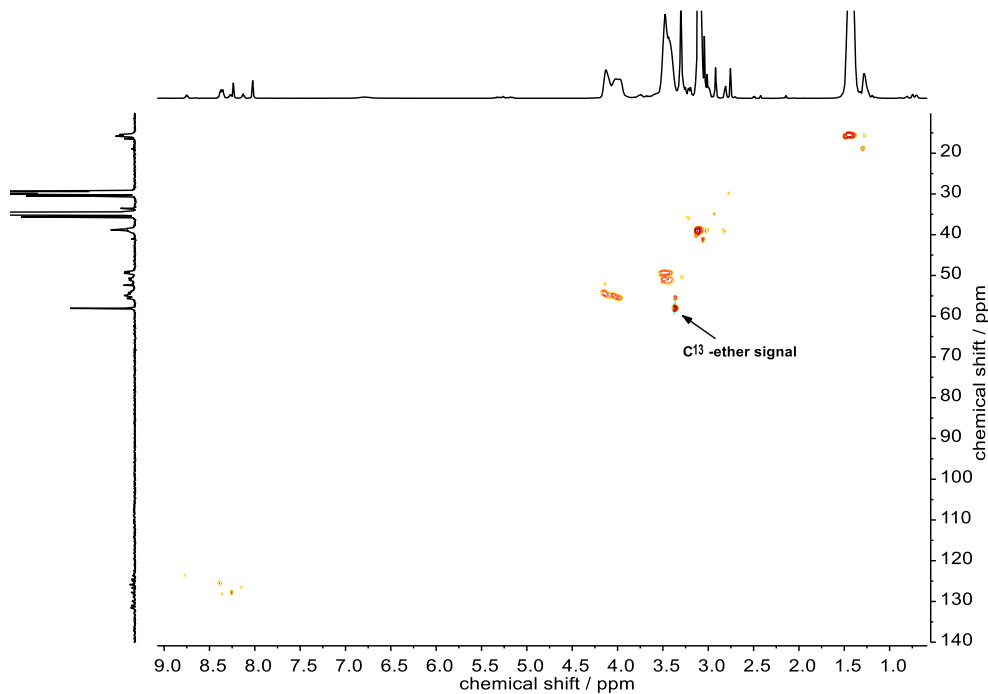


Figure S2.17. HSQC NMR (700, 176 MHz, $\text{DMF-}d_7$) of P(MsMAz), methanol ^{13}C as additive.

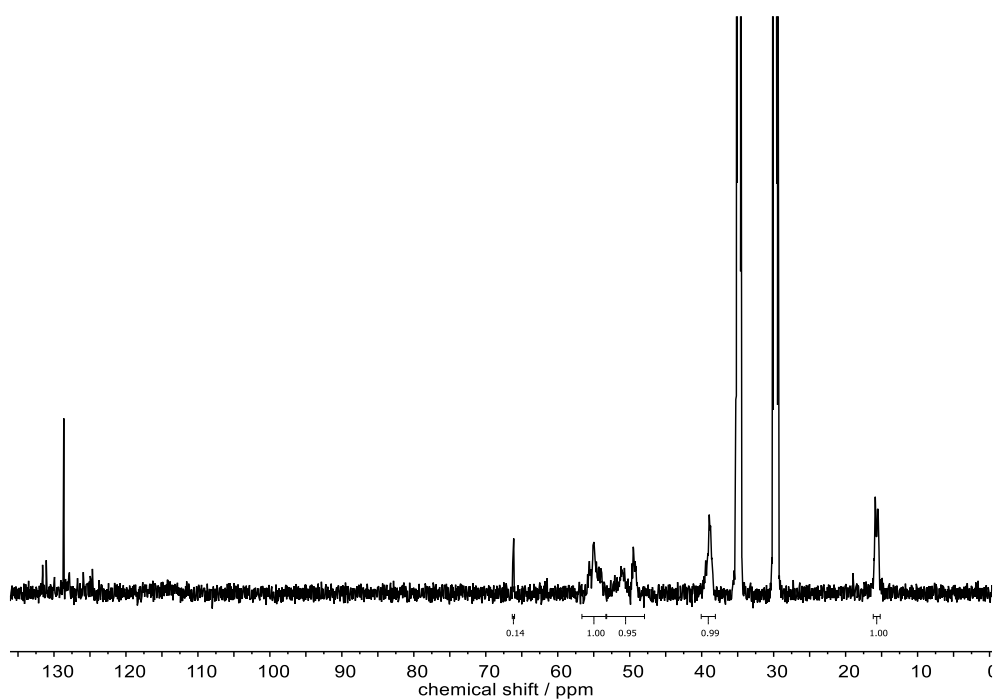


Figure S2.18. ^{13}C NMR, quantitative (176 MHz, 323 K, $\text{DMF-}d_7$) of P(MsMAz), ethanol- $1\text{-}^{13}\text{C}_1$ as additive. δ [ppm] = 66.06 (s 0.20, ethyl- $1\text{-}^{13}\text{C}_1$ -ether), 56.06-53.20 (m, 1C, backbone), 51.87 – 48.62 (m, 1C, backbone) 40.13-37.96 (m, 1C, mesyl- CH_3), 16.86-14.81 (m, 1C, backbone- CH_3). The signal at 57.4 ppm belongs to residual ethanol- $1\text{-}^{13}\text{C}_1$.

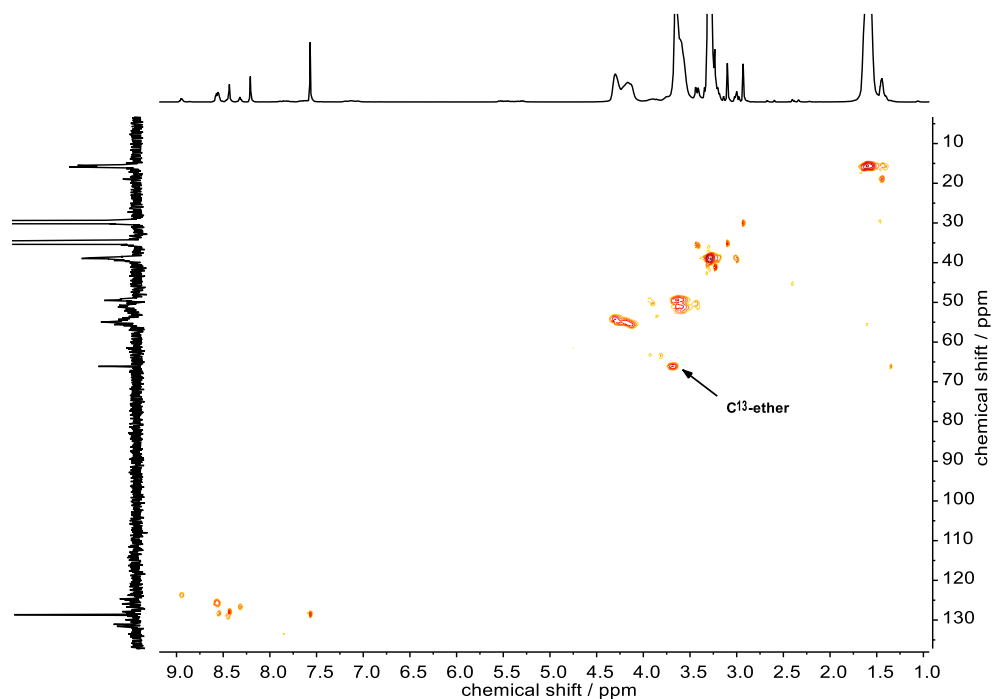


Figure S2.19. HSQC NMR (700, 176 MHz, $\text{DMF-}d_7$) of P(MsMAz), ethanol- $1\text{-}^{13}\text{C}_1$ as additive.

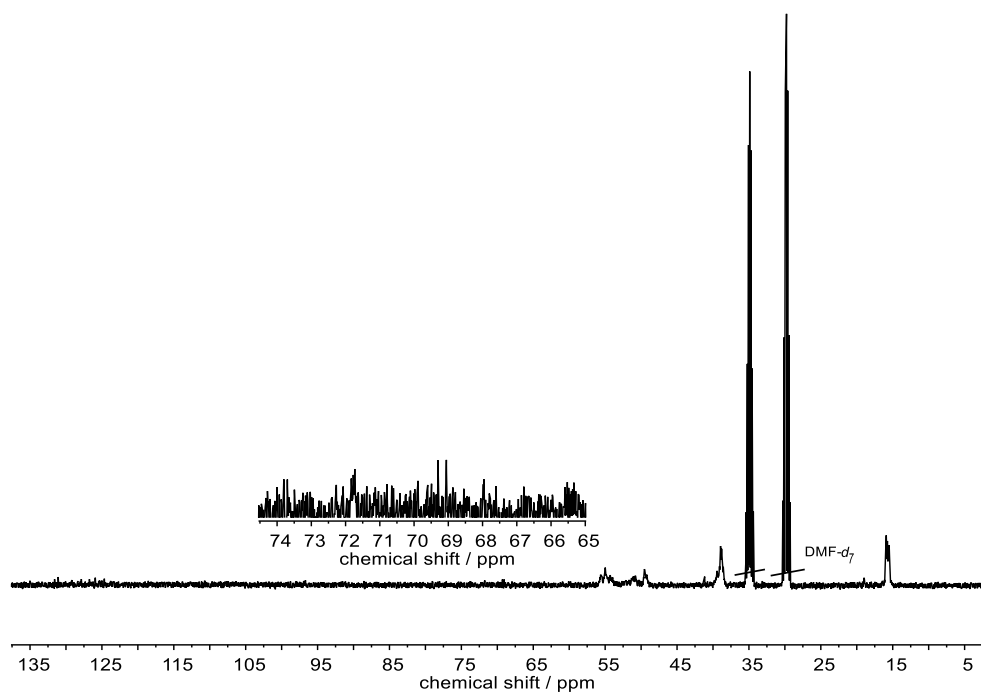


Figure S2.20. ^{13}C NMR, quantitative (176 MHz, 323 K, DMF- d_7) of P(MsMAz), isopropanol-2- $^{13}\text{C}_1$ as additive. δ [ppm] = 71.8 (m, 0.01, isopropyl- $^{13}\text{C}_1$ -ether), 56.06-53.20 (m, 1C, backbone), 51.87 – 48.62 (m, 1C, backbone) 40.13-37.96 (m, 1C, mesyl- CH_3), 16.86-14.81 (m, 1C, backbone- CH_3).

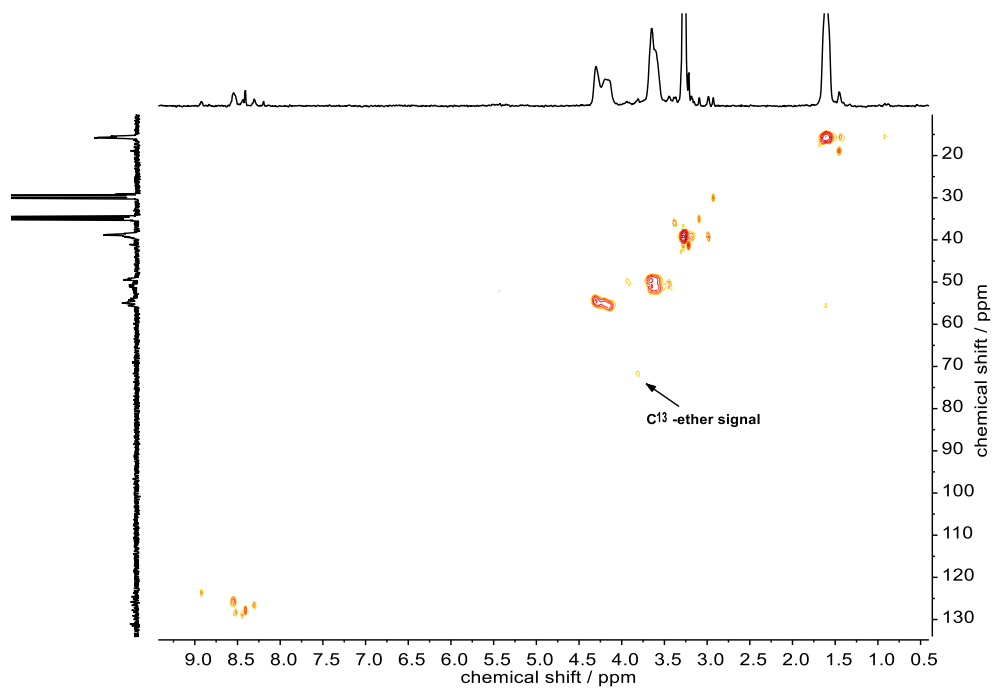


Figure S21. HSQC NMR (700, 176 MHz, DMF- d_7) of P(MsMAz), isopropanol-2- $^{13}\text{C}_1$ as additive.

2.10 Section D. Polymerization in open vials

2.10.1 P(MsMAz)

MsMAz (1) (100 mg, 0.739 mmol) in 1 mL DMF, BnNHMs (5) (2.8 mg, 0.015 mmol) and KHMDS (3.0 mg, 0.015 mmol) in 0.1 mL DMF at 50 °C. Samples taken after 24, 48 and 120 hours.

Table S2.4. Overview of the performed polymerizations of MsMAz (1) in DMF with different amounts of water as an additive, including SEC-analyses.

Monomer	MsMAz (1)	MsMAz (1)	MsMAz (1)
Additive	H ₂ O	H ₂ O	H ₂ O
V / μ L	50	100	200
Equivalents (to initiator)	185	370	740
M_n^a / g mol ⁻¹	1400	900	500
\mathcal{D}^a	1.48	1.37	> 2
Reaction time / h	<120	<120	>120
Conversion / %	~95	~95	~60
Name	P(Ms)-H ₂ O-50- μ L	P(Ms)-H ₂ O-100- μ L	P(Ms)-H ₂ O-200- μ L

^a Number-average molecular weight and molecular weight dispersity determined *via* SEC in DMF (vs. PEO standards).

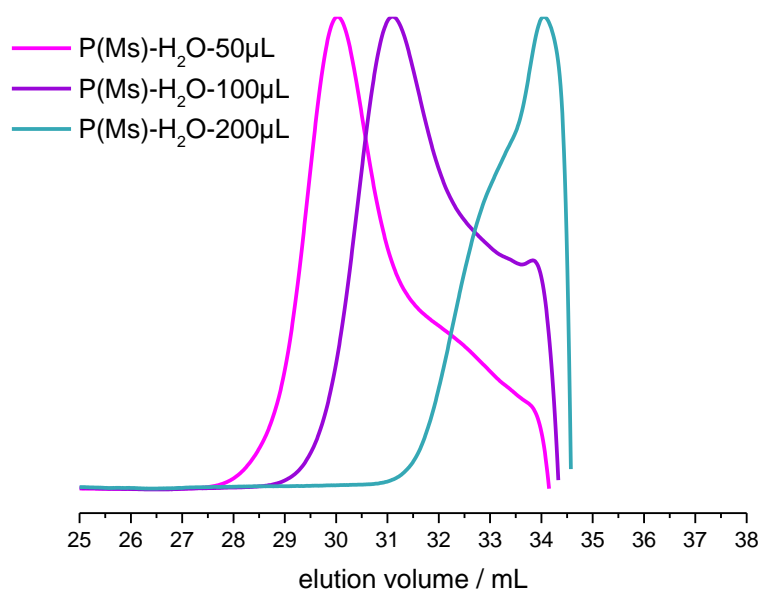


Figure S2.22. SEC traces of P(MsMAz) with water (50, 100, 200 μ L) as an additive in DMF (RI signal).

Table S2.5. Overview of the performed polymerizations of MsMAz (1) in DMF with different amounts of methanol as an additive, including SEC-analyses.

Monomer	MsMAz (1)	MsMAz (1)	MsMAz (1)
Additive	MeOH	MeOH	MeOH
V / μL	50	100	200
Equivalents (to initiator)	115	229	458
M_n^a / g mol^{-1}	2800	1700	800
\mathcal{D}^a	1.23	1.27	1.29
Reaction time / h	<24	<48	<120
Conversion / %	>99	~95	~95
Name	P(Ms)-MeOH- 50- μL	P(Ms)-MeOH- 100- μL	P(Ms)-MeOH- 200- μL

^a Number-average molecular weight and molecular weight dispersity determined *via* SEC in DMF (vs. PEO standards).

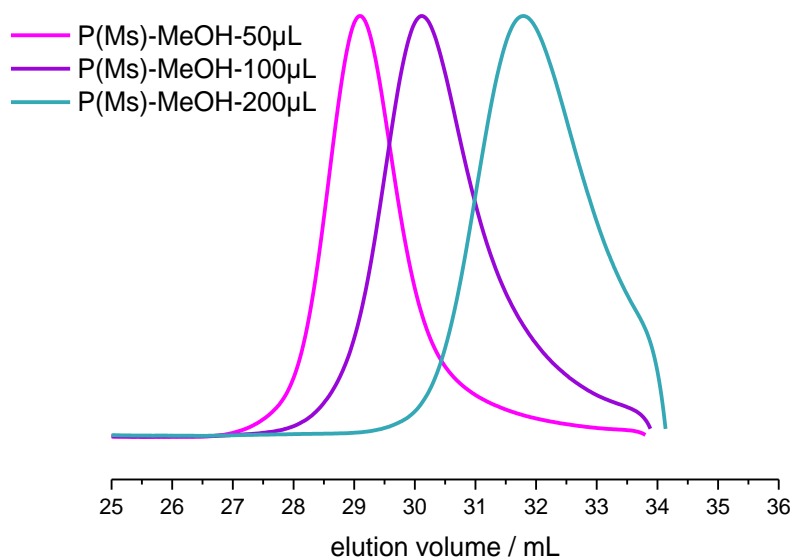
**Figure S2.23. SEC traces of P(MsMAz) with methanol (50, 100, 200 μL) as an additive in DMF (RI signal).**

Table S2.6. Overview of the performed polymerizations of MsMAz (1) in DMF with different amounts of ethanol as an additive, including SEC-analyses.

Monomer	MsMAz (1)	MsMAz (1)	MsMAz (1)	MsMAz (1)
Additive	EtOH	EtOH	EtOH	EtOH
V / μL	50	100	200	400
Equivalents (to initiator)	57	114	228	457
M_n^a / g mol^{-1}	3500	2100	2900	1900
\mathcal{D}^a	1.15	1.24	1.19	1.22
Reaction time / h	<24	<24	<48	<24
Conversion / %	>99	>99	~95	~95
Name	P(Ms)-EtOH-50- μL	P(Ms)-EtOH-100- μL	P(Ms)-EtOH-200- μL	P(Ms)-EtOH-400- μL

^a Number-average molecular weight and molecular weight dispersity determined *via* SEC in DMF (vs. PEO standards).

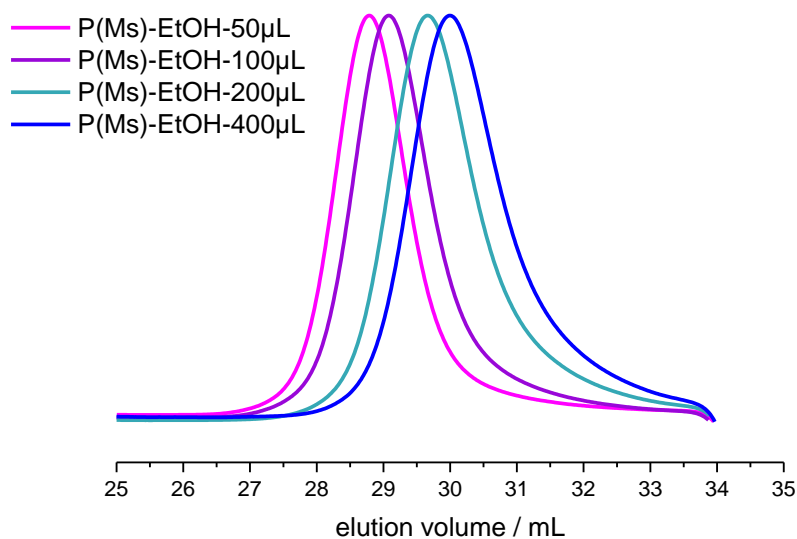
**Figure S2.24. SEC traces of P(MsMAz) with ethanol (50, 100, 200, 400 μL) as an additive in DMF (RI signal).**

Table S2.7. Overview of the performed polymerizations of MsMAz (1) in DMF in an open vial and with isopropanol as an additive, including SEC-analyses.

Monomer	MsMAz (1)	MsMAz (1)
Additive	Open	iPrOH
V / μL	---	400
Equivalents (to initiator)	---	349
M_n^a / g mol^{-1}	3400	2900
\mathcal{D}^a	1.09	1.15
Reaction time / h	<24	<24
Conversion / %	>99	~95
Name	P(Ms)-open vial	P(Ms)-iPrOH-400- μL

^a Number-average molecular weight and molecular weight dispersity determined *via* SEC in DMF (vs. PEO standards).

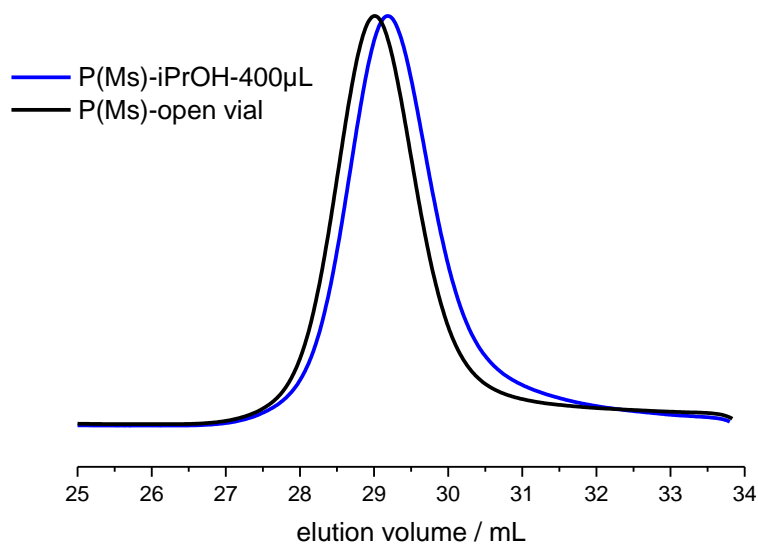


Figure S2.25. SEC traces of P(MsMAz) in an open vial and with isopropanol (400 μL) as an additive in DMF (RI signal).

2.10.2 P(TsMAz)

TsMAz (2) (100 mg, 0.473 mmol) in 1 mL DMF, BnNHMs (5) (1.75 mg, 0.0095 mmol) and KHMDs (1.89 mg, 0.0095 mmol) in 0.1 mL DMF at 50 °C. Samples taken after 24, 44 and 48 hours.

Table S2.8. Overview of the performed polymerizations of TsMAz (2) in DMF with different amounts of water as an additive, including SEC-analyses.

Monomer	TsMAz (2)	TsMAz (2)	TsMAz (2)	TsMAz (2)	TsMAz (2)	TsMAz (2)
Additive	H ₂ O	H ₂ O	H ₂ O	H ₂ O	H ₂ O	H ₂ O
V / μ L	0.17	1.7	17	50	100	200
Equivalents (to initiator)	1	10	100	292	584	1170
M_n^a / g mol ⁻¹	4400	4000	3600	2700	2000	1200
\mathcal{D}^a	1.15	1.16	1.27	1.25	1.41	1.31
Reaction time / h	<40	<40	<40	<24	<24	>48
Conversion / %	>99	>99	>99	>99	~95	~60
Name	P(Ts)-H ₂ O-1eq	P(Ts)-H ₂ O-10eq	P(Ts)-H ₂ O-100eq	P(Ts)-H ₂ O-50- μ L	P(Ts)-H ₂ O-100- μ L	P(Ts)-H ₂ O-200- μ L

^a Number-average molecular weight and molecular weight dispersity determined *via* SEC in DMF

(vs. PEO standards).

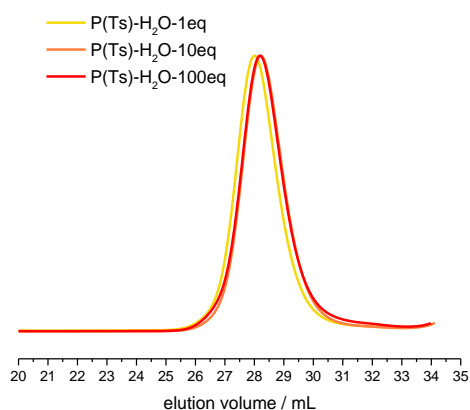


Figure S2.26. SEC traces of P(TsMAz) with water (1, 10, 100 eq.) as an additive in DMF (RI signal).

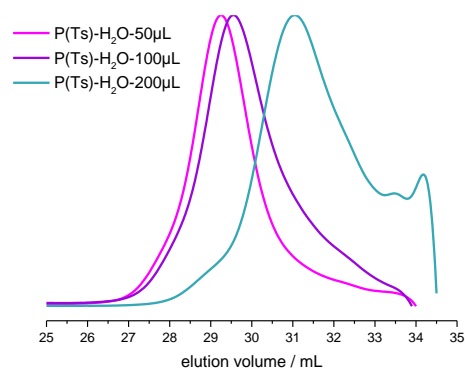


Figure S2.27. SEC traces of P(TsMAz) with water (50, 100, 200 μ L) as an additive in DMF (RI signal).

Table S2.9. Overview of the performed polymerizations of TsMAz (2) in DMF with different amounts of dry methanol as an additive, including SEC-analyses.

Monomer	TsMAz (2)	TsMAz (2)	TsMAz (2)	TsMAz (2)
Additive	MeOH	MeOH	MeOH	MeOH
V / μL	38	50	100	200
Equivalents (to initiator)	100	181	362	724
M_n^a / g mol^{-1}	4000	3400	2600	1500
\mathcal{D}^a	1.21	1.25	1.25	1.28
Reaction time / h	<40	<24	<24	>48
Conversion / %	>99	>99	>99	>99
Name	P(Ts)-MeOH-100eq	P(Ts)-MeOH-50- μL	P(Ts)-MeOH-100- μL	P(Ts)-MeOH-200- μL

^a Number-average molecular weight and molecular weight dispersity determined *via* SEC in DMF (vs. PEO standards).

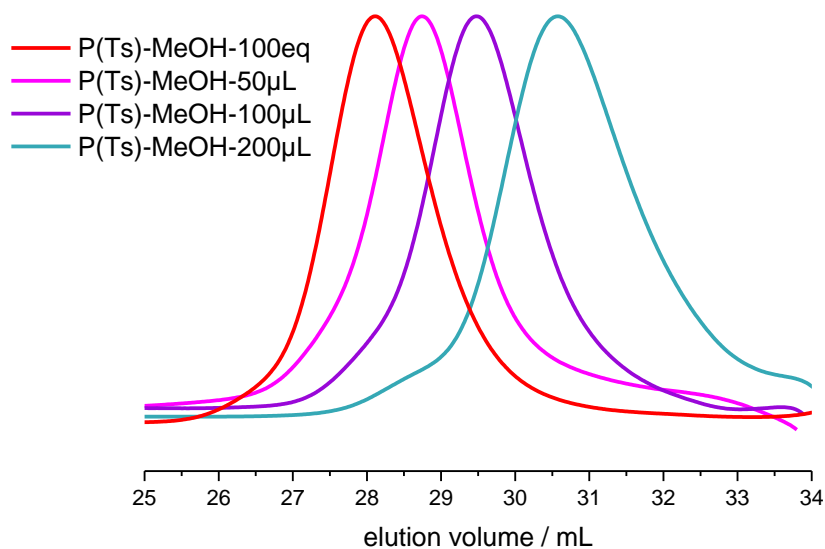
**Figure S2.28. SEC traces of P(TsMAz) with methanol (100 eq., 50, 100, 200 μL) as an additive in DMF (RI signal).**

Table S2.10. Overview of the performed polymerizations of TsMAz (2) in DMF with different amounts of dry ethanol as an additive, including SEC-analyses.

Monomer	TsMAz (2)	TsMAz (2)	TsMAz (2)	TsMAz (2)
Additive	EtOH	EtOH	EtOH	EtOH
V / μL	50	55	100	200
Equivalents (to initiator)	90	100	180	361
M_n^a / g mol^{-1}	3800	3700	3600	3100
\mathcal{D}^a	1.16	1.18	1.20	1.21
Reaction time / h	<24	<40	<24	>48
Conversion / %	>99	>99	>99	>99
Name	P(Ts)-EtOH- 50- μL	P(Ts)-EtOH- 100eq	P(Ts)-EtOH- 100- μL	P(Ts)-EtOH- 200- μL

^a Number-average molecular weight and molecular weight dispersity determined *via* SEC in DMF (vs. PEO standards).

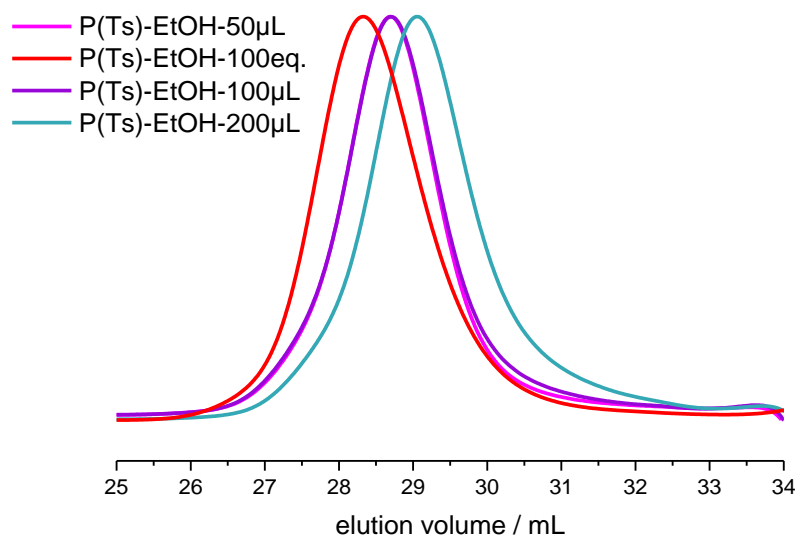


Figure S2.29. SEC traces of P(TsMAz) with ethanol (100 eq., 50, 100, 200 μL) as an additive in DMF (RI signal).

Table S2.11. Overview of the performed polymerizations of TsMAz (2) in DMF with different amounts of dry isopropanol as an additive, including SEC-analyses. In case of 1000 μL iPrOH, the monomer was only dissolved in iPrOH, only the initiator was added from a stock solution in DMF.

Monomer	TsMAz (2)	TsMAz (2)	TsMAz (2)
Additive	iPrOH	iPrOH	iPrOH
V / μL	73	200	1000
Equivalents (to initiator)	100	275	872
M_n^a / g mol^{-1}	3900	3800	2500
\mathcal{D}^a	1.18	1.16	1.23
Reaction time / h	<40	<24	<48
Conversion / %	>99	~60	~95
Name	P(Ts)-iPrOH-100-eq	P(Ts)-iPrOH-200- μL	P(Ts)-iPrOH-1000- μL

^a Number-average molecular weight and molecular weight dispersity determined *via* SEC in DMF (vs. PEO standards).

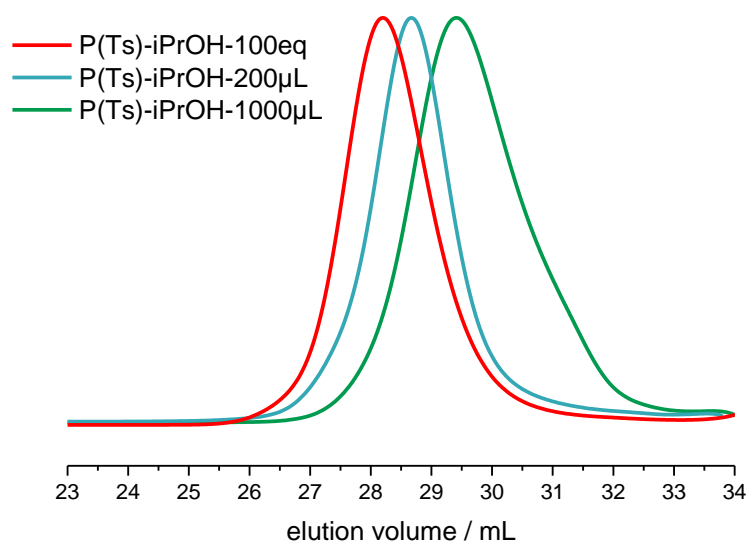


Figure S2.30. SEC traces of P(TsMAz) with isopropanol (100 eq., 200, 1000 μL) as an additive in DMF (RI signal).

Table S2.12. Overview of the performed polymerizations of TsMAz (2) in DMF in an open vial and with dry acetone and ethyl acetate (EtOAc) as an additive, including SEC-analyses. In case of 1000 μL solvent, the monomer was only dissolved in the respective solvent, only the initiator was added from a stock solution in DMF.

Monomer	TsMAz (2)	TsMAz (2)	TsMAz (2)
Additive	Open	Acetone	Ethyl acetate
V / μL	---	1000	1000
M_n^a / g mol^{-1}	4400	6400*	3700
\mathcal{D}^a	1.11	1.16	1.18
Reaction time / h	<40	<24	<24
Conversion / %	>99	>99	>99
Name	P(Ts)-open vial	P(Ts)-acetone-1000- μL	P(Ts)-EtOAc-1000- μL

^a Number-average molecular weight and molecular weight dispersity determined *via* SEC in DMF (vs. PEO standards). * Higher molecular weight, as less than the usual 100 μL of the initiator-solution was added.

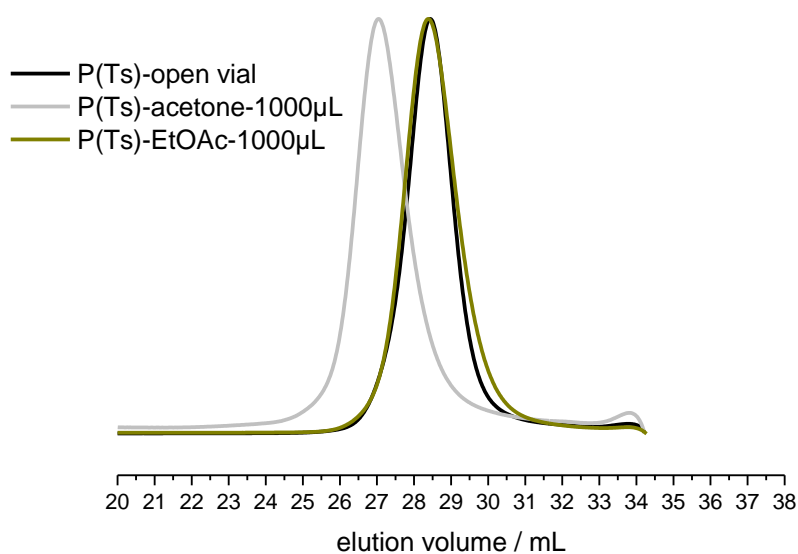


Figure S2.31. SEC traces of P(TsMAz) in an open vial, acetone and ethyl acetate in DMF (RI signal).

TsMAz (2) (100 mg, 0.473 mmol) in 1 mL DMF, BnNHMs (1.75 mg, 0.0095 mmol) and LiHMDS (1.58 mg, 0.0095 mmol) in 0.1 mL DMF at 50 °C.

Table S2.13. Overview of the performed polymerizations of TsMAz (2) from stock solutions in DMF, with Lithium as counterion and different amounts of water as an additive, including SEC-analyses.

Monomer	TsMAz (2)	TsMAz (2)	TsMAz (2)
Additive	H ₂ O	H ₂ O	H ₂ O
V / μ L	0.17	1.7	17
Equivalents (to initiator)	1	10	100
M_n^a / g mol ⁻¹	5700	7700	4600
\mathcal{D}^a	1.14	1.11	1.20
Reaction time / h	<48	<48	<48
Conversion / %	>99	>99	>99
Name	P(Ts)-Li-H ₂ O-1eq	P(Ts)-Li-H ₂ O-10eq	P(Ts)-Li-H ₂ O-100eq

^a Number-average molecular weight and molecular weight dispersity determined *via* SEC in DMF (vs. PEO standards).

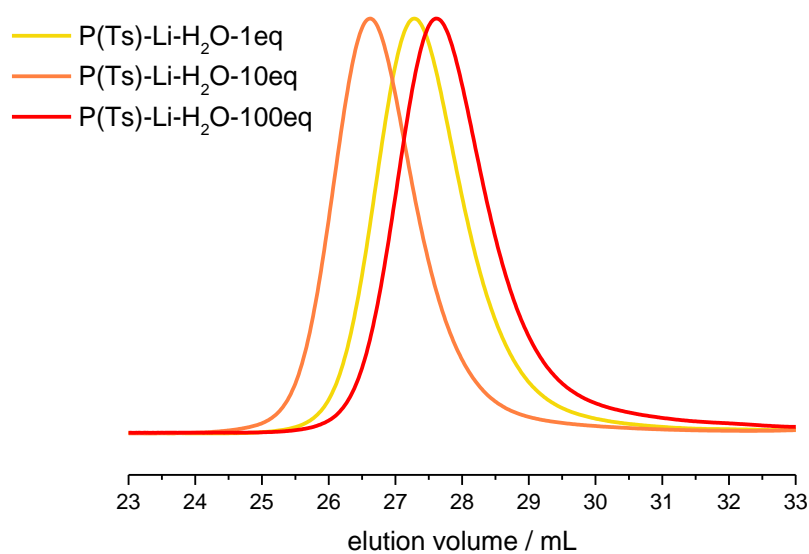
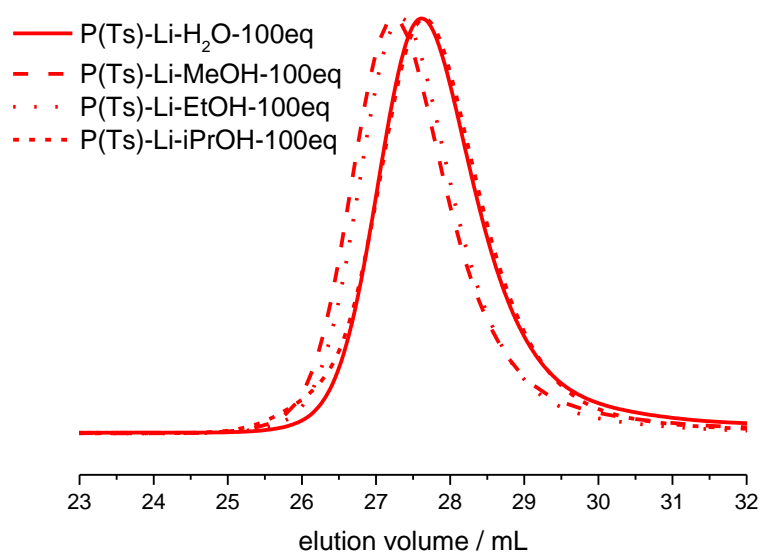


Figure S2.32. SEC traces of P(TsMAz), with lithium as the counterion with water (1, 10, 100 eq.) as an additive in DMF (RI signal).

Table S2.14. Overview of the performed polymerizations of TsMAz (2) in DMF, with lithium as the counterion and different additives, including SEC-analyses.

Monomer	TsMAz (2)	TsMAz (2)	TsMAz (2)	TsMAz (2)
Additive	H ₂ O	MeOH	EtOH	iPrOH
V / μ L	17	38	55	73
Equivalents (to initiator)	100	100	100	100
M_n^a / g mol ⁻¹	4600	5400	5400	5000
\mathcal{D}^a	1.20	1.19	1.16	1.16
Reaction time / h	<48	<48	<48	<48
Conversion / %	>99	>99	>99	>99
Name	P(Ts)-Li-H ₂ O-100eq	P(Ts)-Li-MeOH-100eq	P(Ts)-Li-EtOH-100eq	P(Ts)-Li-iPrOH-100eq

^a Number-average molecular weight and molecular weight dispersity determined *via* SEC in DMF (vs. PEO standards).

**Figure S2.33. SEC traces of P(TsMAz), with lithium as the counterion and different additives (100 eq.) in DMF (RI signal).**

2.11 Section E. MALDI-TOF spectra

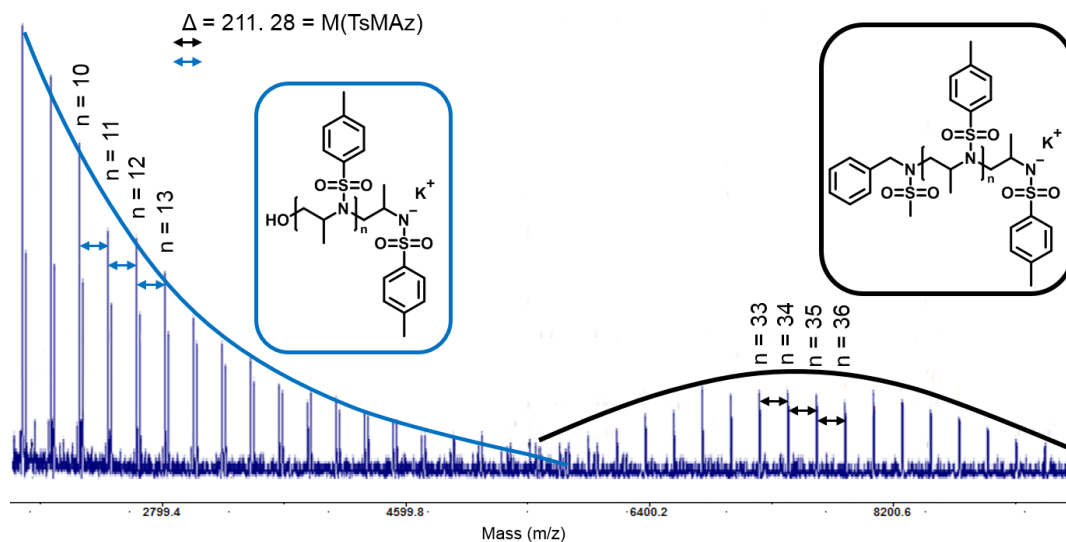
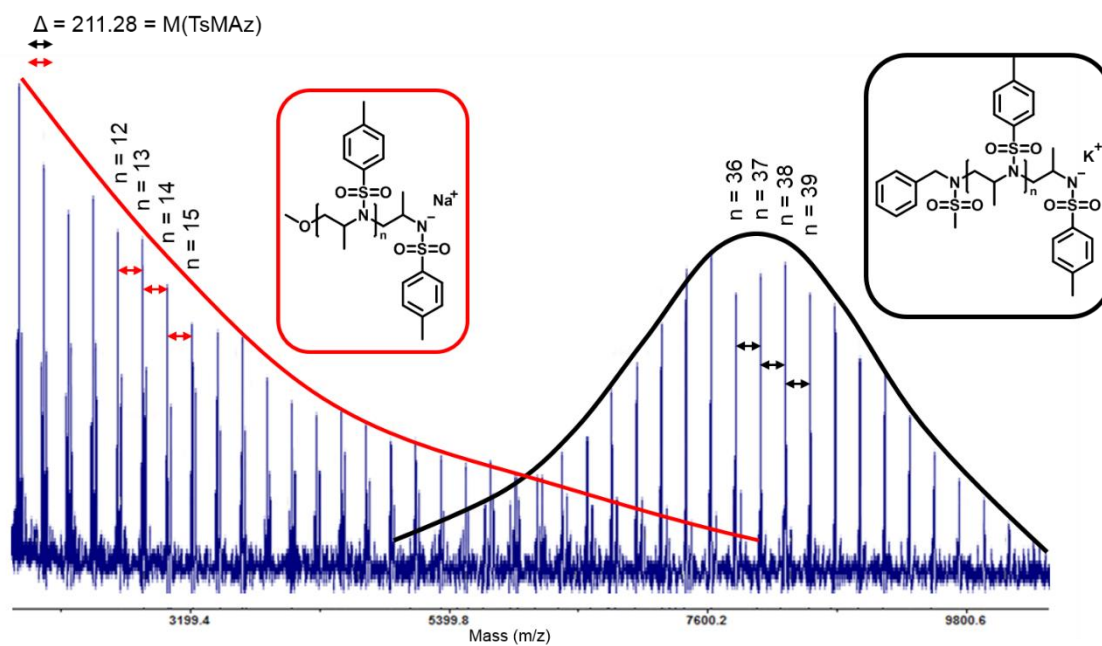
Figure S2.34. MALDI-TOF-spectrum of P(Ts)-H₂O-100eq (Table S7).

Figure S2.35. MALDI-TOF-spectrum of P(Ts)-MeOH-100eq (Table S8).

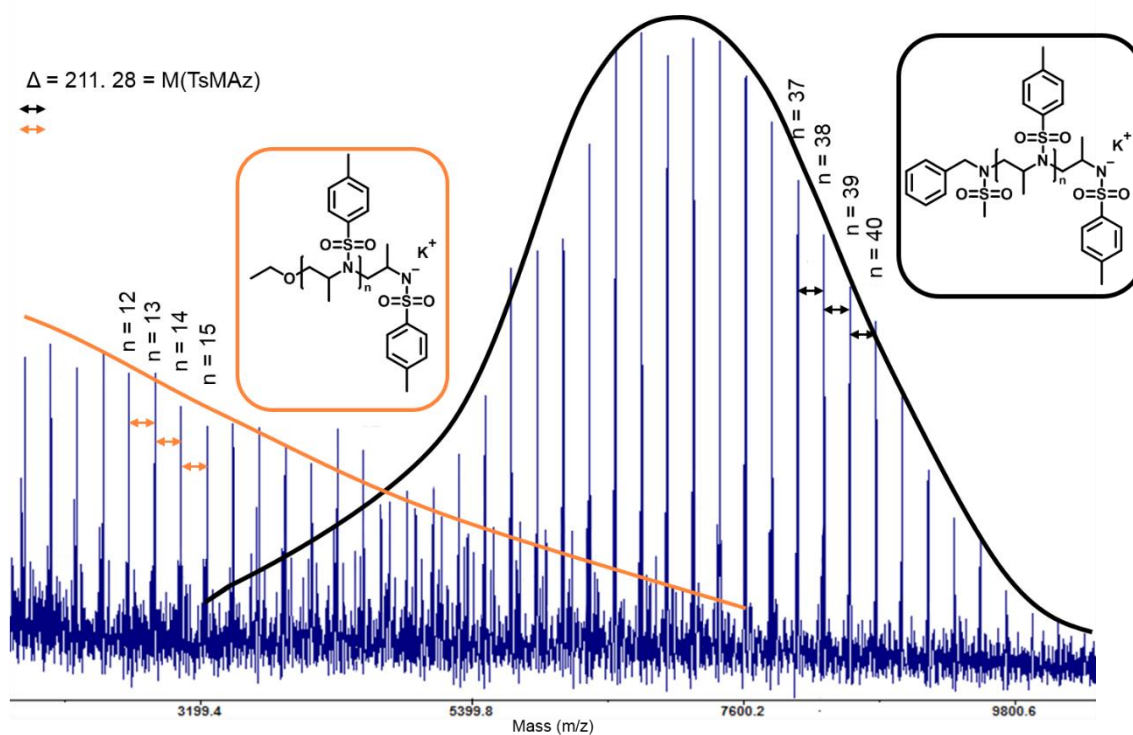


Figure S2.36. MALDI-TOF-spectrum of P(Ts)-EtOH-100eq (Table S9).

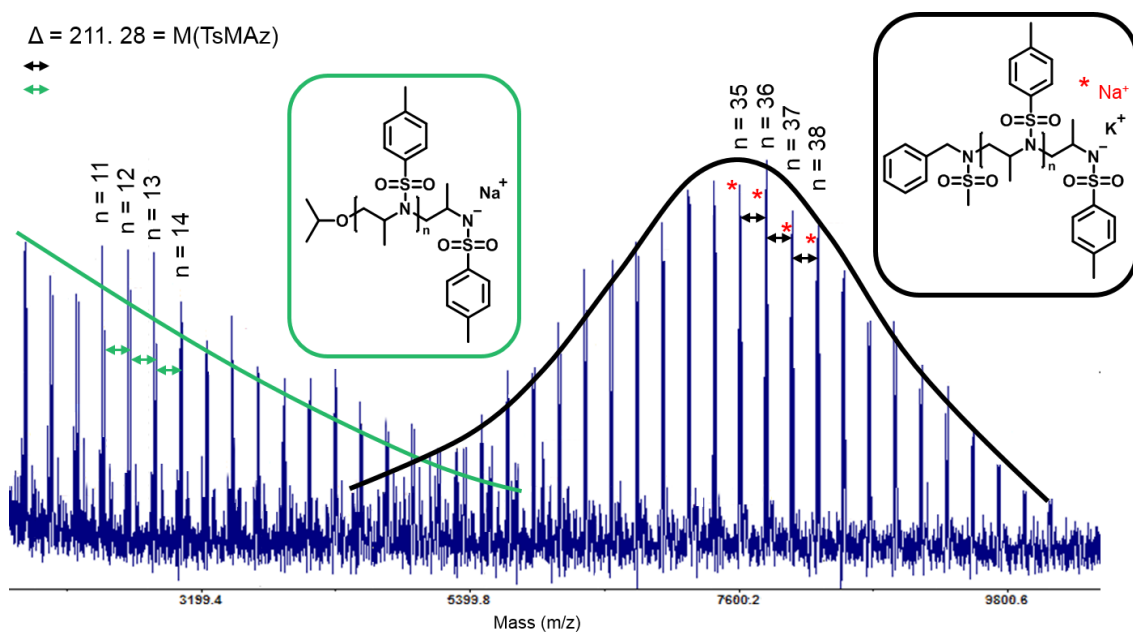


Figure S2.37. MALDI-TOF-spectrum of P(Ts)-iPrOH-100eq (Table S10).

2.12 Section F. Chain extension experiments

For chain extension experiments the polymerizations were carried out in analogy to the procedure above. After stirring the mixtures for at least 18 h, a 100 μL -sample was taken out for further analyses and the second monomer, in 1 mL DMF, was added to the screw cap vial and stirred for further 24 h at the same temperature.

Table S2.15. Overview of the performed chain extension polymerizations of TsMAz (2) in DMF with 100 equivalents water as an additive, including SEC-analyses.

Monomer	TsMAz (2)	TsMAz (2)
Additive	H ₂ O	
V / μL	17	
Equivalents (to initiator)	100	
M_n^a / g mol^{-1}	3700	5800
\mathcal{D}^a	1.16	1.18
Reaction time / h	<24	<24
Conversion / %	>99	>99
Name	P(Ts)-H ₂ O-100eq	P(Ts- <i>b</i> -Ts)-H ₂ O-100eq

^a Number-average molecular weight and molecular weight dispersity determined *via* SEC in DMF (vs. PEO standards).

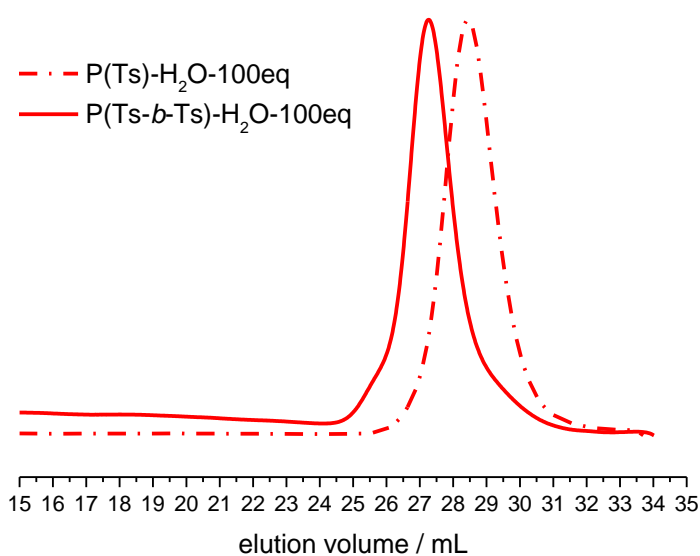


Figure S2.38. SEC traces of the chain extension of P(TsMAz) and P(TsMAz-*b*-TsMAz) with water (100 eq.) as an additive in DMF (RI signal).

Table S2.16. Overview of the performed chain extension polymerizations of TsMAz (2) in DMF with 100 μ L methanol as an additive, including SEC-analyses.

Monomer	TsMAz (2)	TsMAz (2)
Additive	MeOH	
V / μ L	100	
Equivalents (to initiator)	362	
M_n^a / g mol ⁻¹	2600	5400
\mathcal{D}^a	1.25	1.21
Reaction time / h	<24	<24
Conversion / %	>99	>99
Name	P(Ts)-MeOH-100 μ L	P(Ts- <i>b</i> -Ts)-MeOH-100 μ L

^a Number-average molecular weight and molecular weight dispersity determined *via* SEC in DMF (vs. PEO standards).

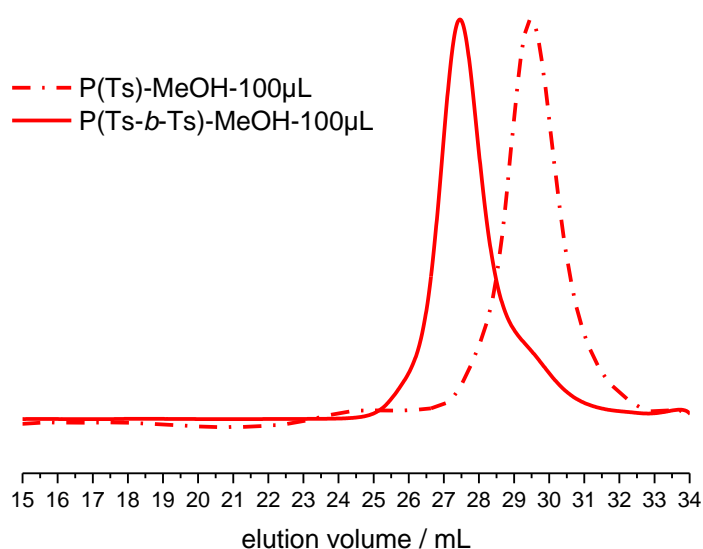


Figure S2.39. SEC traces of the chain extension of P(TsMAz) and P(TsMAz-*b*-TsMAz) with methanol (100 eq.) as an additive in DMF (RI signal).

Table S2.17. Overview of the performed chain extension polymerizations of TsMAz (2) in DMF with 50 μ L ethanol as an additive, including SEC-analyses.

Monomer	TsMAz (2)	TsMAz (2)
Additive	EtOH	
V / μ L	50	
Equivalents (to initiator)	90	
M_n^a / g mol ⁻¹	3800	6200
\mathcal{D}^a	1.16	1.17
Reaction time / h	<24	<24
Conversion / %	>99	>99
Name	P(Ts)-EtOH-50 μ L	P(Ts- <i>b</i> -Ts)-EtOH-50 μ L

^a Number-average molecular weight and molecular weight dispersity determined *via* SEC in DMF (vs. PEO standards).

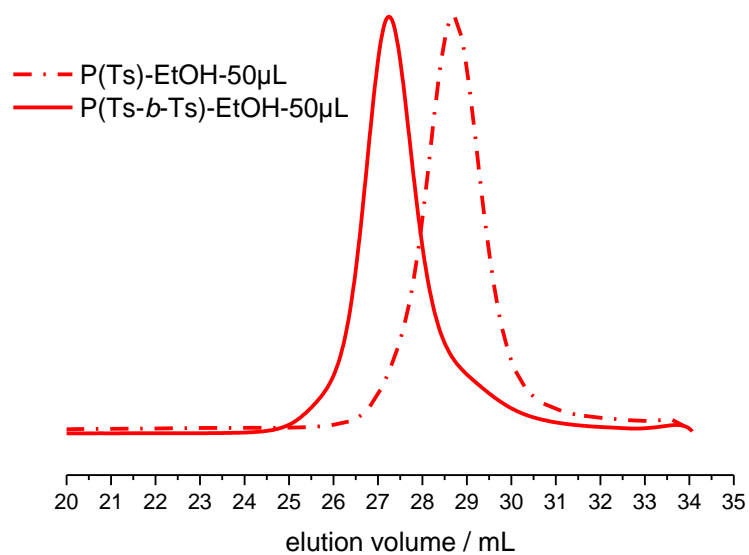


Figure S2.40. SEC traces of the chain extension of P(TsMAz) and P(TsMAz-*b*-TsMAz) with ethanol (50 μ L) as an additive in DMF (RI signal).

Table S2.18. Overview of the performed chain extension polymerizations of TsMAz (2) in DMF with 100 μ L isopropanol as an additive, including SEC-analyses.

Monomer	TsMAz (2)	TsMAz (2)
Additive	iPrOH	
V / μ L	200	
Equivalents (to initiator)	275	
M_n^a / g mol^{-1}	3800	6200
\mathcal{D}^a	1.16	1.20
Reaction time / h	<24	<24
Conversion / %	~60	>99
Name	P(Ts)-iPrOH-200 μ L	P(Ts- <i>b</i> -Ts)-iPrOH-200 μ L

^a Number-average molecular weight and molecular weight dispersity determined *via* SEC in DMF (vs. PEO standards).

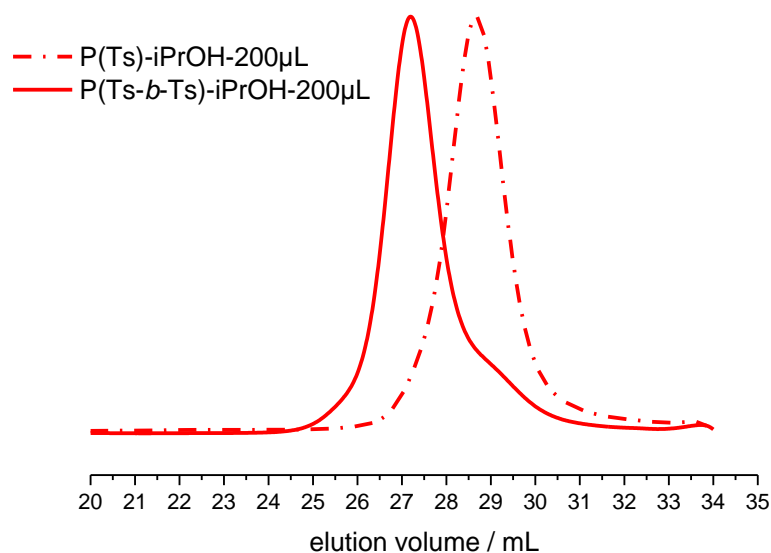


Figure S2.41. SEC traces of the chain extension of P(TsMAz) and P(TsMAz-*b*-TsMAz) with isopropanol (200 μ L) as an additive in DMF (RI signal).

2.13 Section G: Computational Detail

All DFT calculations were carried out with the Gaussian 09 package.⁸ The structures were optimized at the B3LYP level of theory,⁹ with the basis set of 6-31+G*.¹⁰⁻¹¹ The harmonic frequency calculations were performed at the same level of theory to characterize the nature of stationary points, i.e. no imaginary frequencies were found for all optimized structures. The thermostistical contributions to the free energy were obtained from a harmonic oscillator approximation at a temperature of 323.15 K and for 1 atm pressure. Accurate electronic energies were obtained from single point calculations at the B3LYP level upon the optimized structures, in conjunction with the 6-311++G** basis set.^{10, 12} The single point calculations were performed together with PCM (Polarizable Continuum Model) model¹³⁻¹⁵ by employing DMF as the solvent. To calculate the pK_a values, the SMD solvation model¹⁶ was used to compute the solvation Gibbs free energies by employing the gas-phase optimized structures, and with DMF as the solvent. Gibbs free energy of the proton was back corrected by assigning the pK_a value of water equal to 14. Note that the aim of our DFT calculations on pK_a values was not to have accurate numbers compared to the experimental data, but to describe the relative strength of the acidities. IPs and EAs were computed with the solution-phase single point electronic energies while the pKa values with the solution-phase Gibbs free energies which are the summation of gas-phase single point electronic energies, the gas-phase thermostistical contributions and the SMD solvation Gibbs free energies.

The following equations have been used to calculate the interested properties:

$$\mu = -\frac{1}{2}(\text{IP} + \text{EA}) \quad (1)$$

$$\eta = \text{IP} - \text{EA} \quad (2)$$

where IP is ionization potential, EA is electron affinity, η is chemical potential and μ is chemical hardness. The IP and EA were calculated based on the relax geometries of cations and anions.

$$\omega^+ = \frac{\mu^2}{2\eta} \quad (3)$$

$$\omega^- = \frac{1}{2} \frac{(\mu_A - \mu_B)^2}{(\eta_A + \eta_B)^2} \eta_A \quad (4)$$

where ω^+ is electrophilicity index,¹⁷ and ω^- is nucleophilicity index.¹⁸ Details of these two indexes can be found in ref.¹⁹.

The pK_a values were calculated according to equation 5:

$$pK_a = \frac{\Delta G}{2.303 RT} \quad (5)$$

where ΔG is the Gibbs free energy difference of the deprotonation reactions (in kcal mol^{-1}), R is the gas constant ($1.987 \times 10^{-3} \text{ kcal mol}^{-1} \text{ K}^{-1}$), and T is the temperature (in K).

Table S2.19. Calculated ionization potential (IP), electron affinity (EA), the chemical potential (μ), chemical hardness (η), energies of LUMO (ϵ_{LUMO}) and HOMO (ϵ_{HOMO}), electrophilicity index (ω^+) all values are in eV. NBO C atoms.

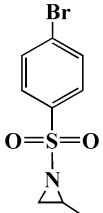
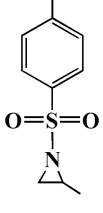
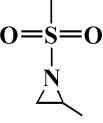
Monomer	IP	EA	μ	η	ϵ_{LUMO}	ω^+	q_c
	7.06	2.22	-4.64	4.84	-1.75	2.22	-0.1937
	6.96	1.95	-4.45	5.01	-1.44	1.98	-0.1952
	7.19	0.80	-3.99	6.39	-0.24	1.25	-0.1945

Table S2.20. Calculated ionization potential (IP), electron affinity (EA), the chemical potential (μ), chemical hardness (η), energies of LUMO (ϵ_{LUMO}) and HOMO (ϵ_{HOMO}), nucleophilicity index (ω^-), all values are in eV. NBO charges on N/O atoms.

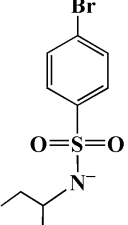
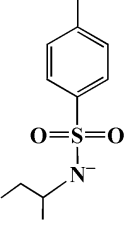
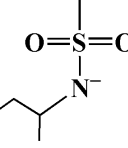
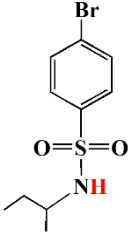
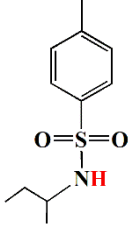
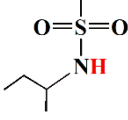
Nucleophile	IP	EA	μ	η	ϵ_{HOMO}	ω^-	N/O
	4.91	-2.76	-1.07	7.67	-5.44	0.27	-1.0303
	4.82	-0.74	-2.04	5.56	-5.36	0.14	-1.0328
	4.81	-0.57	-2.12	5.38	-5.30	0.13	-1.0405
isoPrO ⁻	4.55	-0.42	-2.07	4.97	-4.72	0.14	-1.0525
EtO ⁻	4.37	-0.48	-1.94	4.85	-4.70	0.16	-1.0484
MeO ⁻	4.38	-0.53	-1.93	4.91	-4.67	0.16	-1.0569
HO ⁻	5.16	-0.63	-2.27	5.79	-5.40	0.13	-1.4002

Table S2.21. Calculated ΔG (in kcal mol⁻¹) and pK_a values with DMF as a solvent and at 323.15 K.

Protonated species	ΔG	pK _a
H ₂ O	20.7	14.0
MeOH	17.9	12.1
EtOH	17.8	12.0
isoPrOH	18.5	12.5
	-0.8	-0.5
	2.0	1.4
	2.3	1.5

2.14 Section H. Polymerization of unprotected hydroxyl-functionalized sulfonyl aziridine

2.14.1 Monomer synthesis of 2- ω -propanol-*N*-tosylaziridine (6)

Chloramine-T (7.01 g, 46 mmol, 1 eq.) was dried by freeze-drying with benzene in vacuum overnight. But-3-en-1-ol (12 mL, 138 mmol, 3 eq.) was added together with Chloramine-T and phenyltrimethylammonium tribromide (PTAB) (1.74 g, 4.6 mmol, 0.1 eq.) to the reaction flask, the mixture was dissolved in anhydrous acetonitrile (ACN) (100 mL). The mixture was stirred at room temperature for 3 days. 100 mL of ethyl acetate and water were added to the reaction flask, the organic phase was washed with brine, separated, and dried with Mg_2SO_4 . The organic phase was concentrated at reduced pressure. The crude product was purified by column chromatography over silica gel (Et₂O 100%; R_f : 0.2). The pure product crystallized as white crystals.

¹H NMR (300 MHz, 298K, CD₂Cl₂) δ [ppm] = 7.70 (d, 2H, a), 7.30 (d, 2H, b), 3.61 – 3.46 (m, 2H, c), 2.76 (m, 1H, d), 2.51 (d, 1H, d), 2.37 (s, 3H, f), 2.06 (d, 1H, g), 1.92 – 1.69 (m, 2H, h), 1.37 (m, 1H, i).

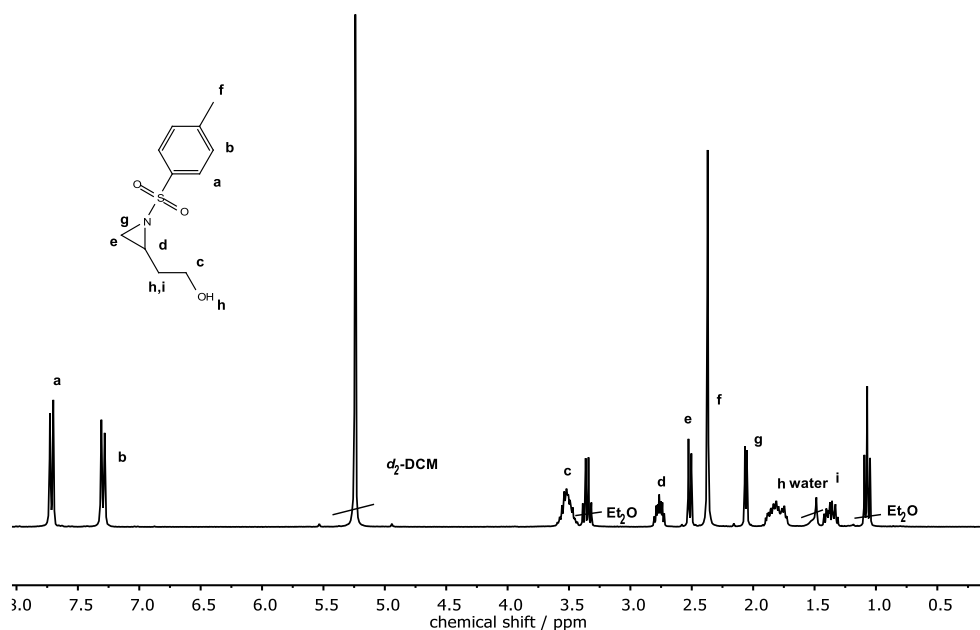


Figure S2.42: ¹H NMR (300 MHz, 298K, DCM-*d*₂) of (6).

2.14.2 Polymerizations: Example for P(6)₂₀

(6) (0.38 mmol, 20 eq.) was dissolved in 1 mL *N,N*-dimethylformamide (DMF). The Initiator (BnNHMs) was dissolved in 1 mL DMF and added to KHMDS (1/1), 1 eq. of the deprotonated initiator was then transferred with a syringe to the reaction flask, containing the monomer. The mixture was stirred at 55 °C for 20 h. The polymer was isolated by removing DMF at reduced pressure (yields: quantitative).

¹H NMR (300 MHz, 298 K, DCM-*d*₂) of P(6)₂₀: δ 7.84 (s, 2H, a), 7.33 (s, 2H, b), 4.50 – 2.67, 1.30-2.12 (m, 7H, c).

¹³C NMR (176 MHz, 323 K, DMF-*d*₇) of P(6)₂₀, δ [ppm] =144.02 (s, 1C, arom.), 137.21 (s, 1C, arom.), 130.40 (s, 2C, arom.), 127.41 (s, 2C, arom.), 59.49-45.72 (m, 4C, backbone), 21.10 (s, 1C, arom-CH₃).

Table S2.22: Overview of performed polymerizations with (6).

Sample	<i>D</i>	<i>M_n</i> (SEC)	<i>M_p</i> (SEC)	<i>M_n</i> (Theory)
P(6) ₂₀	1.26	1600	2000	3300
P(6) ₃₀	1.30	1700	2100	5000
P(6) ₄₀	1.34	2300	2800	6600

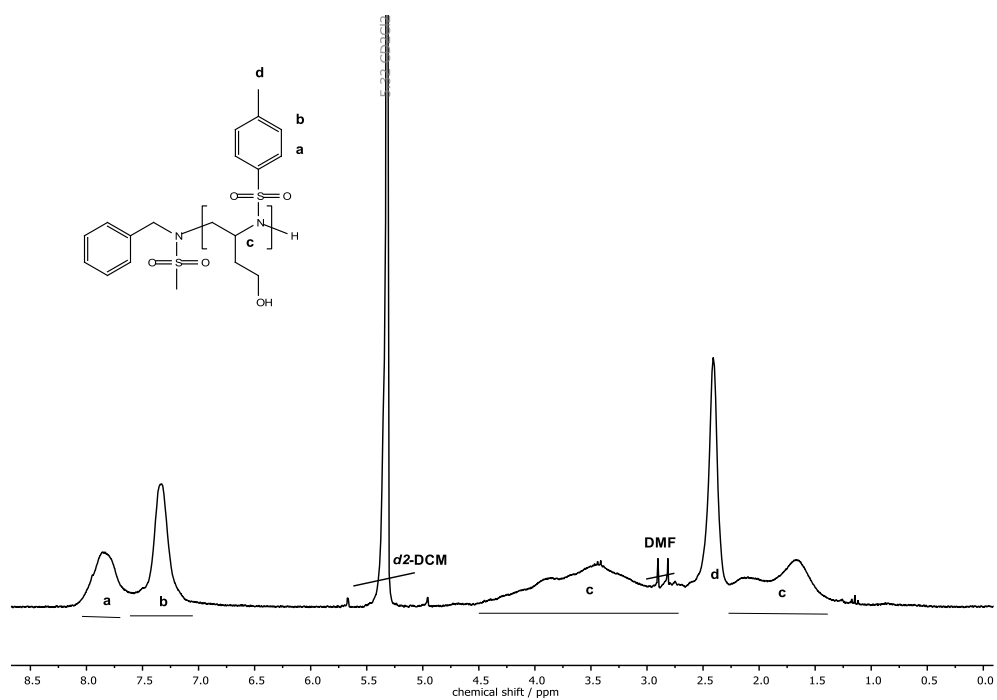


Figure S2.43: ^1H NMR (300 MHz, 298 K, $\text{DCM-}d_2$) of $\text{P}(\mathbf{6})_{20}$.

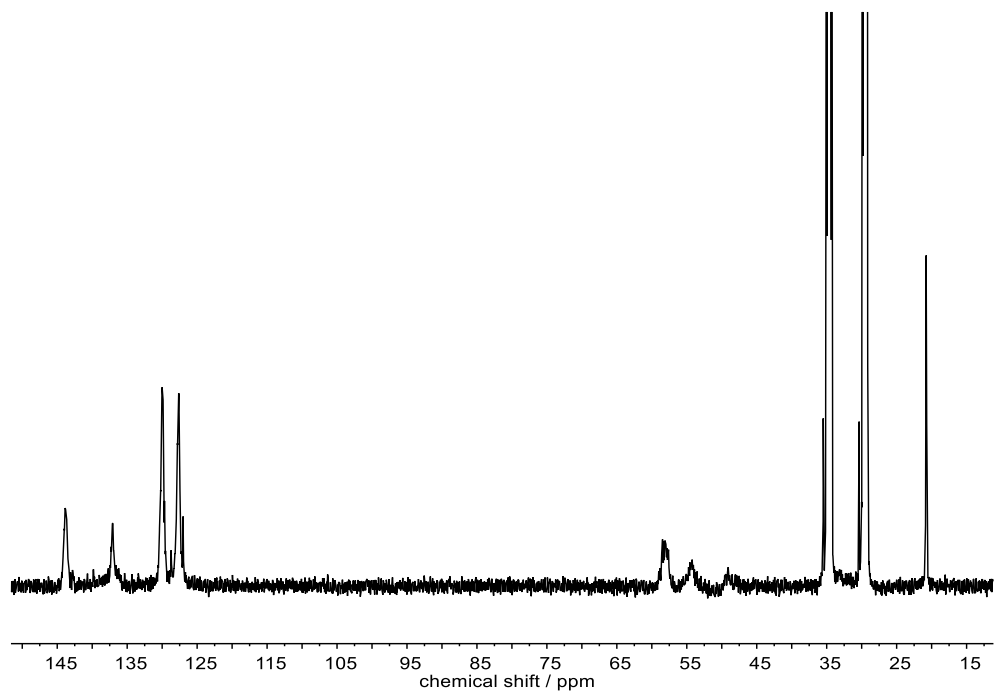


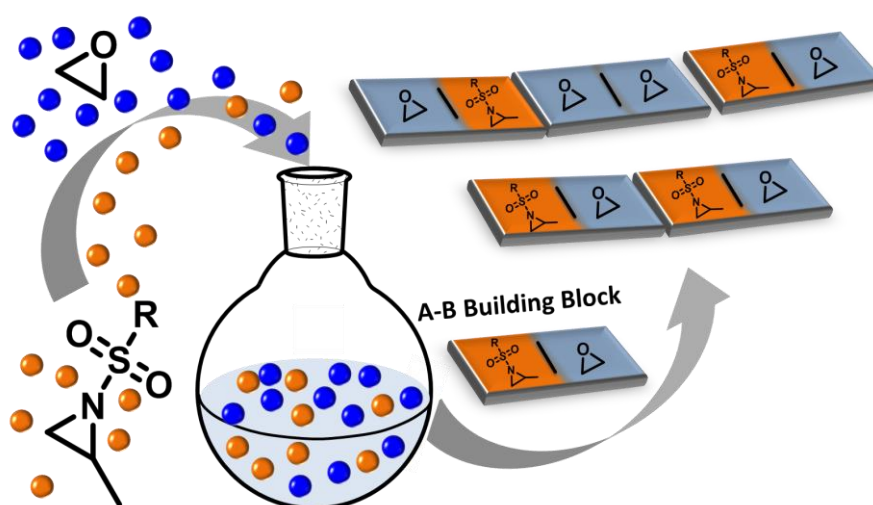
Figure S2.44: ^{13}C NMR (176 MHz, 323 K, $\text{DMF-}d_7$) of $\text{P}(\mathbf{6})_{20}$.

2.15 Additional References Chapter 2

1. Rieger, E.; Alkan, A.; Manhart, A.; Wagner, M.; Wurm, F. R., Sequence-Controlled Polymers via Simultaneous Living Anionic Copolymerization of Competing Monomers. *Macromol Rapid Commun* **2016**, *37* (10), 833-839.
2. Rieger, E.; Manhart, A.; Wurm, F. R., Multihydroxy Polyamines by Living Anionic Polymerization of Aziridines. *ACS Macro Lett.* **2016**, *5* (2), 195-198.
3. Rieger, E.; Gleede, T.; Weber, K.; Manhart, A.; Wagner, M.; Wurm, F. R., The living anionic polymerization of activated aziridines: a systematic study of reaction conditions and kinetics. *Polym. Chem.* **2017**, *8* (18), 2824-2832.
4. Odian, G., *Principles of Polymerization*. 4. ed.; John Wiley & Sons, Inc. : Hoboken, New Jersey, USA, 2004.
5. Freeman, R.; Hill, H.; Kaptein, R., Proton-decoupled NMR. Spectra of carbon-13 With the nuclear overhauser effect suppressed. *Journal of Magnetic Resonance (1969)* **1972**, *7* (3), 327-329.
6. Popov, M., *Modern NMR techniques and their application in chemistry*. CRC Press: 1990.
7. Sotak, C.; Dumoulin, C., Topics in carbon-13 NMR spectroscopy, GC Levy, Ed. *Wiley, New York* **1984**, *4*, 91.
8. Frisch, M.; Trucks, G.; Schlegel, H.; Scuseria, G.; Robb, M.; Cheeseman, J.; Scalmani, G.; Barone, V.; Mennucci, B.; Petersson, G., Gaussian 09, revision D. 01. Gaussian, Inc., Wallingford CT: 2009.
9. Becke, A. D., Density-functional thermochemistry. III. The role of exact exchange. *The Journal of chemical physics* **1993**, *98* (7), 5648-5652.
10. Clark, T.; Chandrasekhar, J.; Spitznagel, G. W.; Schleyer, P. V. R., Efficient diffuse function-augmented basis sets for anion calculations. III. The 3-21+ G basis set for first-row elements, Li-F. *Journal of Computational Chemistry* **1983**, *4* (3), 294-301.
11. Ditchfield, R.; Hehre, W. J.; Pople, J. A., Self-consistent molecular-orbital methods. IX. An extended Gaussian-type basis for molecular-orbital studies of organic molecules. *The Journal of Chemical Physics* **1971**, *54* (2), 724-728.
12. McLean, A.; Chandler, G., Contracted Gaussian basis sets for molecular calculations. I. Second row atoms, Z= 11-18. *The Journal of Chemical Physics* **1980**, *72* (10), 5639-5648.
13. Miertuš, S.; Scrocco, E.; Tomasi, J., Electrostatic interaction of a solute with a continuum. A direct utilization of AB initio molecular potentials for the prevision of solvent effects. *Chemical Physics* **1981**, *55* (1), 117-129.
14. Miertus, S.; Tomasi, J., Approximate evaluations of the electrostatic free energy and internal energy changes in solution processes. *Chemical physics* **1982**, *65* (2), 239-245.
15. Pascual-ahuir, J.-L.; Silla, E.; Tunon, I., GEPOL: An improved description of molecular surfaces. III. A new algorithm for the computation of a solvent-excluding surface. *Journal of Computational Chemistry* **1994**, *15* (10), 1127-1138.
16. Marenich, A. V.; Cramer, C. J.; Truhlar, D. G., Universal solvation model based on solute electron density and on a continuum model of the solvent defined by the bulk dielectric constant and atomic surface tensions. *The Journal of Physical Chemistry B* **2009**, *113* (18), 6378-6396.
17. Parr, R. G.; Szentpaly, L. v.; Liu, S., Electrophilicity index. *Journal of the American Chemical Society* **1999**, *121* (9), 1922-1924.
18. Jaramillo, P.; Pérez, P.; Contreras, R.; Tiznado, W.; Fuentealba, P., Definition of a nucleophilicity scale. *The Journal of Physical Chemistry A* **2006**, *110* (26), 8181-8187.
19. Jhon, Y. H.; Shim, J.-G.; Kim, J.-H.; Lee, J. H.; Jang, K.-R.; Kim, J., Nucleophilicity and accessibility calculations of alkanolamines: applications to carbon dioxide absorption reactions. *The Journal of Physical Chemistry A* **2010**, *114* (49), 12907-12913.

3 *Fast Access to Amphiphilic Multiblock Architectures by the Anionic Copolymerization of Aziridines and Ethylene Oxide*

*Tassilo Gleede, Elisabeth Rieger, Jan Blankenburg, Katja Klein, and
Frederik R. Wurm**



TOC 3: Table of content, symbolizing fast an easy synthesis of amphiphilic multiblock architectures from EO (blue) and Aziridines (orange)

Note: Tassilo Gleede designed, conducted and evaluated the experiments. Katja Klein assisted with the emulsion polymerization. Jan Blankenburg calculated reactivity parameters. Elisabeth Rieger assisted with beneficial discussions regarding reaction setups and data analysis. Frederik R. Wurm supervised the project. Tassilo Gleede and Frederik R. Wurm wrote the manuscript. All authors read and edited the manuscript.

This chapter is based on a published article under the terms of the Copyright this chapter is used with the permission of ACS Publications: Tassilo Gleede, Elisabeth Rieger, Jan Blankenburg, Katja Klein, Frederik R. Wurm, Fast Access to Amphiphilic Multiblock Architectures by the Anionic Copolymerization of Aziridines and Ethylene Oxide, *J. Am. Chem. Soc.* **2018**, 140, 41, 13407-13412

3.1 Abstract

An ideal system for stimuli-responsive and amphiphilic (block) polymers would be the copolymerization of aziridines with epoxides. However, to date, no copolymerization of these two highly strained three-membered heterocycles had been achieved. Herein, we report the combination of the living oxy- and azaanionic ring-opening polymerization of ethylene oxide (EO) and sulfonamide-activated aziridines. In a single step, well-defined amphiphilic block copolymers are obtained by a one-pot copolymerization. Real-time ^1H NMR spectroscopy revealed the highest difference in reactivity ratios ever reported for an anionic copolymerization (with $r_1 = 265$ and $r_2 = 0.004$ for 2-methyl-*N*-tosylaziridine/EO and $r_1 = 151$ and $r_2 = 0.013$ for 2-methyl-*N*-mesylaziridine/EO), leading to the formation of block copolymers with monomodal and moderate molecular weight distributions (M_w/M_n mostly ≤ 1.3). The amphiphilic diblock copolymers were used to stabilize emulsions and to prepare polymeric nanoparticles by miniemulsion polymerization, representing a novel class of nonionic and responsive surfactants. In addition, this unique comonomer reactivity of activated-Az/EO allows fast access to multiblock copolymers, and we prepared the first amphiphilic penta- or tetrablock copolymers containing aziridines in only one or two steps, respectively. These examples render the combination of epoxide and aziridine copolymerizations *via* a powerful strategy for producing sophisticated macromolecular architectures and nanostructures.

3.2 Introduction

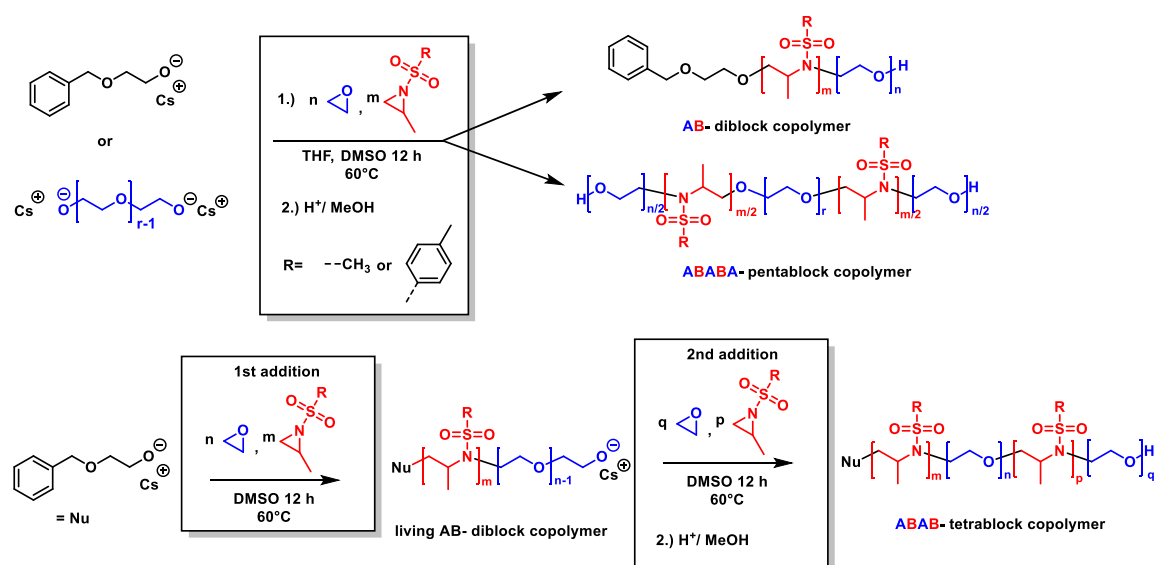
Today, a detailed understanding and control of the monomer sequence distribution during copolymerization and the synthesis of gradient and block copolymers are of growing interest.¹⁻³ Multiblock copolymers have been attracting increased amounts of attention as they have superior properties compared to those of diblock copolymers, for example, in the compatibilization of polymer blends, but also give access to sophisticated nanostructures by self-assembly.⁴⁻⁶ Their synthesis is typically achieved by the sequential monomer addition of each block *via* living or controlled polymerization techniques. Living anionic polymerization (LAP) is the polymerization technique with the highest control over the molecular weight and weight distribution and the highest precision for the synthesis of block copolymers. It also provides a precise way to end-functionalize polymers and other well-defined and complex polymer architectures.⁷⁻⁹ This requires strict purification and inert handling of all reagents to minimize chain termination or other side reactions during the whole multistep process.^{10,11} Several approaches have been recently developed in order to simplify the synthesis protocol. An elegant example was reported by Williams and others, who developed a catalyst that can be switched from the homopolymerization to copolymerization of different monomer families such as epoxides, lactones, anhydrides, and carbon dioxide to produce block copolymers in a one-pot reaction.¹²⁻¹⁴ Coates and Darensbourg's group elegantly used mono- and bimetallic catalysts to selectively synthesize block copolymers from monomer mixtures, resulting in semicrystalline polymers from racemic propylene oxide;¹⁵ multiblock polymers from ethylene and propylene,¹⁶ or ethylene oxide, carbon dioxide, and lactide.¹⁷ The living anionic polymerization of vinyl monomers was used to prepare multisegmented copolymers by the subsequent polymerization of gradient-forming comonomers. This approach reduced the number of steps by a factor of 2; however, tapered structures were obtained.¹⁸ A protocol for reducing the steps and achieving a perfect switch between the segments to prepare multiblock copolymers with a water-soluble block has, to the best of our knowledge, not been reported to date.

An ideal system for stimuli-responsive and amphiphilic polymers would be the copolymerization of aziridines with epoxides, which surprisingly has not been achieved to date. Previous attempts to carry out cationic ring-opening copolymerization of epoxides and *N*-substituted aziridines failed, as reported by Overberger and Tobkes.¹⁹ They also investigated activated tosylated aziridine and other aziridines such as aziridine carboxamide in the cationic copolymerization with epoxides but were not able to produce any copolymers from epoxides and aziridines. The anionic ring-opening polymerization of activated aziridines with sophisticated polymer architectures has been reported: the one-pot synthesis of gradient copolymers in

solution^{20,21} or in emulsion,²² organocatalytic polymerization,^{23–25} and the combination with carbanionic²⁶ or lactide polymerization.²⁷ Other well-defined polysulfonamides and polyamine derivatives with additional functional groups were reported in the last few years by our laboratory^{28,29} and Rupar's group.^{30,31} They are especially interesting because linear poly(ethylenimine) derivatives are important gene transfection agents, which are available only *via* the cationic polymerization of oxazolines with subsequent hydrolysis or as undefined hyperbranched materials.^{32–34}

3.3 Results and Discussion

Herein, we present the first anionic copolymerization of activated aziridines and ethylene oxide. This one-step protocol produces block copolymers of P(aziridine)-*b*-PEO with basically no tapered structures (Scheme 3.1). This monomer pair allows the design of di-, tetra-, or pentablock copolymers in only one or two steps. Such amphiphilic copolymers can be used as responsive surfactants to stabilize emulsion polymerization but also pave the way to well-defined PEO-based transfection or chelating agents or the design of sequence-controlled multiblock copolymers.



Scheme 3.1: Synthesis of Polyaziridine-*b*-poly(ethylene oxide) Block Copolymers by Anionic Copolymerization (2-Methyl-*N*-tosylaziridine (TsMAz), 2-methyl-*N*-mesylaziridine (MsMAz), and *N*-tosylaziridine (TsAz) were used in this study. (Top) In a single step, either AB-diblock or ABABA-pentablock copolymers can be prepared. (Bottom) Sequential addition of aziridine/EO mixture produces ABAB-tetrablock copolymers.

To enable the anionic ROP of aziridines, the ring is activated by amidation at the ring nitrogen with electron-withdrawing substituents such as tosyl or mesyl groups.^{35,36} The electron-deficient aziridines can be ring-opened by different nucleophiles and undergo living polymerization (Scheme 3.1). Here, we used the cesium alkoxide of 2-benzyloxyethanol as the

initiator in order to guarantee an efficient nucleophilic attack of both monomers and to prevent any side reactions during the oxyanionic polymerization of ethylene oxide.³⁶ Copolymers of the sulfonyl aziridines and ethylene oxide with different monomer ratios were obtained by placing both monomers in the reaction flask containing the initiator and the solvent (THF and DMSO). All copolymers were characterized by ¹H NMR spectroscopy and size exclusion chromatography (SEC) (Tables 3.1 and 3.2). After copolymerization, the full conversion of both monomers was determined. The SEC elugrams of all copolymers exhibit moderate to narrow monomodal molecular weight distributions. As SEC is a relative method, no absolute molecular weights were determined, and all molecular weights are apparent vs PEO standards. Presumably, the hydrodynamic radii of PAz are smaller than those of PEO in DMF due to the higher hydrophobicity. Compared to the theoretical molecular weight (Table 3.1), the absolute molecular weight (from NMR) is higher than that measured in SEC under these conditions, which is in accordance with the molecular weight determination *via* ¹H NMR measurements.³⁷ ¹H DOSY NMR further confirmed a successful crossover reaction between tosyl- and mesyl-activated aziridines and ethylene oxide (Figures S3.4 and S3.5). The ¹H NMR spectra show resonances for both PEO and PAz. From the ¹H NMR spectra, the absolute M_n was calculated by comparing the resonances of the initiator (at 7.3–7.2 ppm, 5H and 4.6–4.5 ppm, 2H) to the resonances of both comonomers (7.8–7.5, 2H ppm for TsMAz; 2.1–1.9 ppm, 3H for MsMAz; and 4H for ethylene glycol repeating units). If 2-methyl-*N*-tosylaziridine (TsMAz) is used as the comonomer, polymers with $M_w/M_n \leq 1.23$ were obtained, indicating an efficient crossover reaction from the activated aziridine to EO. 2-Methyl-*N*-mesylaziridine (MsMAz) and EO were polymerized with a narrow molecular weight distribution of $M_w/M_n = 1.12$ for P4. With higher degrees of polymerization of MsMAz (P5 and P6), moderate M_w/M_n ratios of around 1.5 were obtained. (SECs are shown in Figures S3.2, S3.3, S3.6, and S3.7).

Table 3.1: Characterization Data for All Polymers Based on Ethylene Oxide (EO), 2-Methyl-*N*-tosylaziridine (TsMAz), and 2-Methyl-*N*-mesylaziridine (MsMAz)

P#	Polymer ^a	M_n^a	M_n^b	M_w/M_n^b
PTsMAz- <i>b</i> -PEO				
1	P(TsMAZ ₆ - <i>b</i> -EO ₁₁₆)	7200	3700	1.20
2	P(TsMAZ ₃₅ - <i>b</i> -EO ₄₅)	9500	3200	1.23
3	P(TsMAZ ₁₂ - <i>b</i> -EO ₁₉₅)	11300	7900	1.28
PMsMAz- <i>b</i> -PEO				
4	P(MsMAZ ₅ - <i>b</i> -EO ₁₁₆)	5500	4300	1.12
5	P(MsMAZ ₅₀ - <i>b</i> - EO ₁₇₆)	14500	5200	1.56
6	P(MsMAZ ₅₆ - <i>b</i> - EO ₁₆₈)	15000	6400	1.53

^a Absolute Number-average molecular weight (in g/mol) determined *via* ¹H NMR ^b Number-average molecular weight and molecular weight dispersity determined *via* SEC in DMF (*vs.* PEO standards).

Table 3.2: Characterization Data for Multiblock Copolymers of Ethylene Oxide (EO) and 2-Methyl-*N*-tosylaziridine (TsMAz)

P#	Polymer ^a	M_n^a	M_n^b	M_w/M_n^b
Tetra block				
7	P(TsMAZ ₁₅ - <i>b</i> -EO ₂₁₁)	12600	3600	1.33
8	P(TsMAZ ₁₅ - <i>b</i> -EO ₂₁₁ - <i>b</i> -TsMAZ ₇ - <i>b</i> -EO ₁₇₀)	21600	5100	1.25
Penta block				
9	P[(EO ₆₇)] ₂	6000	3300	1.14
10	P[(EO ₆₇ - <i>b</i> -TsMAZ ₅ - <i>b</i> -EO ₉₅)] ₂	16400	4100	1.15

To elucidate the comonomer sequence, the reactivity ratios for ethylene oxide and TsMAz/MsMAz were determined by real-time ¹H NMR kinetics. The copolymerization was performed in sealed NMR tubes, and the resonances of both monomers at 2.05–1.90 ppm for the MsMAz ring protons or at 2.20–2.10 ppm for the TsMAz ring protons were integrated over time and compared to the integral of the resonance of EO (2.6–2.7 ppm) (Figures 3.1A and S3.12 and S3.16 for MsMAz). The highlighted relevant signals of the monomers show the consumption of the monomers over time.

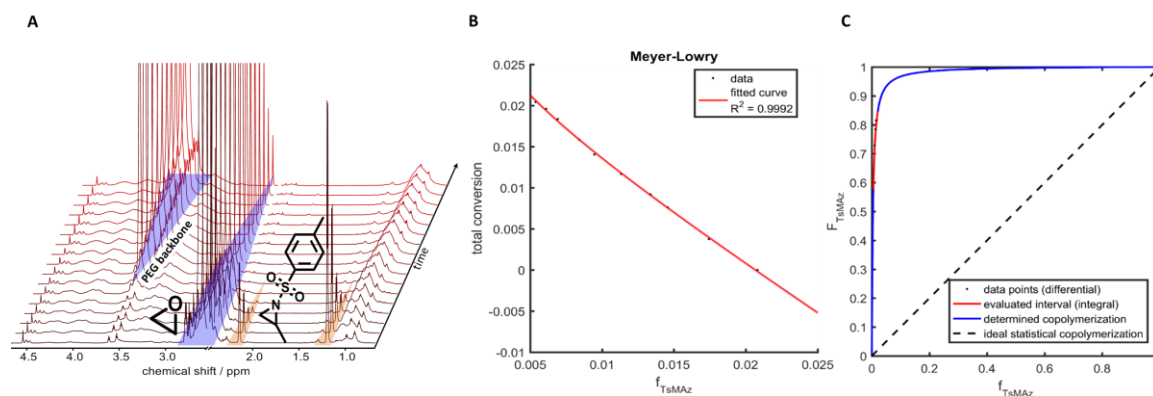


Figure 3.1. (A) Close-up image of the real-time ^1H NMR spectra of the one-pot block polymerization of EO (blue) and TsMAz (orange). (Figure S12 shows the full spectra.) (B) Meyer–Lowry fit of the real-time NMR kinetics of TsMAz and EO. (C) Copolymerization diagram of TsMAz and EO.

Figures S3.18 (MsMAz) and S3.14 (TsMAz) show the individual monomer conversion vs the total conversion of monomers; Figures S3.17 (MsMAz) and S3.13 (TsMAz) show the assembly of the individual monomers in the polymer over time, and direct information on the comonomer incorporation is accessible. In addition, the linearity of these plots underlines the living character of this copolymerization. Both MsMAz and TsMAz confirmed a much faster conversion compared to that for EO. The activated aziridines are consumed first, and EO is ring-opened only after the respective aziridine monomer has been consumed almost completely. This results in a very sharp monomer gradient with basically no tapered structure, that is, a selective polymerization of the activated aziridine first and the formation of block copolymer PAz-*b*-PEO. From the monomer conversion plots (Figures S3.14 and S3.18), only a very slight tapering effect for MsMAz is detected after about 15% conversion. A conversion of ethylene oxide of about 2% was measured, which might also be in the range of errors. For the TsMAz/EO copolymerization, no tapering was detected. In both cases, we assume the formation of block copolymers, and in the following text, we call the products “block copolymers”, even if a very small gradient might be formed. In previous work, we have proven that the sulfonamide group strongly influences the reaction kinetics for aziridines.^{20,36} Because of the electron-withdrawing effect of the sulfonamide on the aziridine ring, nucleophilic ring-opening is favored compared to that on the nonactivated ethylene oxide, resulting in higher propagation rates for the sulfonyl aziridines. This results in the selective polymerization of TsMAz or MsMAz before the propagation of EO is initiated. Thus, the electrophilicity of the activated aziridines determines the reaction rate. This however, might be different for other activating groups. As the tosyl group has a higher electron-withdrawing effect than the mesyl group, the propagation rate of TsMAz ($k_p = 12.15 \times 10^{-4}$ L/mol·s) is ca. 5-fold faster than that of MsMAz ($k_p = 2.49 \times 10^{-4}$ L/mol·s), and the overall reaction time is faster compared to those of MsMAz and EO. The reactivity ratios were determined by Meyer–Lowry (terminal model)

and Jaacks (non-terminal model, with the corresponding fits for TsMAz/EO shown in Figure 3.1B and those for MsMAz/EO shown in Figures S3.20 and S3.21).^{38,39} The reactivity ratios determined by Meyer–Lowry were used to visualize the microstructure of block copolymers for MsMAz and TsMAz (Figure 2). To the best of our knowledge, such a large difference in reactivity ratios has never been reported for anionic copolymerization. The extreme reactivity difference of these monomer pairs leads to the formation of perfect linear block copolymers for TsMAz/EO ($r_{\text{TsMAz}} = 265.0$ and $r_{\text{EO}} = 0.004$) and grafted block copolymers (branching in the SI 3, 3.6.13 and 3.6.14) and for MsMAz/EO ($r_{\text{MsMAz}} = 151.0$, $r_{\text{EO}} = 0.013$). Both methods (Jaacks and Meyer–Lowry) had very similar values for reactivity ratios, and $(r_1 \cdot r_2)$ in all cases very close to 1, confirming an ideal copolymerization and indicating that the influence of the reactive chain end is far inferior to the reactivity of the monomers. In comparison to this extreme difference in monomer reactivity, Frey and co-workers^{18,40} recently reported on the anionic copolymerization of styrene with isoprene, which produces tapered copolymers with a relatively sharp gradient ($r_1 = 11.0$ and $r_2 = 0.049$). This example was long seen as one of the most pronounced gradients reported for living anionic copolymerization. In the case of 4-methylstyrene and isoprene, an even sharper gradient with $r_1 = 25.4$ and $r_{4\text{MS}} = 0.007$ was obtained, which shortens the tapered “midblock” significantly, leading to the formation of more blocklike copolymers. More pronounced reactivity ratios are known only for catalytic polymerizations or the radical copolymerization of a sterically demanding or halogenated monomers.⁴¹

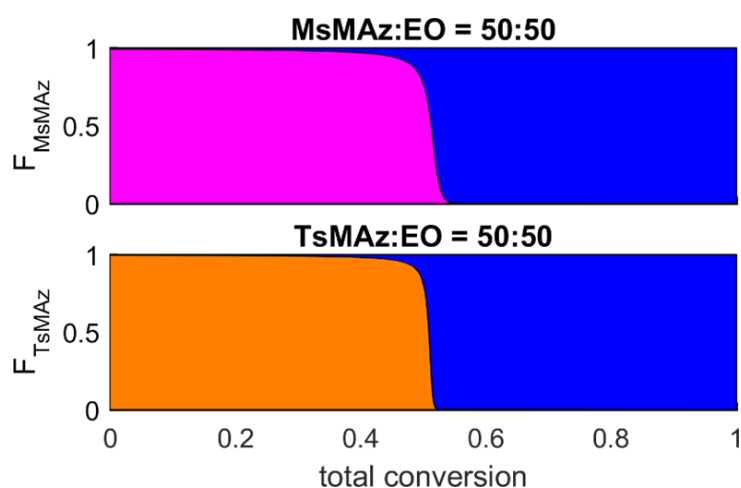


Figure 3.2: Mean composition (F) of the polymer chains versus the total conversion determined by the Meyer–Lowry fit. (Top) Simulated monomer distribution of a 50:50 block copolymer based on the reactivity ratios of MsMAz (pink) and EO (blue). (Bottom:) TsMAz (orange) and EO (blue).

Copolymers containing longer segments of MsMAz (P5 and P6) exhibited a broadened molar mass distribution, which is probably attributed to branching by deprotonation at the CH_3 group in the mesyl activating group from the active chain. This deprotonation was recently postulated by Rupar’s group and others for the anionic polymerization of mesyl-activated

azetidine (Scheme S3.1).⁴² With the fast conversion of MsMAz and the subsequent transfer to the epoxide, the basic living alkoxides chain can deprotonate the mesyl CH₃ group, and the additional PEO arms are grafted. This would lead to P(MsMAz-co-(MsMAz-g-PEO))-b-PEO structures (cf. Scheme S3.1). This grafting of PEO in the case of MsMAz was confirmed by determining the number of hydroxy groups in the copolymer. The terminal OH groups were reacted with 2-chloro-4,4,5,5-tetramethyl-1,3,2-dioxaphospholane, and the number of hydroxy groups was quantified by ³¹P NMR as reported previously.⁴³ Although the number of hydroxy groups ($n(\text{OH})$) in P1 was determined to be close to $n(\text{OH}) \approx 1$ as expected for a linear copolymer, P5 carries $n(\text{OH}) \approx 5$, which is attributed to branching by the proton abstraction of the mesyl group (Table S3.3, Figures S3.27–S3.33). Additionally, quantitative ¹³C NMR spectra of the different polymers further show the branching, and MsMAz as the integral of the terminal CH₂–OH group is 5-fold higher for P5 than for linear polymers as in P1 (Figures S3.32 and S3.33).

Having the one-pot diblock copolymer preparation established, fast access to PEO/PAz multiblock structures is available. After the one-step synthesis of a poly(TsMAz)-b-PEO, a second addition of the TsMAz/EO monomer pair to the living chains leads to an amphiphilic tetrablock copolymer, and with further $n/2$ additions, the synthesis of A-B multiblock polymers with n segments becomes possible. SEC and NMR clearly prove the block transfer and the formation of the ABAB-tetrablock copolymer (Figure 3.3A). The first addition of both monomers yielded a diblock copolymer with PTsMAz₁₅-b-PEO₂₁₁, and after the second addition, the ABAB-tetrablock with a composition of PTsMAz₁₅-b-PEO₂₁₁-b-PTsMAz₇-b-PEO₁₇₀ was obtained.

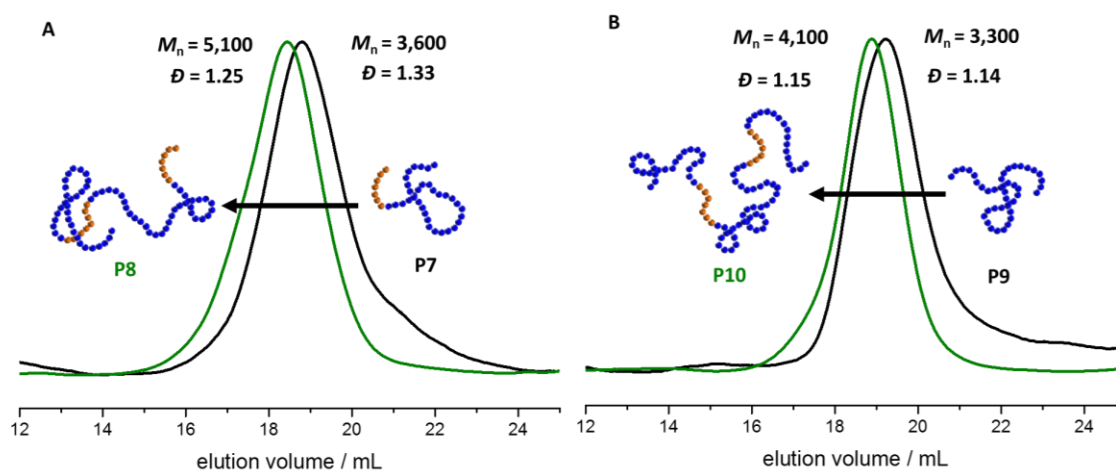


Figure 3.3: (A) SEC traces of P(TsMAz-b-PEO) (black, P7) and a tetrablock of TsMAz and EO (green, P8). (B) SEC traces of P(EO) macroinitiator (black, P9) and a pentablock of TsMAz and EO (green, P10).

ABABA-pentablock copolymers can be prepared even faster: using difunctional PEO as a macroinitiator for the copolymerization of the TsMAz/EO mixture, due to the different reactivity ratios an amphiphilic pentablock copolymer is prepared in a single step, as again confirmed by NMR and SEC (Figure 3.3B). With a PEO₁₃₄ macroinitiator, an ABABA-pentablock with the composition of P[(EO₆₇-*b*-TsMAz₅-*b*-EO₉₅)]₂ and a dispersity of 1.20 was obtained.

Prepared diblock copolymers PAz-*b*-PEO were readily soluble in tetrahydrofuran, dimethyl sulfoxide, chloroform, dichloromethane, and benzene. Except for P2 with a block ratio of 35:45 aziridine to epoxide repeating units, all polymers could be dissolved in water. Because of their amphiphilic nature, micelles are formed in water, rendering those block copolymers as interesting surfactants. The sulfonamide is additionally responsive to changes in the ionic strength of the medium (e.g., by the addition of acid or salts), allowing the block copolymers to be switched to double-hydrophilic materials by the addition of an acid. Surface tension measurements were performed on P1 (HLB = 16) and P5 (HLB = 10) as a result of their similarity to other nonionic surfactants (such as Lutensol, HLB = 18, in which HLB stands for the hydrophilic lipophilic balance).^{44,45} Analyzing the concentration-dependent surface tension showed critical micelle concentration (CMCs) for P1 of 0.05 g/L and P5 of 0.01 g/L, which are comparable to those of commercial nonionic surfactants such as Lutensol AT 50 and 80 with 0.01 g/L (Figures S3.25 and S3.26 and Table S3.2). The surface tension of the tested samples at 1 g/L was extrapolated to almost the same values with 49.3 mN/m for P1 and ca. 55 mN/m for P5 (Lu AT50 = 49.3 mN/m, Lu AT 80 = 48.6 mN/m). As the amphiphilic PAz-*b*-PEO block copolymers exhibit surfactant properties that were similar to those of conventional nonionic surfactants, we tested their capability to stabilize free-radical miniemulsion polymerization in preparing polymer nanoparticles. PAz-*b*-PEO (P1) was selected to stabilize styrene nanodroplets in direct miniemulsion polymerization. P1 was able to sterically stabilize the styrene nanodroplets and the resulting polystyrene nanoparticles effectively. The final dispersion contained well-defined PS nanoparticles with an average diameter of 92 nm (\bar{D} = 0.01, from dynamic light scattering, Figure 3.4, zeta potential = -11 mV, SEM is shown in Figure S3.23). The addition of aqueous HCl resulted in the destabilization of the dispersion resulting from the interaction of the protons with the sulfonamides (Figure S3.24) and thus allowed the film formation of polymer dispersions under acidic conditions and the recovery of the surfactant in the supernatant.

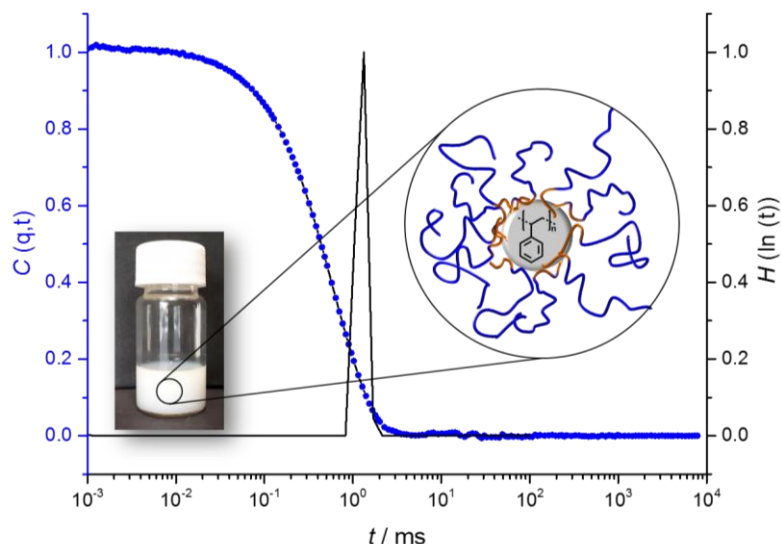


Figure 3.4: Autocorrelation function ($C(q, t)$) of PS particles (blue) and the relaxation time distribution ($H(\ln(t))$) (black). The photograph shows the aqueous dispersion (solid content = 2.0 wt %).

3.4 Summary

The first combination of aza- and oxyanionic ring-opening polymerization was performed by copolymerizing EO and MsMAz or TsMAz. Because of distinct differences in reactivity, the activated aziridines polymerize selectively as the first block and produce block copolymers in a one-pot and one-step reaction. We proved that the sulfonamide anion is able to perform an efficient crossover reaction to EO, i.e., oxyanionic ring-opening polymerization. Difunctional initiators and multiple additions of the monomers further open doors to a variety of amphiphilic ABAB or ABABA-multiblock copolymers in a reduced number of synthesis steps. The amphiphilic block copolymers can be further used as nonionic surfactants for emulsion polymerization or the production of various nanostructures by self-assembly.

3.5 References Chapter 3

1. Shanmugam, S.; Boyer, C. Stereo-, temporal and chemical control through photoactivation of living radical polymerization: synthesis of block and gradient copolymers. *J. Am. Chem. Soc.* **2015**, 137 (31), 9988–9999
2. Matyjaszewski, K.; Ziegler, M. J.; Arehart, S. V.; Greszta, D.; Pakula, T. Gradient copolymers by atom transfer radical copolymerization. *J. Phys. Org. Chem.* **2000**, 13 (12), 775–786.
3. Bates, F. S.; Fredrickson, G. H. Block Copolymers—Designer Soft Materials. *Phys. Today* **1999**, 52 (2), 32–38.
4. O'Reilly, R. K.; Hawker, C. J.; Wooley, K. L. Cross-linked block copolymer micelles: functional nanostructures of great potential and versatility. *Chem. Soc. Rev.* **2006**, 35 (11), 1068–1083.
5. Cui, H.; Chen, Z.; Zhong, S.; Wooley, K. L.; Pochan, D. J. Block copolymer assembly via kinetic control. *Science* **2007**, 317 (5838), 647–650.
6. Bates, F. S.; Hillmyer, M. A.; Lodge, T. P.; Bates, C. M.; Delaney, K. T.; Fredrickson, G. H. Multiblock polymers: panacea or Pandora's box?. *Science* **2012**, 336 (6080), 434–440.
7. Tonhauser, C.; Frey, H. A road less traveled to functional polymers: epoxide termination in living carbanionic polymer synthesis. *Macromol. Rapid Commun.* **2010**, 31 (22), 1938–1947.
8. Baskaran, D.; Müller, A. H. E. Anionic vinyl polymerization - 50 years after Michael Szwarc. *Prog. Polym. Sci.* **2007**, 32 (2), 173–219.
9. Hirao, A.; Goseki, R.; Ishizone, T. Advances in living anionic polymerization: from functional monomers, polymerization systems, to macromolecular architectures. *Macromolecules* **2014**, 47 (6), 1883–1905.
10. Hadjichristidis, N.; Pitsikalis, M.; Pispas, S.; Iatrou, H. Polymers with complex architecture by living anionic polymerization. *Chem. Rev.* **2001**, 101 (12), 3747–3792.
11. Hadjichristidis, N.; Pispas, S.; Floudas, G. Block Copolymers: Synthetic Strategies, Physical Properties, and Applications; *John Wiley & Sons*: **2003**.
12. Paul, S.; Romain, C.; Shaw, J.; Williams, C. K. Sequence Selective Polymerization Catalysis: A New Route to ABA Block Copoly(ester-b-carbonate-b-ester). *Macromolecules* **2015**, 48 (17), 6047–6056.
13. Romain, C.; Zhu, Y.; Dingwall, P.; Paul, S.; Rzepa, H. S.; Buchard, A.; Williams, C. K. Chemoselective Polymerizations from Mixtures of Epoxide, Lactone, Anhydride, and Carbon Dioxide. *J. Am. Chem. Soc.* **2016**, 138 (12), 4120–4131.
14. Stosser, T.; Chen, T. T. D.; Zhu, Y.; Williams, C. K. 'Switch' catalysis: from monomer mixtures to sequence-controlled block copolymers. *Philos. Trans. R. Soc., A* **2018**, 376 (2110), 20170066.
15. Childers, M. I.; Vitek, A. K.; Morris, L. S.; Widger, P. C. B.; Ahmed, S. M.; Zimmerman, P. M.; Coates, G. W. Isospecific, Chain Shuttling Polymerization of Propylene Oxide Using a Bimetallic Chromium Catalyst: A New Route to Semicrystalline Polyols. *J. Am. Chem. Soc.* **2017**, 139 (32), 11048–11054.
16. Eagan, J. M.; Xu, J.; Di Girolamo, R.; Thurber, C. M.; Macosko, C. W.; LaPointe, A. M.; Bates, F. S.; Coates, G. W. Combining polyethylene and polypropylene: Enhanced performance with PE/iPP multiblock polymers. *Science* **2017**, 355 (6327), 814–816.
17. Darensbourg, D. J.; Wu, G. P. A one-pot synthesis of a triblock copolymer from propylene oxide/carbon dioxide and lactide: intermediacy of polyol initiators. *Angew. Chem., Int. Ed.* **2013**, 52 (40), 10602–10606.
18. Grune, E.; Appold, M.; Müller, A. H. E.; Gallei, M.; Frey, H. Anionic Copolymerization Enables the Scalable Synthesis of Alternating (AB)_n Multiblock Copolymers with High Molecular Weight in $n/2$ Steps. *ACS Macro Lett.* **2018**, 7, 807–810.
19. Overberger, C. G. Polymerization Behavior of Aziridines with 1,2-Epoxydes. *J. Polym. Sci., Part A: Gen. Pap.* **1964**, 2 (5), 2181–2187.
20. Rieger, E.; Alkan, A.; Manhart, A.; Wagner, M.; Wurm, F. R. Sequence-Controlled Polymers via Simultaneous Living Anionic Copolymerization of Competing Monomers. *Macromol. Rapid Commun.* **2016**, 37 (10), 833–839.
21. Rieger, E.; Gleede, T.; Weber, K.; Manhart, A.; Wagner, M.; Wurm, F. R. The living anionic polymerization of activated aziridines: a systematic study of reaction conditions and kinetics. *Polym. Chem.* **2017**, 8 (18), 2824–2832.
22. Rieger, E.; Blankenburg, J.; Grune, E.; Wagner, M.; Landfester, K.; Wurm, F. R. Controlling the Polymer Microstructure in Anionic Polymerization by Compartmentalization. *Angew. Chem., Int. Ed.* **2018**, 57 (9), 2483–2487.

23. Bakkali-Hassani, C.; Rieger, E.; Vignolle, J.; Wurm, F. R.; Carlotti, S.; Taton, D. Expanding the scope of N-heterocyclic carbene-organocatalyzed ring-opening polymerization of N-tosyl aziridines using functional and non-activated amine initiators. *Eur. Polym. J.* **2017**, *95*, 746–755.
24. Bakkali-Hassani, C.; Rieger, E.; Vignolle, J.; Wurm, F. R.; Carlotti, S.; Taton, D. The organocatalytic ring-opening polymerization of N-tosyl aziridines by an N-heterocyclic carbene. *Chem. Commun.* **2016**, *52* (62), 9719–9722.
25. Wang, X.; Liu, Y.; Li, Z.; Wang, H.; Gebru, H.; Chen, S.; Zhu, H.; Wei, F.; Guo, K. Organocatalyzed Anionic Ring-Opening Polymerizations of N-Sulfonyl Aziridines with Organic Superbases. *ACS Macro Lett.* **2017**, *6*, 1331–1336.
26. Thomi, L.; Wurm, F. R. Aziridine Termination of Living Anionic Polymerization. *Macromol. Rapid Commun.* **2014**, *35* (5), 585–589.
27. Bakkali-Hassani, C.; Coutouly, C.; Gleede, T.; Vignolle, J.; Wurm, F. R.; Carlotti, S.; Taton, D. Selective Initiation from Unprotected Aminoalcohols for the N-Heterocyclic Carbene-Organocatalyzed Ring-Opening Polymerization of 2-Methyl-N-tosyl Aziridine: Telechelic and Block Copolymer Synthesis. *Macromolecules* **2018**, *51* (7), 2533–2541.
28. Rieger, E.; Manhart, A.; Wurm, F. R. Multihydroxy Polyamines by Living Anionic Polymerization of Aziridines. *ACS Macro Lett.* **2016**, *5* (2), 195–198.
29. Gleede, T.; Rieger, E.; Homann-Müller, T.; Wurm, F. R. 4-Styrenesulfonyl-(2-methyl)aziridine: The First Bivalent Aziridine-Monomer for Anionic and Radical Polymerization. *Macromol. Chem. Phys.* **2018**, *219*, 1700145.
30. Reisman, L.; Mbarushimana, C. P.; Cassidy, S. J.; Rugar, P. A. Living Anionic Copolymerization of 1-(Alkylsulfonyl) aziridines to Form Poly (sulfonylaziridine) and Linear Poly (ethylenimine). *ACS Macro Lett.* **2016**, *5* (10), 1137–1140.
31. Mbarushimana, P. C.; Liang, Q.; Allred, J. M.; Rugar, P. A. Polymerizations of Nitrophenylsulfonyl-Activated Aziridines. *Macromolecules* **2018**, *51* (3), 977–983.
32. Tauhardt, L.; Kempe, K.; Knop, K.; Altuntaş, E.; Jäger, M.; Schubert, S.; Fischer, D.; Schubert, U. S. Linear Polyethyleneimine: Optimized Synthesis and Characterization - On the Way to “Pharmagrade” Batches. *Macromol. Chem. Phys.* **2011**, *1918*–1924.
33. Jager, M.; Schubert, S.; Ochrimenko, S.; Fischer, D.; Schubert, U. S. Branched and linear poly(ethylene imine)-based conjugates: synthetic modification, characterization, and application. *Chem. Soc. Rev.* **2012**, *41* (13), 4755–4767.
34. Monnery, B. D.; Hoogenboom, R. Synthesis and Properties of Polyalkylenimines. Cationic Polymers in Regenerative Medicine; *Royal Society of Chemistry: London*, **2015**; pp 30–61.
35. Stewart, I. C.; Lee, C. C.; Bergman, R. G.; Toste, F. D. Living Ring-Opening Polymerization of N-Sulfonylaziridines: Synthesis of High Molecular Weight Linear Polyamines. *J. Am. Chem. Soc.* **2005**, *127* (50), 17616–17617.
36. Gleede, T.; Rieger, E.; Liu, L.; Bakkali-Hassani, C.; Wagner, M.; Carlotti, S.; Taton, D.; Andrienko, D.; Wurm, F. R. Alcohol- and Water-Tolerant Living Anionic Polymerization of Aziridines. *Macromolecules* **2018**, *51* (15), 5713–5719.
37. Thomi, L.; Wurm, F. R. Living Anionic Polymerization of Functional Aziridines. *Macromol. Symp.* **2015**, *349* (1), 51–56.
38. Blankenburg, J.; Wagner, M.; Frey, H. Well-Defined Multi-Amino-Functional and Stimuli-Responsive Poly (propylene oxide) by Crown Ether Assisted Anionic Ring-Opening Polymerization. *Macromolecules* **2017**, *50* (22), 8885–8893.
39. Rieger, E.; Blankenburg, J.; Grune, E.; Wagner, M.; Landfester, K.; Wurm, F. R. Controlling the polymer microstructure in anionic polymerization by compartmentalization. *Angew. Chem., Int. Ed.* **2017**, *57* (9), 2483–2487.
40. Grune, E.; Johann, T.; Appold, M.; Wahlen, C.; Blankenburg, J.; Leibig, D.; Müller, A. H. E.; Gallei, M.; Frey, H. One-Step Block Copolymer Synthesis versus Sequential Monomer Addition: A Fundamental Study Reveals That One Methyl Group Makes a Difference. *Macromolecules* **2018**, *51* (9), 3527–3537.
41. Brandrup, J.; Immergut, E. H.; Grulke, E. A.; Abe, A.; Bloch, D. R. *Polymer Handbook*; Wiley: New York, **1989**; Vol. 7.
42. Reisman, L.; Rowe, E. A.; Liang, Q.; Rugar, P. A. The anionic ring-opening polymerization of N-(methanesulfonyl) azetidine. *Polym. Chem.* **2018**, *9*, 1618–1625.
43. Balakshin, M.; Capanema, E. On the quantification of lignin hydroxyl groups with ³¹P and ¹³C NMR spectroscopy. *J. Wood Chem. Technol.* **2015**, *35* (3), 220–237.

- 44 Griffin, W. C. Calculation of HLB values of non-ionic surfactants. *J. Soc. Cosmet. Chem.* **1954**, 5 (4), 249– 256.
- 45 Guo, X.; Rong, Z.; Ying, X. Calculation of hydrophile-lipophile balance for polyethoxylated surfactants by group contribution method. *J. Colloid Interface Sci.* **2006**, 298 (1), 441– 450.

3.6 Supporting Information for Fast access to amphiphilic multi-block architectures by anionic copolymerization of aziridines and ethylene oxide

3.6.1 Chemicals.

Solvents and reagents were purchased from Acros Organics, TCI, Sigma-Aldrich or Fluka and used as received unless otherwise stated (2-(benzyloxy)ethan-1-ol, 1,4-bis(hydroxy-methyl)-benzene) methanol, diethylether, anhydrous DMSO, sodium, benzophenone). Deuterated solvents were purchased from Deutero GmbH. 2-methyl-*N*-tosylaziridine (TsMAz) and 2-methyl-*N*-mesylaziridine (MsMAz) were synthesized according to already published procedures and dried by azeotropic distillation from benzene to remove traces of water.¹ Ethylene oxide was purified before use by distillation from dry butyl lithium into a clean and dry ampule. Cesium hydroxide monohydrate was handled inside of a glove box. Tetrahydrofuran was freshly distilled and stored over blank sodium with traces of benzophenone, purple color indicating absence of water.

3.6.2 Methods.

¹H NMR ³¹P NMR and ¹³C NMR spectra were recorded using, a Bruker Avance 300, a Bruker Avance III 500, or a Bruker Avance III 700. All spectra were referenced internally to residual proton signals of the deuterated solvent, ³¹P NMR were referenced to the used standard signal at 148.60 ppm. For P1-P6 SEC measurements in dimethylformamide (DMF) (containing 1.0 g/L of lithium bromide as an additive) an Agilent 1100 Series was used as an integrated instrument, including a GRAM (PSS) column (10000/1000/100 Å), a UV detector (270 nm), and a RI detector at a flow rate of 1 mL/min at 60 °C. Calibration was carried out using PEO standards provided by Polymer Standards Service. For P7-P10 SEC measurements were done in dimethylformamide (DMF) (containing 0.25 g/L of lithium bromide as an additive) an Agilent 1100 Series was used as an integrated instrument, including a PSS HEMA column (106/105/104 g/mol), a UV detector (275 nm), and a RI detector at a flow rate of 1 mL/min at 50 °C. Calibration was carried out using PEO standards provided by Polymer Standards Service.

Differential scanning calorimetry measurements were performed using a Mettler Toledo DSC 823 calorimeter. Three scanning cycles of heating-cooling were performed in the temperature range from -140 to 250 °C. Heating rates of 10 °C/min were employed under nitrogen (30 mL/min). Surface tension measurements to determine the critical micelle concentration were performed using a DCAT 11 EC tensiometer (Dataphysics, Filderstadt,

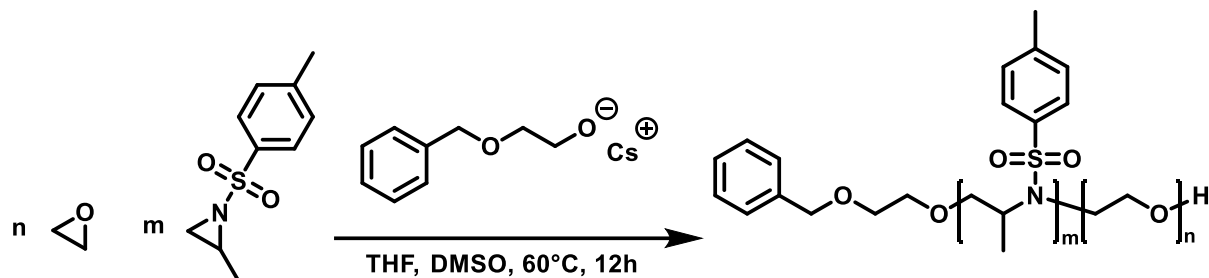
Germany) equipped with a TV 70 temperature control unit, an LDU 1/1 liquid dosing and a refill unit, as well as an RG 11 Du Nouy ring. All solutions were stirred for 120 s at a stirring rate of 50%. The tension values were measured three times after 300 s. The CMC was determined by linear regression of the slopes at high and at low concentration. The point of intersection was determined as the CMC. The Du Nouy ring was washed with water and annealed in a butane flame prior to use.

Scanning electron microscopy (SEM) was performed on a 1530 LEO Gemini microscope (Zeiss, Oberkochen, Germany). The nanoparticle dispersion (10 μL) was diluted in 3 mL of distilled water, drop-cast onto silica wafers, and dried under ambient conditions. Afterward the silica wafers were placed under the microscope and each sample was analyzed at a working distance of ~ 3 mm and an accelerating voltage of 0.2 kV.

Dynamic light scattering measurements (DLS) were performed on an ALV spectrometer consisting of a goniometer and an ALV-5004 multiple-tau full-digital correlator (320 channels) which allows measurements over an angular range from 20° to 150° . A He-Ne Laser operating at a laser wavelength of 632.8 nm was used as light source. For temperature controlled measurements the light scattering instrument is equipped with a thermostat from Julabo. Diluted samples were filtered through PTFE membrane filters with a pore size of 0.45 μm (LCR syringe filters). Measurements were performed at 20°C at different angles ranging from 30° to 150° .

3.6.3 One Pot block polymerization procedure

3.6.3.1 General procedure for the copolymerization of activated aziridines and EO.



Example with the calculated amounts for P1: All glassware was flame-dried at reduced pressure before the reaction. The initiator 2-(benzyloxy)ethan-1-ol (28.8 mg, 190 μmol , 1 eq), and 28.6 mg (170 μmol , 0.9 eq.) cesium hydroxide monohydrate were placed in a 100 mL Schlenk flask and suspended in 10 mL benzene. The mixture is stirred at 60 °C under an argon atmosphere for 1 h, evacuated at 80 °C (10^{-2} mbar) for 3 h to remove benzene and residual water azeotropically and to generate the corresponding cesium alkoxides initiator. Subsequently, approx. 20 mL dry THF were cryo-transferred into the Schlenk flask to dissolve the initiator. 0.9 mL (18 mmol, 95 eq) ethylene oxide were cryo-transferred into a graduated ampule and then into the reaction flask containing the initiator in THF. In a separate flask, the respective amount of the activated aziridine (TsMAz or MsMAz) was dissolved in ca. 3 mL benzene and dried for ca. 4h at reduced pressure to remove traces of water by azeotropic distillation. Then 200 mg (0.95 mmol, 5 eq) TsMAz was added *via* syringe with 1 mL anhydrous DMSO. The reaction mixture was heated to 60 °C and stirred for 12 h before the living chain ends were terminated with methanol and the copolymer was precipitated in cold diethyl ether to remove potentially unreacted monomers and DMSO. The copolymers were obtained as white to a light yellow solid in high yield (82%).

^1H NMR (300 MHz, Chloroform-*d*) δ 7.76 (m, 12H) TsMAz, 7.42 – 7.12 (m, 12H) TsMAz, 4.54 (d, 2H) Initiator, 4.42 – 4.16 (m, 6H) 3.64 (s, 464H) PEO, 2.40 (m, 18H), 1.16 – 0.69 (m, 18H) TsMAz.

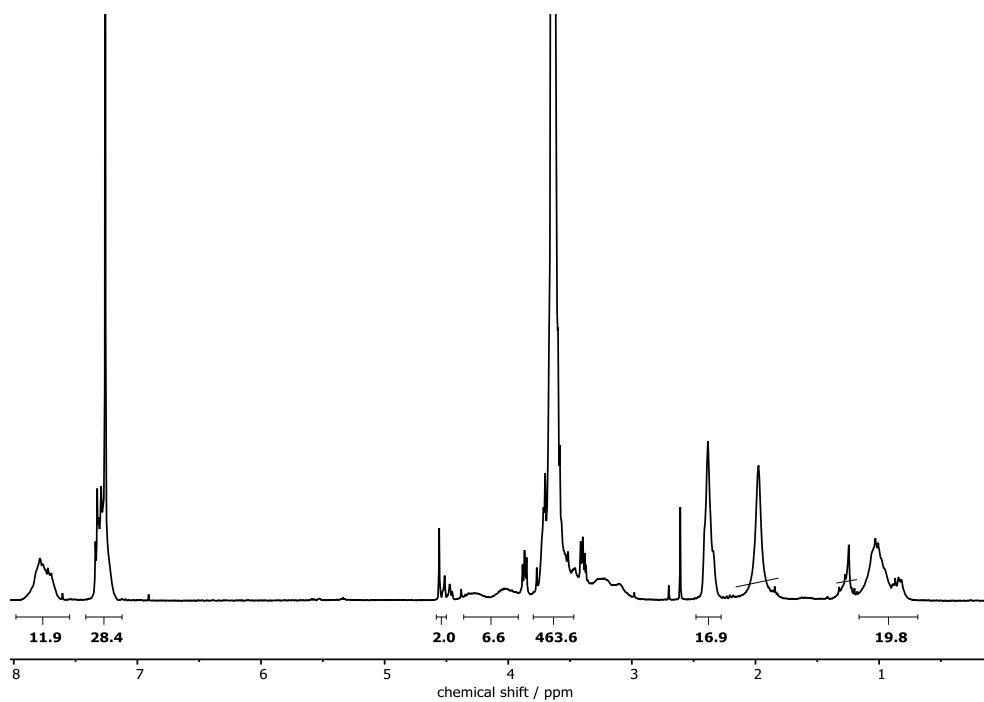


Figure S3.1: ^1H NMR of P1 (300 MHz, Chloroform-*d*).

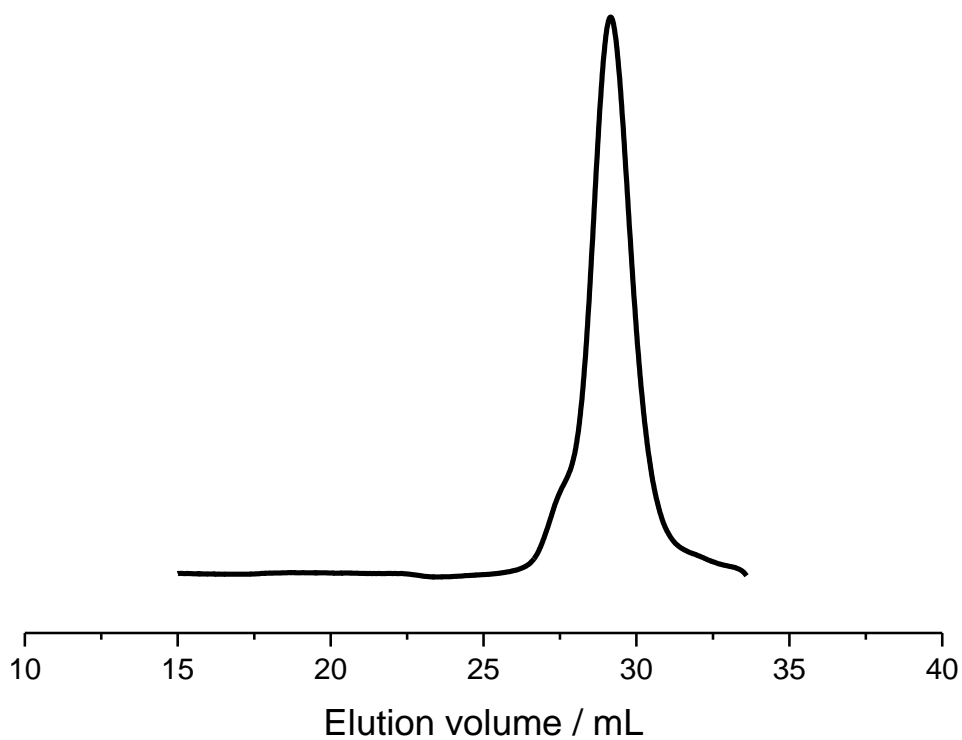


Figure S3.2: SEC trace of P(TsMAz6-b-PEO116) (P1) in DMF, RI-signal.

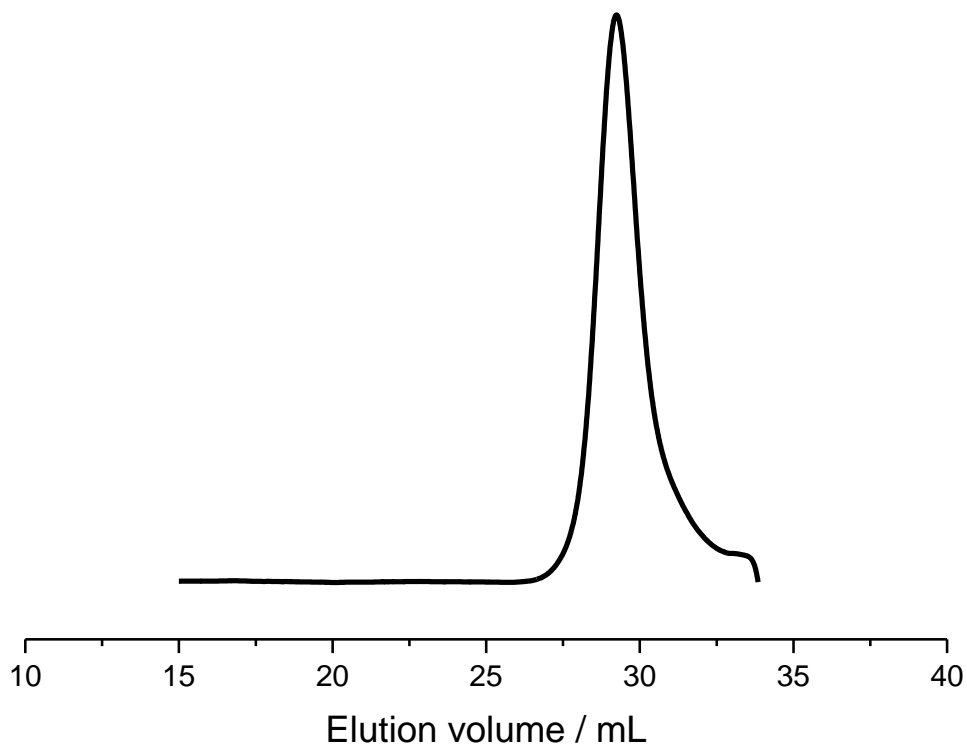


Figure S3.3: SEC trace of P(TsMAz35-b-PEO45) (P2) in DMF, RI-signal.

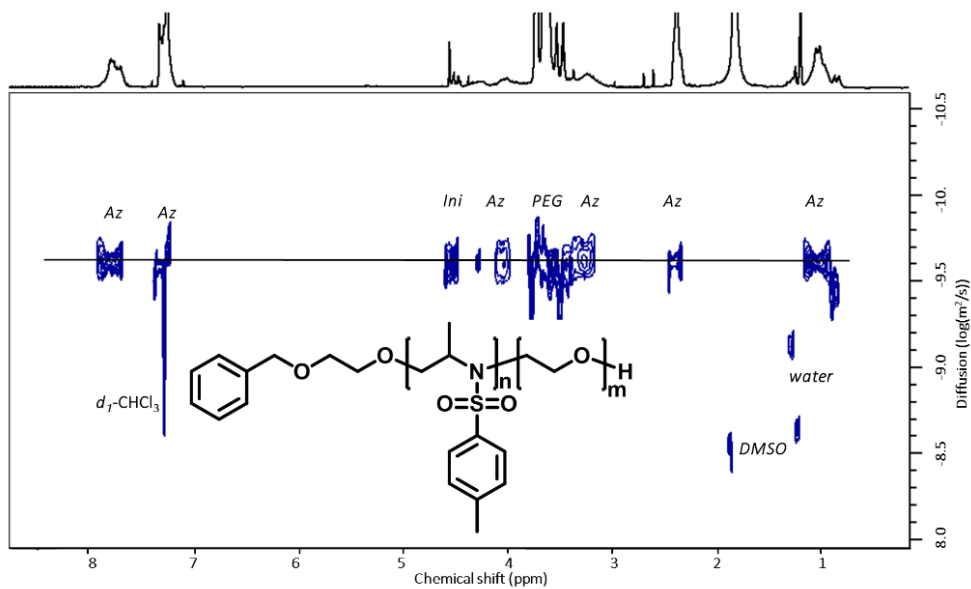


Figure S3.4: ^1H NMR-DOSY (CDCl_3 , 700 MHz, 298K) of P(TsMAz9-b-PEO₁₁₆) (P1).

The copolymerization of MsMAz and EO was performed in direct analogy to TsMAz and EO.

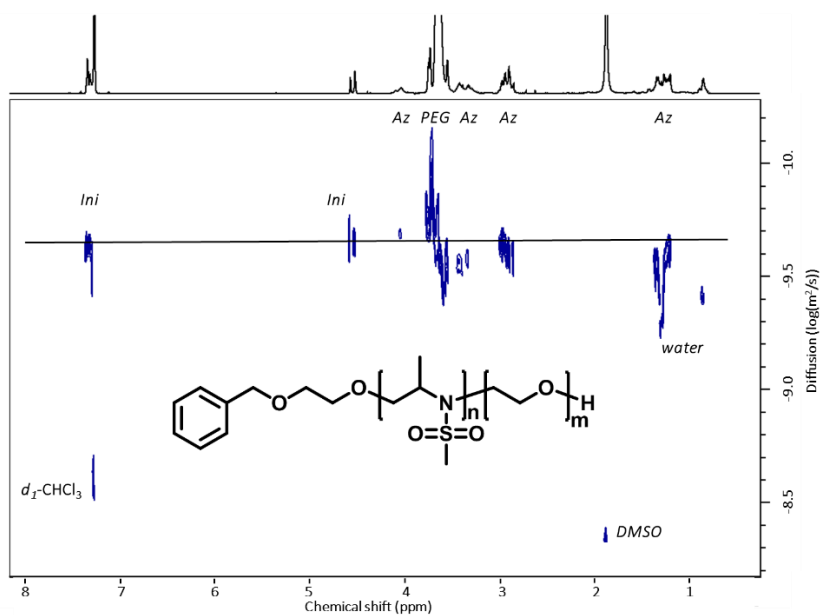


Figure S3.5: ^1H NMR-DOSY (CDCl_3 , 700 MHz, 298K) of $\text{P}(\text{MsMAz}_5\text{-}b\text{-PEO}_{116})$ (P4).

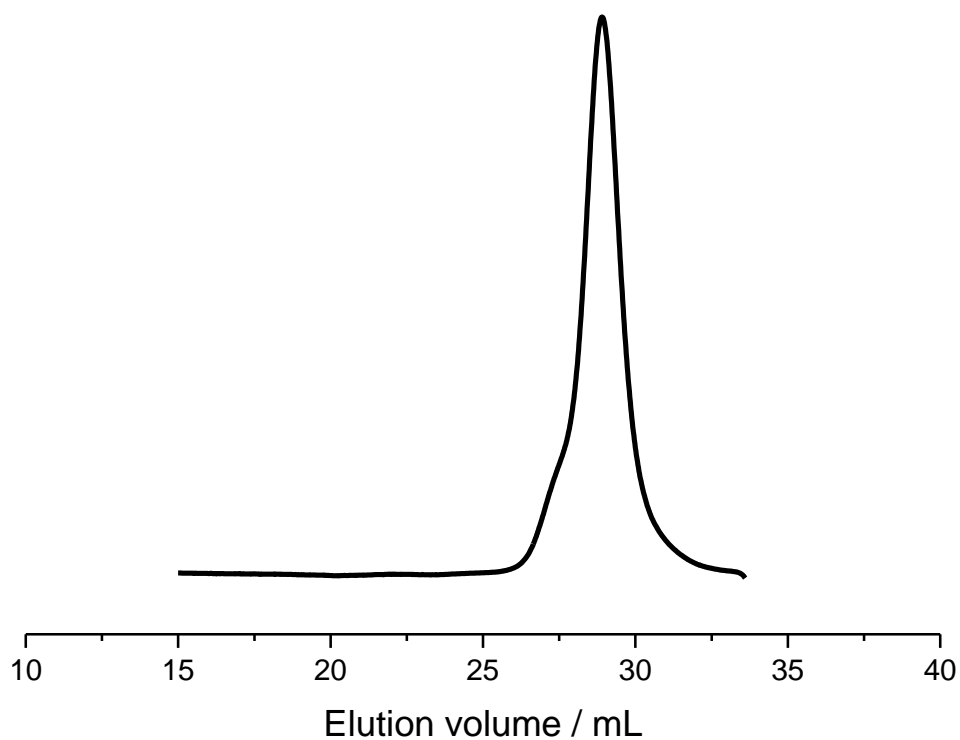


Figure S3.6: SEC trace of $\text{P}(\text{MsMAz}_5\text{-}b\text{-PEO}_{116})$ (P4) in DMF, RI-signal.

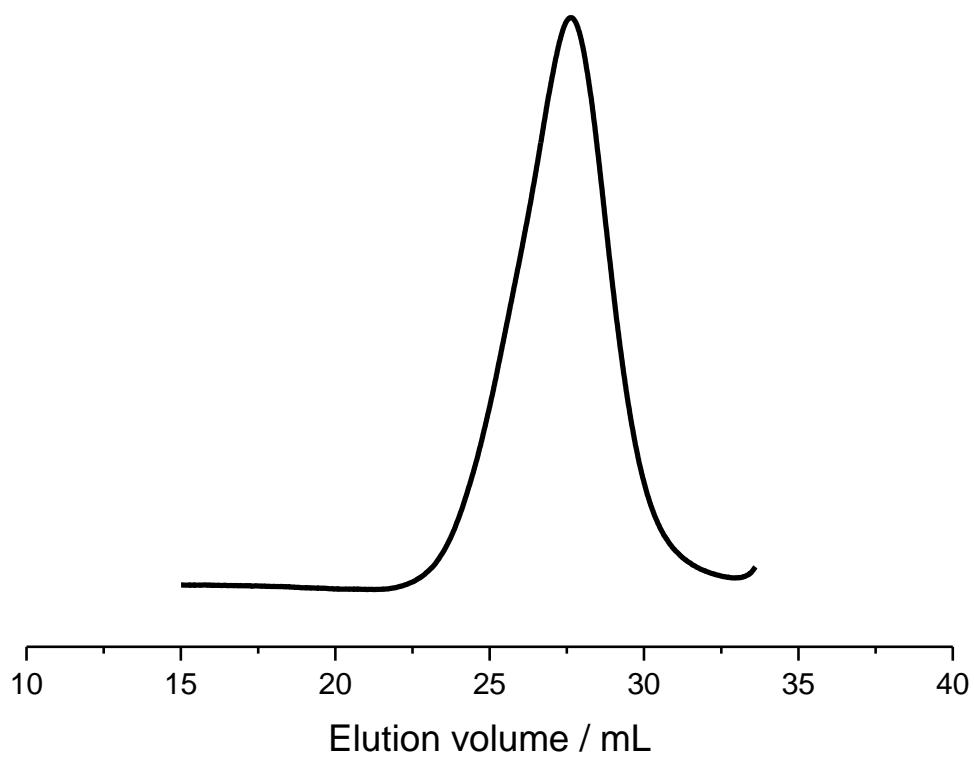
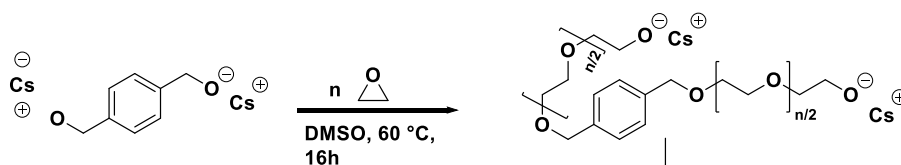


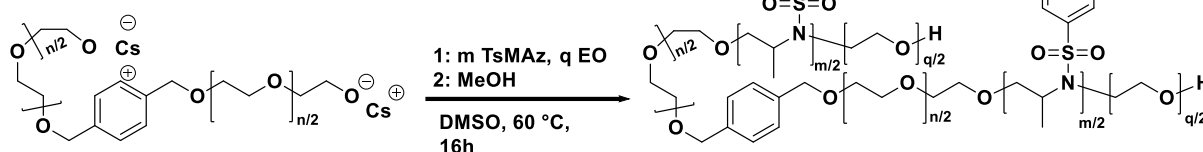
Figure S3.7: SEC trace of P(MsMAz₅₀-*b*-PEO₁₇₆) (P5) in DMF, RI-signal.

3.6.4 General procedure for the synthesis of ABABA-pentablock copolymers with A=PEO and B=PTsMAz.

Macro initiator preparation



Penta-block synthesis



In a flame-dried reaction tube, 28.8 mg of cesium hydroxide monohydrate (0.17 mmol, 1.5 eq) were added to 16 mg of 1,4-bis(hydroxy-methyl)-benzene (0.11 mmol, 1 eq). 2 mL of methanol was added to dissolve the mixture. Then 5 mL of benzene were added and the mixture was stirred for 60 min at 60 °C, methanol, benzene, and water were removed at reduced pressure (ca. 10^{-2} mbar) during 3 h at 60 °C. The drying procedure was repeated with an additional 5 mL of benzene (60°C, 3h, 10^{-2} mbar). The initiator was then dissolved in 5 mL of dry DMSO and 0.5 mL ethylene oxide (10.3 mmol, 90 eq) were added to the reaction flask. The mixture was allowed to stir for 16 h.

To the freshly synthesized difunctional PEO, 0.5 mL ethylene oxide (10.3 mmol, 90 eq) and 0.250 g of predried TsMAz (1.2 mmol, 11 eq) were added in DMSO *via* a gas-tight syringe. The polymerization was continued for 16h at 60°C and terminated by the addition of methanol. The mixture was then diluted with water and dialyzed against deionized water to remove DMSO. Yield: (897 mg, 72%).

^1H NMR of P9 (difunctional PEO) (300 MHz, Chloroform-*d*) δ 7.30 (s, 4H) Initiator, 4.54 (s, 4H) Initiator, 3.64 (s, 532H) PEG.

^1H NMR of P10 (ABABA-pentablock) (300 MHz, Chloroform-*d*) δ 8.05 – 7.55 (m, 20H) TsMAz, 7.46 – 7.09 (m, 20H) TsMAz, 4.53 (s, 4H) Initiator, 4.42 – 4.16 (m, 10H) 3.36 (s, 1296H) PEG, 2.50 – 2.23 (m, 30H) TsMAz, 1.19 – 0.75 (m, 30H) TsMAz.

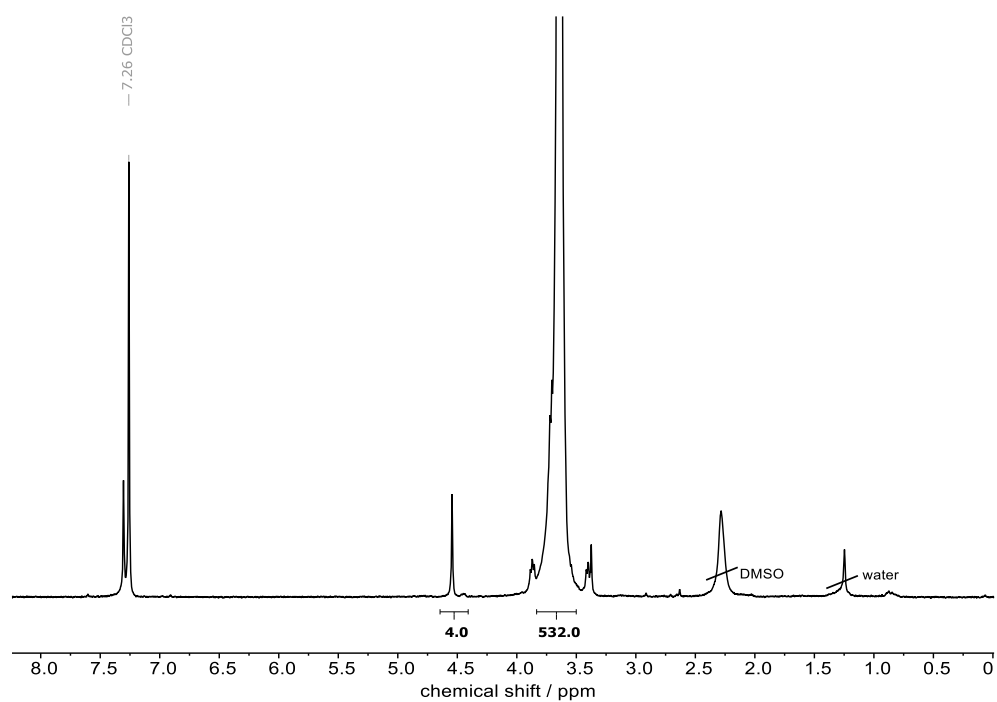


Figure S3.8: ^1H NMR of P9 (300 MHz, Chloroform-*d*).

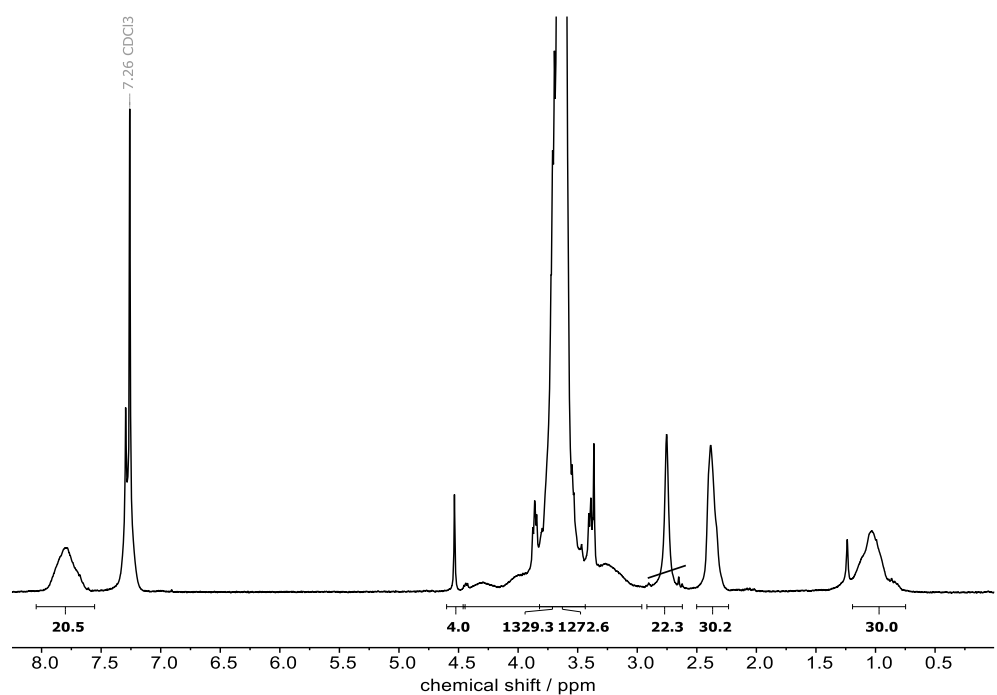
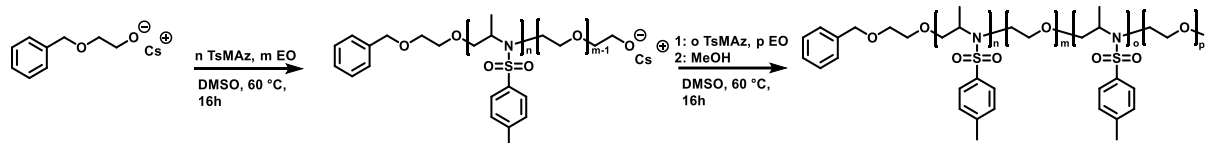


Figure S3.9: ^1H NMR of P10 (300 MHz, Chloroform-*d*).

3.6.5 General procedure for the synthesis of ABAB-tetrablock copolymers with A=PEO and B=PTsMAz.



All glassware was flame-dried at reduced pressure before the reaction. The initiator 2-(benzyloxy)ethanol (16.0 mg, 105 μmol , 1eq) and 15.6 mg (92 μmol , 0.9 eq.) of cesium hydroxide monohydrate were placed in a Schlenk flask and suspended in 5 mL benzene. The mixture was stirred at 60 °C under an argon atmosphere for 1 h, evacuated at 80 °C (10^{-2} mbar) for 3 h to remove benzene and water to generate the corresponding cesium alkoxide. In a separate flask, the respective amount of TsMAz was dissolved in ca. 3 mL benzene and dried for ca. 4h at reduced pressure to remove traces of water by azeotropic distillation. 4 mL of anhydrous DMSO were then added to the freshly generated initiator and 0.5 mL (10.3 mmol, 100 eq) of ethylene oxide were cryo-transferred into the reaction flask and 250 mg (1.2 mmol, 12 eq) TsMAz was added *via* syringe dissolved in 1 mL of anhydrous DMSO. The reaction mixture was heated to 60 °C and stirred for 16h. To the living diblock copolymer solution, 0.5 mL (10.3 mmol, 100 eq) of ethylene oxide were cryo-transferred into the reaction flask and 250 mg (1.2 mmol, 12 eq) of TsMAz was added *via* syringe dissolved in 1 mL of anhydrous DMSO. After 16 h at 60 °C the living chain ends were terminated by the addition of methanol and the copolymer was dialyzed against water to remove DMSO. The copolymer were obtained as white to a light yellow solid with high yield (1.12 g, 84%).

^1H NMR of P 7 (AB-diblock) (300 MHz, Chloroform-*d*) δ 8.10 – 7.56 (m, 30H) TsMAz, 7.55 – 7.12 (m, 30H) TsMAz, 4.56 (s, 2H) Initiator, 4.42 – 4.16 (m, 15H), 3.85 – 3.42 (m, 841H) PEG, 2.57 – 2.15 (m, 45H) TsMAz, 1.25 – 0.68 (m, 45H) TsMAz.

^1H NMR of P 8 (ABAB-tetrablock) (300 MHz, Chloroform-*d*) δ 8.08 – 7.51 (m, 44H) TsMAz, 7.45 – 7.08 (m, 44H) TsMAz, 4.55 (s, 2H) Initiator, 4.42 – 4.16 (m, 22H), 3.85 – 3.42 (m, 1520H) PEG, 2.57 – 2.15 (m, 66H) TsMAz, 1.25 – 0.68 (m, 66H) TsMAz.

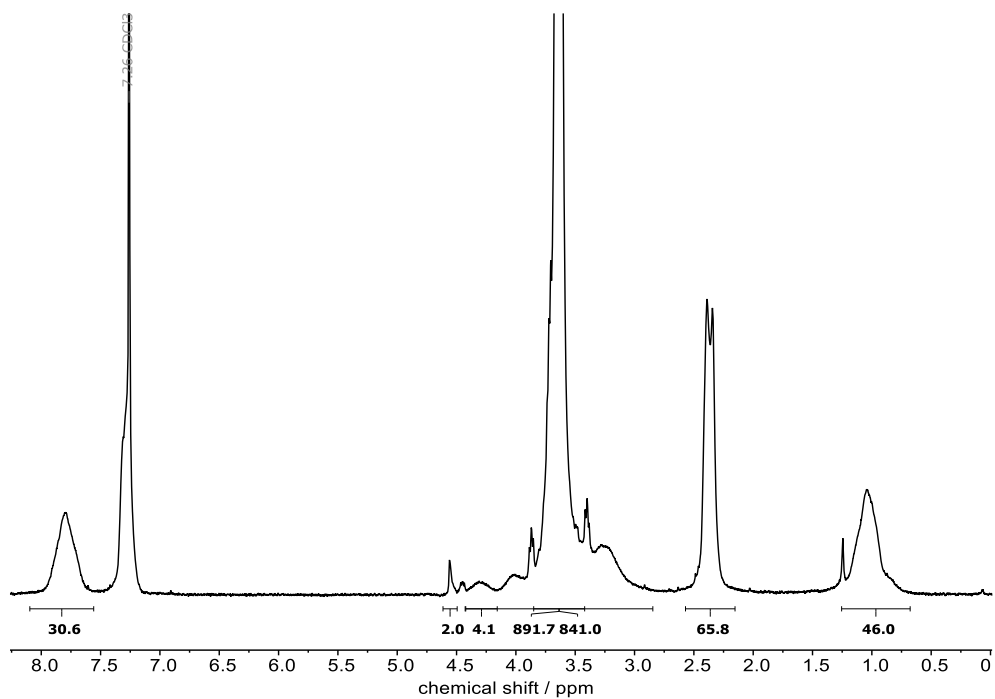


Figure S3.10: ¹H NMR of P 7 (300 MHz, Chloroform-*d*).

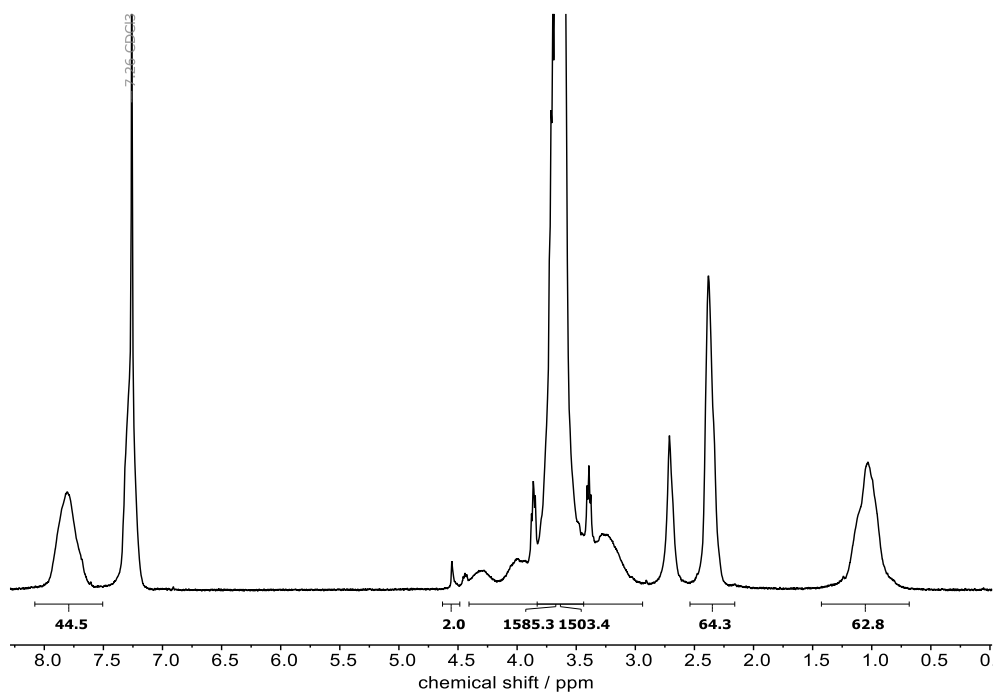


Figure S3.11: ¹H NMR of P 8 (300 MHz, Chloroform-*d*).

3.6.6 Example procedure for the real-time ^1H NMR kinetics: copolymerization of activated aziridines and ethylene oxide.

The initiator 2-(benzyloxy)ethan-1-ol 72.0 mg (10 eq) and 71.0 mg (9 eq) of cesium hydroxide monohydrate were placed in a Schlenk flask and suspended in ca. 3 mL benzene. The mixture was stirred at 60 °C under an argon atmosphere for 1 h, evacuated at 80 °C (10^{-2} mbar) for 3 h to remove benzene and water to generate the corresponding cesium alkoxide. 2.0 mL of anhydrous DMSO- d_6 were added to dissolve the initiator. From this solution, 0.2 mL (1 eq) were added to a dry, valved NMR tube for high-pressure measurements (Wilmad® low pressure/vacuum NMR tube (Wilmad, 507-LPV-7)). Then, a solution of TsMAz (100 mg, 470 μmol) in 0.5 mL DMSO- d_6 was added to the opened NMR tube under argon atmosphere. After solidification of the DMSO- d_6 , the initiator and the aziridine by cooling the NMR tube with liquid nitrogen vacuum (10^{-2} mbar) was applied to the NMR tube. Ethylene oxide (7600 μmol)* was then cryo-transferred to the reaction mixture. The tube was left in liquid nitrogen to be further evacuated (10^{-2} mbar). The NMR tube was sealed by the valve and the mixture was allowed to melt. It was mixed by shaking by hand and placed in the NMR spectrometer to record the first spectrum. The temperature was kept at 40°C with sample spinning turned off for 20 h. Intervals between two measurements were 409 s. Conversion of TsMAz and EO was quantitative.

* Ethylene oxide was directly cryotransfer from the ethylene oxide reservoir, EO amount added to the NMR tube was calculated from the final ^1H NMR of the polymer by comparing the amount TsMAz (100 mg, 470 μmol) and ethylene oxide.

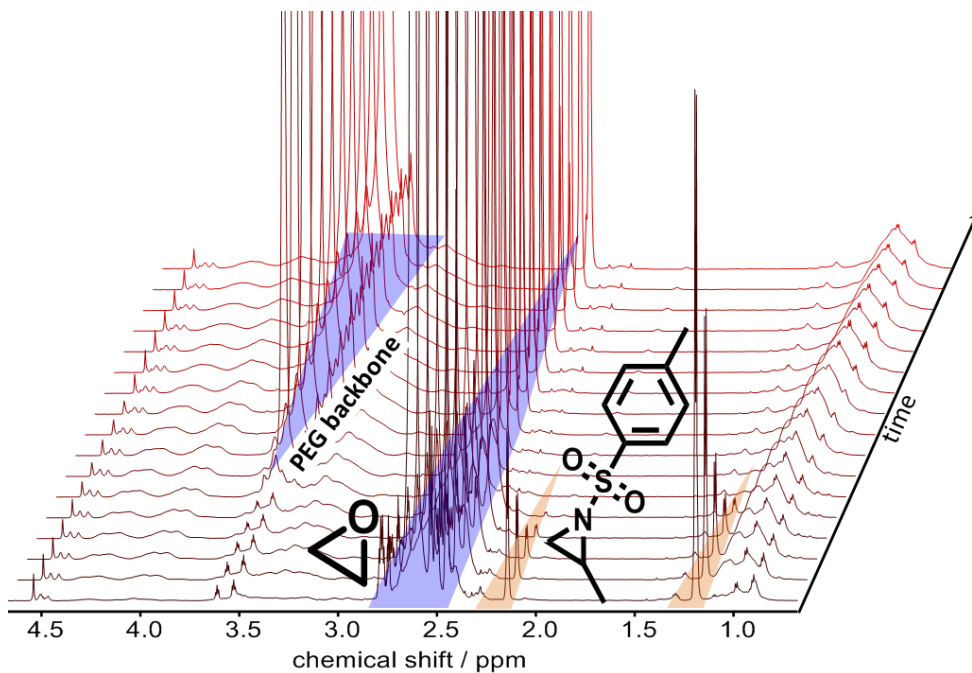


Figure S3.12: A: Zoom into the real-time ¹H NMR spectra of the one pot block polymerization of EO (blue) and TsMAz (orange). Degreasing EO signal is overlaid by DMSO and CH₃- signal.

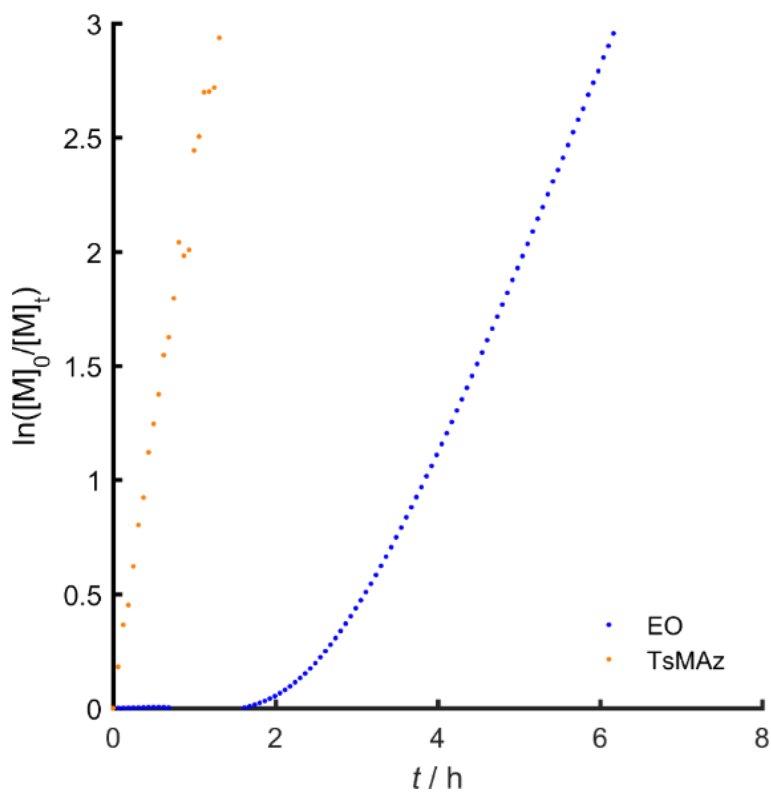


Figure S3.13: Assembly of each monomer in the polymer *versus* reaction time in min. Linearity proves living character of the polymerization.

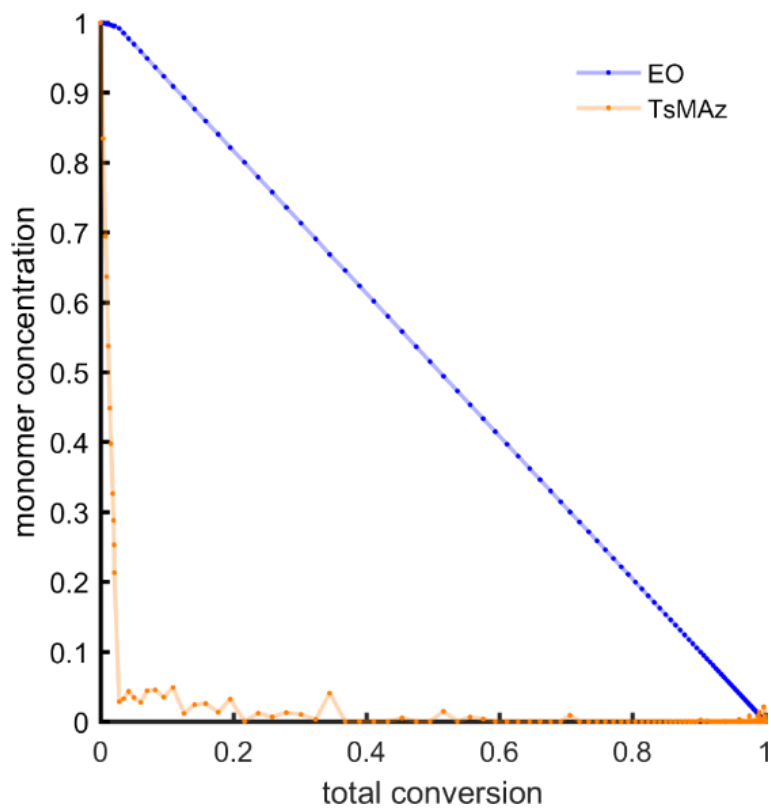


Figure S3.14: Normalized single monomer concentration *versus* total monomer conversion.

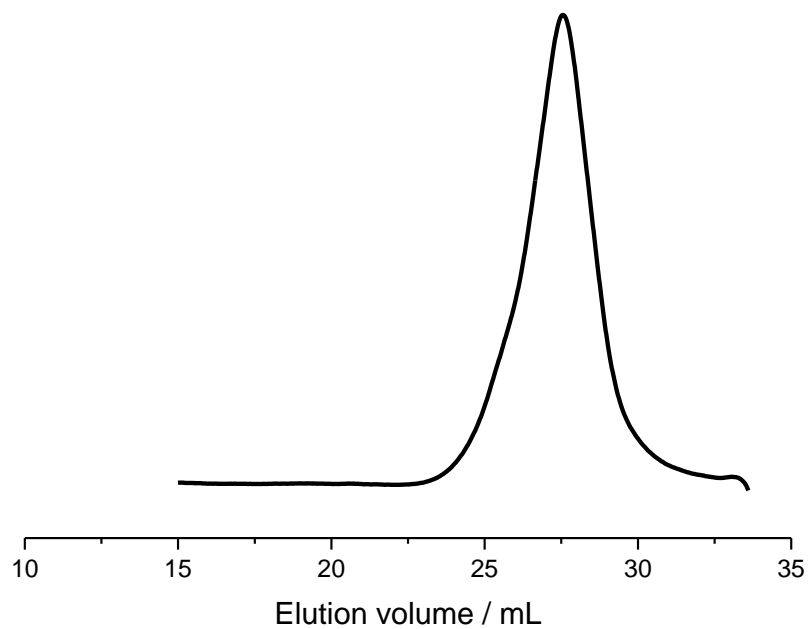


Figure S3.15: SEC trace of P(TsMAz₁₂-*b*-PEO₁₉₅) (P3 from the NMR kinetics) in DMF, RI-signal.

3.6.7 Real-time ^1H NMR kinetics (Data for MsMAz and EO):

The copolymerization of MsMAz and EO was performed in direct analogy to TsMAz and EO.

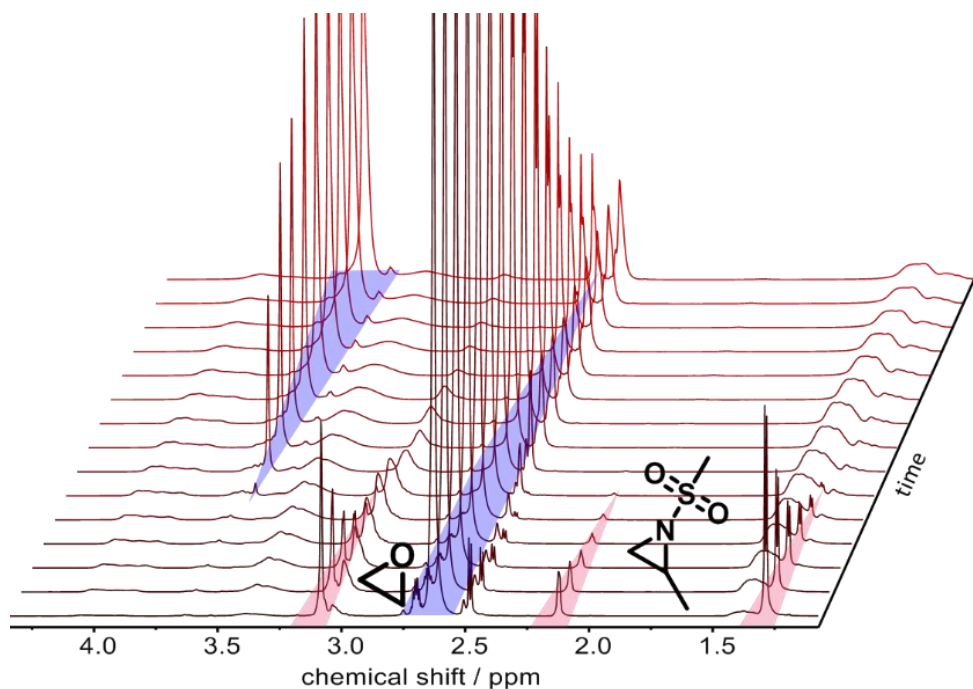


Figure S3.16: Zoom into the real-time ^1H NMR spectra of the one-pot block polymerization of EO (blue) and MsMAz (pink).

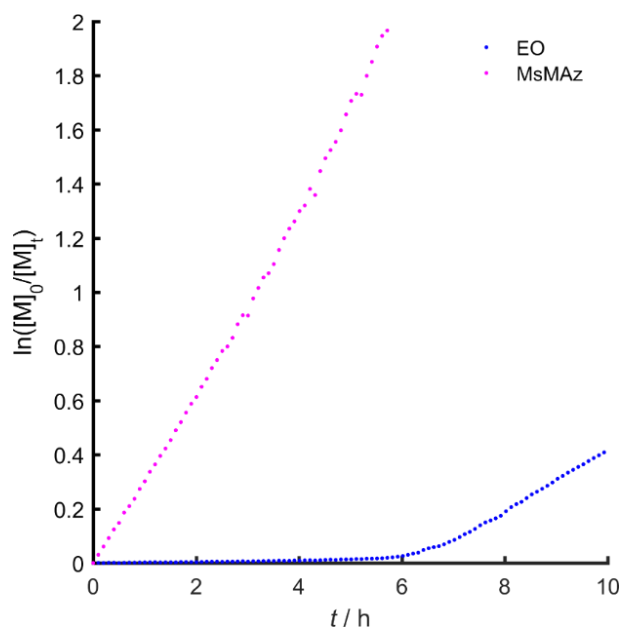


Figure S3.17: Assembly of each monomer in the polymer *versus* reaction time in min. linearity proves lining character of the polymerization.

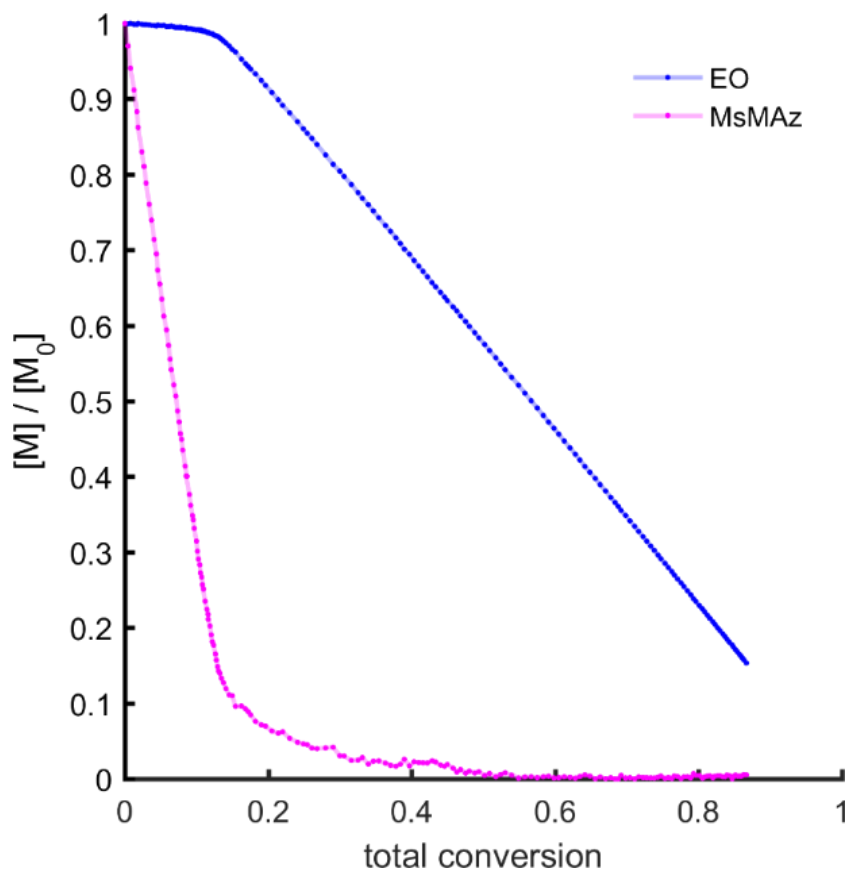


Figure S3.18: Normalized single monomer concentration *versus* total monomer conversion.

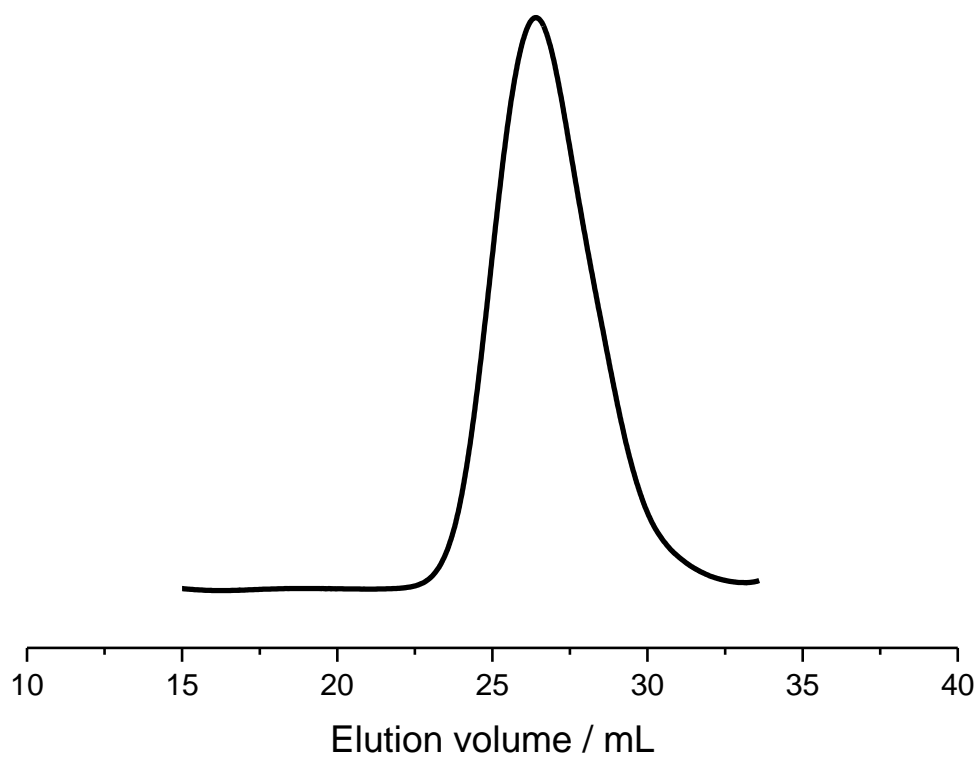


Figure S3.19: SEC trace of P(MsMAz₅₆-*b*-PEO₁₆₈) (P6) in DMF, RI-signal.

3.6.8 Evaluation of reactivity ratios *via* Jaacks assuming an ideal copolymerization

For the ideal case of a copolymerization $r_1 \cdot r_2 = 1$ the copolymerization the copolymerization equation simplifies and is transformed in its integrated form:²

Equation S1: Copolymerization equation of an ideal copolymerization:

$$\frac{d[M_1]}{d[M_2]} = r_1 \frac{[M_1]}{[M_2]}$$

$$\frac{[M_1]}{[M_{1,0}]} = \left(\frac{[M_2]}{[M_{2,0}]} \right)^{r_1}$$

$$\log([M_1]) = r_1 \log([M_2]) + \log\left(\frac{[M_{1,0}]}{[M_{2,0}]}\right)$$

$$r_2 = \frac{1}{r_1}$$

According to Jaacks this equation can be used assuming the copolymerization is ideal to fit the experimental data:³

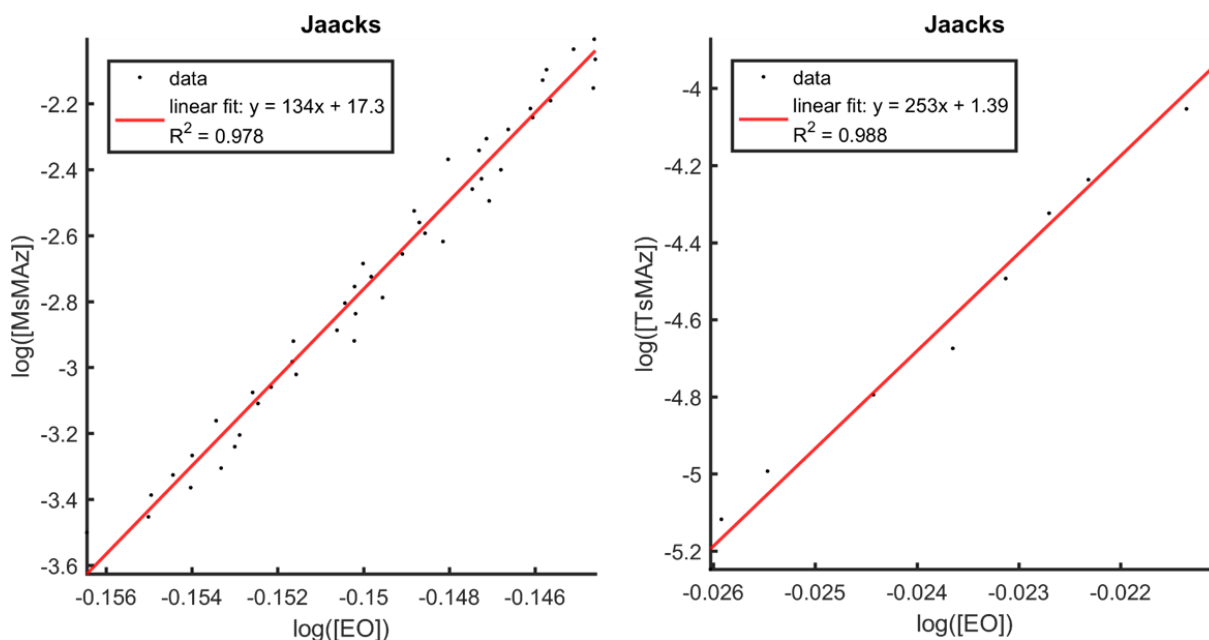


Figure S3.20: Jaacks fit from the real-time NMR data of MsMAz and EO (left), Jaacks fit from the real-time NMR data of TsMAz and EO (right).

3.6.9 Evaluation *via* the Meyer-Lowry equation

The integration of the Mayo Lewis equation introduced by Skeist and first performed analytically by Meyer-Lowry yields the Meyer-Lowry equation. This equation enables the fit of the experimental compositional drift of f_1 during the total conversion X .⁴

Equation S3.2. Meyer-Lowry equation for the evaluation of reactivity ratios.

$$X = 1 - \left(\frac{f_1}{f_{1,0}} \right)^\alpha \left(\frac{1-f_1}{1-f_{1,0}} \right)^\beta \left(\frac{f_1 - \delta}{f_{1,0} - \delta} \right)^\gamma$$

$$\alpha = \frac{r_2}{1-r_2}; \beta = \frac{r_1}{1-r_1}; \gamma = \frac{1-r_1r_2}{(1-r_1)(1-r_2)}; \delta = \frac{1-r_2}{2-r_1-r_2}$$

$$X = 1 - \frac{[M_1] + [M_2]}{[M_{1,0}] + [M_{2,0}]}; f_1 = \frac{[M_1]}{[M_1] + [M_2]}$$

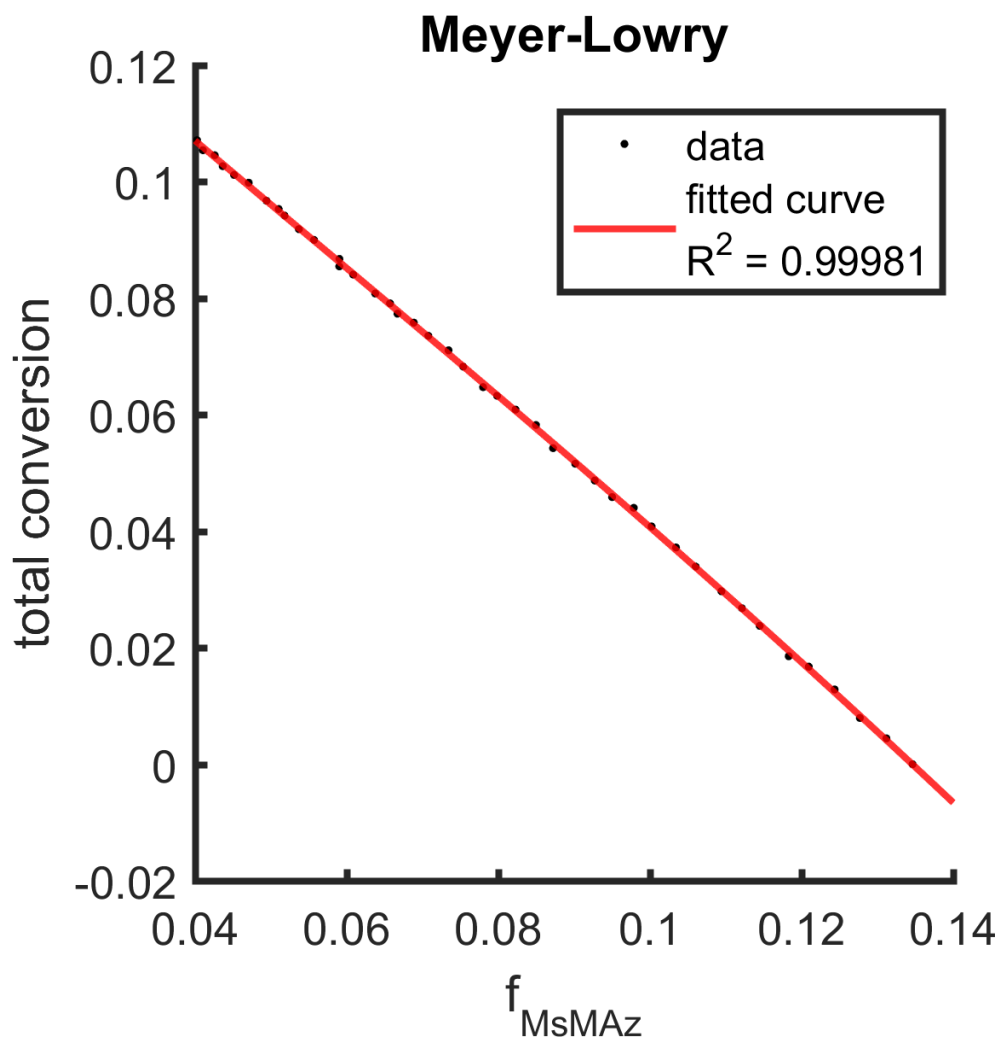


Figure S3.21: Meyer-Lowry fit from the real-time NMR data of MsMAz and EO.

3.6.10 Calculation of the copolymer microstructure.

The resulting microstructure of the copolymers can be calculated by numerical integration according to Skeist or directly with the Meyer Lowry equation in the interval of conversion from 0 to 1 with a given set of reactivity ratios. We used the reactivity ratios determined by the Meyer-Lowry method. This process gives values for total conversion X and fraction of comonomer concentration f_1 . To determine the values of F_1 which corresponds to instantaneous comonomer incorporation, the values of f_1 can be converted by the altered Mayo-Lewis equation using the same reactivity ratios.

$$F_1 = \frac{d[M_1]}{d[M_1] + d[M_2]} = \frac{r_1 f_1^2 + f_1 f_2}{r_1 f_1^2 + 2f_1 f_2 + r_2 f_2^2}$$

The determined slopes y determined above by linear interval fits can be converted to the fractions F_1 incorporated into the polymer by the relationship shown below. The total conversion X is calculated as mentioned above. This process requires no knowledge regarding the reactivity ratios, and it is possible to determine the microstructure from a copolymerization experiment. This enables the comparison of the experimental data with the calculated microstructure.

Equation S3.3. Calculation of F_1 and total conversion X .

$$F_1 = 1 - F_2 = 1 - \frac{d[M_2]}{d[M_1] + d[M_2]} = 1 - \left(\frac{d[M_1] + d[M_2]}{d[M_2]} \right)^{-1} = 1 - \left(\frac{d[M_1]}{d[M_2]} + 1 \right)^{-1}$$

$$F_1 = 1 - (y + 1)^{-1}$$

In this manner, the copolymerization diagram depicted in Figure S 21 and Figure 1C were created.

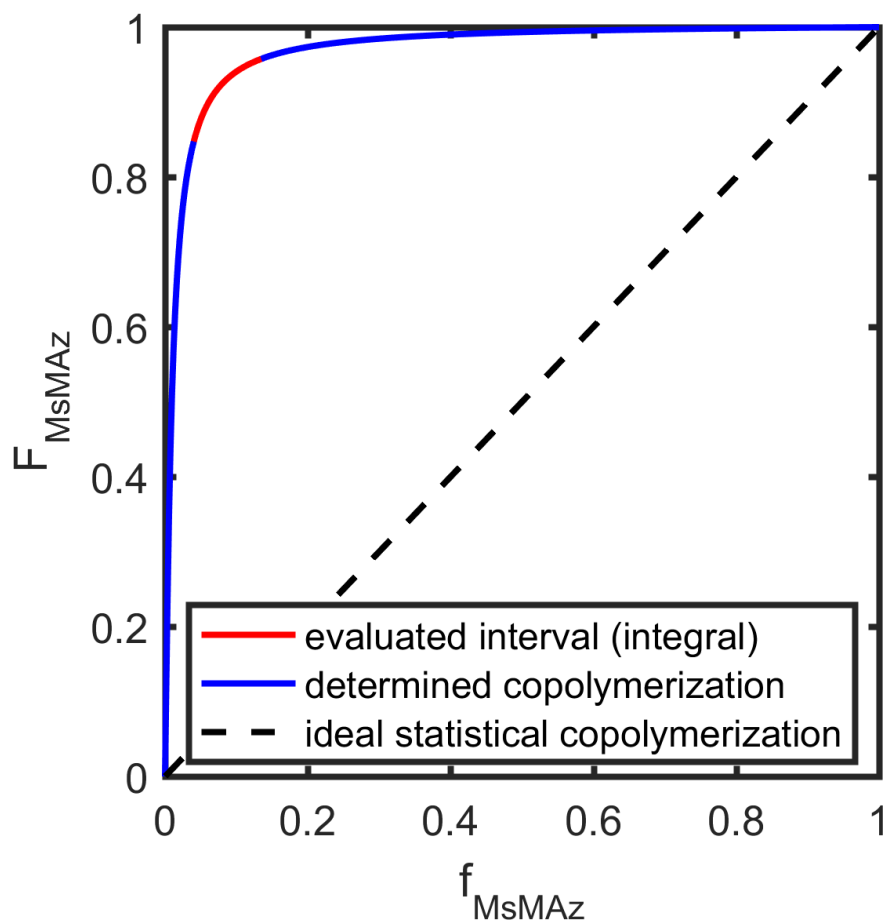


Figure S3.22: Copolymerization diagram of MsMAz and EO.

Table S3.1. Overview of the determined reactivity ratios for the comonomer pairs TsMAz and EO or MsMAz and EO.

	$r(\text{MsMAz})$	$r(\text{EO})$	$r_1 \cdot r_2$	$r(\text{TsMAz})$	$r(\text{EO})$	$r_1 \cdot r_2$
Jaacks Fit	136	0.007	1.0	253	0.004	1.0
Meyer-Lowry Fit	151	0.013	1.9	265	0.004	1.1

3.6.11 General procedure for the miniemulsion polymerization of styrene stabilized by P1.

P1 (541 mg) was dissolved in 24 g of water. A solution of 6.10 g styrene, 253 mg of hexadecane and 103.63 mg of 2,2'-azobis(2-methylbutyronitrile) (V59) was prepared and added dropwise to the vigorous stirring aqueous solution containing P1. The emulsion was stirred for 1 h at 1000 rpm. The emulsion was ultrasonicated (450 W, 2 min, 90% amplitude) to produce a stable miniemulsion and sealed. The miniemulsion was placed in an oil bath at 70°C and the polymerization was allowed to proceed for 24 h. The final nanoparticle dispersion had a solid content of w=19,9%. DLS: Particle size = 92 nm, PDI = 1.01

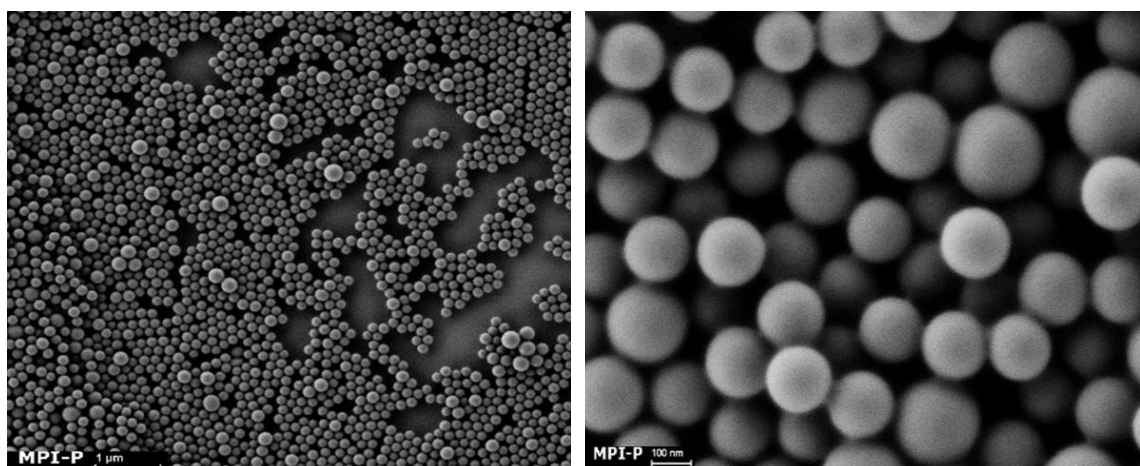


Figure S3.23: SEM images of PS nanoparticles stabilized with P1

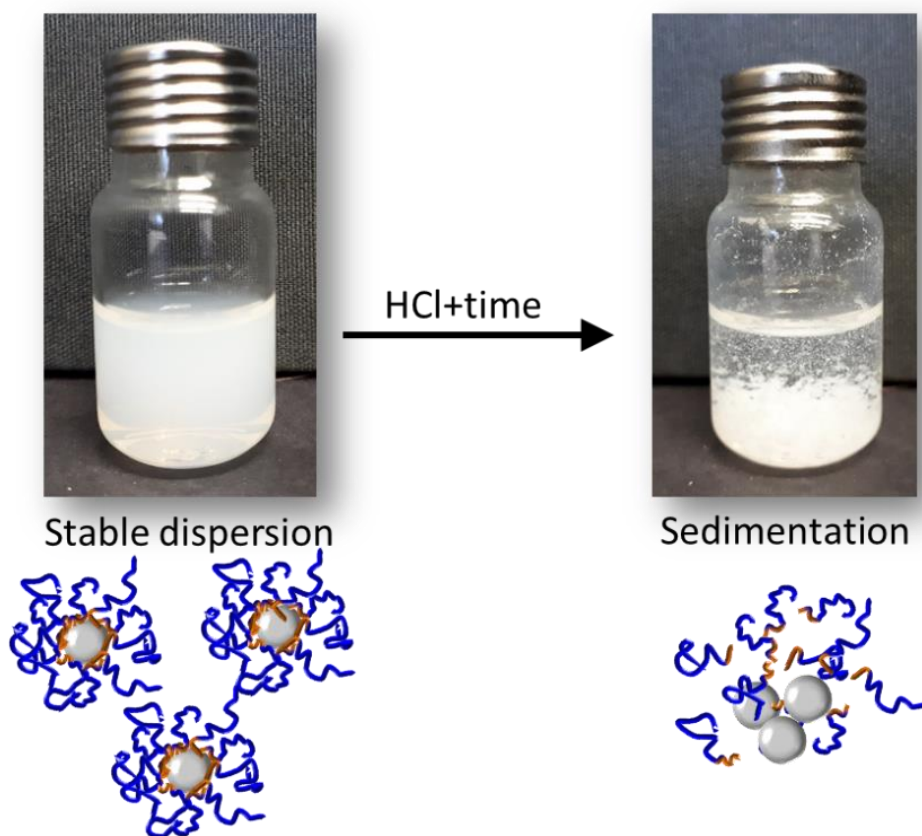


Figure S3.24: PS nanoparticle dispersion stabilized with PTsMAz-*b*-PEO (left), addition of hydrochloric acid destabilizes the dispersion by protonation of the sulfonamide groups (photo taken after 4 days (right)).

3.6.12 Surface Tension Measurements

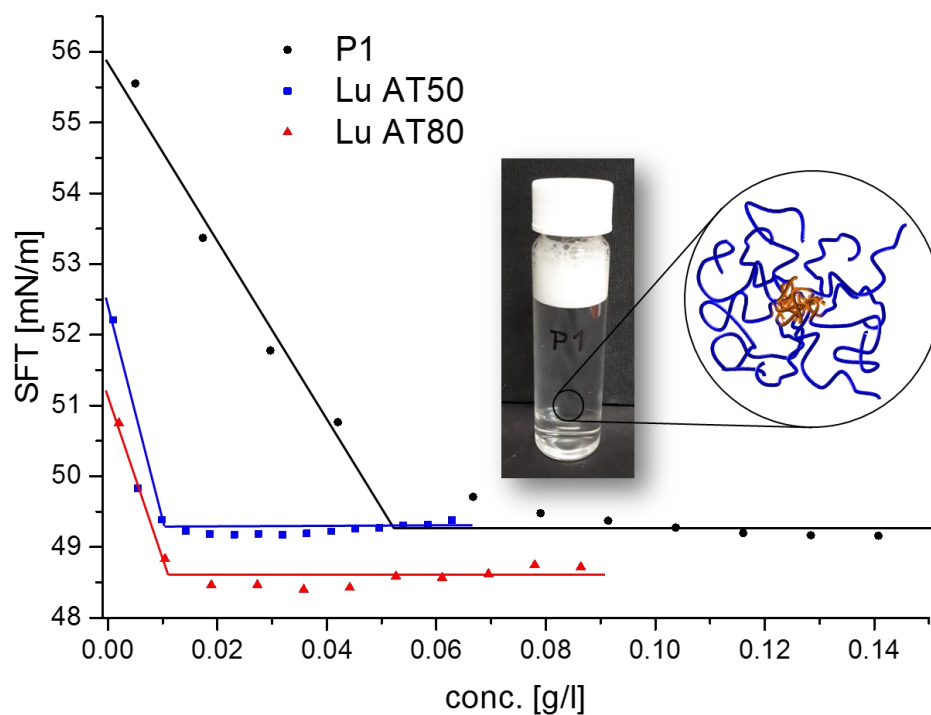


Figure S3.25: Surface tension of P1 (black) and commercially available surfactants (Lu AT50, LU AT80) as comparison at different concentrations. Illustration shows foaming property of aqueous P1 solution (1.5 g/L).

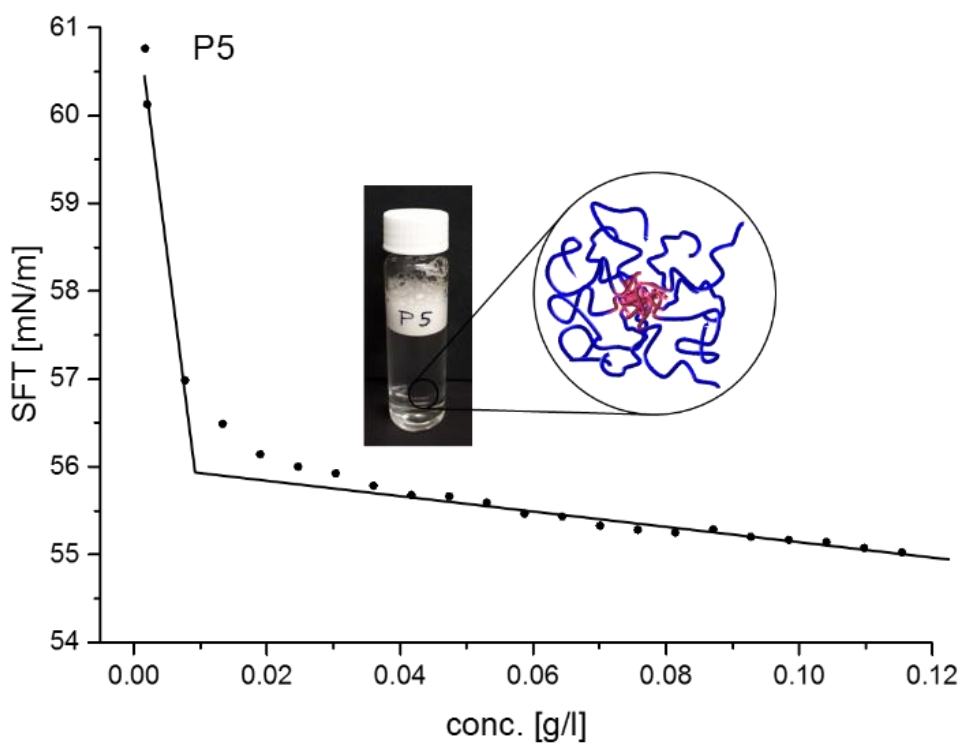


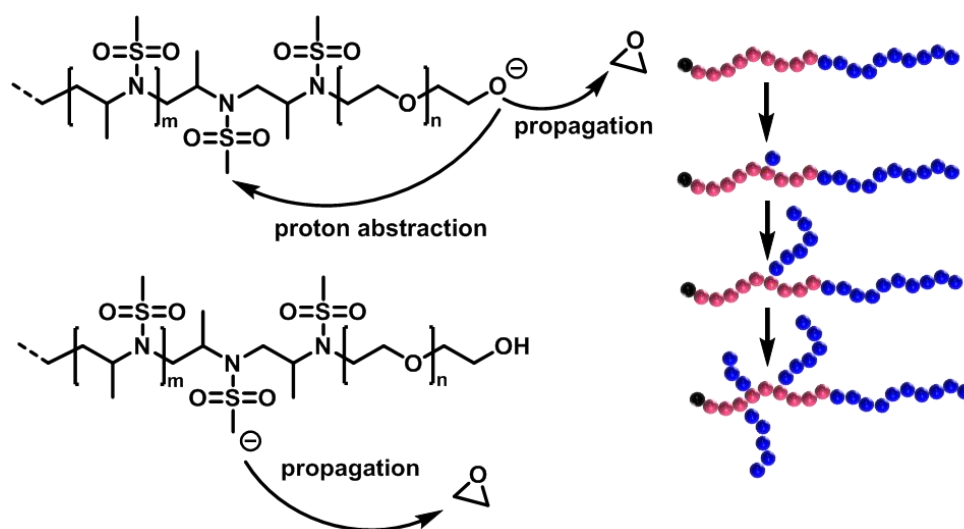
Figure S3.26: Surface tension of P5 (black) at different concentrations. Illustration shows foaming property of aqueous P5 solution (1.5 g/L).

Table S3.2: Surface tension measurements.

Sample	$\sigma^A / \text{mN} \cdot \text{m}^{-1}$	SFT ^B / $\text{mN} \cdot \text{m}^{-1}$	SFT ^C / $\text{mN} \cdot \text{m}^{-1}$
P1	0.05	49.3	n.a.
P5	0.01	55.0	n.a.
Lu AT50	0.01	49.3	48
Lu AT80	0.01	48.6	50

^A CMC, determines by ring tensiometry, ^BSFT, extrapolated value at 1 g/L, ^CSFT from Literature in distilled water at 23 °C at 1 g/L (Technical information BASF SE).

3.6.13 Grafting by deprotonation during MsMAz/EO copolymerization:



Scheme S3.1: Proposed mechanism for the grafting of PEO-arms onto the PMsMAz block during the copolymerization of MsMAz and EO: the CH₃-group from the pendant mesyl groups can be deprotonated by the alkoxides, resulting in grafting of PEO-chains resulting in a P(MsMAz-co-(MsMAz-g-PEO))-b-PEO.

3.6.14 Determination of hydroxyl groups

Hydroxyl groups of the polymers P1, P5 were determined in analogy to M. Balakshin and E. Capanema.⁵ As a control of this method, a sample of mPEG 5k and mPEG 10k were analyzed. The control shows, that this method is able to quantify the amount of hydroxyl groups in polymers with different molecular weights, $n(\text{OH theo})$ and $n(\text{OH exp})$ in Table S3.

Table S3.3: Determination of hydroxyl groups.

polymer	m(polymer / mg) ^a	n(OH theo) / μmol^b	n(added standard) / μmol^c	n(OH exp) / μmol^d
mPEG 5k	41.1	8.2	13.0	9.5
mPEG 10k	40.5	4.1	12.5	4.7
P1	9.9	1.4	10.6	2.9
P5	47.8	3.3	12.9	18.4

^a: Mass of dry polymer in mg added in the NMR tube, ^b: molar amount of polymer corresponding to m(polymer) in the NMR Tube, If the polymer of ideal linear architecture this molarity corresponds exactly to the molarity of hydroxyl groups ($n(\text{OH theo})$). ^c: molar quantity of the added OH standard in the NMR tube, this corresponding ³¹P-signal at 148.60 ppm was normalized. ^d: Molar quantity of determined hydroxyl groups $n(\text{OH exp.})$ in the polymer sample.

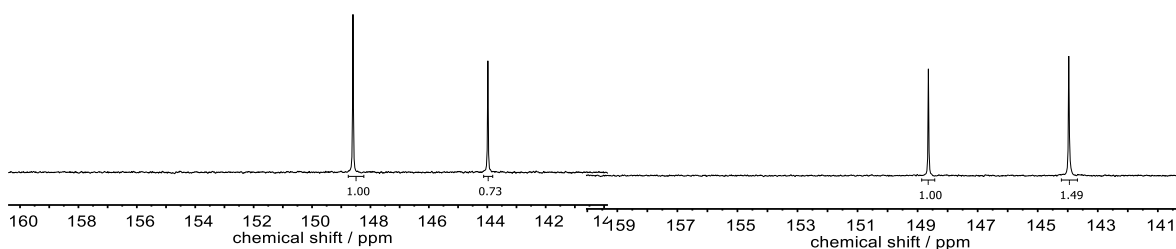


Figure S3.27: ^{31}P NMR of modified mPEG 5k, 121 MHz: Hydroxyl standard: 148.60 ppm, polymeric hydroxy groups: 143.98 ppm.

Figure S3.28: ^{31}P NMR of modified P5, 121 MHz: Hydroxyl standard: 148.60 ppm, polymeric hydroxy groups: 143.98 ppm.

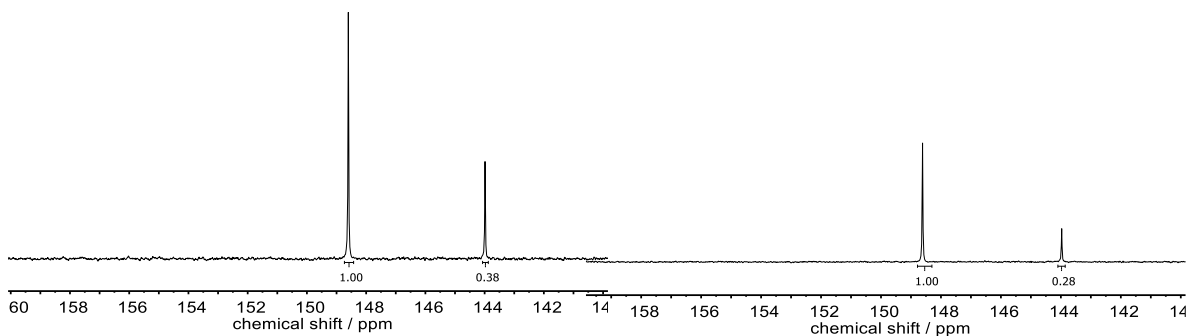


Figure S3.29: ^{31}P NMR of modified mPEG10k, 121 MHz: Hydroxyl standard: 148.60 ppm, polymeric hydroxy groups: 143.98 ppm.

Figure S3.30: ^{31}P NMR of modified P1, 121 MHz: Hydroxyl standard: 148.60 ppm, polymeric hydroxy groups: 143.98 ppm.

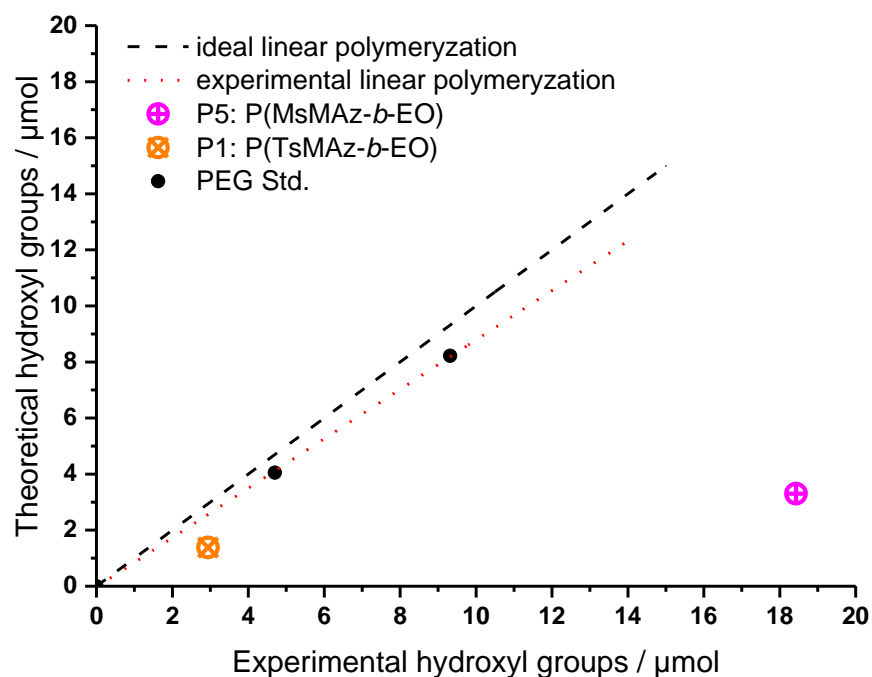


Figure S3.31: Plot of the theoretical and experimental concentration of hydroxyl groups (i.e. PEO chain ends), determined from the reaction of the PAz-PEO copolymers with 2-chloro-4,4,5,5-tetramethyl-1,3,2-dioxaphospholane *via* ^{31}P NMR spectroscopy. The values for TsMAz-*b*-PEO (P1) indicate a linear copolymer (with a single OH end groups), while copolymers of MsMAz and EO (P5) have a higher OH-number, indicating chain grafting as illustrated in Scheme S1.

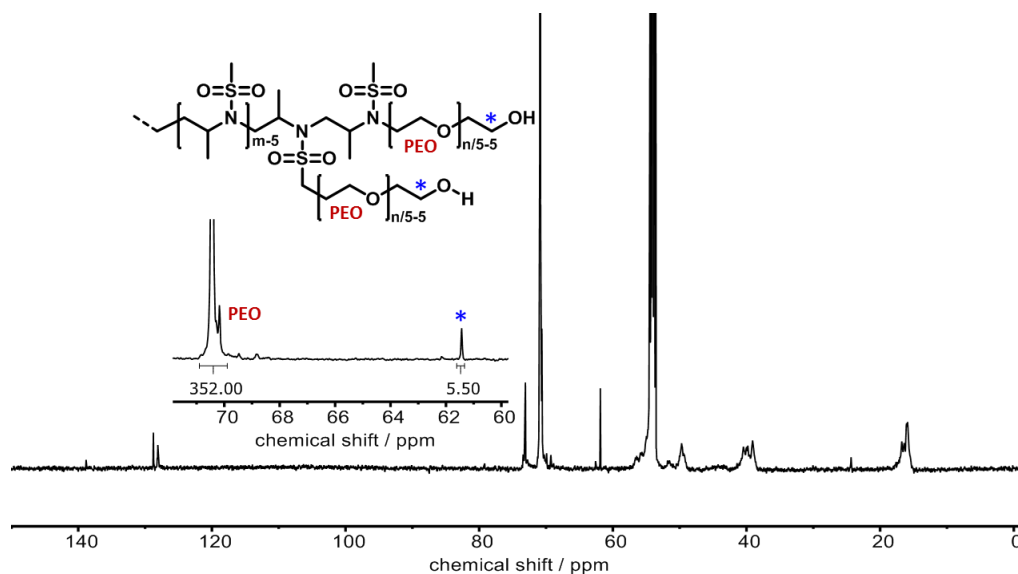


Figure S3.32: Quantitative ^{13}C NMR of P5 (126 MHz, Methylene Chloride- d_2) with zoom in from 72 to 58 ppm showing carbon signal of PEO repeating units at 70.4 ppm (red) and of terminal alcohol carbon at 61.4 ppm (blue).

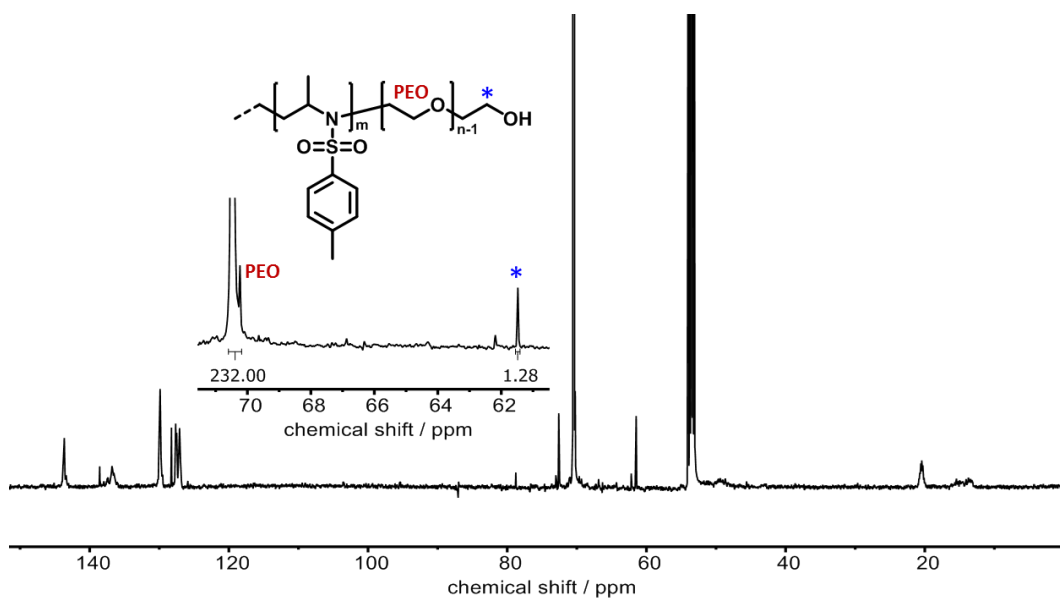


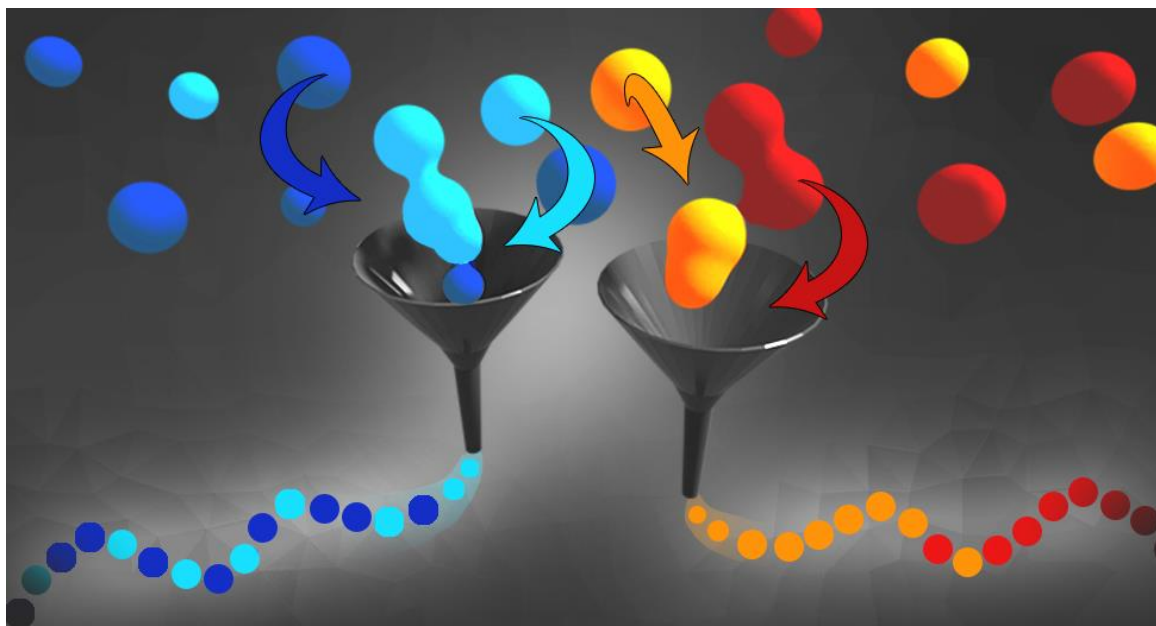
Figure S3.33: Quantitative ^{13}C NMR of P1 (126 MHz, Methylene Chloride- d_2) with zoom in from 72 to 58 ppm showing carbon signal of PEO repeating units at 70.4 ppm (red) and of terminal alcohol carbon at 61.4 ppm (blue).

3.7 Additional References Chapter 3

1. Stewart, I. C.; Lee, C. C.; Bergman, R. G.; Toste, F. D., Living ring-opening polymerization of *N*-sulfonylaziridines: synthesis of high molecular weight linear polyamines. *J. Am. Chem. Soc.* **2005**, 127 (50), 17616-17617.
2. Wall, F. T., The structure of vinyl copolymers. *Journal of the American Chemical Society* **1941**, 63 (7), 1862-1866.
3. Jaacks, V., A novel method of determination of reactivity ratios in binary and ternary copolymerizations. *Macromolecular Chemistry and Physics* **1972**, 161 (1), 161-172.
4. Blankenburg, J.; Wagner, M.; Frey, H., Well-Defined Multi-Amino-Functional and Stimuli-Responsive Poly (propylene oxide) by Crown Ether Assisted Anionic Ring-Opening Polymerization. *Macromolecules* **2017**, 50 (22), 8885-8893.
5. Balakshin, M.; Capanema, E., On the quantification of lignin hydroxyl groups with ³¹P and ¹³C NMR spectroscopy. *Journal of Wood Chemistry and Technology* **2015**, 35 (3), 220-237.

4 *Competitive Copolymerization: Access to Aziridine Copolymers with Adjustable Gradient Strengths*

*Tassilo Gleede, Jens C. Markwart, Niklas Huber Elisabeth Rieger, and
Frederik R. Wurm**



TOC 4: Table of content, symbolizing the combination different monomers for a copolymerization: Depending on the activation difference between two copolymers the microstructure is adjustable from statistical over gradient to block-copolymers.

Note: Jens C. Markwart was responsible for the calculation of the reactivity parameters and the illustrations of the microstructures. Niklas Huber performed the DFT calculations. Elisabeth Rieger kindly provided data of homo- and copolymerizations.

Tassilo Gleede synthesized monomers, conducted polymerization kinetics. Frederik R. Wurm supervised this project. Frederik R. Wurm and Tassilo Gleede wrote the manuscript. All authors edited the manuscript

This chapter is based on a published article under the terms of the Copyright this chapter is used with the permission of ACS Publications: Tassilo Gleede, Jens C. Markwart, Niklas Huber, Elisabeth Rieger, and Frederik R. Wurm, Competitive Copolymerization: Access to Aziridine Copolymers with Adjustable Gradient Strengths, *Macromolecules* **2019**, 52, 24, 9703-9714

4.1 Abstract

Competitive copolymerization gives access to gradient copolymers with simple one-step and one-pot strategies. Due to the living nature of the sulfonyl-aziridine polymerization, gradient copolymers can be obtained with low dispersities and adjustable molar masses. The combination of different sulfonyl activating groups allowed to fine-tune the reactivity difference of the comonomers and thus an exact adjustment of the gradient strength. Sulfonyl-activated aziridines are to date the only monomer class providing access to gradient copolymers with reactivity ratios ranging from: ($1 \leq r_1 \leq 2$; $1 \geq r_2 \geq 0.5$) for statistical- or soft gradient copolymers to block-copolymers ($r_1 \geq 20$, $r_2 \leq 0.02$), only by adjusting the electron-withdrawing effect of the activation groups: The reactivity ratios were calculated by different models for a library of eight comonomers. This library was further used to classify between hard, medium, and soft gradients. From the data obtained from the monomer library, it was possible to predict polymerization rate coefficients (k_p) for aziridines, which were not prepared so far: correlation of the shifts in the ^{13}C NMR spectra, the Hammett Parameters and secondary parameters such as calculated LUMO levels of the monomers and the natural charge at the electrophilic carbon, etc. were used to predict (co)monomer reactivity and the resulting gradient strength. We believe our findings allow to access tailored gradient copolymers with a controlled monomer sequence distribution depending on chemical control of comonomer reactivity. With these systematic data on activated aziridines, also more complex copolymer structures can be predicted and prepared. Such materials might find application as linear polyethylenimine derivatives to act as functional polyelectrolytes, or predesigned compatibilizers and surface-active gradient copolymers by a predictable one-step copolymerization.

4.2 Introduction

The properties of many biopolymers are defined by their monomer sequence. The precise order of monomers, e.g. nucleotides in our DNA and RNA contains our genetic code, the order of amino acids in polypeptides controls the shape of enzymes and thereby determines their activity. Driven by their complex structure, sequence control became a field of research also for artificial polymers, but today's polymer chemistry is still far behind nature's complexity.^{1,2} However, also in several synthetic examples polymer microstructures had a huge impact on materials science.^{3,4}

Herein, we controlled monomer sequence distribution by a competitive, living copolymerization of monomers with adjustable reactivity that will reflect their positioning along the polymer chain, resulting in adjustable gradient copolymers. Nature uses gradient materials to connect soft and hard tissues or surfaces, such as in bone tissue or nacre.⁵ Gradual mineralization or hierarchical pore structures play a crucial role in bio-inspired high-performance materials. Squid beaks are a prominent example representing a natural gradient material consisting of chitin and binding proteins which gradually introduce crosslinking which causes a hydrophobic environment in the chitin/protein network and a much higher break modulus and hardness.^{6,7} The gradient compared to a discrete section material has the advantage, that mechanical mismatches at the interface (weak spot) are avoided.⁵ Graded mechanical properties also exist in byssal threads of marine mussels, which represent a well-studied underwater adhesive material consisting of protein gradients, which allow fascinating properties regarding adhesive, water-resistance and tensile strength.⁸

In artificial copolymers, gradual monomer incorporation had resulted in unique mechanical properties or self-assembled structures.^{9,10} Using the bio-inspired principle of gradient materials to produce graded structures and materials is of high interest in orthopedic implants and other high-performance materials.¹¹ The application of Styrolux® and Styroflex® as gradient materials and polymer blend compatibilizers shows the impact of using gradients copolymers as additives. Such materials are superior to others in terms of impact strength and toughness of polymer films.^{12,13}

Gradient copolymers with different gradient strengths would offer a plethora of possibilities. However, the adjustment of the gradient strength is difficult to achieve, as often chain-end reactivity is limiting the monomers' compatibility or fixed reactivity ratios result in a single gradient profile only. Continuous monomer addition has been reported to control monomer gradients in controlled radical copolymerization (CRP), but this required precise control over the rate of addition and is thus error-prone.¹⁴⁻¹⁶ To further optimize gradient control in CRP,

D'Hooge and coworkers used *in silico* optimizations to get predetermined feeding strategies based on the Mayo-Lewis equation to achieve a high gradient quality.¹⁷ With atom transfer radical polymerization they achieved a linear gradient microstructure of *n*-butyl acrylate and methyl methacrylate via a batch approach. Linear gradients in CRP need an appropriate catalytic system, which leads to low dispersities and high monomer conversions.¹⁸ Figure 4.1A illustrated such a graded polymer microstructure obtained by using continuous monomer addition, resulting in a typical linear monomer feed. Depending on the speed of monomer addition, copolymers with smooth (area a) or up to hard gradients (area c) can be obtained. In this context, the term “gradient” copolymer is often used for materials with very different gradient profiles. We suggest specifying gradient copolymers according to their gradient profile: soft, medium, hard, and block-like with respect to the differences of their reactivity ratios.

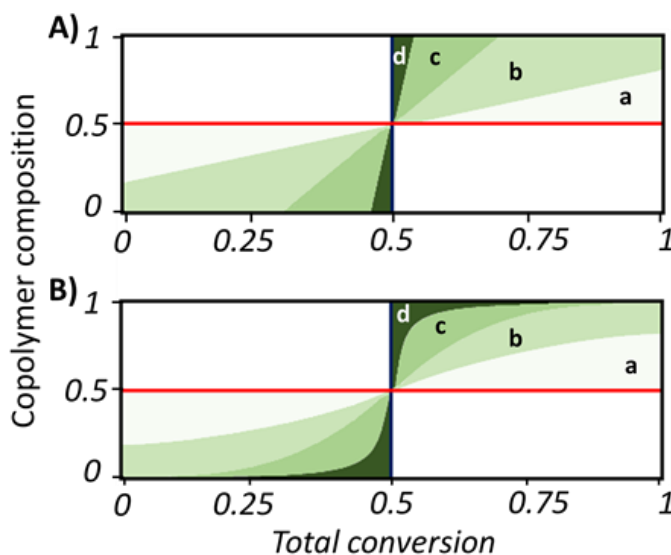
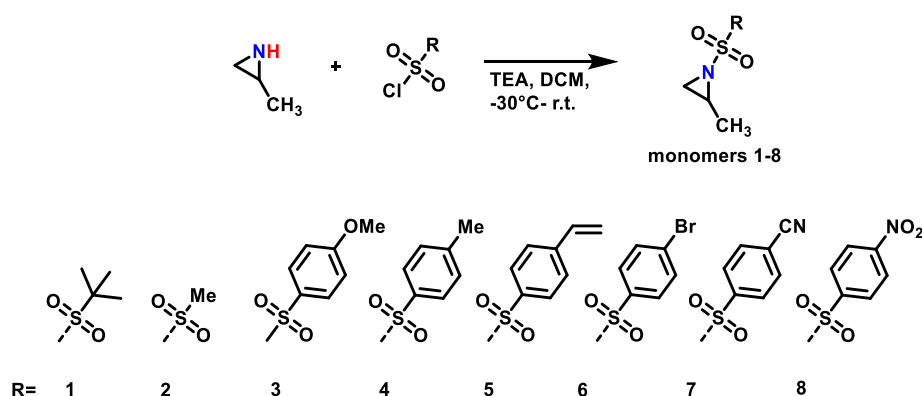


Figure 4.1: Polymer microstructures of gradient copolymers (of two monomers) with different gradient strengths prepared by living / controlled polymerization: plotted is the copolymer composition of monomer 1, against the total conversion of monomers 1 and 2, for living copolymerizations without termination. (A) Synthesized by continuous monomer feeding, with linear gradients. (B) Synthesized by competitive copolymerization of monomer mixtures with different reactivity ratios, with hyperbolic S-shape gradient.

In (competitive) copolymerizations the gradient strength depends on the reactivity ratios of the individual monomers and their crossover reactions. Reactivity ratios of the comonomers describe the reactivity differences for certain reaction conditions. The comonomer reactivity is chemically fixed and thus should be superior to error-prone dosing techniques. We have studied the anionic copolymerization kinetics for sulfonyl activated aziridines in recent years and present herein a systematic library of comonomers with precisely adjusted (co)monomer reactivity ratios covering the overall spectrum of gradient strengths (Figure 4.1B).^{19, 20} The gradients in Figure 4.1B can be distinguished from the linear gradients in Figure 4.1A by its natural S-shape, which can

occur symmetrically or asymmetrically. Ganesan used the term “hyperbolic” for gradients prepared by competitive/ statistical copolymerizations of monomer mixtures.²¹ By the introduction of different sulfonyl activation groups, the (co)monomer’s reactivity is controlled, depending on their electron-withdrawing effect (Scheme 4.2). A combination of different sulfonyl aziridines allows thereby a precise adjustment of the gradient strength in the resulting copolymer. To the best of our knowledge, this is the first example of a comonomer family that allows adjusting the reactivity ratios from perfectly random copolymerization to a formation of block copolymers. If the activating groups are removed after polymerization,^{22,23} a full range of gradient polyamines can be prepared. Further combination with epoxides had resulted in a selective copolymerization sequence with access to multi-block copolymers.²⁴ With this versatile synthesis platform for gradient-copolymers with a variable gradient strength, the terminology of “gradient” needs to be specified. With the *in situ* techniques to follow (co)polymerization reactions reliable methods to calculate reactivity ratios and polymer microstructures have been developed. From the recorded data, reactivity ratios, and Monte-Carlo simulations of the comonomer distributions, are provided. Monte-Carlo simulation as a kinetic model allows illustrating the polymer microstructure. Kinetic models, however, can also determine distributions, chain lengths and many more features of the copolymers.²⁵ Due to the systematic data obtained from our monomer library, also the prediction of reactivity ratios by Hammett parameters or the ¹³C- NMR shift of monomers was feasible. These easy design principles will allow the preparation of functional poly(sulfonyl aziridine)s or (after hydrolysis) polyamines for various applications.^{22,23}



Scheme 4.1: Synthesis of sulfonyl-activated aziridines starting from 2-methyl aziridine and sulfonyl chlorides (1-8). The monomers are sorted by increasing the electron-withdrawing effect of the activation group (AG).

4.3 Experimental Section

4.3.1 Materials

All solvents and reagents were purchased from Sigma-Aldrich, Acros Organics or Fluka and used as received unless otherwise mentioned. All deuterated solvents were purchased from Deutero GmbH and were distilled from CaH_2 or sodium and stored in a glovebox prior to use. All monomers and initiators were dried extensively by azeotropic distillation with benzene prior to polymerization. 2-decyl-*N*-busyl-aziridine (**1**) was synthesized according to previous protocols.¹⁸ 2-methyl-*N*-mesyl-aziridine (**2**), 2-methyl-*N*-tosylaziridine (**4**), 2-methyl-*N*-brosylaziridine (**6**), 2-methyl-*N*-nosylaziridine (**8**), and *N*-benzyl methane sulfonamide (BnNHMs) were synthesized to our previously published protocol.²⁶ 2-decyl-*N*-mesyl-aziridine and 2-decyl-*N*-tosyl-aziridine were synthesized according to a previously published protocol.^{27, 28} **5** was synthesized according to literature.²⁹ 2-methyl-*N*-(4-methoxyphenyl)sulfonyl aziridine (**3**), 2-methyl-*N*-(4-cyanophenyl)sulfonyl aziridine (**7**) were synthesized in analogy to **4** (analytical details below and ¹H NMR, ¹³C NMR in the Supporting Information Section 3).

4.3.2 Instrumentation

NMR: ¹H NMR spectra were recorded using a Bruker Avance 300, a Bruker Avance III 700. All spectra were referenced internally to residual proton or carbon signals of the deuterated solvent, if not noted otherwise. SEC: Size exclusion chromatography (SEC) measurements of polymers were performed in DMF either at 60 °C and a flow rate of 1 mL/min with a PSS SECcurity as an integrated instrument (1 g L⁻¹ LiBr added) with a PSS GRAM 100-1000 column and a refractive index (RI) detector or in DMF (containing 0.25 g L⁻¹ LiBr) on an Agilent 1100 Series as an integrated instrument, including a PSS HEMA column (10⁶/10⁵/10⁴ g mol⁻¹) and a RI detector at a flow rate of 1 mL min⁻¹ at 50 °C. Calibration was carried out using poly(ethylene glycol) standards provided by Polymer Standards Service.

4.3.2.1 Synthesis of **7**

In a dry 250 mL, round bottom flask equipped with a stirring bar the 4-cyanobenzolsulfonylchloride (7.5 g, 36 mmol) was dissolved in 200 mL of dry dichloromethane. The reaction mixture was cooled in a dry-ice acetone bath at -30 °C. 4.5 mL triethylamine (3.3 g,

33 mmol) was added slowly *via* syringe. 2.4 mL freshly distilled methyl aziridine (33 mmol) diluted in 20 mL dry dichloromethane was added dropwise to the reaction mixture. After stirring for 30 min at -30 °C the reaction mixture was further stirred at room temperature for 2 hours. The DCM phase was washed with water (3x 50 mL), 0.2N HCl (1x 50 mL), saturated sodium bicarbonate solution (1x 50 mL) and brine (1x 50 mL). The organic layer was dried over MgSO₄, filtered and concentrated below 30 °C at reduced pressure to give the product as a colorless solid. (Yield: 6.8 g, 93%). Polymerizations were conducted with freshly recrystallized monomer. Therefore the monomer was dissolved in *tert*-butyl methyl ether (1 g in 2 mL) and recrystallized at -20 °C (small amounts of petroleum ether can be added if not crystallization occurs under these conditions); yield 400 mg (40%) purified monomer. Note: The supernatant after recrystallization can be concentrated at reduced pressure and recrystallization can be performed again. Attempted purification by sublimation or column chromatography over silica indicated ring- opened product. ¹H NMR (300 MHz, benzene-*d*₆) δ 7.66 – 7.47 (m, 2H), 6.88 – 6.70 (m, 2H), 2.53 (h, *J* = 5.7 Hz, 1H), 2.24 (dd, *J* = 7.0, 1.6 Hz, 1H), 1.34 (dd, *J* = 4.6, 1.6 Hz, 1H), 0.71 (dd, *J* = 5.6, 1.6 Hz, 3H). ¹³C NMR (176 MHz, chloroform-*d*) δ 142.92, 132.99, 128.52, 117.32, 36.82, 35.56, 16.90

4.3.2.2 Synthesis of 3

In a dry 100 mL, round bottom flask equipped with a stirring bar, 4-methoxybenzolsulfonylchloride (3.0 g, 14.4 mmol, 1 equiv.) was dissolved in 70 mL of dry dichloromethane. The reaction mixture was cooled in a dry-ice acetone bath at -30 °C. 3 mL triethylamine (21 mmol, 1.5 equiv.) was added slowly *via* syringe. Freshly distilled methyl aziridine (1.0 mL, 16 mmol, 1.1 equiv.) diluted in 20 mL dry dichloromethane was added dropwise to the reaction mixture. After stirring for 30 min at -30 °C the reaction mixture was further stirred at room temperature for 2 hours. The DCM phase was washed with water (3x 50 mL), saturated sodium bicarbonate solution (1x 50 mL) and brine (1x 50 mL). The organic layer was then dried over MgSO₄, filtered and the solvent was removed at reduced pressure (yield: 2.5 g, 83%). Further purification by column chromatography over silica can be conducted with petrol ether and ethyl acetate (3:7 volume ratio) *R_f*: 5.4. The product was obtained as a colorless solid.

¹H NMR (300 MHz, chloroform-*d*) δ 7.94 – 7.82 (d, 2H), 7.05 – 6.96 (d, 2H), 3.88 (s, 3H), 2.88 – 2.72 (m, 1H), 2.59 (d, *J* = 7.0 Hz, 1H), 2.01 (d, *J* = 4.6 Hz, 1H), 1.25 (d, *J* = 5.6 Hz, 3H).

¹³C NMR (75 MHz, chloroform-*d*) δ 163.68, 130.11, 130.00, 118.30, 114.40, 55.79, 35.92, 34.84, 16.94.

4.3.2.3 Monitoring polymerizations by *in-situ* ^1H NMR spectroscopy.

Inside of a glovebox in a nitrogen-atmosphere, 100 mg of the respective monomer or monomer mixture was dissolved as a 10 wt% solution with a total volume of 1.0 mL deuterated DMF. A monomer to initiator ratio of $[\text{M}]_0:[\text{I}]_0 = 50:1$ was used in all cases. The initiator-solution in 1 mL deuterated DMF was prepared separately. E.g.: BnNHMs (10 equiv.), Potassium bis(trimethylsilyl)-amide (KHMDs) (10 equiv.) in 1 mL DMF- d_7 . From this 1/10th (1equiv.) was used. A conventional NMR-tube was filled with the monomer(s) in DMF and sealed with a rubber septum. From the initiator stock solution, 100 μL were added to the monomer mixture, mixed quickly and inserted into the spectrometer. All ^1H NMR kinetics were recorded using a Bruker Avance III 700. All spectra were referenced internally to residual proton signals of the deuterated solvent dimethylformamide- d_7 at 8.03 ppm. The $\pi/2$ -pulse for the proton measurements was 13.1 μs . The spectra of the polymerizations were recorded at 700 MHz with 32 scans (equal to 404 s (acquisition time of 2.595 s and a relaxation time of 10 s after every pulse)) until the polymerization was completed. No B-field optimizing routine was used over the kinetic measurement time. The spin-lattice relaxation rate (T1) of the ring-protons, which are used afterward for integration, was measured before the kinetic run with the inversion recovery method.³⁰

4.3.2.4 Determination of reactivity ratios

The reactivity ratios illustrated in Table 4.1 were calculated by three different nonterminal models following the instructions of Jaacks,³¹ Frey,³² or BSL³³ and the Meyer-Lowry³⁴ model as a terminal model. For the anionic polymerization of aziridines, a nonterminal approach should be valid, given our previous studies: the propagating sulfonamide anions do not differ significantly in their size or nucleophilicity,³⁵ indicating a similar chain-end reactivity for all growing chains. We further assume efficient initiation by the activated initiator because the sulfonamide initiator (BnNHMs) is fully deprotonated.

Calculation of reactivity ratios by using the Jaacks model:

The Jaacks model estimates the reactivity ratios under the assumption of an ideal copolymerization $r_1 \cdot r_2 = 1$.³¹ Using this assumption the following equation can be used to fit the experimental data.³⁶

Copolymerization equation of an ideal copolymerization.³⁶

$$\frac{d[M_1]}{d[M_2]} = r_1 \frac{[M_1]}{[M_2]} \quad (\text{equation 1})$$

$$\frac{[M_1]}{[M_{1,0}]} = \left(\frac{[M_2]}{[M_{2,0}]} \right)^{r_1} \quad (\text{equation 2})$$

$$\log \left(\frac{[M_1]}{[M_{1,0}]} \right) = r_1 \log \left(\frac{[M_2]}{[M_{2,0}]} \right) \text{ (equation 3)}$$

$$r_2 = \frac{1}{r_1} \text{ (equation 4)}$$

Calculation of reactivity ratios by using the Meyer-Lowry model:³⁴

$$X = 1 - \left(\frac{f}{f_0} \right)^{\frac{r_2}{1-r_2}} \cdot \left(\frac{1-f}{1-f_0} \right)^{\frac{r_1}{1-r_1}} \cdot \left(\frac{f - \frac{1-r_2}{2-r_1-r_2}}{f_0 - \frac{1-r_2}{2-r_1-r_2}} \right)^{\frac{r_1 r_1 - 1}{(1-r_1)(1-r_2)}} \text{ (equation 5)}$$

Calculation of reactivity ratios by using the Frey model:³²

The ideal integrated model estimated the reactivity ratios under the assumption of a simplified version of an ideal copolymerization and defined $r_1 * r_2 = 1$. This model is mathematically less complex and prevents overfitting. r_2 is calculated with equation 4 and not by fitting. Equation 6 is similar to the first two terms of the Meyer-Lowry equation. However, the exponents, containing the reactivity ratios, only consider a single r-value as its origin is a non-terminal ideal

$$\text{model } (r_1 \cdot r_2 = 1)$$

$$X = 1 - \left(\frac{f}{f_0} \right)^{\frac{1}{r_1-1}} \cdot \left(\frac{1-f}{1-f_0} \right)^{\frac{r_1}{1-r_1}} \text{ (equation 6)}$$

Calculation of reactivity ratios by using the BSL model:

The BSL model is another non-terminal model for the calculation of the reactivity ratios, using the following definition for the monomer conversion using equations 7 and 8 from literature.³³ The equation enables the determination of reactivity ratios at any conversion for copolymerizations, which follow the nonterminal model of copolymerization kinetics.

$$X = 1 - f_{1,0} \left(\frac{M_1}{M_{1,0}} \right) - (1 - f_{1,0}) \left(\frac{M_1}{M_{1,0}} \right)^{r_2} \text{ (equation 7)}$$

$$X = 1 - f_{1,0} \left(\frac{M_2}{M_{2,0}} \right)^{r_1} - (1 - f_{1,0}) \left(\frac{M_2}{M_{2,0}} \right) \text{ (equation 8)}$$

4.3.2.5 Calculation of the copolymer microstructure

The copolymer microstructure can be calculated by the previously obtained reactivity ratios r_1 and r_2 . Therefore, the instantaneous copolymer composition F_1 is plotted against the total monomer conversion X .

Equations used for the calculation of the copolymer microstructure:

$$X = 1 - \frac{[M_1] + [M_2]}{[M_{1,0}] + [M_{2,0}]} \text{ (equation 9)}$$

$$b = \frac{[M_1]}{[M_2]} \text{ (equation 10)}$$

$$\varepsilon = \frac{1+r_1 b}{1+r_2 b^{-1}} \text{ (equation 11)}$$

$$F_1 = \frac{\varepsilon}{1+\varepsilon} \text{ (equation 12)}$$

4.3.2.6 Computational Details

All DFT calculations were carried out with the Gaussian 09 package.³⁷ The structures were optimized at the B3LYP level of theory,³⁸ with the basis set of 6-31+G*.^{39, 40} Accurate electronic energies were obtained from single point calculations at the B3LYP level upon the optimized structures, in conjunction with the 6-311++G** basis set.^{39, 41} The single point calculations were performed together with the PCM (Polarizable Continuum Model) model by employing DMF as the solvent.⁴²⁻⁴⁴ Vertical ionization potentials and electron affinities were computed with the solution-phase single point electronic energies. Population analysis was carried out using the natural bond orbital option within the single point calculations.⁴⁵

The following equations have been used to calculate the interested properties:

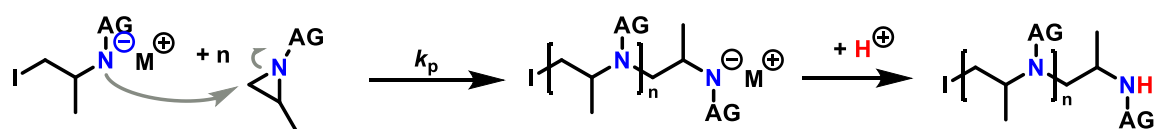
$$\mu = -\frac{1}{2}(IP + EA) \text{ (equation 13)}$$

$$\eta = IP - EA \text{ (equation 14)}$$

with IP is the ionization potential, EA is the electron affinity, η is the chemical potential and μ is the chemical hardness. The IP and EA were calculated based on the relax geometries of cations and anions.

4.4 Results and Discussion

To synthesize gradient copolymers in a batch or one-pot reaction it is essential to use a controlled or living polymerization techniques. Living anionic polymerization of aziridines was conducted in 2005 for the first time by substituting the *N*-proton with a sulfonyl group.⁴⁶ The electron withdrawing nature of the sulfonyl group allows a nucleophilic attack on the non-substituted side of the aziridine ring. Depending on the electron-withdrawing strength of the sulfonyl substituents, the monomer reactivity can be adjusted.²⁰ By choosing functional groups either as a side group in the 2-position^{27, 47} or on the activation group²⁹ multiple functional polyethylenimine derivatives are accessible.



Scheme 4.2: The living anionic ring-opening polymerization of activated aziridines (AG = activation group).

We previously studied the polymerization kinetics of activated aziridines under different conditions. In contrast to epoxide polymerization, different alkali metal counter ions only slightly influenced the polymerization kinetics;⁴⁸ the presence of protic impurities is tolerated by the weakly basic sulfonamide chain-end but slowed down propagation rates.³⁵ Multi-gradient copolymers had been prepared by copolymerization of up to five different activated aziridines in solution²⁰ or adjustable gradient copolymers were prepared by polymerization in emulsion.²⁸

4.4.1 Monomer Synthesis and Polymerization

Monomers **1**, **2**, **4-6**, **8** were prepared according to our previous protocols.^{20, 29, 46} **3** and **7** were synthesized to enlarge the comonomer reactivity library by a similar protocol: the one-step reaction of 2-methyl aziridine and the respective sulfonyl chlorides was applied with yields higher than 80% in most cases.^{20, 29, 46} Both, the novel monomer **7** and monomer **8**²⁰ are highly reactive to moisture and special care has to be taken in their purification and storage (see experimental part for details). Similar findings were reported by Rupar and coworkers for other nitrosyl aziridines.⁴⁹ To suppress spontaneous polymerization of **7** or **8**, it proved to be essential to remain the temperatures below 30 °C during workup and to use mild recrystallization for purification. The polymerizations were conducted in an NMR tube, resulting in well-defined polysulfonamides with narrow molar mass distributions and monomodal SEC elugrams (representative examples for P(**3**) and P(**7**) are reported in Figures S4.15 and S4.17).

4.4.2 Prediction of the monomer reactivity and a forecast on the polymer microstructure

The electron-withdrawing (EWD) behavior of the sulfonyl groups in the monomer library (1-8) was quantified (Scheme 4.1): To predict comonomer gradient profiles, the ^{13}C NMR shifts of the ring carbons can be used easily to illustrate the electron-withdrawing strength of the different sulfonamides. Figure 4.2A shows a zoom into the ^{13}C NMR spectra of the monomers. For a better comparison between the different electron withdrawing groups, the chemical shift of the pendant methyl group was set as a reference. The relative chemical shifts of the electrophilic carbons in the 2- and 3-position clearly shifted downfield, with increasing EWD strength of the substituents from 1 to 8. The Hammett parameter (σ), a substituent constant correlating originally to the reaction coefficient of benzoic acid derivatives, correlates also with the carbon shift of the ^{13}C NMR spectra, allowing to quantify and to predict the copolymerization behavior. Figure 4.2B illustrates the relation of the Hammett parameter of each monomer with the chemical shifts determined from the ^{13}C NMR spectra. A similar linear relation of the Hammett parameter with the β -carbon shifts of different vinyl monomers was reported by Ishizone *et al.*⁵⁰ We here observed this trend for monomers which undergo ring-opening polymerization, to the best of our knowledge a similar reactivity profile has not been reported for oxiranes, thiiranes, cyclic esters or other cyclic monomers for ring-opening polymerization.

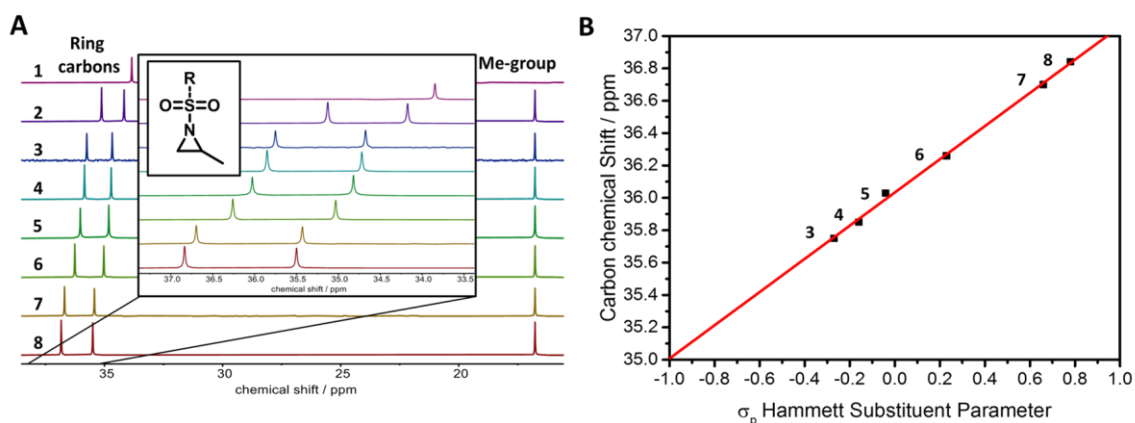


Figure 4.2: A: Zoom into the ^{13}C NMR spectra of activated aziridines 1-8 ordered from top to bottom with increasing EWD behavior (note: the chemical shift of the pendant methyl group was used as a reference), B: Correlation between the ^{13}C NMR shift and the Hammett substituent parameter σ . (Note: Values for monomers 1 and 2 are not listed, as they carry aliphatic sulfonamides.)

The propagation rate coefficient (k_p) for the polymerizations of monomers **1-8** (except **5**) were determined from *in-situ* ^1H NMR spectroscopy by a previously reported method.²⁰ The k_p -values correspond to the electron-withdrawing effect of the sulfonyl group in the order **1** (slow) to **8** (fast), ^1H NMR data for the new P3 and P7 are summarized in Figure S4.16, S4.18. Table 4.1 summarizes the kinetic data for the polymerizations, the ^{13}C NMR shifts, and the Hammett parameters (σ) for all monomers. Section 3 in the Supporting Information summarizes the theoretical and experimental molar masses and the dispersities (determined by SEC). The apparent molar masses from SEC of polyaziridines (e.g. **3** and **7**) are underestimated compared to the theoretical molar mass on our setup, which might be attributed to the hydrophobic character of the polymers. Also the relatively high molar mass of the pendant chains does not increase the hydrodynamic radii of the polymers, which further decreases the apparent molar masses in SEC.

Table 4.1: Relative ^{13}C NMR shifts and Hammett parameters for monomers 1-8 and kinetic data and molar mass characteristics of for P1-P8.*

Monomer	(1)*	(2)*	(3)	(4)	(5)**	(6)***	(7)	(8)***
<i>reference</i>	²⁰	²⁰	<i>This work</i>	²⁰	²⁹	²⁰	<i>This work</i>	²⁰
$\text{C}_2\text{-}^{13}\text{C}$ NMR shift	34.03	35.13	35.75	35.85	36.03	36.26	36.70	36.84
Hammett Parameter σ	---	---	-0.27	-0.17	-0.04	0.23	0.66	0.78
$k_p / 10^{-3} \text{ L mol}^{-1} \text{ s}^{-1}$	5	15	37	41	50	71	90	97

* calibration to solvent signal (77.16 ppm). ** k_p value of **5** was determined *via* a correlation method using equation 15. *** k_p values were taken from the literature. Polymerizations conducted with 10 wt% monomer concentration, with 50 equivalents monomer to 1 equivalent initiator at 50 °C in DMF- d_7 ,

Besides the ^{13}C NMR shift of each monomer, also the propagation rate coefficient (k_p) correlated in the same trend to the Hammett parameters (Figure 4.3; note: monomers having a non-aromatic activation group (1 and 2) are shown in grey, not included in the fit). Based on the ^{13}C NMR shifts and/or the Hammett parameters, prediction of the propagation rates of other activated aziridines becomes feasible by the following fit equations calculated from the experimental data (from Figures 4.3A and 4.3B):

$$k_p = 58 \cdot \sigma + 52 \text{ (equation 15)}$$

$$k_p = 56 \cdot {}^{13}\text{C shift} - 1973 \text{ (equation 16)}$$

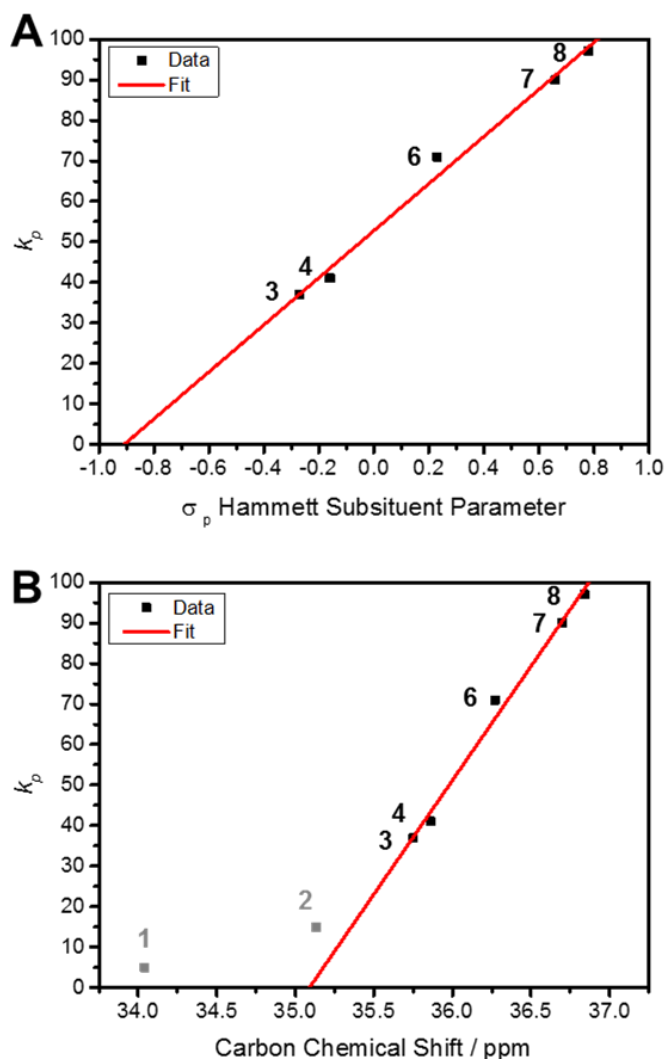


Figure 4.3: (A) Correlation between the determined k_p values and the Hammett Substituent Parameter. (B) Correlation between k_p values and ^{13}C shift of the 3 positioned ring carbon (in gray the aliphatic activation groups, excluded from the linear fit).

The k_p value for monomer 5 was calculated exemplarily: equation 15 gave $k_p = 50 \cdot 10^{-3} \text{ L mol}^{-1} \text{ s}^{-1}$, while equation 16 gave a very similar $k_p = 52 \cdot 10^{-3} \text{ L mol}^{-1} \text{ s}^{-1}$, indicating that both relations can be used to estimate polymerization kinetics, which corresponded well with its copolymerization behavior (cf. Table 4.3). Figure 4.4 shows several predicted values for aromatic sulfonyl-activated aziridines based on the Hammett parameters of the substituents (Table S4.1 summarizes the Hammett parameters according to reference⁵¹ and the calculated k_p values according to equation 15. Note: the Hammett parameters are only valid for aromatic sulfonamides, the aliphatic sulfonamides, however, seem to follow the same trend of reactivity controlled by the EWD of the respective group).

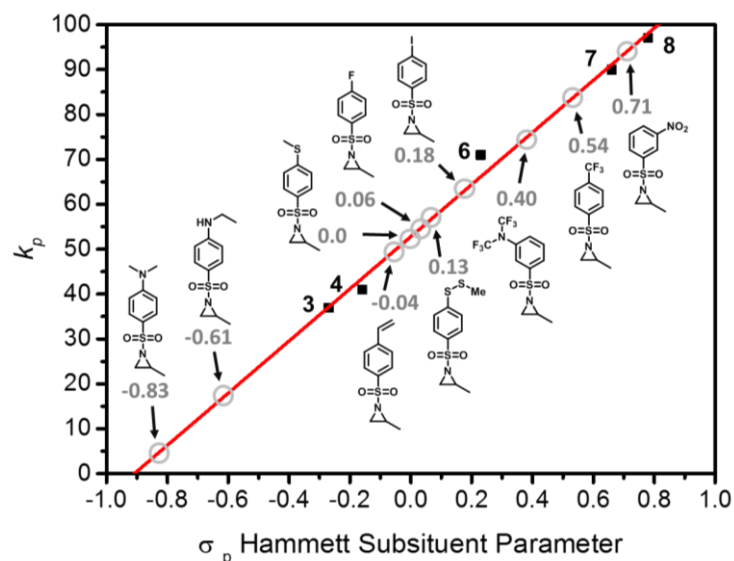


Figure 4.4: Prediction of propagation rate constants (k_p) of various sulfonyl aziridines vs. Hammett parameters (black squares: measured, grey circles: Hammett parameters are taken from literature and estimated k_p value).

In addition to NMR data and Hammett parameters, DFT calculations were conducted to quantify the electron-withdrawing behavior and correlate this to the monomer reactivity. Calculations were performed employing the Gaussian self-consistent reaction field (SCRF) option with *N,N*-dimethylformamide as solvent. Details on this option can be found here <https://gaussian.com/scrf/> and details on the overall setup of the calculations can be provided in the section to computational details. To assess the monomers' reactivity, LUMO and HOMO energies of the sulfonyl aziridines, bond lengths of the N-S bond and the natural charge of the electrophilic site of the activated aziridines were used (cf. Table S4.2). In all cases, also these calculated values allow sorting sulfonyl-activated aziridines to their expected ^{13}C NMR shifts or propagation rates (Figure S4.1). Figure S4.1A shows, the LUMO and HOMO energies of all monomers. As LUMO energies decrease with increasing EWD, this calculation allows a quick estimation of monomer reactivity. The data indicated that a potential monomer with a reactivity higher than monomer **8** has a LUMO energy which is lower than -3.5 eV and thereby probably very unstable and plagued by spontaneous polymerization. The nitrosyl monomers prepared by Rupar *et. al.*⁴⁹ are an example of such highly reactive sulfonyl aziridines as they spontaneously ring-opened. Such findings are supported by data from Stanetty and coworkers, who reported on dinosyl activated aziridines that ring-opened rapidly in the presence of alcohols.⁵² As Figures S4.1B and S4.1D illustrate the N-S bond distance shortens systematically, which correlates with the explanations that the free electron pair of the nitrogen compensated the electron loss on the sulfur caused by the activation group. The natural charge at the electropositive carbon in Figure S4.1 C and S4.1E represent the electrophilicity of the 3-positioned carbon caused by the EWD

nature of the activation groups, with very reactive monomers having a higher natural charge. In summary, sulfonyl activated aziridines allow a systematic adjustment of comonomer reactivity and thus the preparation of a variety of gradient copolymers.

4.4.3 Copolymers: Reactivity ratios and variation of polymer gradient strength

The monomer sequence distribution in copolymers of sulfonyl aziridines depends on the different EWD group of each comonomers. Hoogenboom and coworkers recently studied cationic ring-opening copolymerizations of oxazolines and oxazines and reported that the reactivity ratios depended on the nucleophilicity of the monomers and less on the electrophilicity of the chain end.^{53, 54} For anionic polymerization, the comonomer reactivity depends mostly on the electrophilic nature of the monomers but not on the nucleophilicity of the active chain end.³⁵ Copolymers with different gradient profiles had been reported from carbanionic,⁵⁵⁻⁵⁷ oxyanionic,^{32, 58} and azaanionic copolymerization.^{20, 28} In general, reactivity ratios can be calculated from copolymerization data via different models. The oldest methods to extract reactivity ratios were developed by Wall,³¹ followed by Alfrey and Goldfinger,⁵⁹ as well as Mayo and Lewis.⁶⁰ They can be used for either terminal or nonterminal polymerizations. However, the differential equations are replaced by modern integrated fitting models. Meyer and Lowry applied an integrated Mayo-Lewis equation. The Meyer-Lowry model can directly fit the experimental data; comonomers composition (f) in the reaction mixture depending on the total comonomers conversion (X) in the form of a compositional drift.³⁴ Meyer-Lowry and other integrated models are further distinguished by being nonterminal or terminal models, meaning that the nature of the active chain end has or has no effect on the polymerization. Modern *in silico* modeling techniques can also consider the influence of the monomer sequence just before the active chain end, e.g. two monomers (penultimate), three monomers (pen-penultimate).^{25, 61} Reactivity ratios were calculated by nonterminal models; Recently, Lynd and coworkers suggested that reliable reactivity ratios could be calculated either *via* the Meyer-Lowry (if the terminal model is required) or the Beckingham-Sanoja-Lynd method (BSL / nonterminal model) because the integrated methods are more accurate than linearized models. The authors also pointed out the importance of choosing the right method to distinguish between non-terminal and terminal copolymerizations to determine accurate reactivity ratios.⁶² Non-terminal models like BSL should be preferred for the oxyanionic ring-opening polymerization.^{32, 33} In addition to the existing non-terminal methods, the authors introduced a method to calculate reactivity ratios based on a simplified version of the Meyer-Lowry equation. The original Meyer-Lowry approach

fits both reactivity ratios, while the adapted version fits only one and calculates the other from the reciprocal of r_1 (see equations 5 and 6). This fitting plot has the same axis as the Meyer-Lowry method (an integrated form of Mayo Lewis), which allows direct comparison of non-terminal with a terminal model³² In 1972, Jaacks reported an elegant method, which does not use the Meyer-Lowry equation to extract reactivity ratios. His approximate terminal model is also applicable to copolymerizations like the one of styrene and methacrylate, which require a terminal model.³⁶ In contrast to most literature, in which typically only a single calculation method is used, which might lead to inaccurate results, we used four models to calculate the reactivity ratios for our copolymerizations. We monitored all copolymerizations by *in situ* ^1H NMR and extracted the monomer conversions by selecting one or more distinct proton resonances. To calculate the reactivity ratios, we applied different methods on the data (varying the conversions to minimize the difference of the obtained values). Therefore, we calculated the respective reactivity ratios by the different methods at different conversions (usually up to 40%) to minimize the difference of the resulting reactivity ratios by the linear least square method (data, which was not used to determine the fit function is illustrated in grey in the plots in the Supporting Information or Figure 4.5). In most cases at least three methods resulted in very similar reactivity ratios (Tables 4.2 and 4.3), which also correlate with the reactivity of each monomer expected from the electron-withdrawing effects of the sulfonamide activating groups. To the best of our knowledge, this calculation and optimization of reactivity ratios by different methods and varying conversion has not been reported before. The electron-withdrawing effects of the sulfonamides, i.e. the electrophilicity of each comonomer allows prediction of the expected reactivity ratios and is an additional control over the calculated values. To visualize the polymer microstructures, we used the reactivity ratios based on the method reported recently (Tables 4.2 and 4.3)³² using the equation for comonomers composition (F_1) :

$$F_1 = \frac{d[M_1]}{d[M_1]+d[M_2]} = \frac{r_1f_1^2+f_1f_2}{r_1f_1^2+2f_1f_2+r_2f_2^2} \text{ (equation 17)}$$

We present two visual illustrations of the monomer distribution in the copolymers: the monomer fraction (F) was plotted against the total conversion for a theoretical 50:50 mixture of both comonomers. This plot easily allows predicting the copolymer microstructure visualizing the gradient strength (Table 4.2 and 4.3 middle plot). In addition, we performed Monte Carlo simulations to better visualize the comonomer incorporation. We used the monomer reactivities and plotted a theoretical monomer distribution of 10 individual copolymer chains vs. the degree of polymerization. In contrast to previous visualizations for comonomer sequence distributions calculated by Monte Carlo simulations,³² we set the molar mass dispersity to unity to exclude chain length effects on the visualization. Both plots, allow estimating the percentage of the

tapered part in the polymer and the actual gradient strength. Table 4.2 shows the copolymer compositions of tosyl- and mesyl activated aziridines with varying side chains. This set of copolymerizations underline that the monomer reactivity is dominated by the electron withdrawing effect of the activation group, while the side group in the 2-position of the aziridines had only little influence on the comonomer reactivity in those cases. If tosyl monomers were copolymerized with mesyl activated aziridine (Table 4.2, entries 1 and 2), copolymers with a medium gradient strength were obtained. No significant difference for the reactivity ratios ($r_1 \approx 5$ and $r_2 \approx 0.2$) and microstructures was determined in both cases. In contrast, for copolymerization of aziridines with the same activation groups, random copolymers were obtained (Entries 3 and 4 of Table 4.2).

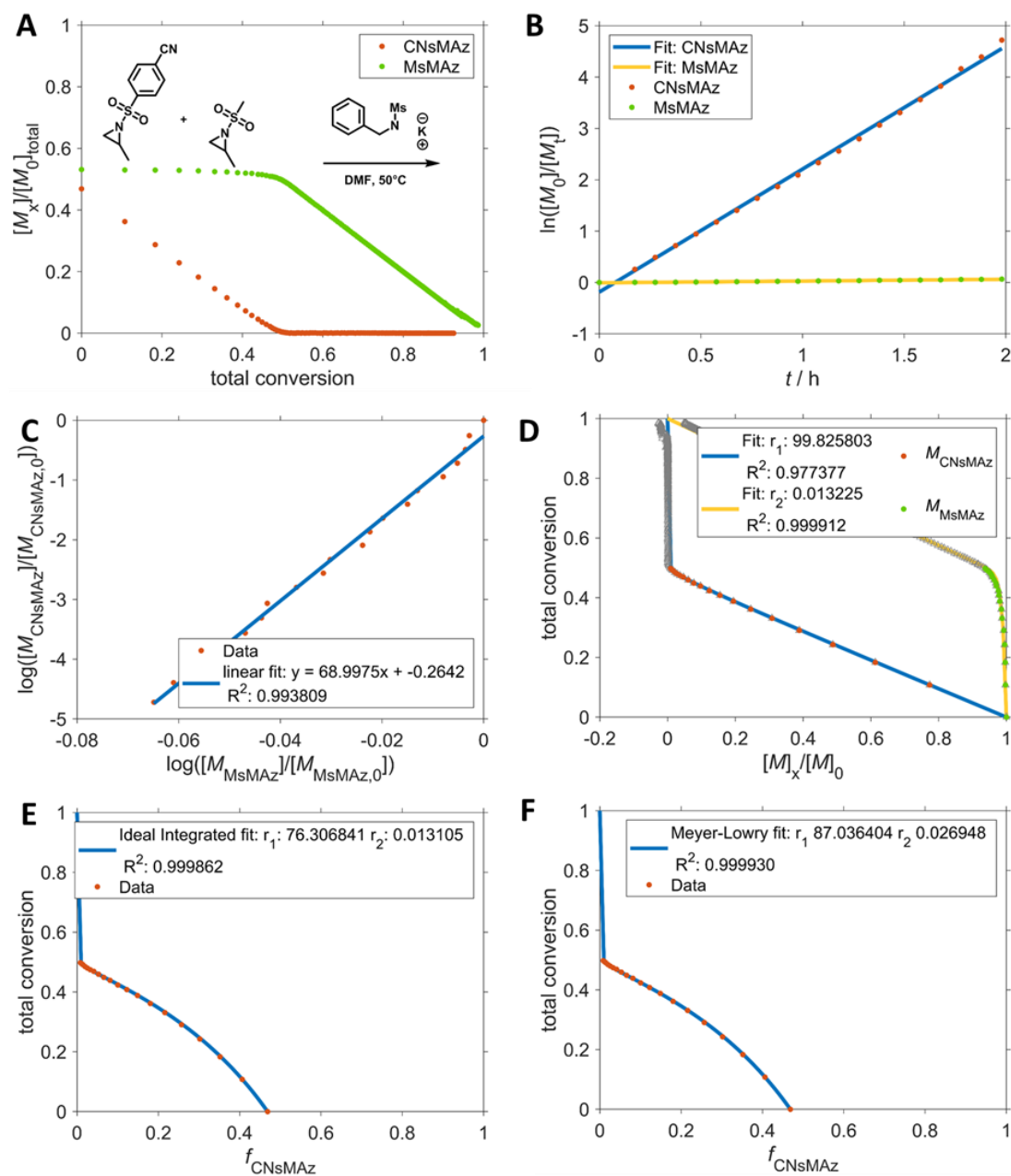
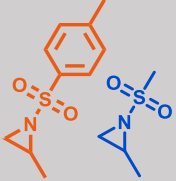
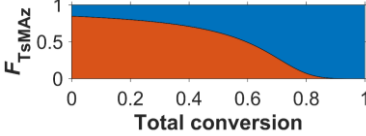
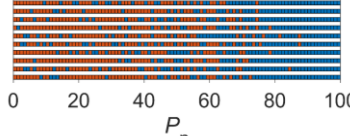
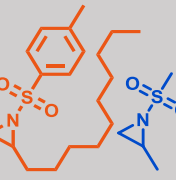
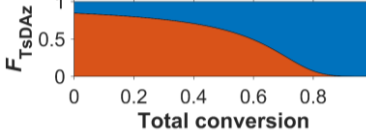
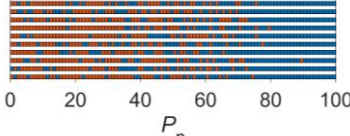
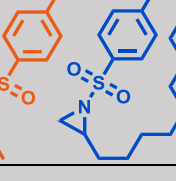
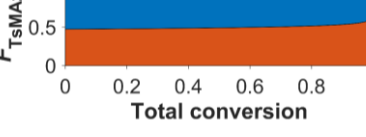
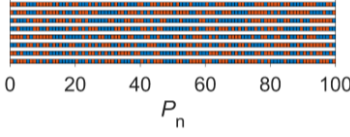
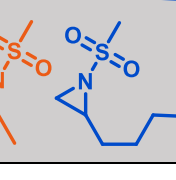
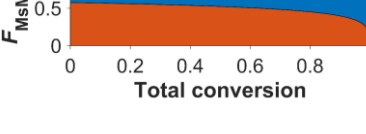
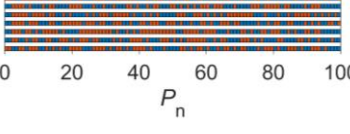


Figure 4.5: Copolymerization data for the combination of monomers 2 and 7. **A:** Monomer concentration as function of total conversion; **B:** logarithmic plot of monomer consumption over time (linearity proves living character); **C:** Jaacks fit on *in-situ* NMR data of the copolymerization; **D:** BSL fit on *in-situ* NMR data of the copolymerization; **E:** Frey fit on *in-situ* NMR data of the copolymerization; **F:** Meyer-Lowry fit on *in-situ* NMR data of the copolymerization. All methods used data from 0 to 50% conversion to determine reactivity values.

Table 4.2: Comonomer reactivity and distributions for copolymerizations of sulfonyl aziridines with different activating groups and the reactivity ratios calculated with nonterminal models from Jaacks,³⁶ Frey,³² BSL,^{33, 62} and Meyer-Lowry³⁴ (M-L). Visualization of the copolymer compositions calculated from the reactivity ratios and via Monte Carlo simulated microstructure of the copolymers.

Co-Monomers	Reactivity ratios		Illustrations of microstructures	
	Method	r_1, r_2	Monomer fraction F plotted against total conversion	Monte Carlo simulation of comonomer distribution
	Jaacks	5.476, 0.182		
	Frey	5.526, 0.180		
	BSL	5.540, 0.181		
	M-L	5.634, 0.190		
	Jaacks	5.508, 0.181		
	Frey	5.493, 0.182		
	BSL	5.487, 0.182		
	M-L	5.461, 0.178		
	Jaacks	0.929, 1.074		
	Frey	0.900, 1.110		
	BSL	0.903, 1.106		
	M-L	n. c.		
	Jaacks	1.354, 0.737		
	Frey	1.359, 0.735		
	BSL	1.359, 0.735		
	M-L	1.428, 0.784		

n. c. not calculated. M-L did not give reasonable reactivity ratios for the fitted data with any monomer conversion

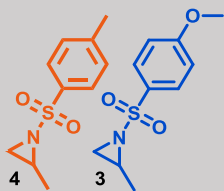
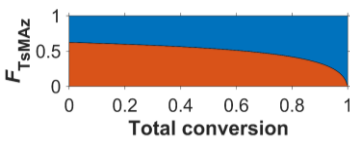
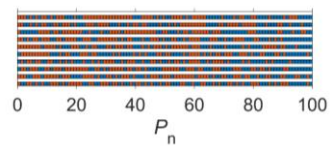
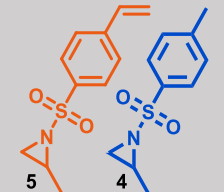
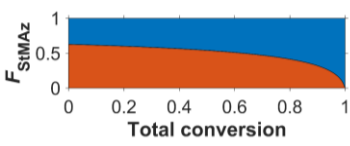
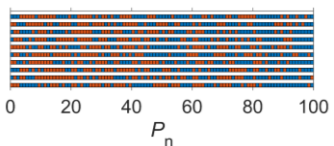
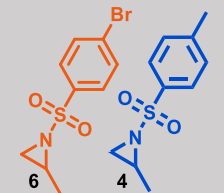
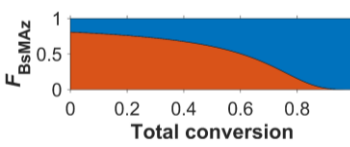
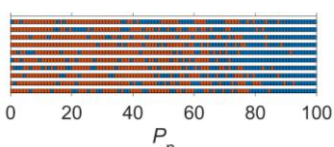
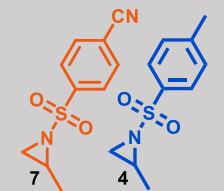
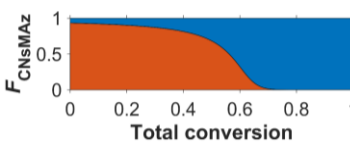
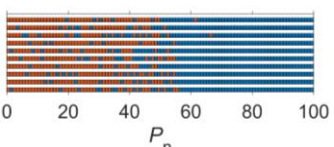
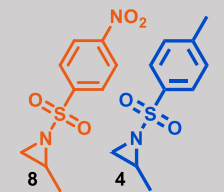
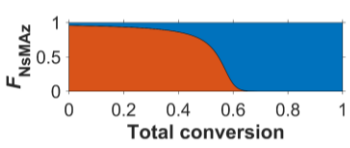
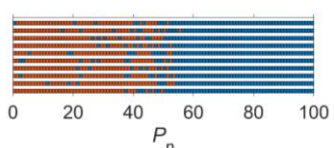
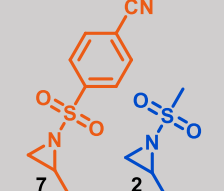
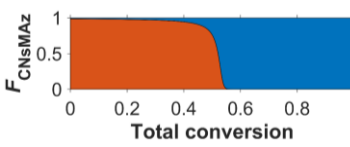
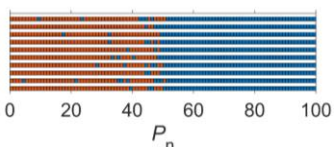
Besides these random and medium gradients (region b in Figure 4.1), activated aziridines allowed the preparation of other gradient profiles as well. Copolymers with soft gradients were accessible for example, when **(3)** and **(4)** with reactivity ratios of 1.75 and 0.57 were copolymerized. The gradient with **5** represented with similar reactivity ratios also a copolymer with a soft gradient. We suggest defining a soft gradient for reactivity ratios of $r_1: \leq 2$ and $r_2: \geq 0.5$.

Increasing the slope of the tapered block further leads to medium gradient copolymers (region b in Figure 4.1). During the final stages of the copolymerization exclusively to the less reactive monomers is reacting and building a separated block (cf. Table 4.2, entries 1 and 2). The properties of copolymers with a medium gradient microstructure differ measurably from random copolymers. Copolymers with medium gradients had been reported as compatibilizers in polymer blends which decreased domain size significantly when compared to block copolymers.^{14, 21, 63, 64}

As **(6)** has a stronger EWD group, it generated, like MsMAz **(2)** with TsMAz **(4)**, a more pronounced gradient yielding in a polymer with exclusively consisting of the less active monomer **(4)** in the terminal 10%, which is illustrated by the Monte Carlo simulation and the monomer fraction plot. Other soft gradient copolymers were reported for the carb-anionic copolymerization of isoprene with myrcene.⁵⁶ Reactivity ratios of r_1 : 4.4 and r_2 : 0.23 formed a soft gradient with a smoothly increasing concentration of isoprene over the total conversion towards a novel bio-based natural rubber. The cationic polymerization also gives examples for the formation of gradients, oxazolines, for example, are known to form soft to medium gradient copolymers, depending on either on steric hindrance or electron pushing or withdrawing behavior of the oxazoline side group.^{65, 66}

Further increase of slope of the tapered microstructure led to polymers which can be seen as “triblock” copolymers consisting of a monomer “A” block at the beginning and a monomer “B” block at the end, connected by a mixed block composed of A and B, as illustrated in the green region c in Figure 4.1.^{13, 67} Due to the tapered middle block, the chemical interface is smoothed out, which had been detected by electron microscopy.^{64, 68} We suggest using the term hard gradient copolymer, whenever the structure for a triblock copolymer is clearly visible. Reactivity ratios leading to hard gradients are typically in the order of around r_1 : 7.5-25 and r_2 : 0.13-0.04. Such hard gradient copolymers were obtained in poly(7-co-4) and poly(8-co-4) (entries 4 and 5, Table 4.3), proving that ca. 30 to 40 % of the terminal blocks consist exclusively of the monomer with the lower reactivity. The “middle block” exhibits a hard gradient and spans over 20-30% of the total degree of polymerization.

Table 4.3: Comonomer reactivity and distributions for copolymerizations of sulfonyl aziridines of monomers with different activating groups and the reactivity parameters calculated with nonterminal models from Jaacks,³⁶ Frey,³² BSL^{33, 62} and Meyer-Lowry³⁴ (M-L). Visualization of the copolymer compositions calculated from the reactivity ratios and via Monte Carlo simulated microstructure of the copolymers.

Co-Monomers	Reactivity ratios		Visualization of copolymer microstructures	
	Method	r_1, r_2	Monomer Fraction F plotted against total conversion	Monte Carlo simulation of comonomer distribution
	Jaacks	1.674, 0.596		
	Frey	1.752, 0.570		
	BSL	1.759, 0.573		
	M-L	n. c.		
	Jaacks	1.681, 0.590		
	Frey	1.682, 0.594		
	BSL	1.675, 0.590		
	M-L	1.477, 0.495		
	Jaacks	4.245, 0.235		
	Frey	4.245, 0.235		
	BSL	4.245, 0.235		
	M-L	4.251, 0.236		
	Jaacks	13.791, 0.072		
	Frey	14.021, 0.071		
	BSL	14.084, 0.071		
	M-L	17.625, 0.199		
	Jaacks	22.664, 0.044		
	Frey	23.347, 0.042		
	BSL	23.801, 0.043		
	M-L	28.880, 0.132		
	Jaacks	68.997, 0.014		
	Frey	76.306, 0.013		
	BSL	99.825, 0.013		
	M-L	87.036, 0,027		

n. c. not calculated. M-L did not give reasonable reactivity ratios for the fitted data with any monomer conversion.

If the reactivity ratio difference further increases, the gradient profile in this “middle block” gets even harder and a block-like copolymer is obtained, which is probably not to distinguish from a “real” block copolymer, prepared by sequential monomer addition. In the aziridine family, such block copolymers can be obtained by a competitive copolymerization of a highly activated (**7**) and a less activated monomer (**2**) (entry 6 in Table 4.3). Poly(7-co-2) copolymers proved a tapered middle segment of only 5% and reactivity ratios of $r_1=76.31$ and $r_2=0.01$. A further increase in reactivity differences was achieved in a previous study by our group when sulfonyl aziridines were copolymerized with ethylene oxide. This comonomer mixture produced block copolymers with the largest difference in comonomer reactivity reported for anionic polymerization to date ($r_1=151$, $r_2=0.013$ (2 and EO) and $r_1=265$, $r_2=0.004$ (3 and EO)).

Grune *at. al.* conducted recently copolymerization studies of 4-methylstyrene and isoprene and observed the formation of a hard gradient copolymer with a tapered section of around 10% for reactivity ratios of $r_1: 25.4$, $r_2: 0.0007$.⁵⁵ Carbanionic copolymerization of the rapid polymerizing myrcene with styrene showed to give a hard gradient copolymer.⁵⁶ Reactivity ratios of $r_1: 36$, $r_2: 0.028$ formed a block-polymer with a tapered section less than 10% (hard gradient) while the copolymerization of myrcene with an even less reactive partner (4-methylstyrene) formed a block-copolymer without visible tapering effect ($r_1: 140$, $r_2: 0.0074$).⁵⁶ To form block like copolymers according to a one-step polymerization on a monomer mixture, reactivity ratios of $r_1 \geq 20$, $r_2 \leq 0.02$ are required. An actual difference in the polymer microstructure is not visible if reactivity ratios become extremer than $r_1: \sim 100$ and $r_2: \sim 0.01$. Figure 4.6 illustrates the effect of the increasing reactivity difference of the comonomer set plotted as a copolymerization diagram (the grey dashed line shows an ideal statistical copolymerization, at any time the monomer ratios in the solution is similar to the monomer content in the polymer). With an increasing reactivity difference between the monomers the curves deviate further from the ideal statistical copolymerization, i.e. the more reactive monomer is converted into the polymer faster than the less reactive one.

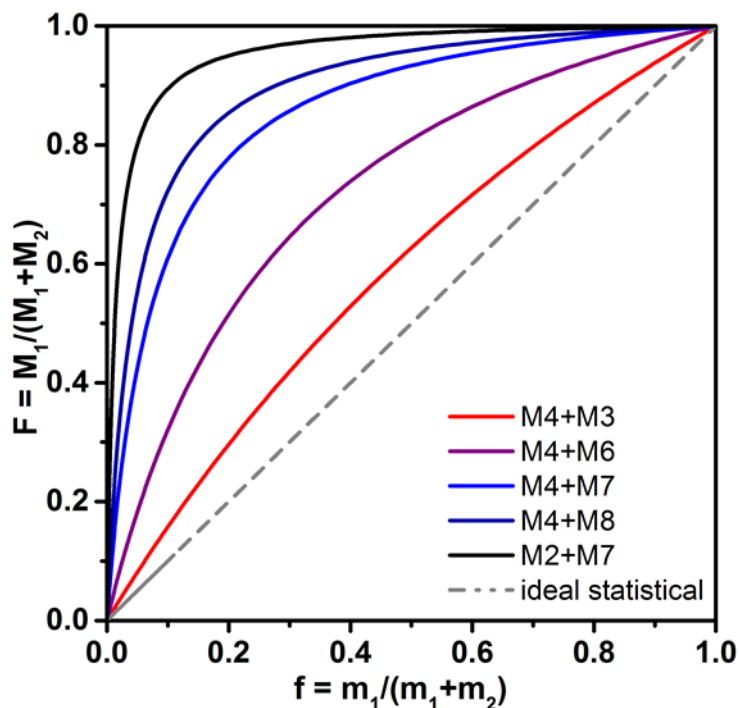


Figure 4.6: Copolymerization diagram of different comonomer pairs (reactivity ratios are listed in Table 4.3).

4.5 Conclusion

Gradient copolymers further expand the properties of copolymers in polymer science. Adjusting the gradient strength by the chemical design of the comonomer reactivity gives access to a variety of new copolymer structures. The family of sulfonyl-activated aziridines was used to prepare a series of gradient copolymers with adjustable gradient profile, by adjusting the electron withdrawing effect of the sulfonyl group. The determination of the reactivity ratios of all copolymerizations was conducted by four different methods. The similarity of the results proves that the AROP of aziridines can be described with terminal and non-terminal models. The comonomer library used herein further allowed prediction of the comonomer reactivity of other activated aziridines and will result in the preparation of even more gradient structures with the potential to be used as compatibilizers or polyelectrolytes after removal of the activating group.

4.6 References Chapter 4

1. Roy, R. K.; Meszynska, A.; Laure, C.; Charles, L.; Verchin, C.; Lutz, J.-F., Design and synthesis of digitally encoded polymers that can be decoded and erased. *Nature communications* **2015**, *6*, 7237.
2. Zamfir, M.; Lutz, J.-F., Ultra-precise insertion of functional monomers in chain-growth polymerizations. *Nature communications* **2012**, *3*, 1138.
3. Shen, M.; Bever, M., Gradients in polymeric materials. *Journal of Materials science* **1972**, *7* (7), 741-746.
4. Kokkinis, D.; Bouville, F.; Studart, A. R., 3D printing of materials with tunable failure via bioinspired mechanical gradients. *Advanced Materials* **2018**, *30* (19), 1705808.
5. Claussen, K. U.; Scheibel, T.; Schmidt, H.-W.; Giesa, R., Polymer Gradient Materials: Can Nature Teach Us New Tricks? *Macromolecular Materials and Engineering* **2012**, *297* (10), 938-957.
6. Cai, H.; Gabryelczyk, B.; Manimekalai, M. S. S.; Gruber, G.; Salentinig, S.; Miserez, A., Self-coacervation of modular squid beak proteins - a comparative study. *Soft Matter* **2017**, *13* (42), 7740-7752.
7. Tan, Y.; Hoon, S.; Guerette, P. A.; Wei, W.; Ghadban, A.; Hao, C.; Miserez, A.; Waite, J. H., Infiltration of chitin by protein coacervates defines the squid beak mechanical gradient. *Nat Chem Biol* **2015**, *11* (7), 488-495.
8. Harrington, M. J.; Waite, J. H., How Nature Modulates a Fiber's Mechanical Properties: Mechanically Distinct Fibers Drawn from Natural Mesogenic Block Copolymer Variants. *Advanced Materials* **2009**, *21* (4), 440-444.
9. Alam, M. M.; Jack, K. S.; Hill, D. J. T.; Whittaker, A. K.; Peng, H., Gradient copolymers – Preparation, properties and practice. *European Polymer Journal* **2019**, *116*, 394-414.
10. Zheng, C., Gradient copolymer micelles: an introduction to structures as well as structural transitions. *Soft Matter* **2019**, *15* (27), 5357-5370.
11. Thomopoulos, S.; Birman, V.; Genin, G. M., *Structural Interfaces and Attachments in Biology*. Springer-Verlag: New York, 2013.
12. Knoll, K.; Niessner, N. In *Styroflex: A New Transparent Styrene-Butadiene Copolymer with High Flexibility Synthesis, Applications, and Synergism with Other Styrene Polymers*, ACS Symposium Series, American Chemical Society: 1998; pp 112-128.
13. Ruzette, A.-V.; Leibler, L., Block copolymers in tomorrow's plastics. *Nature materials* **2005**, *4* (1), 19.
14. Matyjaszewski, K.; Tsarevsky, N. V., Nanostructured functional materials prepared by atom transfer radical polymerization. *Nature Chemistry* **2009**, *1*, 276.
15. Lutz, J.-F., *Sequence-Controlled Polymers*. John Wiley & Sons: 2018.
16. Ouchi, M.; Sawamoto, M., Sequence-controlled polymers via reversible-deactivation radical polymerization. *Polymer Journal* **2017**, *50*, 83-94.
17. D'Hooge, D.; Van Steenberge, P.; Reyniers, M.-F.; Marin, G., Fed-Batch Control and Visualization of Monomer Sequences of Individual ICAR ATRP Gradient Copolymer Chains. *Polymers* **2014**, *6* (4), 1074-1095.
18. Van Steenberge, P. H. M.; D'hooge, D. R.; Wang, Y.; Zhong, M.; Reyniers, M.-F.; Konkolewicz, D.; Matyjaszewski, K.; Marin, G. B., Linear Gradient Quality of ATRP Copolymers. *Macromolecules* **2012**, *45* (21), 8519-8531.
19. Gleede, T.; Reisman, L.; Rieger, E.; Mbarushimana, P. C.; Rupar, P. A.; Wurm, F. R., Aziridines and azetidines: building blocks for polyamines by anionic and cationic ring-opening polymerization. *Polymer Chemistry* **2019**, *10* (24), 3257-3283.
20. Rieger, E.; Alkan, A.; Manhart, A.; Wagner, M.; Wurm, F. R., Sequence-Controlled Polymers via Simultaneous Living Anionic Copolymerization of Competing Monomers. *Macromol. Rapid Commun.* **2016**, *37* (10), 833-839.
21. Ganesan, V.; Kumar, N. A.; Pryamitsyn, V., Blockiness and Sequence Polydispersity Effects on the Phase Behavior and Interfacial Properties of Gradient Copolymers. *Macromolecules* **2012**, *45* (15), 6281-6297.
22. Reisman, L.; Mbarushimana, C. P.; Cassidy, S. J.; Rupar, P. A., Living Anionic Copolymerization of 1-(Alkylsulfonyl)aziridines to Form Poly(sulfonylaziridine) and Linear Poly(ethylenimine). *ACS Macro Letters* **2016**, *5* (10), 1137-1140.
23. Rieger, E.; Gleede, T.; Manhart, A.; Lamla, M.; Wurm, F. R., Microwave-Assisted Desulfonylation of Polysulfonamides toward Polypropylenimine. *ACS Macro Letters* **2018**, 598-603.

24. Gleede, T.; Rieger, E.; Blankenburg, J.; Klein, K.; Wurm, F. R., Fast Access to Amphiphilic Multiblock Architectures by the Anionic Copolymerization of Aziridines and Ethylene Oxide. *J Am Chem Soc* **2018**, *140* (41), 13407-13412.
25. Fierens, S. K.; Van Steenberge, P. H. M.; Reyniers, M. F.; D'Hooge, D. R.; Marin, G. B., Analytical and advanced kinetic models for characterization of chain-growth copolymerization: the state-of-the-art. *Reaction Chemistry & Engineering* **2018**, *3* (2), 128-145.
26. Rieger, E.; Alkan, A.; Manhart, A.; Wagner, M.; Wurm, F. R., Sequence-Controlled Polymers via Simultaneous Living Anionic Copolymerization of Competing Monomers. *Macromolecular rapid communications* **2016**, *37* (10), 833-839.
27. Thomi, L.; Wurm, F. R., Living Anionic Polymerization of Functional Aziridines. *Macromol. Symp.* **2015**, *349* (1), 51-56.
28. Rieger, E.; Blankenburg, J.; Grune, E.; Wagner, M.; Landfester, K.; Wurm, F. R., Controlling the polymer microstructure in anionic polymerization by compartmentalization. *Angew Chem Int Ed Engl* **2017**, *57* (9), 2483-2487.
29. Gleede, T.; Rieger, E.; Homann-Müller, T.; Wurm, F. R., 4-Styrenesulfonyl-(2-methyl)aziridine: The First Bivalent Aziridine-Monomer for Anionic and Radical Polymerization. *Macromolecular Chemistry and Physics* **2018**, 1700145.
30. Freeman, R.; Hill, H. D. W.; Kaptein, R., Proton-Decoupled NMR Spectra of Carbon-13 With the Nuclear Overhauser Effect Suppressed. *J. Magn. Reson.* **1972**, *7*, 327-329.
31. Wall, F. T., The structure of vinyl copolymers. *Journal of the American Chemical Society* **1941**, *63* (7), 1862-1866.
32. Blankenburg, J.; Kersten, E.; Maciol, K.; Wagner, M.; Zorbakhsh, S.; Frey, H., The poly(propylene oxide-co-ethylene oxide) gradient is controlled by the polymerization method: determination of reactivity ratios by direct comparison of different copolymerization models. *Polymer Chemistry* **2019**, *10* (22), 2863-2871.
33. Bryan S. Beckingham, G. E. S., and Nathaniel A. Lynd, Simple and Accurate Determination of Reactivity Ratios Using a Nonterminal Model of Chain Copolymerization. *Macromolecules* **2015**, *48*, 6922-6930.
34. Meyer, V. E.; Lowry, G. G., Integral and differential binary copolymerization equations. *Journal of Polymer Science Part A: General Papers* **1965**, *3* (8), 2843-2851.
35. Gleede, T.; Rieger, E.; Liu, L.; Bakkali-Hassani, C.; Wagner, M.; Carlotti, S.; Taton, D.; Andrienko, D.; Wurm, F. R., Alcohol- and Water-Tolerant Living Anionic Polymerization of Aziridines. *Macromolecules* **2018**, *51* (15), 5713-5719.
36. Jaacks, V., A novel method of determination of reactivity ratios in binary and ternary copolymerizations. *Macromolecular Chemistry and Physics* **1972**, *161* (1), 161-172.
37. Frisch, M.; Trucks, G.; Schlegel, H.; Scuseria, G.; Robb, M.; Cheeseman, J.; Scalmani, G.; Barone, V.; Mennucci, B.; Petersson, G., 09, Revision D. 01. *Gaussian, Inc., Wallingford CT* **2009**.
38. Becke, A. D., Density-functional thermochemistry. III. The role of exact exchange. *The Journal of chemical physics* **1993**, *98* (7), 5648-5652.
39. Clark, T.; Chandrasekhar, J.; Spitznagel, G. W.; Schleyer, P. V. R., Efficient diffuse function-augmented basis sets for anion calculations. III. The 3-21+ G basis set for first-row elements, Li-F. *Journal of Computational Chemistry* **1983**, *4* (3), 294-301.
40. Ditchfield, R.; Hehre, W. J.; Pople, J. A., Self-consistent molecular-orbital methods. IX. An extended Gaussian-type basis for molecular-orbital studies of organic molecules. *The Journal of Chemical Physics* **1971**, *54* (2), 724-728.
41. McLean, A.; Chandler, G., Contracted Gaussian basis sets for molecular calculations. I. Second row atoms, Z= 11-18. *The Journal of Chemical Physics* **1980**, *72* (10), 5639-5648.
42. Miertuš, S.; Scrocco, E.; Tomasi, J., Electrostatic interaction of a solute with a continuum. A direct utilization of AB initio molecular potentials for the prevision of solvent effects. *Chemical Physics* **1981**, *55* (1), 117-129.
43. Miertus, S.; Tomasi, J., Approximate evaluations of the electrostatic free energy and internal energy changes in solution processes. *Chemical physics* **1982**, *65* (2), 239-245.
44. Pascual-Ahuir, J.-L.; Silla, E.; Tunon, I., GEPOL: An improved description of molecular surfaces. III. A new algorithm for the computation of a solvent-excluding surface. *Journal of Computational Chemistry* **1994**, *15* (10), 1127-1138.
45. Foster, J.; Weinhold, F., Natural hybrid orbitals. *Journal of the American Chemical Society* **1980**, *102* (24), 7211-7218.

46. Stewart, I. C.; Lee, C. C.; Bergman, R. G.; Toste, F. D., Living ring-opening polymerization of *N*-sulfonylaziridines: synthesis of high molecular weight linear polyamines. *J. Am. Chem. Soc.* **2005**, *127* (50), 17616-17617.
47. Rieger, E.; Manhart, A.; Wurm, F. R., Multihydroxy Polyamines by Living Anionic Polymerization of Aziridines. *ACS Macro Lett.* **2016**, *5* (2), 195-198.
48. Rieger, E.; Gleede, T.; Weber, K.; Manhart, A.; Wagner, M.; Wurm, F. R., The living anionic polymerization of activated aziridines: a systematic study of reaction conditions and kinetics. *Polym. Chem.* **2017**, *8* (18), 2824-2832.
49. Mbarushimana, P. C.; Liang, Q.; Allred, J. M.; Rugar, P. A., Polymerizations of Nitrophenylsulfonyl-Activated Aziridines. *Macromolecules* **2018**, *51* (3), 997-983.
50. Takashi Ishizone, A. H., Seiichi Nakahama, Anionic Polymerization of Monomers Containing Functional Groups. 6. Anionic Block Copolymerization of Styrene Derivatives Para-Substituted with Electron-Withdrawing Groups. *Macromolecules* **1993**, *26*, 6964-6975.
51. Hansch, C.; Leo, A.; Taft, R. W., A Survey of Hammett Substituent Constants and Resonance and Field Parameters. *Chemical Reviews* **1991**, *91* (2), 165-195.
52. Stanetty, C.; Blaukopf, M. K.; Lachmann, B.; Noe, C. R., The Dinosyl Group: A Powerful Activator for the Regioselective Alcoholysis of Aziridines. *European Journal of Organic Chemistry* **2011**, *2011* (17), 3126-3130.
53. Sedlacek, O.; Lava, K.; Verbraeken, B.; Kasmi, S.; De Geest, B. G.; Hoogenboom, R., Unexpected Reactivity Switch in the Statistical Copolymerization of 2-Oxazolines and 2-Oxazines Enabling the One-Step Synthesis of Amphiphilic Gradient Copolymers. *J Am Chem Soc* **2019**, *141*, 9617-9622.
54. Van Steenberge, P. H. M.; Sedlacek, O.; Hernandez-Ortiz, J. C.; Verbraeken, B.; Reyniers, M. F.; Hoogenboom, R.; D'Hooge D, R., Visualization and design of the functional group distribution during statistical copolymerization. *Nat Commun* **2019**, *10* (1), 1-41.
55. Grune, E.; Johann, T.; Appold, M.; Wahlen, C.; Blankenburg, J.; Leibig, D.; Müller, A. H. E.; Gallei, M.; Frey, H., One-Step Block Copolymer Synthesis versus Sequential Monomer Addition: A Fundamental Study Reveals That One Methyl Group Makes a Difference. *Macromolecules* **2018**, *51* (9), 3527-3537.
56. Grune, E.; Bareuther, J.; Blankenburg, J.; Appold, M.; Shaw, L.; Müller, A. H. E.; Floudas, G.; Hutchings, L. R.; Gallei, M.; Frey, H., Towards bio-based tapered block copolymers: the behaviour of myrcene in the statistical anionic copolymerisation. *Polymer Chemistry* **2019**, *10* (10), 1213-1220.
57. Grune, E.; Appold, M.; Müller, A. H. E.; Gallei, M.; Frey, H., Anionic Copolymerization Enables the Scalable Synthesis of Alternating (AB)_n Multiblock Copolymers with High Molecular Weight in *n*/2 Steps. *ACS Macro Letters* **2018**, 807-810.
58. Herzberger, J.; Leibig, D.; Liermann, J. C.; Frey, H., Conventional Oxyanionic versus Monomer-Activated Anionic Copolymerization of Ethylene Oxide with Glycidyl Ethers: Striking Differences in Reactivity Ratios. *ACS Macro Letters* **2016**, *5* (11), 1206-1211.
59. Alfrey Jr, T.; Goldfinger, G., The mechanism of copolymerization. *The Journal of Chemical Physics* **1944**, *12* (6), 205-209.
60. Mayo, F. R.; Lewis, F. M., Copolymerization. I. A basis for comparing the behavior of monomers in copolymerization; the copolymerization of styrene and methyl methacrylate. *Journal of the American Chemical Society* **1944**, *66* (9), 1594-1601.
61. D'hooge, D. R.; Van Steenberge, P. H.; Derboven, P.; Reyniers, M.-F.; Marin, G. B., Model-based design of the polymer microstructure: bridging the gap between polymer chemistry and engineering. *Polymer Chemistry* **2015**, *6* (40), 7081-7096.
62. Lynd, N. A.; Ferrier, R. C.; Beckingham, B. S., Recommendation for Accurate Experimental Determination of Reactivity Ratios in Chain Copolymerization. *Macromolecules* **2019**, *52* (6), 2277-2285.
63. Malik, R.; Hall, C. K.; Genzer, J., Effect of copolymer compatibilizer sequence on the dynamics of phase separation of immiscible binary homopolymer blends. *Soft Matter* **2011**, *7* (22) 10620-10630.
64. Mok, M. M.; Torkelson, J. M., Imaging of phase segregation in gradient copolymers: Island and hole surface topography. *Journal of Polymer Science Part B: Polymer Physics* **2012**, *50* (3), 189-197.
65. Verbraeken, B.; Monnery, B. D.; Lava, K.; Hoogenboom, R., The chemistry of poly(2-oxazoline)s. *European Polymer Journal* **2017**, *88*, 451-469.
66. Hoogenboom, R.; Lambermont-Thijs, H. M. L.; Jochems, M. J. H. C.; Hoeppener, S.; Guerlain, C.; Fustin, C.-A.; Gohy, J.-F.; Schubert, U. S., A schizophrenic gradient copolymer: switching and

- reversing poly(2-oxazoline) micelles based on UCST and subtle solvent changes. *Soft Matter* **2009**, 5 (19), 3590-3592.
67. Kryszewski, M., Gradient polymers and copolymers. *Polymers for Advanced Technologies* **1998**, 9 (4), 244-259.
68. Singh, N.; Tureau, M. S.; Epps III, T. H., Manipulating ordering transitions in interfacially modified block copolymers. *Soft Matter* **2009**, 5 (23).

4.7 Supporting Information for: Competitive Copolymerization: Access to Aziridine Copolymers with Adjustable Gradient Strengths

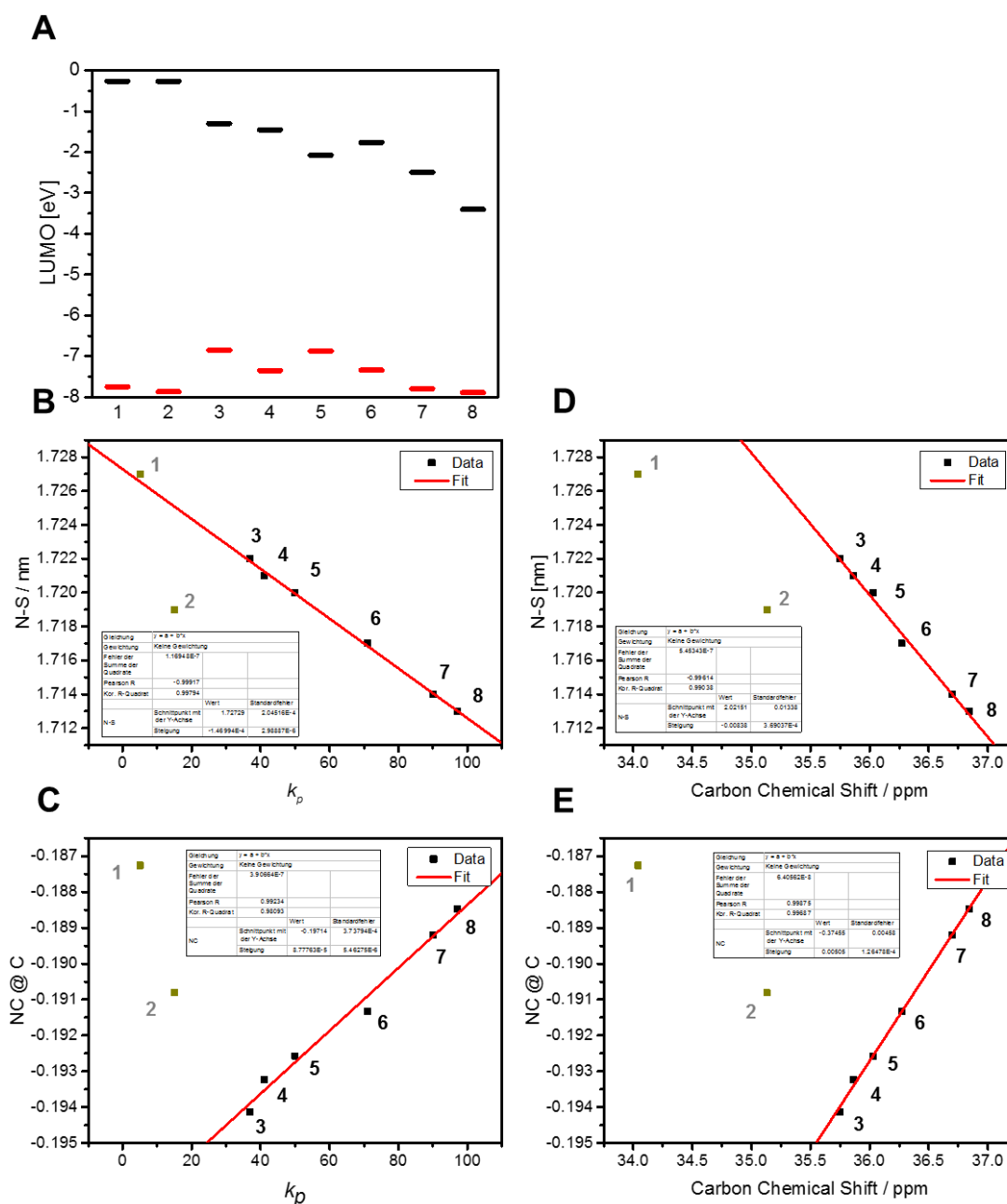
4.7.1 Section 1: DFT results & further correlations

Table S4.1: Substituents of the aromatic activating group of the aziridines with corresponding Hammett parameters (taken from reference¹)

Substituent in para position	σ_p	k_p
-CF ₃	0.54	84.1
-I	0.18	63.2
-F	0.06	56.3
-CH=CH ₂	-0.04	50.4
-S-Me	0.0	52.8
-SS-Me	0.13	60.3
-NH-Et	-0.61	17.3
-NMe ₂	-0.83	4.6
Substituent in metha position	σ_m	k_p
-N(CF ₃) ₂	0.40	76.0
-NO ₂	0.71	94.0

Table S4.2: Overview of the different monomers with their carbon shifts (taken from ^{13}C spectra), Hammett Parameters (taken from reference ¹) E_{HOMO} and E_{LUMO} (calculated), Bond lengths between nitrogen and sulfur (calculated), electrophilicity index ω^+ (calculated).

Monomer	(1)	(2)	(3)	(4)	(5)	(6)	(7)	(8)
E_{HOMO} / eV	-7.747	-7.872	-6.852	-7.348	-6,873	-7.339	-7.795	-7.886
E_{LUMO} / eV	-0.263	-0.268	-1.297	-1.453	-2,071	-1.766	-2.492	-3.402
N-S bond length	1.727	1.719	1.722	1.721	1,720	1.717	1.714	1.713
NC@C	-0.191	-0.191	-0.194	-0.193	-0.193	-0.19133	-0.189	-0.188

**Figure S4.1: HOMO and LUMO energies of the individual aziridines with the activation groups 1-8 (A) Correlation of reactivity parameter k_p with (B) nitrogen-sulfur bond distance N-S, (C) Natural charge at the electropositive carbon (NC@C). And Correlation of carbon chemical shift in ppm with (D) nitrogen-sulfur bond distance N-S, (E) NC@C.**

4.7.2 Section 2: Analytical details / Analysis of reactivity ratios

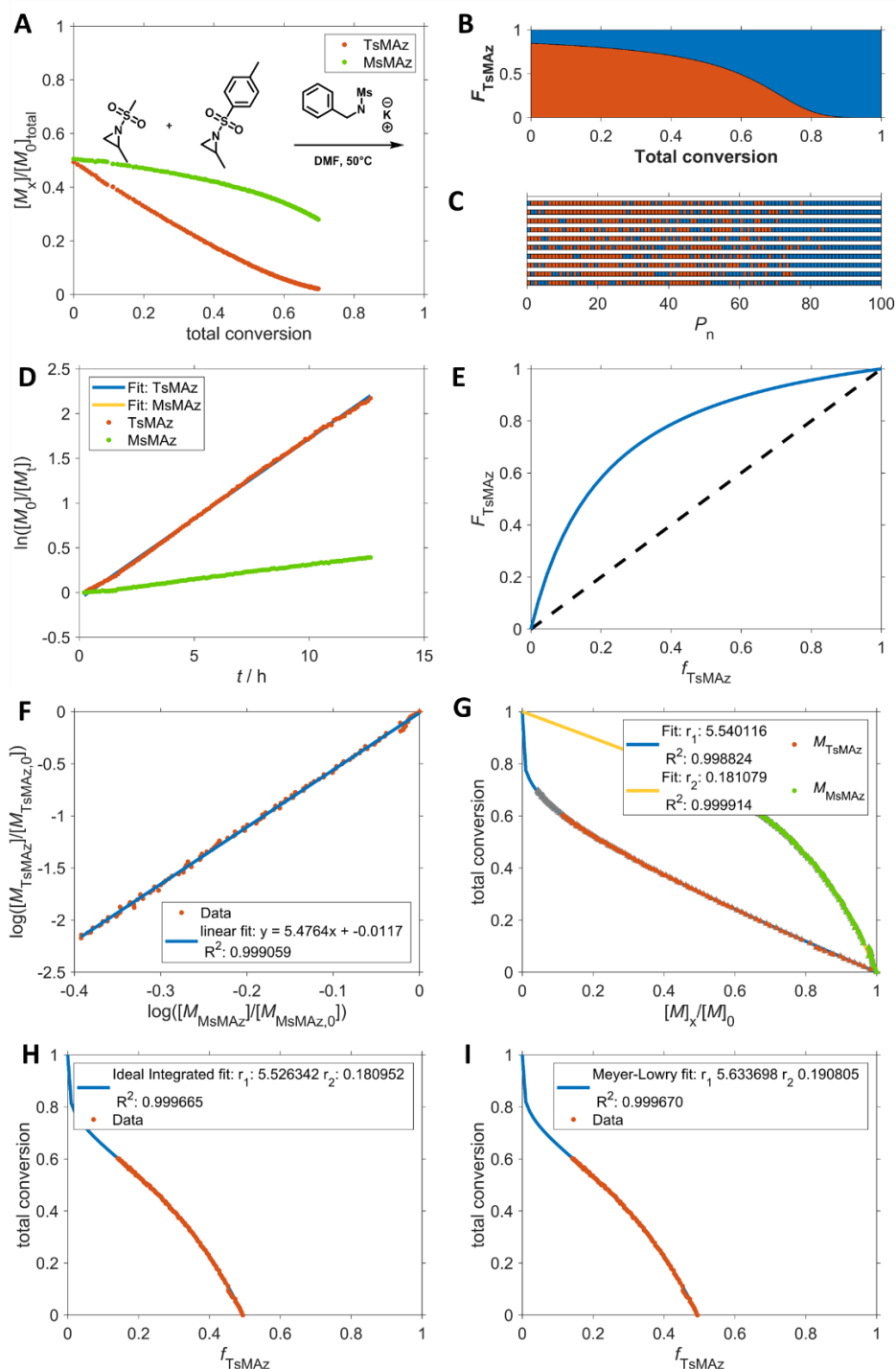


Figure S4.2; A: Monomer concentration as function of total conversion of activated aziridines (2 and 4); **B:** Mean composition (F) of 2 and 4 at 50:50 feed ratios versus total conversion (reactivity ratios calculated with equation 8); **C:** Individual copolymer chains of polymerization mixture assuming an ideal AROP ($\mathcal{D}=1.0$), simulated by kinetic Monte-Carlo simulations (red: less reactive monomer); **D:** Logarithmic plot of monomer consumption over time (linear nature proves living polymerization); **E:** Copolymerization diagram (dashed line corresponds to ideal statistical copolymerization) **F:** Jaacks fit on *in situ* NMR data of monomers; **G:** BSL fit on *in situ* NMR data of monomers. **H:** Frey fit on *in situ* NMR data of monomers; **I:** Meyer-Lowry fit on *in situ* NMR data. All methods used *in situ* NMR data until 60% conversion to extract reactivity ratios.

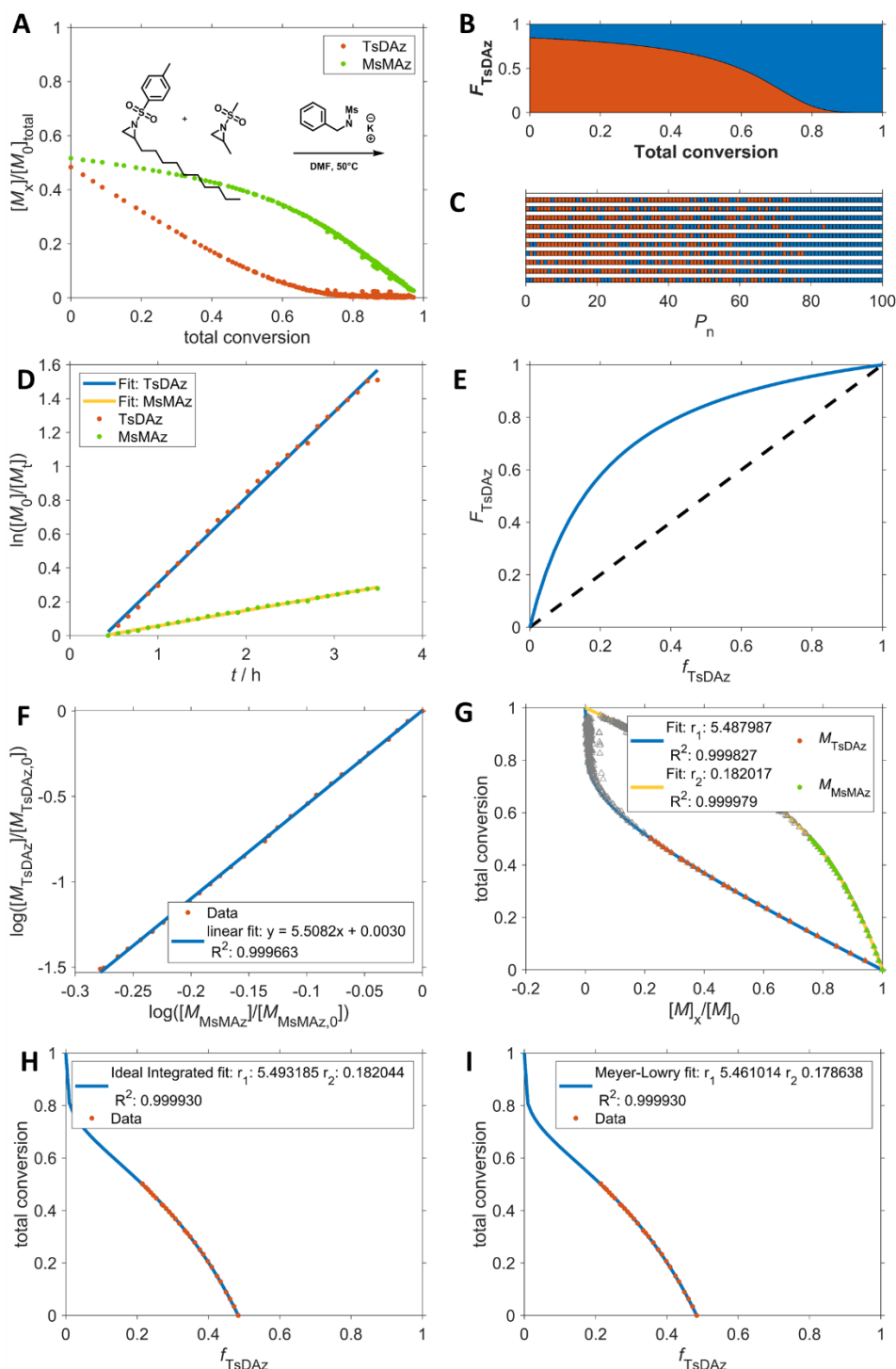


Figure S4.3:A: Monomer concentration as function of total conversion of activated aziridines with and without alkyl chain (activation group 2 and 4 were used); **B:** Mean composition (F) of 2 and 4 at 50:50 feed ratios versus total conversion (reactivity ratios calculated with equation 8); **C:** Individual copolymer chains of polymerization mixture assuming an ideal AROP ($\bar{D}=1.0$), simulated by kinetic Monte-Carlo simulations (red: less reactive monomer); **D:** Logarithmic plot of monomer consumption over time (linear nature proves living polymerization); **E:** Copolymerization diagram (dashed line corresponds to ideal statistical copolymerization) **F:** Jaacks fit on *in situ* NMR data of monomers; **G:** BSL fit on *in situ* NMR data of monomers. **H:** Frey fit on *in situ* NMR data of monomers; **I:** Meyer-Lowry fit on *in situ* NMR data. All methods used *in situ* NMR data until 51% conversion to extract reactivity ratios.

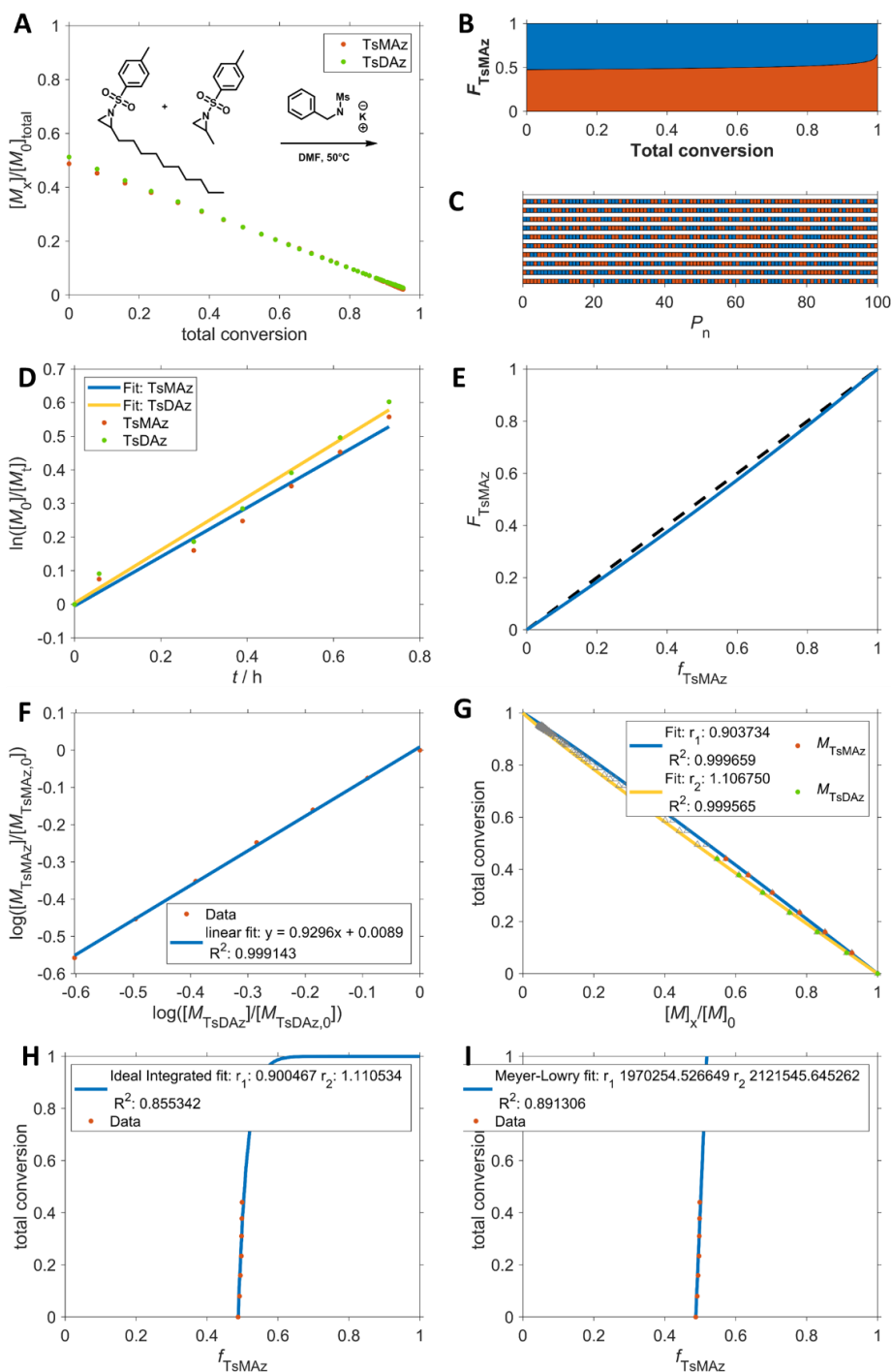


Figure S4.4: A: Monomer concentration as function of total conversion of activated aziridines with and without alkyl chain (activation group of 4 were used); B: Mean composition (F) of both monomers at 50:50 feed ratios versus total conversion (reactivity ratios calculated with equation 8); C: Individual copolymer chains of polymerization mixture assuming an ideal AROP ($\bar{D}=1.0$), simulated by kinetic Monte-Carlo simulations (red: less reactive monomer); D: Logarithmic plot of monomer consumption over time (linear nature proves living polymerization); E: Copolymerization diagram (dashed line corresponds to ideal statistical copolymerization) F: Jaacks fit on *in situ* NMR data of monomers; G: BSL fit on *in situ* NMR data of monomers. H: Frey fit on *in situ* NMR data of monomers; I: Meyer-Lowry fit on *in situ* NMR data. All methods used *in situ* NMR data until 47% conversion to extract reactivity ratios. Comment to M-L: *in situ* NMR data was varied from 0 to 100% conversion. In all cases M-L method gave no reasonable reactivity ratios for this system.

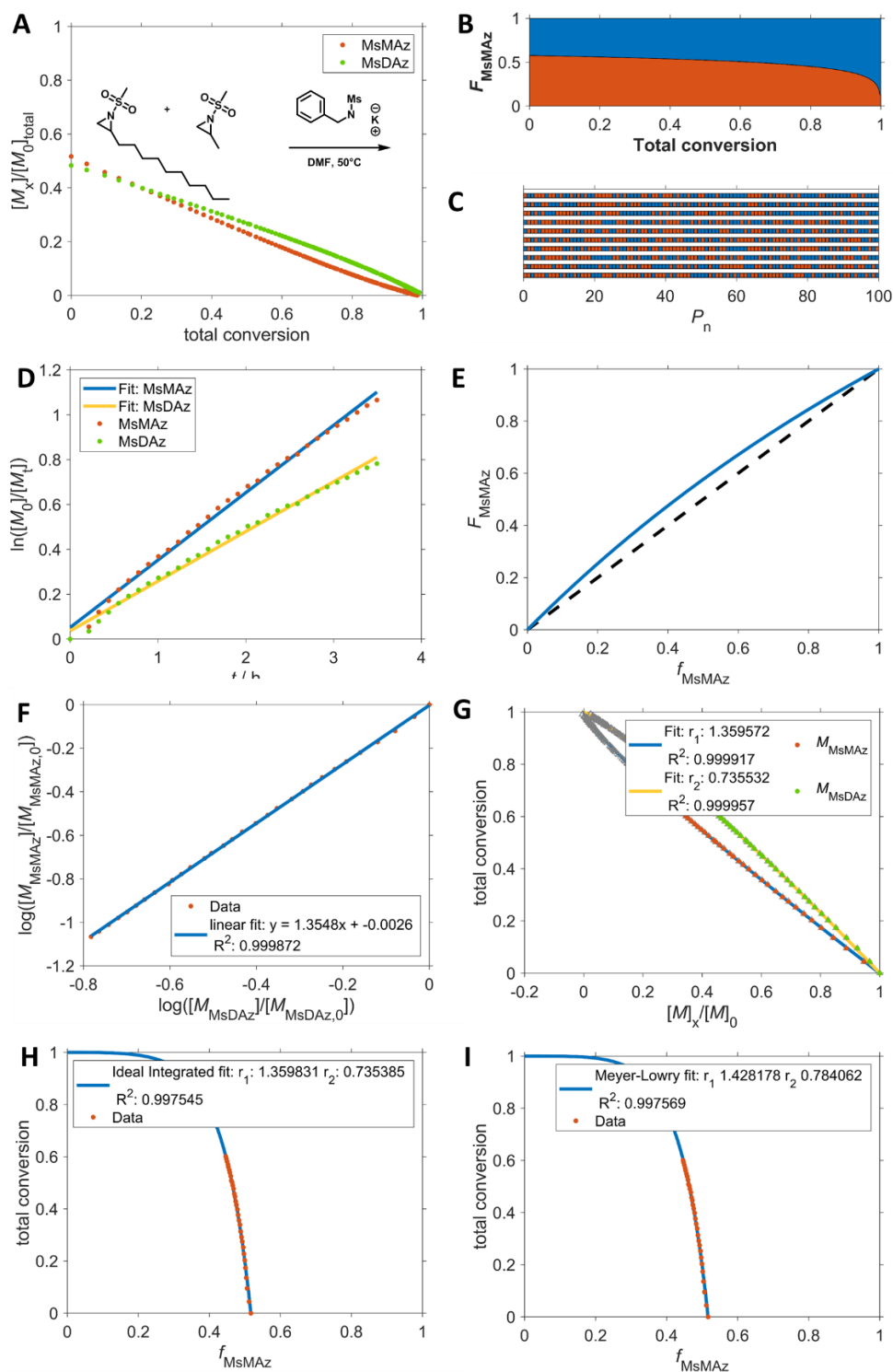


Figure S4.5: A: Monomer concentration as function of total conversion of activated aziridines with and without alkyl chain (activation group of 2 were used); B: Mean composition (F) of both monomers at 50:50 feed ratios versus total conversion (reactivity ratios calculated with equation 8); C: Individual copolymer chains of polymerization mixture assuming an ideal AROP ($\bar{D}=1.0$), simulated by kinetic Monte-Carlo simulations (red: less reactive monomer); D: Logarithmic plot of monomer consumption over time (linear nature proves living polymerization); E: Copolymerization diagram (dashed line corresponds to ideal statistical copolymerization) F: Jaacks fit on *in situ* NMR data of monomers; G: BSL fit on *in situ* NMR data of monomers. H: Frey fit on *in situ* NMR data of monomers; I: Meyer-Lowry fit on *in situ* NMR data. All methods used *in situ* NMR data until 61% conversion to extract reactivity ratios.

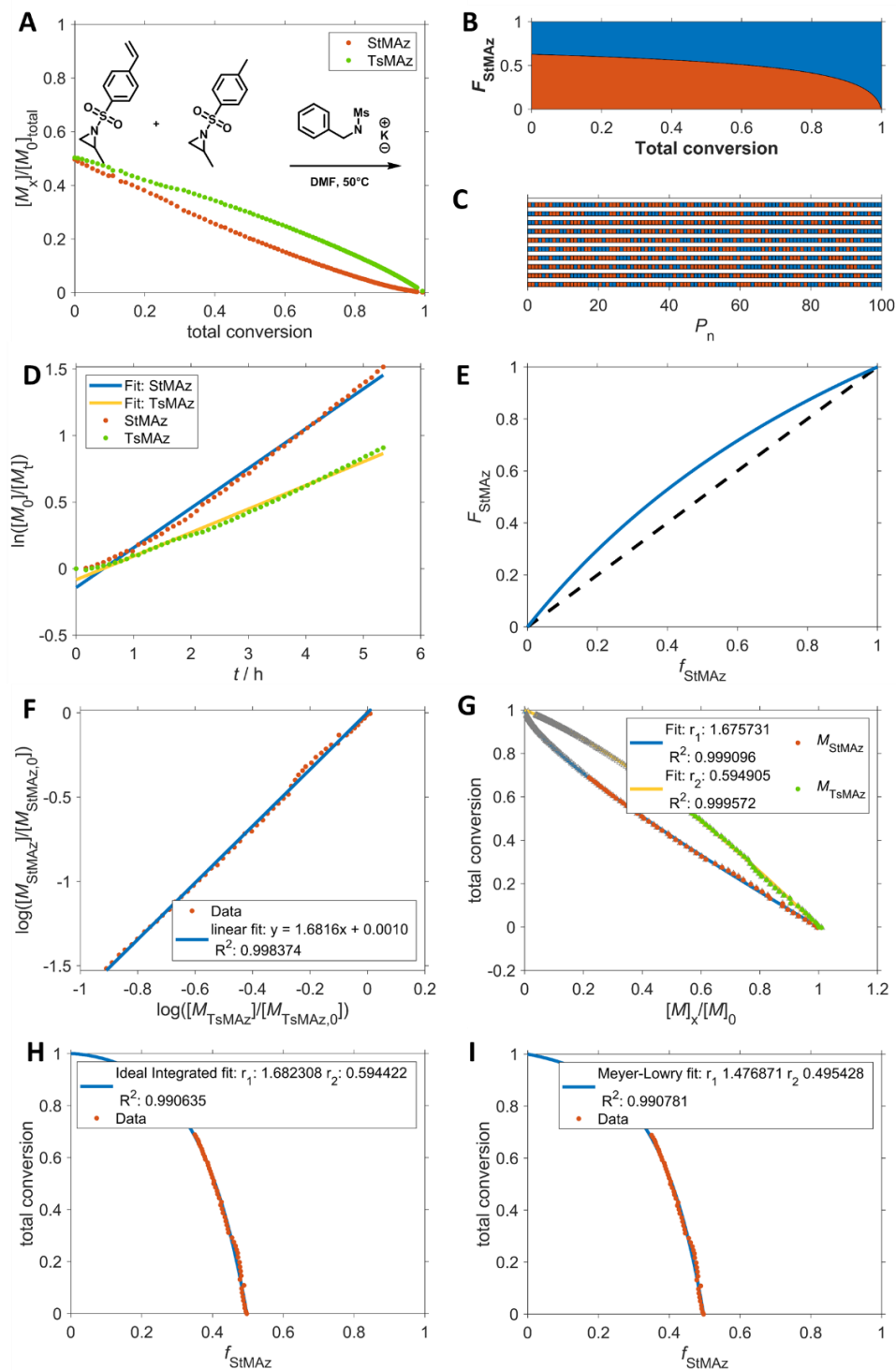


Figure S4.6: A: Monomer concentration as function of total conversion of activated aziridines (activation group of 4 and 5 were used); B: Mean composition (F) of both monomers at 50:50 feed ratios versus total conversion (reactivity ratios calculated with equation 8); C: Individual copolymer chains of polymerization mixture assuming an ideal AROP ($D=1.0$), simulated by kinetic Monte-Carlo simulations (red: less reactive monomer); D: Logarithmic plot of monomer consumption over time (linear nature proves living polymerization); E: Copolymerization diagram (dashed line corresponds to ideal statistical copolymerization) F: Jaacks fit on *in situ* NMR data of monomers; G: BSL fit on *in situ* NMR data of monomers. H: Frey fit on *in situ* NMR data of monomers; I: Meyer-Lowry fit on *in situ* NMR data. All methods used *in situ* NMR data until 69% conversion to extract reactivity ratios.

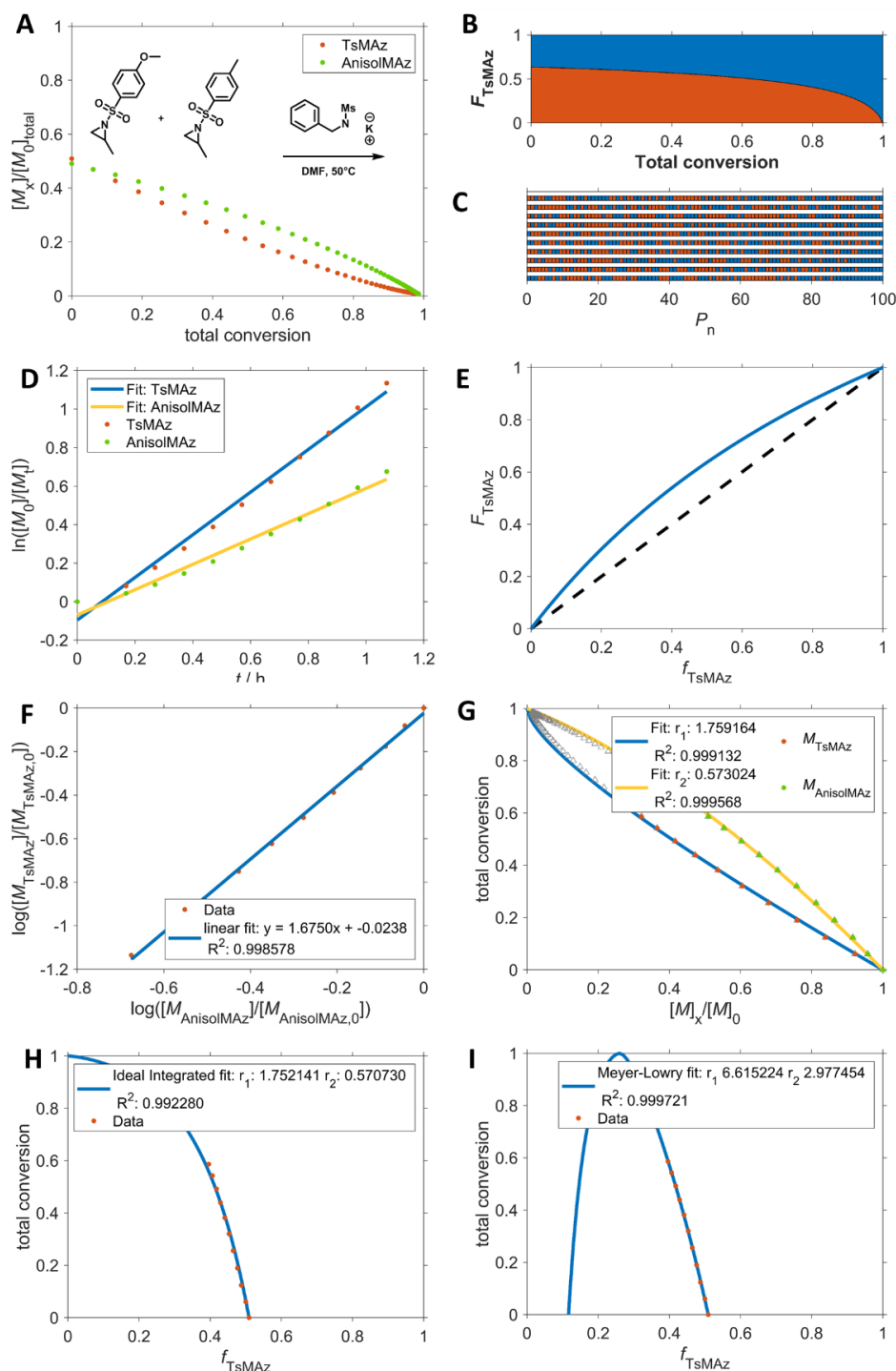


Figure S4.7: A: Monomer concentration as function of total conversion of activated aziridines (activation group of 3 and 4 were used); B: Mean composition (F) of both monomers at 50:50 feed ratios versus total conversion (reactivity ratios calculated with equation 8); C: Individual copolymer chains of polymerization mixture assuming an ideal AROP ($\bar{D}=1.0$), simulated by kinetic Monte-Carlo simulations (red: less reactive monomer); D: Logarithmic plot of monomer consumption over time (linear nature proves living polymerization); E: Copolymerization diagram (dashed line corresponds to ideal statistical copolymerization) F: Jaacks fit on *in situ* NMR data of monomers; G: BSL fit on *in situ* NMR data of monomers. H: Frey fit on *in situ* NMR data of monomers; I: Meyer-Lowry fit on *in situ* NMR data. All methods used *in situ* NMR data until 60% conversion to extract reactivity ratios. Comment to M-L: *in situ* NMR data was varied from 0 to 100% conversion. In all cases M-L method gave no reasonable reactivity ratios for this system.

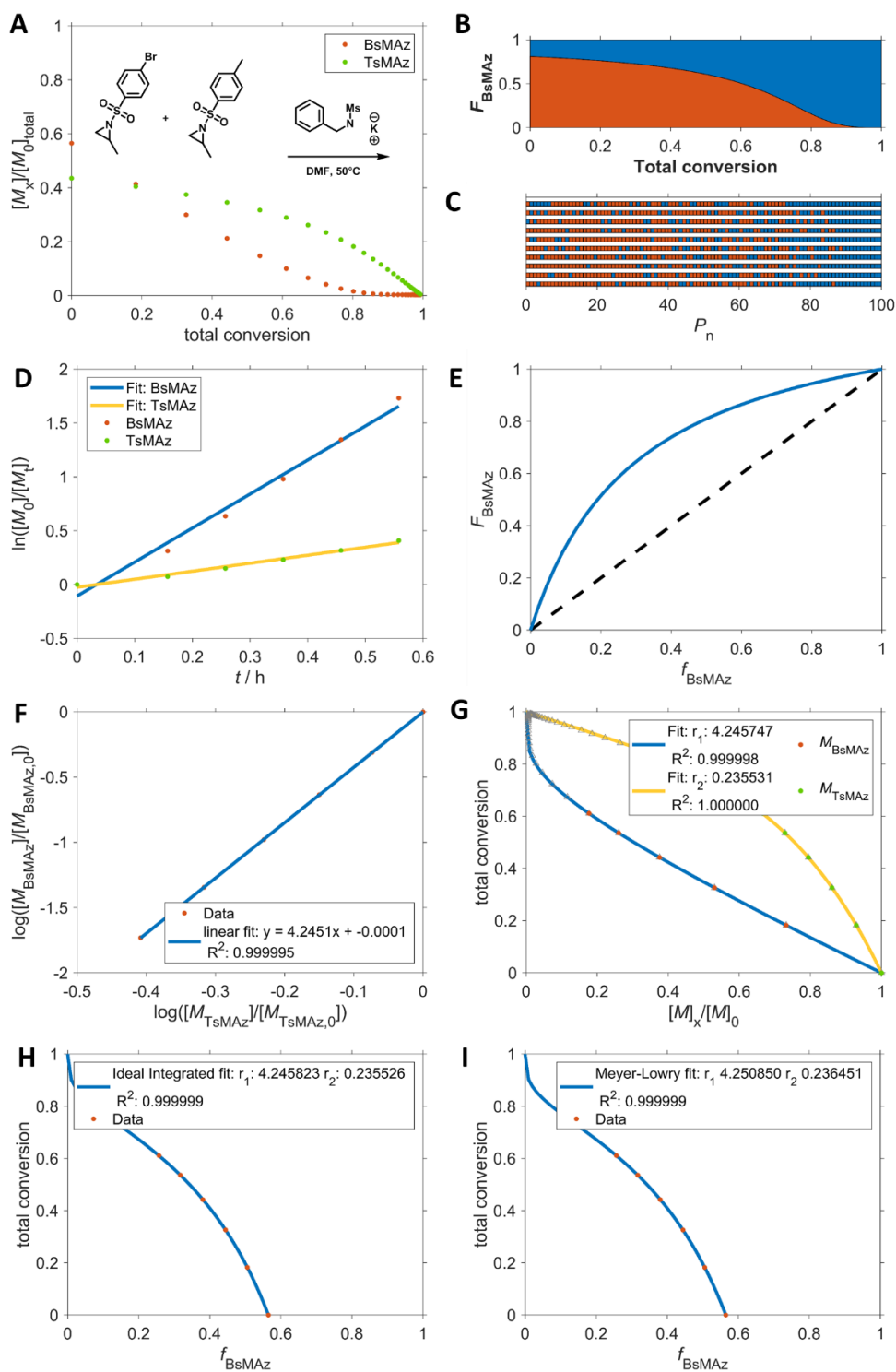


Figure S4.8: A: Monomer concentration as function of total conversion of activated aziridines (activation group of 4 and 6 were used); B: Mean composition (F) of both monomers at 50:50 feed ratios versus total conversion (reactivity ratios calculated with equation 8); C: Individual copolymer chains of polymerization mixture assuming an ideal AROP ($\bar{D}=1.0$), simulated by kinetic Monte-Carlo simulations (red: less reactive monomer); D: Logarithmic plot of monomer consumption over time (linear nature proves living polymerization); E: Copolymerization diagram (dashed line corresponds to ideal statistical copolymerization) F: Jaacks fit on *in situ* NMR data of monomers; G: BSL fit on *in situ* NMR data of monomers. H: Frey fit on *in situ* NMR data of monomers; I: Meyer-Lowry fit on *in situ* NMR data. All methods used *in situ* NMR data until 66% conversion to extract reactivity ratios.

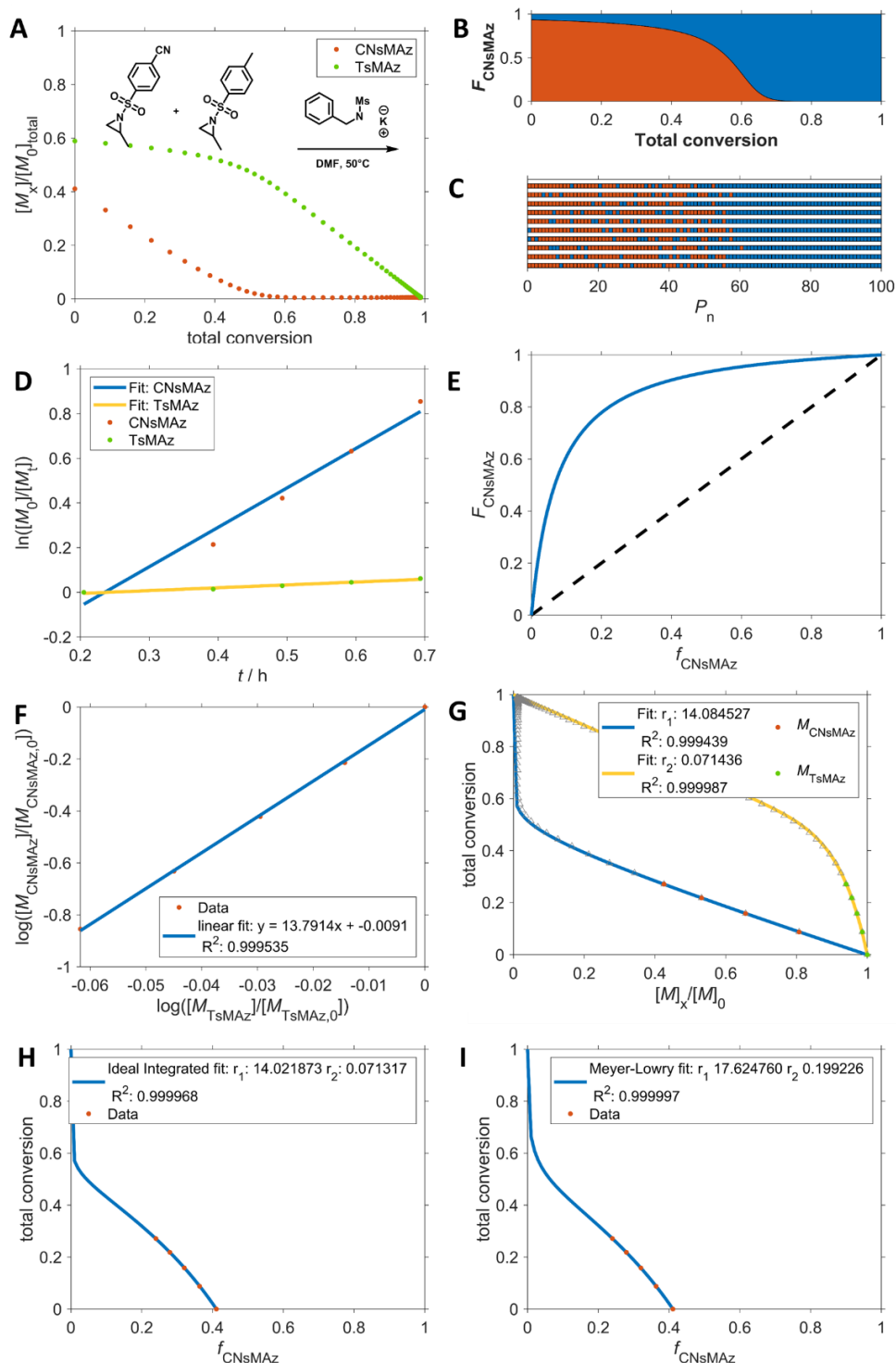


Figure S4.9: A: Monomer concentration as function of total conversion of activated aziridines (activation group of 4 and 7 were used); B: Mean composition (F) of both monomers at 50:50 feed ratios versus total conversion (reactivity ratios calculated with equation 8); C: Individual copolymer chains of polymerization mixture assuming an ideal AROP ($\bar{D}=1.0$), simulated by kinetic Monte-Carlo simulations (red: less reactive monomer); D: Logarithmic plot of monomer consumption over time (linear nature proves living polymerization); E: Copolymerization diagram (dashed line corresponds to ideal statistical copolymerization) F: Jaacks fit on *in situ* NMR data of monomers; G: BSL fit on *in situ* NMR data of monomers. H: Frey fit on *in situ* NMR data of monomers; I: Meyer-Lowry fit on *in situ* NMR data. All methods used *in situ* NMR data until 30% conversion to extract reactivity ratios.

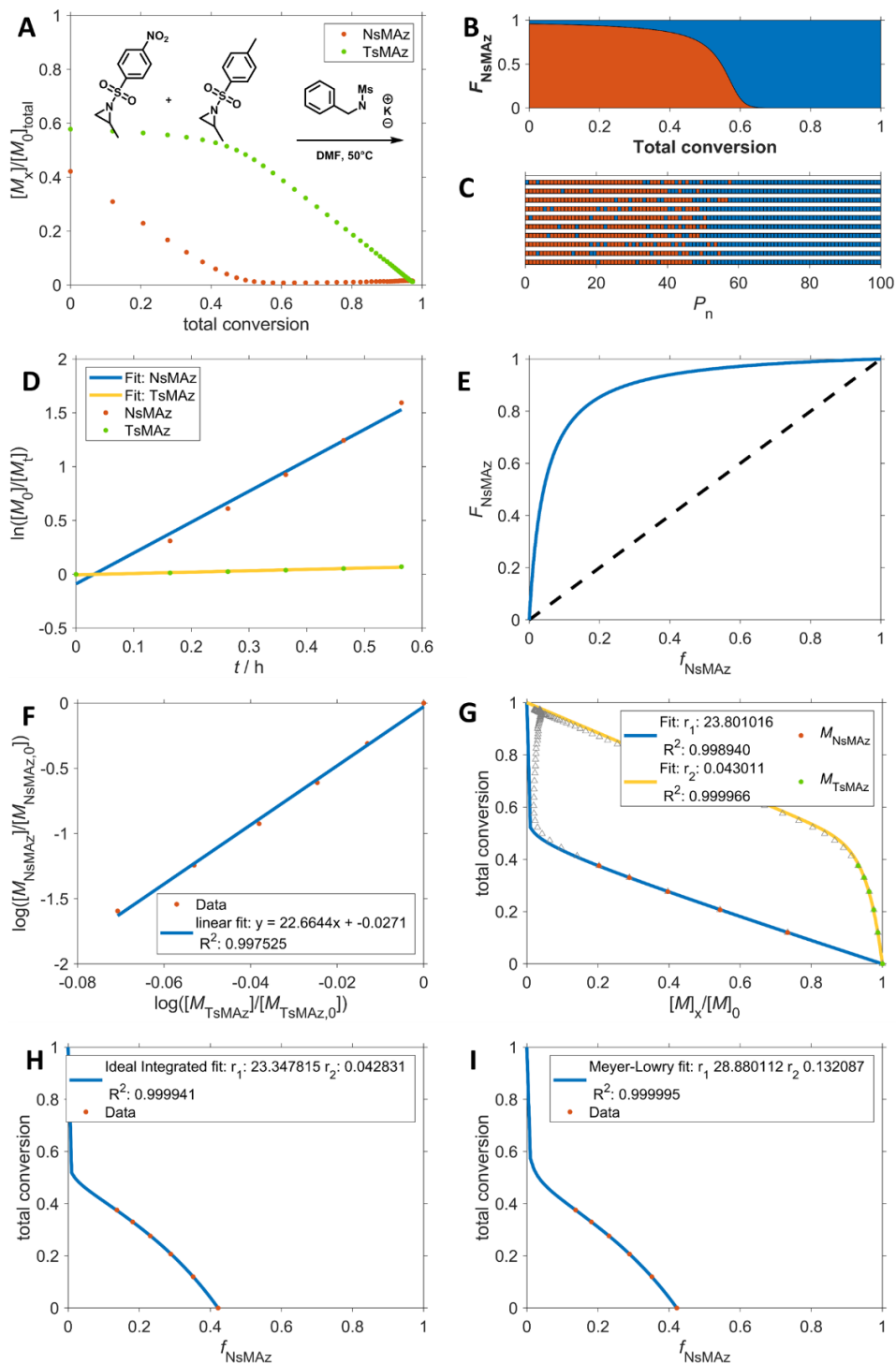


Figure S4.10: A: Monomer concentration as function of total conversion of activated aziridines (activation group of 4 and 8 were used); B: Mean composition (F) of both monomers at 50:50 feed ratios versus total conversion (reactivity ratios calculated with equation 8); C: Individual copolymer chains of polymerization mixture assuming an ideal AROP ($\bar{D}=1.0$), simulated by kinetic Monte-Carlo simulations (red: less reactive monomer); D: Logarithmic plot of monomer consumption over time (linear nature proves living polymerization); E: Copolymerization diagram (dashed line corresponds to ideal statistical copolymerization) F: Jacks fit on *in situ* NMR data of monomers; G: BSL fit on *in situ* NMR data of monomers. H: Frey fit on *in situ* NMR data of monomers; I: Meyer-Lowry fit on *in situ* NMR data. All methods used *in situ* NMR data until 40% conversion to extract reactivity ratios.

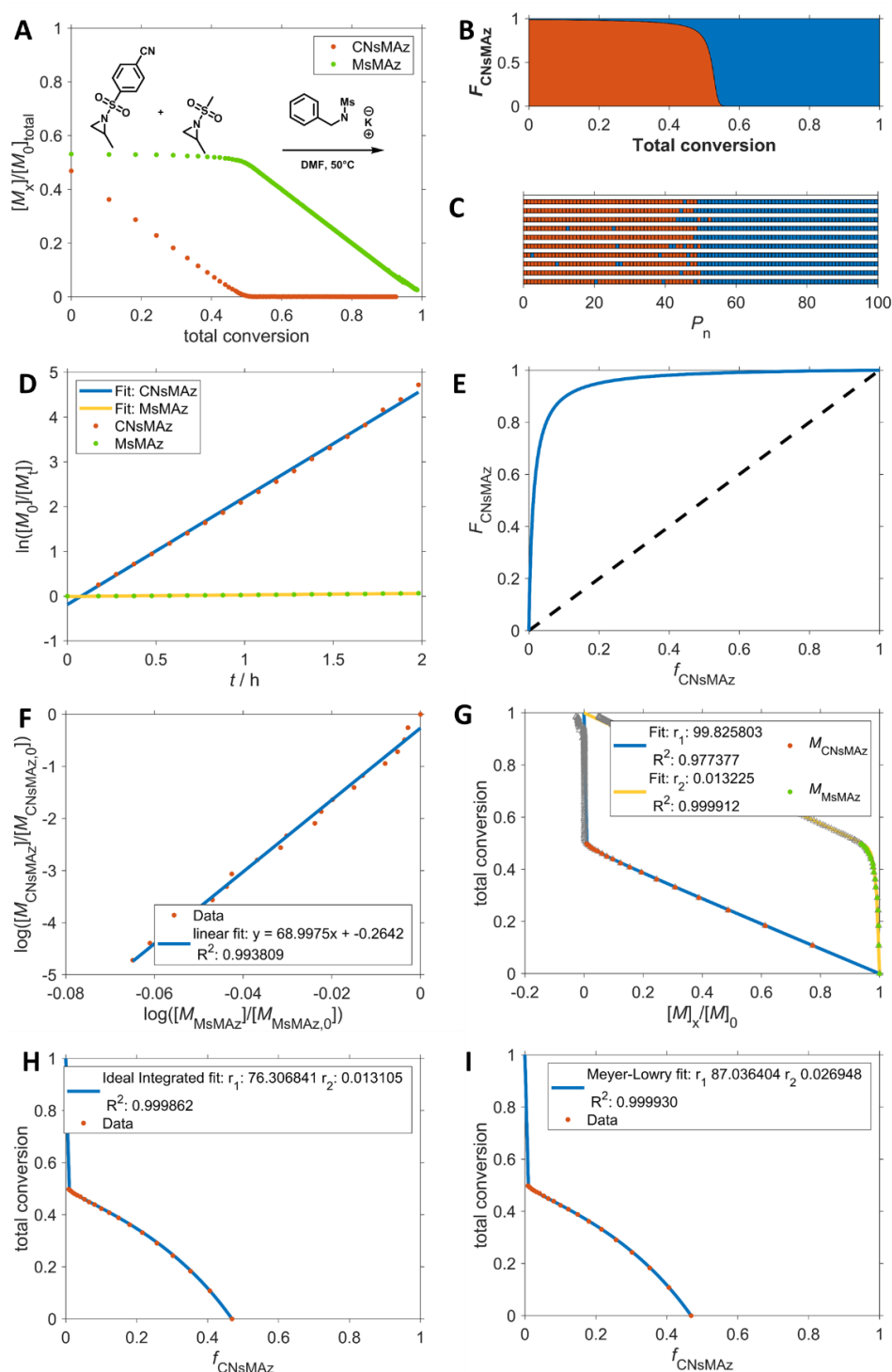
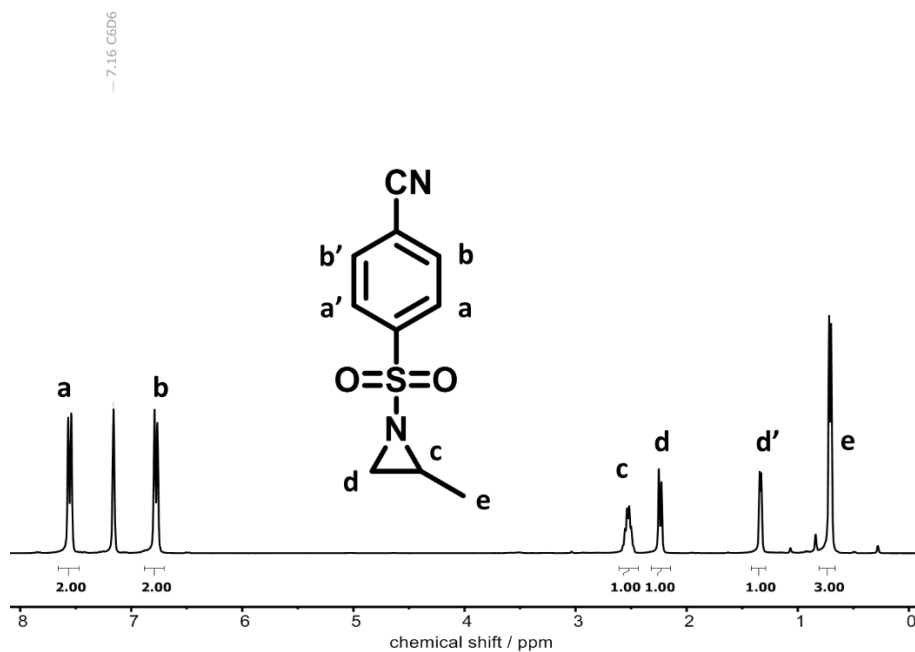
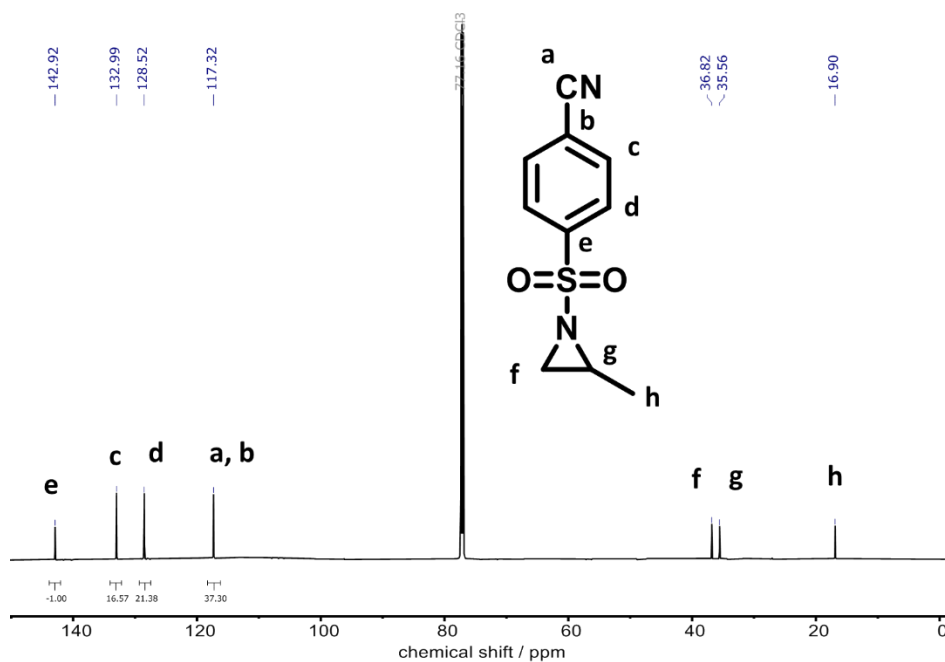
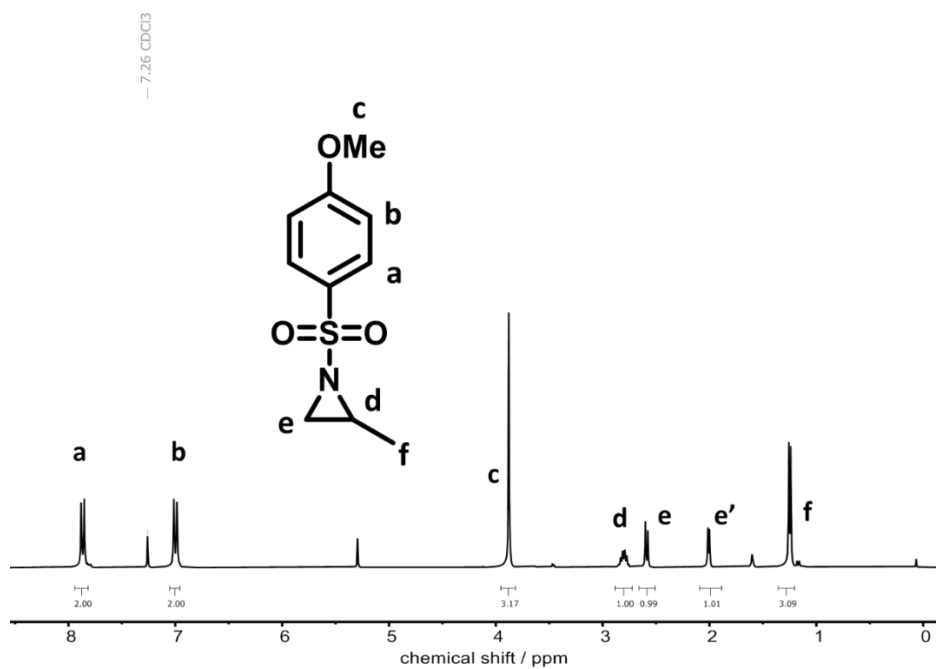
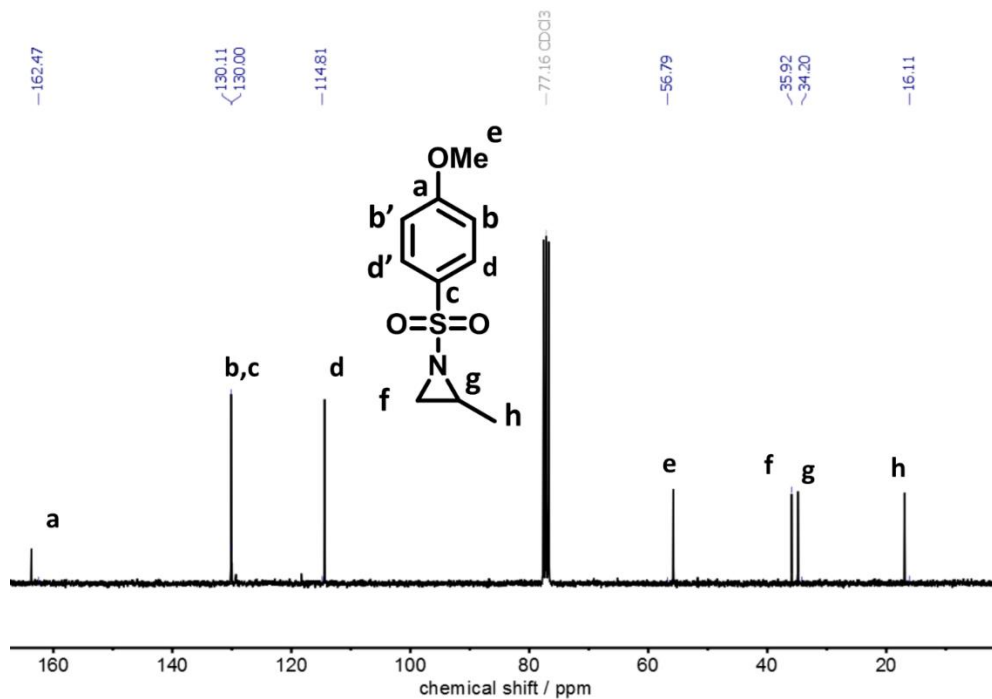
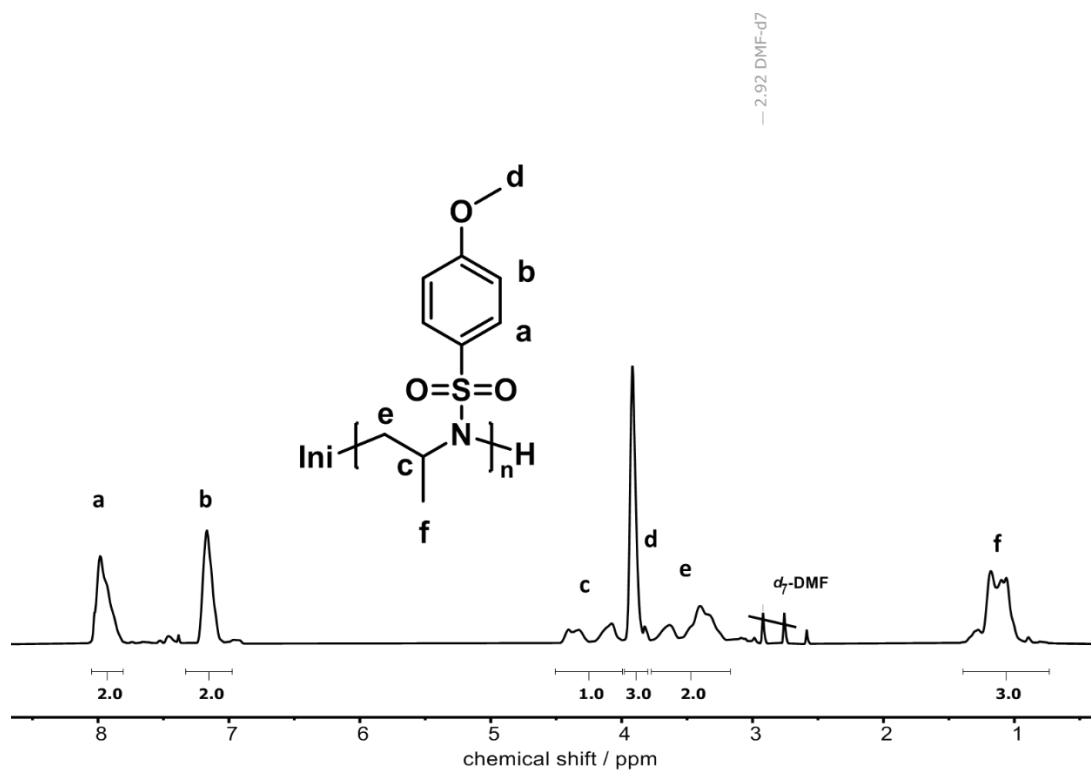
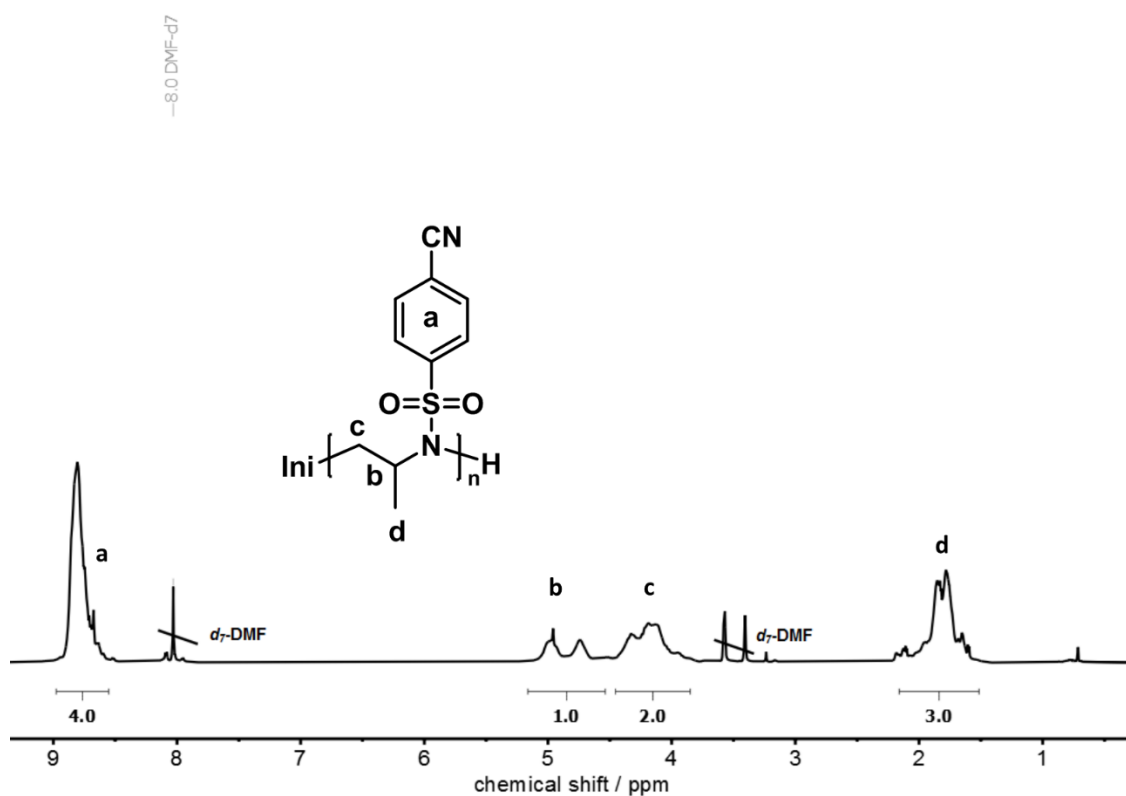


Figure S4.11: A: Monomer concentration as function of total conversion of activated aziridines (activation group of 2 and 7 were used); B: Mean composition (F) of both monomers at 50:50 feed ratios versus total conversion (reactivity ratios calculated with equation 8); C: Individual copolymer chains of polymerization mixture assuming an ideal AROP ($\bar{D}=1.0$), simulated by kinetic Monte-Carlo simulations (red: less reactive monomer); D: Logarithmic plot of monomer consumption over time (linear nature proves living polymerization); E: Copolymerization diagram (dashed line corresponds to ideal statistical copolymerization) F: Jaacks fit on in situ NMR data of monomers; G: BSL fit on in situ NMR data of monomers. H: Frey fit on in situ NMR data of monomers; I: Meyer-Lowry fit on in situ NMR data. All methods used in situ NMR data until 50% conversion to extract reactivity ratios.

4.7.3 Section 3 / Analytical details & NMR

Figure S4.12 ^1H NMR (300 MHz, Benzene- d_6) of 1-((4-cyanophenyl)sulfonyl)-2-methylaziridine.Figure S4.13: ^{13}C NMR (176 MHz, Chloroform- d) of 1-((4-cyanophenyl)sulfonyl)-2-methylaziridine.

Figure S4.14: ¹H NMR (300 k-d) of 1-((4-methoxyphenyl)sulfonyl)-2-methylaziridine.Figure S4.15: ¹³C NMR (75 MHz, Chloroform-d) of 1-((4-methoxyphenyl)sulfonyl)-2-methylaziridine.

Figure S4.16: ^1H NMR (700 MHz, $\text{DMF-}d_7$) of Poly (3).Figure S4.17: ^1H NMR (700 MHz, $\text{DMF-}d_7$) of Poly (6).

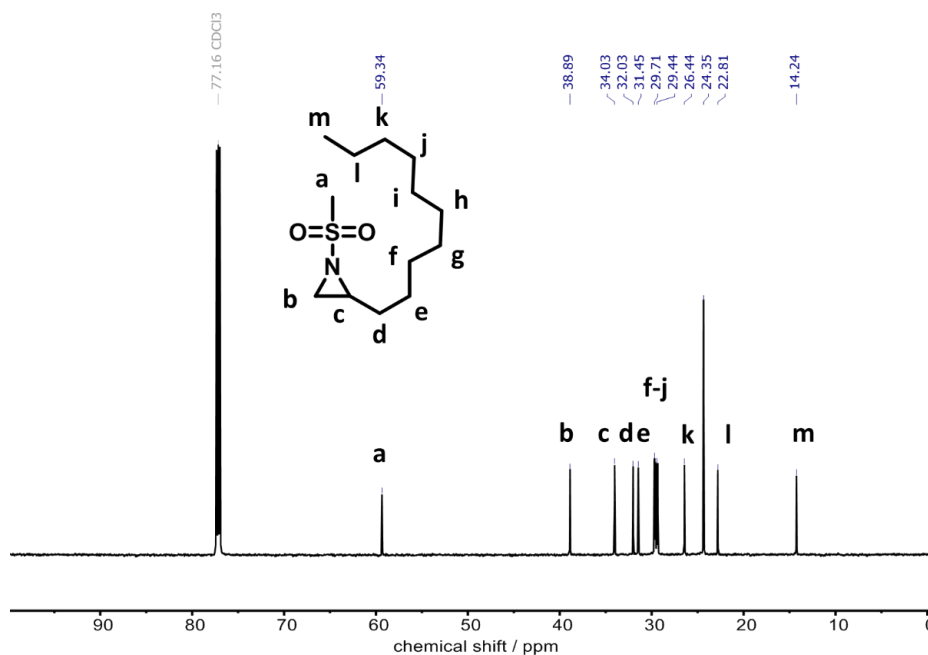
¹³C NMR spectra (raw data) of previously reported activated aziridines:

Figure S4.18: ¹³C NMR of *tert*-BusDecAz (1) (176 MHz, Chloroform-*d*) δ 59.34, 38.89, 34.03, 32.03, 31.45, 29.71, 29.66, 29.58, 29.44, 29.34, 26.44, 24.35, 22.81, 14.24.

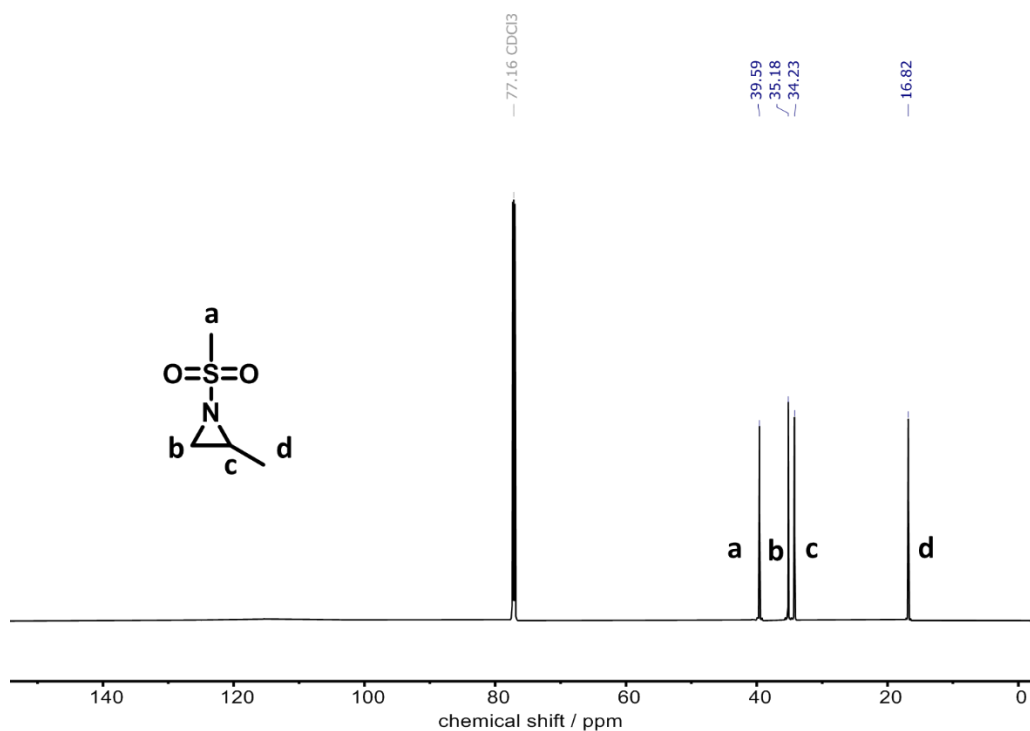


Figure S4.19: ¹³C NMR of MsMAz (2) (176 MHz, Chloroform-*d*) δ 39.59, 35.18, 34.23, 16.82.

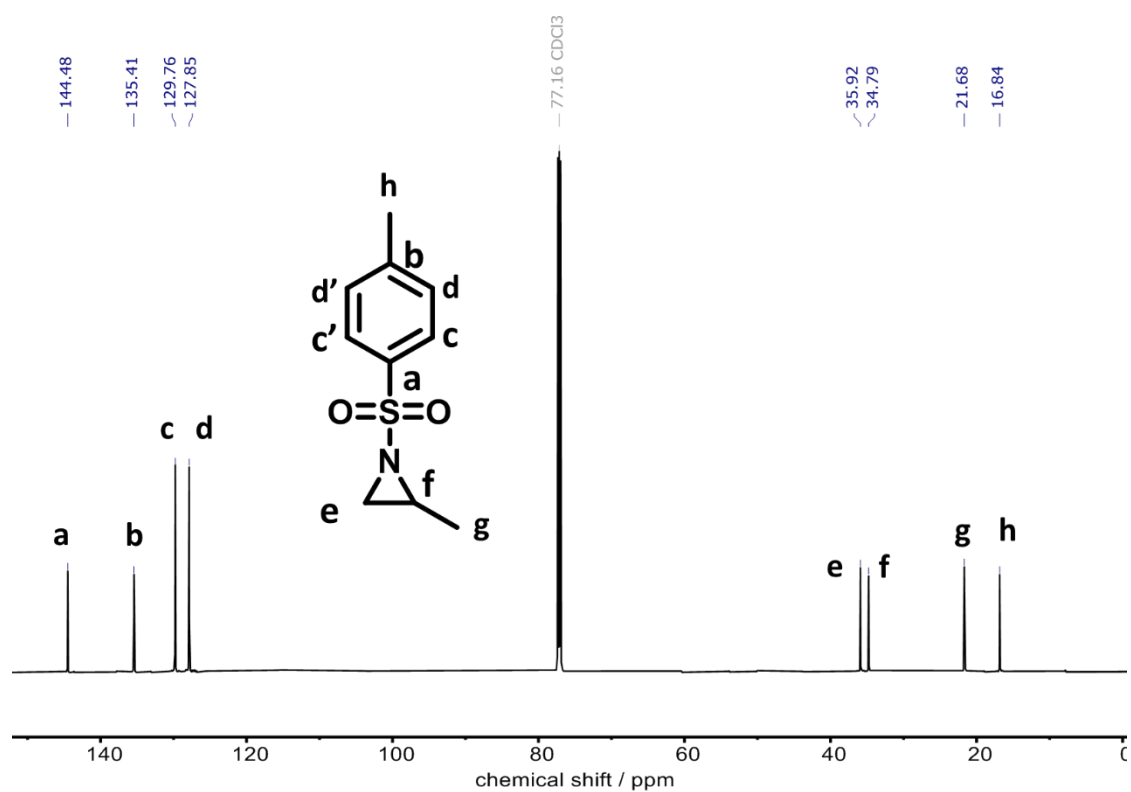


Figure S4.20: ^{13}C NMR of TsMAz (4) (176 MHz, Chloroform-*d*) δ 144.48, 135.41, 129.76, 127.85, 35.92, 34.79, 21.68, 16.84.

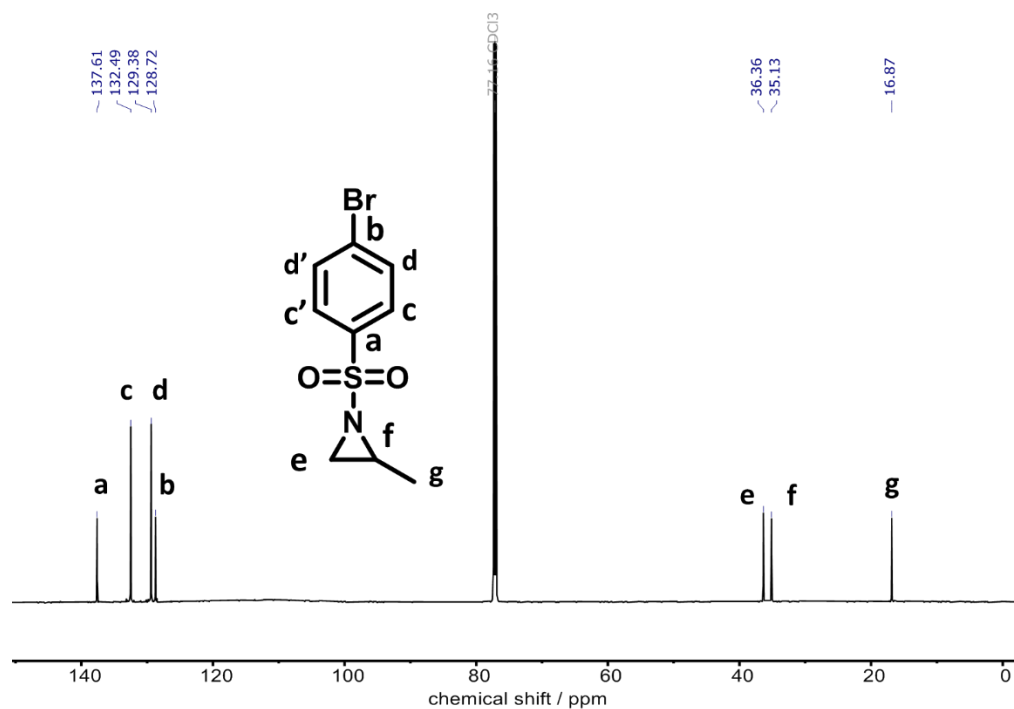


Figure S4.21: ^{13}C NMR of BsMAz (6) (176 MHz, Chloroform-*d*) δ 137.61, 132.49, 129.38, 128.72, 36.36, 35.13, 16.87.

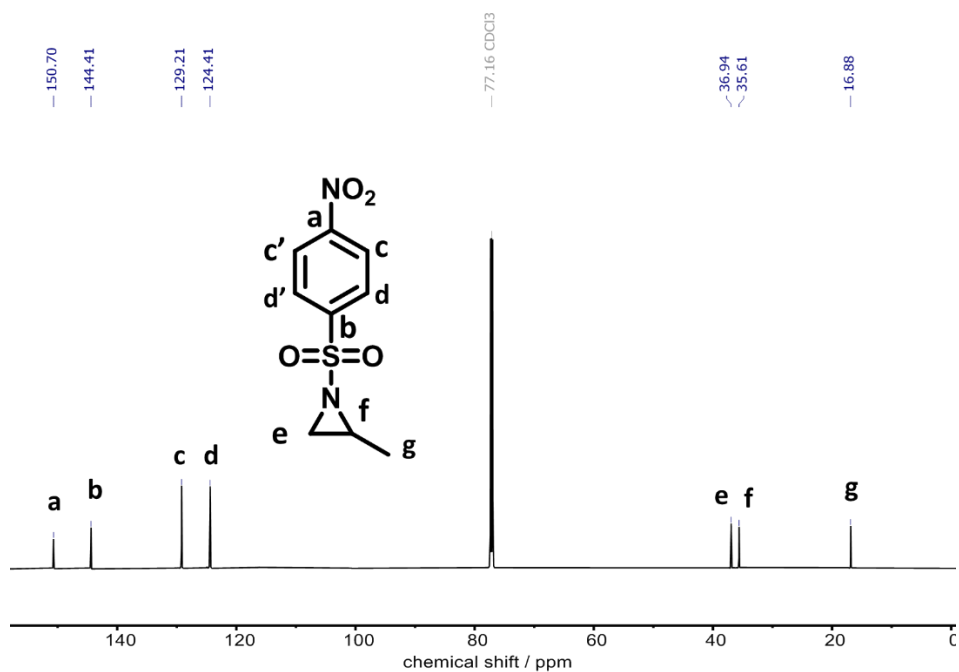
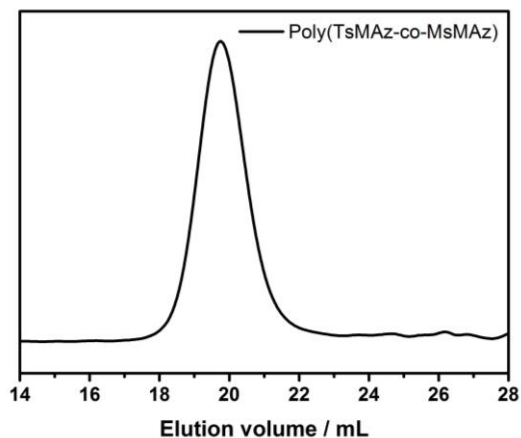
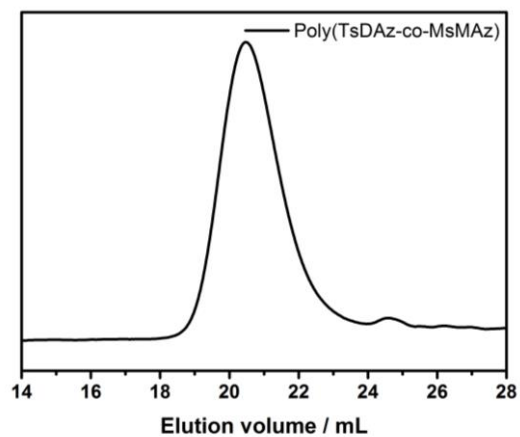


Figure S4.23: ¹³C NMR of NsMAz (8) (176 MHz, Chloroform-*d*) δ 150.70, 144.41, 129.21, 124.41, 36.94, 35.61, 16.88.

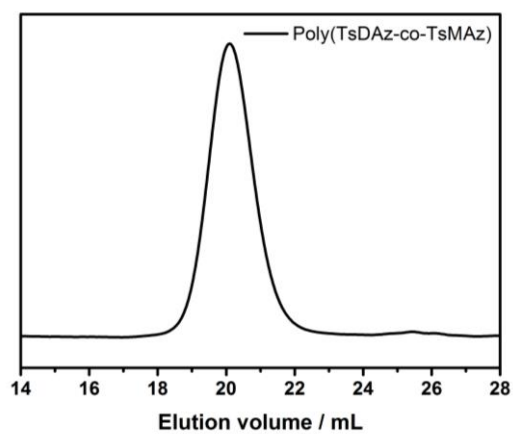
SECs corresponding to copolymerizations in Table 2



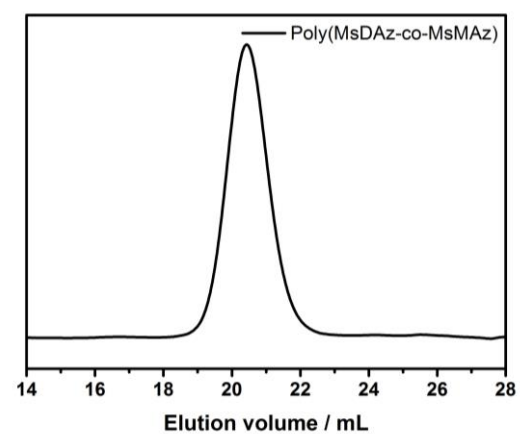
M_n (theo): 8835, M_n (SEC): 3400, \mathcal{D} : 1.11



M_n (theo): 11985, M_n (SEC): 2400, \mathcal{D} : 1.14

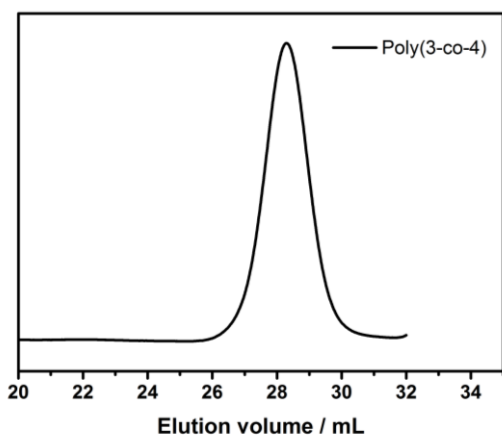


M_n (theo): 13885, M_n (SEC): 3000, \mathcal{D} : 1.10

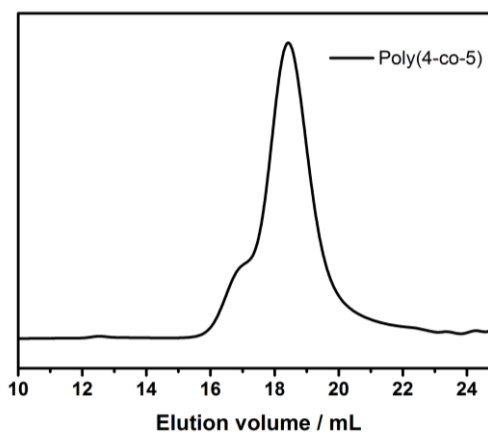


M_n (theo): 10085, M_n (SEC): 2100, \mathcal{D} : 1.06

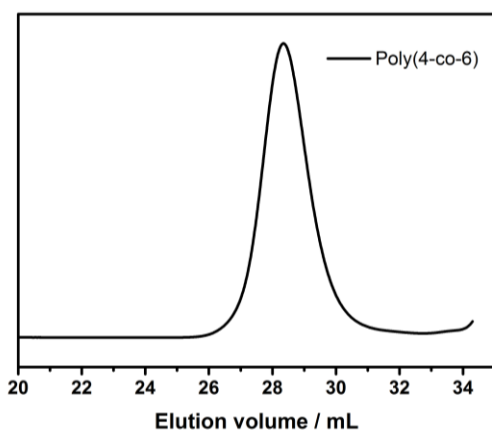
SECs corresponding to copolymerizations of Table 4.3*



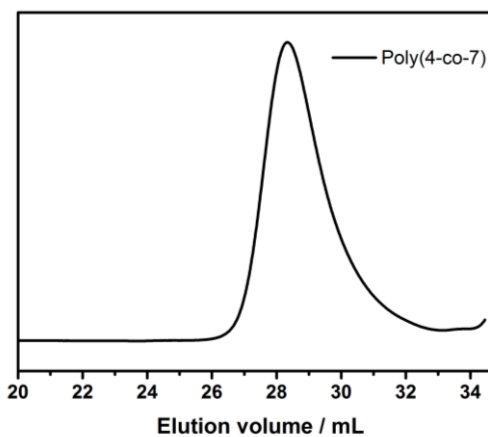
$M_n(\text{theo}): 11135, M_n(\text{SEC}): 3100, \bar{D}: 1.13$



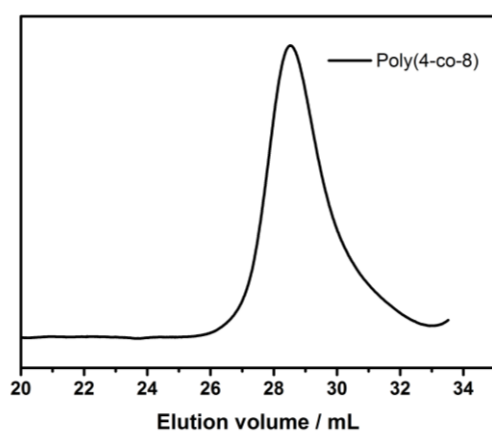
$M_n(\text{theo}): 21885, M_n(\text{SEC}): 5000, \bar{D}: 1.15$



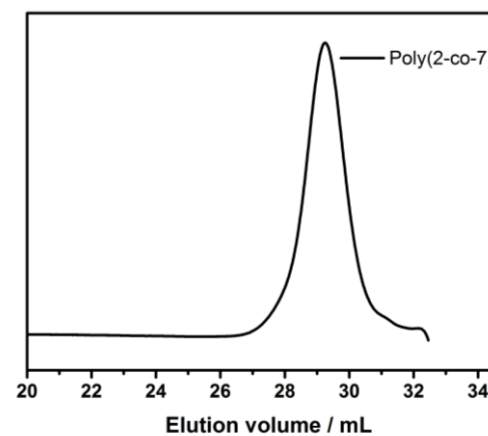
$M_n(\text{theo}): 12360, M_n(\text{SEC}): 3900, \bar{D}: 1.12$



$M_n(\text{theo}): 11010, M_n(\text{SEC}): 3000, \bar{D}: 1.32$



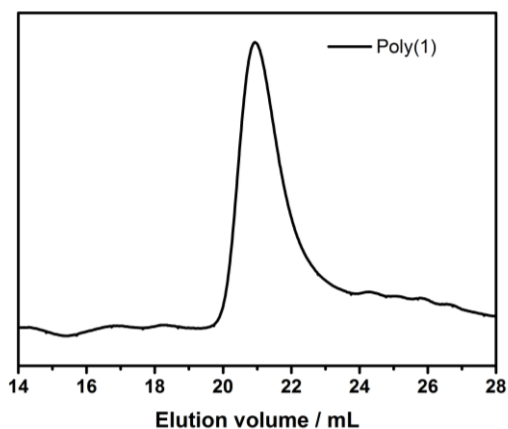
$M_n(\text{theo}): 11510, M_n(\text{SEC}): 2900, \bar{D}: 1.28$



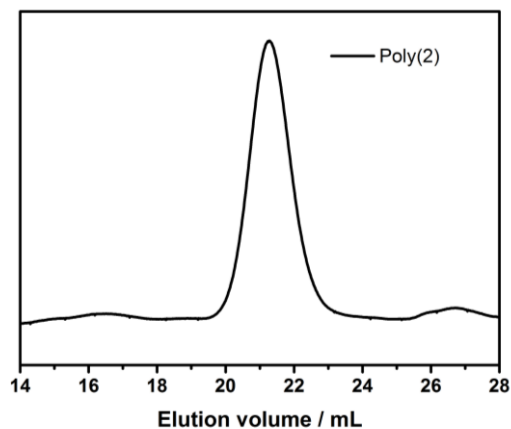
$M_n(\text{theo}): 9110, M_n(\text{SEC}): 1900, \bar{D}: 1.16$

*Note: SECs performed on two different setups

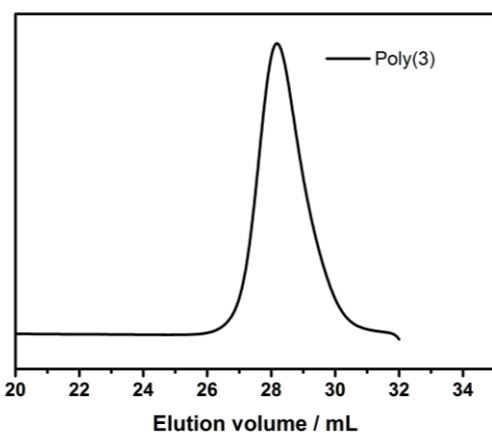
SECs of Homopolymerizations corresponding to Table 4.1*



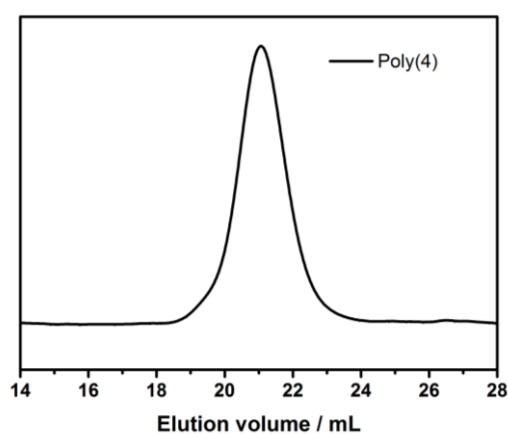
M_n (theo): 15335, M_n (SEC): 2100, D : 1.14



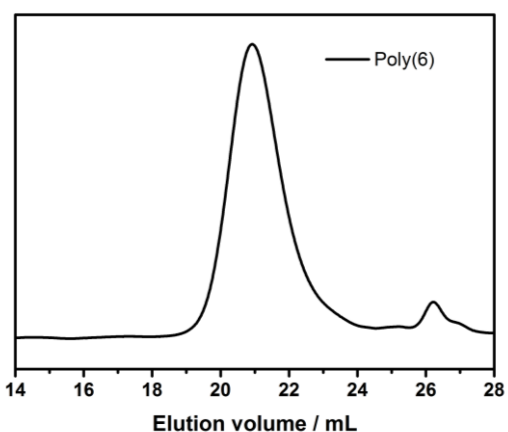
M_n (theo): 6935, M_n (SEC): 2200, D : 1.07



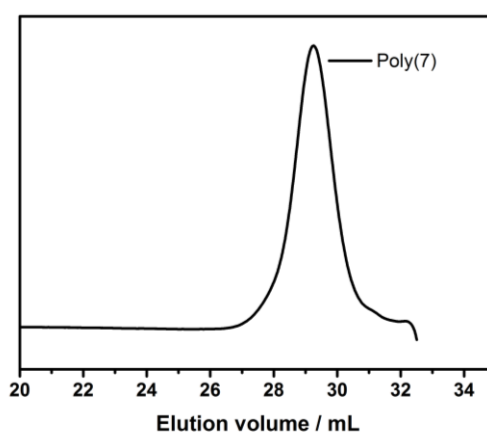
M_n (theo): 11535, M_n (SEC): 2800, D : 1.17



M_n (theo): 10735, M_n (SEC): 2300, D : 1.09

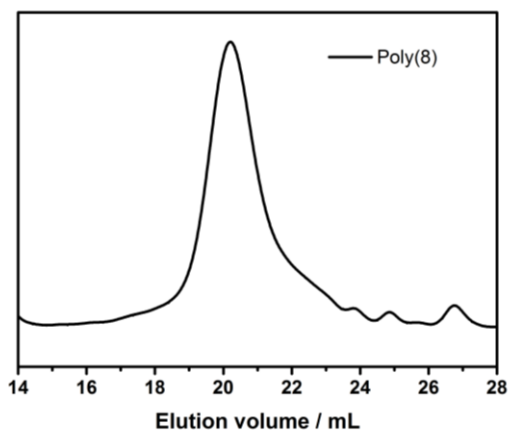


M_n (theo): 13880, M_n (SEC): 3000, D : 1.19



M_n (theo): 11285, M_n (SEC): 1900, D : 1.16

*Note: SECs performed on two different setups.



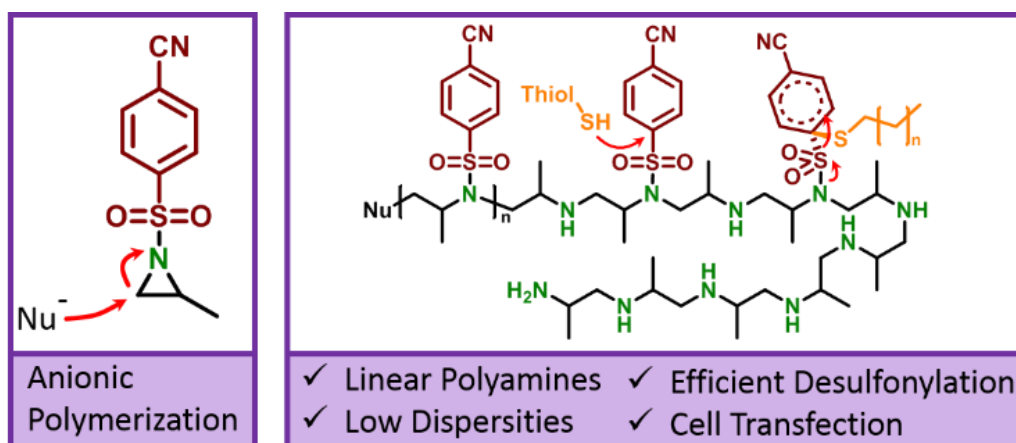
$M_n(\text{theo})$: 12285, $M_n(\text{SEC})$: 3000, D : 1.16

4.7.4 Additional References Chapter 4

1. Hansch, C.; Leo, A.; Taft, R. W., A Survey of Hammett Substituent Constants and Resonance and Field Parameters. *Chemical Reviews* **1991**, *91* (2), 165-195.

5 *Linear well-defined polyamines via anionic ring-opening polymerization of activated aziridines: from mild desulfonylation to cell transfection*

Tassilo Gleede, Fangzhou Yu, Ying-Li Luo, Youyong Yuan, Jun Wang and
Frederik R. Wurm*



TOC 5: The TOC illustrates the desulfonylation of the polysulfonamide, which was polymerized by anionic ring-opening polymerization.

Note: Fangzhou Yu, Ying-Li Luo, Youyong Yuan supervised by Jun Wang conducted all biological assays and edited this part in the manuscript. Frederik R. Wurm supervised the project. Tassilo Gleede did the synthetic work. Tassilo Gleede and Frederik R. Wurm wrote and edited the manuscript.

This chapter is based on a published article under the terms of the Copyright this chapter is used with the permission of ACS Publications: Tassilo Gleede, Fangzhou Yu, Ying-Li Luo, Youyong Yuan, Jun Wang and Frederik R. Wurm, Linear Well-Defined Polyamines via Anionic Ring-Opening Polymerization of Activated Aziridines: From Mild Desulfonylation to Cell Transfection, *ACS Macro Lett.* **2020**, 9, XXX, 20-25

5.1 Abstract

Linear polyethylenimine (L-PEI), a standard for non-viral gene delivery, is usually prepared by hydrolysis from poly(2-oxazoline)s. Lately, anionic polymerization of sulfonamide-activated aziridines had been reported as an alternative pathway towards well-defined L-PEI and linear polyamines. However, desulfonylation of the poly(sulfonyl aziridine)s typically relied on harsh conditions (acid, microwave) or used a toxic solvent (e.g. hexamethylphosphoramide). In addition, the drastic change of polarity requires solvents, which keep poly(sulfonyl aziridine)s as well as L-PEI in solution and only a limited number of strategies were reported. Herein, we prepared 1-(4-cyanobenzenesulfonyl) 2-methyl-aziridine (**1**) as a monomer for the anionic ring-opening polymerization. It was polymerized to well-defined and linear poly(sulfonyl aziridine)s. The 4-cyanobenzenesulfonyl-activating groups were removed under mild conditions to linear polypropylenimine (L-PPI). Using dodecanethiol and diazabicyclo-undecene (DBU) allowed $\geq 98\%$ desulfonylation and a reliable purification towards polyamines with high purity and avoiding main-chain scission. This method represents a fast approach in comparison to previous methods used for post-polymerization desulfonylation and produces linear well-defined polyamines. The high control over molecular weight and dispersities achieved by living anionic polymerization are the key advantages of our strategy, especially if used for biomedical applications, in which molecular weight might correlate with toxicity. The synthesized polypropylenimine was further tested as cell-transfection-agent and proved with 16.1 % transfection efficiency of the cationic nanoparticles to be an alternative to L-PEI obtained from the 2-oxazoline route. This general strategy will allow the preparation of complex macromolecular architectures containing polyamine segments, which were not accessible before.

5.2 Introduction

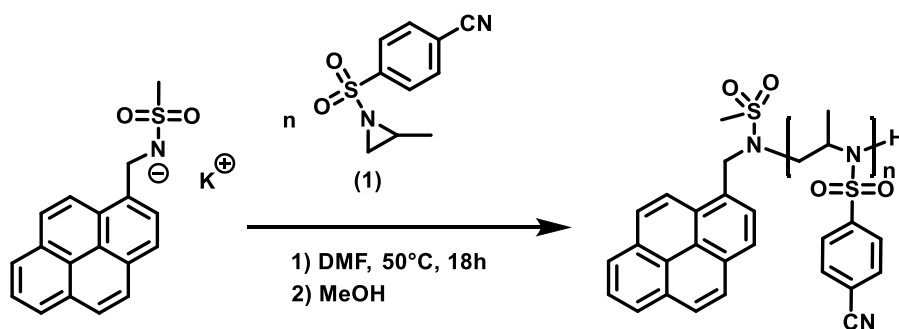
Linear polyamines, especially polyethylen- or propylenimine, would be ideal building blocks for macromolecular architectures for pH-responsive or metal-chelating (nano)materials. However, to date, only a very limited number of polymers with well-defined polyamine-segments have been reported.¹ Living anionic polymerization (LAP) is the superior method, when it comes to the synthesis of well-defined polymers with low dispersity and complex architectures. In direct analogy to the oxy-anionic ring-opening polymerization of epoxides, LAP of sulfonyl-activated aziridines gives access to well-defined linear poly(sulfonyl aziridine)s, where *N*-substituted nitrogen is part of the polymer backbone.² However, the free polyamines are only obtained, after removal of the sulfonamides under typically harsh conditions, which potentially resulted in the scission of the main chain and incomplete desulfonylation or by using toxic solvents, such as hexamethylphosphoramide (HMPA).³

LAP of sulfonyl aziridines stands out from oxy- and carbanionic polymerization by its unique tolerance against water and other protic additives due to the low nucleophilicity of the growing chain end.⁴ Polymerization of sulfonyl aziridines was also achieved by organo-catalyzed polymerization with a variety of superbases⁵ and carbenes, recently.⁶⁻⁸ The electron- withdrawing effect of the activating *N*-substituent directly correlates to the propagation rates coefficient and allowed the design of sequence-controlled gradient copolymers by competing copolymerization of different aziridines in a one-pot synthesis.^{9, 10} Sulfonyl aziridines copolymerized with ethylene oxide gave access to amphiphilic block copolymers by a fast one-pot polymerization procedure, due to highly different propagation rates.¹¹ Those amphiphilic block copolymers were used as emulsifiers and for the preparation of multi-block copolymers. A similar protocol for a one-step synthesis was more recently established by Rupar and coworkers, to access block copolymers from sulfonyl-activated azetidines and aziridines.¹² Block-polyamines with defined N-N distances of 2 or 3 CH₂-groups were prepared. Other block copolymers of aziridines with styrene¹³ or lactide⁶ were also prepared recently, relying on sequential monomer addition

Even though poly(sulfonyl aziridine)s could be beneficial materials for several applications, in which hydrophobicity or high thermal resistance might be beneficial, to date they are mainly considered as intermediates to polyamines after removal of the sulfonyl groups. Linear polyethylenimine (L-PEI) of well-defined size and dispersity are important for non-viral gene transfection.¹⁴ L-PEI is also used in applications such as anti-fouling coatings,¹⁵ chelation,¹⁶ or CO₂ capture.^{17, 18} However, only a limited number of synthetic strategies give access to L-PEI: the cationic ROP of aziridines only provides branched polymers and probably the most common pathway towards L-PEI is the acidic or basic hydrolysis of poly(2-oxazoline)s.¹⁹⁻²² Synthesis of

poly(2-oxazoline)s was developed more than 50 years ago and was continuously improved.^{23, 24} Today, CROP of 2-oxazolines can be conducted as living cationic polymerization providing well-defined polymers with low dispersities.²⁵⁻²⁷ Other methods are rare and, one to be mentioned is the mild acidic hydrolysis of poly(*N*-pyranyl ethylenimine)s.²⁸ However, the cationic ring-opening (CROP) suffered from chain transfer and termination reactions and this strategy was not further continued.

We developed a strategy based on living anionic ROP to linear polyamines. LAP avoids termination reactions and gives access to complex polymer architectures. Several monomer classes are polymerized by LAP and aziridines might be a powerful addition to this monomer set for additional complex structures. Sulfonyl aziridines gave access to polyamines by different desulfonylation strategies.^{3, 29, 30} However, the need for toxic solvents or harsh reaction conditions (e.g. highly acidic, microwave,²⁹ or lithium metal in HMPA³⁰) made this strategy less attractive compared to the oxazoline route. Additionally, chain-scission had reported and the work-up procedures reduced yields in some cases. Sulfonamides, however, have adjustable stability depending on their substitution pattern, which can be utilized to tailor desulfonylation conditions.³¹ While tosyl groups need strong acids or reducing conditions to be removed from the polymer, desulfonylation of nitrophenylsulfonyl groups had been removed under much milder conditions, recently.³² However, the purity and yield of the obtained L-PEI were lower compared to L-PEI from poly(2-oxazoline)s. Further, the nitrophenylsulfonyl activated monomer proved to be highly reactive and spontaneous polymerization was reported.³²



Scheme 5.1: Anionic ring-opening polymerization of 1-(4-cyanobenzenesulfonyl) 2-methyl-aziridine (1).

5.3 Results and Discussion

Here, we present the synthesis and polymerization of the activated sulfonyl aziridine (**1**) (Scheme 5.1). The monomer **1** was prepared by the reaction of 2-methyl aziridine with 4-cyanobenzenesulfonyl chloride and purified crystallization from *tert*-butyl methyl ether. The monomer was obtained as a white powder with a 93% yield and was bench-stable over several weeks without polymerization.

The ^1H NMR spectrum of **1** revealed the typical resonance pattern for a 2-substituted sulfonyl aziridine with resonances from 3.53 ppm (m), 2.24 ppm (d) and 1.34 ppm (d) (Figure S5.1). In the ^{13}C NMR spectrum, the resonances of the ring-carbons were detected at 36.8 and 35.6 ppm, respectively, indicating a stronger electron-withdrawing effect of the cyanobenzenesulfonyl group compared to other sulfonyl aziridines (Figure S2, note: the tosyl-substituted analog exhibited ^{13}C NMR resonances at higher field (ca. 35.9, 34.7 ppm)).³³ ESI mass spectrometry proved the successful preparation of **1** with a single mass peak for the protonated monomer at 223.1 Da (MH^+ , Figure S3).³³ For the polymerization of **1**, the monomer was freshly recrystallized, and dissolved in DMF at 50°C. After the addition of the initiator, the polymerization followed living characteristics and in all cases, full monomer conversion was achieved.

The polymers were purified by precipitation from the crude reaction mixture into cold methanol or diethyl ether and gave yields of 68 – 96 %. Polymers with degrees of polymerization (DP) from 25 to 200 repeating units, $M_n = 6,300\text{--}44,700 \text{ gmol}^{-1}$ were synthesized with narrow to moderate molecular weight distributions ($D = 1.15 - 1.43$, Figure 5.1 and Table 5.1). The increased molar mass dispersities with increasing degree of polymerization might be caused by decreased solubility of the polymers as we had encountered for previous poly(sulfonyl aziridine)s. ^1H NMR spectroscopy proved the successful formation of the polymer, with typical resonances for poly(sulfonyl aziridine)s (cf. Figure 5.2 and labels in the spectra).

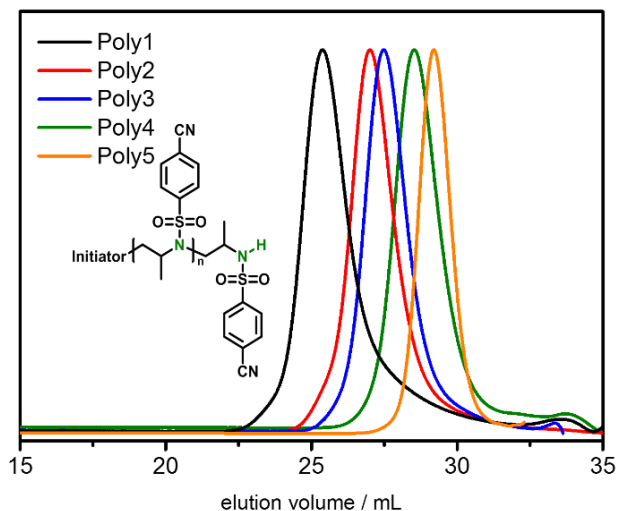


Figure 5.1: Size exclusion chromatograms of Poly1-Poly5 (in DMF).

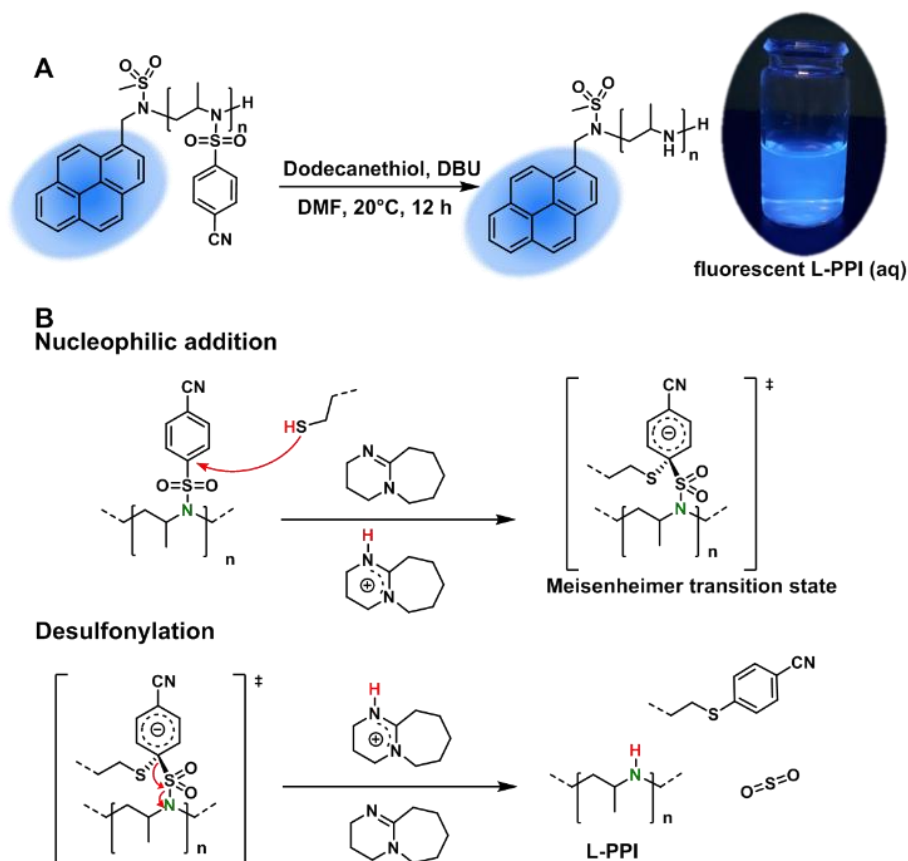
The polyamines were released by a mild desulfonylation *via* a nucleophilic attack to the electron-deficient 4-cyanophenylsulfonyl group by a thiolate forming a Meisenheimer-complex (Scheme 5.2). Desulfonylation was performed in DMF with a 5-fold excess of dodecanethiol and DBU as base (note: the cyanobenzenesulfonyl groups can be removed directly after the polymerization by adding DBU and the thiol or after work-up of the intermediate poly(sulfonyl aziridine)).

Linear polypropyleneimine (L-PPI) was isolated after the addition of ethyl acetate to the crude mixture and extraction with water. L-PPI was obtained after subsequent dialysis and lyophilization with ca. 40% yield. As the desulfonylation occurred under very mild conditions, also the SEC traces of the linear PPIs exhibited narrow molar mass dispersities, comparable to the starting materials. In addition, the fluorescent initiator remained intact (Scheme 5.2A), proving the possibility to install further functionalities at the alpha-position of the polymer chain end. The PPIs (1, 2, and 5) eluted at earlier elution volumes compared to the precursors Poly-1 and Poly-2 and Poly-2 (compare SEC in HFIP Figures S5.4 and S5.5), which is probably related to a larger hydrodynamic radius than the precursor polymer in HFIP. The desulfonylation was reproducible also for high molar mass PPIs (Table 5.2, PPI-1), indicating that during the process chain scission was avoided.

Table 5.1. Molar mass characterization of different polymers based on monomer 1.

#	DP	M_n^a / gmol^{-1}	$M_n^{b,c} / \text{gmol}^{-1}$	$\rho^{b,c}$
Poly-1	200*	44,700*	8,600 ^b	1.45 ^b
Poly-2	90	20,500	6,500 ^b	1.14 ^b
Poly-3	79	17,500	5,200 ^b	1.18 ^b
Poly-4	42	9,300	3,500 ^b	1.15 ^b
Poly-5	30*	6,300*	1900 ^b	1.12 ^b
PPI-1	215	12,400	17,800 ^c	1.22 ^c
PPI-2	83	5,000	12,100 ^c	1.29 ^c
PPI-5	30*	1,800*	5,600 ^c	1.16 ^c

^a: determined via ¹H NMR, ^b: determined via SEC (DMF),
^c: determined via SEC in hexafluoroisopropanol (HFIP)*:
theoretical value.



Scheme 5.2: (A) Desulfonation of Poly(1) to linear PPI (the photo shows the fluorescence of the PPI in water (2 mg / mL, 266 nm)). (B) Mechanism of desulfonation by nucleophilic addition of the thiolate *via* a Meisenheimer intermediate, followed by the release of sulfur dioxide, thioether and the polyamine.

The purified L-PPI was analyzed by ^1H NMR (Figures 5.2, S5.6) and ^{13}C NMR spectroscopy (Figure S5.7) proving that a high to quantitative desulfonation of at least 98% was achieved. Similar values are reported for the hydrolysis of commercially available L-PEI from poly(2-oxazoline)s with 92-93% hydrolysis.²⁷ Laboratory produced L-PEI from poly(2-oxazoline)s is with 99% to quantitative hydrolysis efficiency for L-PEI was reported,²⁷ similar to the herein reported L-PPI from poly(sulfonyl aziridine)s. MALDI ToF MS of PPI-2 (Figure S5.8) underlines the effective desulfonation. All main signals in the spectrum were attributed to PPI confirming the removal of the cyanobenzenesulfonyl groups and showing only the repeating unit of propyleneimine (with 57.1 gmol^{-1}). Other peaks for molar masses referring to partly deprotected polymer were not detected. Compared to the result of SEC and ^1H NMR, the MALDI ToF MS analysis underestimated the mass of the polymer, only smaller fractions of polyamine were detected, which is probably due to mass discrimination effects. It was reported that the multiple charges on polyamines resulted in complexation to impurities during the sample preparation and adhesion to the metal substrate and thus reducing the resolution of mass spectra.³⁴

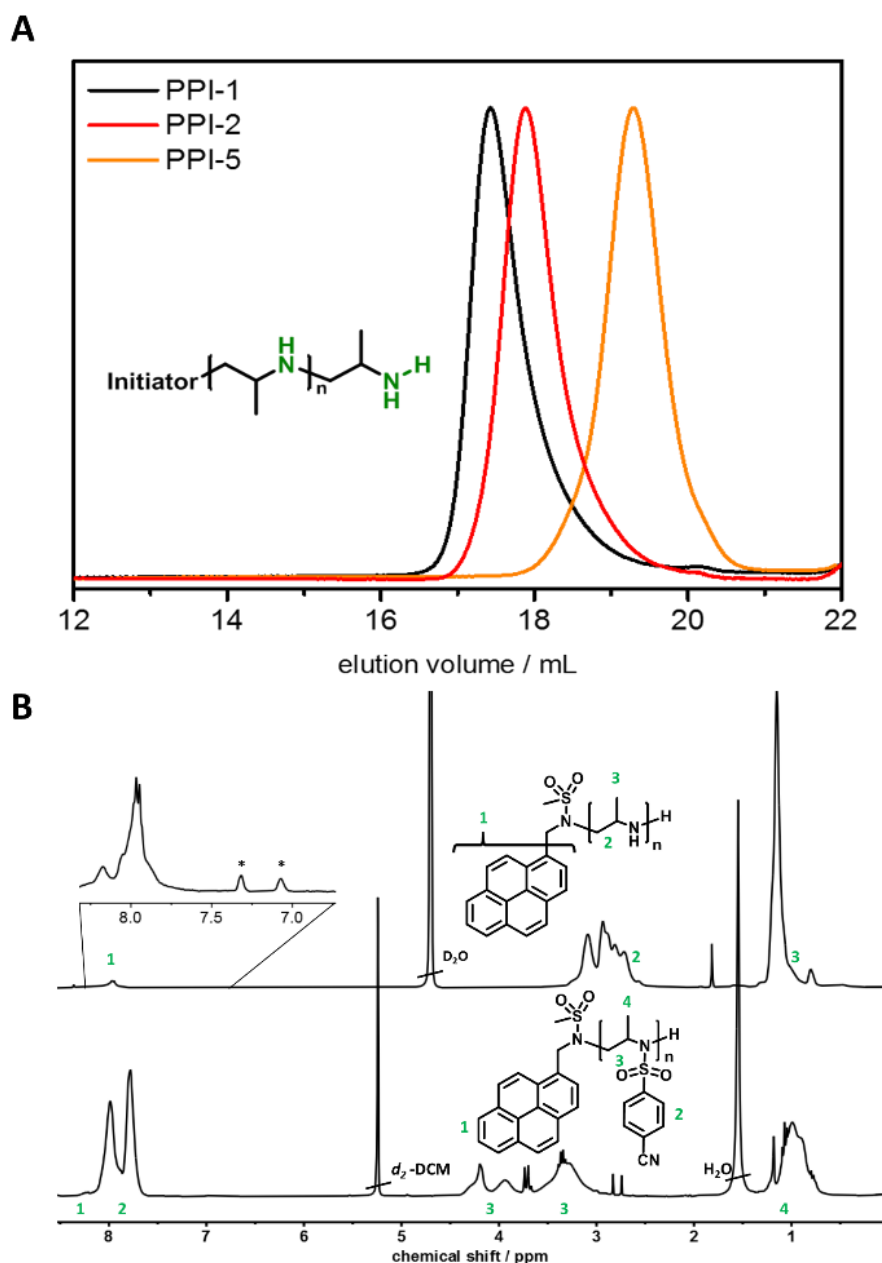


Figure 5.2. Desulfonation of Poly-2: (A) SEC traces of poly propylene imines PPI-1 (black), PPI-2 (red) PPI-5 (orange) in HFIP. (B) Overlay of the ^1H NMR spectra of Poly-2 (in CD_2Cl_2) and PPI-2 (in D_2O). * Residues of aromatic signals.

The linear PPI-5 was used to study cellular transfection efficiency. The gene-loaded cationic PPI-5 nanoparticles (abbreviated as PPI5-DNA-NPs below) were obtained by means of electrostatic attraction between the anionic plasmid DNA and the cationic PPI. Figure S5.9 shows the representative size distribution profiles and zeta potentials of the nanoparticles. The particle size and polydispersity index (PDI) of PPI5-DNA-NPs (N/P=40) were 89 nm and 0.206, respectively, demonstrating a relatively narrow particle size distribution. In addition, as N/P increased, the surface charge with zeta potential change from -20.8 to 24.5 mV were measured. The results of agarose gel electrophoresis (Figure S5.10) proved that PPI5-DNA-NPs binds with DNA to various

degrees with different N/P-ratio in the complex. There was decreasing free DNA present in the lane with the increase of the ratio of PPI5/DNA. When the N/P of NPs reached 20:1 or above, almost all DNA was combined with NPs without free DNA bands in the lane visible. Detection of expression of EGFP was carried out using inverted fluorescent microscope (Figure S5.12) and flow cytometry (Figure 5.3). The results underlined that PPI5-DNA-NPs successfully transferred plasmid DNA into 293T cells, and the transfection efficiency can reach 16.1% when the N/P of PPI5-DNA-NPs is 50:1 (Figure 5.3). To the best of our knowledge, this is the first example for a gene transfection conducted with a polyamine, prepared from poly(sulfonyl aziridine)s.

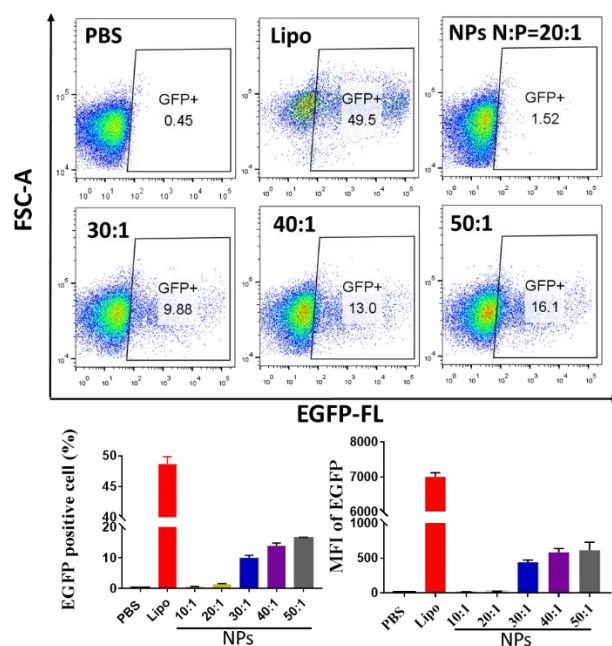


Figure 5.3: GFP expression levels after transfection using Lipofectamine and PPI5-DNA-NPs (N:P=20:1, 30:1, 40:1, 50:1).

5.4 Summary

In summary, we present a novel activated sulfonyl aziridine, **1**, a monomer for the living anionic ring-opening polymerization. Similar to other monomers of the family of sulfonyl aziridines, well-defined linear poly(sulfonyl aziridine)s were obtained by ROP. In contrast to previously reported highly activated aziridines, **1**, was stable and did not undergo spontaneous polymerization. More importantly, mild desulfonylation *via* a nucleophilic aromatic substitution removed the 4-cyanobenzenesulfonyl groups almost quantitatively and linear polypropylenimines were obtained. We believe this strategy is to date the fastest and mildest pathway to well-defined linear polyamines. The reaction conditions avoid very low or high temperatures, harsh reaction conditions, toxic solvents (such as HMPA) and exhibit an easy work-up procedure, to access linear polyamines by anionic ring-opening polymerization, which further allows the combination with other anionic polymerization techniques for macromolecular architectures. We further demonstrated the successful application of PPI as cell transfection agent; the cationic L-PPI can bind DNA through electrostatic attraction, and the gene vectors PPI5-DNA-NPs were used successfully to transfer reporter gene EGFP to 293T cells, leading to gene expression and subsequent protein synthesis. We believe this general strategy will broaden the synthetic toolbox for the preparation of complex macromolecular architectures containing well-defined polyamine segments.

5.5 References Chapter 5

1. Gleede, T.; Reisman, L.; Rieger, E.; Mbarushimana, P. C.; Rupar, P. A.; Wurm, F. R., Aziridines and azetidines: building blocks for polyamines by anionic and cationic ring-opening polymerization. *Polymer Chemistry* **2019**, *10* (24), 3257-3283.
2. Stewart, I. C.; Lee, C. C.; Bergman, R. G.; Toste, F. D., Living Ring-Opening Polymerization of *N*-Sulfonylaziridines: Synthesis of High Molecular Weight Linear Polyamines. *Journal of the American Chemical Society* **2005**, *127* (50), 17616-17617.
3. Rieger, E.; Gleede, T.; Manhart, A.; Lamla, M.; Wurm, F. R., Microwave-Assisted Desulfonylation of Polysulfonamides toward Polypropylenimine. *ACS Macro Letters* **2018**, 598-603.
4. Gleede, T.; Rieger, E.; Liu, L.; Bakkali-Hassani, C.; Wagner, M.; Carlotti, S.; Taton, D.; Andrienko, D.; Wurm, F. R., Alcohol- and Water-Tolerant Living Anionic Polymerization of Aziridines. *Macromolecules* **2018**, *51* (15), 5713-5719.
5. Wang, X.; Liu, Y.; Li, Z.; Wang, H.; Gebru, H.; Chen, S.; Zhu, H.; Wei, F.; Guo, K., Organocatalyzed Anionic Ring-Opening Polymerizations of *N*-Sulfonyl Aziridines with Organic Superbases. *ACS Macro Letters* **2017**, 1331-1336.
6. Bakkali-Hassani, C.; Coutouly, C.; Gleede, T.; Vignolle, J.; Wurm, F. R.; Carlotti, S.; Taton, D., Selective Initiation from Unprotected Aminoalcohols for the *N*-Heterocyclic Carbene-Organocatalyzed Ring-Opening Polymerization of 2-Methyl-*N*-tosyl Aziridine: Telechelic and Block Copolymer Synthesis. *Macromolecules* **2018**, *51* (7), 2533-2541.
7. Bakkali-Hassani, C.; Rieger, E.; Vignolle, J.; Wurm, F. R.; Carlotti, S.; Taton, D., The organocatalytic ring-opening polymerization of *N*-tosyl aziridines by an *N*-heterocyclic carbene. *Chem. Commun.* **2016**, *52* (62), 9719-9722.
8. Bakkali-Hassani, C.; Rieger, E.; Vignolle, J.; Wurm, F. R.; Carlotti, S.; Taton, D., Expanding the scope of *N*-heterocyclic carbene-organocatalyzed ring-opening polymerization of *N*-tosyl aziridines using functional and non-activated amine initiators. *European Polymer Journal* **2017**, *95*, 746-755.
9. Rieger, E.; Alkan, A.; Manhart, A.; Wagner, M.; Wurm, F. R., Sequence-Controlled Polymers via Simultaneous Living Anionic Copolymerization of Competing Monomers. *Macromol. Rapid Commun.* **2016**, *37* (10), 833-839.
10. Rieger, E.; Blankenburg, J.; Grune, E.; Wagner, M.; Landfester, K.; Wurm, F. R., Controlling the Polymer Microstructure in Anionic Polymerization by Compartmentalization. *Angewandte Chemie International Edition* **2018**, *57* (9), 2483-2487.
11. Gleede, T.; Rieger, E.; Blankenburg, J.; Klein, K.; Wurm, F. R., Fast Access to Amphiphilic Multiblock Architectures by the Anionic Copolymerization of Aziridines and Ethylene Oxide. *J Am Chem Soc* **2018**, *140* (41), 13407-13412.
12. Reisman, L.; Rowe, E. A.; Jackson, E. M.; Thomas, C.; Simone, T.; Rupar, P. A., Anionic Ring-Opening Polymerization of *N*-(tolylsulfonyl)azetidines To Produce Linear Poly(trimethylenimine) and Closed-System Block Copolymers. *Journal of the American Chemical Society* **2018**, *140* (46), 15626-15630.
13. Thomi, L.; Wurm, F. R., Aziridine Termination of Living Anionic Polymerization. *Macromol Rapid Commun* **2014**, *35* (5), 585-589.
14. Jager, M.; Schubert, S.; Ochrimenko, S.; Fischer, D.; Schubert, U. S., Branched and linear poly(ethylene imine)-based conjugates: synthetic modification, characterization, and application. *Chem Soc Rev* **2012**, *41* (13), 4755-4767.
15. Francolini, I.; Vuotto, C.; Piozzi, A.; Donelli, G., Antifouling and antimicrobial biomaterials: an overview. *Apmis* **2017**, *125* (4), 392-417.
16. Kobayashi, S.; Hiroishi, K.; Tokunoh, M.; Saegusa, T., Chelating properties of linear and branched poly(ethylenimines). *Macromolecules* **1987**, *20* (7), 1496-1500.
17. Didas, S. A.; Choi, S.; Chaikittisilp, W.; Jones, C. W., Amine-oxide hybrid materials for CO₂ capture from ambient air. *Accounts of chemical research* **2015**, *48* (10), 2680-2687.
18. Shen, X.; Du, H.; Mullins, R. H.; Kommalapati, R. R., Polyethylenimine applications in carbon dioxide capture and separation: from theoretical study to experimental work. *Energy Technology* **2017**, *5* (6), 822-833.
19. Lambermont-Thijs, H. M. L.; van der Woerd, F. S.; Baumgaertel, A.; Bonami, L.; Du Prez, F. E.; Schubert, U. S.; Hoogenboom, R., Linear Poly(ethylene imine)s by Acidic Hydrolysis of Poly(2-oxazoline)s: Kinetic Screening, Thermal Properties, and Temperature-Induced Solubility Transitions. *Macromolecules* **2010**, *43* (2), 927-933.

20. Tauhardt, L.; Kempe, K.; Knop, K.; Altuntaş, E.; Jäger, M.; Schubert, S.; Fischer, D.; Schubert, U. S., Linear Polyethyleneimine: Optimized Synthesis and Characterization - On the Way to "Pharmagrade" Batches. *Macromolecular Chemistry and Physics* **2011**, 212 (17) 1918-1924.
21. Tauhardt, L.; Kempe, K.; Schubert, U. S., Toward the design of LPEI containing block copolymers: Improved synthesis protocol, selective hydrolysis, and detailed characterization. *Journal of Polymer Science Part A: Polymer Chemistry* **2012**, 50 (21), 4516-4523.
22. Monnery, B. D.; Hoogenboom, R., CHAPTER 2. Synthesis and Properties of Polyalkylenimines. **2014**, 30-61.
23. Hoogenboom, R., 50 years of poly(2-oxazoline)s. *European Polymer Journal* **2017**, 88, 448-450.
24. Verbraeken, B.; Monnery, B. D.; Lava, K.; Hoogenboom, R., The chemistry of poly(2-oxazoline)s. *Eur. Polym. J.* **2017**, 88, 451-469.
25. Hoogenboom, R.; Fijten, M. W.; Thijs, H. M.; van Lankvelt, B. M.; Schubert, U. S., Microwave-assisted synthesis and properties of a series of poly (2-alkyl-2-oxazoline) s. *Designed monomers and polymers* **2005**, 8 (6), 659-671.
26. Wiesbrock, F.; Hoogenboom, R.; Leenen, M. A.; Meier, M. A.; Schubert, U. S., Investigation of the living cationic ring-opening polymerization of 2-methyl-, 2-ethyl-, 2-nonyl-, and 2-phenyl-2-oxazoline in a single-mode microwave reactor. *Macromolecules* **2005**, 38 (12), 5025-5034.
27. Perevyazko, I.; Gubarev, A. S.; Tauhardt, L.; Dobrodumov, A.; Pavlov, G. M.; Schubert, U. S., Linear poly(ethylene imine)s: true molar masses, solution properties and conformation. *Polymer Chemistry* **2017**, 8 (46), 7169-1779.
28. Weyts, K. F.; Goethals, E. J., New synthesis of linear polyethyleneimine. *Polymer Bulletin* **1988**, 19 (1), 13-19.
29. Rieger, E.; Manhart, A.; Wurm, F. R., Multihydroxy Polyamines by Living Anionic Polymerization of Aziridines. *ACS Macro Lett.* **2016**, 5 (2), 195-198.
30. Reisman, L.; Mbarushimana, C. P.; Cassidy, S. J.; Rugar, P. A., Living Anionic Copolymerization of 1-(Alkylsulfonyl)aziridines to Form Poly(sulfonylaziridine) and Linear Poly(ethylenimine). *ACS Macro Letters* **2016**, 5 (10), 1137-1140.
31. Javorskis, T.; Orentas, E., Chemoselective Deprotection of Sulfonamides Under Acidic Conditions: Scope, Sulfonyl Group Migration, and Synthetic Applications. *J. Org. Chem.* **2017**, 82 (24), 13423-13439.
32. Mbarushimana, P. C.; Liang, Q.; Allred, J. M.; Rugar, P. A., Polymerizations of Nitrophenylsulfonyl-Activated Aziridines. *Macromolecules* **2018**, 51 (3), 997-983.
33. Rieger, E.; Alkan, A.; Manhart, A.; Wagner, M.; Wurm, F. R., Sequence-Controlled Polymers via Simultaneous Living Anionic Copolymerization of Competing Monomers. *Macromol. Rapid Commun.* **2016**, 37 (10), 833-839.
34. Altuntaş, E.; Knop, K.; Tauhardt, L.; Kempe, K.; Crecelius, A. C.; Jäger, M.; Hager, M. D.; Schubert, U. S., Tandem mass spectrometry of poly (ethylene imine) s by electrospray ionization (ESI) and matrix-assisted laser desorption/ionization (MALDI). *Journal of Mass Spectrometry* **2012**, 47 (1), 105-114.

5.6 Supporting Information for Linear well-defined polyamines via anionic ring-opening polymerization of activated aziridines: from mild desulfonation to cell transfection

5.7 Materials and analytic methods

5.7.1 Chemicals.

Solvents and reagents were purchased from Acros Organics, TCI, Sigma-Aldrich or Fluka and used as received unless otherwise stated (methanol, diethylether, anhydrous DMF, DCM, 4-Cyanobenzenesulfonyl chloride, CaH₂, CaSO₄, *tert*-butyl methyl ether, Dodecane thiol). Deuterated solvents were purchased from Deutero GmbH. 2-Methylaziridine was synthesized according to already published procedures¹ DBU and 2-methylaziridine were purified by distillation from CaH₂ to remove traces of water. DBU was than stored over molecular sieve 3 Å and 4 Å. 2-Methyl-*N*-tosylaziridine (TsMAz) and 2-methyl-*N*-mesylaziridine (MsMAz), PyNHMs-initiator were synthesized according to already published procedures and dried by azeotropic distillation from benzene to remove traces of water.¹

Fetal bovine serum (FBS) was purchased from Excell Bio (Shanghai, China). Dulbecco's Modified Eagle Medium (DMEM) was purchased from Thermo Fisher Scientific (Suzhou, China) Methyl thiazol tetrazolium (MTT) was obtained from Sigma-Aldrich (St Louis, MO). LipofectamineTM 3000 Reagent were obtained from Invitrogen (Carlsbad, CA). GelRed and Orange Loading Buffer was obtained from TSINGKE Biological Technology (Beijing, China). All the other chemicals and reagents used were of analytical purity grade or higher, obtained commercially.

5.7.2 Cell culture

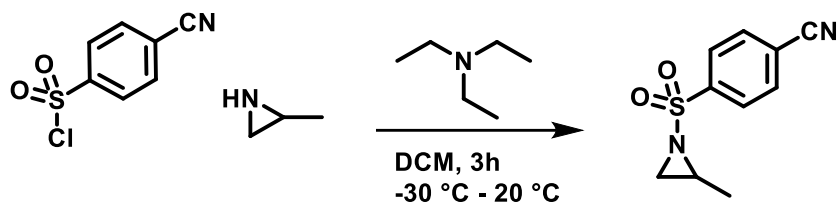
The 293T cell line was obtained from the Type Culture Collection of the Chinese Academy of Sciences (Shanghai, China) and maintained in DMEM with 10% FBS under a humidified atmosphere containing 5% CO₂ at 37 °C.

5.7.3 Analytic methods.

¹H NMR and ¹³C NMR spectra were recorded using, a Bruker Avance 300, a Bruker Avance III 500, or a Bruker Avance III 700. All spectra were referenced internally to residual proton signals of the deuterated solvent. For all polymers SEC measurements in dimethylformamide (DMF) (containing 1.0 g/L of lithium bromide as an additive) an Agilent 1100 Series was used as an integrated instrument, including a GRAM (PSS) column (10000/1000/100 Å), a UV detector (270 nm), and a RI detector at a flow rate of 1 mL/min at 60 °C. Calibration was carried out using PEO standards provided by Polymer Standards Service. Deprotected Polyamines and their corresponding polysulfonamides were additionally analyzed with hexafluoroisopropanol (HFIP) as eluent. HFIP SEC measurements were performed in HFIP (3 g/L potassium trifluoroacetate (KTFA) added) at 40 °C and a flow rate of 0.8 mL min⁻¹. The columns were packed with modified silica (PFG columns particle size: 7 µm, porosity: 100 Å and 1000 Å). Calibration was carried out using PMMA standards (provided by Polymer Standards Service) with toluene as an internal standard. A refractive index (RI) detector (G1362A RID) and a UV/VIS detector (at 230 nm; Jasco UV-2075 Plus) were used for polymer detection. MALDI-FTICR. The PPI was characterized by MALDI-FTICR-MS using a solariX mass spectrometer (Bruker). The samples were prepared using a dried droplet method with *trans*-3-indoleacrylic acid (IAA) (40 mg mL⁻¹ in THF) as a matrix. ESI MS. Monomer mass was determined by Advion Expression CMS *via* direct injection Analysis from methanolic sample solution (c = 1 mg / mL).

5.8 Synthesis Procedures

5.8.1 Synthesis of 1



The synthesis of 1 is orientated of previous synthesized monomers such as MsMAz and TsMAz. In a pre-dried 250 mL round bottom flask equipped with a stirring bar the 4-cyanobenzenesulfonylchlorid (7.00 g, 33 mmol) was dissolved in 150 mL of dry dichloromethane. The Reaction mixture was cooled in a dry ice acetone bath at -30 °C. 4.35 g trimethylamine (33 mmol) was added slowly *via* syringe. Freshly distilled methylaziridine (2.4 mL, 33 mmol) diluted in 20 mL dry dichloromethane was added dropwise to the reaction mixture. After stirring for 30 min at -30 °C the reaction mixture was further stirred at room temperature for 2 hours. The DCM phase was washed with water (3x 50 mL) 0.2N HCl (1x 50 mL), saturated sodium bicarbonate solution (1x 50 mL) and Brine (1x 50 mL). The organic phase was than dried over MgSO₄, filtered and concentrated below 30 °C under vacuum to give the product. (yield: 93%). Polymerization was done with freshly recrystallized monomer. Therefor the monomer was solved in *tert*-butyl methyl ether and recrystallized at -20 °C after the addition of small amounts of petrol ether. Purification by sublimation or column chromatography over silica showed to ring open the product.

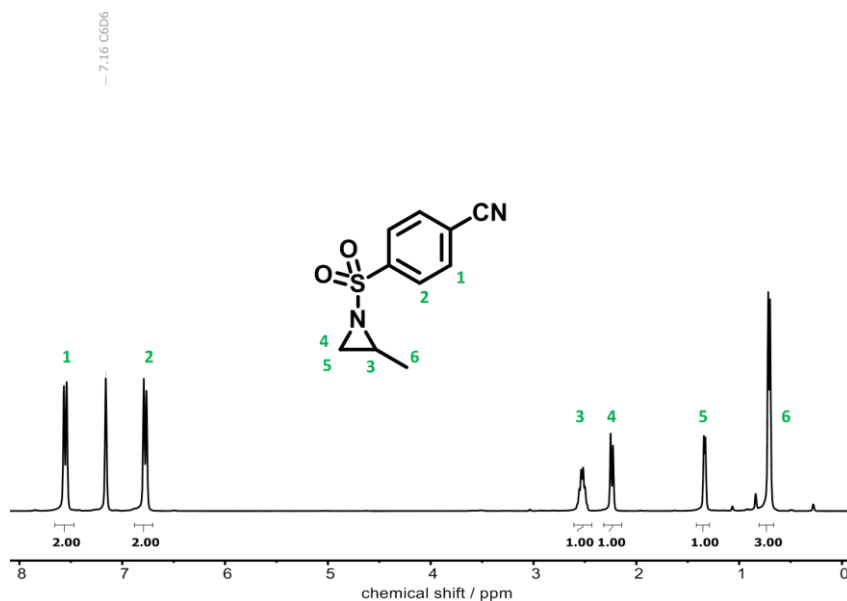


Figure S5.1 ¹H NMR (300 MHz, Benzene-d₆ of 1) δ 7.66 – 7.47 (d, 2H), 6.88 – 6.70 (d, 2H), 2.53 (h, J = 5.7 Hz, 1H), 2.24 (dd, J = 7.0, 1.6 Hz, 1H), 1.34 (dd, J = 4.6, 1.6 Hz, 1H), 0.71 (dd, J = 5.6, 1.6 Hz, 3H).

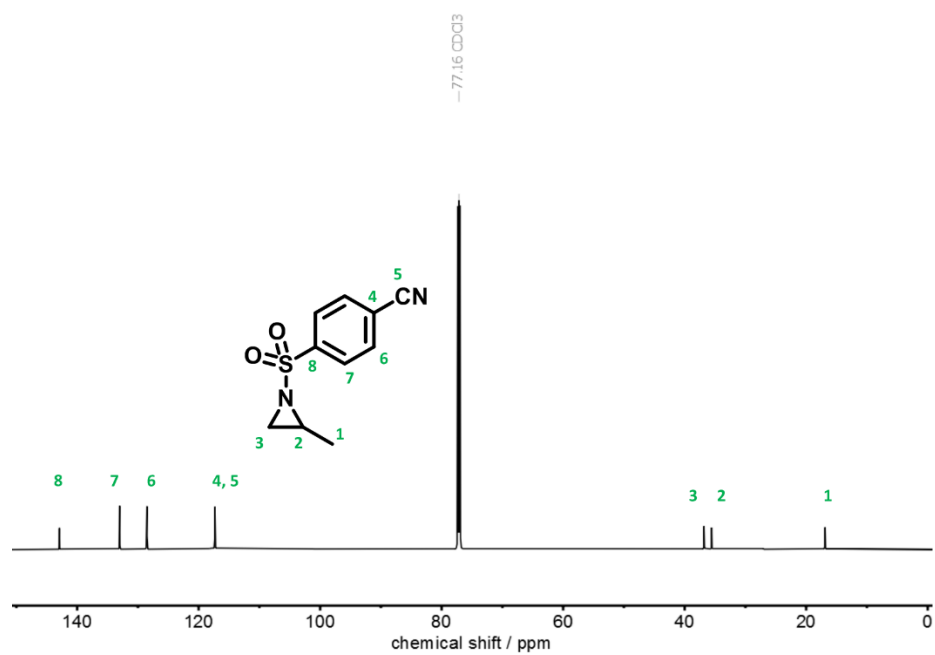


Figure S5.2: ^{13}C NMR (176 MHz, Chloroform-d) of (1) δ 142.92, 128.52, 117.32, 36.82, 35.56, 16.90.

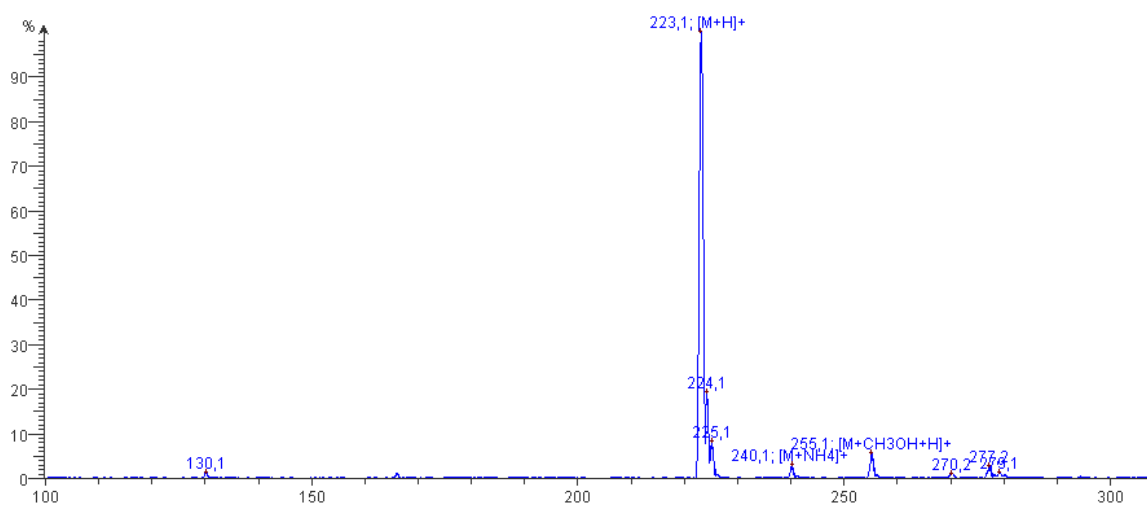
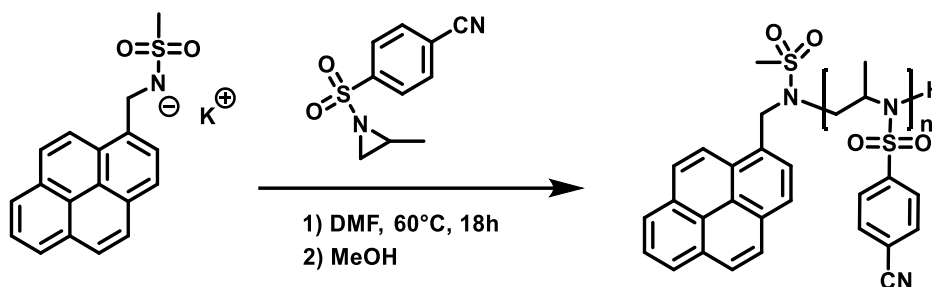


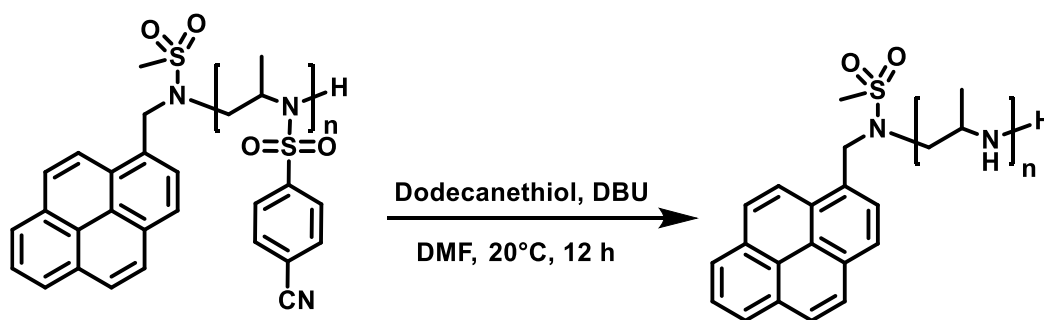
Figure S5.3: Spectrum of (1) background subtracted. Main fraction corresponds to monomer mass + H^+ of 223.1 g/mol.

5.8.2 General procedure for the azaanionic polymerization of 1.



All glassware (Schlenk flasks) was flame-dried by *in vacuo* for at least three times. All reactants (except potassium bis(trimethylsilyl)amide (KHMDs)) were dried from benzene *in vacuo* for at least 4 h. The monomers were dissolved in anhydrous *N,N*-dimethylformamide (DMF) to give a 10 wt% solution, the PyNHMs-initiator were dissolved in 1 mL DMF. The initiator solution was activated by adding it to KHMDs under argon-atmosphere. From the initiator-solution, the appropriate volume was added to the monomer solution. The mixture was stirred at 60 °C over night. To terminate the polymers, 0.5 mL acidic methanol was added and the reaction mixture was precipitated in ca. 30 mL methanol or diethylether. The pale white solids were collected by centrifugation and dried at room temperature *in vacuo*, yields: 95-98%.

5.8.3 Procedure for Desulfonation of Poly(CNsMAz)



The desulfonation can be performed either directly after the polymerization or after purification of the polymer. In case for P4 500 mg polymer (1 equiv. corresponding to sulfonamide unit) of the poly(sulfonylaziridine) remained in 3 mL dry DMF, to the polymer solution 1.6 mL dry DBU (4.7 equiv.) and 2.6 mL dodecanethiol (5 equiv) was added. Thereby the clear solution turns into a pale yellow solution. The solution is then allowed to stir over night to full conversion. For purification, the organic phase was diluted with ethyl acetate (10 mL) and washed with water (3x10 mL). The aqueous phase, containing the PPI and DBU was further washed with ethyl acetate and petrol ether (10 mL) and freeze dried to concentrate the product. By dialysis (MWCO = 3000 g/mol) against Milli-Q water DBU was removed and the polymer was obtained after freeze drying as pale yellow solid with 40% yield

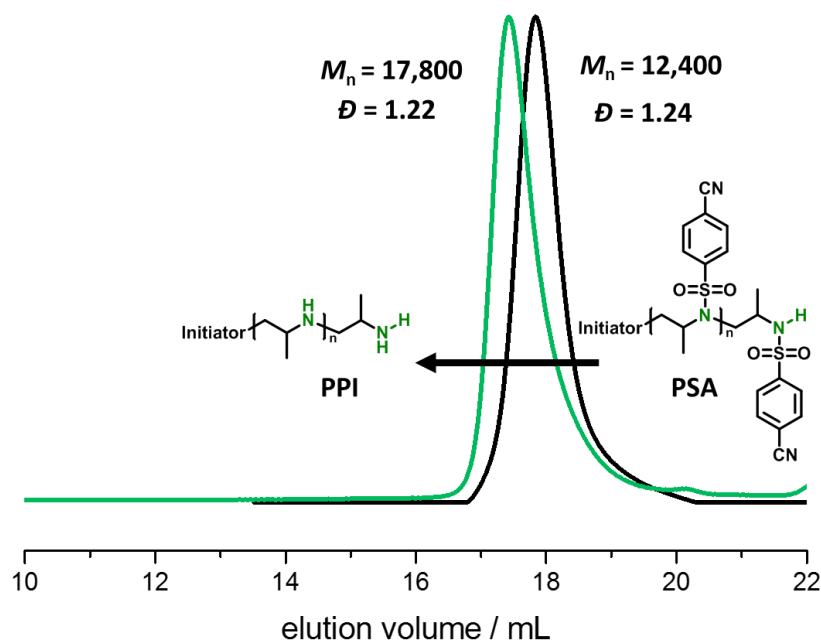


Figure S5.4: Overlay of SEC traces, P(4) (black) and the corresponding L-PPI (PPI-4, green) in HFIP

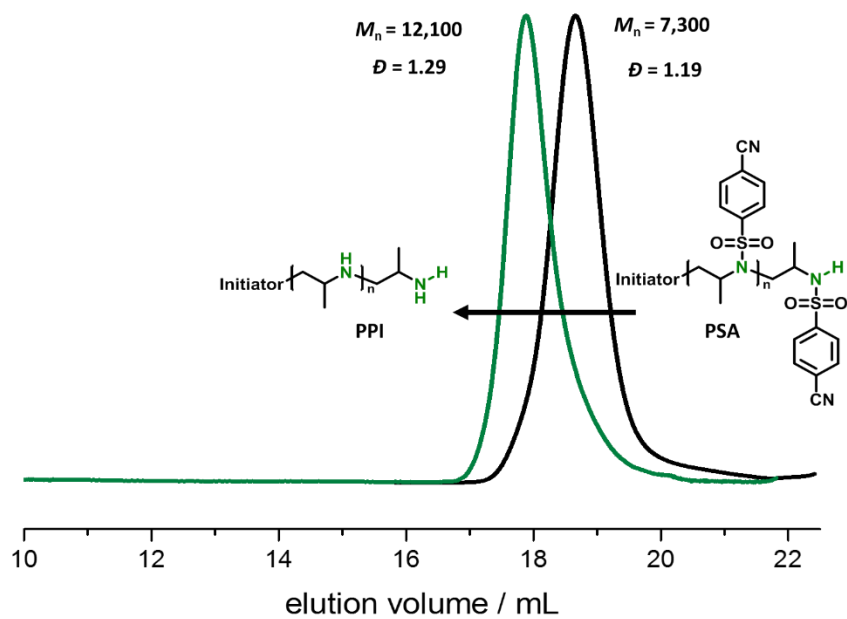


Figure S5.5: Overlay of SEC traces, Poly-2 (black) and the corresponding L-PPI (PPI-2, green) in HFIP

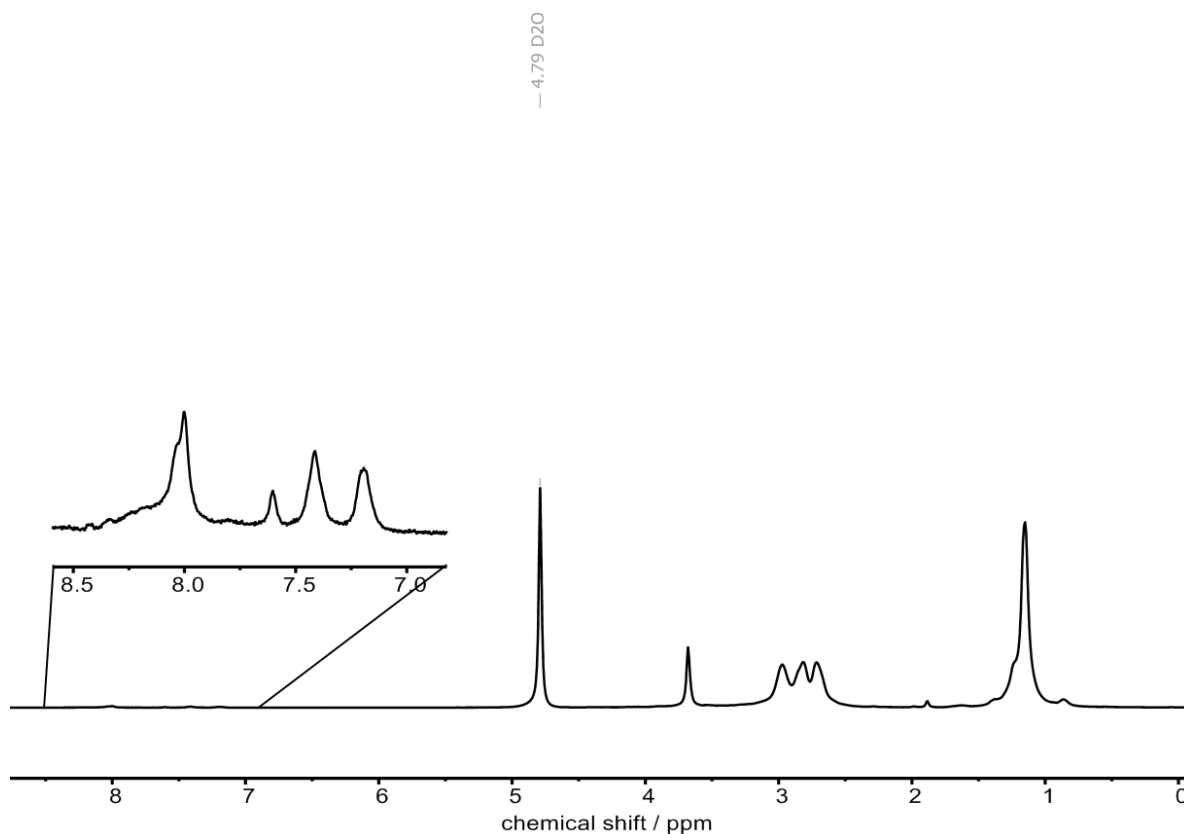


Figure S5.6: ^1H NMR of P1 (500 MHz, water- d_2) with zoom in from 6.9 to 8.5 ppm. PPI-3

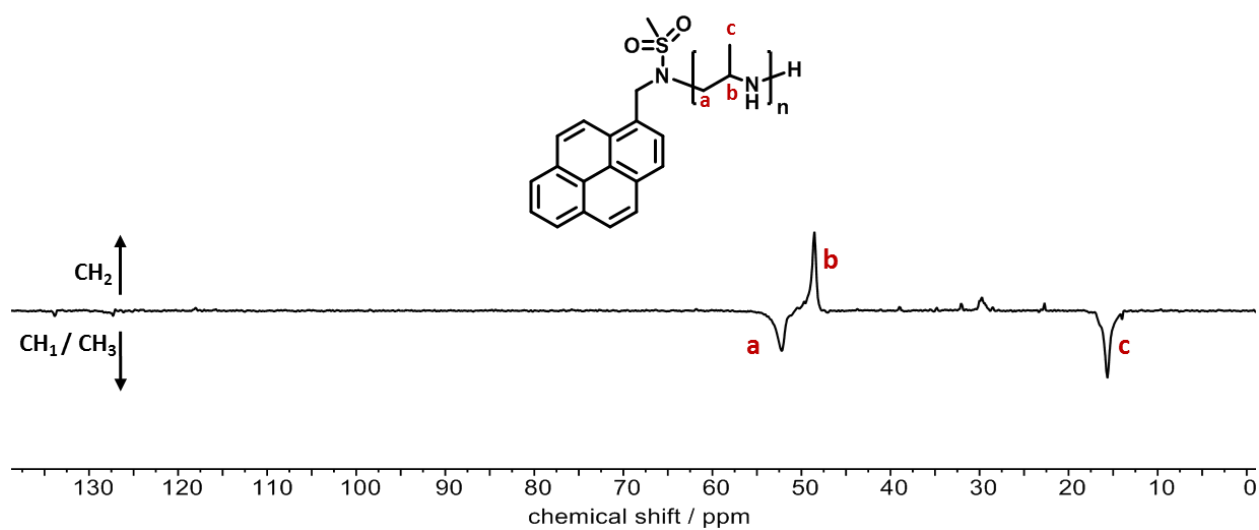


Figure S5.7: ^{13}C NMR of PPI (126 MHz, water- d_2)

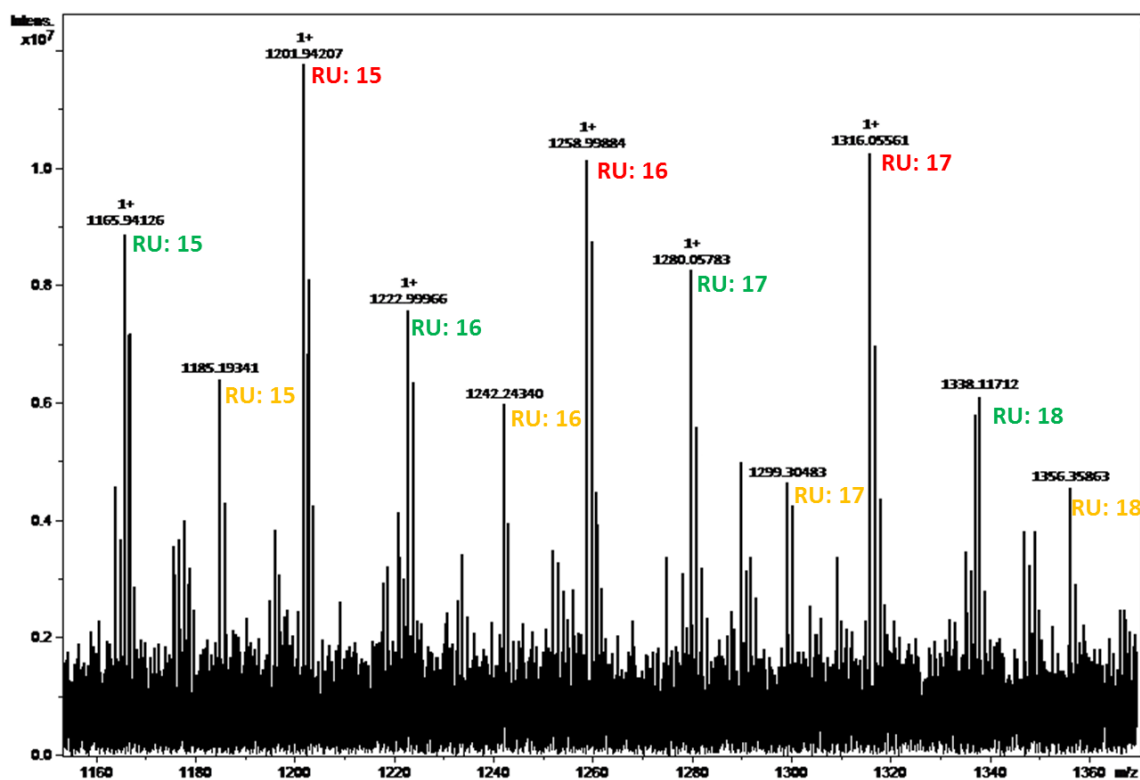


Figure S5.8: MALDI ToF MS spectrum of PPI-3: Individual superimposition labeled with number of repeating units (RU): red: $Py-CH_2-NMs[PI_{RU}]\cdot K^+$, yellow: $Py-CH_2-NMs[PI_{RU}]\cdot Na^+$, green: $Py-CH_2-NMs[PI_{RU}]\cdot H^+$,

5.8.4 Formation of PPI5-DNA-NPs

The gene loaded cationic PPI-5 nanoparticles (abbreviated as PPI5-DNA-NPs below) were obtained by means of electrostatic attraction between the anionic plasmid DNA and the cationic PPI-5. Firstly, accurately weighed (10 mg) liner-PPI-5 was dissolved into 1 mL DNAase-free water under sonication; PX458 plasmid DNA(30 μ g) was dissolved into 1 mL DNAase-free water. According to Table S5.1, after diluting PPI-5 to corresponding concentration, the plasmid DNA solution was added into PPI-5 solution at an equal volume under vortex. The mixture was kept for 30 min at room temperature, the resultant PPI5-DNA NPs were stored at 4 °C and directly used for further study. The diameter and zeta potential of PPI5-DNA-NPs were characterized using a Malvern Zetasizer Nano ZS90 system (Worcestershire, UK) see figure S9.

Table S5.1: Quality Ratio of PPI-5 to DNA in Nanoparticles with different N/P

N/P (molar)	m(PPI5)/m(DNA)
2.5	11:60
5	22:60
10	44:60
20	88:60
30	132:60
40	176:60
50	220:60
60	264:60
80	352:60

5.8.5 Determination of DNA Binding Efficiency

In order to investigate the binding efficiency between PPI-5 and DNA, the PPI5-DNA-NPs were analyzed by agarose gel electrophoresis. The gels were prepared with 1.0% (w/v) agarose in 20 mL TAE buffer (40 mM Tris, 40 mM Acetic acid, 1 mM EDTA, pH 8.5) containing 2 μ L GelRed (10,000 \times) as stains. The PPI5-DNA NPs with different N\|P and control plasmid DNA were applied to gel electrophoresis at a constant 100 V for 40 min. After the electrophoresis, images were obtained using UV transilluminator (Alpha Imagers EC, Alpha Innotech Corporation) to show the location of DNA.

5.8.6 Cell Viability Test of PPI5-DNA-NPs

The cytotoxicity of PPI5-DNA-NPs was evaluated by MTT method in 293T cell line. Briefly, the cells were seeded into a 96-well microtiter plates at a density of 5×10^3 cells per well in 0.1 mL of DMEM culture medium supplemented with 10% fetal bovine serum (FBS) in 5% CO₂ incubator at 37 °C for 24 h. After that, the culture medium was replaced by 0.1 mL fresh complete DMEM medium with different concentrations of the nanoparticles (expressed as PPI-5 concentration, 0.20, 0.39, 0.78, 1.56, 3.13, 6.25, 12.50, 25.00 and 50.00 μ g/mL). The result of Cell Viability Test was showed in Figure S11.

5.8.7 Detection of the EGFP expression efficiency in vitro

The transfection activity of PPI5-DNA-NPs were evaluated in 293T cell lines using plasmid DNA, encoding enhanced green fluorescence protein (EGFP) as reporter gene in the transfection studies. The cells were seeded into 24-well plates at a density of about 5×10^4 cells per well in 0.5 mL of DMEM culture medium with 10% FBS, 24 h prior to transfection. At a confluence level of 50–60%, cells were washed twice with PBS, then incubated with 0.5 mL of serum-free media containing 1.0 μ g of DNA in transfection vectors at 37°C. Lipofectamine 3000 (Invitrogen) was used as positive control, equal volume PBS was used as negative control. The formulation of Lipofectamine/DNA complex was carried out according to the manufacturer's protocols and the PPI5-DNA-NPs prepared as previous describe was adjusted to equal penetration using PBS (10 \times). The cells were incubated with the vectors for 6 h. The transfection media was then replaced with 0.5 mL of fresh complete culture media, and the cells were incubated sequentially until 72 h post transfection. Transfection experiments were performed in triplicates.

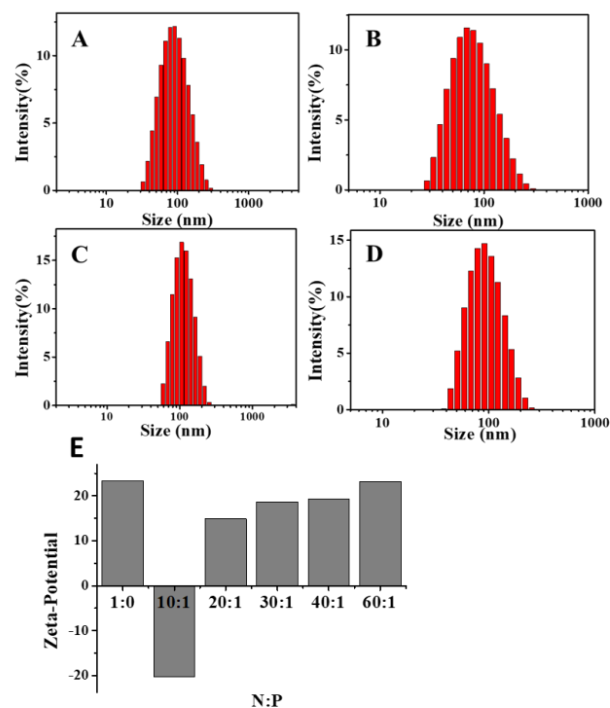


Figure S5.9: (A) size distribution profile for PPI5-DNA-NPs with N:P 10:1. (83.03 nm, PDI=0.177) (B) size distribution profile for PPI5-DNA-NPs with N:P 30:1 (112.8 nm, PDI=0.193) (C) size distribution profile for PPI5-DNA-NPs with N:P 40:1 (89.04 nm, PDI=0.206) (D) size distribution profile for PPI5-DNA-NPs with N:P 60:1 (71.72 nm, PDI=0.195) (E) the surface charge with zeta potential of PPI5-DNA-NPs with different N/P.

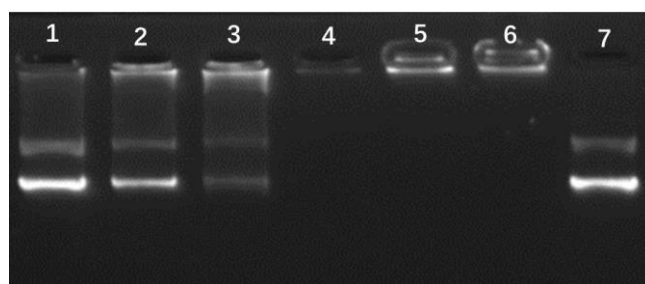


Figure S5.10: Agarose gel electrophoresis of PPI1-DNA-NPs. Lane 1–6: PPI1-DNA-NPs with different N/P at 2.5, 5, 10, 20, 40, 80, respectively; Lane 7: free DNA control

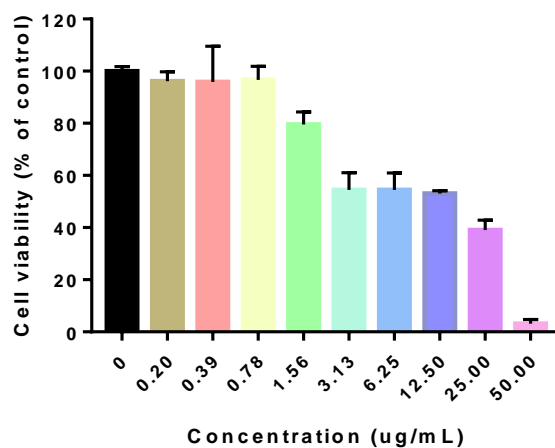


Figure S5.11 : Cell viability of PPI1-DNA-NPs against 293T cell line by MTT assay (n =5)

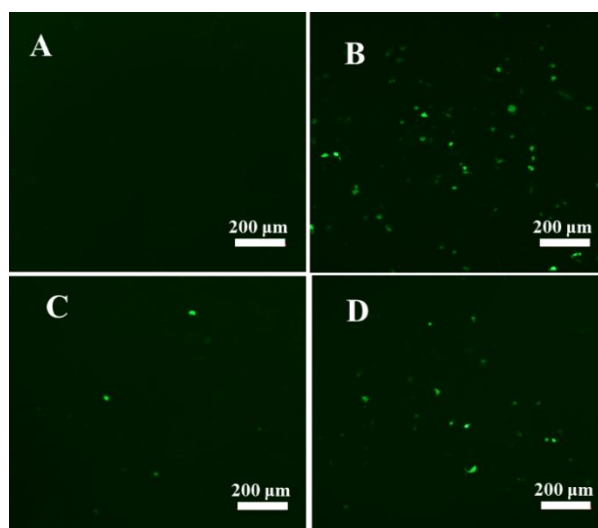


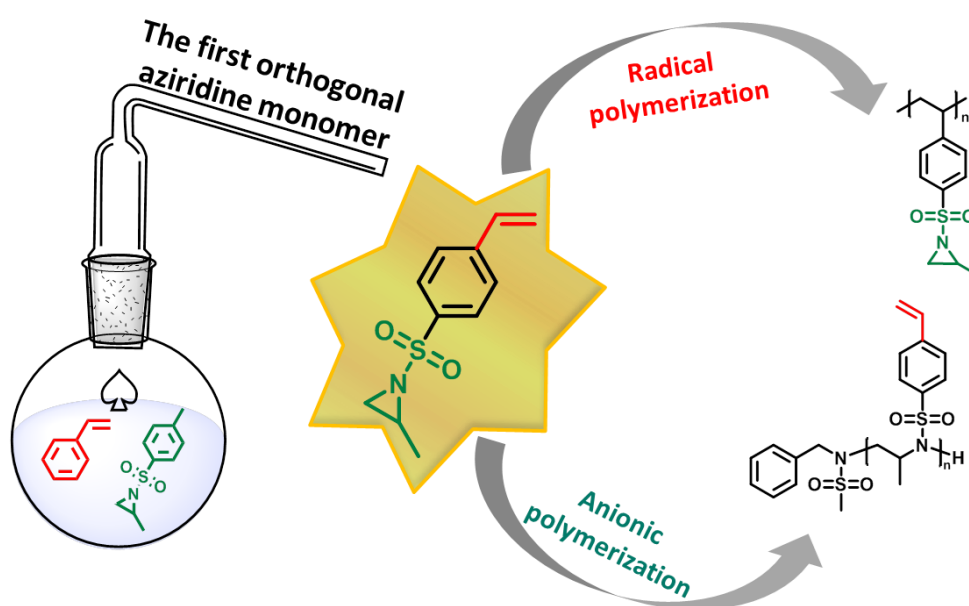
Figure. S5.12: Fluorescence microscopy of 293T cells after gene transfection of plasmid DNA ($\times 100$) (A) The transfection results of PBS blank control; (B) The transfection results of Lipofectamine 3000 positive control; (C) The transfection results of PPI5-DNA-NPs ($N \setminus P=20$); (D) The transfection results of PPI5-DNA-NPs ($N \setminus P=40$).

5.9 Additional References Chapter 5

1. Stewart, I. C.; Lee, C. C.; Bergman, R. G.; Toste, F. D., Living ring-opening polymerization of *N*-sulfonylaziridines: synthesis of high molecular weight linear polyamines. *J. Am. Chem. Soc.* **2005**, *127* (50), 17616-17617.
2. Wall, F. T., The structure of vinyl copolymers. *Journal of the American Chemical Society* **1941**, *63* (7), 1862-1866.
3. Jaacks, V., A novel method of determination of reactivity ratios in binary and ternary copolymerizations. *Macromolecular Chemistry and Physics* **1972**, *161* (1), 161-172.
4. Blankenburg, J.; Wagner, M.; Frey, H., Well-Defined Multi-Amino-Functional and Stimuli-Responsive Poly (propylene oxide) by Crown Ether Assisted Anionic Ring-Opening Polymerization. *Macromolecules* **2017**, *50* (22), 8885-8893.
5. Balakshin, M.; Capanema, E., On the quantification of lignin hydroxyl groups with ³¹P and ¹³C NMR spectroscopy. *Journal of Wood Chemistry and Technology* **2015**, *35* (3), 220-237.

6 4-Styrenesulfonyl-(2-methyl)aziridine: The First Bivalent Aziridine-Monomer for Anionic and Radical Polymerization

Tassilo Gleede, Elisabeth Rieger, Tatjana Homann-Müller and Frederik R. Wurm*



TOC 6: Table of content, symbolizing the combination of two different monomers (Styrene and tosyl activated 2-methylaziridine) to access bivalent monomer with orthogonal moieties for radical (red) and anionic (green) polymerization.

Note: Elisabeth Rieger assisted with helpful discussions around the reaction setups and analytics. Tatjana Homann-Müller synthesized this new monomer during her master thesis and conducted first polymerizations. Tassilo Gleede optimized the monomer synthesis conducted polymerizations, post polymerization modifications and wrote the manuscript. Frederik R. Wurm supervised the manuscript. All authors edited the manuscripts

This chapter is based on an open access article under the terms of the Creative Commons Attribution-Non Commercial License: Tassilo Gleede, Elisabeth Rieger, Tatjana Homann-Müller, Frederik R. Wurm, 4-Styrenesulfonyl-(2-methyl)aziridine: The First Bivalent Aziridine-Monomer for Anionic and Radical Polymerization. *Macromol. Chem. Phys.* **2018**, 219, 1700145

6.1 Abstract

4-Styrenesulfonyl-(2-methyl)aziridine (StMAz), the first orthogonal aziridine monomer, for both anionic ring-opening and radical polymerization is presented. Both polymerization pathways are accessible without using protective groups. Aza-anionic ring-opening polymerization (AAROP) of StMAz and other methyl-aziridine derivatives provide multifunctional polyaziridines. Molecular weights between 3000 and 13 000 g mol⁻¹ are obtained with low molecular weight dispersities ($\bar{M}_w/\bar{M}_n = 1.1$). The amount of vinyl groups in linear polyaziridines from AAROP depends on the monomer/comonomer ratio. The vinyl groups of P(StMAz)- homo- or copolymers are entirely convertible by thiol-ene addition. This allows modification with multiple functional groups. Free radical polymerization of StMAz leads to polyalkylenes with aziridine side groups, which are known to be efficiently addressable *via* nucleophiles. Polysulfonamides still belong to a rather new class of polymers accessible by anionic polymerization. Enlarging the scope of postpolymerization modifications on polyaziridines/-sulfonamides is important for further macromolecular architectures. The aziridine and the vinyl group are combined to develop the first orthogonal monomer for aza-anionic polymerization and radical polymerization.

6.2 Introduction

Nitrogen-containing polymers (N-polymers) are often favored for drug delivery issues regarding cell targeting, like gene delivery studies show.^{1,2} Additionally, they are applied in water refinery^{3,4} and can serve as direct catalysts by stabilizing transition metals.⁵ To fulfill the goals of current scientific challenges, functionalizable groups at N-polymers are essential for fine adjustment of polymer properties. Radical polymerization of vinyl monomers allows fast access to a variety of highly functional polymer materials based on various monomers. On the other side, living ionic polymerization allows the highest control over molecular weights and distributions.⁶ Ionic polymerizations of epoxides or aziridines can be used to prepare polyethers and polyamines, but most functional groups need to be protected. An outstanding class of monomers, the so-called “bivalent or orthogonal monomers,” is polymerized chemoselectively by different mechanisms while maintaining the other group. To date, only few of such monomers have been reported.⁸⁻¹⁰

Aziridinyl ethyl methacrylate (AEMA), for example, can be selectively polymerized by radical or carbanionic polymerization of the acrylate and by cationic polymerization of the aziridine ring, functional polyamines are obtained. AEMA represents to the best of our knowledge the first orthogonal aziridine-containing monomer.⁸ However, anionic polymerization of the aziridine cannot be conducted on such structure as the aziridine ring is not activated. The well-known glycidyl methacrylate is similar to AEMA polymerizable *via* radical and an ionic mechanism.⁹ Vinyl ferrocenyl glycidyl ether represents a monomer which, besides radical polymerization, is suitable for anionic ring-opening polymerization (AROP). The nature of the ferrocene-functionality in the polymer is advantageous for applications where redox response is required.^{11,12} Bivalent monomers are applied in industry as additives in several polyacrylates example wise for pigment coating;^{13,14} additionally, they are of interest for scientific aspects; with an orthogonal polymerizable or addressable group, those materials can be used for the preparation of graft-polymers, cross-linked gels, or surface modifications.^{10,15-17} However, only few bifunctional chemoselective monomers have been reported.

Herein, we report the first bivalent monomer for the aza-anionic ring-opening, carrying an activated aziridine, combined with vinyl functionality for radical polymerization. 4-Styrenesulfonyl-(2-methyl)aziridine (StMAz) is polymerized by two different protocols, free radical and aza-anionic ring-opening polymerization. ¹H NMR proved that both protocols allowed a selective reaction with one functional group and maintained the other for postmodifications. Additional to the earlier reported robust way to obtain multihydroxy polyamines from acetals, as protected monomers,¹⁸ we demonstrated, that various functional groups can be added to obtain

multihydroxy or carboxy polyamines *via* a thiol-ene postmodification. The use of different thiols makes the polysulfonamides a platform for various modifications.^{19, 20}

StMAz showed similar reactivity to previously reported aziridine monomers,^{21, 22} which allowed us to prepare copolymers with nonfunctional aziridines to further adjust the degree of functionalization. In addition, the free radical polymerization of StMAz leaves the aziridine-group untouched as a potential receptive for nucleophiles. Thermal analyses of the (co)polymers by differential scanning calorimetry (DSC) and thermogravimetric analyses (TGA) proved a remarkably high char yield of $\approx 50\%$ for both, polyalkylene- and polyethylamine-(StMAz), which indicated a heat induced cross-linking. We believe that StMAz further enriches the toolbox of aziridine monomers, which can be used for the preparation of functional and well-defined architectures by living anionic polymerization.

6.3 Experimental Section

6.3.1 Materials

Solvents and reagents were purchased from Acros Organics, TCI, Sigma-Aldrich, or Fluka and used as received, unless otherwise stated. Deuterated solvents were purchased from Deutero GmbH. *N*-benzyl methanesulfonamide (BnNHMs), 2-methyl-*N*-tosylaziridine (TsMAz), and 2-methyl-*N*-mesylaziridine (MsMAz) were synthesized according to already published procedures and dried by azeotropic distillation from benzene to remove traces of water.²³ 2-Methylaziridine was distilled from CaH₂ prior use.

6.3.2 Methods

6.3.2.1 Analyses

¹H NMR and ¹³C NMR spectra were recorded using, a Bruker Avance 300, a Bruker Avance III 500, a Bruker Avance III 700. All spectra were referenced internally to residual proton signals of the deuterated solvent.

For SEC measurements in dimethylformamide (DMF) (containing 0.25 g L⁻¹ of lithium bromide as an additive), an Agilent 1100 Series was used as an integrated instrument, including a PSS HEMA column (106/105/104 g mol⁻¹), a UV detector (275 nm), and a RI detector at a flow rate of 1 mL min⁻¹ at 50 °C. Calibration was carried out using PEO standards provided by Polymer Standards Service.

Matrix-assisted laser desorption/ionization time-of-flight (MALDI-ToF) measurements were performed using a Shimadzu Axima CFR MALDI-TOF mass spectrometer, employing dithranol (1,8-dihydroxy-9(10H)-anthracenone) as a matrix.

Thermogravimetric analysis was performed with the Mettler Toledo ThermoSTAR TGA /SDTA 851-Thermowaage in the temperature range from 25 to 1000 °C with a heating rate of 10 °C min⁻¹.

Differential scanning calorimetry measurements were performed using a Mettler Toledo DSC 823 calorimeter. Three scanning cycles of heating-cooling were performed in the temperature range from -140 to 250 °C. Heating rates of 10 °C min⁻¹ were employed under nitrogen (30 mL min⁻¹).

For infrared spectroscopy, the polymers were pressed with KBr to form a pellet and the absorption between 4000 and 400 cm⁻¹ was recorded in a Spectrum BX spectrometer from PerkinElmer.

6.3.2.2 Polymerizations

All glassware was flame-dried at reduced pressure prior use. The monomers were dissolved in ≈1 mL benzene and dried for ≈4 h at reduced pressure to remove traces of water by azeotrope distillation. The monomers were then dissolved in DMF (final concentration 10 wt%). With BnNHMs used as initiator, the sulfonamide anion was generated in a separate flask by deprotonation with potassium bis(trimethylsilyl)amide (KHMDS) in DMF, a calculated amount of this initiator stock solution was added to the monomer solution at 50 °C and the reaction was stirred until completion (typically 15 h). After the polymerization has reached completion, the living anion was terminated by the addition of methanol and precipitated into a tenfold excess of methanol. The polymers were recovered by centrifugation in typically quantitative yield.

6.3.3 Synthesis

Synthesis of StMAz

The 4-vinylbenzene-1-sulfonyl chloride was synthesized according to literature procedure.²⁴ The product was used without further purification. The 4-vinylbenzene-1-sulfonyl chloride was converted to StMAz with following procedure. *Rac*-2-methylaziridine (2.0 g, 35 mmol) and 6.6 mL (48 mmol) *N,N*-diisopropylethylamine were dissolved in 25 mL dry toluene and cooled to -30 °C. 4-vinylbenzene-1-sulfonyl chloride (6.5 g, 32 mmol) was dissolved in 10 mL dry toluene and added dropwise over a period of 20 min to the reaction. The mixture was stirred for

additional 90 min at $-30\text{ }^{\circ}\text{C}$ and allowed to warm up to room temperature and stirred overnight. 20 mL saturated sodium hydrogen carbonate solution was added and stirred for 60 min. The aqueous phase was removed and the organic layer was washed again with brine, dried over magnesium sulfate, and evaporated to dryness. 7.1 g (quantitative yield) of off-white oil was obtained. The monomer structure was further confirmed by NMR (Figures S6.1–S6.3, Supporting Information) and MALDI-ToF mass analysis (325.21 g mol^{-1} (StMAz*H-NEt₃⁺), 224.06 g mol^{-1} StMAz*H⁺). To inhibit spontaneous polymerization, 2,6-di-*tert*-butyl-4-methylphenol (BHT) could be added. The compound was stored at $-20\text{ }^{\circ}\text{C}$. If necessary, the compound could be purified with column chromatography on silica gel (PE/EA 5:1, $R_f = 0.4$). For radical and anionic polymerization, the compound was used without further purification.

Synthesis of P(StMAz) via AROP

Example procedure: 100 mg (0.444 mmol, 10 eq) of StMAz and 300 mg (2.2 mmol, 50 eq) of MsMAz were placed in a Schlenk flask and dissolved in 2 mL benzene. The monomers were dried by azeotrope freeze drying in vacuum ($\approx 4\text{ h}$). In a separated Schlenk flask, the initiator was generated. 8.2 mg (0.044 mmol, 1 eq) BnNHMs was dried by azeotrope freeze drying in vacuum with benzene. 8.8 mg KHMDs (0.044 mmol, 1 eq) dissolved in 3 mL dry DMF was added to BnNHMs. This solution was then added to the monomer mixture. The reaction was performed at $50\text{ }^{\circ}\text{C}$ overnight under argon atmosphere. The polymerization was terminated by addition of acidic methanol. Until termination, standard Schlenk conditions were applied. For purification, the polymer was precipitated in large amount of methanol (see Figures S6.9 and S6.13 in the Supporting Information for analytical data).

Modification via Thiol-ene Reaction

General procedure: 52 mg of the polymer P6 (0,073 mmol, 1 eq regarding the vinyl groups) and 9 mg (0,055 mmol, 0.75 eq) azobis(isobutyronitrile) (AIBN) were placed in a 10 mL Schlenk flask. Then, 114 mg mercaptoethanol (1.5 mmol, 20 eq) was added with 1 mL of DMF. After two freeze–pump–thaw cycles, the mixture was stirred at $75\text{ }^{\circ}\text{C}$ under argon overnight. For purification, the polymer was precipitated in diethylether (Et₂O), dissolved in dichloromethane (DCM), and precipitated again in Et₂O. Drying in vacuum gave pure product (see Figures S6.7–S6.17 in the Supporting Information for analytical data).

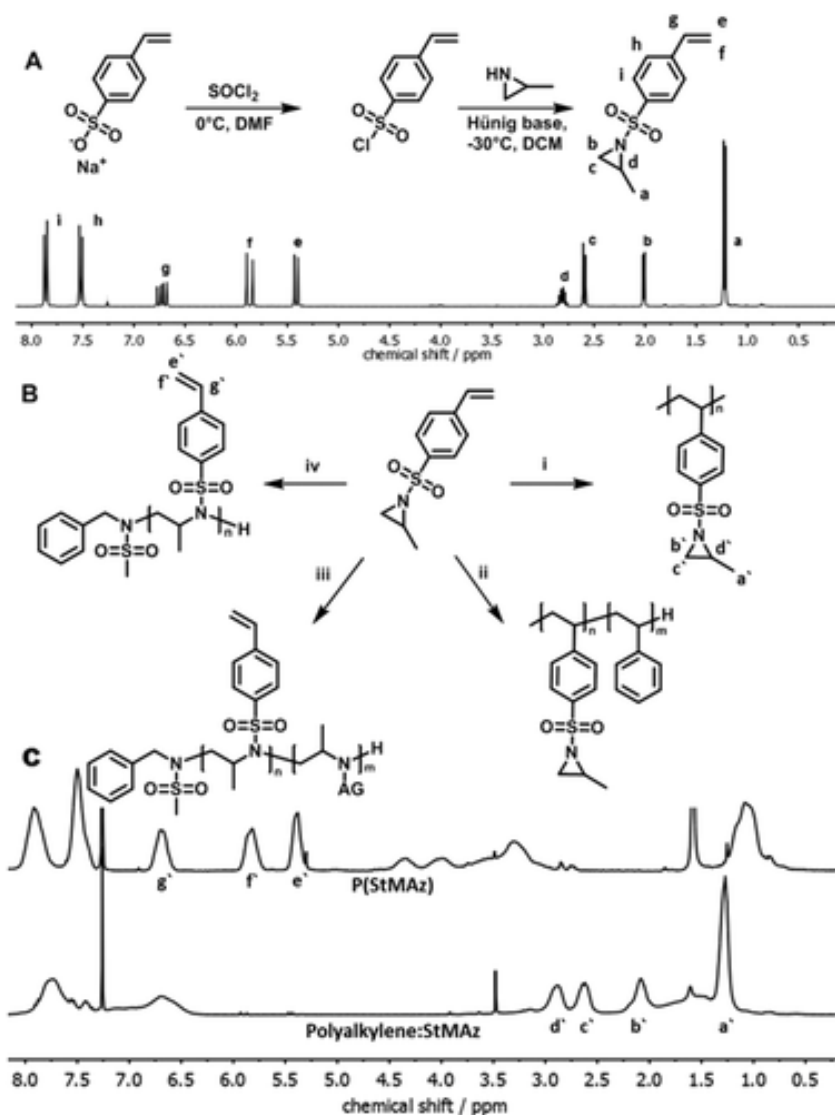
Synthesis of Polyalkylene:StMAz via Free Radical Polymerization

StMAz (150 mg, 0.671 mmol) was placed in UV-quartz glass cuvette equipped with a stirring bar. 2,2-Dimethoxy-2-phenylacetophenone (5.75 mg, 22.4 μmol) was dissolved in 2 mL of degassed benzene and transferred into the quartz glass cuvette. The polymerization was performed by irradiation with 6 W UV254 nm light for 5 h. Temperatures did not exceed room temperature during polymerization. Copolymerization with styrene was conducted analogous to the procedure for homopolymers. For purification, the polymer was precipitated in methanol (see Figures S6.4 and S6.18 in the Supporting Information for analytical data).

6.4 Results and Discussion

6.4.1 Monomer Synthesis

The activated aziridine monomers have two potential positions, which can be used in order to adjust the polymer properties. First, the variation of the alkyl chain at the 2-position of the aziridine ring allows to attach functional or solubilizing groups. We demonstrated that steric groups such as C-10 chains or bulky phenyl groups do not hamper the polymerization.^{22, 25} In addition, the electron withdrawing group, which is attached to the aziridine ring by a cleavable sulfonamide, can be used as a handle to control chemical function.^{18, 26} The electron withdrawing behavior activates the aziridine and thereby influences the polymerization kinetics.²² StMAz is estimated to have a similar electron withdrawing behavior as the TsMAz. Thereby, the distribution of the reactive vinyl group in polysulfonamides can be adjusted. Polysulfonamides with vinyl groups at the termini, in the middle, or randomly distributed can be obtained by this method. The synthesis of StMAz starts from commercially available sodium 4-vinylbenzenesulfonate (Scheme 6.1A). StMAz was produced in a two-step synthesis; the monomer was obtained with an overall yield of 80%. In the first step, 4-styrene sulfonic acid is converted with thionyl chloride to the corresponding sulfonyl chloride. In a second step, the sulfonyl chloride was converted to StMAz by amidation with 2-methylaziridine under basic conditions in dry DCM. Beneficially, StMAz was pure enough for the anionic polymerization after extraction from the reaction mixture (note: to avoid unwanted radical polymerization, BHT can be added as a stabilizer to the monomer).



Scheme 6.1: A) Synthesis route to 4-styrenesulfonyl-(2-methyl)aziridine (StMAz). B) Polymerization of StMAz: (i) free radical polymerization with 2,2-dimethoxy-2-phenylacetophenone in benzene (P7, P9), (ii) free radical copolymerization with styrene, 2,2-dimethoxy-2-phenylacetophenone in benzene (P8), (iii) anionic copolymerization of StMAz with sulfonamide-activated aziridines (P3, P4, P5, P6, P10), (iv) homopolymerization of StMAz with KHMDS, BnNHMs in DMF at 50°C (P1, P2). C) The ^1H NMR spectra of the different homo(StMAz) polymers. P(StMAz) (P1, anionic polymerization), polyalkylene:StMAz (P7, free radical polymerization).

6.4.2 Polymerization Kinetics

The anionic copolymerization of StMAz with TsMAz was monitored by real-time ^1H NMR spectroscopy. Figure 6.1 shows the individual monomer conversion versus total conversion of monomers; Figure S6.21 (Supporting Information) shows the assembly of the monomers in the polymer over time. For the real-time polymerization kinetics, the reaction should proceed in a suitable timescale, usually from minutes to hours. The observed component has to have distinguishable resonances in the ^1H NMR spectrum which are consumed during the reaction. The resonances of 1.65–1.62 and 1.61–1.59 ppm (see Figure S6.22 in the Supporting Information) belong to the aziridine ring of the StMAz and TsMAz. A zoom-in to the relevant signals of the monomer is showing the consumption of the monomers. Due to a sufficient chemical shift of the different resonances, the ring protons are predestined to monitor the anionic polymerization. Due to a more pronounced negative mesomeric effect, the electron withdrawing behavior of StMAz is stronger compared to TsMAz. Therefore, we see in Figure 6.1 a slightly faster monomer consumption of StMAz. Nevertheless, this difference compared to monomers of previous studies is comparatively weak compared to other activating groups.²² Concluding the polymerization behavior of StMAz with other monomers is similar to TsMAz.

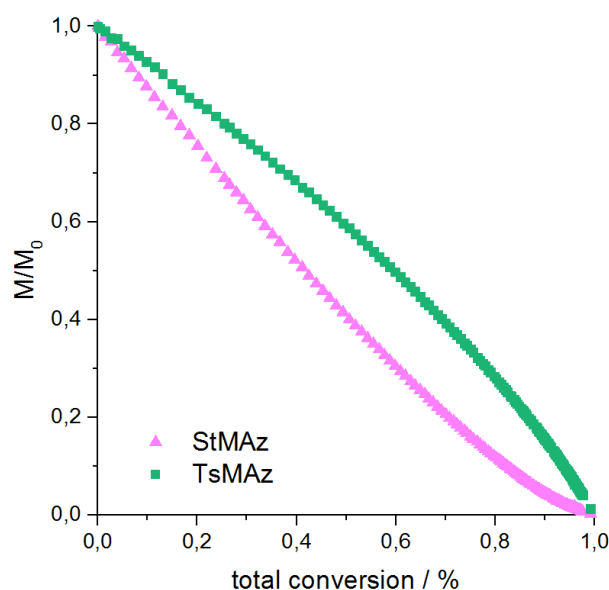


Figure 6.1: Normalized monomer concentration versus total conversion of the aza-anionic copolymerization of StMAz and TsMAz with BnNKMs as initiator in DMF-d₇, at 50 °C (P10-kinetic).

6.4.3 Polymerization of StMAz

Aziridines as such were used due to their affinity to nucleophilic ring-opening as side groups in polyacrylates and others. For instance, nucleophiles like alcohols can react efficiently.²⁷ This is known to be a novel method for postmodification of polymers, as it was demonstrated on polyacrylates. Cross-linking and postmodification can be performed. The ring-opening reaction of aziridines by nucleophiles was also discussed as a conjugate reaction for clickable polymers.^{28, 29} As comparison, ring-opening reaction of epoxide groups attached at polymers is known to be problematic due to its high reactivity. Mild conditions have to be found to maintain the epoxide and to functionalize the polymer selectively.³⁰ Additionally, moisture induced ring-opening makes storage of epoxides difficult.³¹ Earlier, Kobayashi and co-workers successfully polymerized a bifunctional monomer (AEMA) consisting of a methacrylate linked to an aziridine by different techniques while leaving the other group intact. They successfully polymerized the MMA-group *via* free radical and anionic polymerization and the aziridine *via* cationic polymerization.^{8, 32} The cationic ring-opening leads to 80% polymer yield and observed molecular weight distributions of $\bar{D} = 2.2$. Nevertheless, the anionic polymerization of the aziridine functionality of AEMA was not possible.

StMAz was successfully polymerized *via* AROP as homo- and copolymers with TsMAz (P3, P4) and MsMAz (P5, P6) as the respective comonomers. The SEC elugrams confirmed monomodal size and narrow distributions with $M_w/M_n \approx 1.1$ for the copolymers and $M_w/M_n \approx 1.2$ for the homopolymers (Figure 6.2B and Figure S6.15 (Supporting Information)). Full monomer conversion was confirmed *via* ^1H NMR (Figure 6.2A). MALDI-ToF mass spectrometry proves the formation of the envisioned StMAz (Figure S6.5, Supporting Information). The main distribution can be calculated to contain the mass of the initiator and the monomer mass with a distance of 223 g mol^{-1} (marked with arrows), the molar mass of StMAz. The incorporation of comonomers (MsMAz) was also confirmed by MALDI-ToF MS (Figure S6.6, Supporting Information): a linear combination of the monomer masses of both repeating units can be detected in the spectrum.

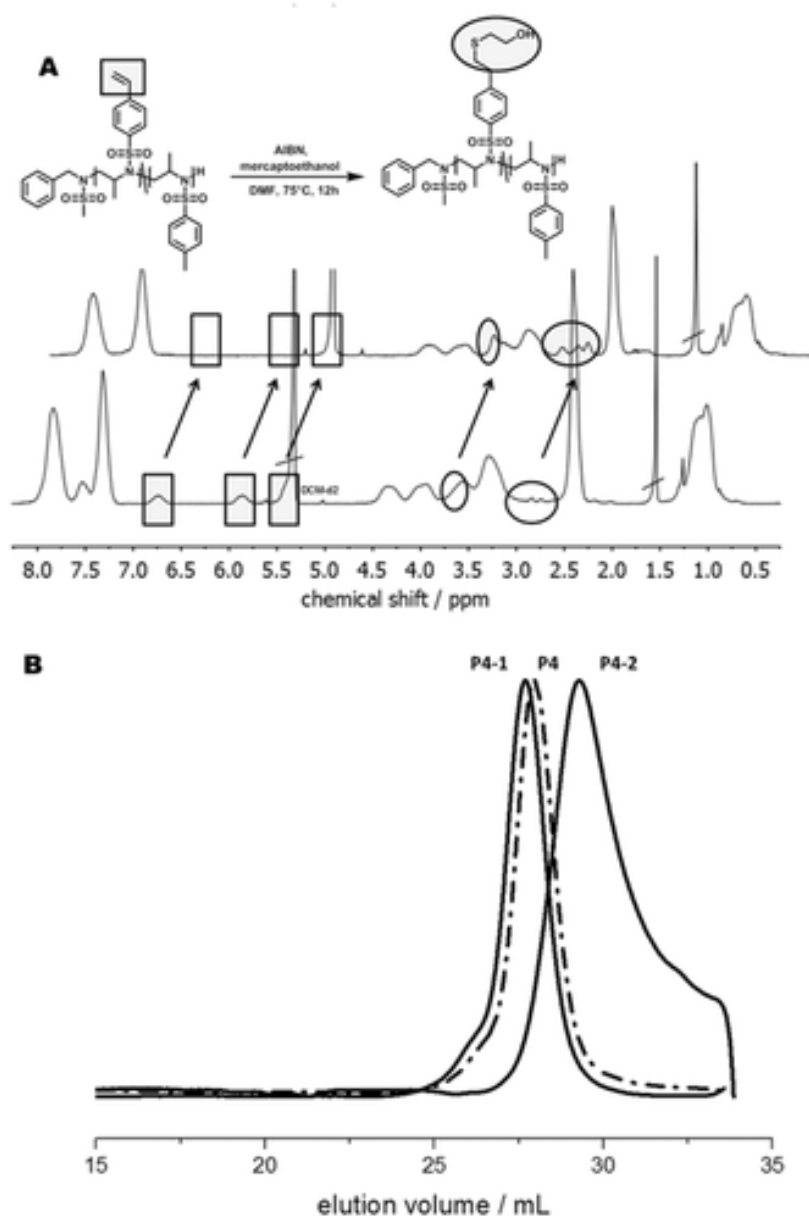


Figure 2: A) ^1H NMR of $\text{P(TsMAz}_{50}\text{-co-StMAz}_{10})$ before and after thiol-ene addition of mercaptoethanol. Circles highlight the signals of the thioether group. Squares highlight the disappearing vinyl signals. B) SEC traces of $\text{P(TsMAz}_{50}\text{-co-StMAz}_{10})$ (P4) and the modified polymer with hydroxyl (P4-1) and carboxy groups (P4-2).

6.4.4 Thiol-ene-Postpolymerization Modification

The remaining vinyl groups of all synthesized polyaziridines were proven to be intact after polymerization *via* ^1H NMR and postmodification. In an additional step, complete conversion to functionalized thioether was performed with radical thiol-ene addition. To avoid cross-linking of the polymers during the thiol-ene reaction, a 20 equivalent excess of thiols regarding one equivalent of vinyl groups was used. As the modified polymers were soluble in DMF and as the molecular weight distributions of the modified polymers are unchanged after modification, cross-linking was not observed. The ^1H NMR spectrum of P4 shows the highlighted signals of the vinyl protons in squares (Figure 6.1). After modification with mercaptoethanol (P4-1) (Figure 6.2A) or mercaptopropionic acid (P4-2) (Figure S6.10, Supporting Information), those signals vanish and new signals, marked with circles, can be assigned to the thioether groups. Full conversion of the vinyl groups was confirmed for the mesyl analogous copolymer (P6) (see ^1H NMR spectra in Figures S6.7 and S6.11 in the Supporting Information). The SEC elugrams of P4 and the modified P4-1 show both monomodal and narrow molecular weight distributions. After the modification with mercaptoethanol, the molecular weight distribution slightly shifts to lower elution times, indicating an increase of the molecular weight. In contrast, the same polymer, modified with mercaptopropionic acid, elutes later (P4-2) under the same chromatographic conditions. This late elution can be assigned to the interactions of the multiple carboxylic acid groups with the column material. This observation was also made for the modified P(MsMAz-*co*-StMAz) derivatives P6-1 and P6-2 (Figures S6.15 and S6.16, Supporting Information). In addition to previous work of our group,¹⁸ this work shows an alternative way to obtain polyhydroxy sulfonamides. Modification of vinyl groups with thiol-ene chemistry has been proven to be a robust and flexible way to introduce various functional groups, such as carboxylic acids, hydroxyl, amines, and many more.^{19, 20}

6.4.5 Free Radical Polymerization

Free radical polymerization of StMAz was performed either by thermal or by UV-light induced initiation (AIBN in DMF (P9) or with 2,2-dimethoxy-2-phenylacetophenone and UV irradiation (P7, P8)). Under these conditions, polymers of 3700 and 8000 g mol⁻¹ were prepared with molecular weight distributions of ≈ 1.7 –2.4 (Figure S6.17 in the Supporting Information shows the SEC of polyalkylene:StMAz). The ¹H NMR spectra of the polyalkylene:StMAz show the characteristic resonances of the aziridine substituents (in Figure S6.4: a, c, d at 2.25, 2.62, and 2.05 ppm), while the vinyl resonances disappeared after the polymerization. The molecular weights determined by SEC in Table 6.1 are known to be underestimated by the factor of 2 to 3 compared to the theoretical weights. This is due to the PEG standard which was used in our set-up.^{18, 32}

Table 6.1: Overview of polymers synthesized from StMAz

#	Polymer ^{a)}	$M_n^a)$ [g mol ⁻¹]	$M_n^b)$ [g mol ⁻¹]	$M_w/M_n^b)$
P1	PStMAz ₃₀	6850	4300	1.27
P1-1	P1-mercaptoethanol	9200	7250	1.14
P1-2	P1-mercaptopropionic acid	10 000	n.a.	n.a.
P2	PStMAz ₅₀	11 300	5000	1.19
P3	P(TsMAz _{50-co} -StMAz ₅)	8050	9000	1.09
P4	P(TsMAz _{50-co} -StMAz ₁₀)	9150	10 250	1.11
P4-1	P4-mercaptoethanol	9900	13 150	1.13
P4-2	P4-mercaptopropionic acid	10 200	5250	1.5
P5	P(MsMAz _{50-co} -StMAz ₅)	11 850	7050	1.16
P6	P(MsMAz _{50-co} -StMAz ₁₀)	12 950	7050	1.22
P6-1	P6-mercaptoethanol	12 600	10 800	1.15
P6-2	P6-mercaptopropionic acid	14 000	5000	1.64
P7	Polyalkylene:StMAz		3700	1.7
P8	Polyalkylene:StMAz-co-St		8000	2.4
P9	Polyalkylene:StMAz		3800	1.7
P10-kinetic	P(TsMAz _{50-co} -StMAz ₅₀)	21700	5000	1.09

^{a)} Theoretical molecular weight

^{b)} Molecular weight and molecular weight dispersity determined *via* SEC in DMF (*vs* PEO standards). Polymers P1–P6 were polymerized by AROP. Polymers P7–P9 were polymerized by free radical polymerization.

6.4.6 Thermal Characterization

The thermal properties of the polymers and copolymers have been analyzed by DSC and TGA. TGA of the different P(StMAz)s and copolymers were measured and compared to the homopolymers P(TsMAz) and polystyrene (Figure 6.3). Decomposition of the polymers, independent of the monomer composition starts at $T_{on}(95\%) = 340\text{ }^{\circ}\text{C}$ and degradation proceeds in a single step due to degradation of the side groups and of the polymeric backbone. At temperatures above $420\text{ }^{\circ}\text{C}$, only slightly further degradation takes place and reaches a char yield at $700\text{ }^{\circ}\text{C}$. Notable is the char yield of the *homo*-P(StMAz) (TGA, P7 and P1) with 48 and 41 wt% remarkably higher compared to polystyrene and also compared to P(TsMAz). This can be explained by thermal cross-linking of the pendant functional groups and thus leads to thermally stable decomposition products, which might be of interest for future applications, e.g., as flame retardant additives.

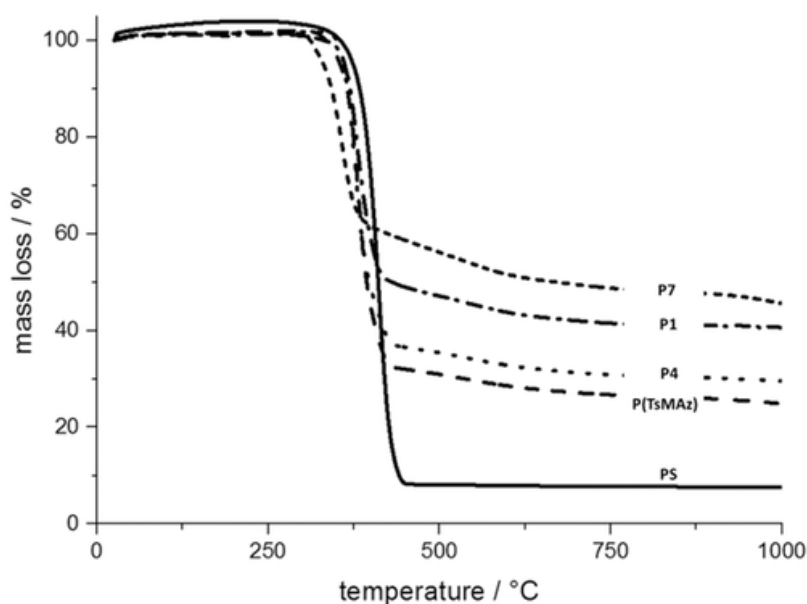


Figure 6.3: Thermogravimetric analyses, $10\text{ }^{\circ}\text{C min}^{-1}$, under nitrogen. 48% ash yield at $750\text{ }^{\circ}\text{C}$ (P7), 41% ash yield at $750\text{ }^{\circ}\text{C}$ (P1), 30% ash yield at $750\text{ }^{\circ}\text{C}$ (P4), 26% ash yield at $750\text{ }^{\circ}\text{C}$ (P(TsMAz)), 8% ash yield at $750\text{ }^{\circ}\text{C}$ (polystyrene).

Crosslinking of the polymers appears to be heat-induced. This was indicated *via* DSC. A precise T_g of P(StMAz) cannot be detected (Figure S6.18). A structural difference was observed by infra-red spectroscopy. Therefore a small amount of P(StMAz) was heated to $250\text{ }^{\circ}\text{C}$ under nitrogen atmosphere. A decrease in intensity of the corresponding bands of the double bond ($=\text{C}-\text{H}$ stretch: $\nu = 3092, 3045$; $\text{C}=\text{C}$ stretch: $\nu = 1633$; $=\text{C}-\text{H}$ bend: $\nu = 920$) in the IR-spectrum (See Figure S6.19) was observed. Furthermore the P(StMAz) is after heating insolubility in all tested solvents (CDCl_3 , DMSO, DMF).

6.4.7 Conclusions

We developed a robust two-step synthesis for StMAz, the first orthogonal monomer for the aza-anionic ring-opening and free radical polymerization. Both polymerization mechanisms lead to highly functional polymers, either carrying reactive vinyl- or aziridine-groups. The living anionic ring-opening polymerization of StMAz leads to polymers with narrow molecular weight distributions and adjustable molecular weights. Also, copolymers with other aziridines were prepared, allowing to control the degree of functionality.

In the presence of thermal or photoinitiators, StMAz undergoes free radical polymerization to form homo- or copolymers, which carry aziridine side groups. They exhibit a cross-linking property during heating, indicated by TGA analysis and ^1H NMR. This and the successful copolymerization with other aziridine monomers confirm StMAz to be a novel, suitable member in the family of anionically polymerizing aziridines. The applicability of this monomer is topic of further studies.

6.5 References Chapter 6

1. S. Taranejoo, J. Liu, P. Verma, K. Hourigan, *Journal of Applied Polymer Science* **2015**, 132.
2. M. A. Mintzer, E. E. Simanek, *Chem. Rev.* **2009**, 109, 259.
3. S. Zhao, Z. Wang, *Journal of Membrane Science* **2017**, 524, 214.
4. Y. Uludag, H. Ö. Özbelge, L. Yilmaz, *Journal of Membrane Science* **1997**, 129, 93.
5. S. Ponnurangam, I. V. Chernyshova, P. Somasundaran, *Adv. Colloid Interface Sci.* **2016**.
6. D. Baskaran, A. H. E. Müller, *Progress in Polymer Science* **2007**, 32, 173.
7. J. Herzberger, K. Niederer, H. Pohlitz, J. Seiwert, M. Worm, F. R. Wurm, H. Frey, *Chem. Rev.* **2016**, 116, 2170.
8. T. Ishizone, T. Takata, M. Kobayashi, *Journal of Polymer Science* **2003**, 41, 1335.
9. D. Luo, P. Li, Y. Li, M. Yang, *Journal of Applied Polymer Science* **2010**, 1527.
10. A. Alkan, L. Thomi, T. Gleede, F. R. Wurm, *Polym. Chem.* **2015**, 6, 3617.
11. A. Alkan, F. R. Wurm, *Macromol Rapid Commun* **2016**, 37, 1482.
12. R. Pietschnig, *Chem Soc Rev* **2016**, 45, 5216.
13. C. Kunszt, N. Loew, T. Farwick, B. Feldmann, *BASF Coatings GmbH, invs.:* **2016**.
14. N. Suemura, K. Yoshitake, T. Takeyama, *Nissan Chem. Ind., LTD., invs.:* **2016**.
15. S. A. B. Nicolay V. Tsarevsky, and Krzysztof Matyjaszewski, *Macromolecules* **2007**, 40, 4439.
16. J. Majer, P. Krajnc, *Macromolecular Symposia* **2010**, 296, 5.
17. A. Bhattacharya, *Progress in Polymer Science* **2004**, 29, 767.
18. E. Rieger, A. Manhart, F. R. Wurm, *ACS Macro Letters* **2016**, 5, 195.
19. A. B. Lowe, *Polym. Chem.* **2010**, 1, 17.
20. M. J. Kade, D. J. Burke, C. J. Hawker, *Journal of Polymer Science Part A: Polymer Chemistry* **2010**, 48, 743.
21. T. Homann-Müller, E. Rieger, A. Alkan, F. R. Wurm, *Polym. Chem.* **2016**, 7, 5501.
22. E. Rieger, A. Alkan, A. Manhart, M. Wagner, F. R. Wurm, *Macromol. Rapid Commun.* **2016**, 37, 833.
23. I. C. Stewart, C. C. Lee, R. G. Bergman, F. D. Toste, *J. Am. Chem. Soc.* **2005**, 127, 17616.
24. J. C. Brendel, F. Liu, A. S. Lang, T. P. Russell, T. M., *ACS Nano* **2013**, 7, 6069.
25. C. Bakkali-Hassani, E. Rieger, J. Vignolle, F. R. Wurm, S. Carlotti, D. Taton, *Chem. Commun.* **2016**, 52, 9719.
26. L. Reisman, C. P. Mbarushimana, S. J. Cassidy, P. A. Rugar, *ACS Macro Letters* **2016**, 5, 1137.
27. X. E. Hu, *Tetrahedron* **2004**, 60, 2701.
28. H.-J. Jang, J. T. Lee, H. J. Yoon, *Polym. Chem.* **2015**, 6, 3387.
29. H. K. Moon, S. Kang, H. J. Yoon, *Polym. Chem.* **2017**, 8, 2287.
30. R. Barbey, H. A. Klok, *Langmuir* **2010**, 26, 18219.
31. A. Apicella, Nicooolals, L., *Ind. Eng. Chem. Prod. Res. Dev.* **1984**, 23, 288.
32. M. Kobayashi, K. Uchino, T. Ishizone, *Journal of Polymer Science Part A: Polymer Chemistry* **2005**, 43, 4126.

6.6 Supporting information for 4-Styrenesulfonyl-(2-methyl)aziridine: The First Bivalent Aziridine-Monomer for Anionic and Radical Polymerization

6.7 Analytical Data of StMAz

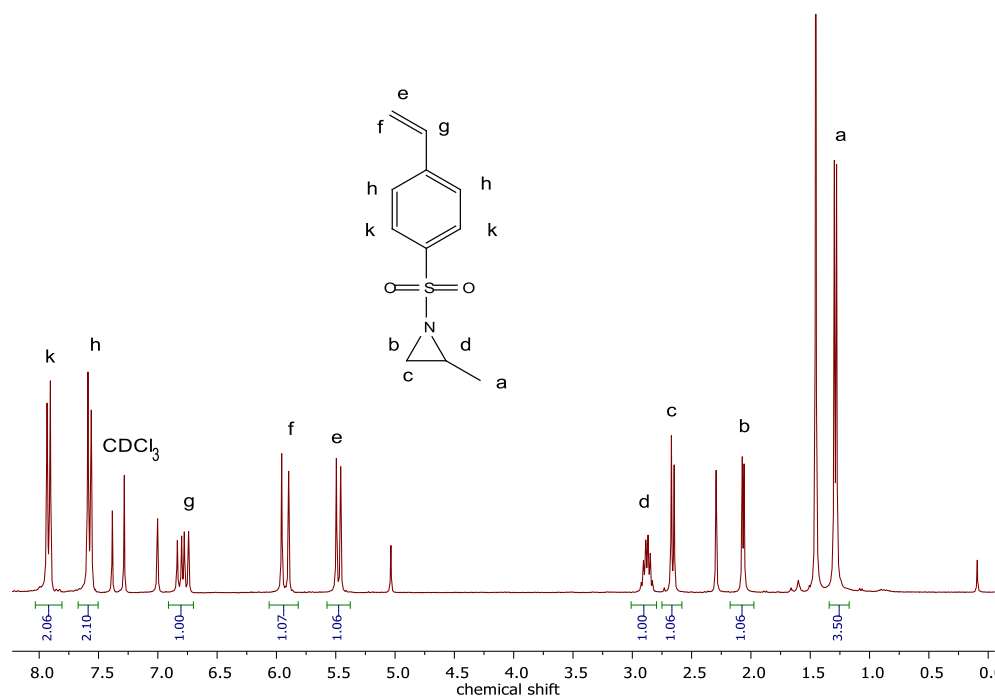


Figure S6.1: ¹H NMR (300 MHz, 298 K, CDCl₃) of StMAz

¹H NMR (300 MHz, CDCl₃): δ [ppm] = 7.92 (d, 2H, k), 7.58 (d, 2H, h), 6.84-6.73 ppm (dd, 1H, g), 5.94 (d, 1H, f), 5.43 ppm (d, 1H, e), 2.95-2.78 (m, 1H, d), 2.66 (d, 1H, c), 2.07 (d, 1H, b), 1.29 (d, 3H, a).

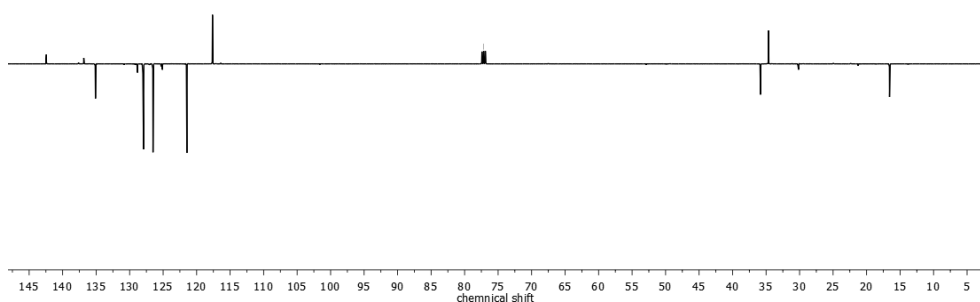


Figure S6.2: ^{13}C NMR (101 MHz, CDCl_3) of StMAz.. δ [ppm] = 135.76, 128.14, 126.69, 117.79, 36.01, 34.85, 16.81.

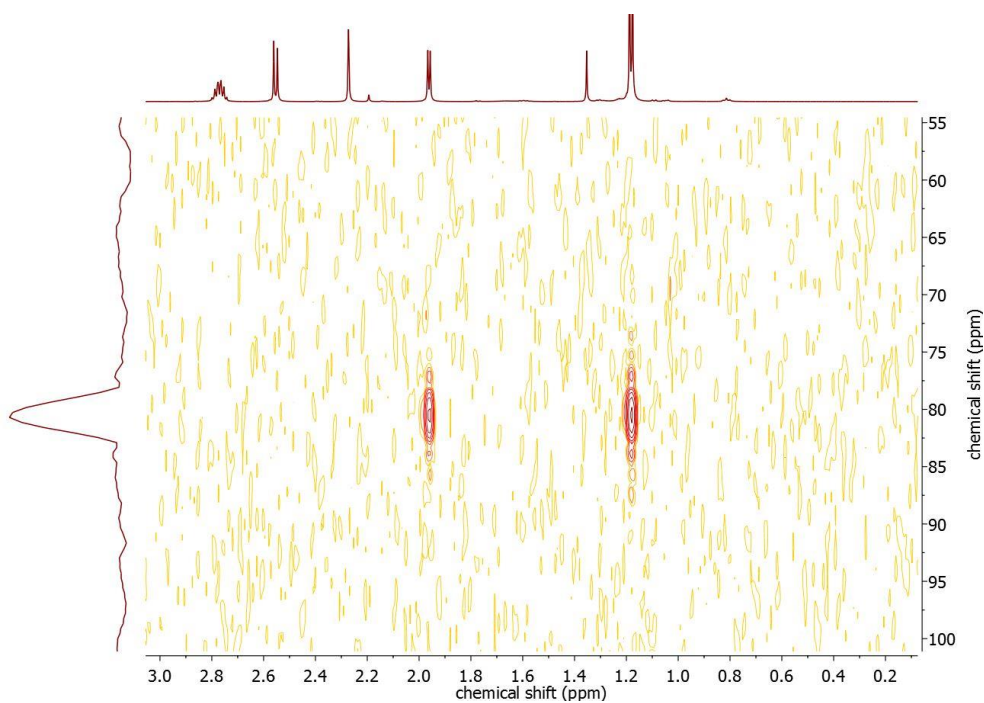


Figure S6.3: ^1H ^{15}N -HMBC (71 MHz, 298 K, CDCl_3) of StMAz. ^1H ^{15}N HMBC (71 MHz, 298 K, CDCl_3): δ [ppm] = 80.51.

6.8 Analytical Data of homo and co-polymers

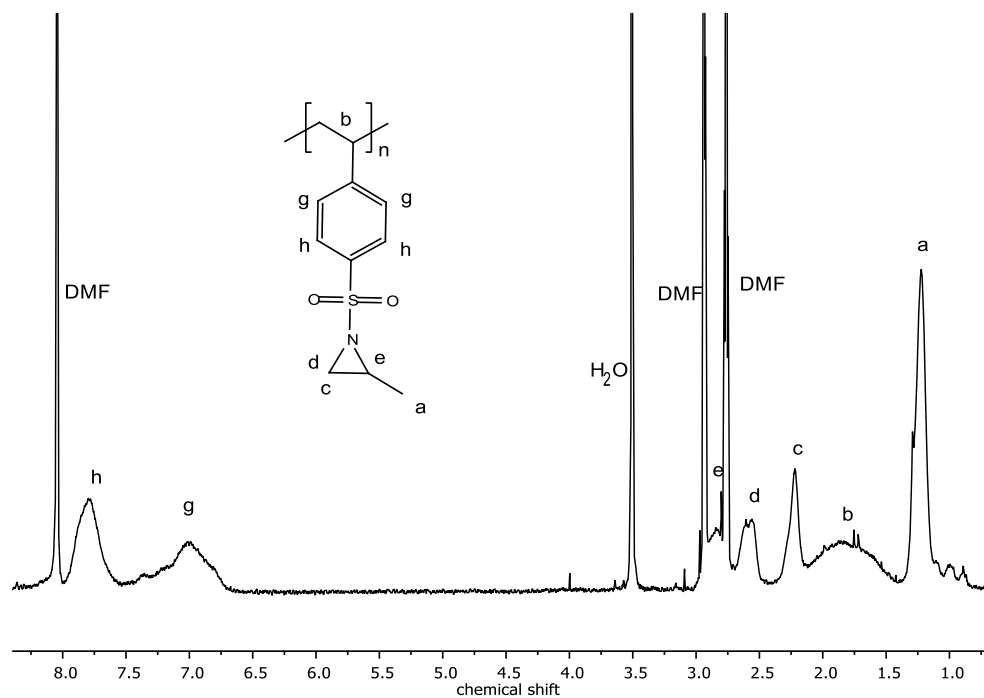
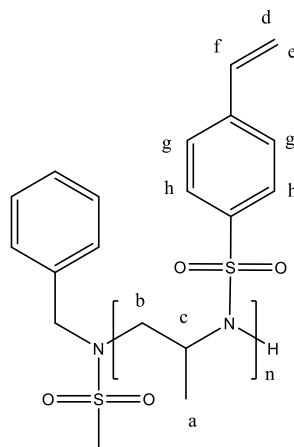
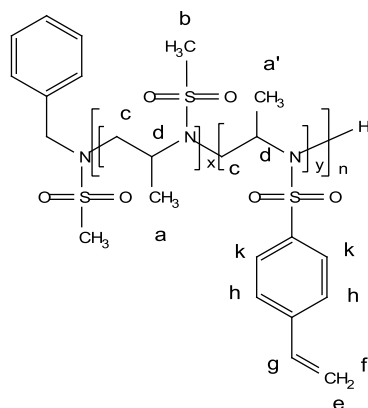


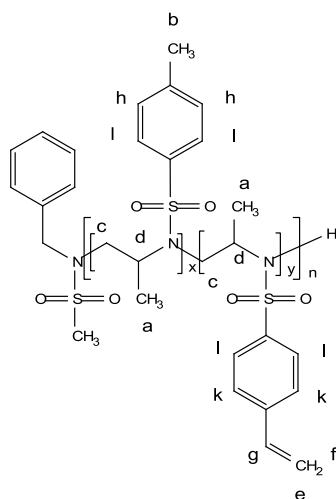
Figure S6.4: ¹H-NMR (300 MHz, CDCl₃) spectrum of P(StMAz). polymerized vinolog. δ [ppm] = 8.00-7.5 (br, h), 7.50-6.65 (br, g), 3.02-2.72 (br, e), 2.69-2.43 (br, d), 2.38-2.13 (br, c), 2.11-1.41 (br, b), 1.40-1.04 (br, a).



¹H NMR (300 MHz, CDCl₃): δ [ppm] = 8.16-7.70 (br, h), 7.70-7.35 (br, g), 6.90-6.52 (br, f), 6.00-5.68 (br, e), 5.50-5.24 (br, d), 4.61-3.67 (br, c), 3.67-2.96 (br, b), 1.42-0.55 (br, a). (For spectrum see Figure SI 9)



$^1\text{H NMR}$ (300 MHz, CDCl_3): δ [ppm] = 8.13-7.71 (br, k), 7.71-7.34 (br, h), 6.89-6.62 (br, g), 6.03-5.71 (br, f), 5.55-5.28 (br, e), 4.53-3.69 (br, d), 3.69-3.09 (br, c), 3.09-2.62 (br, b), 1.55-0.67 (br, a, a'). (For spectrum see Figure SI 7)



$^1\text{H NMR}$ (300 MHz, CDCl_3): δ [ppm] = 8.17-7.66 (br, l), 7.66-7.39 (br, k), 7.39-7.17 (br, h), 6.87-6.57 (br, g), 5.98-5.71 (br, f), 5.54-5.28 (br, e), 4.62-3.84 ppm (br, d), 3.84-2.99 (br, c), 2.50-2.11 (br, b), 1.44-0.55 (br, a). (For spectrum see Figure SI 8)

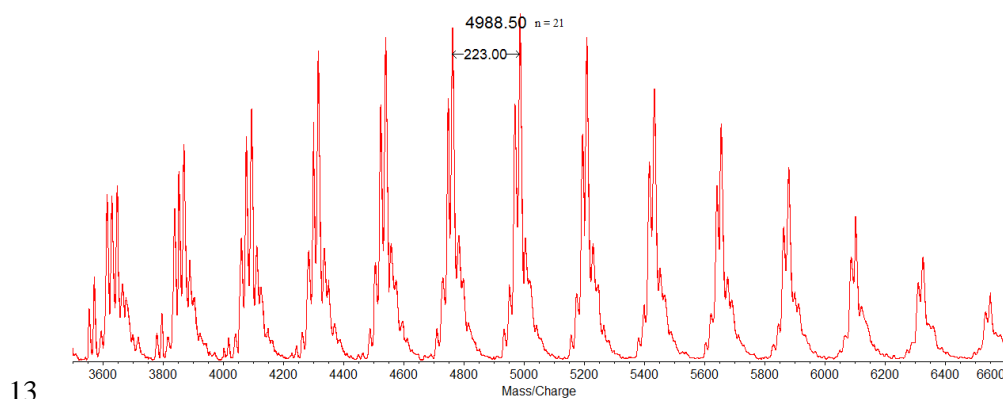


Figure S6.5: MALDI-ToF MS von P(StMAz)30

MALDI-TOF mass spectrometry proves the formation of the envisioned StMAz. The main distribution can be calculated to contain the mass of the initiator and the monomer mass with a

distance of 223 g mol^{-1} , the molar mass of StMAz, up to a detectable molecular weight of ca. 7500 g mol^{-1} . The maximum of the distribution corresponds to the molecular weight of 21 repeating units, the initiator and potassium as a counter ion.

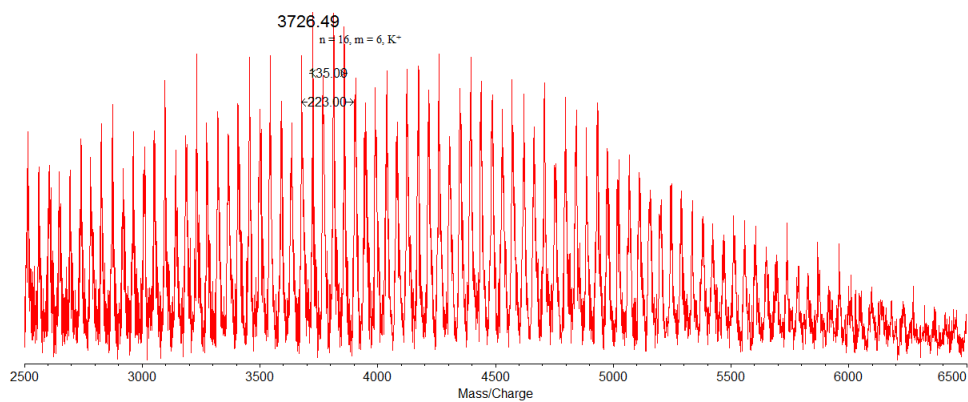


Figure S6.6: Zoom into the MALDI ToF mass spectrum of P(MsMAz-co-StMAz).

6.9 Analytic of Thiol-ene functionalization

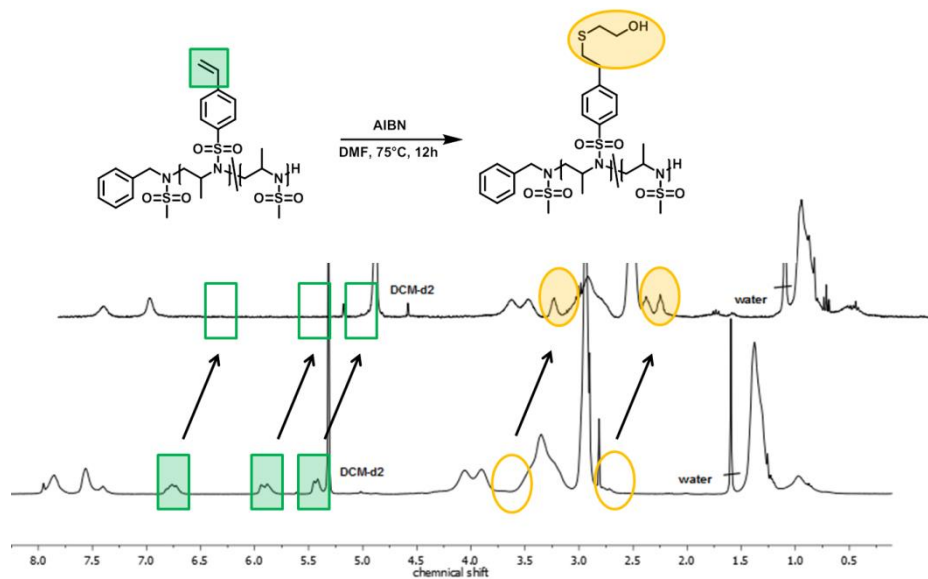


Figure S6.7: ¹H NMR (DCM-d₂, 300 MHz, 298 K) spectra of P6 (unmodified) and P6-1 (after thiol-ene addition with 2-mercaptoethanol).

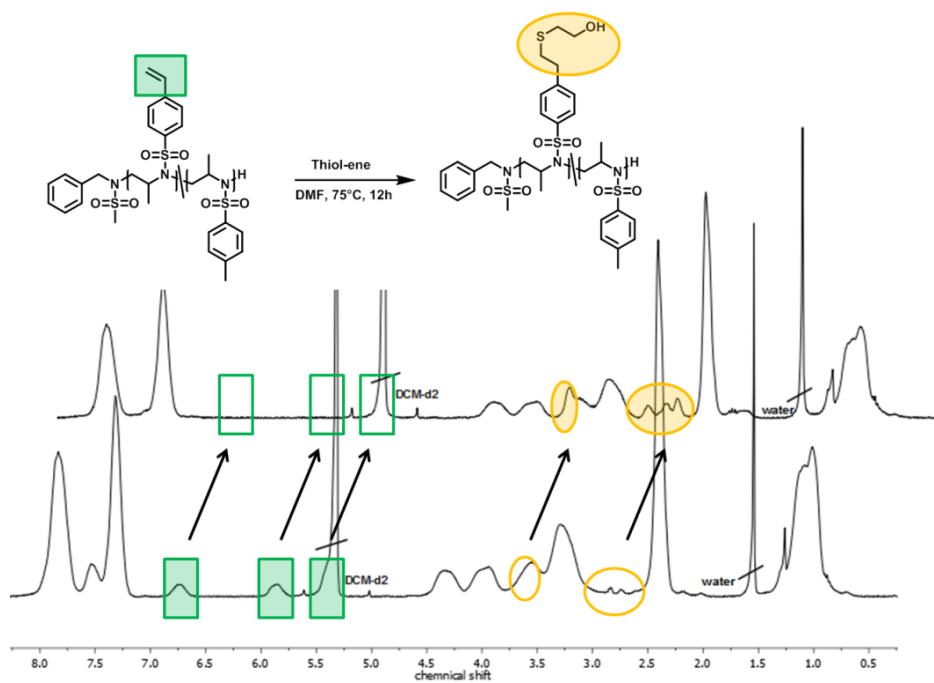


Figure S6.8: ¹H NMR (DCM-d₂, 300 MHz, 298 K) spectra of P4 (unmodified) and P4-1 (after thiol-ene addition with 2-mercaptoethanol).

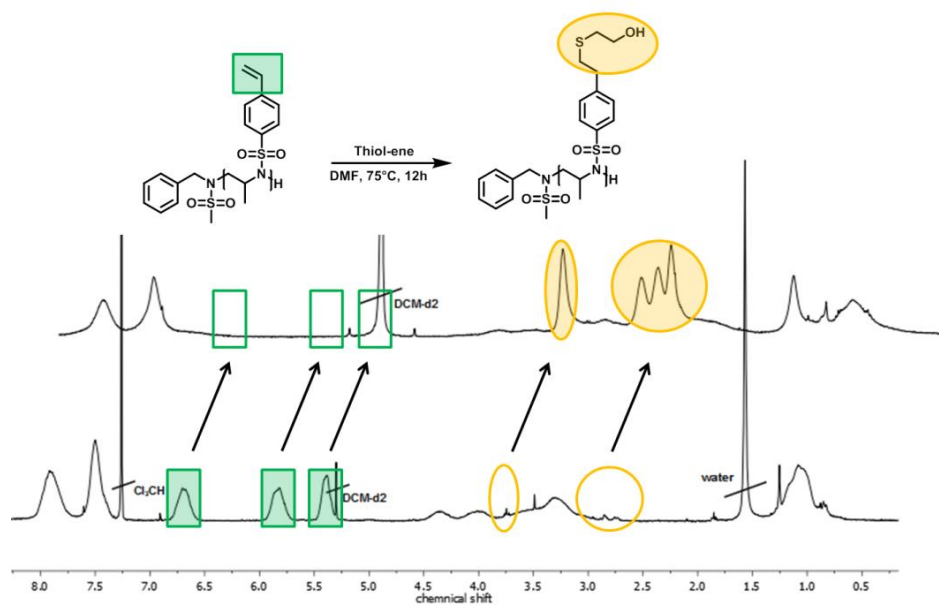


Figure S6.9: ^1H NMR (DCM- d_2 , 300 MHz, 298 K) spectra of P1 (unmodified) and P1-1 (after thiol-ene addition with 2-mercaptoethanol).

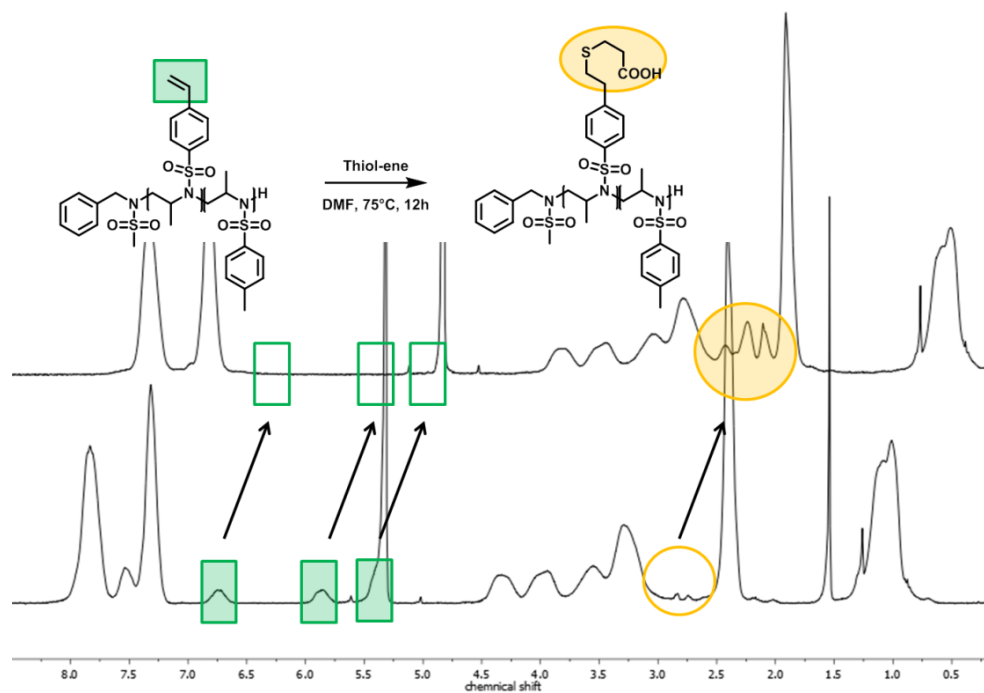


Figure S6.10: ^1H NMR (DCM- d_2 , 300 MHz, 298 K) spectra of P4 (unmodified) and P4-2 (after thiol-ene addition with 3-mercaptopropionic acid).

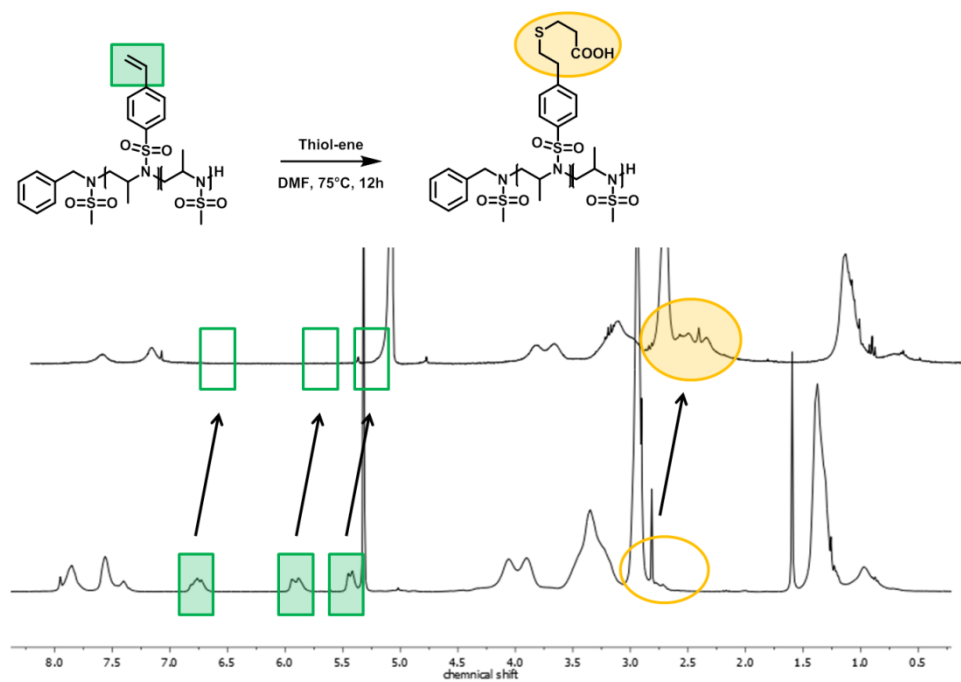


Figure S6.11: ^1H NMR (DCM-d_2 , 300 MHz, 298 K) spectra of P6 (unmodified) and P6-2 (after thiol-ene addition with 3-mercaptopropionic acid).

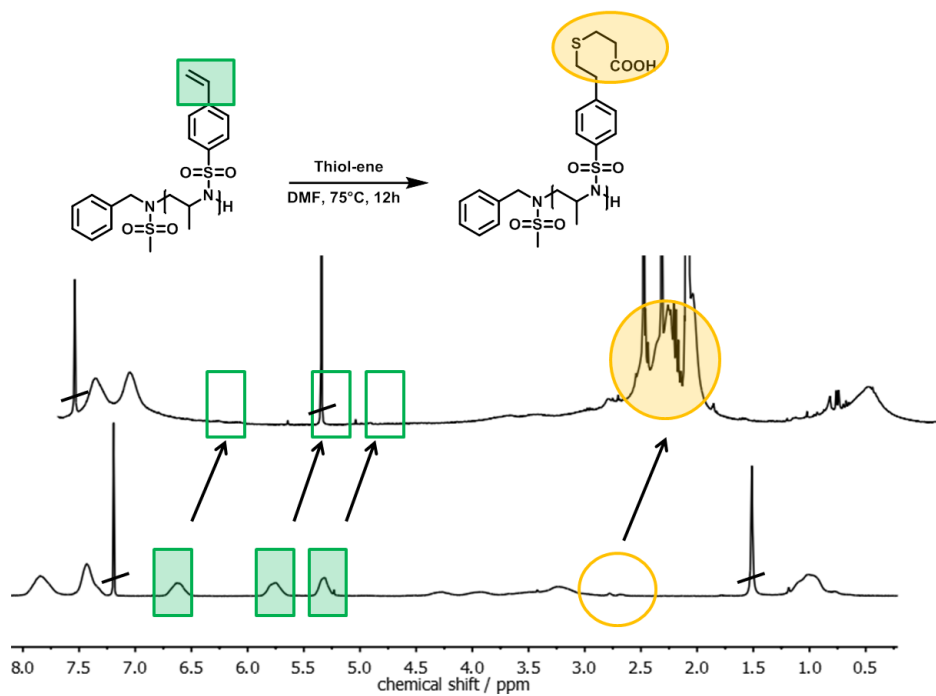


Figure S6.12: ^1H NMR (CDCl_3 / DMSO-d_6 , 300 MHz, 298 K) spectra of P1 (unmodified) and P1-2 (after thiol-ene addition with 3-mercaptopropionic acid).

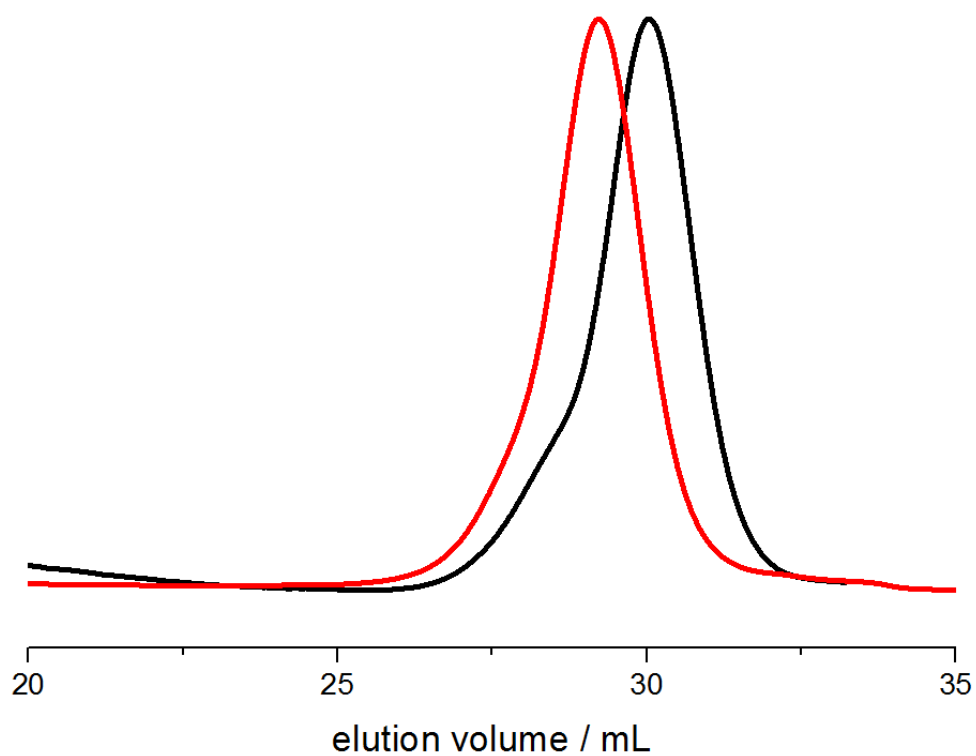


Figure S6.13: SEC traces of P1 (black) and P1-1 (red) in DMF (RI signal)

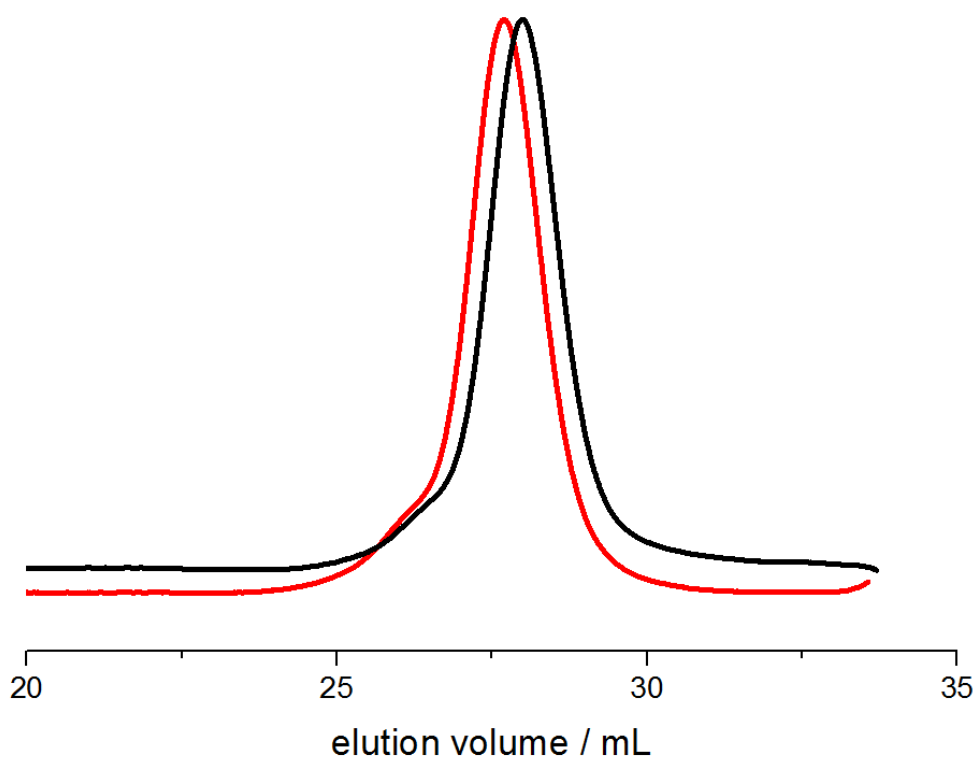


Figure S6.14: SEC traces of P4 (black) and P4-1 (red) in DMF (RI signal)

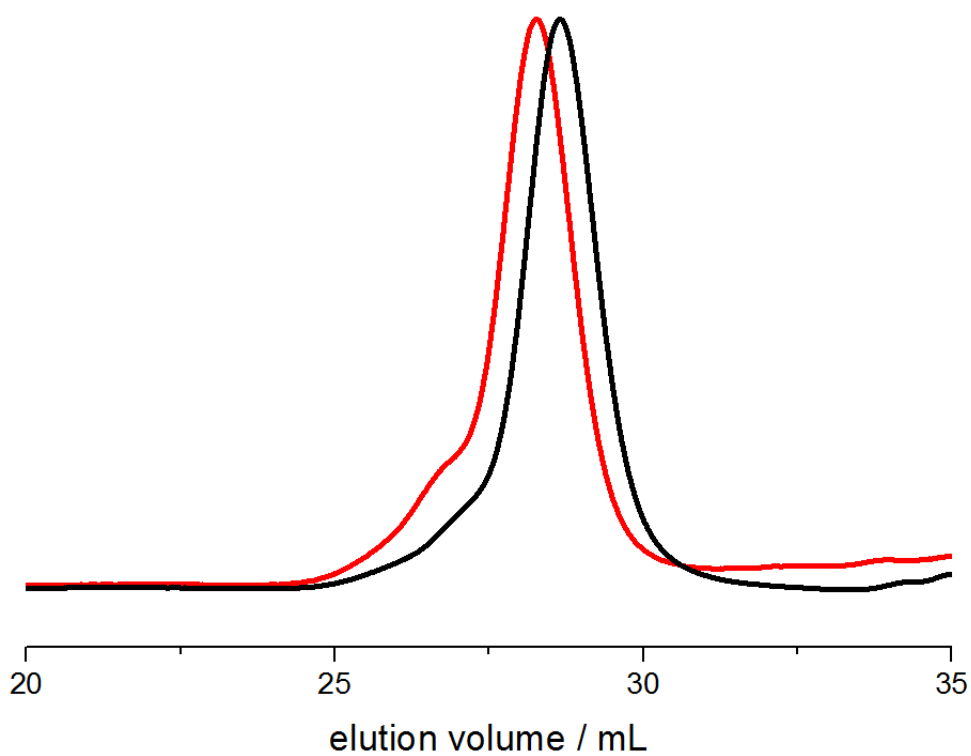


Figure S6.15: SEC traces of P6 (black) and P6-1 (red) in DMF (RI signal)

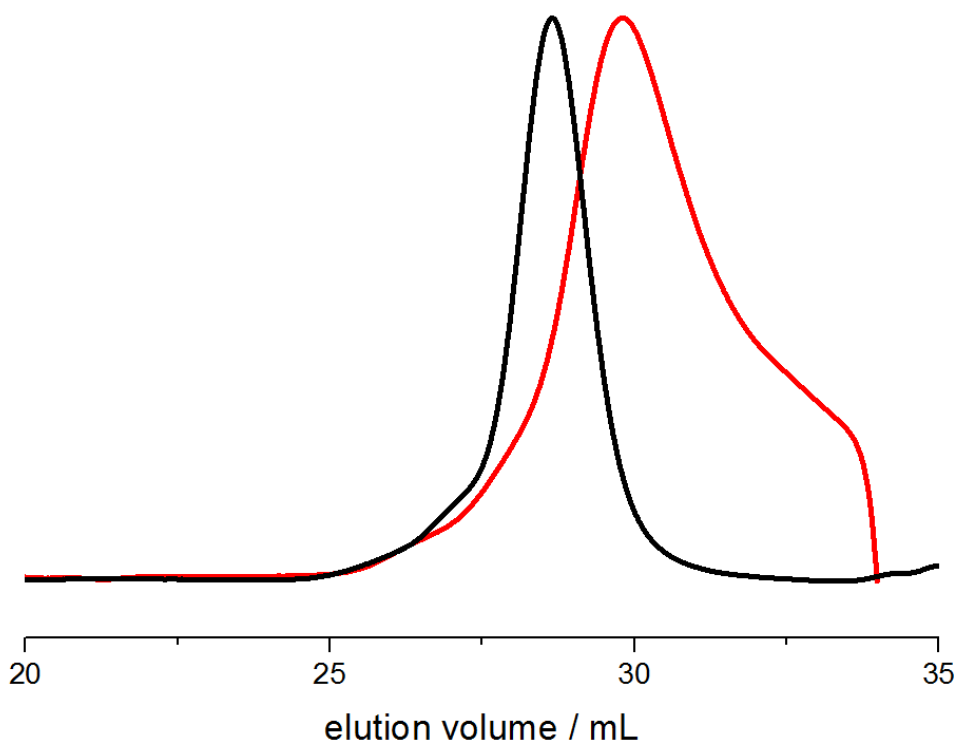


Figure S6.16: SEC traces of P6 (black) and P6-2 (red) in DMF (RI signal)

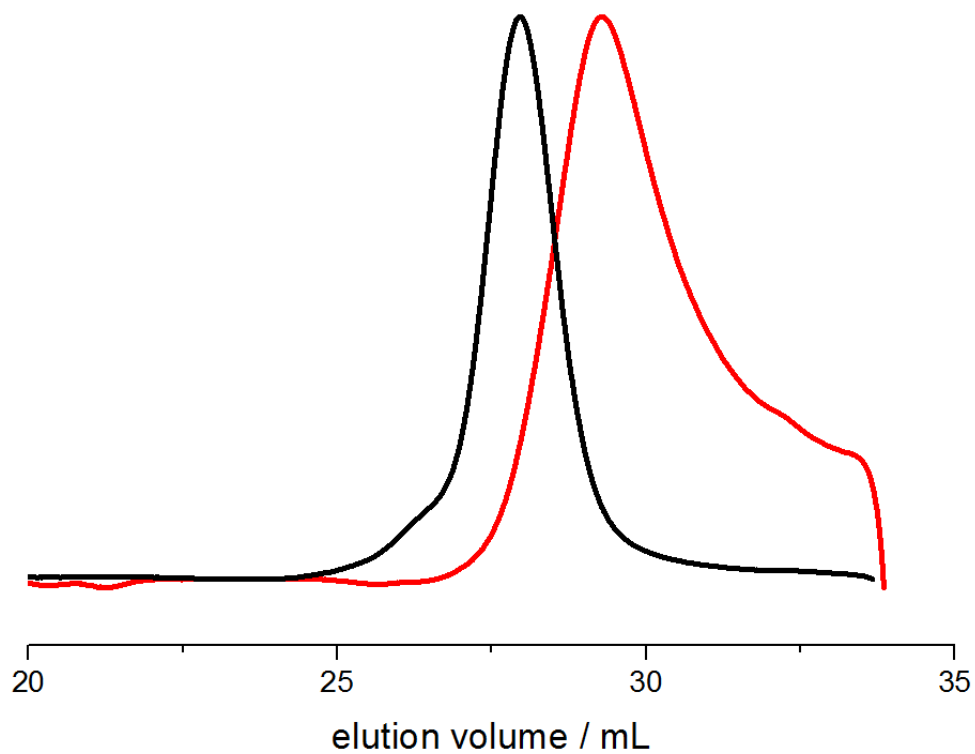


Figure S6.17: SEC traces of P4 (black) and P4-2 (red) in DMF (RI signal)

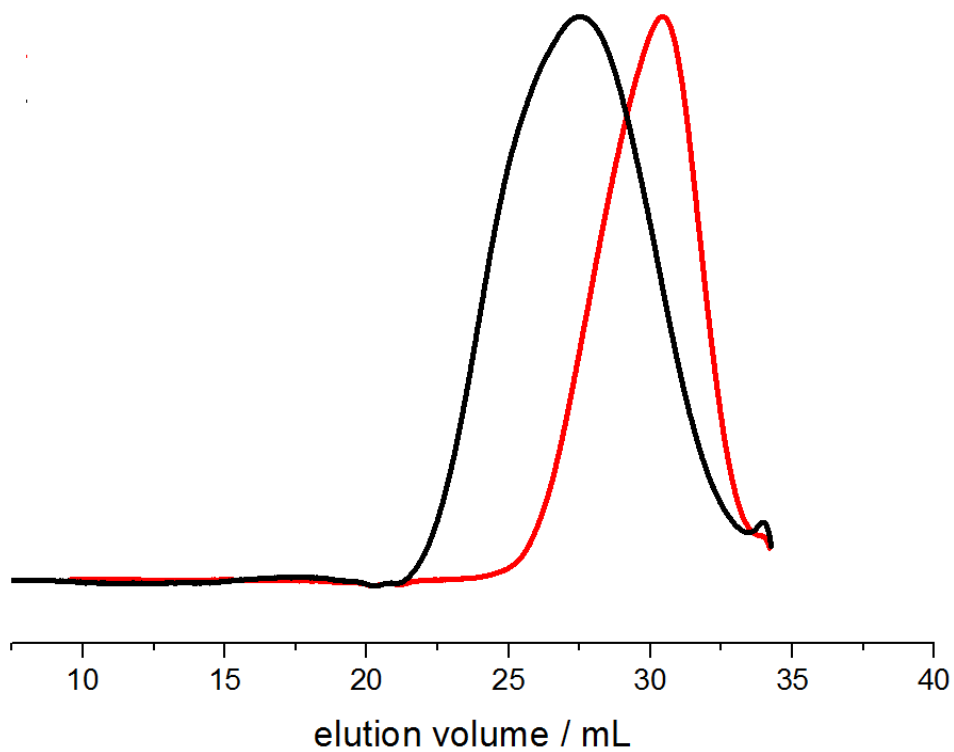


Figure S6.18: SEC traces of P7 and P8 (free radical polymerization)

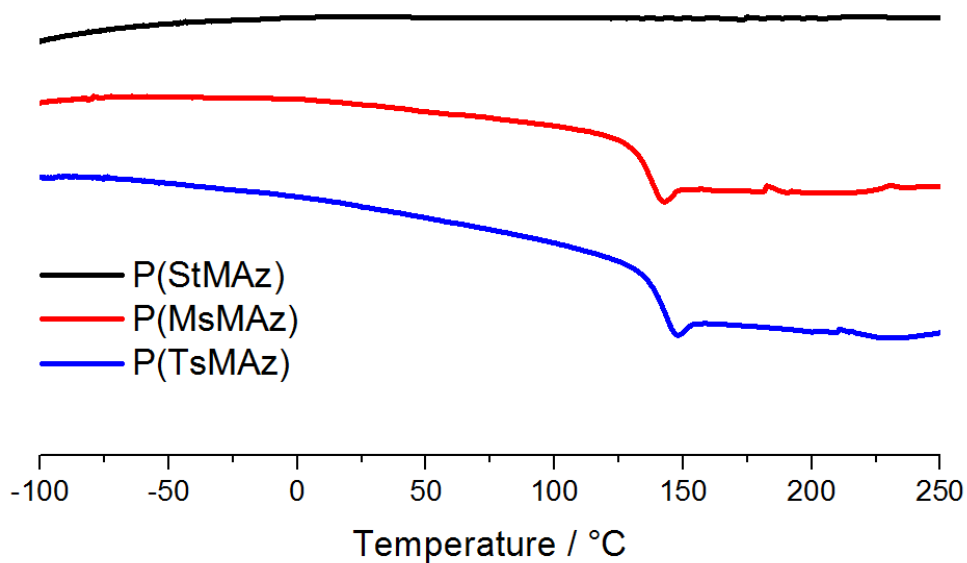


Figure S6.19: DSC curves (second heating) of P(StMAz) (P2) and other homo poly(aziridine)s from MsMAz and TsMAz for comparison. P2: TG=not observed, P(MsMAz)50: TG=140 °C, P(MsMAz)50: TG=142 °C

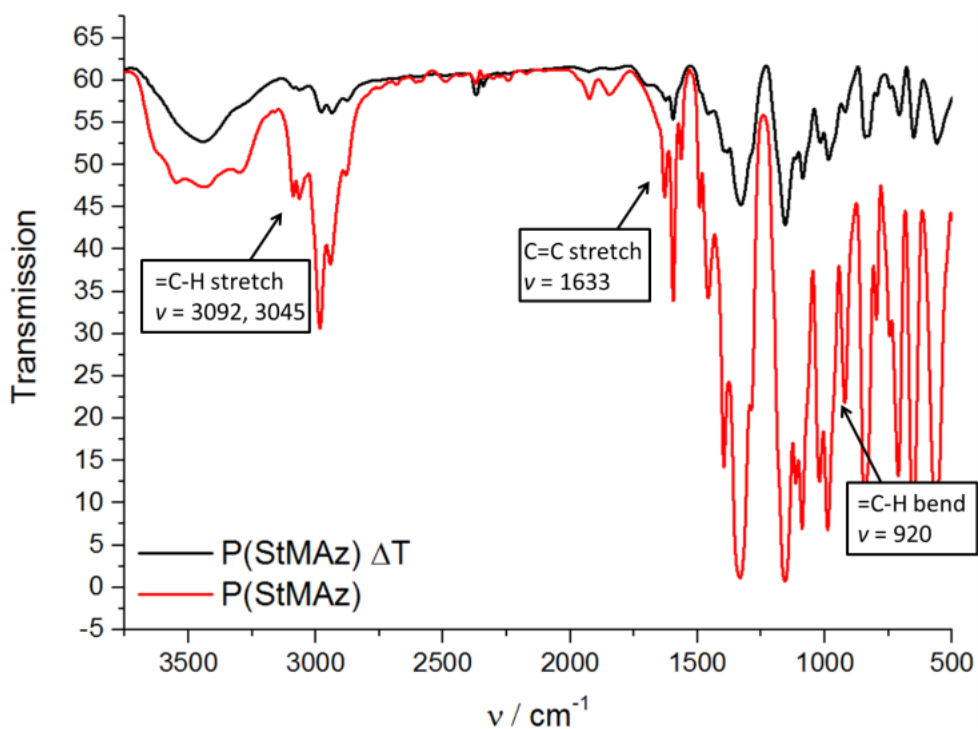


Figure S6.20: IR Spectra of Poly(StMAz) (P1) (red) and P1 after heating to 250°C. Temperature program corresponded to DSC Measurement.

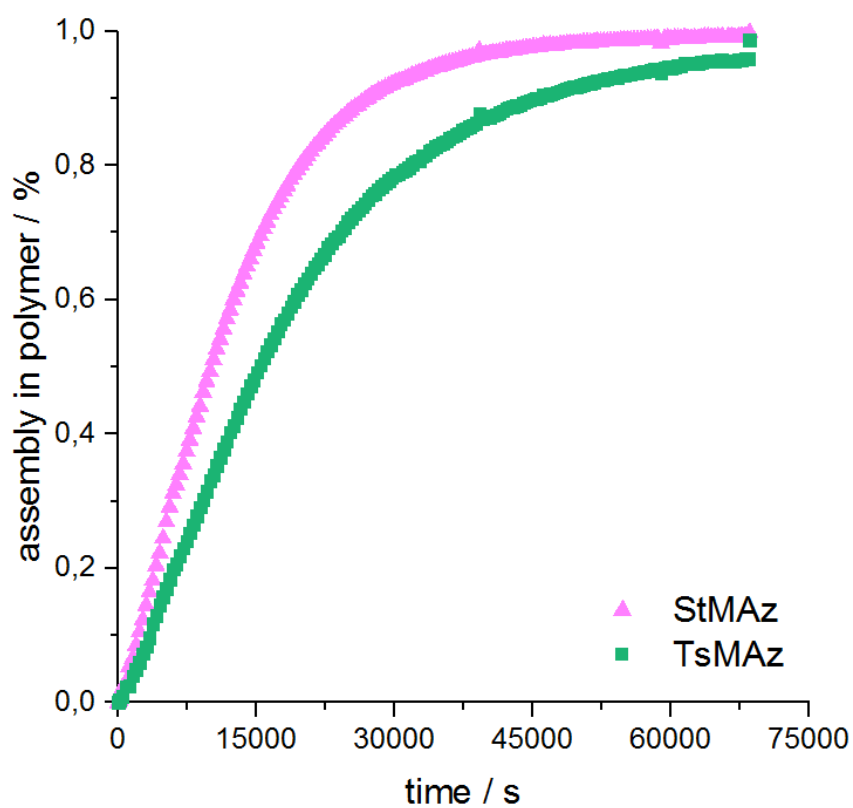


Figure S6.21: Assembly of the monomer in the polymer versus reaction time.

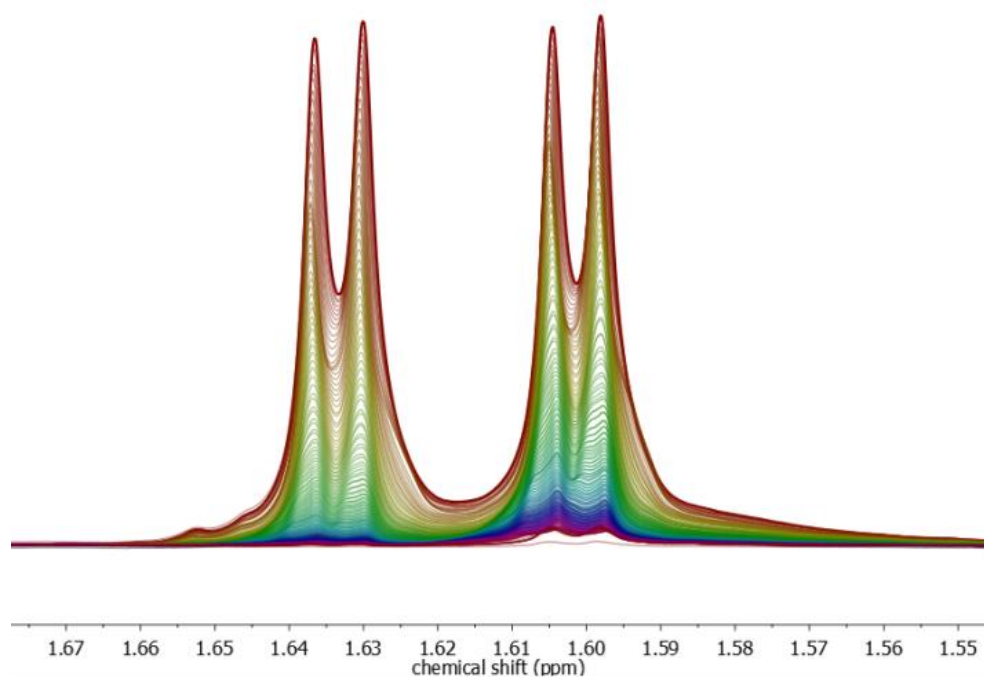


Figure S6.22: Zoom-in of the relevant signals of the monomer ring-protons, showing the consumption of the monomer.

7 Tacticity control in poly(sulfonyl aziridine)s: Towards tuning crystallinity and supramolecular interactions

*Tassilo Gleede and Frederik R. Wurm**

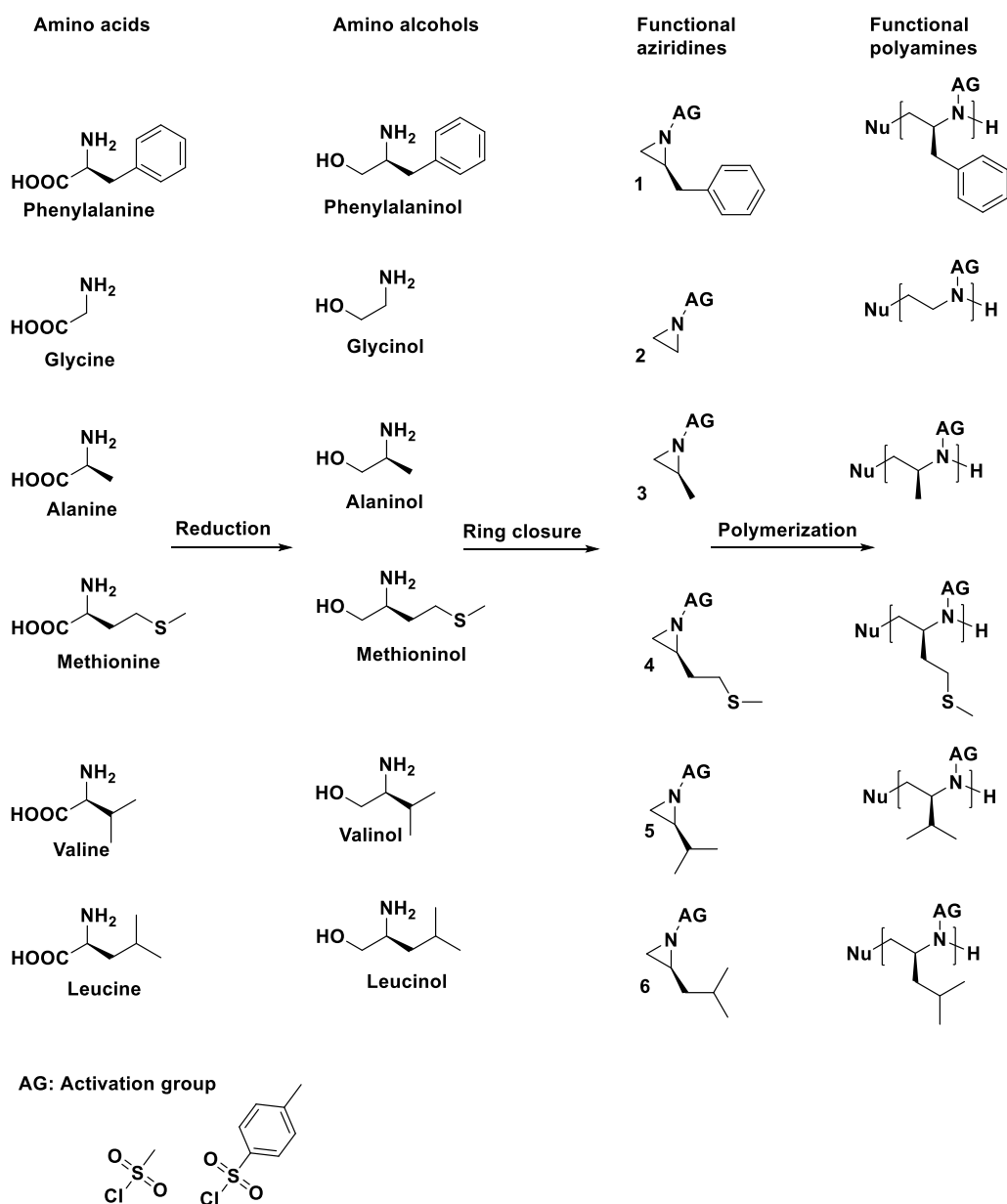
Note: This chapter is based on unpublished results and corresponds to an Outlook. Synthesis and analysis of monomers and polymers is done by Tassilo Gleede, if not noted otherwise. The concept was developed by Frederik Wurm and Tassilo Gleede.

7.1 Introduction

Chirality is an important feature in many biopolymers and particularly relevant for tuning mechanical or thermal properties in synthetic polymers. Chirality is especially important in polypeptides, which are made of natural occurring amino acids (AS). Apart from glycine, naturally-occurring amino acids are *L*-enantiomers. This forces polypeptides into more complex assemblies / secondary structures, such as helices or sheets.³ The helical structure of polypeptides and of DNA was first found by Pauling as well as Watson and Crick in the early 1950's.^{4 1, 2} Natta later found that isotactic polypropylene (PP) also exhibits a helical conformation,⁵ caused by the conformation of the stereocenters in the polymer backbone. Isotactic PP was the first example of a synthetic polymer with helical structure. As a solid material the properties of crystalline isotactic PP differ significantly to atactic amorphous PP in terms of density, x-ray scattering and solubility in ether, heptane and toluene. Unlike polypeptides or other natural chiral helices PP showed to lose its helical conformation by forming a random coil, indicated by viscosity measurements in tetralin.⁵ Since then, different polymers with chiral side groups were synthesized with the goal to maintain their hierarchical structure in solution. This further allows studying the unique properties such as optical rotation values in solution and thermal stability in the solid state⁶⁻⁸. Today artificial hierarchical polymers are seen as promising candidates to study hierarchically assembly in supramolecular structures like coiled-coils,² mimic protein DNA hybrids,⁹ and to synthesize biorthogonal helices and functional superstructures with catalytic activity.

Anionic polymerization as a discipline of modern polymer science, is advantageous to synthesize polymers with different tacticity. The absence of termination reactions, allows the synthesis of polymers with well-defined polymer lengths, which is essential to compare the properties of polymers with different tacticity.¹⁰⁻¹⁵ Using two or more monomers with different reactivities could allow the adjustment of tacticity in the polymer backbone by single step, one-pot reactions.^{16, 17} This may contribute to fine-tuning the degree of tacticity in the polymer backbone. Sulfonyl-activated aziridines as a rather new monomer class undergoes anionic polymerization.^{11, 18} As the monomers consist of a three membered ring, the introduction of functional groups is possible on various sites. The *N*-sulfonyl group influences the monomer reactivity by its electron-withdrawing nature,¹⁶ furthermore it can be removed by hydrolysis or other desulfonylation reactions after polymerization.¹⁹ Side groups at the 2-position introduce a stereocenter and are used to introduce functionalities.²⁰⁻²² In our previous work various functionalities were introduced using a racemic mixture.

Aziridines can be synthesized from amino acids which act as natural source of enantiopurity.²³⁻²⁵ As illustrated in Scheme 7.1, six amino acids can be seen as possible starting compounds to access functional activated aziridines and their polymers. After reduction of the AS, the reduced amino alcohols can be converted to aziridine monomers followed by ring-closure reaction. Enantiopure aziridines would form isotactic polyaziridines, which potentially have a secondary structure similar to polypeptides. The difference between polypeptides and isotactic polyaziridines is that hydrogen bonds, which stabilize the secondary structure in solution, are only present in polypeptides and not in polyaziridines.

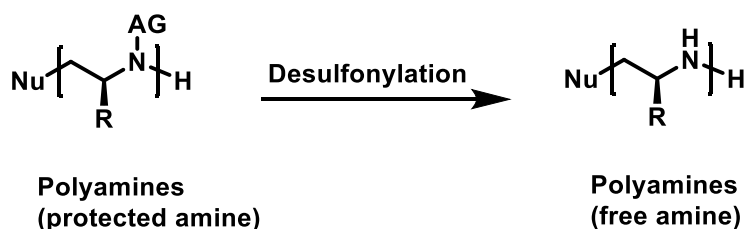


Scheme 7.1: Possible synthesis route of functional aziridines from naturally occurring amino acids towards functional polyamines in analogy to polypeptides.

Toste and Bergmann demonstrated; that polymers based on enantiopure aziridnes have a decreased solubility compared to racemic substituted aziridines.²⁶ Polymers formed from monomer **1** precipitate and are insoluble in all tested organic solvents (DMF, DCM, DMSO, CHCl₃).²⁶

Our group demonstrated, that unsubstituted activated aziridines such as tosylaziridines **2** do not polymerize towards high degree of polymerization. Usually the reaction mixture becomes turbid as polymers start to precipitate and propagation reactions are inhibited.²⁷ This is most likely related to a higher degree of crystallinity caused by a more uniform polymer structure. However, detailed studies are off. Toste and Bergman found, that a racemic mixture of **3**, activated with mesyl or tosyl, can be polymerized up to 200 RU to in DMF soluble polyaziridines. In contrast, enantiopure monomers become insoluble after 25 repeating units or less. Choosing activation groups with different structures is an established method to improve solubility of polysulfonylamides. Rupar *et. al.* used a mixture of different activation groups such as *sec*-busyl- and mesyl-aziridines. The resulting polymer becomes irregular in structure and the solubility is increased.²⁸ They also showed, that the solubility of *ortho*-substituted polysulfonylaziridines is superior to *para*-substituted polysulfonylaziridines, polymers up to 200 and 400 repeating units were synthesized, while homopolymerizations were limited to a maximum of 25 RU.²⁹ Using activation groups with different structural patterns or different side groups on the monomers might also be beneficial to overcome solubility issues. Therefore, copolymerization of monomers with different side chains (**1-6**) may provide polyaziridines with an adequate solubility in organic solvents in the future.

Desulfonylation of polysulfonylaziridines like illustrated in scheme 7.2 is reported in literature for alkylsulfonyl groups,²⁸ aromatic substituents^{19, 30} and highly activated aromatic substituents.^{29, 31} Removing the protecting groups of isotactic polysulfonylaziridines would allow obtaining substituted linear polyethyleneimine in analogy to isotactic polypropyleneoxide³² and polypropylenesulfide³³ for the first time.



Scheme 7.2: Desulfonylation of polysulfonamide leads to linear polyamine derivatives.

Secondary amines, like they are present in the deprotected polymer would promote solubility also in water.^{11, 34} Amines provide further sites for multiple chemical modifications according to amine chemistry. Due to the chiral environment of the secondary amines, this polymer might be of importance for catalytic applications.

Famous examples for enantiopure amines applied in catalytic chemistry is the Hajos-Parrish-Eder-Sauer-Wiechert reaction,^{35, 36} primary amino acids like phenylalanine and others are used as catalyst to perform intramolecular aldol reactions with high enantiomeric excess (*e.e.*). Also 4-Dimethylaminopyridine (DMAP) derivatives find a broad application as nucleophilic catalysts. They promote acylation reactions of secondary alcohols, kinetic resolutions, Michael Additions^{37, 38} etc.. The advantage of DMAP is that the chiral environment and its nucleophilicity is adjustable by substituents. As a result, it is used in many enantioselective reactions.³⁹⁻⁴¹ The steric impact of the substituents in the polymer could then influence catalytic processes like kinetic resolutions. The substituents could be used to tune the catalytic environment for specific reaction.

Expanding the scope of enantiopure aziridines like **5** and **6** as well as their polymerization will be part of future studies. Desulfonylation and the exploration of catalytic properties of the isotactic polyamine will be part of future work as well. To explore first properties of isotactic polyamine derivatives the enantiopure monomer **3** and **4** were synthesized and first polymerizations of **3** were conducted successfully. Polymers with different DP and a different amount of enantiopure monomers were obtained to study the impact of tacticity with CD-spectroscopy and SEM.

7.2 Experimental Section

7.2.1 Chemicals

Solvents and reagents were purchased from Acros Organics, TCI, Sigma-Aldrich or Fluka and used as received unless otherwise stated (methanol, diethylether, anhydrous DMF, DCM, (2S)-2-Amino-1-propanol, DMAP, triethylamine, tosylchloride, CaH₂, MgSO₄). Deuterated solvents were purchased from Deutero GmbH. 2-Methylaziridine was synthesized according to already published procedures.²⁶ 2-Methylaziridine was purified by distillation from CaH₂ to remove traces of water. 2-Methyl-*N*-tosylaziridine (*rac*-TsMAz) and PyNHMs-initiator were synthesized according to already published procedures and dried by azeotropic distillation from benzene to remove traces of water.²⁶ The synthesis of enantiomeric pure TsMAz was adopted from literature.⁴²

7.2.2 Instrumentation

NMR: ^1H NMR spectra were recorded using a Bruker Avance 300, a Bruker Avance III 700. All spectra were referenced internally to residual proton or carbon signals of the deuterated solvent, if not noted otherwise.

SEC: Size exclusion chromatography (SEC) measurements of standard polymers were performed in DMF (1 g L⁻¹ LiBr added) at 60 °C and a flow rate of 1 mL/min with an PSS SECcurity as an integrated instrument, including a PSS GRAM 100-1000 column and a refractive index (RI) detector. Calibration was carried out using poly(ethylene glycol) standards provided by Polymer Standards Service.

HPLC: HPLC was used to determine the enantiomeric excess of the chiral monomers. Using amylose tris(3-chloro-4-methylphenylcarbamate) immobilized on 3 μm silica gel as column material at 25 °C and 1 mL / min in hexane / EtOH 95/5.

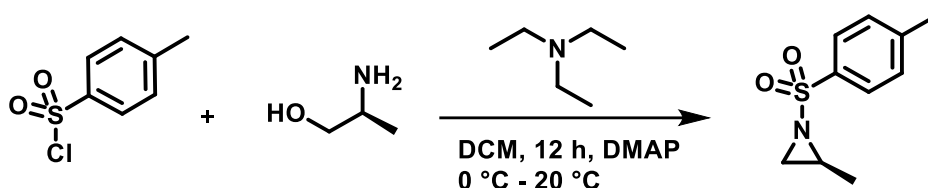
DLS: Dynamic light scattering measurements (DLS) were performed on an ALV spectrometer consisting of a goniometer and an ALV-5004 multiple-tau full-digital correlator (320 channels) which allows measurements over an angular range from 20° to 150°. A He-Ne Laser operating at a laser wavelength of 632.8 nm was used as light source. For temperature-controlled measurements the light scattering instrument is equipped with a thermostat from Julabo. Diluted samples were filtered through PTFE membrane filters with a pore size of 0.45 μm (LCR syringe filters). Measurements were performed at 20 °C at different angles ranging from 30° to 150°.

SEM: Scanning electron microscopy (SEM) was performed on a 1530 LEO Gemini microscope (Zeiss, Oberkochen, Germany). The nanoparticle dispersion (10 μL) was diluted in 3 mL of distilled water, drop-cast onto silica wafers, and dried under ambient conditions. Afterward the silica wafers were placed under the microscope and each sample was analyzed at a working distance of ~ 3 mm and an accelerating voltage of 0.2 kV.

Circular dichroism (CD) spectroscopy: All spectra were recorded using a concentration of 50 μM in acetonitrile using a quartz cell with a path length of 2 mm or 1 mm. CD-spectra were recorded on a J-815 CD-spectrometer (JASCO) using the software Spectra Manager 2.08.04. An average of three scans was reported. All spectra were corrected by the subtraction of the background. All data was processed using Origin Pro 9.1.

7.2.3 Synthetic procedures

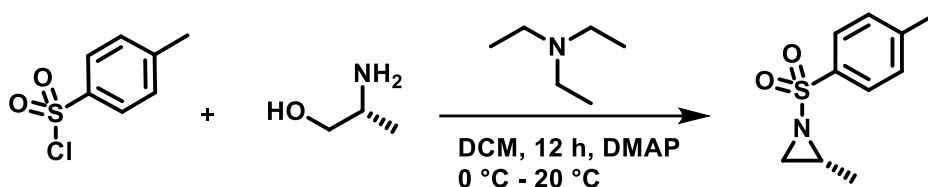
Synthesis of (S)-2-methyl-1-tosylaziridine ((S)3)



In a 500 mL reaction flask, equipped with a dropping funnel, (2S)-2-amino-1-propanol (2.5 g, 1 equiv.) was dissolved in 200 mL dry DCM. To this solution TEA (13.5 g, 4.0 equiv.) was added at 0 °C. Then TsCl (16 g, 2.5 equiv) dissolved in ca 100 mL dry DCM was added dropwise over a period of 30 min at 0 °C. After the addition of the TsCl, a catalytic amount (20 mg) of DMAP was added to the reaction mixture, the mixture was allowed to warm up to room temperature and was stirred for 12 h. 100 mL of saturated NH_4Cl (aq) was added to terminate the reaction, the product was extracted with DCM, the organic phases were combined and dried over Na_2SO_4 . The DCM was evaporated at reduced pressure. 550 mg (7.9%) of pure product was obtained as a colorless solid after purification *via* column chromatography.

^1H NMR (250 MHz, Benzene- d_6) δ 7.83 (d, J = 8.0 Hz, 2H), 6.87 (d, J = 8.0 Hz, 2H), 2.72 – 2.51 (m, 1H), 2.36 (d, J = 6.9 Hz, 1H), 1.95 (s, 3H), 1.51 (d, J = 4.5 Hz, 1H), 0.83 (d, J = 5.6 Hz, 3H).

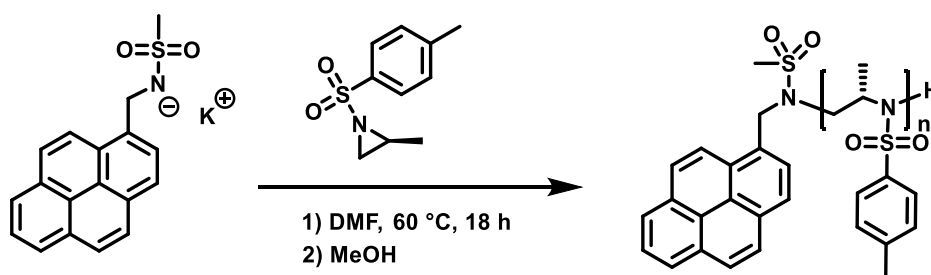
Synthesis of (R)-2-methyl-1-tosylaziridine ((R)3)



The synthesis of (R)3 was done in direct analogy to (S)3, by using (2R)-2-amino-1-propanol as starting compound. 900 mg (13% yield) of the pure product was obtained as a colorless solid after purification *via* column chromatography. To verify the enantiomeric purity of the synthesized chiral monomers, HPLC was conducted with 1 mg/mL solutions of (R)3 and (S)3 and rac-TsMAz in hexane / EtOH 95/5.

^1H NMR (300 MHz, benzene- d_6) δ 7.94 – 7.80 (m, 2H), 6.73 (d, J = 7.9 Hz, 2H), 2.62 (h, J = 5.7 Hz, 1H), 2.40 – 2.30 (m, 1H), 1.84 (s, 3H), 1.37 (d, J = 4.5 Hz, 1H), 0.82 – 0.72 (m, 3H).

General procedure for the azaanionic polymerization of (R)3 and (S)3



All glassware (Schlenk flasks) was flame-dried by *in vacuo* for at least three times. All reactants (except potassium bis(trimethylsilyl)amide (KHMDs)) were dried from benzene *in vacuo* for at least 4 h. The TsMAz was dissolved in anhydrous *N,N*-dimethylformamide to give a 10 wt% solution, the PyNHMs-initiator were dissolved in 1 mL DMF. The initiator solution was activated by adding it to KHMDs under the argon-atmosphere. From the initiator-solution, the appropriate volume was added to the monomer solution. The mixture was stirred at 60 °C overnight. To terminate the polymerization, 0.5 mL acidic methanol was added and the reaction mixture was precipitated in ca. 25 mL diethyl ether. The colorless precipitate was collected by centrifugation and dried at room temperature *in vacuo* to give a colorless powder with moderate yields (71 – 86%).

7.3 Results and Discussion

Monomer synthesis of (S)**3**, (R)**3** and (rac)**3** was performed in analogy to the literature.⁴² Monomer (S)**4** was also synthesized following the literature procedure. To synthesize enantiopure activated aziridines, we chose to use amino alcohols as a natural source of enantiopurity. To determine the final enantiomeric excess of the enantiopure aziridines the racemic mixture of **3** was separated *via* HPLC. Figure S 7.1 shows full baseline separation of the two enantiomers. Using the same HPLC method the enantiopure aziridines (S)**3** and (R)**3** were confirmed to be of high enantiopurity. Figure S 7.2 and S 7.3 show only a single peak corresponding to the specific enantiomer. Therefore, we assume the enantiomeric excess of the activated aziridines is with 98% *e.e.* equal to the *e.e.* of the used amino alcohols. Figure S 7.4 and S 7.5 show the ¹H NMR of tosyl-monomers (R)**3** and (S)**3**.

Monomer (S)**4**, containing a thioether side group was synthesized, activated with a mesyl and a tosyl group. The thioether side group should not inhibit the anionic polymerization and it allows further modification by oxidation, which can be used to adjust the hydrophilicity of the side groups to further increase the solubility. The ¹H NMR's prove both (S)**4** monomers were successfully synthesized activated with a mesyl (figure S7.7) and a tosyl group (figure 7.8). For future studies the thioether monomers need to be polymerized. Then subsequent studies on oxidation behavior, and formation of a secondary structure can follow. Polymer properties could then be further modified by oxidation reactions.

To investigate the impact of the enantiomeric purity on the solubility and the degree of polymerization we polymerized of both TsMAz enantiomers with the goal to study the isotactic polymers in solution. Table 7.1 summarizes the conducted polymerizations of enantiomerically pure TsMAz.

Table 7.1: Summary of conducted homopolymerizations of **3.**

<i>Experiment</i>	<i>e.e.^a / %</i>	<i>DP^b</i>	<i>M_n^b / g mol⁻¹</i>	<i>M_n^c / g mol⁻¹</i>	<i>Đ^c</i>
#1	+98	100	21.400	n.d.	n.d.
#2	+98	50	10.900	n.d.	n.d.
#3	+98	25	5.600	n.d.	n.d.
#4	+98	12.5	3.000	1000	1.09
#5	-98	100	21.400	n.d.	n.d.

Experiments conducted with 10 wt% monomer concentration in DMF. ^a enantiomeric excess of the monomer was determined *via* HPLC. ^b Theoretical value, ^c Number-average molecular weight and molecular weight dispersities determined *via* SEC in DMF (vs. PEO standards). n.d.: not determined

We were able to confirm the finding of Toste and Bergmann; polymers of enantiomeric pure aziridines become insoluble in all tested organic solvents (DMF, DMSO, DCM, CHCl_3). All reaction solutions became turbid several minutes after initiation. Therefore, analysis *via* SEC of the polymers with a DP greater than 12.5 was not possible. #4 with 12.5 repeating units remained soluble enough in DMF and allowed SEC analysis, see Figure 7.11. The determined molecular weight was with 1000 g/mol underestimated by the factor of 3. As PEO standards were used for the SEC an underestimated molecular weight by the factor of 2 – 3 was also reported in our previous publications.^{16, 18, 20}

The obtained DMF dispersions from polymerization #1 – #4 were diluted with DMF to further analyze the milky dispersions by dynamic light scattering. Figure S 7.9 and figure S7.10 show, that the hydrodynamic radii were all around 90 nm over multiple angles. The Independent of the anticipated degree of polymerization (12.5–100) of the enantiopure polymers, the polymers became insoluble and formed structures, with a similar size and homogeneous size distributions in DMF.

Sample #1 was further analyzed by scanning electron microscopy (SEM). Figure 7.1 shows the dried polymer. #1 precipitated in flakes with a size below 1 μm . SEM further visualized a layered structure of the flakes. The size difference between DLS results and the SEM image is most probable explained by agglomeration of the sample during preparation on the SEM grit.

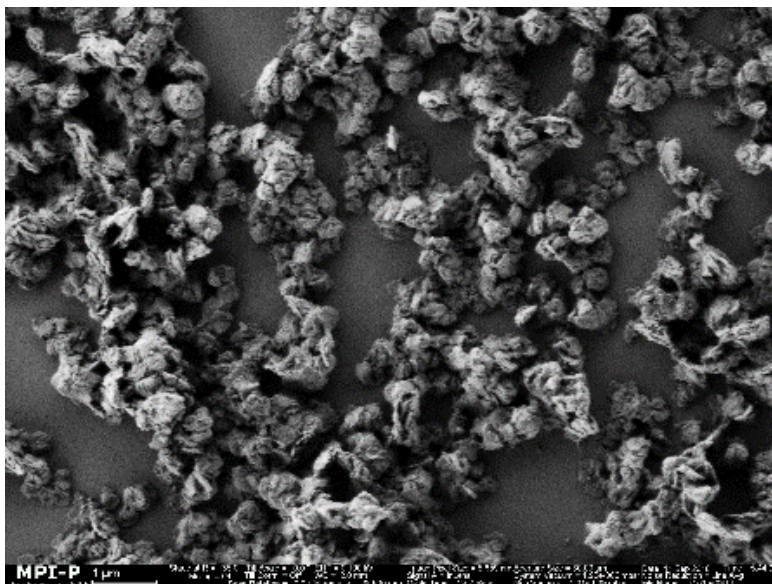


Figure 7.1: SEM of #1. Prepared by drop cast a diluted DMF dispersion of #1 on a SEM grid followed by evaporation of DMF at room temperature.

To mediate the solubility of the polymers the degree of enantiomeric excess was decreases from 98% down to 20% to see, how the tacticity limits the solubility of the polysulonylamines. Table 7.2 shows the conducted polymerizations of the tosyl-activated monomer (S)**3** copolymerized with the racemic monomer rac-TsMAz.

Table 7.2: Summary of conducted co-polymerizations of 3 with varying *e.e.*

Experiment	<i>e.e.</i> ^a / %	DP ^b	M_n^b / g mol ⁻¹	M_n^c / g mol ⁻¹	\bar{D}^c
#1	+98	100	21.400	n.d.	n.d.
#6	+87.5	100	21.400	n.d.	n.d.
#7	+75	100	21.400	n.d.	n.d.
#8	+50	100	21.400	6800	1.12
#9	+20	100	21.400	5700	1.10

Experiments conducted with 10 wt% monomer concentration in DMF. ^a enantiomeric excess of the monomer was determined *via* HPLC; mixing the monomer with its racemic analog gave a reduced *e.e.*. ^b Theoretical value, ^c Number-average molecular weight and molecular weight dispersities determined *via* SEC in DMF (vs. PEO standards). n.d.: not determined

Variation of the enantiomeric excess of the monomers gave consequently polymers with a different amount of isotactic side groups. It appeared, that an *e.e.* above 50% leads to insoluble polymers. An *e.e.* of 50% or lower still allows a proper solubilization in DMF. SEC of the polymers #8 and #9 has an excellent narrow molecular weight distribution (see Figure S 12 and S 13).

To analyse the optical activity of the polymers, CD-spectroscopy was used. The polymers were precipitated into diethyl ether and dried under high vacuum to fully remove traces of DMF. DMF does not allow CD-spectroscopy below 250 nm, as it absorbs light in this region. The obtained powder was then dissolved under ultrasound in dry acetonitrile with 1 g/L to give a milky dispersion. The dispersion was further diluted by 1/10th in ACN. CD-spectra were taken from 180 nm to 350 nm, see figure 7.2.

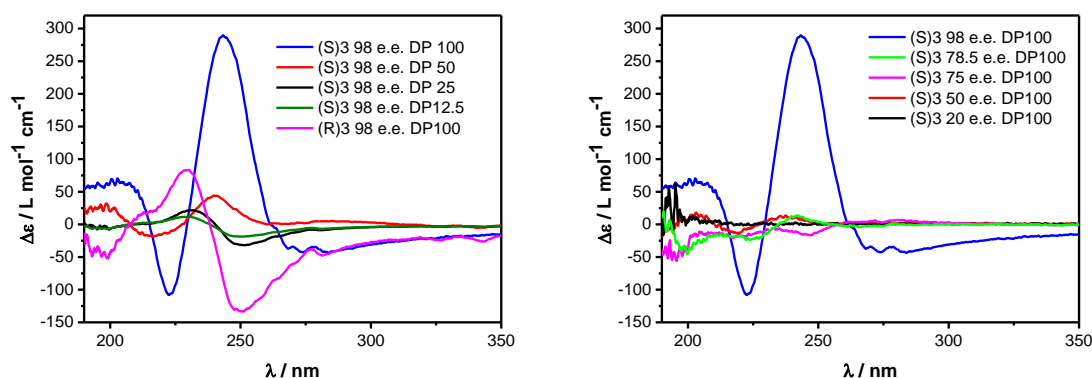


Figure 7.2: CD Absorption spectra of homopolymers with 98%*e.e.* and varying DP from 12.5 to 100 (left side). CD Absorption spectra of copolymers with varying *e.e.* DP: 100 (right side)

This procedure was repeated for all samples. The polymer from (S)**3** with 100 RU (blue spectrum) shows an intense positive signal at 243 nm, followed by a minimum at 222 nm. Two positive signals can be seen additionally at 270 nm and 277 nm, both are weak in intensity. Decreasing the RU of the polymer to 50 RU (red spectrum) shows the similar pattern, but much weaker in intensity. Decreasing the RU even further over 25 to 12.5 RU shows spectra different to the blue spectra and lower in intensity.

The comparison of the CD-spectra of polymers with high *e.e.* and different degree of polymerization shows that a high DP is required to that polyaziridines form a secondary structure. Additionally, shown in figure 7.2 (left side) the maxima and minima of (S)**3** with 100 RU are reversed to the (S)**3** with 100 RU. The mirrored maxima indicate the formation of structure with opposite chirality e.g. a helix. Figure 1 right spectra compares the CD-spectra of Poly(S)**3** with 100 RU and a decreasing enantiomeric excess. The intensity of the maxima decreases significantly if *e.e.* is lower than 98%. This indicates, that polymers do not form any secondary structure if the tacticity of the side groups is not highly isotactic.

7.4 Summary

Different enantiopure aziridines were synthesized and the enantiomeric excess was determined for (R)**3** and (S)**3**. Polymerizations of (R) and (S)**3** activated with tosyl groups were successful. The obtained polymers meet the literature finding that enantiopure polyaziridines are hardly soluble in most solvents. We observed polymers with RU greater than 12.5 cannot be analyzed by standard SEC techniques as solubility is limited. However, we were able to obtain and analyze a homogeneous dispersion of polyaziridine particles in DMF after polymerization of enantiopure aziridines. CD-spectroscopy further proved the polymers to be optical active and showed evidence, that the polymers form a helical structure in ACN. We believe, that using different activation groups and testing other side groups like monomer **4**, **5**, **6** may be useful to overcome the issues of limited solubility of isotactic poly sulfonamides. We further see a huge potential to study chiral polyamides / amines in respect to their potential catalytic activity.

7.5 References Chapter 7

1. A. A. Vedenov, A. M. D., M. D. Frank-Kamenetskii, The Helix-Coil Transition in DNA. *Sov. Phys. Usp.* **1972**, *14* (6), 715-736.
2. Feigon, D. E. G. a. J., Multistrained DNA Structures. **1999**, *9*, 305-314.
3. Bonduelle, C., Secondary structures of synthetic polypeptide polymers. *Polymer Chemistry* **2018**, *9* (13), 1517-1529.
4. Pauling, L.; Corey, R. B.; Branson, H. R., The structure of proteins: two hydrogen-bonded helical configurations of the polypeptide chain. *Proceedings of the National Academy of Sciences* **1951**, *37* (4), 205-211.
5. Natta, G.; Pino, P.; Corradini, P.; Danusso, F.; Mantica, E.; Mazzanti, G.; Moraglio, G., Crystalline high polymers of α -olefins. *Journal of the American Chemical Society* **1955**, *77* (6), 1708-1710.
6. Eiji Yashima, K. M., Chirality-Responsive Helical Polymers. *Macromolecules* **2008**, *41* (1), 3-12.
7. Eiji Yashima, K. M., Hiroki Iida, Yoshio Furusho, and Kanji Nagai, Helical Polymers: Synthesis, Structures, and Functions. *Chem. Rev.* **2009**, *109* (11), 6102-6211.
8. Yashima, E., Synthesis and structure determination of helical polymers. *Polymer Journal* **2010**, *42* (1), 3-16.
9. Cutter, A. R.; Hayes, J. J., A brief review of nucleosome structure. *FEBS Lett* **2015**, *589* (20 Pt A), 2914-22.
10. Odian, G., *Principles of Polymerization*. John Wiley & Sons: New Jersey, USA, 2004.
11. Gleede, T.; Reisman, L.; Rieger, E.; Mbarushimana, P. C.; Rupar, P. A.; Wurm, F. R., Aziridines and azetidines: building blocks for polyamines by anionic and cationic ring-opening polymerization. *Polymer Chemistry* **2019**, *10* (24), 3257-3283.
12. Hadjichristidis, N.; Pitsikalis, M.; Pispas, S.; Iatrou, H., Polymers with complex architecture by living anionic polymerization. *Chemical reviews* **2001**, *101* (12), 3747-3792.
13. Hadjichristidis, N.; Pispas, S.; Floudas, G., *Block copolymers: synthetic strategies, physical properties, and applications*. John Wiley & Sons: 2003.
14. Baskaran, D.; Müller, A. H. E., Anionic vinyl polymerization - 50 years after Michael Szwarc. *Progress in Polymer Science* **2007**, *32* (2), 173-219.
15. Herzberger, J.; Niederer, K.; Pohlit, H.; Seiwert, J.; Worm, M.; Wurm, F. R.; Frey, H., Polymerization of Ethylene Oxide, Propylene Oxide, and Other Alkylene Oxides: Synthesis, Novel Polymer Architectures, and Bioconjugation. *Chem. Rev.* **2016**, *116* (4), 2170-243.
16. Rieger, E.; Alkan, A.; Manhart, A.; Wagner, M.; Wurm, F. R., Sequence-Controlled Polymers via Simultaneous Living Anionic Copolymerization of Competing Monomers. *Macromol. Rapid Commun.* **2016**, *37* (10), 833-9.
17. Rieger, E.; Blankenburg, J.; Grune, E.; Wagner, M.; Landfester, K.; Wurm, F. R., Controlling the Polymer Microstructure in Anionic Polymerization by Compartmentalization. *Angewandte Chemie International Edition*, n/a-n/a.
18. Rieger, E.; Gleede, T.; Weber, K.; Manhart, A.; Wagner, M.; Wurm, F. R., The living anionic polymerization of activated aziridines: a systematic study of reaction conditions and kinetics. *Polym. Chem.* **2017**, *8* (18), 2824-2832.
19. Rieger, E.; Gleede, T.; Manhart, A.; Lamla, M.; Wurm, F. R., Microwave-Assisted Desulfonylation of Polysulfonamides toward Polypropylenimine. *ACS Macro Letters* **2018**, 598-603.
20. Rieger, E.; Manhart, A.; Wurm, F. R., Multihydroxy Polyamines by Living Anionic Polymerization of Aziridines. *ACS Macro Letters* **2016**, *5* (2), 195-198.
21. Thomi, L.; Wurm, F. R., Living Anionic Polymerization of Functional Aziridines. *Macromolecular Symposia* **2015**, *349* (1), 51-56.
22. Gleede, T.; Rieger, E.; Liu, L.; Bakkali-Hassani, C.; Wagner, M.; Carlotti, S.; Taton, D.; Andrienko, D.; Wurm, F. R., Alcohol- and Water-Tolerant Living Anionic Polymerization of Aziridines. *Macromolecules* **2018**, *51* (15), 5713-5719.
23. Sweeney, J. B.; Cantrill, A. A., Preparation and ring-opening reactions of N,O-bis(diphenylphosphinyl) hydroxymethylaziridine ('Di-Dpp'). *Tetrahedron* **2003**, *59* (21), 3677-3690.
24. Sweeney, J. B., Aziridines: epoxides' ugly cousins? *Chem. Soc. Rev.* **2002**, *31* (5), 247-258.
25. Buckley, B. R.; Patel, A. P.; Wijayantha, K. G., Observations on the modified Wenker synthesis of aziridines and the development of a biphasic system. *J Org Chem* **2013**, *78* (3), 1289-92.

26. Stewart, I. C.; Lee, C. C.; Bergman, R. G.; Toste, F. D., Living ring-opening polymerization of N-sulfonylaziridines: synthesis of high molecular weight linear polyamines. *J. Am. Chem. Soc.* **2005**, *127* (50), 17616-7.
27. Thomi, L.; Wurm, F. R., Aziridine Termination of Living Anionic Polymerization. *Macromol Rapid Commun* **2014**, *35* (5), 585-9.
28. Reisman, L.; Mbarushimana, C. P.; Cassidy, S. J.; Rugar, P. A., Living Anionic Copolymerization of 1-(Alkylsulfonyl)aziridines to Form Poly(sulfonylaziridine) and Linear Poly(ethylenimine). *ACS Macro Letters* **2016**, *5* (10), 1137-1140.
29. Mbarushimana, P. C.; Liang, Q.; Allred, J. M.; Rugar, P. A., Polymerizations of Nitrophenylsulfonyl-Activated Aziridines. *Macromolecules* **2018**, *51* (3), 997-983.
30. Reisman, L.; Rowe, E. A.; Jackson, E. M.; Thomas, C.; Simone, T.; Rugar, P. A., Anionic Ring-Opening Polymerization of N-(tolylsulfonyl)azetidines To Produce Linear Poly(trimethylenimine) and Closed-System Block Copolymers. *Journal of the American Chemical Society* **2018**, *140* (46), 15626-15630.
31. Gleede, T. W., R. F., Unpublished
32. Beekmans, L.; Hempenius, M. A.; Vancso, G. J., Morphological development of melt crystallized poly(propylene oxide) by in situ AFM: formation of banded spherulites. *European polymer journal* **2004**, *40* (5), 893-903.
33. N. Spassky, P. S., Stereoselective Polymerization of Propylene Sulphide. *European Polymer Journal* **1971**, *7*, 7-16.
34. Kobayashi, S., Ethyleneimine Polymers. *Prog. Polym. Sci.* **1990**, *15*, 751-823.
35. Hajos, Z. G.; Parrish, D. R., Asymmetric synthesis of bicyclic intermediates of natural product chemistry. *The Journal of Organic Chemistry* **1974**, *39* (12), 1615-1621.
36. Ulrich Eder, G. S., Rudolf Wiechert, New Type of Asymmetric Cyclization to Optically Active Steroid CD Partial Structures. *Angew. Chem.* **1971**, *10* (7).
37. Wang, W.; Ye, L.; Shi, Z.; Zhao, Z.; Li, X., Enantioselective Michael addition of malonates to α,β -unsaturated ketones catalyzed by 1,2-diphenylethanediamine. *RSC Advances* **2018**, *8* (73), 41699-41704.
38. Sonsona, I. G.; Marqués-López, E.; Gimeno, M. C.; Herrera, R. P., First aromatic amine organocatalysed activation of α,β -unsaturated ketones. *New Journal of Chemistry* **2019**, *43* (31), 12233-12240.
39. Xu, L. W.; Luo, J.; Lu, Y., Asymmetric catalysis with chiral primary amine-based organocatalysts. *Chem Commun (Camb)* **2009**, (14), 1807-21.
40. Wurz, R. P., Chiral Dialkylaminopyridine Catalysts in Asymmetric Synthesis. *Chem. Rev.* **2007**, *107* (12), 5570-5595.
41. Stefan France, D. J. G., Scott J. Miller, and Thomas Lectka, Nucleophilic Chiral Amines as Catalysts in Asymmetric Synthesis. *Chem. Rev.* **2003**, *103* (8), 2985-3012.
42. Vicario, J. L.; Badía, D.; Carrillo, L., An improved procedure for the preparation of chiral nonracemic N-tosyl-2-alkylaziridines and N, 2-dialkylaziridines on multigram-scale. *Arkivoc* **2007**, *4*, 304-311.

7.6 Supporting Information for Tacticity control in poly(sulfonyl aziridine)s: Towards tuning crystallinity and supramolecular interactions

7.6.1 HPLC elution volumes of (rac) TsMAz and pure enantiomers

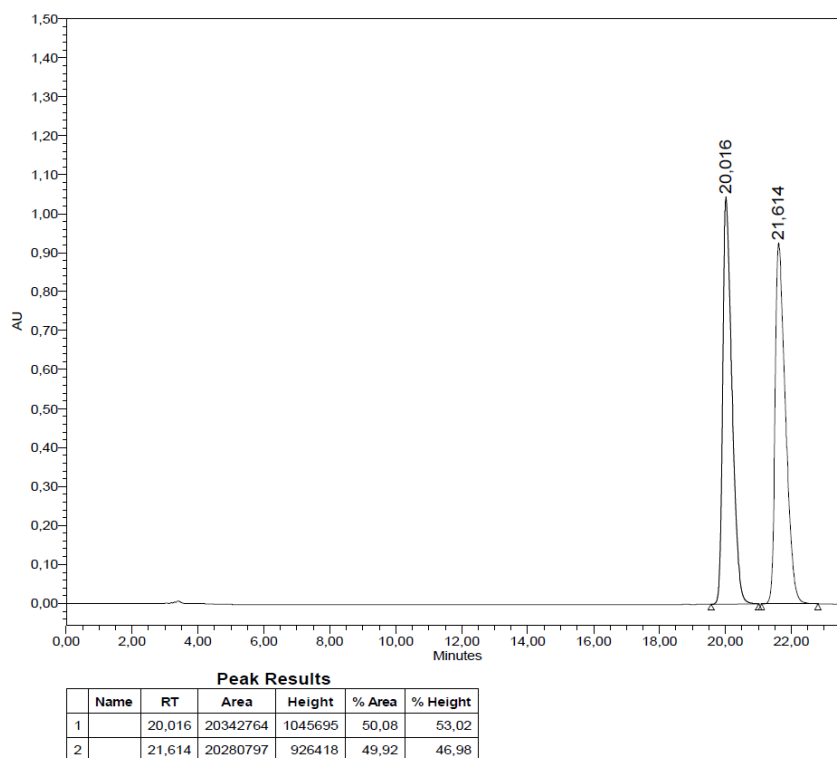


Figure S 7.1: HPLC trace of (rac) TsMAz using Amylose tris(3-chloro-4-methylphenylcarbamate)-immobilized on 3 μ m silica gel at 25°C and 1 mL / min in hexane / EtOH 95/5, showing baseline separation of the two enantiomers at 20.0 min (R3) and 21.6 min (S3).

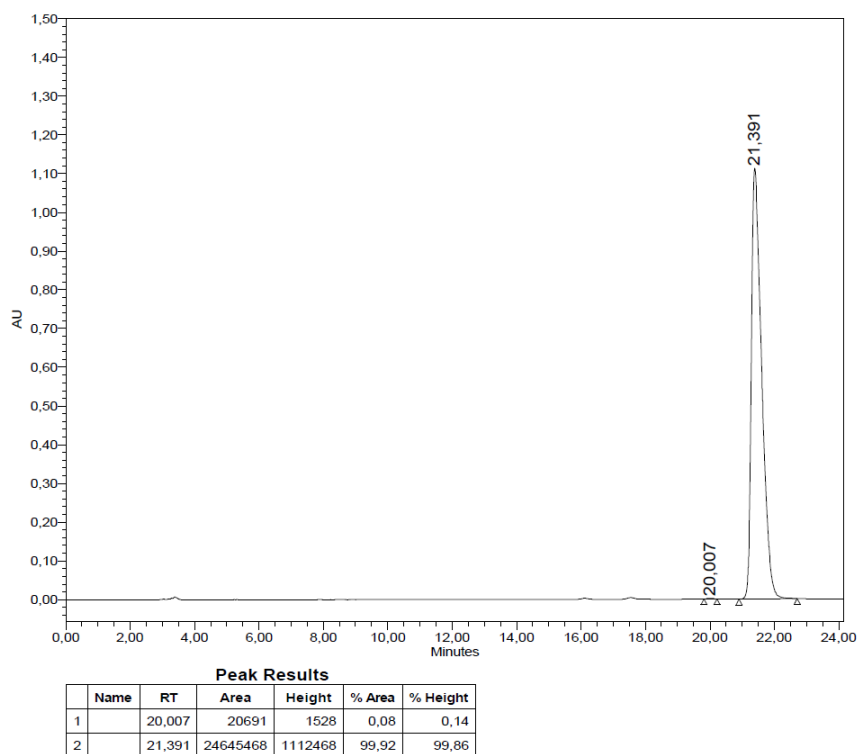


Figure S 7.2: HPLC trace of (S) (+) TsMAz using Amylose tris(3-chloro-4-methylphenylcarbamate)immobilized on 3 μ m silica gel at 25°C and 1 mL / min in hexane / EtOH 95/5, showing the (S3) enantiomer at 21.4 min with an ee of 99%.

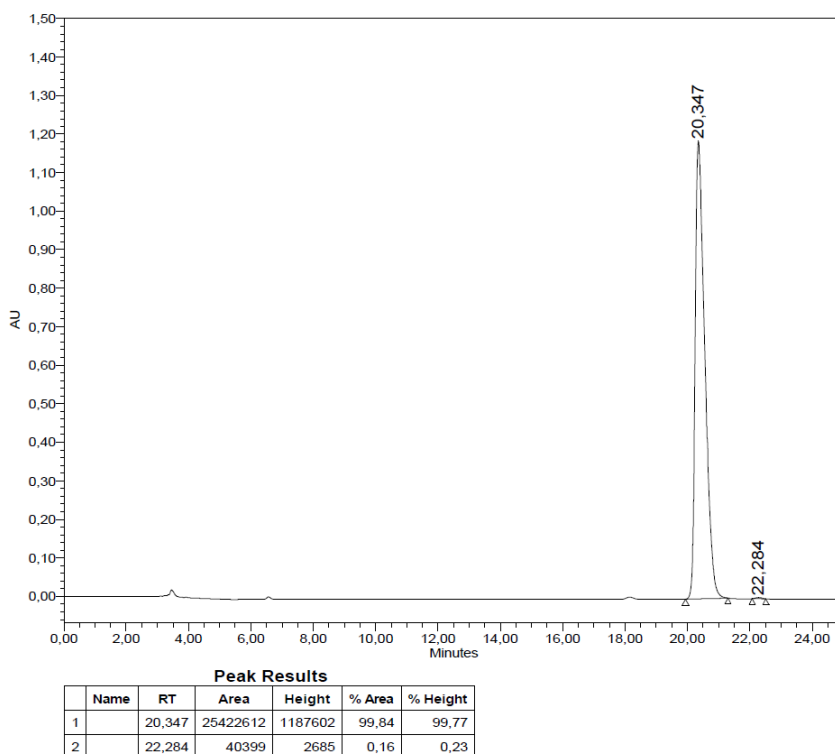


Figure S 7.3: HPLC trace of (S) (-) TsMAz using Amylose tris(3-chloro-4-methylphenylcarbamate)immobilized on 3 μ m silica gel at 25°C and 1 mL / min in hexane / EtOH 95/5, showing the (R3) enantiomer at 20.34 min with an ee of 99%.

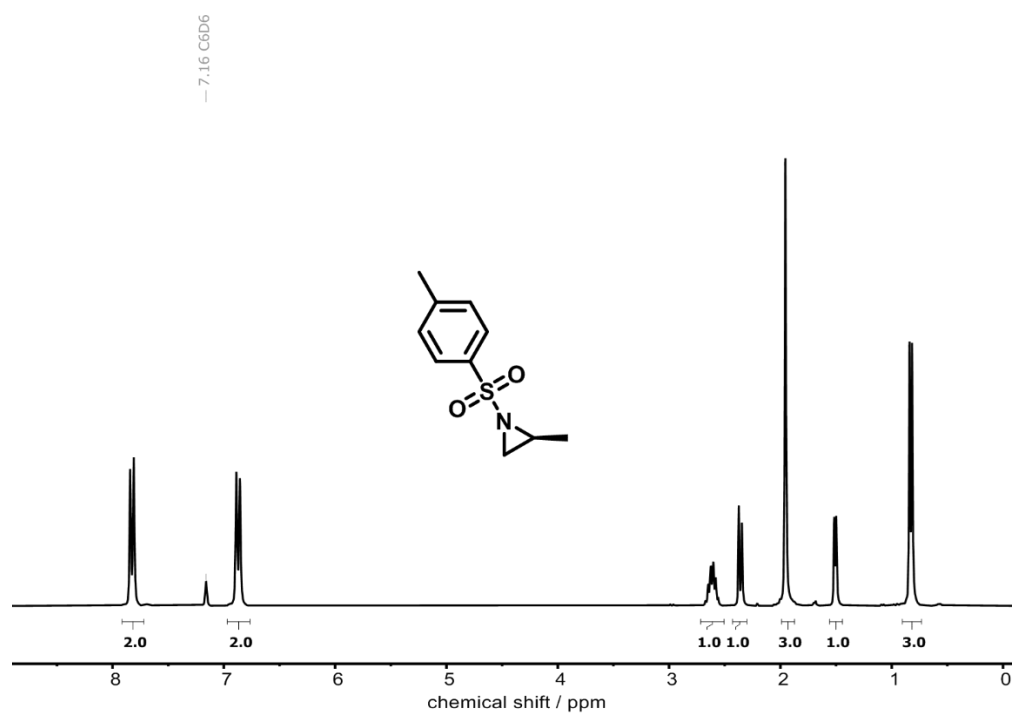
7.6.2 ^1H NMR of monomers

Figure S 7.4: ^1H NMR of (S)3 with a tosyl activating group (250 MHz, Benzene- d_6) δ 7.83 (d, $J = 8.0$ Hz, 2H), 6.87 (d, $J = 8.0$ Hz, 2H), 2.72 – 2.51 (m, 1H), 2.36 (d, $J = 6.9$ Hz, 1H), 1.95 (s, 3H), 1.51 (d, $J = 4.5$ Hz, 1H), 0.83 (d, $J = 5.6$ Hz, 3H)

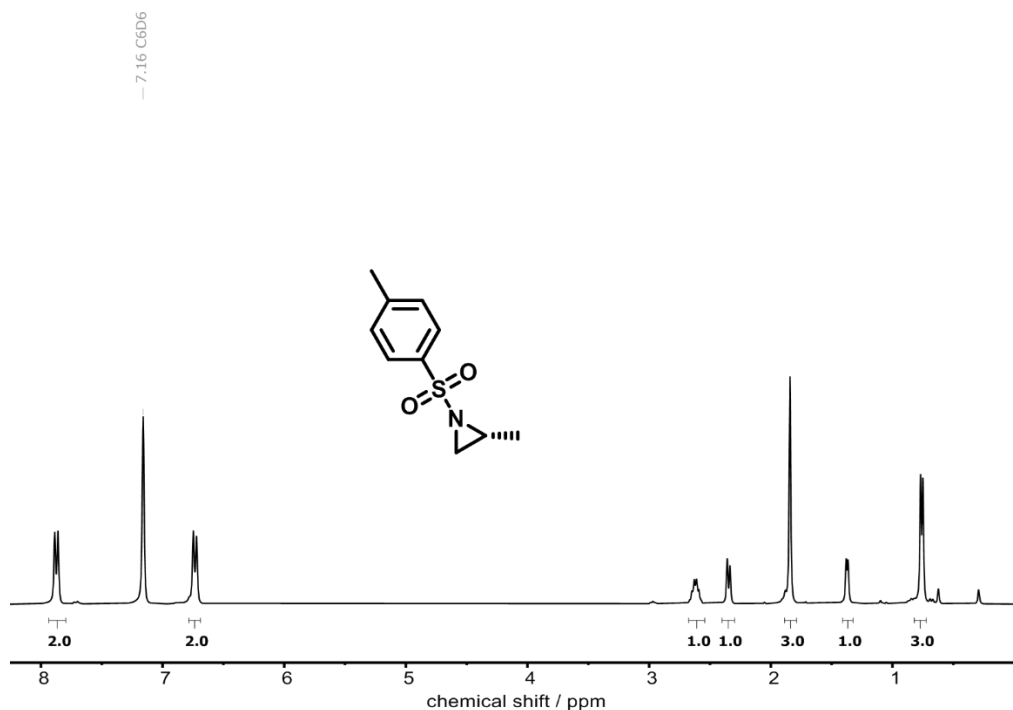


Figure S 7.5: ^1H NMR of (R)3 with a tosyl activating group (300 MHz, Benzene- d_6) δ 7.94 – 7.80 (m, 2H), 6.73 (d, $J = 7.9$ Hz, 2H), 2.62 (h, $J = 5.7$ Hz, 1H), 2.40 – 2.30 (m, 1H), 1.84 (s, 3H), 1.37 (d, $J = 4.5$ Hz, 1H), 0.82 – 0.72 (m, 3H).

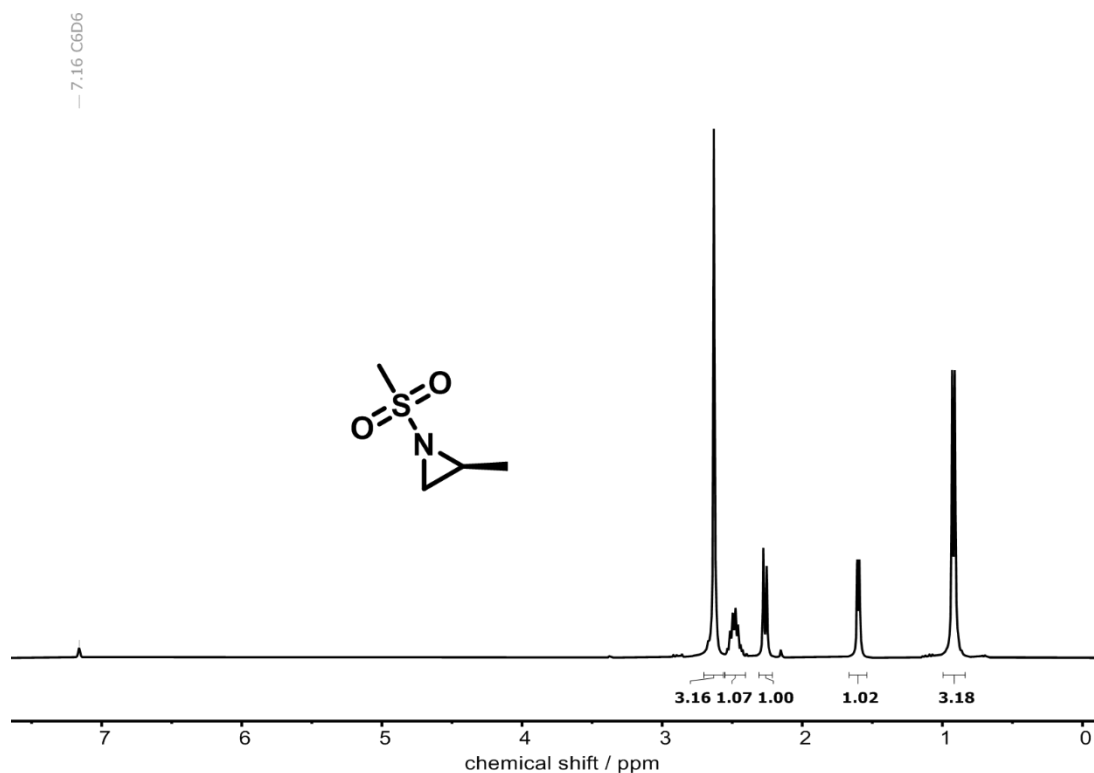


Figure S 7.6: ^1H NMR of (S)3 containing a mesyl activating group (300 MHz, Benzene- d_6) δ 2.63 (s, 3H), 2.55 – 2.39 (m, 1H), 2.27 (d, J = 7.0 Hz, 1H), 1.60 (d, J = 4.6 Hz, 1H), 0.92 (d, J = 5.6 Hz, 3H).

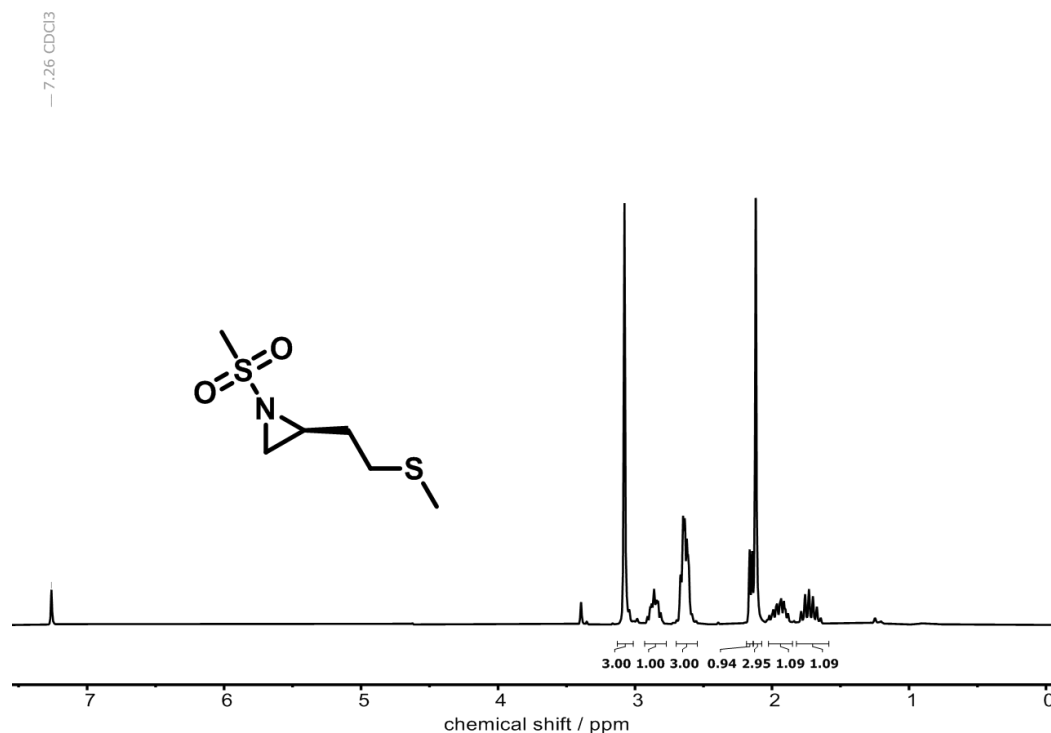


Figure S 7.7: ^1H NMR (250 MHz, Chloroform- d) δ 3.08 (s, 3H), 2.85 (tq, J = 8.4, 4.3, 3.7 Hz, 1H), 2.63 (qd, J = 7.3, 6.0, 3.6 Hz, 3H), 2.15 (d, J = 4.5 Hz, 1H), 2.12 (s, 3H), 1.95 (dtd, J = 14.8, 7.5, 4.8 Hz, 1H), 1.73 (dt, J = 14.3, 7.1 Hz, 1H).

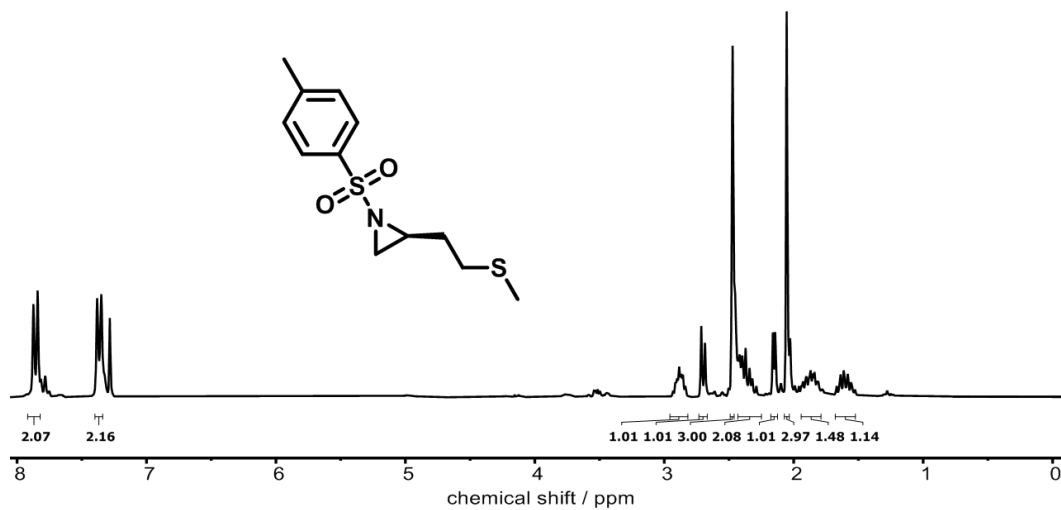


Figure S 7.8: ¹H NMR (250 MHz, Chloroform-*d*) δ 7.86 (d, $J = 8.0$ Hz, 2H), 7.37 (d, $J = 7.9$ Hz, 2H), 2.88 (td, $J = 7.6, 3.8$ Hz, 1H), 2.70 (d, $J = 7.0$ Hz, 1H), 2.43 – 2.25 (m, 2H), 2.15 (d, $J = 4.5$ Hz, 1H), 2.05 (s, 3H), 1.88 (ddd, $J = 15.6, 8.5, 3.9$ Hz, 1H), 1.68 – 1.52 (m, 1H).

7.6.3 Dynamic light scattering of polymer dispersions

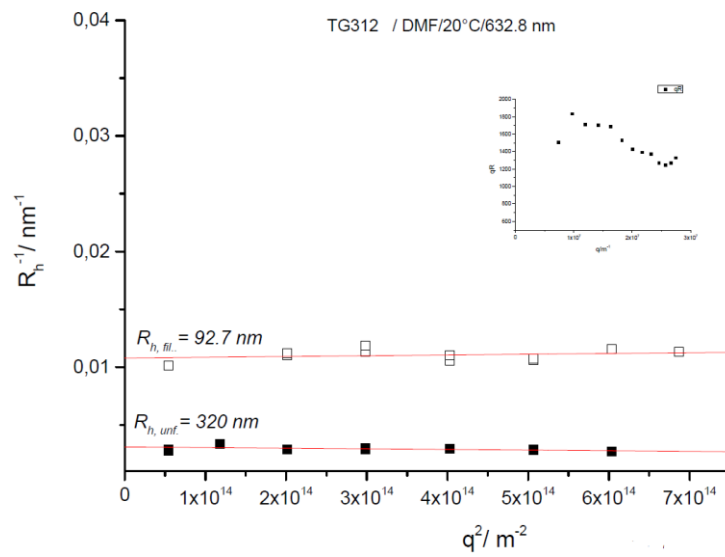


Figure S 7.9: DLS of Poly(S)3, with 100 RU (#1) in DMF.

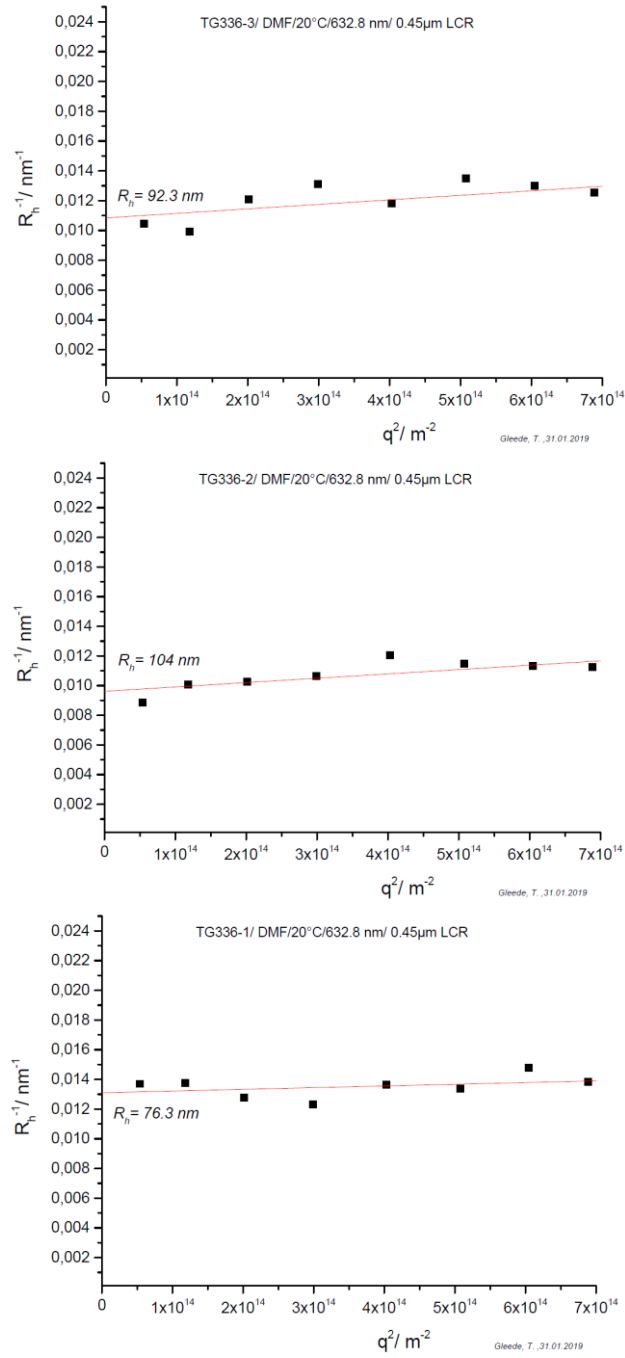


Figure S 7.10: DLS of #4, #3, #2 with 100 RU in DMF.

7.6.4 Size exclusion elugrams of solubil enantio rich polyaziridines

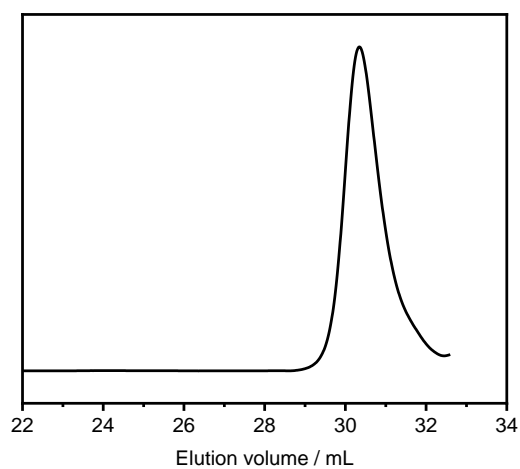


Figure S 7.11: SEC of #4, in DMF.

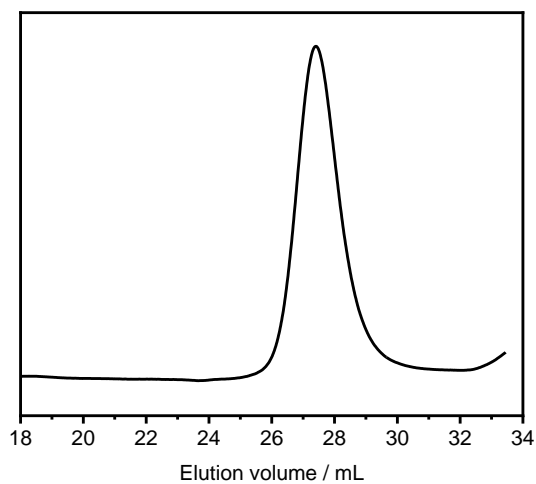


Figure S 7.12: SEC of #9, in DMF.

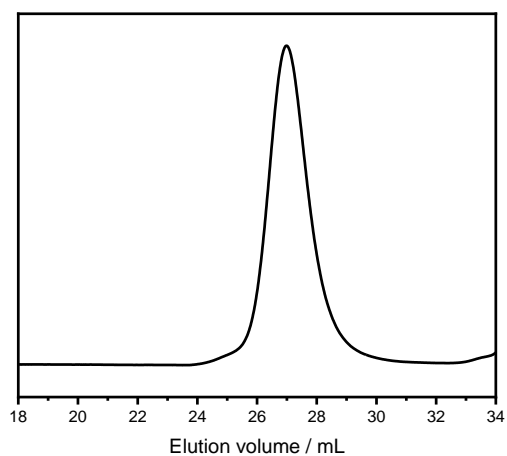


Figure S 7.13: SEC of #10, in DMF.

8 Appendix

8.1 Publications of Cooperation Projects

During the time working on my PhD thesis, several cooperation projects (C. P.), with my participation were conducted. Those that were successfully published are presented in this section in paper format.

C.P. 1: Polymerization kinetics of activated aziridines

“The Living Anionic Polymerization of Activated Aziridines: Systematic Study of Reaction Conditions and Kinetics” published in: *Polymer Chemistry*, 2017, 8, 2824–2832, written by: Elisabeth Rieger, Tassilo Gleede, Katja Weber, Angelika Manhart, Manfred Wagner and Frederik R. Wurm

C.P. 2: Desulfonylation of polysulfonamides

“Microwave-Assisted Desulfonylation of Polysulfonamides toward Polypropylenimine” published in: *ACS Macro. Letters* 2018, 7, (6), 598–603, written by: Elisabeth Rieger, Tassilo Gleede, Angelika Manhart and Frederik R. Wurm

C.P. 3: Carbene catalyzed selective initiation of aziridines

“Selective Initiation from Unprotected Aminoalcohols for the N-Heterocyclic Carbene-Organocatalyzed Ring-Opening Polymerization of 2-Methyl-N-tosyl Aziridine: Telechelic and Block Copolymer Synthesis” published in: *Macromol.* **2018**, 51, (7), 2533–2541., written by: Camille Bakkali-Hassani, Clément Coutouly, Tassilo Gleede, Joan Vignolle, Frederik R. Wurm, Stéphane Carlotti and Daniel Taton

C.P. 4: Ruthenocenyl Glycidyl Ether for anionic polymerization

“Ruthenocenyl Glycidyl Ether: A Ruthenium-Containing Epoxide for Anionic Polymerization” published in: *Organometallics* 2017, 36, 3023–3028, written by: Arda Alkan, Tassilo Gleede, and Frederik R. Wurm

C.P. 1: Polymerization kinetics of activated aziridines

Polymer
Chemistry

PAPER

View Article Online
View Journal | View IssueCite this: *Polym. Chem.*, 2017, **8**,
2824The living anionic polymerization of activated
aziridines: a systematic study of reaction
conditions and kinetics†Elisabeth Rieger, Tassilo Gleede, Katja Weber, Angelika Manhart, Manfred Wagner
and Frederik R. Wurm *

"A living race" – polymerization kinetics of anionic polymerizations depends strongly on the solvent polarity and reactivity of the growing chain end. Both the carb- and oxyanionic polymerization is under control at the university lab and on the industrial level, however, no information for the aza-anionic polymerization of aziridines has been reported systematically. This work studies the polymerization of two activated aziridines (2-methyl-*N*-mesylaziridine (MsMAz) and 2-methyl-*N*-tosylaziridine (TsMAz)) by real-time ¹H NMR spectroscopy. This technique allows monitoring the consumption of the monomer precisely during the polymerization under different conditions (temperature, solvent, initiator and counter-ion variation). From the experimental data, propagation rate constants (k_p) were calculated and analyzed. The polymerization of MsMAz was monitored at different temperatures (20, 50, and 100 °C). The increase of temperature increases the speed of polymerization, but keeps the living behavior. Furthermore, the influence of different solvents on the polymerization speed was examined, proving solvating solvents such as DMSO and DMF as the fastest solvents. Two different initiators, the potassium salts of *N,N'*-(1,4-phenylenebis(methylene))dimethanesulfonamide (BnBis(NHMs)), the first bifunctional initiator for the AROP of aziridines, and of *N*-benzyl-sulfonamide (BnNHMs) were compared. The variation of the counter ions Li⁺, Na⁺, K⁺, and Cs⁺ (generated from the respective bis(trimethylsilyl)amide salts) proved successful polymerization of both monomers with all counter ions. Slight variations have been detected in the order: Cs⁺ > Li⁺ > Na⁺ > K⁺, which is in strong contrast for the AROP of epoxides, shows a strong gegenion-dependent kinetic profile. This allows the use of commercially available initiators, such as BuLi for the synthesis of PAz. With these results in hand, the azaanionic polymerization can be used as a valuable tool in the family of anionic polymerization for the preparation of structurally diverse polysulfonamides and polyamines under a broad variety of conditions, while maintaining the living behavior.

Received 14th March 2017,
Accepted 5th April 2017DOI: 10.1039/c7py00436b
rsc.li/polymers

Introduction

The knowledge of polymerization kinetics allows us to construct complex polymeric architectures by different polymerization techniques. 60 years after the discovery of the living anionic polymerization, their solvent, counter ion and temperature dependencies are taught in introductory polymer classes. Conditions are known for the carb- and oxyanionic polymerization.^{1–3}

However, such detailed and fundamental investigations are missing for the living anionic ring-opening polymerization (AROP) of aziridines and will be presented in this work.

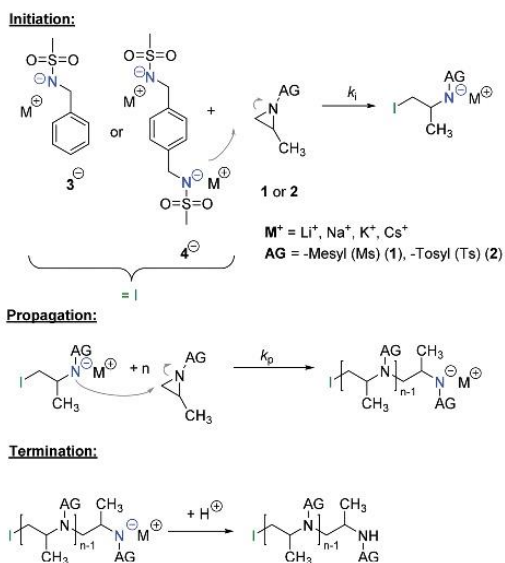
The azaanionic polymerization of activated aziridines was recently established.^{4–9} To enable anionic polymerization of aziridines, the acidic proton at the nitrogen needs to be substituted by an activating group, e.g. a sulfonamide group (Scheme 1). To date, only such activated aziridines undergo anionic polymerization, but also a few other aziridine-containing polymers have been prepared and studied as functional polymers for postmodification.^{10–14}

The AROP of aziridines allows us to prepare well-defined poly(ethylene imine) derivatives.^{4,9} We have developed new monomers and initiator-systems during the last few years, expanding this still rather unexplored approach to polysulfonamides and amines.^{5–8,15,16}

With a similar ring-strain of 111 kJ mol^{−1} for ethylene imine as for ethylene oxide (114 kJ mol^{−1}), the anionic ring-opening polymerization should be feasible.^{17,18} In contrast to unsubstituted ethylene imine, which can only be polymerized

Max-Planck-Institut für Polymerforschung (MPI-P), Ackermannweg 10,
D-55128 Mainz, Germany. E-mail: wurm@mpip-mainz.mpg.de

† Electronic supplementary information (ESI) available. See DOI: 10.1039/c7py00436b



Scheme 1 Mechanism of the living anionic ring-opening polymerization of activated aziridines (AG = activation group).

via a cationic mechanism, leading to branched PEI (poly(ethylene imine)),¹⁹ *N*-protected aziridines can also be polymerized anionically, due to their activating group. The sulfonamide substitutes the acidic proton at the aziridine and acts as an electron-withdrawing group. This results not only in the general possibility for anionic AROP, but further in different reactivities of the monomers, leading to sequential incorporation.⁷

Herein, 2-methyl-*N*-mesyl-aziridine (MsMAz, 1) and 2-methyl-*N*-tosylaziridine (TsMAz, 2) were used to elucidate the polymerization kinetics under different conditions. The results from this study will allow us to use activated aziridines for the preparation of well-defined polymer architectures by anionic polymerization in the future.

Experimental section

Chemicals

All solvents and reagents were purchased from Sigma-Aldrich, Acros Organics or Fluka and used as received unless otherwise mentioned. All deuterated solvents were purchased from Deutero GmbH and were distilled from CaH_2 or sodium and stored in a glovebox prior to use. All monomers and initiators were dried extensively by azeotropic distillation with benzene prior to polymerization. Cesium bis(trimethylsilyl)amide was synthesized according to a literature protocol.^{4,20} 2-Methyl-*N*-mesyl-aziridine (MsMAz, 1), 2-methyl-*N*-tosylaziridine (TsMAz, 2) and *N*-benzyl methanesulfonamide (BnNHMs, 3) were synthesized according to our previously published protocol.⁷ The

synthesis of the bifunctional initiator (BnBis(NHMs), 4) can be found in the ESI†

Methods

NMR. ¹H NMR spectra were recorded using a Bruker Avance III 250, a Bruker Avance 300, a Bruker Avance III 500 or a Bruker Avance III 700. All spectra were referenced internally to residual proton signals of the deuterated solvent.

SEC. Size exclusion chromatography (SEC) measurements of standard polymers were performed in DMF (1 g L⁻¹ LiBr added) at 60 °C and a flow rate of 1 mL min⁻¹ with a PSS SECURITY as an integrated instrument, including a PSS GRAM 100–1000 column and a refractive index (RI) detector. Calibration was carried out using poly(ethylene glycol) standards provided by Polymer Standards Service. For polymers from the NMR-kinetics size exclusion chromatography measurements were performed in DMF (containing 0.25 g L⁻¹ of lithium bromide as an additive) with an Agilent 1100 series as an integrated instrument, including a PSS HEMA column (106/105/104 g mol⁻¹), a UV detector (275 nm), and a RI detector at a flow rate of 1 mL min⁻¹ at 50 °C. Calibration was carried out using PEO standards provided by Polymer Standards Service.

MALDI-TOF. Matrix-assisted laser desorption/ionization time-of-flight (MALDI-TOF) measurements were performed using a Shimadzu Axima CFR MALDI-TOF mass spectrometer, employing DCTB (*trans*-2-[3-(4-*tert*-butylphenyl)-2-methyl-2-propenylidene] malononitrile) as a matrix (5 mg mL⁻¹ in THF).

General procedure for the azaanionic polymerization. All Schlenk flasks were flame dried *in vacuo* at least three times, using the Schlenk technique, as for the following steps. All reactants (except the bis(trimethylsilyl)amide salts) were freeze-dried from benzene *in vacuo* for at least 4 h. The monomers and the initiator were dissolved in 2 and 1 mL anhydrous *N,N*-dimethylformamide (DMF). The bis(trimethylsilyl)amide salt was added quickly in argon-counter flow to the initiator-solution. From the initiator-solution the appropriate volume was added to the monomer solution. The mixture was stirred at the desired temperature and over the desired time (to ensure complete reaction: 18 h reaction time at 50 °C). The polymers were obtained as colorless powders after precipitation of the reaction mixture into 30 mL methanol and drying at reduced pressure. For chain extension experiments the polymerizations were carried out in analogy to the conventional procedure. After stirring the mixtures for at least 18 h, a 100 μL-sample was taken out for further analyses and the second monomer, in 1 mL DMF, was added and stirred for further 24 h at the same temperature (SEC traces are summarized in the ESI†).

Monitoring polymerizations by real-time ¹H NMR spectroscopy. All polymerizations were carried out in analogy to the conventional procedure in a Schlenk flask. Inside a glove box under a nitrogen-atmosphere the respective monomer was dissolved as a *ca.* 10 wt% solution in a total volume of 0.7 mL of the respective deuterated solvent, calculated for a monomer to initiator of $[M]_0 : [I]_0 = 30 : 1$, if not otherwise stated. The

initiator-solution in 1 mL deuterated solvent was prepared separately (exemplarily for the polymerization of MsMAz (**1**) (70 mg) in 0.7 mL DMF- d_7 and the initiator-system: BnNHMs (**3**) ((32.0 mg), potassium bis(trimethylsilyl)-amide (KHMS) (34.4 mg) in 1 mL DMF- d_7). A conventional NMR-tube was filled with the reaction mixture and sealed with a rubber-septum. Prior to initiation, the pure monomer-solvent mixture was measured at 50 °C. From the stock solution of the initiator, 100 μ L were added to the monomer mixture, mixed quickly and inserted into the spectrometer. All ^1H NMR kinetics were recorded using a Bruker Avance III 700. All spectra were referenced internally to residual proton signals of the deuterated solvent dimethylformamide- d_7 at 8.03 ppm, dimethylsulfoxide- d_6 at 2.50 ppm, tetrahydrofuran- d_8 at 3.58 ppm, benzene- d_6 7.16 ppm, and cyclohexane- d_{12} at 1.38 ppm. The $\pi/2$ -pulse for the proton measurements was 13.1 μ s. The spectra of the polymerizations were recorded at 700 MHz with 32 scans (equal to 404 s (acquisition time of 2.595 s and a relaxation time of 10 s after every pulse)) over a period of at least 3 h. No B-field optimizing routine was used over the kinetic measurement time. The spin-lattice relaxation rate (T_1) of the ring-protons, which are used afterwards for integration, was measured before the kinetic run with the inversion recovery method.²¹

Results and discussion

The AROP of *N*-activated aziridines can be initiated by a deprotonated secondary sulfonamide, which can be formed *in situ* e.g. by the use of bis(trimethylsilyl)amides. This freshly prepared nucleophile opens the ring most likely at its less substituted side and thus forms the propagating sulfonamide anion.⁴ Propagation occurs *via* nucleophilic attack of this azanion at the next monomer and it continues, as long as the monomer is available. As it is a living polymerization, no termination occurs, in the absence of impurities, and controlled termination by adding an electrophile is possible (Scheme 1).^{4,7}

All propagation rates are calculated from the linear first-order kinetic plots, using the equations shown below for living polymerizations (eqn (I) and (II)). Eqn (I) shows the reduction of the monomer concentration $[M]$ over time, $[P^-]$ stands for the number of growing chains and is equivalent to the initiator concentration $[I]$, because in the living anionic polymerization (LAP) each initiating site starts a growing polymer chain ($[P^-] = [I]$). Integration gives the linear eqn (II), therefore plotting $\ln([M]_0/[M]_t)$ versus time results in a straight line, where the slope (k_{app}) gives the propagation rate (k_p), when divided by the original initiator concentration $[I]_0$. First-order kinetics, which are required for simplification of the equation, are evidenced if $\ln([M]_0/[M]_t)$ increases linearly and has already been reported for the LAP of some sulfonyl aziridines.^{2,4}

$$-\frac{d[M]}{dt} = k_p[P^-][M] = k_p[I][M] \quad (\text{I})$$

$$\ln \frac{[M]_0}{[M]_t} = k_{\text{app}}t = k_p[I]_0t \quad (\text{II})$$

However, a systematic kinetic investigation of the AROP has not been reported to date. Here we chose 2-methyl-*N*-mesylaziridine (MsMAz, **1**) and 2-methyl-*N*-tosylaziridine (TsMAz, **2**) as two monomers with different activating groups that alter the monomer reactivity, to study the polymerization in different solvents, namely dimethylsulfoxide (DMSO- d_6), dimethylformamide (DMF- d_7), tetrahydrofuran (THF- d_8), benzene- d_6 and cyclohexane- d_{12} (CyHex) at a constant temperature of 50 °C. In DMF- d_7 also different temperatures (20, 50, and 100 °C) were investigated. Two sulfonamide-based initiators were used and the influence of the counter ions on propagation rates was studied. *N*-Benzyl methanesulfonamide (BnNHMs, **3**), deprotonated by lithium (LiMDS), sodium (NaMDS), potassium (KMDS) and cesium (CsMDS) bis(trimethylsilyl)amide, was used as a monofunctional initiator. *N,N'*-(1,4-Phenylenebis(methylene))dimethanesulfonamide (NBis(NHMs), **4**) was designed as a novel bifunctional initiator for the AROP and also deprotonated with KMDS, which will allow the preparation of ABA triblock copolymers and is currently under investigation in our lab.

Real-time ^1H NMR spectroscopy was used to monitor the polymerization under these different conditions.^{2,2,23} Requirements for this method are reaction times in the range of minutes to hours and reagents with distinguishable resonances in their spectrum (Fig. 1). In *N*-sulfonyl-aziridines, the three ring-protons are detected as two doublets (CH_2) and one multiplet (CH) in the region from 3 to 2 ppm of the ^1H NMR spectrum (Fig. 1A). These chemical shifts are sensitive probes for the monomer reactivity: the more they are shifted downfield in the spectrum, the stronger the activation, *i.e.* the electron-withdrawing effect of the sulfonamide. This allowed us to use the different monomer reactivities and to prepare sequenced copolymers.⁷ As the monomer is consumed during the polymerization, the monomer signals vanish and simultaneously the growing polymer-backbone emerges between 3.5 and 4.5 ppm (Fig. 1B). By integration of the well-separated monomer peaks over time and normalization to the amount of unreacted monomer, plotting of the monomer conversion *vs.* the reaction time or the total conversion is possible (Fig. 1C and D).

The azaanionic polymerization proceeds in a living manner which was proven by chain extension experiments. Both the formation of diblock copolymers of **1** and **2**, and the chain extension of **2** resulted in a complete shift of the molecular weight distributions in SEC experiments and thus underlines the living character of the chain ends (Fig. S16–S19†).

The propagation rate constants k_p were calculated from the integrals of the monomer signals of the first 13 spectra (*ca.* 1.5 h reaction time). For “fast” polymerizations (100% conversion in less than 1 h) only the first 4 values were used for the determination of the slope (equivalent to the apparent propagation rate constant (k_{app})) of the linear fits. Division of

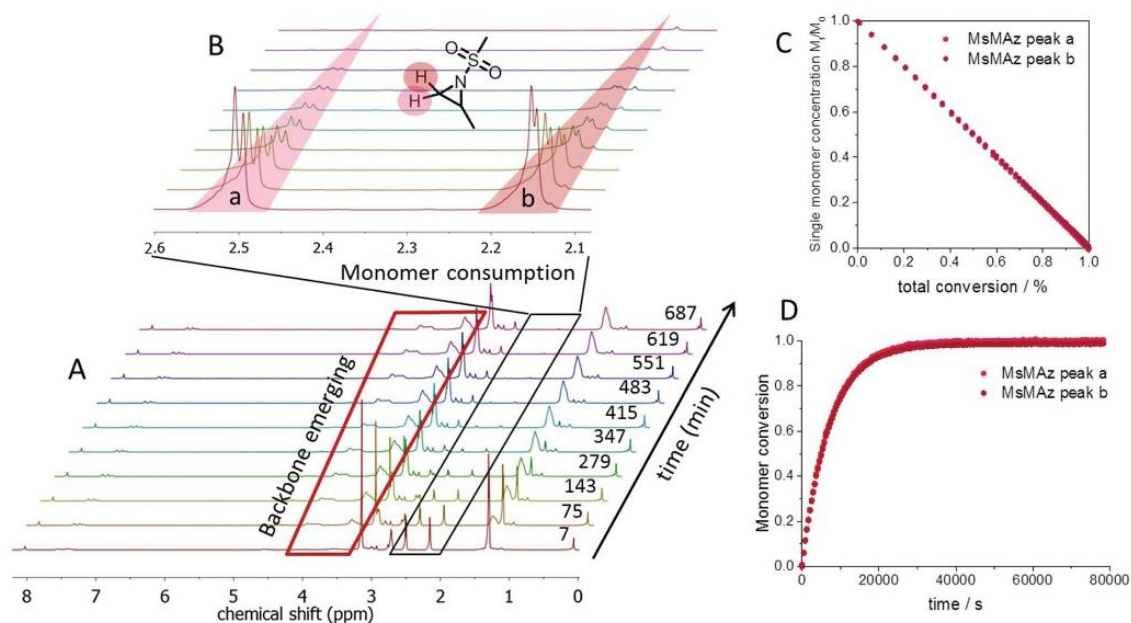


Fig. 1 (A) Selection of the ¹H NMR spectra of the azaanionic polymerization of MsMAz (**1**) with BnNKMs (**3**) as the initiator in DMF-*d*₇, at 50 °C. (B) Relevant signals of the monomer ring-protons, showing the consumption of the monomer. (C) Normalized single monomer concentration versus total conversion. (D) Monomer conversion versus reaction time.

k_{app} with the initial initiator-concentration reveals the initiator-independent propagation rate coefficient k_p .

From every reaction in the NMR tube a small aliquot was taken and analyzed by size exclusion chromatography (SEC). All polymers exhibited monomodal and narrow molecular weight distributions (D typically < 1.1, Tables 1–4 and the ESI†) and reached full monomer conversion in most cases (see below). The molecular weights of the PAZ determined from SEC are underestimated on our setup compared to the absol-

ute values calculated from NMR by end group analysis (Tables 1–4). Since for all SEC analyses PEO-standards were used for conventional calibration, the molecular weights calculated from NMR-data should be considered for comparisons.

Temperature variation

The polymerization of MsMAz (**1**) was initiated with BnNHMs (**3**)/KMDS in DMF-*d*₇ at 20, 50 and 100 °C (Table 1; note: under these conditions 1 eq. hexamethyldisilazane (HMDS) is present as an inherent additive in the polymerization mixture, its influence will be discussed later on). At 20 °C after 17 hours the conversion reached 60% with a propagation rate of $k_p = 0.98 \times 10^{-3} \text{ L mol}^{-1} \text{ s}^{-1}$. At 50 °C full conversion was achieved after ca. 8 hours, revealing a k_p of $10.53 \times 10^{-3} \text{ L mol}^{-1} \text{ s}^{-1}$, which is ca. ten times higher compared to 20 °C. When the polymerization was performed at 100 °C, full conversion was achieved after 30 min with a k_p -value of ca. $123.85 \times 10^{-3} \text{ L mol}^{-1} \text{ s}^{-1}$ (Fig. S1†). At all temperatures, the polymerization remains living, and the addition of new monomer allows the formation of block copolymers.^{7,8,15}

Solvent variation

The solvent polarity and the solvation of the living chain ends have a tremendous influence on the propagation rate in ionic polymerizations.^{2,3,24} For the azaanionic ROP of MsMAz (**1**) at 50 °C, polar solvents such as DMSO-*d*₆ ($k_p = 13.17 \pm 0.7 \times 10^{-3} \text{ L mol}^{-1} \text{ s}^{-1}$ (mean value from repeated measurements I

Table 1 Overview of the performed anionic polymerizations of 2-methyl-*N*-mesyl-aziridine at different temperatures in *N,N*-dimethylformamide

Initiator	BnNKMs (3-K)	BnNKMs (3-K)	BnNKMs (3-K)
Ratio [I]:[M]	01:30	01:30	01:30
Monomer	MsMAz (1)	MsMAz (1)	MsMAz (1)
Additive	HMDS	HMDS	HMDS
Solvent	DMF- <i>d</i> ₇	DMF- <i>d</i> ₇	DMF- <i>d</i> ₇
<i>T</i> /°C	100	50	20
$k_p/10^{-3} \text{ L mol}^{-1} \text{ s}^{-1}$	123.85	10.53	0.98
$M_n^a/g \text{ mol}^{-1}$	2000	2200	2000
$M_n^b/g \text{ mol}^{-1}$	4000	3600	2200
D^c	1.08	1.06	1.08
Reaction time/h	0.50	8.00	17.00
Conversion/%	>99	>99	60

^a Number-average molecular weight and molecular weight dispersity determined via SEC in DMF (vs. PEO standards). ^b Number-average molecular weight determined by NMR analyses.

Table 2 Overview of the performed anionic polymerizations of 2-methyl-*N*-mesyl-aziridine in different solvents

Initiator	BnNKMs (3-K)	BnNKMs (3-K)	BnNKMs (3-K)	BnNKMs (3-K)	BnNKMs (3-K)	BnNKMs (3-K)	BnNKMs (3-K)
Ratio [I]:[M]	01:30	01:30	01:30	01:30	01:30	01:30	01:30
Monomer	MsMAz (1)	MsMAz (1)	MsMAz (1)	MsMAz (1)	MsMAz (1)	MsMAz (1)	MsMAz (1)
Additive	HMDS	HMDS	HMDS	HMDS	HMDS	HMDS	HMDS
Solvent ^a	DMSO- <i>d</i> ₆ -1 ^a	DMSO- <i>d</i> ₆ -II ^a	DMF- <i>d</i> ₇	THF- <i>d</i> ₈ -1 ^a	THF- <i>d</i> ₈ -II ^a	Benzene- <i>d</i> ₆	CyHex- <i>d</i> ₁₂
<i>T</i> /°C	50	50	50	50	50	50	50
<i>k</i> _p /10 ⁻³ L mol ⁻¹ s ⁻¹	13.87	12.46	10.53	0.87	0.65	0.56	—
<i>M</i> _n ^a /g mol ⁻¹	2100	2500	2200	1600	1500	700	—
<i>M</i> _n ^b /g mol ⁻¹	4100	5100	3600	1500 ^d	1700 ^d	— ^d	— ^d
<i>D</i> ^a	1.11	1.09	1.06	1.09	1.09	1.17	—
Reaction time/h	8.00	8.00	8.00	>17	>17	>17	>17
Conversion/%	>99	>99	>99	30	n.d.	n.d.	n.d.

^aTwo identical polymerization mixtures (I or II). ^bNumber-average molecular weight and molecular weight dispersity determined *via* SEC in DMF (vs. PEO standards). ^cNumber-average molecular weight determined by NMR. ^dSamples taken after 17 h reaction, no full conversion.

Table 3 Overview of the performed anionic polymerizations of 2-methyl-*N*-mesyl-aziridine using different initiators

Initiator	BnNKMs (3-K)	BnBis(NKMs) (4-K)	BuLi
Ratio [I]:[M]	01:30	01:50	01:30
Monomer	MsMAz (1)	MsMAz (1)	MsMAz (1)
Additive	HMDS	HMDS	—
Solvent	DMF- <i>d</i> ₇	DMF- <i>d</i> ₇	DMF- <i>d</i> ₇
<i>T</i> /°C	50	50	50
<i>k</i> _p /10 ⁻³ L mol ⁻¹ s ⁻¹	10.53	9.02	18.08
<i>M</i> _n ^a /g mol ⁻¹	2200	2700	2200
<i>M</i> _n ^b /g mol ⁻¹	3600	3700	n.d.
<i>D</i> ^a	1.06	1.09	1.08
Reaction time/h	8	6	5
Conversion/%	99	>99	>99

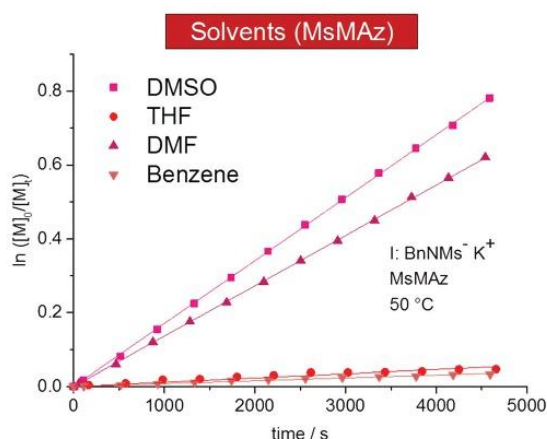
^aNumber-average molecular weight and molecular weight dispersity determined *via* SEC in DMF (vs. PEO standards). ^bNumber-average molecular weight determined by NMR analyses.

Table 4 Overview of the performed anionic polymerizations of 2-methyl-*N*-tosyl-aziridine in *N,N*-dimethylformamide with different gegenions

Initiator	BnNLiMs (3-Li)	BnNNaMs (3-Na)	BnNKMs (3-K)	BnNCsMs (3-Cs)
Ratio [I]:[M]	01:30	01:30	01:30	01:30
Monomer	TsMAz (2)	TsMAz (2)	TsMAz (2)	TsMAz (2)
Additive	HMDS	HMDS	HMDS	HMDS
Solvent	DMF- <i>d</i> ₇	DMF- <i>d</i> ₇	DMF- <i>d</i> ₇	DMF- <i>d</i> ₇
<i>T</i> /°C	50	50	50	50
<i>k</i> _p /10 ⁻³ L mol ⁻¹ s ⁻¹	90.30	60.91	39.79	98.69
<i>M</i> _n ^a /g mol ⁻¹	3000	2900	2300	2800
<i>M</i> _n ^b /g mol ⁻¹	n.d.	n.d.	n.d.	n.d.
<i>D</i> ^a	1.09	1.09	1.09	1.06
Reaction time/h	8	8	8	8
Conversion/%	>99	>99	>99	>99

^aNumber-average molecular weight and molecular weight dispersity determined *via* SEC in DMF (vs. PEO standards). ^bNumber-average molecular weight determined by NMR analyses.

and II) and DMF-*d*₇ (10.53 × 10⁻³ L mol⁻¹ s⁻¹) are the suitable solvents and reach full conversion after *ca.* 8 hours and with narrow molecular weight distributions (Fig. 2 and Table 2).

**Fig. 2** Kinetic plots of $\ln([M]_0/[M]_t)$ vs. time of MsMAz (1), BnNKMs (3) at 50 °C in different solvents (data listed in Table 2).

The polymerization in THF-*d*₈ was remarkably slower with $k_p = 0.76 \pm 0.11 \times 10^{-3} \text{ L mol}^{-1} \text{ s}^{-1}$ (mean value from repeated measurements I and II). Also in benzene-*d*₆ only slow propagation was detected ($k_p = 0.56 \times 10^{-3} \text{ L mol}^{-1} \text{ s}^{-1}$). After 17 h a conversion of 30% was reached. Cyclohexane-*d*₁₂, a typical solvent for carbanionic polymerization, did not result in chain growth. This trend directly reflects the solvation of the living chains and reveals aprotic polar solvents such as DMSO and DMF as the solvents of choice for the AROP of sulfonyl aziridines. However, also in the other solvents the polymerizations remain living and might be considered for special monomers.

Initiator variation

Deprotonated sulfonamides are used as the initiators for the azaanionic ROP of activated aziridines. KMDS was previously used for this series of experiments at 50 °C in DMF-*d*₇ (Table 3). It has to be noted, that in all cases an equimolar amount of HMDS is produced during the initiator formation (also compare sections below).

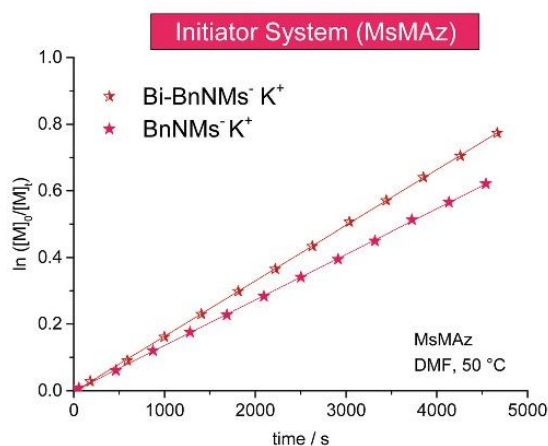


Fig. 3 Kinetic plots of $\ln([M]_0/[M]_t)$ vs. time for the azaanionic polymerization of MsMAz (**1**) with different initiators at 50 °C (data listed in Table 3).

Comparing different sulfonamide initiators, (Fig. 3) the potassium salt of *N*-benzyl methanesulfonamide (BnNKM_s, **3**) ($k_p = 10.53 \times 10^{-3} \text{ L mol}^{-1} \text{ s}^{-1}$) and the novel bifunctional initiator (BnBis(NKM_s), **4**) exhibit a propagation constant of k_p (BnBis(NKM_s)) = $9.02 \times 10^{-3} \text{ L mol}^{-1} \text{ s}^{-1}$. MALDI-ToF mass spectrometry of the polymers prepared with both initiators proves their successful incorporation in the polymer chain and the absence of any additional distribution (Fig. S11 and S12†). This allows the synthesis of ABA triblock-copolymers based on aziridines which is currently under investigation.

As the studies with different counter ions revealed (see below) that also lithium cations can propagate the AROP of aziridines, *n*-butyllithium (*n*-BuLi) was tested as a commercially available initiator for the AROP of MsMAz (**1**) which demonstrated the fastest reaction rate under these conditions ($k_p = 18.08 \times 10^{-3} \text{ L mol}^{-1} \text{ s}^{-1}$, cf. Fig. S4† and discussion for counter ions). MALDI-ToF mass spectrometry proved the incorporation of the butyl chain and shows a single mass distribution (Fig. S13†).

Influence of counter-ions

It is known from ionic polymerizations that the solvation of the growing chain and the respective counter ion plays an important role in the polymerization kinetics: the stronger the binding between the growing chain and the counter ion (and the lower the solvation efficiency of the solvent), the slower the propagation. For the anionic polymerization of styrene, for example, lithium counter ions show an increase of the polymerization kinetics compared to sodium counter ions. For epoxides, typically potassium and cesium show the highest propagation rates, while lithium alkoxides do not or only very slowly propagate, as they coordinate strongly to the Pearson-hard alkoxide.^{2,25–32} In the case of sulfonamide anions such studies had not been performed; in previous work, potassium

salts proved to be efficient. We studied the polymerization of **1** and **2** (DMF-*d*₇, 50 °C, BnNHMs (**3**) as the initiator) with different counter ions by deprotonating **3** with different bis(trimethylsilyl)amide salts (lithium, sodium, potassium salts are commercially available, CsMDS was prepared according to the literature^{4,20}). For both monomers, propagation with all counter ions was observed (Fig. 4, S2† and Table 4), probably due to the rather soft nature of the propagating anion. Under these conditions the order of $\text{Cs}^+ > \text{Li}^+ > \text{Na}^+ > \text{K}^+$ was found for both monomers (Fig. 4A).

For MsMAz (**1**) as a less reactive monomer the same trend was observed ($\text{Cs}^+ > \text{Li}^+ > \text{Na}^+ > \text{K}^+$), however, the differences were less pronounced (Fig. S2† and Table 5). Noteworthy, in all cases living polymerization with reasonable polymerization rates of the activated aziridines is observed (cf. Fig. 4B, S14 and 15†). This indicates a higher solvation of the propagating azaanion chains under these conditions, in contrast to the epoxide polymerization, where hardly propagation is observed with lithium as a counter ion, also in highly solvating solvents.

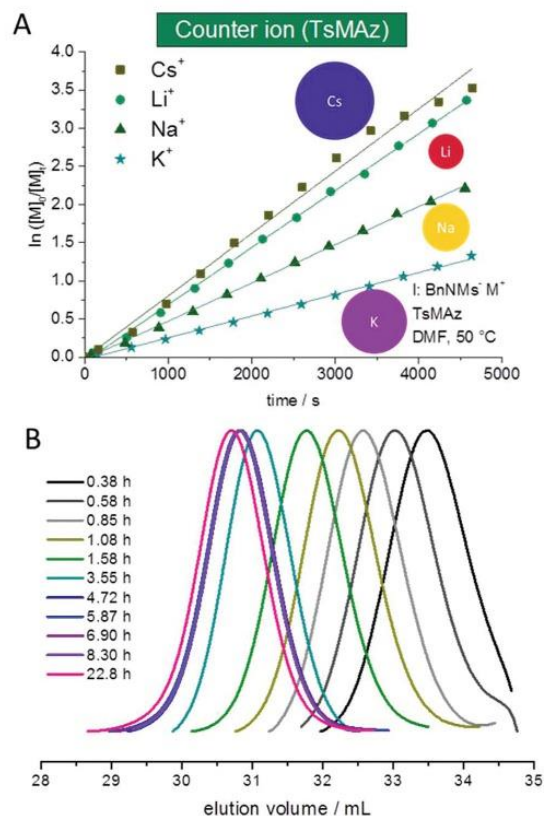


Fig. 4 (A) Kinetic plots of $\ln([M]_0/[M]_t)$ vs. time for the azaanionic polymerization of TsMAz (**2**) with BnNHMs (**3**, initiator) in DMF-*d*₇ at 50 °C with different bis(trimethylsilyl)amide-salts. (B) SEC-kinetics of MsMAz (**1**) and BnNKM_s (**3**) at 50 °C in DMF (RI-signal, PEO-standard), (Table 5).

Table 5 Overview of the performed anionic polymerizations of 2-methyl-*N*-mesyl-aziridine with different gegenions and amounts of hexamethyldisilazane

Initiator	BnNLiMs (3-Li)	BnNNaMs (3-Na)	BnNKMs (3-K)	BnNCsMs (3-Cs)	BnNKMs ^c (3-K)	BnNKMs (3-K)
Ratio[I]:[M]	01:30	01:30	01:30	01:30	01:30	01:30
Monomer	MsMAz (1)	MsMAz (1)	MsMAz (1)	MsMAz (1)	MsMAz (1)	MsMAz (1)
Additive	HMDS	HMDS	HMDS	HMDS	—	2 eq. HMDS
Solvent	DMF- <i>d</i> ₇	DMF- <i>d</i> ₇	DMF- <i>d</i> ₇	DMF- <i>d</i> ₇	DMF- <i>d</i> ₇	DMF- <i>d</i> ₇
<i>T</i> /°C	50	50	50	50	50	50
<i>k</i> _p /10 ⁻³ L mol ⁻¹ s ⁻¹	15.39	11.66	10.53	15.74	11.19	8.45
<i>M</i> _n ^a /g mol ⁻¹	2400	2400	2200	2100	2200	2000
<i>M</i> _n ^b /g mol ⁻¹	4000	3900	3600	3800	3700	4000
<i>D</i> ^a	1.07	1.06	1.06	1.08	1.07	1.10
Reaction time/h	8.00	7.00	8.00	7.00	8.00	9.00
Conversion/%	>99	>99	97	>99	98	>99

^a Number-average molecular weight and molecular weight dispersity determined *via* SEC in DMF (vs. PEO standards). ^b Number-average molecular weight determined by NMR analyses. ^c Prepared by deprotonation with KOH.

Also the cation dependence on the polymerization kinetics, which does not follow the cation size can be explained by the Pearson acid base concept³³ that the sulfonamide anion is weakly coordinated by its respective cation compared to an alkoxide, which strongly binds to lithium cations also in polar organic solvents as mentioned above. The “softer” sulfonamide anion exhibits higher binding to intermediate sized cations sodium and potassium, but less binding to the hard lithium and soft cesium cations. In addition, comparing the two monomers **1** and **2**, with the smaller electron withdrawing effect of the mesyl group in MsMAz (**1**) compared to the tosyl group in **2**, a more nucleophilic growing chain end is produced. This leads to the less expressed trend in the propagation rate of the different counter ions, as the interaction between the azaanion at the chain end and the cationic counter ion is stronger.

To identify the influence of the inherent additive hexamethyldisilazane (HMDS), which is generated in a molar amount after the deprotonation of BnHMs (**3**) by the bis(trimethylsilyl)amide salt, on the chain end reactivity, polymerizations of **1** with different amounts of HMDS were performed (note: MALDI ToF mass spectrometry revealed that only polymers, initiated by **3** are produced under these conditions, cf. the ESI†).

To study the influence of HMDS on the polymerization kinetics several experiments were conducted: (i) **3** was deprotonated with KMDS (*i.e.* one equivalent of HMDS is produced with respect to the initiator); (ii) to exclude HMDS in the polymerization, BnNHMs (**3**) was deprotonated with potassium hydroxide (KOH) and dried by azeotropic removal of the emerging water with benzene before adding the monomers; (iii) another polymerization was conducted under the same conditions, however with two equivalents of HMDS with respect to the initiator. Comparing the propagation rate constants of these three polymerizations in the presence of 1 or 2 eq. or without HMDS, a decrease of the polymerization kinetics with an increasing amount of HMDS was detected (BnNKMs in DMF (no HMDS) at 50 °C *k*_p = 11.19 × 10⁻³ L mol⁻¹ s⁻¹, BnNKMs, 1 eq. HMDS in DMF at 50 °C *k*_p = 10.53 × 10⁻³

L mol⁻¹ s⁻¹, BnNKMs, 2 eq. HMDS in DMF at 50 °C *k*_p = 8.45 × 10⁻³ L mol⁻¹ s⁻¹). These results prove that HMDS influences the polymerization kinetics, probably due to coordination to the anionic chain end and the formation of a complex. The same trend was observed for the polymerization of **1** with lithium as the counter ion: for MsMAz, 50 °C, DMF, BuLi (no HMDS) a *k*_p = 18.1 × 10⁻³ L mol⁻¹ s⁻¹ was determined (Table 3), while the presence of HMDS in the system reduced the *k*_p to 15.4 × 10⁻³ L mol⁻¹ s⁻¹ (Table 5 first entry, MsMAz, 50 °C, DMF, BnNLiMs, HMDS).

To examine the influence of DMF as a highly solvating solvent, polymerizations with lithium, potassium and cesium, with the “standard procedure”, *i.e.* BnNHMs (**3**), the respective bis(trimethylsilyl)amide salt, at 50 °C, were carried out in THF. In all cases the polymerization proceeds much slower in THF compared to DMF, irrespective of which counter ion was used (Table 6 and Fig. S3†). This indicates a lower solvation of the living chain ends in THF, reducing the polymerization kinetics

Table 6 Overview of the performed anionic polymerizations of 2-methyl-*N*-mesyl-aziridine with different gegenions in tetrahydrofuran

Initiator	BnNLiMs (3-Li)	BnNKMs (3-K)	BnNKMs (3-K)	BnNCsMs (3-Cs)
Ratio [I]:[M]	01:30	01:30	01:30	01:30
Monomer	MsMAz (1)	MsMAz (1)	MsMAz (1)	MsMAz (1)
Additive ^a	HMDS	HMDS-I	HMDS-II	HMDS
Solvent	THF- <i>d</i> ₈	THF- <i>d</i> ₈	THF- <i>d</i> ₈	THF- <i>d</i> ₈
<i>T</i> /°C	50	50	50	50
<i>k</i> _p /10 ⁻³ L mol ⁻¹ s ⁻¹	0.72	0.87	0.65	1.36
<i>M</i> _n ^b /g mol ⁻¹	700	1600	1500	1400
<i>M</i> _n ^c /g mol ⁻¹	1300 ^d	1500 ^d	1700 ^d	2500 ^d
<i>D</i> ^a	1.17	1.09	1.09	1.08
Reaction time/h	>24	>17	>17	>18
Conversion/%	33	38	43	63

^a In the case of KMDS the measurements were repeated and are marked with I, respectively II. ^b Number-average molecular weight and molecular weight dispersity determined *via* SEC in DMF (vs. PEO standards). ^c Number-average molecular weight determined by NMR analyses. ^d Samples taken after minimum 17 h reaction, no full conversion.

(at least by a factor of 10). In contrast, the conventional oxyanionic polymerization and the recently reported organocatalytic ring-opening polymerization of sulfonylaziridines¹⁶ proceed smoothly in THF and reach full conversion in the course of several hours.

With these results in hand, the combination of the azaanionic polymerization with other ionic polymerization techniques will be used to produce various macromolecular architectures and the use of commercially available lithium-based initiators (*e.g.* butyllithium).

Conclusions

We report on the systematic polymerization kinetics of the living anionic polymerization of *N*-activated aziridines, exemplarily with MsMAz and TsMAz, two activated aziridines of different reactivities, by real-time ¹H NMR spectroscopy. We found that their polymerization follows living conditions at temperatures between 20 and 100 °C. The comparison of different solvents for the polymerization proved that polar aprotic solvents exhibit the fastest polymerization kinetics with the order of DMSO ≥ DMF ≫ THF ≥ benzene, and no propagation in cyclohexane, depending on the solvation of the living chain end. The use of different initiators, namely sulfonamides BnNHMs and a novel bifunctional sulfonamide (BnBis(NHMs)) were compared with each other and we additionally identified *n*-butyllithium as a potent commercial alternative.

However, the sulfonamide initiators are ideal to study the influence of the counter ion on the polymerization kinetics. The sulfonamide initiator was deprotonated with the respective metal bis(trimethylsilyl)amide (Li, Na, K, or Cs). In all cases fast propagation of the anionic polymerization was observed, which is in strong contrast to epoxide polymerization, where lithium alkoxides show only very slow propagation rate constants. For activated aziridines the following trend was observed: Cs⁺ > Li⁺ > Na⁺ > K⁺ with reasonable *k*_p values in all cases in DMF, indicating a high solvation of all propagating azaanions in DMF, with a less pronounced effect of the counter ion compared to alkoxide chains. In contrast, in THF only a weak counter ion dependency and low reaction kinetics have been observed.

We believe that this fundamental work will help to further understand and foster the field of the anionic polymerization of aziridines. In particular, the less pronounced counter ion effect compared to the well-known anionic polymerization of epoxide makes the AROP of sulfonylaziridines easy and switching for example from carb- to aza-anionic polymerization or the use of simple commercially available butyllithium. *N*-Sulfonyl-activated aziridines undergo AROP under various conditions producing well-defined polysulfonamides and -amines after hydrolysis. This defined access to such structures was not possible to date and we believe that aziridines will become a valuable tool for combinations with other anionic polymerizations for diverse applications, for example as a well-defined alternative for branched poly(ethylene imine)s.

Acknowledgements

The authors thank the Deutsche Forschungsgemeinschaft (DFG WU750/7-1) for support. The authors thank Stefan Spang for the NMR measurements. E. R. thanks the BMBF/MPG network MaxSynBio. Open Access funding provided by the Max Planck Society.

References

- 1 M. Szwarc, M. Levy and R. Milkovich, *J. Am. Chem. Soc.*, 1956, **78**, 2656–2657.
- 2 G. Odian, *Principles of Polymerization*, John Wiley & Sons, New Jersey, USA, 2004.
- 3 N. Hadjichristidis and A. Hiraio, *Anionic Polymerization: Principles, Practice, Strength, Consequences and Applications*, Springer Japan, 2015.
- 4 I. C. Stewart, C. C. Lee, R. G. Bergman and F. D. Toste, *J. Am. Chem. Soc.*, 2005, **127**, 17616–17617.
- 5 L. Thomi and F. R. Wurm, *Macromol. Rapid Commun.*, 2014, **35**, 585–589.
- 6 L. Thomi and F. R. Wurm, *Macromol. Symp.*, 2015, **349**, 51–56.
- 7 E. Rieger, A. Alkan, A. Manhart, M. Wagner and F. R. Wurm, *Macromol. Rapid Commun.*, 2016, **37**, 833–839.
- 8 E. Rieger, A. Manhart and F. R. Wurm, *ACS Macro Lett.*, 2016, **5**, 195–198.
- 9 L. Reisman, C. P. Mbarushimana, S. J. Cassidy and P. A. Rugar, *ACS Macro Lett.*, 2016, **5**, 1137–1140.
- 10 M. Kobayashi, K. Uchino and T. Ishizone, *J. Polym. Sci., Part A: Polym. Chem.*, 2005, **43**, 4126–4135.
- 11 A. P. Spork and T. J. Donohoe, *Org. Biomol. Chem.*, 2015, **13**, 8545–8549.
- 12 H.-J. Jang, J. T. Lee and H. J. Yoon, *Polym. Chem.*, 2015, **6**, 3387–3391.
- 13 D. C. McLeod and N. V. Tsarevsky, *Macromol. Rapid Commun.*, 2016, **37**, 1694–1700.
- 14 H. K. Moon, S. Kang and H. J. Yoon, *Polym. Chem.*, 2017, **8**, 2287–2291.
- 15 T. Homann-Müller, E. Rieger, A. Alkan and F. R. Wurm, *Polym. Chem.*, 2016, **7**, 5501–5506.
- 16 C. Bakkali-Hassani, E. Rieger, J. Vignolle, F. R. Wurm, S. Carlotti and D. Taton, *Chem. Commun.*, 2016, **52**, 9719–9722.
- 17 J. B. Sweeney, *Chem. Soc. Rev.*, 2002, **31**, 247–258.
- 18 M. Bednarek, P. P. Kubisa and S. Penczek, *Macromolecules*, 1999, **32**, 5257–5263.
- 19 B. D. Monnery and R. Hoogenboom, in *Cationic Polymers in Regenerative Medicine*, The Royal Society of Chemistry, 2015, pp. 30–61.
- 20 S. Neander and U. Behrens, *Z. Anorg. Allg. Chem.*, 1999, **625**, 1429–1434.
- 21 R. Freeman, H. D. W. Hill and R. Kaptein, *J. Magn. Reson.*, 1972, **7**, 327–329.

Paper

Polymer Chemistry

- 22 A. Alkan, A. Natalello, M. Wagner, H. Frey and F. R. Wurm, *Macromolecules*, 2014, **47**, 2242–2249.
- 23 A. Natalello, A. Alkan, P. von Tiedemann, F. R. Wurm and H. Frey, *ACS Macro Lett.*, 2014, **3**, 560–564.
- 24 M. Van Beylen, D. N. Bhattacharyya, J. Smid and M. Szwarc, *J. Phys. Chem.*, 1966, **70**, 157–161.
- 25 K. S. Kazanskii, A. A. Solovyanov and S. G. Entelis, *Eur. Polym. J.*, 1971, **7**, 1421–1433.
- 26 M. Szwarc, in *Living Polymers and Mechanisms of Anionic Polymerization*, Springer, Berlin, Heidelberg, Germany, 1983, vol. 49, pp. 1–177.
- 27 K. Matyjaszewski and A. H. E. Müller, *Controlled and Living Polymerizations: From Mechanisms to Applications*, John Wiley & Sons, Weinheim, Germany, 2009.
- 28 J. Herzberger, K. Niederer, H. Pohlit, J. Seiwert, M. Worm, F. R. Wurm and H. Frey, *Chem. Rev.*, 2016, **116**, 2170–2243.
- 29 M. van Beylen, S. Bywater, G. Smets, M. Szwarc and D. J. Worsfold, *Adv. Polym. Sci.*, 1988, **86**, 87–143.
- 30 H. Jeuck and A. H. E. Müller, *Makromol. Chem.*, 1982, **3**, 121–125.
- 31 F. S. Dainton, G. C. East, G. A. Harpell, N. R. Hurworth, K. J. Ivin, R. T. Laflair, R. H. Pallen and K. M. Hui, *Makromol. Chem.*, 1965, **89**, 257–262.
- 32 J. E. L. Roovers and S. Bywater, *Trans. Faraday Soc.*, 1966, **62**, 701–706.
- 33 A. F. Holleman and E. Wiberg, *Lehrbuch der Anorganischen Chemie*, Walter de Gruyter Co., Berlin, Germany, 34th edn, 1995.

C.P. 2: Desulfonation of polysulfonamides

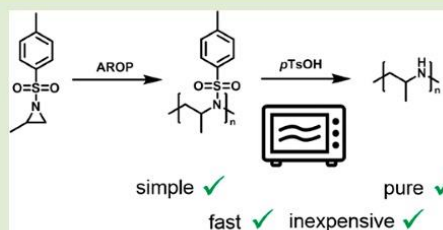
Microwave-Assisted Desulfonation of Polysulfonamides toward Polypropylenimine

Elisabeth Rieger,[†] Tassilo Gleede,[†] Angelika Manhart,[†] Markus Lamla,[‡] and Frederik R. Wurm^{*†‡}[†]Max-Planck-Institut für Polymerforschung (MPI-P), Ackermannweg 10, 55128 Mainz, Germany[‡]Institute for Organic Chemistry III/Macromolecular Chemistry, University of Ulm, Albert-Einstein-Allee 11, 89081 Ulm, Germany

Supporting Information

ABSTRACT: Linear polyethylenimine (L-PEI) has been the gold standard for gene delivery and is typically prepared by hydrolysis from poly(2-oxazoline)s. Recently, also the anionic polymerization of activated aziridines was reported as a potential pathway toward linear and well-defined polyamines. However, only sulfonamide-activated aziridines so far undergo the living anionic polymerization and their desulfonation was only reported scarcely. This is mainly due to the relatively high stability of the sulfonamides and the drastic change in solubility during the desulfonation. Herein, we investigated the desulfonation of such poly(aziridine)s prepared from tosylated or mesylated propyleneimine to afford linear polypropylenimine (L-PPI)

as an alternative to L-PEI. Different desulfonation strategies for tosylated (Ts) and mesylated (Ms) PPI were studied. The reductive cleavage of the sulfonamide with sodium bis(2-methoxy ethoxy) aluminum hydride yielded 80% of deprotected amine groups. Quantitative conversion to L-PPI was obtained, when the tosylated PPI was hydrolyzed under acidic conditions with *p*TsOH under microwave (MW) irradiation. The same treatment removed 90% of the mesyl groups from the mesylated PPI analog. The MW-assisted acidic hydrolysis represents a fast, inexpensive and easy approach in comparison to other methods, where complex reaction conditions and tedious purifications are major drawbacks, however some chain scission may occur. The high purity of the obtained products, in combination with the versatility of the activated aziridine chemistry, demonstrate many advantages of our strategy, especially for future biomedical implementations.



The living anionic polymerization (LAP) of activated aziridines, that is, sulfonyl aziridines, gives access to polysulfonamides with various structures. This azaanionic polymerization, first reported in 2005, and revived by our group in 2013, allows the synthesis of polymers with sulfonylated nitrogen atoms in the polymer backbone, which were not accessible before.^{1–5} Recent publications studied the mechanism^{6–8} or the formation of sequence-controlled materials by competing copolymerization of several activated aziridines,^{9,10} thriving the understanding of azaanionic polymerization, next to the well-known oxy- and carbanionic polymerizations.^{11,12} The interest in polyaziridines (PAz), that is, the polysulfonamides, which are obtained after the polymerization of sulfonyl-aziridines, is mainly motivated by the possibility to prepare various polyamines after their desulfonation. Well-defined polyamines are interesting materials as polyelectrolytes, in surfactants, or as transfection agents. Today, linear polyethylenimine (L-PEI) is extensively used for nonviral gene transfection, due to its high efficiency.^{13,14} However, its synthesis via the cationic polymerization of oxazolines,^{15,16} also requires a hydrolysis step, which is often not complete and molecular characterization of commercial PEI batches (linear and branched from the cationic polymerization of aziridine) is challenging.¹⁷ Concerns about the high toxicity of PEI make research for less toxic alternatives necessary. The anionic

polymerization of activated aziridines might be a powerful strategy to meet the needs, as it can be combined with other anionic polymerization techniques and the broad monomer scope might result in efficient, but less toxic alternatives to PEI.

Surprisingly, the focus of research on nonviral transfection agents was almost exclusively on L-PEI, while linear polypropylenimine (L-PPI), with one more methyl-group, has not been considered to date, even though a reasonable synthesis had been reported already decades ago.¹⁸ Compared to living anionic polymerization, cationic polymerizations are often limited, especially for high molecular weights.¹² However, also PAz needs a reasonable desulfonation strategy, in order to prepare the polyamines. Several strategies to remove sulfonamides in low molecular weight compounds, especially for toluene-sulfonamides, have been reported.^{19,20} Classic routes employ sodium or lithium naphthalenide,^{19–24} sodium or lithium in liquid ammonia,^{19,20,25} strong acids,^{19,20,25,26} and sodium amalgam.^{20,27,28} Several other methods, such as the mild samarium(II)-iodide (SmI₂),^{19,20,29–32} electrochemistry,^{20,25,32–36} microwave (MW) irradiation,^{20,37,38} tributyltin hydride/azoisobutyronitrile (Bu₃SnH/AIBN),^{20,31} trimethylsil-

Received: March 5, 2018

Accepted: May 2, 2018

yl iodide (TMSI),^{20,39} different titanium-compounds,^{20,31,40,41} magnesium in methanol,^{19,20,42} other metal complexes,^{20,43} photolysis,^{20,44,45} tetra-*n*-butylammonium fluoride (TBAF),^{20,46,47} or trifluoroacetic acid⁴⁸ have been reported. Some of those methodologies only cleave very “active” sulfonamides, that is, with additional electron withdrawing groups (e.g., nosyl)^{49,50} or secondary sulfonamides.²⁰

This broad scope of desulfonation reactions has not been applied to PAz so far. However, for PAz additional issues for the desulfonation step need to be addressed. Especially, the change in solubility from the hydrophobic polysulfonamide to the very hydrophilic polyamine make the choice of reaction conditions and subsequent purification more challenging than for low molecular weight compounds. Therefore, many desulfonation strategies might not be applicable for polymeric structures. Only in four publications, the deprotection of PAz has been reported. Acidic hydrolysis of tosyl groups was achieved on a poly(styrene-*b*-tosylaziridine) with hydrobromic acid and phenol in refluxing THF.⁵¹ Bergman and Toste reported the desulfonation with lithium naphthalene (LiNp), but did not show details on the obtained products, for example, molecular weight distribution or NMR spectra of the product.⁵ The group of Rupar was able to remove the sulfonyl groups, using elemental lithium and *tert*-butanol (*t*-BuOH) in hexamethylphosphoramide (HMPA) and tetrahydrofuran (THF) to obtain L-PEL.³ This is a reasonable method with good yields, but with lithium metal and the toxicity of HMPA and the low temperatures (−20–5 °C), this strategy is not attractive for larger scales. We recently reported the desulfonation of polyaziridines under reductive conditions with sodium bis(2-methoxy ethoxy)aluminum hydride (Red-Al) in toluene. Under these conditions, ca. 80% of desulfonation was achieved and further acetal-protected alcohols remained intact.⁴

Herein, we investigated different methods for the desulfonation of polyaziridines, namely, P(TsMAz)₆₀, P(MsMAz)₄₇, and copolymers of P((TsMAz)₂₅-*co*-(MsMAz)₂₅). The goal was to find a facile methodology, which prevents toxic additives and without the need for heavy metals. Especially for biomedical applications, removal of heavy metals might be challenging and their use should be avoided. Besides reduction with Red-Al, now also applied for mesylated polymers, the acidic hydrolysis with toluene sulfonic acid under microwave irradiation was found to meet most of those requirements and is highlighted herein.

The polyaziridines were synthesized via the living anionic ring-opening polymerization of sulfonyl aziridines (2-methyl-*N*-mesyl-aziridine (MsMAz, 1) and 2-methyl-*N*-tosylaziridine (TsMAz, 2)), initiated by *N*-pyrene-methanesulfonamide (PyNHMs) according to literature (Scheme 1).^{4,6,9,10}

Experimental details and analytical data of the obtained polymers P(MsMAz)₄₇ (P1), P(TsMAz)₆₀ (P2), and P-

((TsMAz)₂₅-*co*-(MsMAz)₂₅) (P(2-*co*-1)) are summarized in Table 1 and the Supporting Information (pp S3–S6). The repeating units, given as a subscript number, were determined via end group analysis from the ¹H NMR-spectra. All polymers have monomodal molecular weight distributions with $\bar{D} \leq 1.11$ with full monomer conversion and quantitative yield.

The desulfonation was investigated via electrochemistry, arene radicals (NaNp), reduction with samarium(II) iodide (SmI₂), Red-Al, and via the acidic hydrolysis under microwave irradiation. Electrochemical reduction of low molecular weight sulfonamides had been reported in the literature.²⁰ This rather mild and easy to conduct procedure was attempted (in analogy to literature reports) in DMF, which is both a good solvent for the polysulfonamide and the polyamine. Different conditions were investigated (cf. Supporting Information, section G for details), but under these conditions, neither P1 nor P2 could be desulfonated. After 3–5 h of reaction, a dark unidentified material was deposited on the platinum-electrodes, indicating that insolubility issues might have inhibited the reaction (potentially, amide anions could be formed, which might also be insoluble in DMF). Conversely, when sodium naphthalene (NaNp)^{8,19–21} or SmI₂^{19,20,29–32} were employed, NMR spectroscopy indicated a successful removal of the sulfonamides from P2 (indicated by sharp resonances of a tosyl derivative). However, in both cases, the color of the crude was brown (probably due to partial oxidation) and the purification of the polyamine was challenging and not further attempted. Both methods might be reinvestigated, however, as our aim was to establish a fast and convenient pathway to polyamines, we continued with other procedures.

The reduction with Red-Al was reported as a mild method for acetal-protected polytosylaziridines with ca. 80% of desulfonation, without hydrolysis of the acetals.⁴ We conducted experiments with the mesylated, the tosylated, and the copolymer to assess the applicability of Red-Al for general desulfonation of polysulfonamides (Scheme 2b and the Supporting Information, section E for experimental details). P(TsMAz) (P2) was treated with Red-Al in refluxing toluene and ca. 80% of the tosyl groups were removed (cf. SI, Figures S7 and S8 for P2–1). Removal of aluminum side products from the crude mixture was difficult and some inorganic residues remained in the products (cf. the ¹H NMR spectra in Figures S7 and S9). In contrast, P(MsMAz) (P1) was insoluble in toluene and THF and no reaction with Red-Al after refluxing the suspension at 110 °C overnight was observed, probably due to its low solubility. When the copolymer (P(2-*co*-1)) was treated with Red-Al, the NMR spectra of the reaction mixture indicated again the removal of most of the tosyl groups, while the mesyl groups were also partially removed. However, purification of the materials from the inorganic side products was challenging and NMR spectra showed broad resonances, from which the degree of deprotection can only be estimated (the resonances belonging to the remaining mesyl groups are labeled with a star (*), compare Figure S9). Overall, the reductive deprotection via Red-Al was able to remove the sulfonamides partly under the investigated conditions, but probably solubility and aggregation hamper a complete desulfonation.

Acidic hydrolysis of sulfonamides is an attractive method to release the polyamines. The acid-catalyzed cleavage of various low molecular weight sulfonamides follows a general mechanism similar to amide cleavage and is literature-known.⁵² In order to overcome solubility issues, we used a

Scheme 1. Azaanionic Ring-Opening Polymerization of Activated Aziridines

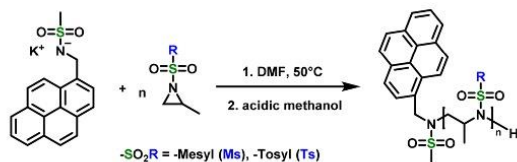
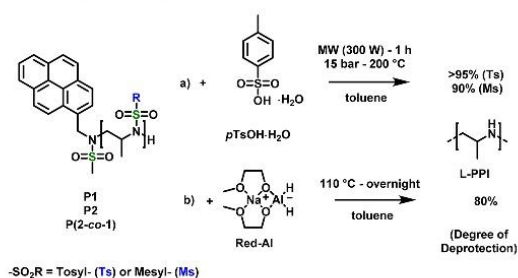


Table 1. Characterization Data of Polyaziridines

polymer	#	M_n (th) ^a	M_n ^b	M_n ^c	M_w/M_n ^c
P(MsMAz) ₄₇	P1	7100	6700	8000	1.10
P(TsMAz) ₆₀	P2	10900	13000	20500	1.10
P((TsMAz) ₂₅ -co-(MsMAz) ₂₅)	P(2-co-1)	9000	9000	12600	1.11

^aTheoretical number-average molecular weight (g/mol). ^bNumber-average molecular weight determined by end group analysis from ¹H NMR spectroscopy. ^cNumber-average molecular weight and molecular weight dispersity determined via SEC in HFIP (vs. PMMA standards).

Scheme 2. Desulfonation of Polyaziridines via (a) Hydrolytic Cleavage under Microwave Irradiation, >95% Linear Polypropyleneimine (L-PPI), and (b) Reductive Removal with Red-Al, about 80% L-PPI



suspension of the starting materials in combination with the microwave-assisted acidic hydrolysis in the presence of *p*-toluenesulfonic acid. Similar strategies have been successfully employed for the deprotection of poly(2-oxazoline)s to obtain L-PEI.⁵³ When hydrochloric acid (HCl) or sulfuric acid (H₂SO₄) were used and the PAz suspended in the respective acid, only a very low degree of desulfonation was achieved which is probably attributed to solubility issues. With *p*TsOH·H₂O as the acidic catalyst, the polymer was suspended in toluene and the reaction was performed under MW irradiation of 300 W, at different temperatures, with a maximum pressure of 15 bar. After the desired reaction time (cf. Table 2), the crude solid inside the microwave reactor was dissolved in water and washed with chloroform. Performing the reaction at 180 or 200 °C, 83% or >95% desulfonation was achieved,

respectively. The polymer was purified by an anionic exchange resin, yielding quantitatively deprotected L-PPI (P2–2, after reaction at 200 °C) in the case of P(TsMAz) (P2) (Figure 1 and Scheme 2a). Table 2 summarizes literature and current attempts for desulfonation of PAz. The ratio of the integrals of the doublet at 1.04 ppm, belonging to the methyl side chain and the multiplet at 3.04–2.36 ppm from the backbone is 1:1, which is in agreement to expectations.¹⁸ Furthermore, no aromatic signals were detected, proving full desulfonation and also indicating the partial removal of the initiator, which might occur under these conditions (Figure 1A). SEC-data shows a clear shift of the elution volume for the deprotected polymer P2–2 to higher elution volumes, indicating the decrease in molecular weight, due to desulfonation (Figure 1B). The monomodal molecular weight distribution remained intact, but the dispersity increased to 1.39 for the desulfonation performed at 200 °C and to 1.20 for the desulfonation performed at 180 °C, which might be due to chain scission during the acid treatment or also interactions with the column material during the SEC experiment (Figures 1B and S17). ¹H DOSY NMR of the product shows the polymers diffusion is clearly separated from the solvent diffusion of water proving no low molecular weight fragments in the product (Figure S14). The MALDI -spectrum confirms the presence of the repeating unit of propyleneimine (PI, 57 g/mol) in the product (see Figure S18). Calculating the absolute composition of the different distributions further indicate fragmentation of the polymer and the presence of the initiator in some subdistributions. However, as fragmentation of L-PEI during mass spectrometry was reported, MALDI cannot fully confirm the presence of chain scission in the product (e.g., no olefin signals were detected in the NMR spectra).⁵⁴ A certain amount of chain scission was proven by reacting the desulfonated

Table 2. Overview of Desulfonation Reactions for Polyaziridines (Literature and Current Work)

activ. group	solvent	reagent	conditions	purification	product	depro. (%)	ref.	comment
unspec. ^a	n.d.	LiNp	RT, over- night	filtration	L-PPI	n.d.	8	no data shown
Ms- ^b Bus	HMPA, THF	Li, <i>t</i> -BuOH	–20–5 °C, 6.5 h	precipitation and washing	L-PEI	>95	3	laborious, toxic solvent
Ms- ^b Bus- <i>b</i> -Ms ^c	HMPA, THF	Li, <i>t</i> -BuOH	–20–5 °C, 6.5 h	precipitation and washing	L-PEI- <i>b</i> -PPI	>95	3	laborious, toxic solvent
Ts	toluene	Red-Al	110 °C, overnight	filtration, dialyses	polyhydroxy amine	~80	4	complex purification, intact acetal groups
Ts (P2)	toluene	Red-Al	110 °C, overnight	filtration, dialyses	L-PPI (P2–1)	~80	e	complex purification
Ts-Ms ^d (P(2-co-1))	toluene	Red-Al	110 °C, overnight	filtration, dialyses	L-PPI (P(2-co-1)-1)	~80	e	complex purification
Ts (P2)	toluene	<i>p</i> TsOH	180 °C, 1 h, 300 W, max. 15 bar	extraction, ion exchange resin	L-PPI (P2–2)	83	e	fast, pure, chain scission?
Ts (P2)	toluene	<i>p</i> TsOH	200 °C, 1 h, 300 W, max. 15 bar	extraction, ion exchange resin	L-PPI (P2–2)	>95	e	fast, pure, chain scission?
Ms (P1)	toluene	<i>p</i> TsOH	200 °C, 1.5 h, 300 W, max. 15 bar	extraction, ion exchange resin	L-PPI (P1–2)	~90	e	fast, pure, chain scission?

^aactivating groups not specified, tosyl- (Ts) or mesyl- (Ms) group. ^bPoly(mesyl-co-(*sec*-butylsulfanyl)aziridine). ^cPoly((mesyl-co-(*sec*-butylsulfanyl))-*block*-mesyl)aziridine. ^dPoly(tosyl-co-(mesyl)aziridine). ^eThis work.

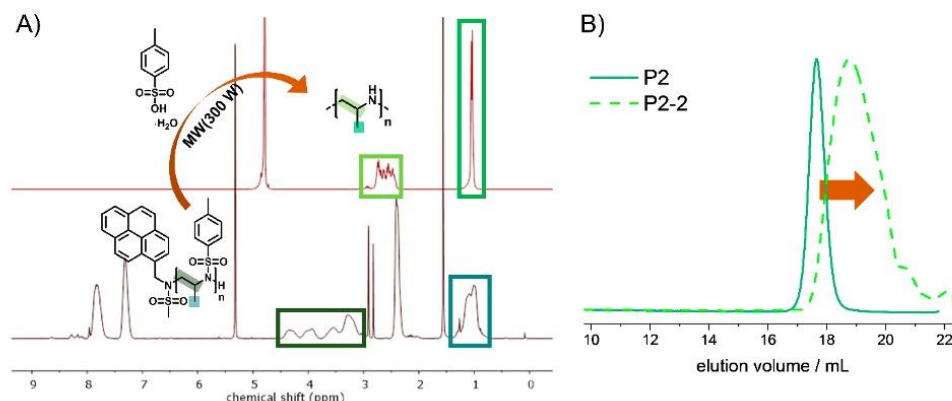


Figure 1. (A) Overlay of the ¹H NMR spectra and (B) SEC traces of P(TsMAz) (P2) and L-PPI (P2-2) derived from P2 from acidic hydrolysis under microwave irradiation at 200 °C.

polymer (P2-2), obtained as fully protected PPI, with tosyl chloride back to PTsMAz (cf. Supporting Information, section I). The SEC data proves that the molecular weight of the tosylated product was reduced compared to the initial material due to chain scission (Figure S25). This correlates to the reduced molar masses detected by MALDI MS spectrometry of the desulfonated polymers. Similar findings have been reported for the acidic cleavage of amides in poly(2-oxazoline)s, but 180 °C proved to be sufficient for hydrolysis with minor chain scission.⁵³

When P(MsMAz) (P1) was suspended in toluene together with *p*-toluenesulfonic acid and reacted under the same conditions for 1.5 h, ¹H NMR spectra show that about 10% mesyl units remained intact (cf. SI, Figure S17); a slightly lower degree of desulfonation was obtained, when repeated under the same conditions, but only 1 h of reaction time. SEC data shows a monomodal distribution with $\bar{D} = 1.36$, also shifted to higher elution times, indicating the desulfonation. However, the MALDI-spectrum of P1-2 showed exclusively the repeating unit of PPI, no mesyl unit can be assigned, potentially due to a partial ionization during the measurement (Figure S22). For both polymers, lower temperatures during the desulfonation in the microwave were investigated but did not result in any optimization. All tested conditions and the results are summarized in Table S1. The acidic hydrolysis under microwave irradiation is a nonselective method for desulfonation and the experimental handling is very simple (no inert atmosphere, no extra steps or low-temperature conditions are necessary) and additionally inexpensive. Furthermore, the purification is straightforward and no heavy metal compound is involved. However, due to the harsh reaction conditions, chain-scission occurs to a certain extent both at 180 and 200 °C, which might limit the process and makes new activating groups for aziridines necessary. More activated sulfonamides were installed very recently but did not produce the desulfonated products.⁵⁵

In summary, we present the deprotection of polyaziridines via a reductive mechanism using Red-Al, which leads to a desulfonation of about 80% for the tosyl groups. The MW-assisted acidic hydrolysis resulted in fully deprotected L-PPI for P(TsMAz) and 90% of P(MsMAz). The acidic hydrolysis via microwave irradiation is a cost-efficient, simple, and nontoxic

method in terms of reaction conditions and purification, as all byproducts are easily removed. However, a certain extent of chain scission cannot be avoided under these conditions. This makes further strategies for desulfonation for PAz necessary. The use of other activating groups than mesyl or tosyl are currently under investigation in our lab to prepare PAz, which can be desulfonated under milder and more selective methods and will be reported in a full paper soon.

■ ASSOCIATED CONTENT

Supporting Information

The Supporting Information is available free of charge on the ACS Publications website at DOI: 10.1021/acsmacrolett.8b00180.

Experimental details (PDF).

■ AUTHOR INFORMATION

Corresponding Author

*E-mail: wurm@mpip-mainz.mpg.de.

ORCID

Frederik R. Wurm: 0000-0002-6955-8489

Notes

The authors declare no competing financial interest.

■ ACKNOWLEDGMENTS

The authors thank Prof. Dr. Katharina Landfester for continuous support. The authors thank the Deutsche Forschungsgemeinschaft (DFG WU750/7-1). E.R. thanks Regina Holm (Johannes Gutenberg-University, Mainz, Germany) for the HFIP-SEC-measurements, Barbara Riehl (Johannes Gutenberg-University, Mainz, Germany) and Prof. Dr. Siegfried R. Waldvogel (Johannes Gutenberg-University, Mainz, Germany) for discussions and providing the equipment and conducting the electrochemical reactions.

■ REFERENCES

- Gleede, T.; Rieger, E.; Homann-Müller, T.; Wurm, F. R. 4-Styrenesulfonyl-(2-methyl)aziridine: The First Bivalent Aziridine-Monomer for Anionic and Radical Polymerization. *Macromol. Chem. Phys.* **2018**, *219*, 1700145.

- (2) Homann-Müller, T.; Rieger, E.; Alkan, A.; Wurm, F. R. *N*-Ferrocenylsulfonyl-2-methylaziridine: the first ferrocene monomer for the anionic (co)polymerization of aziridines. *Polym. Chem.* **2016**, *7* (35), 5501–5506.
- (3) Reisman, L.; Mbarushimana, C. P.; Cassidy, S. J.; Ruper, P. A. Living Anionic Copolymerization of 1-(Alkylsulfonyl)aziridines to Form Poly(sulfonylaziridine) and Linear Poly(ethylenimine). *ACS Macro Lett.* **2016**, *5* (10), 1137–1140.
- (4) Rieger, E.; Manhart, A.; Wurm, F. R. Multihydroxy Polyamines by Living Anionic Polymerization of Aziridines. *ACS Macro Lett.* **2016**, *5* (2), 195–198.
- (5) Thomi, L.; Wurm, F. R. Living Anionic Polymerization of Functional Aziridines. *Macromol. Symp.* **2015**, *349* (1), 51–56.
- (6) Rieger, E.; Gleede, T.; Weber, K.; Manhart, A.; Wagner, M.; Wurm, F. R. The living anionic polymerization of activated aziridines: a systematic study of reaction conditions and kinetics. *Polym. Chem.* **2017**, *8* (18), 2824–2832.
- (7) Wang, X.; Liu, Y.; Li, Z.; Wang, H.; Gebru, H.; Chen, S.; Zhu, H.; Wei, F.; Guo, K. Organocatalyzed Anionic Ring-Opening Polymerizations of *N*-Sulfonyl Aziridines with Organic Superbases. *ACS Macro Lett.* **2017**, *6* (12), 1331–1336.
- (8) Stewart, I. C.; Lee, C. C.; Bergman, R. G.; Toste, F. D. Living ring-opening polymerization of *N*-sulfonylaziridines: Synthesis of high molecular weight linear polyamines. *J. Am. Chem. Soc.* **2005**, *127* (50), 17616–17617.
- (9) Rieger, E.; Alkan, A.; Manhart, A.; Wagner, M.; Wurm, F. R. Sequence-Controlled Polymers via Simultaneous Living Anionic Copolymerization of Competing Monomers. *Macromol. Rapid Commun.* **2016**, *37* (10), 833–839.
- (10) Rieger, E.; Blankenburg, J.; Grune, E.; Wagner, M.; Landfester, K.; Wurm, F. R. Controlling the Polymer Microstructure in Anionic Polymerization by Compartmentalization. *Angew. Chem., Int. Ed.* **2018**, *57*, 2483.
- (11) Hadjichristidis, N.; Hiraio, A. *Anionic Polymerization*; Springer: Japan, 2015; p 1082.
- (12) Odian, G. *Principles of Polymerization*, 4th ed.; John Wiley & Sons, Inc.: Hoboken, New Jersey, U.S.A., 2004.
- (13) Boussif, O.; Lezoualc'h, F.; Zanta, M. A.; Mergny, M. D.; Scherman, D.; Demeneix, B.; Behr, J.-P. A versatile vector for gene and oligonucleotide transfer into cells in culture and in vivo: poly-ethylenimine. *Proc. Natl. Acad. Sci. U. S. A.* **1995**, *92* (16), 7297–7301.
- (14) Islam, M. A.; Park, T. E.; Singh, B.; Maharjan, S.; Firdous, J.; Cho, M.-H.; Kang, S.-K.; Yun, C.-H.; Choi, Y. J.; Cho, C.-S. Major degradable polycations as carriers for DNA and siRNA. *J. Controlled Release* **2014**, *193*, 74–89.
- (15) Jaeger, M.; Schubert, S.; Ochrimenko, S.; Fischer, D.; Schubert, U. S. Branched and linear poly(ethylene imine)-based conjugates: synthetic modification, characterization, and application. *Chem. Soc. Rev.* **2012**, *41* (13), 4755–4767.
- (16) Verbraeken, B.; Monnery, B. D.; Lava, K.; Hoogenboom, R. The chemistry of poly(2-oxazoline)s. *Eur. Polym. J.* **2017**, *88*, 451–469.
- (17) Perevyazko, I.; Gubarev, A. S.; Tauhardt, L.; Dobrodumov, A.; Pavlov, G. M.; Schubert, U. S. Linear poly(ethylene imine)s: true molar masses, solution properties and conformation. *Polym. Chem.* **2017**, *8* (46), 7169–7179.
- (18) Saegusa, T.; Kobayashi, S.; Ishiguro, M. A New Route to Optically Active Linear Poly(propylenimine). *Macromolecules* **1974**, *7* (6), 958–959.
- (19) Alonso, D. A.; Andersson, P. G. Deprotection of sulfonyl aziridines. *J. Org. Chem.* **1998**, *63* (25), 9455–9461.
- (20) Senboku, H.; Nakahara, K.; Fukuhara, T.; Hara, S. Hg cathode-free electrochemical detosylation of *N,N*-disubstituted *p*-toluenesulfonamides: mild, efficient, and selective removal of *N*-tosyl group. *Tetrahedron Lett.* **2010**, *51* (2), 435–438.
- (21) Ji, S.; Gortler, L. B.; Waring, A.; Battisti, A. J.; Bank, S.; Closson, W. D.; Wriede, P. A. Cleavage of sulfonamides with sodium naphthalene. *J. Am. Chem. Soc.* **1967**, *89* (20), 5311–5312.
- (22) Bergmeier, S. C.; Seth, P. P. A general method for deprotection of *N*-toluenesulfonyl aziridines using sodium naphthalenide. *Tetrahedron Lett.* **1999**, *40* (34), 6181–6184.
- (23) Henry, J. R.; Marcin, L. R.; McIntosh, M. C.; Scola, P. M.; Davis Harris, G.; Weinreb, S. M. Mitsunobu reactions of *n*-alkyl and *n*-acyl sulfonamides—an efficient route to protected amines. *Tetrahedron Lett.* **1989**, *30* (42), 5709–5712.
- (24) Alonso, E.; Ramón, D. J.; Yus, M. Reductive deprotection of allyl, benzyl and sulfonyl substituted alcohols, amines and amides using a naphthalene-catalysed lithiation. *Tetrahedron* **1997**, *53* (42), 14355–14368.
- (25) Roemmele, R. C.; Rapoport, H. Removal of *N*-arylsulfonyl groups from hydroxy. α -amino acids. *J. Org. Chem.* **1988**, *53* (10), 2367–2371.
- (26) Kudav, D. P.; Samant, S. P.; Hosangadi, B. D. Perchloric Acid-Acetic Acid: A Reagent System for Detosylation. *Synth. Commun.* **1987**, *17* (10), 1185–1187.
- (27) Chavez, F.; Sherry, A. A simplified synthetic route to polyaza macrocycles. *J. Org. Chem.* **1989**, *54* (12), 2990–2992.
- (28) Forshee, P. B.; Sibert, J. W. Sodium Amalgam: A Highly Efficient Reagent for the Detosylation of Azathiocrown Ethers. *Synthesis* **2006**, *2006* (05), 756–758.
- (29) Szostak, M.; Spain, M.; Procter, D. J. Recent advances in the chemoselective reduction of functional groups mediated by samarium (ii) iodide: a single electron transfer approach. *Chem. Soc. Rev.* **2013**, *42* (23), 9155–9183.
- (30) Vedejs, E.; Lin, S. Deprotection of Arenesulfonamides with Samarium iodide. *J. Org. Chem.* **1994**, *59* (7), 1602–1603.
- (31) Knowles, H. S.; Parsons, A. F.; Pettifer, R. M.; Rickling, S. Desulfonylation of amides using tributyltin hydride, samarium diiodide or zinc/titanium tetrachloride. A comparison of methods. *Tetrahedron* **2000**, *56* (7), 979–988.
- (32) Goulaouic-Dubois, C.; Guggisberg, A.; Hesse, M. Protection of Amines by the Pyridine-2-sulfonyl Group and Its Cleavage under Mild Conditions (SmI₂ or Electrolysis). *J. Org. Chem.* **1995**, *60* (18), 5969–5972.
- (33) Mairanovsky, V. G. Electro-Deprotection—Electrochemical Removal of Protecting Groups. *Angew. Chem., Int. Ed. Engl.* **1976**, *15* (5), 281–292.
- (34) Coeffard, V.; Thobie-Gautier, C.; Beaudet, I.; Le Grogne, E.; Quintard, J.-P. Mild Electrochemical Deprotection of *N*-Phenylsulfonyl *N*-Substituted Amines Derived from (R)-Phenylglycinol. *Eur. J. Org. Chem.* **2008**, *2008* (2), 383–391.
- (35) Scialdone, O.; Belfiore, C.; Filardo, G.; Galia, A.; Sabatino, M. A.; Silvestri, G. Direct electrochemical detosylation of tetraosylcyclohexanone to cyclen with carbon cathodes. *Electrochim. Acta* **2005**, *51* (4), 598–604.
- (36) Kossai, R.; Emir, B.; Simonet, J.; Mousset, G. The cathodic cleavage of aromatic sulphonamides: an elegant way to produce amino radicals themselves fully characterized by means of the spin marking technique. *J. Electroanal. Chem. Interfacial Electrochem.* **1989**, *270* (1), 253–260.
- (37) Kubrakova, I. V.; Formanovsky, A. A.; Mikhura, I. V. Facile hydrolytic cleavage of a sulfonamide bond under microwave irradiation. *Mendeleev Commun.* **1999**, *9* (2), 65–66.
- (38) Wellner, E.; Sandin, H.; Pääkkönen, L. Synthesis of 6, 6-difluorohomopiperazines via microwave-assisted detosylation. *Synthesis* **2003**, *2003* (02), 0223–0226.
- (39) Sabitha, G.; Reddy, B. V. S.; Abraham, S.; Yadav, J. S. Deprotection of sulfonamides using iodotrimethylsilane. *Tetrahedron Lett.* **1999**, *40* (8), 1569–1570.
- (40) Vellemäe, E.; Lebedev, O.; Mäeorg, U. A mild method for cleavage of *N*-Tos protected amines using mischmetal and TiCl₄. *Tetrahedron Lett.* **2008**, *49* (8), 1373–1375.
- (41) Nayak, S. K. A Facile Route to the Deprotection of Sulfonate Esters and Sulfonamides with Low Valent Titanium Reagents. *Synthesis* **2000**, *2000* (11), 1575–1578.

- (42) Nyasse, B.; Grehn, L.; Ragnarsson, U. Mild, efficient cleavage of arenesulfonamides by magnesium reduction. *Chem. Commun.* **1997**, *11*, 1017–1018.
- (43) Uchiyama, M.; Matsumoto, Y.; Nakamura, S.; Ohwada, T.; Kobayashi, N.; Yamashita, N.; Matsumiya, A.; Sakamoto, T. Development of a Catalytic Electron Transfer System Mediated by Transition Metal Ate Complexes: Applicability and Tunability of Electron-Releasing Potential for Organic Transformations. *J. Am. Chem. Soc.* **2004**, *126* (28), 8755–8759.
- (44) Hamada, T.; Nishida, A.; Yonemitsu, O. Selective removal of electron-accepting p-toluene- and naphthalenesulfonyl protecting groups for amino function via photoinduced donor acceptor ion pairs with electron-donating aromatics. *J. Am. Chem. Soc.* **1986**, *108* (1), 140–145.
- (45) Urjasz, W.; Celewicz, L. Photochemical removal of the tosyl group from the 5′N position of 5′-aminopyrimidine nucleosides: synthetic applications. *J. Phys. Org. Chem.* **1998**, *11* (8–9), 618–621.
- (46) Yasuhara, A.; Sakamoto, T. Deprotection of N-sulfonyl nitrogen-heteroaromatics with tetrabutylammonium fluoride. *Tetrahedron Lett.* **1998**, *39* (7), 595–596.
- (47) Yasuhara, A.; Kameda, M.; Sakamoto, T. Selective Mono-desulfonylation of N, N-Disulfonylarylamines with Tetrabutylammonium Fluoride. *Chem. Pharm. Bull.* **1999**, *47* (6), 809–812.
- (48) Javorskis, T.; Orentas, E. Chemoslective Deprotection of Sulfonamides Under Acidic Conditions: Scope, Sulfonyl Group Migration, and Synthetic Applications. *J. Org. Chem.* **2017**, *82* (24), 13423–13439.
- (49) Fukuyama, T.; Cheung, M.; Jow, C.-K.; Hidai, Y.; Kan, T. 2, 4-Dinitrobenzenesulfonamides: A simple and practical method for the preparation of a variety of secondary amines and diamines. *Tetrahedron Lett.* **1997**, *38* (33), 5831–5834.
- (50) Fukuyama, T.; Jow, C.-K.; Cheung, M. 2- and 4-Nitrobenzenesulfonamides: Exceptionally versatile means for preparation of secondary amines and protection of amines. *Tetrahedron Lett.* **1995**, *36* (36), 6373–6374.
- (51) Thomi, L.; Wurm, F. R. Aziridine termination of living anionic polymerization. *Macromol. Rapid Commun.* **2014**, *35* (5), 585–9.
- (52) Searles, S.; Nukina, S. Cleavage And Rearrangement Of Sulfonamides. *Chem. Rev.* **1959**, *59* (6), 1077–1103.
- (53) Tauhardt, L.; Kempe, K.; Knop, K.; Altuntaş, E.; Jäger, M.; Schubert, S.; Fischer, D.; Schubert, U. S. Linear Polyethyleneimine: Optimized Synthesis and Characterization – On the Way to “Pharmagrade” Batches. *Macromol. Chem. Phys.* **2011**, *212* (17), 1918–1924.
- (54) Altuntaş, E.; Knop, K.; Tauhardt, L.; Kempe, K.; Crecelius, A. C.; Jäger, M.; Hager, M. D.; Schubert, U. S. Tandem mass spectrometry of poly(ethylene imine)s by electrospray ionization (ESI) and matrix-assisted laser desorption/ionization (MALDI). *J. Mass Spectrom.* **2012**, *47* (1), 105–114.
- (55) Mbarushimana, P. C.; Liang, Q.; Allred, J. M.; Rugar, P. A. Polymerizations of Nitrophenylsulfonyl-Activated Aziridines. *Macromolecules* **2018**, *51* (3), 977–983.

C. P. 3. Carbene catalyzed selective initiation of aziridines

Macromolecules

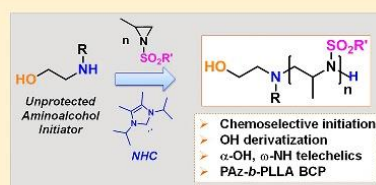
Cite This: *Macromolecules* XXXX, XXX, XXX–XXX

Article

Selective Initiation from Unprotected Aminoalcohols for the *N*-Heterocyclic Carbene–Organocatalyzed Ring-Opening Polymerization of 2-Methyl-*N*-tosyl Aziridine: Telechelic and Block Copolymer SynthesisCamille Bakkali-Hassani,[†] Clément Coutouly,[†] Tassilo Gleede,[‡] Joan Vignolle,[†] Frederik R. Wurm,^{‡,§} Stéphane Carlotti,^{*,†} and Daniel Taton^{*,†}[†]Centre National de la Recherche Scientifique, Laboratoire de Chimie des Polymères Organiques, 16 avenue Pey-Berland, F-33607 Pessac Cedex, France[‡]Max-Planck-Institut für Polymerforschung, Ackermannweg 10, D-55128 Mainz, Germany

Supporting Information

ABSTRACT: Commercial aminoalcohols, namely, 2-(methyl amino)ethanol (1) and diethanolamine (2), are investigated as direct initiators, i.e., with no need of protection of the hydroxyl groups, for the *N*-heterocyclic carbene-organocatalyzed ring-opening polymerization (NHC-OROP) of 2-methyl-*N*-*p*-toluenesulfonyl aziridine. NHC-OROP's are performed at 50 °C in tetrahydrofuran, in the presence of 1,3-bis(isopropyl)-4,5-dimethylimidazol-2-ylidene (^{Me}S-IPr) as organocatalyst. Thus, nonprotected and nonactivated aminoalcohol initiators 1 and 2 provide a direct access to metal-free α -hydroxy- ω -amino- and α,α' -bis-hydroxy- ω -amino telechelics on the basis of polyaziridine (PAz), respectively. Excellent control over molar masses, narrow dispersities ($D \leq 1.20$), and high chain-end fidelity are evidenced by combined analyses, including NMR spectroscopy, size exclusion chromatography, and MALDI ToF mass spectrometry. The amino-initiated NHC-OROP is therefore tolerant to the presence of nonprotected hydroxyl group(s). The as-obtained hydroxyl-ended PAz can be further derivatized in reaction with phenyl isocyanate, highlighting the accessibility of the hydroxyl groups in α -position. Moreover, block copolymer synthesis can be readily achieved by sequential NHC-OROP of 2-methyl-*N*-*p*-toluenesulfonyl aziridine and *L*-lactide, from 1 used in this case as a double-headed initiator. Remarkably, each of the two NHC-OROP steps proves highly chemoselective, with PAz and poly(*L*-lactide) (PLLA) segments being grown from the secondary amino- and the primary hydroxy- function, respectively. In this way, a well-defined PAz-*b*-PLLA diblock copolymer is synthesized in the presence of the same ^{Me}S-IPr organocatalyst, i.e., following a completely metal-free strategy.



INTRODUCTION

In the past 15 years, organocatalysts have been introduced in macromolecular synthesis for producing polymer materials free of any metallic residues, with a potential use in high-value applications, such as biomedical and personal beauty care applications, microelectronic devices, or food packaging.^{1,2} Several classes of organic activators, including Brønsted/Lewis acids or bases and mono- or bicomponent bifunctional catalytic systems, have been utilized, both for step-growth and chain-growth polymerizations, and for depolymerization reactions as well. Several general reviews or highlights on organo-catalyzed polymerizations are available,^{2–6} while other reviews have dealt with more specific aspects, e.g., the ring-opening polymerization (ROP),^{7–9} the group-transfer polymerization (GTP) of acrylics and methacrylics,^{10,11} the zwitterionic polymerization,¹² or organo-catalyzed polymerizations induced by H-bond components.^{13–15}

In this context, *N*-heterocyclic carbenes (NHCs) have been among the first organocatalysts employed for polymer synthesis, providing a straightforward synthetic strategy to a wide

range of polymers.^{5,6,12,16–18} This is obviously related to the near unlimited structural diversity of NHCs, which allows finely tuning their steric and electronic properties and using them either as Brønsted and/or Lewis bases.^{19–22} Cyclic esters (e.g., lactide and lactones) have been by far the most investigated monomer substrates in NHC-organocatalyzed ROP (NHC-OROP).^{16,23–25} However, the range of monomers amenable to polymerization by a NHC catalysis has largely been expanded to the ROP of other heterocycles, including five-membered *O*-carboxyanhydrides,²⁶ *N*-substituted carboxyanhydrides,^{27–29} phosphoesters,³⁰ carbonates,^{31,32} siloxanes and carbosiloxanes,³³ lactams,^{34,35} epoxides,^{36,37} and *N*-activated aziridines,^{38,39} also to the polymerization of alkyl (meth)acrylates,^{40–43} and finally to some polymerizations proceeding by a step-growth process, such as polyurethane⁴⁴ or polyepoxide⁴⁵ synthesis. Besides their role as true catalysts,

Received: November 25, 2017

Revised: February 24, 2018

ACS Publications

© XXXX American Chemical Society

A

DOI: 10.1021/acs.macromol.7b02493
Macromolecules XXXX, XXX, XXX–XXX

Table 1. NHC-OROP of 2-Methyl-*N*-*p*-toluenesulfonyl Aziridine Using Aminoalcohol 1 or 2 as Initiator (THF, 50 °C, 24 h)

Run	Initiator	[Az]/[Initiator]/[NHC]	Conv. ^(a) (%)	$\overline{Mn}_{\text{THEO}}^{(b)}$	$\overline{Mn}_{\text{SEC}}^{(c)}$	$D^{(c)}$
1		10/1/0.1	100	2 100	2 650	1.10
2		20/1/0.1	100	4 200	3 750	1.08
3		50/1/0.1	100	10 600	7 800	1.15
4		100/1/0.1	100	21 100	16 600	1.09
5		20/1/0.1	100	4 200	17 000	1.23
6		10/1/0.1	100	2 100	2 400	1.18
7		20/1/0.1	100	4 200	3 800	1.18
8		50/1/0.1	100	10 600	6 500	1.10
9		100/1/0.1	100	21 100	13 200	1.11

^aConversion was calculated by ¹H NMR. ^b $\overline{Mn}_{\text{THEO}} = ([\text{Az}]/[\text{Initiator}]) \times M_{\text{Az}} \times \text{conv.}$ (in g mol⁻¹). ^cNumber-average molar mass (in g mol⁻¹) and dispersity determined by size exclusion chromatography in THF (PS calibration).

i.e., in organo-catalyzed polymerizations, some NHCs can operate as direct nucleophilic initiators in the absence of an initiator, i.e., in organo-initiated polymerization, for instance, through ring-opening of heterocyclic monomers^{2–6,12,16,36} or through 1,4-conjugate addition of some (meth)acrylic substrates.^{46–48} In many cases, NHCs provide high polymerization rates, excellent chain-end fidelity, and control over molar masses of resulting polymers and also allow achieving cyclic polymer structures.^{5,6,17}

Inspired by seminal works by Toste and Bergman et al.⁴⁹ and later on by Wurm et al. and Rupar et al. on the organometallic-type anionic ROP of *N*-sulfonyl aziridines,^{50–53} we have recently shown that these three-membered ring heterocycles can be subjected to a controlled NHC-OROP.^{38,39} Typically, catalytic amounts of 1,3-bis(isopropyl)-4,5(dimethyl)imidazol-2-ylidene (^{Me}S-Ipr) as NHC organocatalyst and THF as solvent have been employed at 50 °C. In this case, an *N*-activated secondary amine mimicking the growing chains has been selected as an initiator. Metal-free polyaziridines (PAz), as well as PAz-based block copolymers, have thus been achieved, with excellent control over molar masses (up to 20,000 g·mol⁻¹) and low dispersities ($D < 1.15$). In another contribution, we have shown that the NHC-OROP is tolerant to functional initiators, such as an α -allyl *N*-sulfonyl amine or trimethylsilyl azide, enabling a direct access to α -functionalized PAz.³⁹ In addition, we have demonstrated that activation of the amino-containing initiator is eventually not required for the controlled NHC-OROP to proceed. A nonactivated secondary amine, namely, di-*n*-butylamine, can indeed directly initiate the NHC-OROP of *N*-tosylaziridines.³⁹ As discussed in previous reports,^{49–53} poly(*n*-alkyl aziridine)s are precursors of choice of well-defined linear poly(ethylene imine), for potential applications in the biomedical field. While preparing this manuscript, Guo et al. have reported that some “organic superbases”, such as phosphazene (*t*Bu-P₄) and the Verkade’s base (P-

(*i*PrNCH₂CH₂)₃N), can be employed to catalyze the controlled/living AROP of 2-methyl-*N*-tosylaziridine.⁵⁴ In this contribution, we resort for the first time to nonprotected nonactivated aminoalcohols as direct initiators for the synthesis of both α -hydroxy- ω -amino- and α,α' -bis-hydroxy- ω -amino telechelics based on PAz. Of particular interest, such PAz precursors can serve as macroinitiators for further chain extension. Thus, α -hydroxy- ω -amino PAz enables block copolymer synthesis by sequential NHC-OROP of 2-methyl-*N*-*p*-toluenesulfonyl aziridine and L-lactide (L-LA) in this order, from the secondary amine and from the primary hydroxyl, respectively, yielding PAz-*b*-PLLA block copolymers. Overall, this *N*-activated aziridine NHC-OROP method warrants high chain-end fidelity and high control over molar masses and dispersities, providing a path breaking to metal-free and hydroxylated PAz and to novel block copolymers.

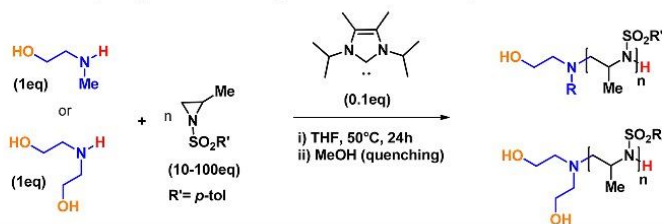
EXPERIMENTAL SECTION

Instrumentation. NMR spectra were recorded on a Bruker Avance 400 (¹H, ¹³C, 400.2 and 100.6 MHz, respectively) in appropriate deuterated solvents. Molar masses were determined by size exclusion chromatography (SEC) in THF (1 mL/min) with trichlorobenzene as a flow marker, using both refractometric (RI) and UV detectors. Analyses were performed using a three-column TSK gel TOSOH (G4000, G3000, G2000) calibrated with polystyrene standards. MALDI ToF spectra were performed by the CESAMO (Bordeaux, France) on a Voyager mass spectrometer (Applied Biosystems). Spectra were recorded in the positive-ion mode using the reflectron and with an accelerating voltage of 20 kV. Samples were dissolved in THF at 10 mg/mL. The matrix solution (*trans*-3-indoleacrylic acid, IAA) was prepared by dissolving 10 mg in 1 mL of THF. A MeOH solution of cationization agent (NaI, 10 mg/mL) was also prepared. Solutions were combined in a 10:1:1 volume ratio of matrix to sample to cationization agent.

Materials. THF was dried over sodium/benzophenone and distilled prior to use. 2-(Methylamino) ethanol (Sigma-Aldrich,

B

DOI: 10.1021/acs.macromol.7b02493
Macromolecules XXXX, XXX, XXX–XXX

Scheme 1. NHC-OROP of 2-Methyl *N*-*p*-Toluenesulfonyl Aziridine Initiated by Aminoalcohols

>98.0%) was dried over refluxed KOH pellets and distilled prior to use. Toluene was dried over CaH₂, refluxed overnight, distilled, and stored over polystyryllithium. Diethanolamine (Sigma-Aldrich, >98.0%) was dried by azeotropic distillation with dry toluene (three times) and further dried under a vacuum overnight at 50 °C. (L)-Lactide (Sigma-Aldrich, 98.0%) was recrystallized three times from dry toluene. 1,3-Bis(isopropyl)-4,5(dimethyl)imidazol-2-ylidene (^{Me}S-IPr) was prepared according to the procedure already reported by Kuhn et al.⁵⁵ 2-Methyl-*N*-tosylaziridine was prepared according to the procedure described by Wurm et al.^{50,51} The ¹H NMR spectrum of 2-methyl *N*-*p*-toluenesulfonyl aziridine is provided in the Supporting Information (Figure S1). Phenyl isocyanate (Sigma-Aldrich, >98.0%) and hexamethylene diisocyanate (Sigma-Aldrich, >99.0%) were used as received. All polymerizations were conducted under an argon atmosphere at 50 °C.

General Polymerization Procedure. In a typical procedure, 0.5 mg (2.9 μmol) of ^{Me}S-IPr, 150 μL (0.2 M in THF) of 2-(methylamino) ethanol, and 850 μL of dried THF were added in a flame-dried Schlenk flask in the glovebox. After homogenization, the solution was cooled down to 0 °C, and a solution containing 120 mg (0.57 mmol) of 2-methyl *N*-tosylaziridine in 1 mL of THF was added under an argon flux. After 24 h at 50 °C, an aliquot of the polymerization mixture was taken to determine the conversion by ¹H NMR (THF-*d*8). The reaction was quenched with 1 mL of degassed MeOH and stirred for 30 min. The crude product was analyzed by SEC in THF, purified by precipitation in MeOH (twice), and then washed with ether. The PAz derivative was recovered as a white solid after drying under a vacuum at room temperature (12 h). Note that this polymerization can be implemented at the gram scale under these experimental conditions. ¹H NMR PAz (400 MHz, 298 K, THF-*d*8): δ (ppm) = 8.10–7.70 (br, 2H, CH(Ar)); 7.50–7.20 (br, 2H, CH(Ar)); 4.50–3.80 (br, 1H, CH(backbone)); 3.80–3.00 (br, 2H, CH₂(backbone)); 2.38 (s, 3H, CH₃(tosyl)); 1.20–0.90 (br, 3H, CH₃). ¹³C NMR PAz (100.6 MHz, 298 K, THF-*d*8; see Figures S2 and S3): δ (ppm) = 143.90; 137.75; 130.20; 127.84; 55.18; 49.82; 16.05; 14.83; 13.70.

Functionalization of α-Hydroxy-ω-aminotelechelic PAz Using Phenyl Isocyanate. In a flame-dried Schlenk flask were added 40 mg (9.5 μmol) of α-hydroxy-ω-aminotelechelic PAz (run 1, Table 1) dried by three azeotropic distillations with toluene. Phenyl isocyanate (21 μL, 0.19 mmol, 20 equiv) was then added under an argon flux, and the mixture was heated up to 70 °C for 24 h. The reaction was monitored by ¹H NMR (THF-*d*8), and the crude product was purified by precipitation twice in MeOH and dried under a vacuum at room temperature (8 h).

¹H NMR (400 MHz, 298 K, THF-*d*8). δ (ppm) = 8.66 (br, NH, 1H); 8.10–7.70 (br, 40H, CH(tosyl)); 7.50–7.20 (br, 40H, CH(tosyl) + 4H (phenyl)); 6.90 (m, 1H, CH(phenyl)); 4.50–3.80 (br, 20H, CH(backbone)); 3.80–3.00 (br, 40H, CH₂(backbone)); 2.38 (s, 60H, CH₃(tosyl)); 1.20–0.90 (br, 60H, CH₃).

Polymerization of L-Lactide Initiated from the α-Hydroxy-ω-aminotelechelic PAz. In the glovebox, 40.0 mg of α-hydroxy-ω-aminotelechelic PAz (run 1, Table 1), dried by three azeotropic distillations with toluene, 0.2 mg (1.1 μmol) of ^{Me}S-IPr, and 1 mL of dried THF were added in a flame-dried Schlenk flask. After homogenization, the solution was cooled down to 0 °C, and a solution containing 130 mg (0.91 mmol) of (L)-lactide in 1 mL of

THF was added under argon. After 24 h at 50 °C, an aliquot of the polymerization mixture was taken to determine the conversion by ¹H NMR in THF-*d*8 (conv. 52% after 24 h). The reaction was quenched with a solution containing 10 mg of benzoic acid in 1 mL of MeOH and stirred for 30 min. The crude product was analyzed by SEC (THF), purified by precipitation in MeOH at low temperature (0 °C), and then washed with ether. PAz-*b*-poly(lactide) was recovered as a white solid after drying under a vacuum at room temperature (12 h). ¹H NMR PAz-*b*-PLA (400 MHz, 298 K, THF-*d*8): δ (ppm) = 8.10–7.70 (br, 40H, CH(tosyl)); 7.50–7.20 (br, 40H, CH(tosyl)); 5.16 (m, 30H, CH(PLA)); 4.50–3.80 (br, 20H, CH(PAz)); 3.80–3.00 (br, 40H, CH₂(PAz)); 2.38 (s, 60H, CH₃(tosyl)); 1.51 (m, 90H, CH₃(PLA)); 1.20–0.90 (br, 60H, CH₃).

Functionalization of α,α'-Bishydroxy-ω-aminotelechelic PAz with Phenyl Isocyanate. In a flame-dried Schlenk were added 40 mg (32.0 μmol) of α,α'-hydroxy-ω-aminotelechelic PAz (Run 6, Table 1) dried by three azeotropic distillations with toluene. Phenyl isocyanate (69 μL, 0.64 mmol, 20 equiv) was added under argon and the mixture was heated up to 70 °C during 24h. The reaction was monitored by ¹H NMR spectroscopy (THF-*d*8). The crude product was purified by precipitation twice in MeOH and dried under vacuum at room temperature (8h). ¹H NMR (400 MHz, 298K, THF-*d*8): δ(ppm) = 8.60 (br, NH, 1H) 8.10–7.70 (br, 20H, CH(tosyl)); 7.50–7.20 (br, 20H, CH(tosyl) + 4H (phenyl)); 6.88 (m, 1H, CH(phenyl)) 4.50–3.80 (br, 10H, CH(backbone)); 3.80–3.00 (br, 20H, CH₂(backbone)); 2.38 (s, 30H, CH₃(tosyl)); 1.20–0.90 (br, 30H, CH₃).

RESULTS AND DISCUSSION

As we have previously reported, a simple nonactivated secondary amine can directly initiate the ^{Me}S-IPr-OROP of 2-methyl-*N*-*p*-toluenesulfonyl aziridine.³⁹ Here, two different commercially available hydroxyl-containing nonactivated amines⁵⁶ were examined as novel initiators to directly prepare α-hydroxy-ω-aminotelechelic poly(*N*-tosyl aziridine)s, as depicted in Scheme 1. Reactions were carried out at 50 °C in THF, with 10 mol % of 1,3-bis(isopropyl)-4,5(dimethyl)-imidazol-2-ylidene (^{Me}S-IPr) relative to the initiator. Table 1 summarizes the different polymerization experiments. Indeed, very well-defined polyazirines (PAz) were obtained using 2-(methyl amino)ethanol (1) under those conditions (entries 1–4, Table 1), excellent control over molar masses (up to 16 600 g·mol⁻¹), and low dispersities (*D* < 1.20, see Figure 1) being achieved, with symmetrical and monomodal size exclusion chromatography (SEC) traces. In addition, apparent molar masses, as determined by SEC, increased when increasing the initial monomer to the initiator molar ratio (Figure 1, runs 1–4, and Table 1).

The ¹H NMR spectrum of a typical PAz initiated from 1 showed all signals due to the resonance of the protons of the repeating unit (Figure 2a). However, the presence of the hydroxyl group in the α-position of PAz chains could not be directly detected. Thus, further derivatization of this PAz precursor using an excess of phenyl isocyanate (20 equiv) led to

C

DOI: 10.1021/acs.macromol.7b02493
Macromolecules XXXX, XXX, XXX–XXX

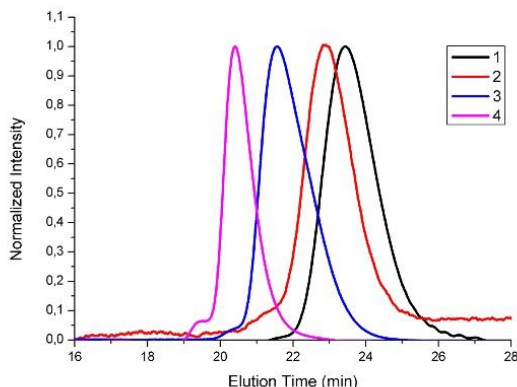


Figure 1. SEC traces (RI detection) of poly(2-methyl *N-p*-toluenesulfonyl aziridine)s initiated by 2-methyl aminoethanol (runs 1–4, Table 1).

an α -urethane PAz, the characterization of which by SEC showed a slight shift toward the higher molar masses due to the introduction of the carbamate moiety in PAz chain-ends (Figure 3d), with retention of a low dispersity. Characteristic signals in the aromatic region at 6.90–7.50 ppm and around 8.60 ppm, assigned to the phenyl ring and to the NH of the carbamate moiety, respectively, were unambiguously detected by ^1H NMR after this postchemical modification step (Figure 2b). This attested to the presence of the hydroxyl group in the parent PAz derived from **1**, also confirming that PAz chains were grown from the secondary ω -NH(Ts) amino functionality in a controlled manner, with no interference of the hydroxyl group. In addition, PAz molar mass could be precisely estimated by comparing the relative intensity of the urethane

signals with those corresponding to the main chain protons, assuming that the modification reaction was quantitative. Agreement between experimental molar masses and theoretical values (Table 1) supported that both the initiation of NHC-OROP and the derivatization of $-\text{OH}$ end groups into $-\text{O}(\text{C}=\text{O})\text{N}(\text{H})\text{Ph}$ were highly efficient. As already noted in our previous works on NHC-OROP of *N*-activated aziridines,^{38,39} apparent molar masses as determined by SEC using PS standards were lower than those predicted.

In Figure 3b is displayed the MALDI ToF mass spectrum of the carbamate-functionalized PAz. The isotopic distribution perfectly matched the expected structure, supporting the accessibility of the hydroxy function in the α -position through quantitative derivatization of the α -OH PAz precursor. All of these results thus demonstrated that 2-methyl aminoethanol **1** initiated the NHC-OROP of 2-methyl *N*-tosylaziridine in THF at 50 °C from the secondary amino group in a highly chemoselective manner, with the unprotected primary OH group remaining inactive.

A reaction was performed under the same conditions in the presence of allyl alcohol, in order to figure out whether this simple primary alcohol could somehow affect the polymerization outcome. Although polymerization did take place (entry 5, Table 1), forming a PAz with a higher molar mass than expected, $M_n = 17\,000\text{ g}\cdot\text{mol}^{-1}$ and $D = 1.23$, ^1H NMR analysis of this polymer did not show any evidence of the incorporation of allyl alcohol; no diagnostic signal due to the allylic protons was detected. A control experiment directly utilizing $^{\text{Me}}\text{5-IPr}$ and the monomer, i.e., in the absence of any other reagent, also formed a PAz derivative with in this case a M_n value of 60 000 $\text{g}\cdot\text{mol}^{-1}$ and $D = 1.25$ (Figure S4), very likely via the so-called zwitterionic ring-opening polymerization (ZROP) mechanism.^{2–6,12,16,36} In other words, due to its nucleophilic character, $^{\text{Me}}\text{5-IPr}$ was able to directly initiate the ROP 2-

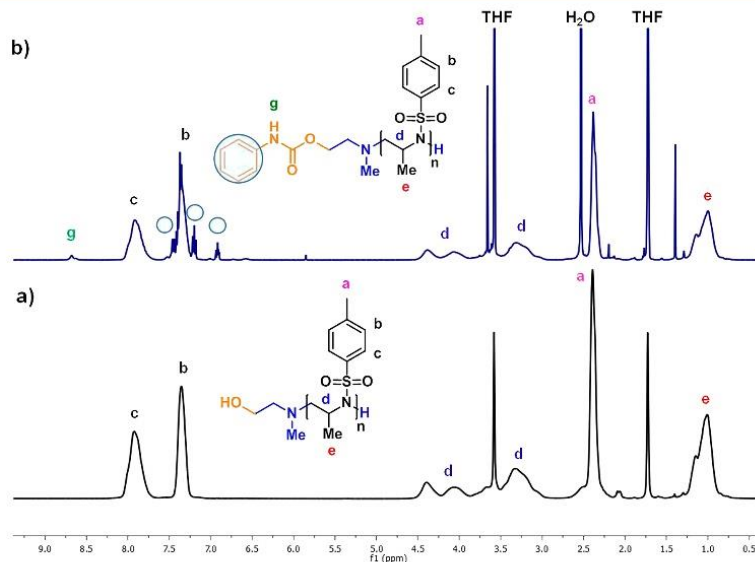


Figure 2. ^1H NMR spectrum of an α -hydroxy- ω -NH(tosyl) poly(2-methyl *N-p*-toluenesulfonyl aziridine) initiated by 2-methyl aminoethanol (run 1, Table 1) and its α -carbamate derivative obtained after postfunctionalization (b).

D

DOI: 10.1021/acs.macromol.7b02493
Macromolecules XXXX, XXX, XXX–XXX

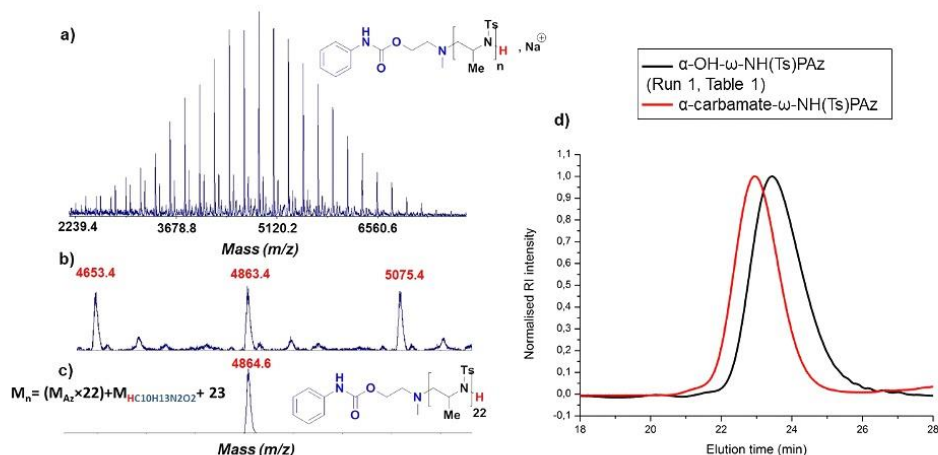
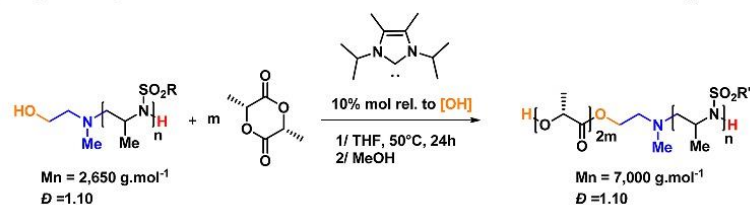


Figure 3. (a) Experimental and (b, c) computed MALDI ToF mass spectrum of a α -carbamate- ω -NH(Ts) poly(2-methyl *N-p*-toluenesulfonyl aziridine) obtained by postfunctionalization and (d) SEC traces of α -hydroxy-poly(2-methyl *N-p*-toluenesulfonyl aziridine) before (in black) and after (in red) derivatization by phenylisocyanate.

Scheme 2. Synthesis of Poly(2-methyl *N-p*-toluene sulfonyl aziridine)-*b*-Poly(L-lactide) Block Copolymer by Sequential NHC-OROP Using 2-(Methyl amino)ethanol as a Double-Headed Initiator and ^{Me}S-IPr as the Same Organocatalyst



methyl *N*-tosylaziridine. However, the presence of allyl alcohol somehow affected the ROP kinetics: longer reaction times were indeed needed to reach complete conversion in this case, compared to a direct ZROP experiment (see the proposed mechanism in Scheme S1).⁵⁷

The synthesis of well-defined α -functionalized PAz by NHC-OROP, and evidence of the easy accessibility of the OH group through quantitative derivatization, prompted us to derive a novel family of block copolymers using this precursor as a macroinitiator. Synthetic strategies to block copolymers generally include (i) sequential polymerization, i.e., consecutive addition of at least two monomers, (ii) coupling of preformed homopolymers with antagonist end groups, (iii) switch from one to another polymerization mechanism, and (iv) use of a “double-headed” initiator.^{58–61} In our initial paper, all PAz-based block copolymers have been successfully obtained by sequential NHC-OROP, using an *N*-activated amine initiator.³⁸ Here, we envisioned that 2-(methyl amino)ethanol could serve as a double-headed initiator to grow two types of polymer chains, namely, a PAz chain and a poly(L-lactide) (PLLA) from the secondary amino and hydroxyl groups, respectively. Thus, we took advantage of the presence of the OH group in the α -position of the α -hydroxy- ω -aminotelechelic PAz precursor to grow a PLLA block in the presence of the same ^{Me}S-IPr organocatalyst. As a proof of concept, L-lactide (L-LA) was added onto a THF solution of the preformed α -hydroxy PAz initiated by **1** and catalyzed by ^{Me}S-IPr, playing here the role of

a macroinitiator. It was thus expected that initiation of the NHC-OROP of LA selectively took place from the primary hydroxyl, in this case with no interference by the secondary ω -NH(Ts) amino end group of the PAz precursor (see Scheme 2). After stirring the solution overnight at 50 °C, the SEC trace of the resulting compound clearly shifted to the higher molar masses, while the dispersity remained very low, attesting to a highly effective crossover reaction from PAz to PLLA (Figure 4). Analysis by ¹H NMR confirmed the presence of both PAz and PLA blocks. The overall composition of the PAz-*b*-PLLA block copolymer could be estimated, knowing the molar mass of the α -OH PAz precursor, from the relative integrations of characteristic signals of both blocks at 7.70–8.10 ppm (*Ar*) and at 5.16 ppm (*Me*) for PAz and PLLA blocks, respectively. A value of 8600 g·mol⁻¹, vs 7000 g·mol⁻¹ by SEC analysis, was thus calculated for a total molar mass of 4300 and 4300 g·mol⁻¹ for the PAz and PLA blocks, respectively (Figure 5). The latter value agreed with the expected molar mass based on a quantitative initiation from the α -OH PAz precursor. Thus, block copolymer synthesis could be readily achieved by sequential NHC-OROP of aziridine and LA, using 2-methyl aminoethanol as a double-headed initiator. Intriguingly, the sequential growth by NHC-OROP occurs with a high selectivity, with PAz and PLA blocks being grown from the secondary ω -NH(Ts) amino- and primary hydroxy- functions, respectively. This fully metal-free synthetic strategy enables

E

DOI: 10.1021/acs.macromol.7b02493
Macromolecules XXXX, XXX, XXX–XXX

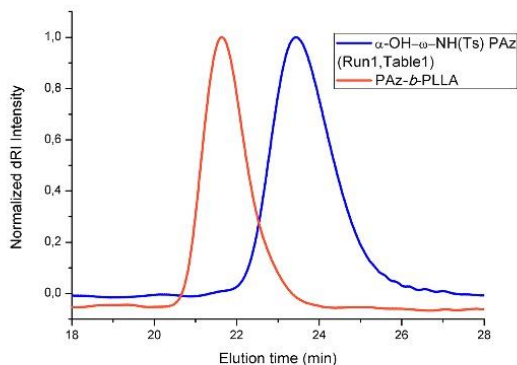


Figure 4. SEC traces of α -hydroxy-poly(2-methyl *N*-*p*-toluenesulfonyl aziridine) and poly(2-methyl *N*-*p*-toluenesulfonyl aziridine)-*b*-poly(L-lactide) obtained by sequential NHC-OROP.

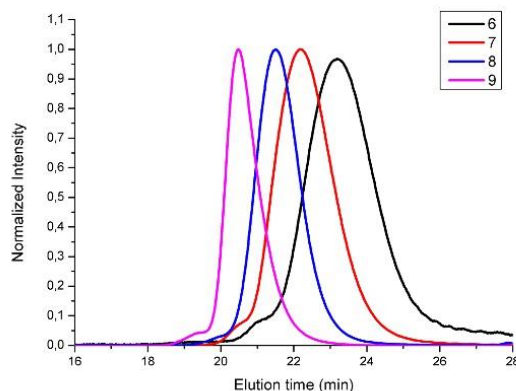


Figure 6. SEC traces of poly(2-methyl *N*-*p*-toluene sulfonyl aziridine) initiated by diethanolamine (runs 6–9, Table 1).

synthesis of well-defined and unprecedented PAz-*b*-PLLA diblock copolymers from the same NHC organocatalyst.

We then resorted to another commercially available hydroxyamino-containing compound, namely, diethanolamine (**2**, Scheme 1), to initiate the NHC-OROP of 2-methyl *N*-tosylaziridine. In the latter case, it was expected that α,α' -bis-hydroxy- ω -amino PAz telechelics could be synthesized. Different ratios between the monomer and the initiator were employed (entries 6–9, Table 1). Remarkably, well-defined polymers could also be obtained in this case, with molar masses in the range 3200–13 200 g·mol⁻¹ and $\bar{D} < 1.20$, and with no need for protection of the two hydroxyl groups of **2** (Figure 6). As in the case of the α -OH- ω -NH(Ts) PAz obtained from **1**, the presence of the primary hydroxyl groups could not be

directly evidenced by ¹H NMR (see Figure S4 for peak assignments). However, MALDI ToF MS analysis of a low molar mass PAz obtained in this way (entry 7, Table 1) revealed a single population consistent with the formation of a cationized PAz, with a peak-to-peak mass increment of 211.3 g·mol⁻¹ corresponding to the molar mass of one monomer unit (Figure 7). Discrete peaks appeared at $m/z = 211.3n + M_{(\text{HOCH}_2\text{CH}_2)_2\text{N}} + M_{\text{H}} + 23$, where n was the degree of polymerization, 23 was the molar mass of Na⁺ generated during ionization, and $M_{(\text{HOCH}_2\text{CH}_2)_2\text{N}}$ and M_{H} were the molar mass of end groups introduced in the α - and ω -position, respectively. Simulations giving the theoretical isotope distributions were in perfect agreement with experimental distributions attributed to the cationized adduct of the α -diethanolamino, ω -NH(Ts) PAz.

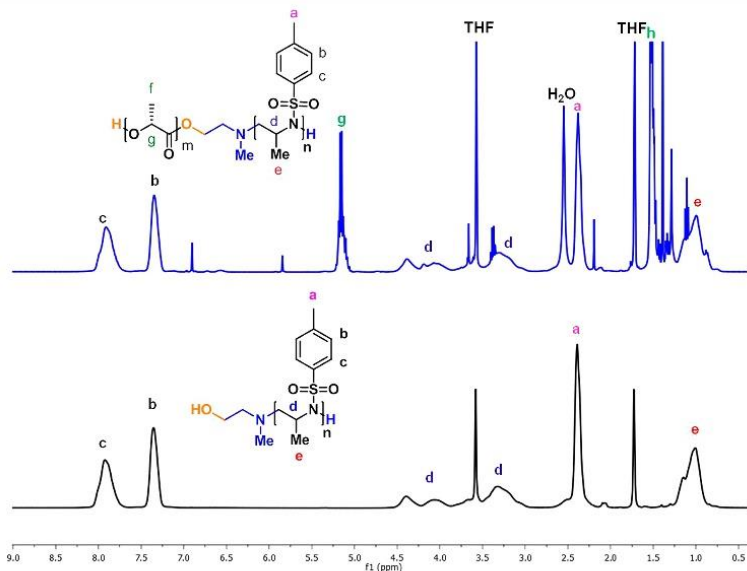


Figure 5. ¹H NMR (THF-*d*₈) spectrum of α -hydroxy-poly(2-methyl *N*-*p*-toluenesulfonyl aziridine) and poly(2-methyl *N*-*p*-toluenesulfonyl aziridine)-*b*-poly(lactide) obtained by sequential NHC-OROP.

F

DOI: 10.1021/acs.macromol.7b02493
Macromolecules XXXX, XXX, XXX–XXX

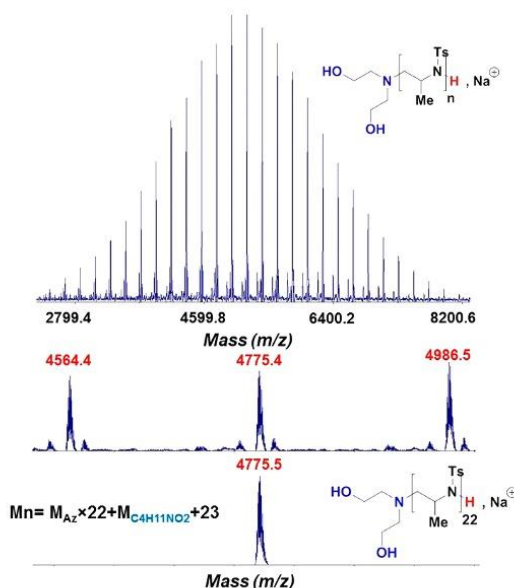


Figure 7. Experimental and computed MALDI ToF mass spectrum of an α,α' -bishydroxy, ω -NH(tosyl) poly(2-methyl *N*-*p*-toluenesulfonyl aziridine).

This result unambiguously attested to the presence of both hydroxyl groups in the α -position of PAz chains, i.e., to the formation of a α,α' -bis-hydroxy PAz telechelic.

To further illustrate the reactivity of the geminal hydroxy chain ends, the latter PAz was also reacted with 2 equiv of phenyl isocyanate, leading to a telechelic α,α' -bis-carbamate PAz telechelic. This was supported by ^1H NMR analysis showing the diagnostic signal at 8.6 ppm, due to the NH of the carbamate group (Figure S5). In Figure S6 are also displayed SEC traces before and after urethanization, with a slight increase in molar mass after addition of phenyl isocyanate, while the dispersity remains very low. MALDI ToF MS analysis of the low molar mass α,α' -bis-carbamate PAz telechelic revealed a single population consistent with the formation of a cationized PAz, with a peak-to-peak mass increment of $211.3\text{ g}\cdot\text{mol}^{-1}$ corresponding to the molar mass of one monomer unit (Figure S7). Simulations giving the theoretical isotope distributions were flawlessly matched experimental distributions attributed to the cationized adduct of the α -dicarbamate, ω -NH(Ts) PAz (Figure S7).

CONCLUSION

The *N*-heterocyclic carbene-organocatalyzed ring-opening polymerization (NHC-OROP) of 2-methyl-*N*-*p*-toluenesulfonyl aziridine can be controlled at $50\text{ }^\circ\text{C}$ in THF in the presence of aminoalcohols as multifunctional initiators. This provides a facile and direct synthetic access to metal-free α -hydroxy, ω -amino and α,α' -bis-hydroxy, ω -amino poly(*N*-tosyl aziridine) telechelics, with no need for tedious protection–deprotection chemistry. As evidenced by combined characterizations, including NMR spectroscopy, SEC, and MALDI ToF mass spectrometry, this NHC-OROP process proves highly chemoselective and guarantees high chain-end fidelity, as well as a

high level of control over molar masses and dispersity. Given the accessibility and versatility of the hydroxyl function, both for postfunctionalization reactions and as an initiating fragment for a wide range of polymerization reactions, this synthetic strategy utilizing commercially available nonactivated hydroxy-containing amines further expands the scope of NHC-mediated polymerizations for macromolecular engineering of polyaziridines. This is demonstrated here with the preparation of poly(*N*-tosyl aziridine)-*b*-poly(*L*-lactide) block copolymer by sequential and selective NHC-OROP using the same NHC organocatalyst. Future work will focus on aminoalcohol-initiated NHC-OROP of other *N*-substituted aziridine monomers, and on the synthesis and investigations of the properties of various block copolymers.

ASSOCIATED CONTENT

Supporting Information

The Supporting Information is available free of charge on the ACS Publications website at DOI: 10.1021/acs.macromol.7b02493.

Additional ^1H and ^{13}C NMR and MALDI ToF spectra for polymers and proposed polymerization mechanism (PDF)

AUTHOR INFORMATION

Corresponding Authors

* (S.C.) E-mail: carlotti@enscbp.fr.

* (D.T.) E-mail: taton@enscbp.fr

ORCID

Frederik R. Wurm: 0000-0002-6955-8489

Stéphane Carlotti: 0000-0002-0086-4955

Daniel Taton: 0000-0002-8539-4963

Notes

The authors declare no competing financial interest.

ACKNOWLEDGMENTS

The authors gratefully thank the French Ministry of Education and Research for financial support of C.B.-H. F.R.W. thanks the Deutsche Forschungsgemeinschaft (WU 750/7-1) for funding.

REFERENCES

- MacMillan, D. W. C. The Advent and Development of Organocatalysis. *Nature* **2008**, *455*, 304–308.
- Kiesewetter, M. K.; Shin, E. J.; Hedrick, J. L.; Waymouth, R. M. Organocatalysis: Opportunities and Challenges for Polymer Synthesis. *Macromolecules* **2010**, *43*, 2093–2107.
- Ottou, W. N.; Sardon, H.; Mecerreyes, D.; Vignolle, J.; Taton, D. Update and Challenges in Organo-Mediated Polymerization Reactions. *Prog. Polym. Sci.* **2016**, *56*, 64–115.
- Hu, S.; Zhao, J.; Zhang, G.; Schlaad, H. Macromolecular Architectures through Organocatalysis. *Prog. Polym. Sci.* **2017**, *74*, 34–77.
- Fèvre, M.; Pinaud, J.; Gnanou, Y.; Vignolle, J.; Taton, D. *N*-Heterocyclic Carbenes (NHCs) as Organocatalysts and Structural Components in Metal-Free Polymer Synthesis. *Chem. Soc. Rev.* **2013**, *42*, 2142–2172.
- Naumann, S.; Dove, A. P. *N*-Heterocyclic Carbenes for Metal-Free Polymerization Catalysis: An Update. *Polym. Int.* **2016**, *65*, 16–27.
- Kamber, N. E.; Jeong, W.; Pratt, R. C.; Lohmeijer, B. G.; Hedrick, J. L.; Waymouth, R. M. Organocatalytic Ring-Opening Polymerization. *Chem. Rev.* **2007**, *107*, 5813–5840.

- (8) Dove, A. P. Organic Catalysis for Ring-Opening Polymerization. *ACS Macro Lett.* **2012**, *1*, 1409–1412.
- (9) Mespouille, L.; Coulembier, O.; Kawalec, M.; Dove, A. P.; Dubois, P. Implementation of Metal-Free Ring-Opening Polymerization in the Preparation of Aliphatic Polycarbonate. *Prog. Polym. Sci.* **2014**, *39*, 1144–1164.
- (10) Chen, Y.; Kakuchi, T. Organocatalyzed Group Transfer Polymerization. *Chem. Rec.* **2016**, *16*, 2161–2183.
- (11) Takada, K.; Ito, T.; Kitano, K.; Tsuchida, S.; Takagi, Y.; Chen, Y.; Satoh, T.; Kakuchi, T. Synthesis of Homopolymers, Diblock Copolymers, and Multiblock Polymers by Organocatalyzed Group Transfer Polymerization of Various Acrylate Monomers. *Macromolecules* **2015**, *48*, 511–519.
- (12) Brown, H. A.; Waymouth, R. M. Zwitterionic Ring-Opening Polymerization for the Synthesis of High Molecular Weight Cyclic Polymers. *Acc. Chem. Res.* **2013**, *46*, 2585–2596.
- (13) Thomas, C.; Bibal, B. Hydrogen-Bonding Organocatalyst for Ring-Opening Polymerization. *Green Chem.* **2014**, *16*, 1687–1699.
- (14) Chuma, A.; Horn, H. W.; Swope, W. C.; Pratt, R. C.; Zhang, L.; Lohmeijer, B. G. G.; Wade, C. G.; Waymouth, R. M.; Hedrick, J. L.; Rice, J. E. The Reaction Mechanism for the Organocatalytic Ring-Opening Polymerization of L-Lactide Using a Guanidine-Based Catalyst: Hydrogen-Bonded or Covalently Bound? *J. Am. Chem. Soc.* **2008**, *130*, 6749–6754.
- (15) Zhang, X.; Jones, G. O.; Hedrick, J. L.; Waymouth, R. M. Fast and Selective Ring-Opening Polymerizations by Alkoxides and Thioureas. *Nat. Chem.* **2016**, *8*, 1047–1053.
- (16) Connor, E. F.; Nycy, G. W.; Myers, M.; Möck, A.; Hedrick, J. L. First Example of N-Heterocyclic Carbenes as Catalysts for Living Polymerization: Organocatalytic Ring-Opening Polymerization of Cyclic Esters. *J. Am. Chem. Soc.* **2002**, *124*, 914–915.
- (17) Naumann, S.; Dove, A. P. N-Heterocyclic Carbenes as Organocatalysts for Polymerizations: Trends and Frontiers. *Polym. Chem.* **2015**, *6*, 3185–3200.
- (18) Naumann, S.; Buchmeiser, M. R. Latent and Delayed Action Polymerization Systems, *Macromol. Rapid Commun.* **2014**, *35*, 682–701.
- (19) Bourissou, D.; Guerret, O.; Gabbai, F. P.; Bertrand, G. Stable Carbenes. *Chem. Rev.* **2000**, *100*, 39–92.
- (20) Marion, N.; Diez-Gonzalez, S.; Nolan, S. P. N-Heterocyclic Carbenes as Organocatalysts. *Angew. Chem., Int. Ed.* **2007**, *46*, 2988–3000.
- (21) Enders, D.; Niemeier, O.; Henseler, A. Organocatalysis by N-Heterocyclic Carbenes. *Chem. Rev.* **2007**, *107*, 5606–5655.
- (22) Hopkinson, M. N.; Richter, C.; Schedler, M.; Glorius, F. An Overview of N-Heterocyclic Carbenes. *Nature* **2014**, *510*, 485–496.
- (23) Coulembier, O.; Dove, A. P.; Pratt, R. C.; Sentman, A. C.; Culkun, D. A.; Mespouille, L.; Dubois, P.; Waymouth, R. M.; Hedrick, J. L. Latent Thermally Activated Organic Catalysts for the On-Demand Living Polymerization of Lactide. *Angew. Chem., Int. Ed.* **2005**, *44*, 4964–4968.
- (24) Brown, H. A.; Xiong, S.; Medvedev, G. A.; Chang, Y. A.; Abu-Omar, M. M.; Caruthers, J. M.; Waymouth, R. M. Zwitterionic Ring-Opening Polymerization: Models for Kinetics of Cyclic Poly(ϵ -caprolactone) Synthesis. *Macromolecules* **2014**, *47*, 2955–2963.
- (25) Chang, Y. A.; Waymouth, R. M. Ion Pairing Effects in the Zwitterionic Ring Opening Polymerization of δ -Valerolactone. *Polym. Chem.* **2015**, *6*, 5212–5218.
- (26) Xia, H.; Kan, S.; Li, Z.; Chen, J.; Cui, S.; Wu, W.; Ouyang, P.; Guo, K. N-Heterocyclic Carbenes as Organocatalysts in Controlled/Living Ring-Opening Polymerization of O-Carboxyanhydrides Derived from L-Lactic Acid and L-Mandelic Acid. *J. Polym. Sci., Part A: Polym. Chem.* **2014**, *52*, 2306–2315.
- (27) Guo, L.; Zhang, D. Cyclic Poly(α -peptoid)s and Their Block Copolymers from N-Heterocyclic Carbene-Mediated Ring-Opening Polymerizations of N-Substituted N-Carboxyanhydrides. *J. Am. Chem. Soc.* **2009**, *131*, 18072–18074.
- (28) Guo, L.; Lahasky, S. H.; Ghale, K.; Zhang, D. N-Heterocyclic Carbene-Mediated Zwitterionic Polymerization of N-Substituted N-Carboxyanhydrides toward Poly(α -peptoid)s: Kinetic, Mechanism, and Architectural Control. *J. Am. Chem. Soc.* **2012**, *134*, 9163–9171.
- (29) Lahasky, S. H.; Serem, W. K.; Guo, L.; Garino, J. C.; Zhang, D. Synthesis and Characterization of Cyclic Brush-Like Polymers by N-Heterocyclic Carbene-Mediated Zwitterionic Polymerization of N-Propargyl N-Carboxyanhydride and the Grafting-to Approach. *Macromolecules* **2011**, *44*, 9063–9074.
- (30) Stukenbroeker, T. S.; Solis-Ibarra, D.; Waymouth, R. M. Synthesis and Topological Trapping of Cyclic Poly(alkylene phosphates). *Macromolecules* **2014**, *47*, 8224–8230.
- (31) Nederberg, F.; Lohmeijer, B. G. G.; Leibfarth, F.; Pratt, R. C.; Choi, J.; Dove, A. P.; Waymouth, R. M.; Hedrick, J. L. Organocatalytic Ring Opening Polymerization of Trimethylene Carbonate. *Biomacromolecules* **2007**, *8*, 153–160.
- (32) Venkataraman, S.; Ng, V. W. L.; Coady, D. J.; Horn, H. W.; Jones, G. O.; Fung, T. S.; Sardon, H.; Waymouth, R. M.; Hedrick, J. L.; Yang, Y. Y. A Simple and Facile Approach to Aliphatic N-Substituted Functional Eight-Membered Cyclic Carbonates and Their Organocatalytic Polymerization. *J. Am. Chem. Soc.* **2015**, *137*, 13851–13860.
- (33) Brown, H. A.; Chang, Y. A.; Waymouth, R. M. Zwitterionic Polymerization to Generate High Molecular Weight Cyclic Poly(carbosiloxane)s. *J. Am. Chem. Soc.* **2013**, *135*, 18738–18741.
- (34) Naumann, S.; Epple, S.; Bonten, C.; Buchmeiser, M. R. Polymerization of ϵ -Caprolactam by Latent Precatalysts Based on Protected N-Heterocyclic Carbenes. *ACS Macro Lett.* **2013**, *2*, 609–612.
- (35) Naumann, S.; Schmidt, F. G.; Frey, W.; Buchmeiser, M. R. Protected N-Heterocyclic Carbene as Latent Pre-Catalyst for the Polymerization of ϵ -Caprolactone. *Polym. Chem.* **2013**, *4*, 4172–4181.
- (36) Raynaud, J.; Absalon, C.; Gnanou, Y.; Taton, D. N-Heterocyclic Carbene-Induced Zwitterionic Ring-Opening Polymerization of Ethylene Oxide and Direct Synthesis of α , ω -Difunctionalized Poly(ethylene oxide)s and Poly(ethylene oxide)-b-poly(ϵ -caprolactone) Block Copolymers. *J. Am. Chem. Soc.* **2009**, *131*, 3201–3209.
- (37) Raynaud, J.; Ottou, W. N.; Gnanou, Y.; Taton, D. Metal-Free and Solvent-Free Access to α , ω -heterodifunctionalized Poly(propylene oxide)s by N-Heterocyclic Carbene-Induced Ring Opening Polymerization. *Chem. Commun.* **2010**, *46*, 3203–3205.
- (38) Bakkali-Hassani, C.; Rieger, E.; Vignolle, J.; Wurm, F. R.; Carloti, S.; Taton, D. The Organocatalytic Ring-Opening Polymerization of N-tosyl Aziridines by an N-Heterocyclic Carbene. *Chem. Commun.* **2016**, *52*, 9719–9722.
- (39) Bakkali-Hassani, C.; Rieger, E.; Vignolle, J.; Wurm, F. R.; Carloti, S.; Taton, D. Expanding the Scope of N-Heterocyclic Carbene-Organocatalyzed Ring-Opening Polymerization of N-Tosyl Aziridines using Functional and Non-Activated Amine Initiators. *Eur. Polym. J.* **2017**, *95*, 746–755.
- (40) Raynaud, J.; Ciolino, A.; Baccaredo, A.; Destarac, M.; Bonnette, F.; Kato, T.; Gnanou, Y.; Taton, D. Harnessing the Potential of N-Heterocyclic Carbenes for the Rejuvenation of Group-Transfer Polymerization of (Meth)Acrylics. *Angew. Chem.* **2008**, *120*, 5470–5473.
- (41) Scholten, M. D.; Hedrick, J. L.; Waymouth, R. M. Group Transfer Polymerization of Acrylates Catalyzed by N-Heterocyclic Carbenes. *Macromolecules* **2008**, *41*, 7399–7404.
- (42) Raynaud, J.; Gnanou, Y.; Taton, D. Group Transfer Polymerization of (Meth)acrylic Monomers Catalyzed by N-Heterocyclic Carbenes and Synthesis of All Acrylic Block Copolymers: Evidence for an Associative Mechanism. *Macromolecules* **2009**, *42*, 5996–6005.
- (43) Raynaud, J.; Liu, N.; Gnanou, Y.; Taton, D. Expanding the Scope of Group Transfer Polymerization Using N-Heterocyclic Carbenes as Catalysts: Application to Miscellaneous (Meth)acrylic Monomers and Kinetic Investigations. *Macromolecules* **2010**, *43*, 8853–8861.
- (44) Sardon, H.; Pascual, A.; Mecerreyes, D.; Taton, D.; Cramail, H.; Hedrick, J. L. Synthesis of Polyurethanes Using Organocatalysis: A Perspective. *Macromolecules* **2015**, *48*, 3153–3165.
- (45) Naumann, S.; Speiser, M.; Schowner, R.; Giebel, E.; Buchmeiser, M. R. Air Stable and Latent Single-Component Curing of Epoxy/

Anhydride Resins Catalyzed by Thermally Liberated N-Heterocyclic Carbene. *Macromolecules* **2014**, *47*, 4548–4556.

(46) Zhang, Y.; Chen, E. Y.-X. Conjugate-Addition Organopolymerization: Rapid Production of Acrylic Bioplastics by N-Heterocyclic Carbenes. *Angew. Chem., Int. Ed.* **2012**, *51*, 2465–2469.

(47) Hong, M.; Tang, X.; Falivene, L.; Caporaso, L.; Cavallo, L.; Chen, E. Y.-X. Proton-Transfer Polymerization by N-Heterocyclic Carbenes: Monomer and Catalyst Scopes and Mechanism for Converting Dimethacrylates into Unsaturated Polyesters. *J. Am. Chem. Soc.* **2016**, *138*, 2021–2035.

(48) Falivene, L.; Cavallo, L. Guidelines to Select the N-Heterocyclic Carbene for the Organopolymerization of Monomers with a Polar Group. *Macromolecules* **2017**, *50*, 1394–1401.

(49) Stewart, I. C.; Lee, C. C.; Bergman, R. G.; Toste, F. D. Living Ring-Opening Polymerization of N-Sulfonylaziridines: Synthesis of High Molecular Weight Linear Polyamines. *J. Am. Chem. Soc.* **2005**, *127*, 17616–17617.

(50) Rieger, E.; Manhart, A.; Wurm, F. R. Multihydroxy Polyamines by Living Anionic Polymerization of Aziridines. *ACS Macro Lett.* **2016**, *5*, 195–198.

(51) Rieger, E.; Gleede, T.; Weber, K.; Manhart, A.; Wagner, M.; Wurm, F. R. The Living Anionic Polymerization of Activated Aziridines: A Systematic Study of Reaction Conditions and Kinetics. *Polym. Chem.* **2017**, *8*, 2824–2832.

(52) Gleede, T.; Rieger, E.; Homann-Müller, T.; Wurm, F. R. 4-Styrenesulfonyl-(2-methyl)aziridine: The First Bivalent Aziridine-Monomer for Anionic and Radical Polymerization. *Macromol. Chem. Phys.* **2018**, *219*, 1700145.

(53) Reisman, L.; Mbarushimana, C. P.; Cassidy, S. J.; Rupar, P. A. Living Anionic Copolymerization of 1-(Alkylsulfonyl)aziridines to Form Poly(sulfonylaziridine) and Linear Poly(ethylenimine). *ACS Macro Lett.* **2016**, *5*, 1137–1140.

(54) Wang, X.; Liu, Y.; Li, Z.; Wang, H.; Gebru, H.; Chen, S.; Zhu, H.; Wei, F.; Guo, K. Organocatalyzed Anionic Ring-Opening Polymerizations of N-Sulfonyl Aziridines with Organic Superbases. *ACS Macro Lett.* **2017**, *6*, 1331–1336.

(55) Kuhn, N.; Kratz, T. Synthesis of Imidazol-2-ylidenes by Reduction of Imidazole-2(3H)-thiones. *Synthesis* **1993**, *1993*, 561–562.

(56) Aminoalcohols have recently been used to initiate the ROP of N-substituted glycine, leading to α -hydroxyl- ω -aminotelechelic polypeptides under certain conditions: Tao, X.; Zheng, B.; Bai, T.; Zhu, B.; Ling, J. Hydroxyl Group Tolerated Polymerization of N-Substituted Glycine N-Thiocarboxyanhydride Mediated by Aminoalcohols: A Simple Way to α -Hydroxyl- ω -aminotelechelic Polypeptides. *Macromolecules* **2017**, *50*, 3066–3077.

(57) A detailed investigation into the NHC-mediated ZROP of 2-alkyl-N-tosyl aziridines will be the topic of a forthcoming publication.

(58) Yagci, Y.; Atilla Tasdelen, M. Mechanistic Transformations Involving Living and Controlled/Living Polymerization Methods. *Prog. Polym. Sci.* **2006**, *31*, 1133–1170.

(59) Bernaerts, K. V.; Du Prez, F. E. Dual/Heterofunctional Initiators for the Combination of Mechanistically Distinct Polymerization Techniques. *Prog. Polym. Sci.* **2006**, *31*, 671–722.

(60) Chagneux, N.; Trimaille, T.; Rollet, M.; Beaudoin, E.; Gérard, P.; Bertin, D.; Gigmes, D. Synthesis of Poly(n-butyl acrylate)-b-poly(ϵ -caprolactone) through Combination of SG1-Nitroxide-Mediated Polymerization and Sn(Oct)2-Catalyzed Ring-Opening Polymerization: Study of Sequential and One-Step Approaches from a Dual Initiator. *Macromolecules* **2009**, *42*, 9435–9442.

(61) Aydogan, C.; Kutahya, C.; Allushi, A.; Yilmaz, G.; Yagci, Y. Block Copolymer Synthesis in One Shot: Concurrent Metal-Free ATRP and ROP Processes Under Sunlight. *Polym. Chem.* **2017**, *8*, 2899–2903.

C.P. 4: Ruthenocenyl Glycidyl Ether for anionic polymerization

ORGANOMETALLICS


Article

pubs.acs.org/Organometallics

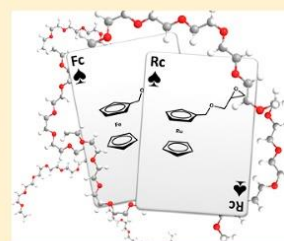
Ruthenocenyl Glycidyl Ether: A Ruthenium-Containing Epoxide for Anionic Polymerization

Arda Alkan, Tassilo Gleede, and Frederik R. Wurm*

Max Planck Institute for Polymer Research (MPIP), Ackermannweg 10, 55128 Mainz, Germany

 Supporting Information

ABSTRACT: Ruthenocenyl glycidyl ether (rcGE) is a novel monomer for the anionic polymerization and copolymerization with ethylene oxide to water-soluble, thermo-, and redox-responsive organometallic poly(ethylene glycol)s (PEGs). The polymers exhibit adjustable molecular weights, comonomer ratios, and narrow molecular weight distributions (typically $M_w/M_n < 1.2$). Real-time ^1H NMR copolymerization kinetics prove random incorporation of rcGE into the polyether backbone in analogy to its ferrocene analog. The rcGE-co-EO copolymers are water-soluble with a lower critical solution temperature, depending on the rcGE content. Terpolymerization of ferrocenyl glycidyl ether, ethylene oxide, and rcGE produces the first random PEG derivatives with multiple redox response. Ruthenocenyl glycidyl ether broadens the field of organometallics, especially ruthenium-containing polymers, and these copolymers might find applications in catalysis, as redox-active surfactants, or as staining reagents in electron microscopy.



INTRODUCTION

Organometallic polymers combine the properties of inorganic elements with those of synthetic polymers. Most of them are hydrophobic, while water-soluble organometallic polymers are scarce. Poly(ethylene glycol) (PEG) is the polymer when applications in water are demanded. It is one of the most often used synthetic water-soluble polymers. PEG dominates the food industry and cosmetic and medical applications as well as being used as soft segment in polyurethanes and in various other applications.^{1,2}

To date, no report on ruthenocene (rc)-functionalized PEG is found in the literature. The incorporation of metals into such polymers might be interesting for installing novel properties into organic materials,^{3,4} such as redox response, catalytic activity, or being used in biomedical applications.^{5–7} Metallocenes are attractive to be combined with organic polymeric materials, with ferrocene (fc) being the most studied derivative,⁸ but polymers with cobaltocene,^{9–13} rhodocene,¹⁴ nickelocene,^{15,16} or rc¹⁷ have been reported. The placement of metals into such materials might also enable them to be used as an imaging reagent in electron microscopy. Amphiphilic systems like hydrophilic polymers with an alkyl anchor or block polymers could be of special interest as a staining reagent. They can improve contrast to liposomes or colloidal systems if used as surfactant.¹⁸

Ruthenium is of special interest in catalysis and redox chemistry.¹⁹ However, only few examples of ruthenium-containing polymers have been reported.^{17,20–22} Ruthenocene was incorporated as side chains into poly(methacrylate)s,¹⁷ poly(phosphazene)s,²¹ or in the polymer backbone after ring-opening polymerization of [1]ruthenocenophanes.²⁰ Even more rare in the literature are water-soluble organometallic

polymers.²³ In our continuous research on the development of precise and water-soluble metallocene-containing polymers,^{23,24} we expanded our monomer design to ruthenium.

Herein, we prepare the first rc-containing epoxide (rcGE) that can undergo ring-opening polymerization. By the living anionic polymerization, organometallic polyethers and well-defined copolymers with ethylene oxide are available for the first time. We recently reported on the design of iron-containing polyethylene glycols, carrying pendant fc groups along the polyether, which were used as triple-responsive polymers for surface coatings or for the preparation of organometallic hyperbranched polyglycerol.^{25–28} In contrast to fc, which can be incorporated into polymers as side or main chain element,²³ rc in polymers is much less studied.²³ This might be attributed to the difficulty of polymerizing redox sensitive compounds, the less expressed redox reversibility of rc, or simply the high costs of the starting rc compared to fc.

The synthesis of a novel monomer that can be copolymerized with ethylene oxide, i.e., rc glycidyl ether (rcGE), is the key to generating rc-loaded PEGs. These materials were studied with respect to their thermal properties in aqueous solution and redox profile. In addition, “bimetallic” copolymers carrying both fc as well as rc-moieties along the polyether backbone were prepared by terpolymerization of ethylene oxide (EO), ferrocenyl glycidyl ether (fcGE), and rc glycidyl ether (rcGE). Additionally, this is the first report to date on bimetallic PEG. We believe that rcGE broadens the scope of organometallic monomers for the production of various other structures, such as the design of future smart materials in water.

Received: April 12, 2017

Published: August 16, 2017

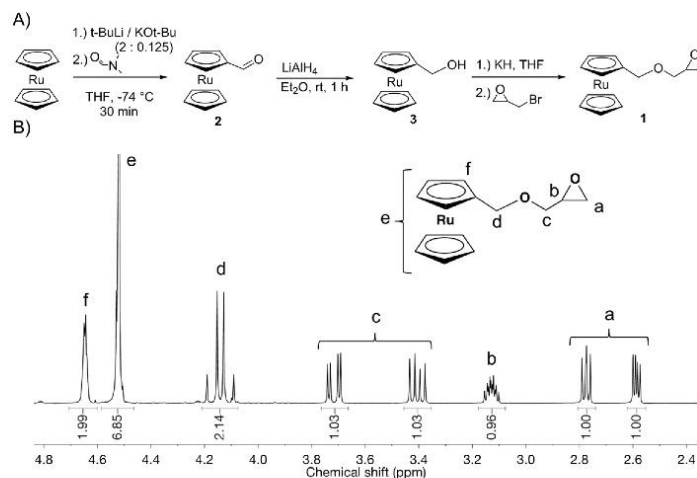


Figure 1. (A) Synthesis of ruthenocenyl glycidyl ether (rcGE). (B) ^1H NMR spectrum of rcGE (1) (300 MHz, $\text{chloroform-}d_1$).

Table 1. Characterization Data for rcGE-co-EO and rcGE-co-fcGE-co-EO Copolymers

no.	formula	rcGE (mol %) ^a	fcGE (mol %) ^a	M_n (g mol ⁻¹) ^a	M_n (g mol ⁻¹) ^b	D^b
Terpolymers						
P1	$\text{BnOCH}_2\text{CH}_2\text{OP}[\text{EO}_{277}\text{-co-fcGE}_{17}\text{-co-rcGE}_{16}]$	5.2	5.4	21800	2200	1.15
P2	$\text{BnOCH}_2\text{CH}_2\text{OP}[\text{EO}_{359}\text{-co-fcGE}_7\text{-co-rcGE}_8]$	10.3	9.8	7000	2100	1.10
P3	$\text{BnOCH}_2\text{CH}_2\text{OP}[\text{EO}_{392}\text{-co-fcGE}_4\text{-co-rcGE}_4]$	1.3	1.3	15200	4000	1.09
P4	$\text{BnOCH}_2\text{CH}_2\text{OP}[\text{EO}_{125}\text{-co-fcGE}_2\text{-co-rcGE}_2]$	1.7	1.2	6600	4000	1.12
Copolymers						
P5	$\text{BnOCH}_2\text{CH}_2\text{OP}[\text{EO}_{213}\text{-co-rcGE}_{18}]$	7.6		15000	4300	1.10
P6	$\text{BnOCH}_2\text{CH}_2\text{OP}[\text{EO}_{372}\text{-co-rcGE}_7]$	1.9		18600	1900	1.15
P7	$\text{BnOCH}_2\text{CH}_2\text{OP}[\text{EO}_{105}\text{-co-rcGE}_6]$	5.4		6500	2500	1.12
With R = 1,2-Bis(hexadecyl)glycerol						
P8	$\text{R}[\text{EO}_{107}\text{-co-rcGE}_1]$	1.0		6300	1600	1.10
P9	$\text{R}[\text{EO}_{95}\text{-co-rcGE}_2]$	2.5		5600	2000	1.10
Copolymerization Kinetics						
P10	$\text{BnOCH}_2\text{CH}_2\text{OP}[\text{EO}_{125}\text{-co-rcGE}_{16}]$	11.2		10400	3400	1.20

^aDetermined from ^1H NMR spectroscopy. ^bDetermined by size exclusion chromatography in DMF vs PEG standards. $D = M_w/M_n$

RESULTS AND DISCUSSION

Monomer Synthesis. Ruthenocenyl glycidyl ether (1) was synthesized in a three-step protocol starting from rc (Figure 1 A). In the first step, rc is deprotonated by the use of the Schlosser's base, a mixture of *tert*-butyllithium (*t*-BuLi) and potassium *tert*-butoxide (*t*-BuOK). The intermediate rc carboxaldehyde (2) is obtained after the reaction of dimethylformamide (DMF) with the carbanion.²⁹ In the second step, rc carboxaldehyde (2) is reduced with lithium aluminumhydride to ruthenocenyl methanol (3).³⁰ Ruthenocenyl glycidyl ether (1) is obtained after deprotonation of the alcohol with potassium hydride and reaction with epibromohydrine, similar to the protocol described previously for other glycidyl ethers.²⁸ The monomer is obtained as a light yellow liquid in an overall yield of ca. 68% after purification via column chromatography. See the Supporting Information for a detailed synthesis protocol. Figure 1B shows the ^1H NMR spectrum of 1 in $\text{chloroform-}d_1$; ^{13}C (Figure S1), ^{13}C DEPT (Figure S2), HSQC (Figure S3), HMBC (Figure S4), and COSY (Figure S5) NMR spectra with the respective assignments are listed in

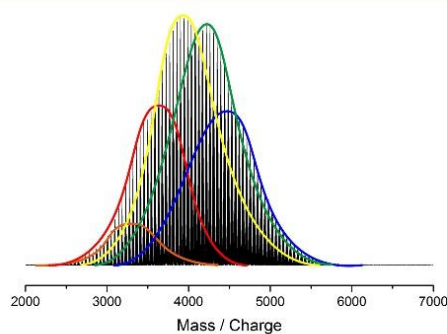


Figure 2. Individual superposition of P7MALDI ToF MS spectrum: orange: $\text{BnOCH}_2\text{CH}_2\text{OP}[\text{EO}_2\text{-co-rcGE}_1]\cdot\text{Ag}^+$, Red: $\text{BnOCH}_2\text{CH}_2\text{OP}[\text{EO}_3\text{-co-rcGE}_2]\cdot\text{Ag}^+$, yellow: $\text{BnOCH}_2\text{CH}_2\text{OP}[\text{EO}_4\text{-co-rcGE}_3]\cdot\text{Ag}^+$, green: $\text{BnOCH}_2\text{CH}_2\text{OP}[\text{EO}_5\text{-co-rcGE}_4]\cdot\text{Ag}^+$, blue: $\text{BnOCH}_2\text{CH}_2\text{OP}[\text{EO}_x\text{-co-rcGE}_5]\cdot\text{Ag}^+$.

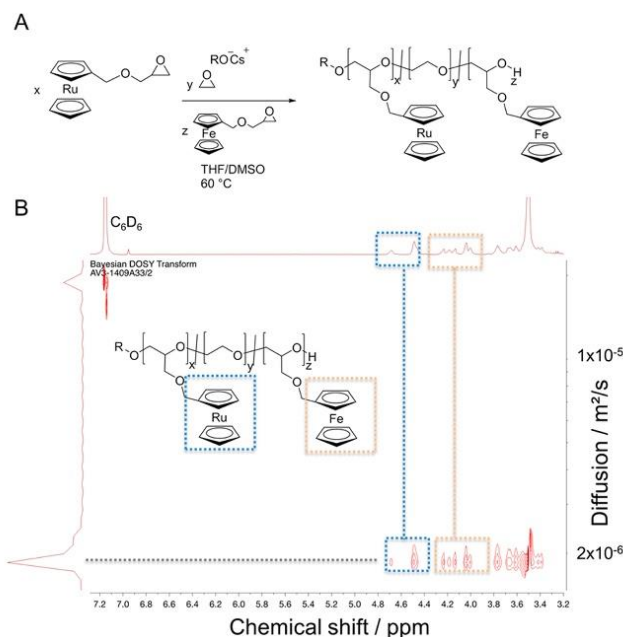


Figure 3. (A) Scheme for the anionic terpolymerization of rcGE, fcGE, and EO. (B) ^1H DOSY NMR spectrum (in benzene- d_6) of the terpolymer P(rcGE-*co*-fcGE-*co*-EO), proving the incorporation of the three monomers in the terpolymer.

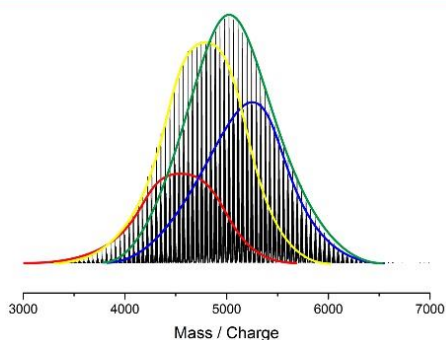


Figure 4. Individual superposition of P4MALDI ToF MS spectrum: red: $\text{BnOCH}_2\text{CH}_2\text{OP}[\text{EO}_x\text{-}co\text{-fcGE}_0\text{-}co\text{-rcGE}_1]\cdot\text{Cs}^+$, yellow: $\text{BnOCH}_2\text{CH}_2\text{OP}[\text{EO}_x\text{-}co\text{-fcGE}_1\text{-}co\text{-rcGE}_1]\cdot\text{Cs}^+$, green: $\text{BnOCH}_2\text{CH}_2\text{OP}[\text{EO}_x\text{-}co\text{-fcGE}_{1+n}\text{-}co\text{-rcGE}_{1+(n-1)}]\cdot\text{Cs}^+$, blue: $\text{BnOCH}_2\text{CH}_2\text{OP}[\text{EO}_x\text{-}co\text{-fcGE}_2\text{-}co\text{-rcGE}_2]\cdot\text{Cs}^+$.

the Supporting Information proving the signal assignments. The multiplets at 2.6, 2.8, and 3.1 ppm prove the formation of the epoxide monomer. In addition, the characteristic signals for a monosubstituted rc derivative are detected at 4.5 and ca. 4.6 ppm.

Polymerization. Water-soluble copolymers of rcGE and ethylene oxide were prepared by the anionic ring-opening polymerization following literature conditions for other EO copolymerizations.²⁸ In brief, after deprotonation of the initiator benzyloxyethanol with cesium hydroxide to its cesium

alkoxide, the copolymerization of rcGE and EO was conducted in a THF/DMSO mixture at 60 °C. Molecular weights of the copolymers were calculated by end-group analysis from the ^1H NMR spectra (Figure S6). The aromatic initiator resonances (at ca. 7.2 ppm) were compared to the resonances of both repeat units in the polymer to give (i) the overall molecular weight and (ii) the copolymer composition. Both are typically in accordance to the theoretical values, as the polymerization proceeds under living conditions. The molar ratio of rcGE in the copolymers matched well with the feed ratio and was determined from the ^1H NMR resonances of the rc-units between 3.8 and 4.2 ppm and the PEO backbone at ca. 3.5 ppm.

Molecular weights from 1900 to 4300 g mol^{-1} were synthesized. The molar fraction of rcGE was varied from 1.9 to 7.8% to ensure the water-solubility of the copolymers. As the rcGE units introduce hydrophobicity into the PEG backbone, the comonomer feed was kept below 10% rcGE; otherwise, water-insoluble copolymers are obtained, as reported for fcGE-EO copolymers (compare below).²⁷ The narrow molecular weight dispersities ($D = M_w/M_n$) range from 1.10 to 1.15 and are listed in Table 1, as determined by size exclusion chromatography (SEC). Molecular weights determined via SEC appear to be smaller compared to molecular weights determined from ^1H NMR spectroscopy. This is a typical finding for organometallic PEG copolymers and other PEG-*co*-polymers with hydrophobic comonomers; it is related to the different solvation of the copolymers compared to the SEC standard PEG.^{28,31}

Matrix-assisted laser desorption/ionization time-of-flight mass spectrometry measurements (MALDI ToF MS) was

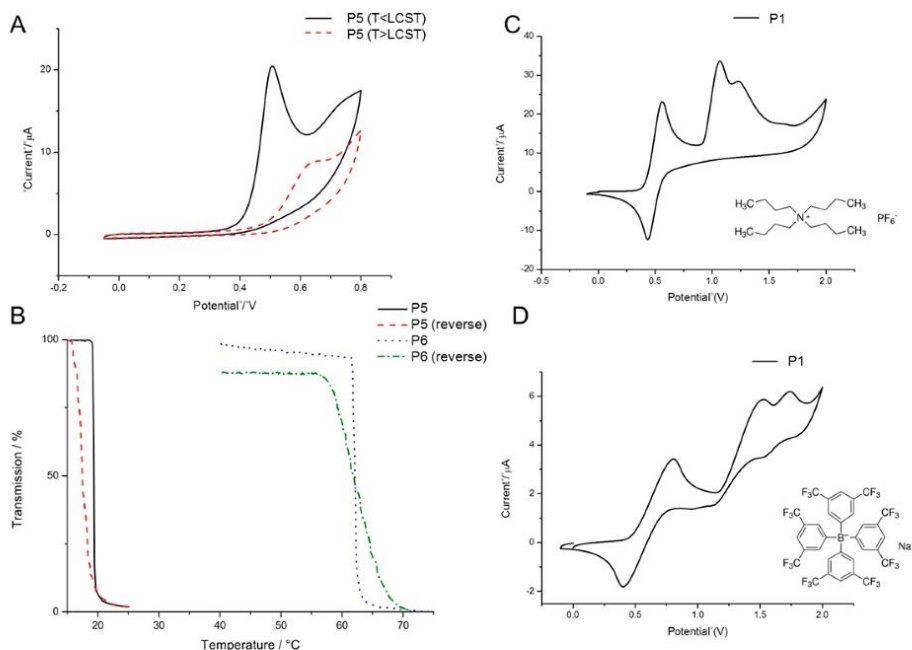


Figure 5. (A) Cyclic voltammogram of P5 in water below (15 °C) and above (25 °C) LCST with KCl as electrolyte. (B) Turbidity measurements of P5 and P6. (C, D) Cyclic voltammograms of P1 in dichloromethane with NBu_4PF_6 (C) and NaBArF_{24} (D) as electrolyte (vs Ag/AgCl).

used to assess the incorporation of both monomers into the copolymer. MALDI MS of organometallic compounds has been reviewed recently.³² P7 and P4 were studied exemplarily, proving the stability of the rc units under these conditions (Figure 2). Molecular weight data is in good agreement with the SEC measurements listed in Table 1. The MALDI spectrum in Figure 2 shows the different compositions of the polymers; it confirms the repeating unit of EO with 44.05 g mol⁻¹ distance in each frame as well as the repeating unit of rcGE of 317.35 g mol⁻¹. The individual masses found in the spectrum were assigned to the polymer cationized with a Ag-ion. The silver triflate added during sample preparation suppressed the Cs-ions completely (which might be detected as counterion during the MALDI experiment as Cs-alkoxides are the propagating species during the polymerization). Each superposition colored individually proving the incorporation of rcGE in the polyether structure (see Figure S7 for original data).

In addition to the copolymers prepared from **1** and EO, terpolymers with **1**, the fc analog (fcGE), and EO were prepared. The terpolymers combine the redox properties of both metallocenes and exhibit defined molecular structures with narrow molecular weight distributions. Figure 3 shows the reaction conditions and the ¹H DOSY NMR spectrum of a representative terpolymer. The resonances for both metallocenes, i.e., rc units (4.4–4.6 ppm) and fc units (4.0–4.2 ppm), are detected at the same diffusion coefficient with the polyether backbone at ca. 3.5 ppm, proving the successful formation of the terpolymer.

Furthermore, the terpolymer P4 was analyzed by MALDI-ToF MS. Figure 4 illustrates the different superposition of the

terpolymer. Each polymer with individual units of fcGE and rcGE and varying units of EO is highlighted by individual colors. The spectrum confirms the repeating unit of EO of 44.05 g mol⁻¹ in each frame. The repeating units of rcGE (317.35 g mol⁻¹) and fcGE (272.13 g mol⁻¹) were also confirmed between the different modes. The individual masses found for in the spectrum correspond to the polymer and Cs-ion. Cs as counterion can be explained as no additive was used for the sample preparation; thus, Cs-ions remaining from the polymer synthesis acted as ionizing species. No masses corresponding to polymer or other ions like Na⁺ were found (see Figure S8 for original data).

As reported previously for fcGE-co-EO copolymers, such structures exhibit a lower critical solution temperature, depending on the comonomer ratio. Exemplarily, Figure 5 shows the turbidity measurements of P5 (with 7.6% rcGE) and P6 (with 1.9% rcGE). Sharp phase separation temperatures at 20 °C (for P5) or 63 °C (for P6) are detected during the heating of the aqueous polymer solution. During the cooling process, this process is fully reversible, and only a slight hysteresis is observed in both cases. This LCST-type phase separation from an aqueous solution might be an additional feature of these novel organometallic polyethers for future applications.

Electrochemical characterization of P5 as a representative water-soluble rc-containing polymer was performed below and above the cloud point. Cloud point signifies the temperature where the polymer becomes insoluble in water or where the transmitted light is decreased to 50% intensity. With the fully water-soluble polymer (below the phase separation temperature), the oxidation wave of rc is detected by cyclic

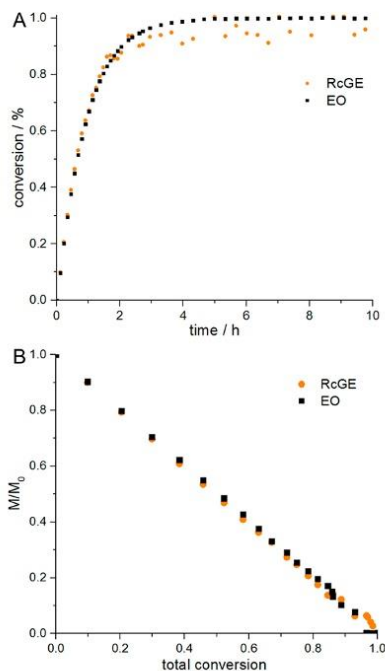


Figure 6. Real-time ^1H NMR kinetics of the copolymerization of ethylene oxide and rcGE (12 mol %) at 40 °C measured in $\text{DMSO-}d_6$. (A) Monomer conversion vs time plot. (B) Monomer conversion of EO and rcGE vs total monomer conversion.

voltammogram (CV) in water (Figure 5A). In contrast to the fully reversible redox behavior of fc, rc does not undergo a reversible reduction in the reverse curve under such conditions, which has been reported previously for other rc-based redox materials.³³ Interestingly, after heating the aqueous polymer solution above the cloud point, the oxidation potential is almost completely lost, as the polymer precipitates from solution. This indicates that the precipitated polymer can no longer undergo an electrochemical reaction (Figure 5A).

In the case of terpolymers, P1 was chosen as a representative terpolymer; the CV measurements were performed in DCM, due to low solubility in water. The reversible oxidation of fc is detected at ca. 0.6 V with a single redox peak (Figure 5C). In addition, the Ru(II) species in rcGE units are oxidized at potentials above 1.0 V as two sets of irreversible redox peaks. In this case, a two-wave oxidation is observed, which might be attributed to the bis(ruthenocenium) dication,³⁴ which was reported for low-molecular-weight rc-compounds earlier under these CV conditions.³⁵ With TBAPF_6 as the supporting electrolyte (Figure 5C), the redox process of rcGE is not reversible with the oxidation peak at ca. 1.1 V and the reduction almost invisible. The irreversible reduction from Ru(III) to Ru(II) could be explained by additional follow-up reactions or ion pairing of the cationic ruthenocenium units with PF_6^- .³⁵

Using a less coordinating anion than PF_6^- in the CV experiment, i.e., tetrakis[(3,5-trifluoromethyl)phenyl]borate (NaBARF_{34}) as electrolyte, a reversible redox behavior of fc (at E_{pc} ca. 0.8 V with i_{pa} and $i_{pc} = 3 \mu\text{A}$) is detected. For rc, a

nonreversible two-wave oxidation at ca. $E_{pc} = 1.5$ V and $E_{pc,2} = 1.75$ V is again detected under such conditions, similar to other metallocene-containing materials.^{14,17,35}

Real-Time ^1H NMR Spectroscopy Copolymerization.

To confirm the random nature of the copolymerization of EO and rcGE during the anionic polymerization, real-time ^1H NMR spectroscopy was used³⁶ (detailed experimental details can be found in the Supporting Information). Briefly, a solution of the initiator in $\text{DMSO-}d_6$ and a mixture of rcGE (11 mol %) and EO (89 mol %) in $\text{DMSO-}d_6$ were separately transferred into a NMR tube under an argon atmosphere and quickly frozen with liquid nitrogen. The cold NMR tube was evacuated and sealed; the polymerization was subsequently initiated by warming the tube to 40 °C in the NMR spectrometer. The growth of the polymer backbone as well as the consumption of both monomers was followed over time by the decrease of the epoxide resonances at 2.61 ppm for the methylene protons of EO and at 3.10–3.18 ppm for the methine resonance of rcGE (signal b, Figure 1).

Figure 6A shows a representative example for the monomer conversion in the course of the polymerization with comonomer content of 11 mol % rcGE. The copolymerization at 40 °C requires 4 h to reach full conversion. Figure 6B illustrates the consumption of the monomers during polymerization, revealing a random incorporation of rcGE and EO into the growing polymer chain. Throughout the polymerization, the molar ratio of rcGE and EO units in the polymer chain remains constant and there is no deviation from the initial ratio of the comonomer feed. As shown for fcGE before, the rc analog does not alter the reactivity of the glycidyl ether structure. This proves the formation of random copolymers of EO and rcGE by anionic copolymerization under the copolymerization conditions studied. It was previously reported that fcGE and EO undergo random copolymerization under these conditions,²⁸ so it can be stated that the nature of the metal (Fe or Ru) in the sandwich complex does not alter the reactivity of the monomers during the anionic copolymerization. Thus, random copolymers are prepared for binary (rcGE or fcGE and EO) and ternary (rcGE + fcGE + EO) monomer mixtures.

CONCLUSIONS

We presented the first ruthenocene-containing epoxide monomer (rcGE) for the anionic polymerization. RcGE was prepared in a three-step protocol from rc. Water-soluble and thermoresponsive materials were prepared by copolymerization with ethylene oxide (EO) by adjusting the comonomer ratio (rcGE/EO). The copolymerization produces well-defined copolymers with adjustable molecular weights and narrow molecular weight distributions (typically $M_w/M_n < 1.2$). Real-time ^1H NMR kinetics proved the random comonomer incorporation. The rcGE-containing PEGs show redox-active behavior in both water and organic solution; however, the reversibility is dependent on the conditions of the oxidation, which is typical for rc-based materials. In addition, by increasing the temperature of the solution above the cloud point temperature, the polymer precipitates from solution and thus allows a reversible on/off switch of its redox-response. In addition, terpolymers containing both ruthenium and iron were prepared by simultaneous copolymerization of EO, rcGE, and fcGE, which allowed the generation of water-soluble bimetallic PEGs with multiple redox responses. Such thermoresponsive ruthenium- and iron-containing polyethers broaden the scope

of organometallic polymers and might find application in catalysis or as covalent staining reagents of PEG-chains for electron microscopy, due to the high electron density of rc.

■ ASSOCIATED CONTENT

● Supporting Information

The Supporting Information is available free of charge on the ACS Publications website at DOI: 10.1021/acs.organomet.7b00278.

Additional schemes, experimental and characterization data (PDF)

■ AUTHOR INFORMATION

Corresponding Author

*E-mail: wurm@mpip-mainz.mpg.de. Phone: 0049 6131 379 581. Fax: 0049 6131 370 330.

ORCID

Frederik R. Wurm: 0000-0002-6955-8489

Notes

The authors declare no competing financial interest.

■ ACKNOWLEDGMENTS

We thank Angelika Manhart (MPIP) for synthetic assistance and Prof. Dr. Andreas Kilbinger (University of Fribourg) for MALDI-ToF measurements. F.R.W. thanks the Max Planck Graduate Center (MPGC) for support.

■ REFERENCES

- Herzberger, J.; Niederer, K.; Pohlitz, H.; Seiwert, J.; Wurm, M.; Wurm, F. R.; Frey, H. *Chem. Rev.* **2016**, *116*, 2170–2243.
- Klein, R.; Wurm, F. R. *Macromol. Rapid Commun.* **2015**, *36*, 1147–65.
- Neuse, E. W.; Rosenberg, H. J. *Macromol. Sci., Polym. Rev.* **1970**, *4*, 1–145.
- Zhou, J.; Whittell, G. R.; Manners, I. *Macromolecules* **2014**, *47*, 3529–3543.
- Nguyen, P.; Gómez-Elipe, P.; Manners, I. *Chem. Rev.* **1999**, *99*, 1515–1548.
- Yan, Y.; Zhang, J.; Ren, L.; Tang, C. *Chem. Soc. Rev.* **2016**, *45*, 5232–5263.
- Fouda, M. F. R.; Abd-Elzaher, M. M.; Abdelsamaia, R. A.; Labib, A. A. *Appl. Organomet. Chem.* **2007**, *21*, 613–625.
- Hudson, R. D. A. *J. Organomet. Chem.* **2001**, 637–639, 47–69.
- Zhang, J.; Chen, Y. P.; Miller, K. P.; Ganewatta, M. S.; Bam, M.; Yan, Y.; Nagarkatti, M.; Decho, A. W.; Tang, C. *J. Am. Chem. Soc.* **2014**, *136*, 4873–4876.
- Zhang, J.; Ren, L.; Hardy, C. G.; Tang, C. *Macromolecules* **2012**, *45*, 6857–6863.
- Ciganda, R.; Gu, H.; Castel, P.; Zhao, P.; Ruiz, J.; Hernandez, R.; Astruc, D. *Macromol. Rapid Commun.* **2016**, *37*, 105.
- Yan, Y.; Zhang, J.; Qiao, Y.; Tang, C. *Macromol. Rapid Commun.* **2014**, *35*, 254–9.
- Yan, Y.; Zhang, J.; Tang, C. *ACS Symp. Ser.* **2015**, *1188*, 15–27.
- Yan, Y.; Deaton, T. M.; Zhang, J.; He, H.; Hayat, J.; Pageni, P.; Matyjaszewski, K.; Tang, C. *Macromolecules* **2015**, *48*, 1644–1650.
- Köhler, F. H.; Schell, A.; Weber, B. *Chem. - Eur. J.* **2002**, *8*, 5219–5227.
- Rosenblum, M.; Nugent, H. M.; Jang, K. S.; Labes, M. M.; Cahalane, W.; Klemarczyk, P.; Reiff, W. M. *Macromolecules* **1995**, *28*, 6330–6342.
- Yan, Y.; Zhang, J.; Qiao, Y.; Ganewatta, M.; Tang, C. *Macromolecules* **2013**, *46*, 8816–8823.
- Alkan, A.; Wald, S.; Louage, B.; De Geest, B. G.; Landfester, K.; Wurm, F. R. *Langmuir* **2017**, *33*, 272–279.
- White, R. E.; Hanusa, T. P. Ruthenium: Organometallic Chemistry. In *Encyclopedia of Inorganic Chemistry*; King, R. B., Ed.; John Wiley & Sons, Ltd.: Hoboken, NJ, 2006.
- Vogel, U.; Lough, A. J.; Manners, I. *Angew. Chem., Int. Ed.* **2004**, *43*, 3321–3325.
- Allcock, H. R. *J. Inorg. Organomet. Polym. Mater.* **2005**, *15*, 57–65.
- Okada, K.; Yamaguchi, B.; Fujisaka, T. *Kobunshi Ronbunshu* **1997**, *54*, 209–216.
- Alkan, A.; Wurm, F. R. *Macromol. Rapid Commun.* **2016**, *37*, 1482–1493.
- Homann-Mueller, T.; Rieger, E.; Alkan, A.; Wurm, F. R. *Polym. Chem.* **2016**, *7*, 5501–5506.
- Alkan, A.; Thomi, L.; Gleede, T.; Wurm, F. R. *Polym. Chem.* **2015**, *6*, 3617–3624.
- Alkan, A.; Steinmetz, C.; Landfester, K.; Wurm, F. R. *ACS Appl. Mater. Interfaces* **2015**, *7*, 26137–26144.
- Alkan, A.; Natalello, A.; Wagner, M.; Frey, H.; Wurm, F. R. *Macromolecules* **2014**, *47*, 2242–2249.
- Tonhauser, C.; Alkan, A.; Schömer, M.; Dingels, C.; Ritz, S.; Mailänder, V.; Frey, H.; Wurm, F. R. *Macromolecules* **2013**, *46*, 647–655.
- Sanders, R.; Mueller-Westerhoff, U. T. *J. Organomet. Chem.* **1996**, *512*, 219–224.
- Barlow, S.; Cowley, A.; Green, J. C.; Brunker, T. J.; Hascall, T. *Organometallics* **2001**, *20*, 5351–5359.
- Niederer, K.; Schüll, C.; Leibig, D.; Johann, T.; Frey, H. *Macromolecules* **2016**, *49*, 1655–1665.
- Wyatt, M. F. *J. Mass Spectrom.* **2011**, *46*, 712–719.
- Gubin, S. P.; Smirnova, S. A.; Denisovich, L. I.; Lubovich, A. A. *J. Organomet. Chem.* **1971**, *30*, 243–255.
- Trupia, S.; Nafady, A.; Geiger, W. E. *Inorg. Chem.* **2003**, *42*, 5480–5482.
- Swarts, J. C.; Nafady, A.; Roudebush, J. H.; Trupia, S.; Geiger, W. E. *Inorg. Chem.* **2009**, *48*, 2156–2165.
- Rieger, E.; Gleede, T.; Weber, K.; Manhart, A.; Wagner, M.; Wurm, F. R. *Polym. Chem.* **2017**, *8*, 2824–2832.